EUROPEAN WATER RESOURCES ASSOCIATION

12th World Congress of EWRA

on Water Resources and Environment

[EWRA 2023]

Managing Water-Energy-Land-Food under Climatic, Environmental and Social Instability

27 June - 1 July 2023, Thessaloniki, Greece

PROCEEDINGS

Editors

Athanasios Loukas

Harris Vangelis

Dimitris Tigkas

Pantelis Sidiropoulos

2023

EUROPEAN WATER RESOURCES ASSOCIATION

12th World Congress of EWRA
on Water Resources and Environment
[EWRA 2023]

Managing Water-Energy-Land-Food under Climatic, Environmental and Social Instability

27 June – 1 July 2023, Thessaloniki, Greece

PROCEEDINGS

Editors

Athanasios Loukas
Harris Vangelis
Dimitris Tigkas
Pantelis Sidiropoulos

2023

ISBN: 978-618-84419-1-0

Managing Water-Energy-Land-Food under Climatic, Environmental and Social Instability
Proceedings of the 12th World Congress of EWRA on Water Resources and Environment
[EWRA 2023]
27 June – 1 July 2023, Thessaloniki, Greece

Editors:
Athanasios Loukas, Harris Vangelis, Dimitris Tigkas, Pantelis Sidiropoulos

EWRA Editorial Office:
Iroon Polytechniou 9, 157 80, Athens, Greece
e-mail: puboffice@ewra.net

Cite this publication as:
Loukas A., Vangelis H., Tigkas D., Sidiropoulos P. (eds.) 2023. Managing Water-Energy-Land-Food under Climatic, Environmental and Social Instability. Proceedings of the 12th World Congress of EWRA on Water Resources and Environment, 27 June – 1 July 2023, Thessaloniki, Greece.

Aegis

Hellenic Republic | Ministry of Climate Crisis and Civil Protection

Organising Bodies

Principal Organiser
Aristotle University of Thessaloniki | Faculty of Engineering | School of Rural and Surveying Engineering

Co-Organiser
Technical Chamber of Greece | Section of Central Macedonia

Sponsors

Platinum Sponsor

Gold Sponsor

Silver Sponsors

Sponsors

Scientific Committee

Ahi, Y.	Ankara University	Turkey
Akratos, C.	Democritus University of Thrace	Greece
Angelides, P.	Democritus University of Thrace	Greece
Aronica, G.	University of Messina	Italy
Assaf, H.	American University of Ras Al Khaimah	U.A.E.
Baltas, E.	National Technical University of Athens	Greece
Bellos, V.	Democritus University of Thrace	Greece
Bonaccorso, B.	University of Messina	Italy
Bresci, E.	University of Florence	Italy
Cancelliere, A.	University of Catania	Italy
Cetinkaya, C.	Dokuz Eylul University	Turkey
Dercas, N.	Agricultural University of Athens	Greece
Efstratiadis, A.	National Technical University of Athens	Greece
Findikakis, A.	Bechtel Corp. – Stanford University	U.S.A.
Franchini, M.	University of Ferrara	Italy
Garrote, L.	Technical University of Madrid	Spain
Georgiou, P.	Aristotle University of Thessaloniki	Greece
Gitau, M.	Purdue University	U.S.A.
Gul, A.	Dokuz Eylul University	Turkey
Hatzimitsis, D.	Technical University of Cyprus	Cyprus
Iglesias, A.	Technical University of Madrid	Spain
Kallioras, A.	National Technical University of Athens	Greece
Kangalou, I.	Democritus University of Thrace	Greece
Karatzas, G.	Technical University of Crete	Greece
Karavitis, C.	Agricultural University of Athens	Greece
Karpouzos, D.	Aristotle University of Thessaloniki	Greece
Katsifarakis, K.	Aristotle University of Thessaloniki	Greece
Kavvas, L.	University of California-Davis	U.S.A.
Khonova, S.	Slovak Technical University of Bratislava	Slovakia
Kjeldsen, T.	University of Bath	U.K.
Kolokytha, E.	Aristotle University of Thessaloniki	Greece
Koutroulis, A.	Technical University of Crete	Greece
Kungolos, A.	Aristotle University of Thessaloniki	Greece
Langousis, A.	University of Patras	Greece
Laspidou, C.	University of Thessaly	Greece

Latinopoulos, D.	Aristotle University of Thessaloniki	Greece
Llasat, C.M.	University of Barcelona	Spain
Loucks, P.	Cornell University	U.S.A.
Maia, R.	University of Porto	Portugal
Makropoulos, C.	National Technical University of Athens	Greece
Mallios, Z.	Aristotle University of Thessaloniki	Greece
Maris, F.	Democritus University of Thrace	Greece
Mediero, L.	Technical University of Madrid	Spain
Mylopoulos, N.	University of Thessaly	Greece
Nalbantis, I.	National Technical University of Athens	Greece
Nikolaidis, N.	Technical University of Crete	Greece
Nohara, D.	Kajima Technical Research Institute	Japan
Noto, V.	University of Palermo	Italy
Panagopoulos, I.	Aristotle University of Thessaloniki	Greece
Papadopoulou, M.	National Technical University of Athens	Greece
Papaioannou, G.	Democritus University of Thrace	Greece
Papalexiou, S.M.	University of Calgary	Canada
Papamichail, D.	Aristotle University of Thessaloniki	Greece
Psilovikos, A.	University of Thessaly	Greece
Sapountzis, M.	Aristotle University of Thessaloniki	Greece
Sechi, G.	University of Cagliari	Italy
Simonovic, S.	Western University	Canada
Spiliotis, M.	Democritus University of Thrace	Greece
Srdjevic, Z.	University of Novi Sad	Serbia
Sylaios, G.	Democritus University of Thrace	Greece
Szolgay, J.	Slovak Technical University of Bratislava	Slovakia
Tayfur, G.	Izmir Institute of Technology	Turkey
Teegavarapu, R.	Florida Atlantic University	U.S.A.
Teodosiu, C.	Gheorghe Asachi Technical University of Iasi	Romania
Theodossiou, N.	Aristotle University of Thessaloniki	Greece
Vagiona, D.	Aristotle University of Thessaloniki	Greece
Vasiliades, L.	University of Thessaly	Greece
Vicente-Serrano, S.	Spanish National Research Council	Spain
Voudouris, K.	Aristotle University of Thessaloniki	Greece
Werner, M.	IHE Delft	The Netherlands
Wu, J.	Nanjing Institute of Geology and Limnology	China
Xenarios, S.	Nazarbayev University	Kazakhstan
Xu, J.	Louisiana State University	U.S.A.
Zouboulis, A.	Aristotle University of Thessaloniki	Greece

Organising and Scientific Committee

Loukas, A. (Chair)	Aristotle University of Thessaloniki
Oikonomou, E.	Aristotle University of Thessaloniki
Papaevangelou, G.	Aristotle University of Thessaloniki
Sidiropoulos, P.	Aristotle University of Thessaloniki
Chatzigiannis, A.	Technical Chamber of Greece - Section of Central Macedonia
Tsakiris, G.	National Technical University of Athens
Tsihrintzis, V.	National Technical University of Athens
Vangelis, H.	National Technical University of Athens
Tigkas, D.	National Technical University of Athens
Kourtis, I.	National Technical University of Athens

Editors' Preface

The European Water Resources Association (EWRA) is an international non-profit association, established in 1992, aiming at enhancing cooperation and exchanges in research and application in the field of water resources. The organization of a bi-annual World Congress is one of the diverse activities of EWRA, providing a forum of discussions between scientists and professional engineers. After the successful 11th World Congress of EWRA in Madrid, the next Congress, initially scheduled to be held in 2021, was postponed due to the worldwide negative impacts of the Covid-19 pandemic.

This volume of Proceedings includes the papers presented at the 12th World Congress of EWRA on Water Resources and Environment that was held in Thessaloniki, Greece, 27 June – 1 July 2023, under the title "Managing Water-Energy-Land-Food under Climatic, Environmental and Social Instability". The principal organiser of the Congress was the Aristotle University of Thessaloniki - Faculty of Engineering, School of Rural and Surveying Engineering and the co-organiser was the Technical Chamber of Greece - Section of Central Macedonia. The Congress was origanised under the auspices of the Greek Ministry of Climate Crisis and Civil Protection.

The aim of the Congress was to discuss innovation in water resources management to address current and future challenges: growing uncertainty, greater extremes, increasing demand, water scarcity and global change. While traditional management practice is still effective, new technologies and approaches are emerging to better protect, regulate, allocate and recycle water resources. Sustainable management of water resources in the 21st Century requires a comprehensive understanding of the interaction of complex natural and social components in a changing context. The Congress aimed to seek scientifically sound and economically-efficient solutions that are environmentally friendly, socially acceptable and climate-proof.

The Congress intended to be a forum for scientists and engineers from diverse cultures around the world to discuss their understanding of water resources systems at a diversity of scales and to promote environmentally sustainable water resources management. The Proceedings contain a compilation of peer-reviewed papers describing the communications presented at the Congress, including a wide range of topics addressing the most critical aspects of water resources management.

The Proceedings are organised following the twelve specialised conferences of the Congress:

I. Hydrological Extremes and Hazards under Climatic Instability
II. Water Related Hazards and risks
III. Water Quality and Advanced Water Treatment
IV. Hydrological Modelling of Complex River Basins
V. Urban and Agricultural Water Systems
VI. Water-Energy-Land-Food Nexus
VII. Ecosystems and Environmental Processes
VIII. Groundwater Contamination and Management

IX. Geoinformatics, Remote Sensing and Big Data Handling
X. Transboundary River Basin Management and Hydro-diplomacy
XI. Socioeconomic Aspects and Water Resources Policies and Governance
XII. Global Water Security

All the papers presented at the Congress will be assessed for possible invitation to be extended and enhanced, so as to be published after peer review process in the journals of EWRA (*Water Resources Management*, *Environmental Processes*, *European Water* and *Water Utility Journal*).

The editors would like to thank:

- The Aristotle University of Thessaloniki for hosting the Congress, providing the academic space to share ideas and interchange opinions
- The authors of the papers and the participants of the Congress, for their knowledge and contributions.
- The members of the Scientific and Organizing Committees for their efforts devoted to prepare the structure of the Congress, to supervise peer-review of the contributions and to conduct the sessions in an efficient way.
- The sponsors of the Congress for their financial support.

The Editors

Table of Contents

Keynote Speekers

I. Hydrological Extremes and Hazards under Climatic Instability

II. Water Related Hazards and Risks

III. Water Quality and Advanced Water Treatment

IV. Hydrological Modelling of Complex River Basins

V. Urban and Agricultural Water Systems

VI. Water-Energy-Land-Food Nexus

VII. Ecosystems and Environmental Processes

VIII. Groundwater Contamination and Management

IX. Geoinformatics, Remote Sensing and Big Data Handling

X. Transboundary River Basin Management and Hydro-diplomacy

XI. Socioeconomic Aspects and Water Resources Policies and Governance

XII. Global Water Security

Keynote Speekers

Water and the question of sustainability and/or growth

Angelos Findikakis
Stanford University / Bechtel Corporation, United States of America

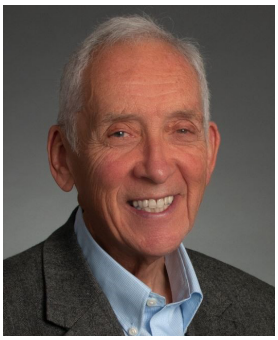

Angelos Findikakis has spent most of his career with Bechtel Corporation working in studies supporting the licensing, design and construction of industrial and civil infrastructure projects in the United States and around the world. He specializes in water resources, hydraulics and hydrology. As a Bechtel Fellow he has an active role in Bechtel's technical excellence program.
As Adjunct Professor at Stanford University he taught water resources management for several years.
He has been active in different national and international professional associations, currently serving as Editor of the quarterly magazine Hydrolink and as IAHR's Liaison to the UN Water program.

Coupled human-nature systems: Greater than the sum of their parts?

Kaveh Madani
United Nations University, Institute for Water, Environment and Health, Canada

Prof. Kaveh Madani is a globally recognized scientist, educator, and activist, working on complex human-water systems at the interface of science, policy, and society. He is currently the Director of the United Nations University Institute for Water, Environment and Health (UNU-INWEH), *aka* the UN think tank on water.
He has previously served as the Deputy Head of Iran's Department of Environment, Vice President of the UN Environment Assembly Bureau, Chief of Iran's Department of Environment's International Affairs and Conventions Center, Head of the Resource Nexus Research Programme at the United Nations University, and a tenured faculty member of the Centre for Environmental Policy at Imperial College London.
Prof. Madani is an expert in applying mathematical and economic methods to complex human-water problems to derive policy and governance insights. He has over 200 publications and is a Fellow of AGU and EWRI. He has received numerous awards and recognitions for his fundamental research contributions, teaching innovations, as well as outreach and humanitarian activities, including the New Face of Civil Engineering (ASCE), Arne Richter Award for Outstanding Young Scientists (EGU), Hydrologic Sciences Early Career Award (AGU), Walter Huber Civil Engineering Research Prize (ASCE), and Ambassador Award (AGU).

Flood management challenges in the framework of the SDG 13

María Carmen Llasat
University of Barcelona, Spain

María Carmen Llasat is Full Professor of Atmospheric Physics at the University of Barcelona (UB) and leads the GAMA Group since 1995. Her research and activity focus on climate change and hydrometeorological risks (mainly floods) from a multidisciplinary approach, fields in which she has more than 200 scientific peer review publications.
She was president of the Natural Hazards Section of the European Geophysical Society and founder and editor-in-chief of Natural Hazards and Earth System Science. She has been member of numerous international committees and projects as well as member of the Advisory Council for Sustainable Development (CADS) of the Generalitat de Catalunya for more than 10 years. Nowadays she is member of the steering committee of the Mediterranean Experts group on Climate and Environmental Change (MedECC), among others. She has had a strong participation in the First Mediterranean Assessment Report and nowadays is one of the coordinators of the Special Report on Coastal Risks of MedECC. Besides her research activity, she develops a strong outreach activity, and acts as mentor of a high number of PhD students.

Sustainable coastal groundwater management through innovative governance in a changing climate

George Karatzas
Technical University of Crete, Greece

Professor George P. Karatzas received his Ph.D. in 1992 from the Department of Civil Engineering and Environmental Engineering at Rutgers University, USA in a combined Ph.D. program with Princeton University, USA. At the present time he is a Full Professor in the School of Chemical and Environmental Engineering at the Technical University of Crete, Greece (1998-today) where he has served as Chairman and Dean of the Department. Prior to that position he worked as a postgraduate at the Research Center for Groundwater Remediation Design at the University of Vermont (1992-1994) and as an assistant professor at the Civil and Environmental Engineering Department at the University of Vermont (1994-1999).
His area of research includes numerical simulation in porous media, subsurface hydrology and contaminant transport, groundwater management, subsurface remediation techniques, global optimization techniques, surface water modeling and floods. He is the author of 113 journal publications, 87 conference proceedings, one book and 5 book chapters. He has been principal investigator and co-investigator in several national and international research projects related to groundwater flow and contaminant transport, groundwater management, surface hydrology and floods.

I. Hydrological Extremes and Hazards under Climatic Instability

Estimation of rainfall intensity-duration-frequency curves in future climate change scenarios based on hourly climate model projections

G. Buonacera*, N. Palazzolo, A. Cancelliere, D.J. Peres
Department of Civil Engineering and Architecture, University of Catania, Via S. Sofia 64, 95123, Catania, Italy
** e-mail: gaetano.buonacera@phd.unict.it*

Introduction

The magnitude and frequency of heavy rainfall events is expected to be altered in the future due to climate change (Arnell et al. 2001). Identifying and assessing potential changes to the magnitude of extreme rainfall is of key importance for the design of urban hydraulic systems, as well as for flood assessments. Rainfall intensity-duration-frequency (IDF) curves are one of the most widely used tools for multiple hydraulic engineering purposes. The future impacts of climate change on IDF curves can be estimated using climate projections from regional climate models (RCMs) nested within global climate models (GCMs) under different emission scenarios (Representative concentration pathways – RCPs of the Fifth IPCC assessment report). Some previous studies derive future IDF curves based on projections at the daily time scale which require the application of statistical downscaling approaches (e.g., Forestieri et al. 2018). Here we propose and apply a simple approach to derive future IDF curves based on change factors derived from RCMs to be applied to the first moments (e.g., mean and standard deviation) of observed annual maxima data. The methodology is applied to hourly projections, so it does not involve temporal statistical downscaling. We apply the methodology to Sicily Island (southern Italy), where the evidence of statistically significant trends of extreme rainfall at daily and sub-daily time scales have been showcased (Bonaccorso and Aronica 2016).

Materials and methods

As schematically illustrated in Figure 1, the proposed methodology follows two parallel paths aimed at deriving both observed and RCM IDF curves through the simple scaling method (Burlando and Rosso 1996). Specifically, on one side we used the observed maxima annual precipitation data at 1h, 3h, 6h, 12h, 24h, and the sample means are calculated ($m_O(t)$) at the five durations. Thus, dividing each value the by the sample mean of the respective duration, a dimensionless series is derived. A probability distribution (e.g., Extreme Value, Log-normal) is then fitted to the dimensionless series, and its parameters are estimated using method of moments. Finally, the dimensionless quantile $h^*_{T,0}$ is calculated for the return period T of interest. The five $m_O(t)$ values are then approximated by fitting a power law by the least squares method $m_O(t) = bt^n$. The combination of the dimensionless quantile with the power law, provides the IDF curves (Eq. 1), for the observed series:

$$h_T^O = h^*_{T,0}\, bt^n = at^n \quad (1)$$

On the other side, the projected annual maxima precipitation data for the 5 mentioned durations are derived from using the hourly precipitation data provided RCMs. The sample means are estimated at the five durations, $m_c(t)$ and $m_f(t)$ for the control period and the future one, respectively, as well as the dimensionless standard deviations σ_c and σ_f. Therefore, change factors, i.e., the five factors for the means ($CF_m = m_f(t)/ m_c(t)$), and for the dimensionless standard deviation ($CF_\sigma = \sigma_f / \sigma_c$), are derived and multiplied to their observed counterparts to derive future moments (Eqs. 2, 3):

$$m_f'(t) = m_O(t)\, CF_m \quad (2)$$

$$\sigma_f' = \sigma_0\, CF_\sigma \quad (3)$$

Finally, using the future moments of Eqs. 2 and 3, the dimensionless distribution's parameters are estimated, as well as the dimensionless quantile of future precipitation $h^*_{T,f}$. Through the regression of

$m_f'(t)$ values ($m_f'(t) = b't^{n'}$), future IDF curves are derived (Eq. 4):

$$h_T^f = h^*_{T,f}\, b't^{n'} = a't^{n'} \quad (4)$$

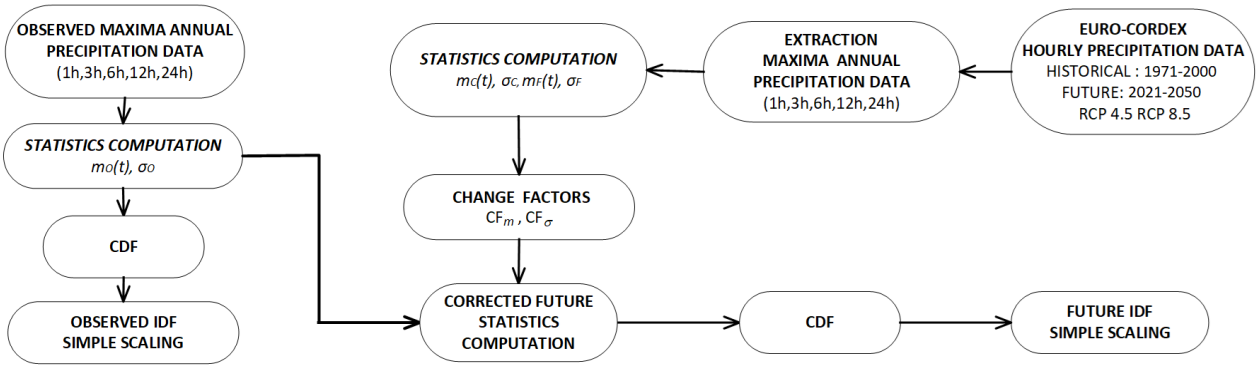

Figure 1. Methodology for deriving rainfall intensity-duration-frequency curves in future climate change scenarios.

Results and concluding remarks

The presented methodology was applied using the precipitation data provided by seven rain gauges stations distributed in 3 different climatic areas of Sicily (Peres et al. 2020), for which both the simple-scaling and the goodness of fit of the lognormal distribution was successfully passed. Several GCM-RCM EuroCORDEX combinations were used to derive the IDF curves in both emission scenarios RCP 4.5 (intermediate) and RCP 8.5 (extreme). Here we present, for brevity, the results relative to the "MPI-M-MPI-ESM-LR_r1i1p1_SMHI-RCA4" model (which, based on preliminary analyses, seems the most accurate), future period (from 2021 to 2050) and return period of 50 years. Table 1 summarizes the main results, namely the coefficients of observed IDF curves, and of the future ones, for each analyzed rain gauge. Overall, with exception of Catania rain gauge, there is a general increase of the IDF curves. Specifically, the greatest increase is observed for the worst-case climate scenario RCP 8.5.

Table 1. Parameters of the IDF curves computed for both observed and future precipitation.

Rain gauge	Observed		RCP 4.5		RCP 8.5	
	a	*n*	*a'*	*n'*	*a'*	*n'*
Castroreale	36.54	0.53	37.90	0.55	41.36	0.52
Catania	37.17	0.58	30.88	0.59	33.55	0.56
Corleone	28.78	0.48	30.00	0.48	33.45	0.47
Gela	26.45	0.49	27.83	0.49	30.60	0.47
Lentini	33.18	0.47	35.17	0.54	37.65	0.50
Mineo	26.45	0.49	30.00	0.50	30.60	0.52
Ragusa	32.87	0.54	33.81	0.57	40.50	0.58

Future analysis will consider the uncertainty of projections as well as the application to a wider set of gauges in Sicily.

References

Arnell N, Liu C, Compagniucci R, Cunha L, Hanaki K, Howe C, Mailu G, Shiklomanov I, Stakhiv E (2001) Climate Change 2001: impacts, adaptation and vulnerability. Chapter 4, Hydrology and Water Resources 3745: 193–233

Bonaccorso B, Aronica GT (2016) Estimating Temporal Changes in Extreme Rainfall in Sicily Region (Italy). Water Resources Management 30(15): 5651–5670

Burlando P, Rosso R (1996) Scaling and muitiscaling models of depth-duration-frequency curves for storm precipitation. Journal of Hydrology 187(1): 45–64

Forestieri A, Arnone E, Blenkinsop S, Candela A, Fowler H, Noto LV (2018) The impact of climate change on extreme precipitation in Sicily, Italy. Hydrological Processes 32(3): 332–348

Peres DJ, Senatore A, Nanni P, Cancelliere A, Mendicino G, Bonaccorso B (2020) Evaluation of EURO-CORDEX historical simulations by high-quality observational datasets in southern Italy: insights on drought assessment. Nat Hazards Earth Syst Sci 20: 3057–3082

Economic benefits of including drought information in water resources management

A. Sordo-Ward[1*], P. Bianucci[1], A. Iglesias[2], L. Garrote[1]
[1] Dep. Civil Engineering: Hydraulics, Energy and Environment, Universidad Politécnica de Madrid, Madrid, Spain
[2] Dep. Agricultural Economics and Social Sciences, Universidad Politécnica de Madrid, Madrid, Spain
* e-mail: alvaro.sordo.ward@upm.es

Introduction

This study analyses the potential economic benefits of including the forecast of drought as a relevant factor in the decision process. Water managers could use it to reduce uncertainty and increase their profits. We quantify the value of the drought forecast and analyse the expected gain in a decision outcome. We propose to conduct an economic analysis comparing the gains versus the costs of providing the information. The results depend on the accuracy of the drought forecast (accounted for the hit rate) and the approach of the stakeholders to risk management, called risk aversion (Quiroga et al. 2011). The methodology is applied to different regulated water resources systems in Spain. The objective of the study is to answer two main questions: 1) How do we know that advanced drought information is currently helping decisions? and 2) What is the value of information in the decision process?

Materials and methods

As stated in FAO 33 (1979), water is essential for crop production and the use of available water should prioritize efficient crop production and high yields. In this study we considered two kinds of crops: horticulture and cereals. The relationship between water supply and crop yield was estimated (FAO 33 1979). Given a total water allocation for farmers, horticulture shows higher productivity than cereals. As the water deficit increases (water supply decreases), horticultural productivity decreases until both curves cross. Therefore, there is a range of high water availability levels for which horticulture is selected. For lower water availability, the cereal productivity becomes higher than that of horticulture; thus, cereal is selected.

In Spain, most irrigation systems are supplied with water regulated in dams and reservoirs. First, to perform the reservoir risk analysis we need to quantify, objectively, the probability of having water shortages to make the decision. Thus, we determine the probability distribution of the deficit as a function of the available storage in a specific month (April in this study). Based on the historical series of monthly flow (56 years, length of the sample), and by assuming different values of storage (in April) as a percentage of the total existing storage in the system, we determine the non exceedance probability distribution deficit, as a percentage of the total water allocation for the farmer.

Following the same procedure, we estimate different relationships among the stored volume, deficit and risk aversion. Defined a value of acceptable deficit (25% for this study), we compute, for the month when the decision is made (April in this study, and for each year of the data series), the available storage in the system that is required to satisfy the required fraction of the demand in a time horizon (usually until the end of the irrigation season) and with a given probability (threshold that describes risk aversion). In this study, we decided to select cereals when the probability of not being able to supply 75% of the demand during the irrigation season is more than a threshold. The threshold defines the "risk aversion" of the stakeholder.

The results also depend on the accuracy of drought forecast and it is accounted for the hit rate. In this study, we assume that a seasonal drought forecast is available. The forecast is able to classify streamflow in the irrigation season in one of three categories: wet season (top 33% of streamflow seasonal historical observed data), average season (middle 33%) and dry season (low 33%). The forecast quality is defined by the hit rate. We named perfect forecast the case where the hit rate is 100%. It is based on the historic

observed series where, each year, we know in advance the category of the following months.

The proposed methodology was applied to nine regulated water resource systems in Spain. The systems were selected to evaluate a wide range of climates and regulation of the systems. Streamflow data were taken from the results of the SIMPA model (Simulation – Precipitation – Runoff)(Estrela and Quintas 1996). SIMPA is a hydrological distributed model (cells 500 x 500 meters) with a monthly time step. A total of 56 years of monthly time series were available, spanning the hydrological year 1960–61 to 2016–17. The topology of the models, the data and the economic return were obtained from the different River Basin Plans for Spain for the cycle 2022–2027. We assumed the same relationships for all regulated water resource systems. The behaviour of the irrigated systems was evaluated by applying the Water Availability and Adaptation Policy Analysis (WAAPA) model (Garrote 2017). WAAPA is a model that simulates water allocation in a water resource system. WAAPA performs the simulations on a monthly time scale. The basic components of WAAPA are reservoirs, inflows and demands. These components are linked to nodes in the river network. WAAPA allows simulation of reservoir operation and computation of supply to demands from an individual reservoir or from a system of reservoirs accounting for ecological flows and evaporation losses. From the time series of supply volumes, supply reliability can be computed according to different criteria. In this study we utilized the criteria of gross volume reliability. We evaluated the performance of the systems under the management hypothesis named local management. This hypothesis assumes that every reservoir in the sub-basin supplies only local demands. Downstream reservoirs can only use uncontrolled spills from upstream basins and return flows from upstream demands.

Results and concluding remarks

The results show that the percentage of gross income in drought years was improved by using the drought information for the irrigation systems analysed: 17.7% in Adaja-Cega, 6.2% in Pisuerga-Carrión, 13% in Jalón, 3% in Guadalope, 9.5% in Guadiana Menor, 3.3% in Jaén, 20% in Alto Genil, 11% in Alagón and 1.9% in Tormes irrigation system. Results are consistent for different values of forecast quality. The results also show that the risk aversion factor has a high impact on the results. The best risk values ranged from 0.10 to 0.40. The main conclusion is that a significant fraction of the reduced income from the risk of water scarcity is offset by using the forecast. Finally, the application of the framework to Spanish case studies shows that information benefits exceed costs when drought frequency is 20-40% above normal values; below these uncertainty values in the decisions dominate the results; above these values, management decisions are limited even with perfect information.

Acknowledgments: This research was funded by the Spanish Ministry of Science and Innovation, grant number PID2019-105852RA-I00: “Simulation of climate scenarios and adaptation in water resources systems (SECA-SRH)”.

References

Estrela Monreal T, Quintas Ripoll L (1996) El sistema integrado de modelización Precipitación-Aportación SIMPA. Revista Digital Del Cedex 104: 43

FAO 33 (1979) Irrigation and Drainage paper. Food and Agriculture Organization of the United Nations, Rome

Garrote L (2017) Managing Water Resources to Adapt to Climate Change: Facing Uncertainty and Scarcity in a changing context. Water Resour Manag 31: 2951–2963

Quiroga S, Garrote L, Iglesias A et al. (2011) The economic value of drought information for water management under climate change: a case study in the Ebro basin. Nat Hazards Earth Syst Sci 11: 1–9. https://doi.org/10.5194/nhess-11-1-2011

Spatial distribution of mean annual precipitation in Crete using geostatistical methods

G. Kampouris[1,2], S. Kontinis[1,2*], A. Loukas[1], A. Spyridis[2]
[1] Laboratory of Hydraulic Works and Environmental Management, Department of Transportation and Hydraulic Engineering, School of Rural & Surveying Engineering - A.U.Th., Thessaloniki, Greece
[2] YAS Studies-Research-Consultant Services, Thessaloniki, Greece
* e-mail: kontinis@topo.auth.gr

Introduction

Natural phenomena have been a subject of human observation for thousands of years. These phenomena exhibit spatial variation and distribution. The variables, which characterize the natural phenomena, are called Regionalized Variables according to the geostatistical approach.

These variables present great difficulties in their study, as there are divergences and instability in spatial variability due to the types of anisotropies and discontinuities. Journel and Huijbregts (1978) argued that the interpretation of the arithmetic values of a regional variable z(x) and z(x_i) as independent realizations of a random function Z(x), is not acceptable. This is because this interpretation does not take into account spatial autocorrelation between the two neighboring values z(x+h) and z(x). This reason prompted the scientists working in the field of geostatistics to define the Random Function, which consists of two independent aspects, spatial structure and randomness, which define the regional variables (Matheron 1970).

Materials and methods

In this paper, the phenomenon of precipitation and more specifically, the Mean Annual Precipitation of thirty-six (36) hydrological years 1973-74 to 2008-09 (MAP_{36}) (Tigkas et al. 2022) was analyzed. The study area is the island of Crete, Greece. Crete, in recent years, experienced periods of severe drought episodes causing many problems to human activities, crops and infrastructure. The data sample used consists of the MAP_{36} values measured at sixty-two (62) rain gauge stations.

The spatial distribution of MAP_{36} was studied using geostatistical methods and the results have been evaluated using Cross Validation and Indipendent Validation. Specifically, two different Independent Validations were performed, the first one using two stations in Heraklion and Lasithi, which have the same data period as the analysis stations (i.e. 1973-74 to 2008-09). In the second Independent Validation, sixteen (16) stations across Crete were used but they had available data for up to eleven (11) hydrological years.

The coordinates of the stations and MAP_{36} were used to design the experimental semivariogram with both data being derived from the sample. In selecting the theoretical semivariogram, a total of twenty (20) theoretical models have been considered from which the Spherical Model was selected as the one showing the optimal fit among the others. In all the semivariograms it was observed that there was a high variability at a distance between pairs of about 175 km. After digging, four (4) pairs with large differences in MAP_{36} were identified. This phenomenon is justified because the stations are located between the mountainous areas of Chania and the lowland areas of Lasithi where such behavior is expected.

The next step was to investigate the anisotropy. Initially, a survey was carried out in the basic directions of 0^o, 45^o, $90^o$and 135^o. To ensure sample coverage, an angular tolerance equal to 45^o was chosen. During the tests strong differences were found in the 45^o and 90^o directions and therefore an analysis was carried out in the directions between them. Eventually, the direction of the anisotropy was identified in 55^o. The values of the ratio of anisotropy that led to a better match for the different angular tolerances were between 1.5 and 2.5. For a better fit and non-distortion of the sample, a degree of anisotropy equal to 1.8 was selected as it was observed that its results were acceptable for all directions.

After selecting the appropriate theoretical semivariogram model, the optimal geostatistical

interpolation methods, kriging, was used. In particular, the methods of Ordinary Kriging, Universal Kriging (with linear and quadratic drift) and External Drift Kriging have been applied. In the latter, external drift was applied via EU-DEM, of Copernicus Land Monitoring Service which is an elevation dataset covering Europe at a 25 m resolution with a vertical accuracy is ±7 m. In addition, Point and Block Kriging have been investigated. The Universal Kriging method provided superior results with linear than quadratic drift and in each case the results of Point Kriging were superior to those of Block Kriging. For these reasons it was chosen to use three methods, Ordinary Point, Universal Point with linear drift and External Drift Point Kriging.

Results and concluding remarks

The results of the indicators produced by the Ordinary and Universal Kriging methods were similar, with the indicators of Universal being slightly better. It is observed that the use of External Drift Kriging provides best results for the set of indicators compared to the other two methods, which also demonstrates the direct correlation between precipitation and ground morphology and elevation.

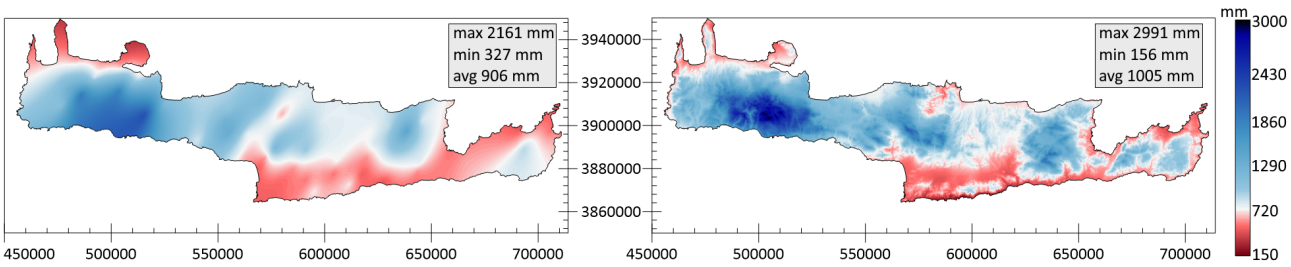

Figure 1. Distribution map of MAP36 using two Kriging methods, on the left with Ordinary Kriging and on the right with External Drift Kriging (in Greek Coordinate reference system GGRS87).

Regarding the MAP_{36} values obtained from the kriging methods, while Ordinary and Universal have a similar distribution, it turns out that Universal Kriging results in more extreme values. The values obtained from External Drift Kriging are noticeably higher due to the influence of altitude, and in areas with relatively high altitude, a higher precipitation is observed than for the other methods. The Cross Validation and Independent Validation of the results indicated that the External Drift Kriging gave the best results compared to the other two kriging methods.

In this paper, the geostatistical approach is used for the spatial distribution of MAP_{36} in Crete and the best-fitted theoretical semivariogram (spherical) to the experimental semivariogram is selected. The spatial anisotropy of MAP_{36} has been investigated and the direction of the anisotropy was identified in 55^{o}. The results from the previous analysis have been implemented to estimate the spatial distribution of MAP_{36} using three kriging methods (namely, Ordinary Kriging, Universal Kriging (with linear and quadratic drift) and External Drift Kriging). The results of kriging application have been validated using Cross Validation and Independent Validation and indicated that the External Drift Kriging method gives the best results. This paper presents the results found in the Diploma Engineering Thesis of Kampouris and Kontinis (Kampouris and Kontinis 2023).

References

Journel AG, Huijbregts CJ (1978) Mining Geostatistics. Academic Press, San Diego

Matheron GFPM (1970) Theory of regionalized variables, and its applications. École Nationale Supérieure des Mines des Paris, Fontaineblau

Kampouris G, Kontinis S (2023) Spatial distribution of Mean Annual Precipitation in Crete using geostatistical methods. Diploma Engineering Thesis, School of Rural and Surveying Engineering, Aristotle University of Thessaloniki, Thessaloniki (in Greek)

Tigkas D, Kourtis I, Proutsos N, Tsakiris VC, Vangelis H, Tsakiris G (2022) Comparative Application of the Agricultural Drought Indicator aSPI in Crete. 15th Panhellenic Conference of the Greek Hydrotechnical Union, 2-3 June 2022, Thessaloniki, Greece (in Greek)

Characterization of 1-hour maximum rainfall values in Calabria, southern Italy, by means of the ERA-5 reanalysis

F. Chiaravallloti[1], R. Coscarelli[1*], T. Caloiero[2]
[1] *CNR-IRPI, Rende (CS), Italy*
[2] *CNR-ISAFOM, Rende (CS), Italy*
** e-mail: roberto.coscarelli@irpi.cnr.it*

Introduction

Heavy precipitation events are likely to become more frequent in most parts of Europe; yet, records of hourly precipitation are often insufficient to study trends and changes in heavy rainfall. Atmospheric reanalyses are an important source of long-term meteorological data, often considered as a solution to overcome the unavailability of direct measurements. The reanalysis procedure makes use of a large amount of heterogeneous historical observations, both sensed and remotely measured (in situ, satellite, etc.), assimilated within a dynamical model to reconstruct the state of the atmosphere, land surface and oceans in the past. Among the available reanalyses, the ERA5 dataset (Hersbach et al. 2020), released by the ECMWF, can be considered one of the state-of-the-art products. Atmospheric and surface variables are provided hourly, from 1950 to almost real time, with a horizontal resolution of 31 km. The land model of the ERA5, driven by the downscaled meteorological forcing from the lowest ERA5 model level, and with an elevation correction for the thermodynamic near-surface state (Dutra et al. 2020), is also used to derive the ERA5-land dataset, characterized by a higher spatial resolution (9 km) and finer precipitation distribution details (Muñoz-Sabater et al. 2021).

In this paper, data from the ERA5-land reanalysis dataset were first used to detect possible trends in the 1-hour maximum yearly rainfall values in a region of southern Italy and then the monthly distribution of these values has been analysed.

Materials and methods

In this work, the total precipitation field of the ERA5-Land reanalysis dataset, downloaded from the Copernicus Climate Change Service (C3S), was used for each of the 141 cells (dimension 9x9 km^2) in the Calabria region (southern Italy) to derive the time series of hourly precipitation amount from 1950 until 2020. This parameter represents the accumulated liquid and frozen water, comprising rain and snow, falling to the Earth's surface, and it includes both large-scale and convective precipitation. The sequence of months in which the annual maximum of hourly rainfall occurs was then calculated for each cell, obtaining a succession of 71 values for each of them. To check the rainfall trend, the widely recognized non-parametric Mann–Kendall test (Mann 1945; Kendall 1962) and the Theil–Sen slope estimator (Sen 1968) have been employed at monthly, seasonal and annual scales considering a significant level equal to 95%. Finally, the time frame 1961-2020 was divided into three intervals, and for each one, considering the entire study area (141 cells), the frequency distribution of the months recording the annual maxima was calculated.

Results and concluding remarks

Results regarding trends reveal a global positive tendency of the maximum 1-hr rainfall on a yearly scale, involving 27.7% of the total number of cells. This tendency is not uniform for all the seasons: positive in spring, summer and autumn, positive for winter but with a few number of cells involved (Figure 1). These not-uniform tendencies are also confirmed on a monthly scale. While September is the month with the highest number of cells (about 62%) having positive tendencies, followed by April, July and March, months such as January and October show negative tendencies, instead. The tendency on the temporal distribution of the occurrence of the yearly maximum 1-hr rainfall (Figure 2) also confirms these results. In the first sub-

period, the maximum values mostly occurred in October; in the more recent sub-period September is the month with the highest number of occurrence of the yearly maximum 1-hr rainfall values.

The occurrence of the catastrophic geo-hydrological events in Calabria, with losses and damages, mainly caused by short and extreme rainfall, also confirm the results of this study. In the last decades, these events have often occurred in September.

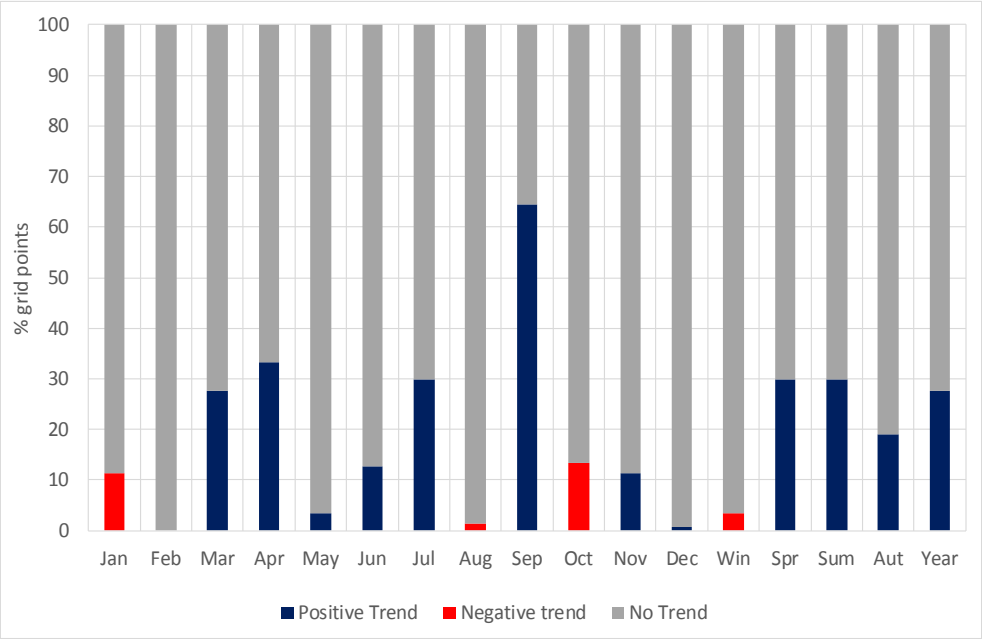

Figure 1. Percentages of grid points presenting positive or negative trend.

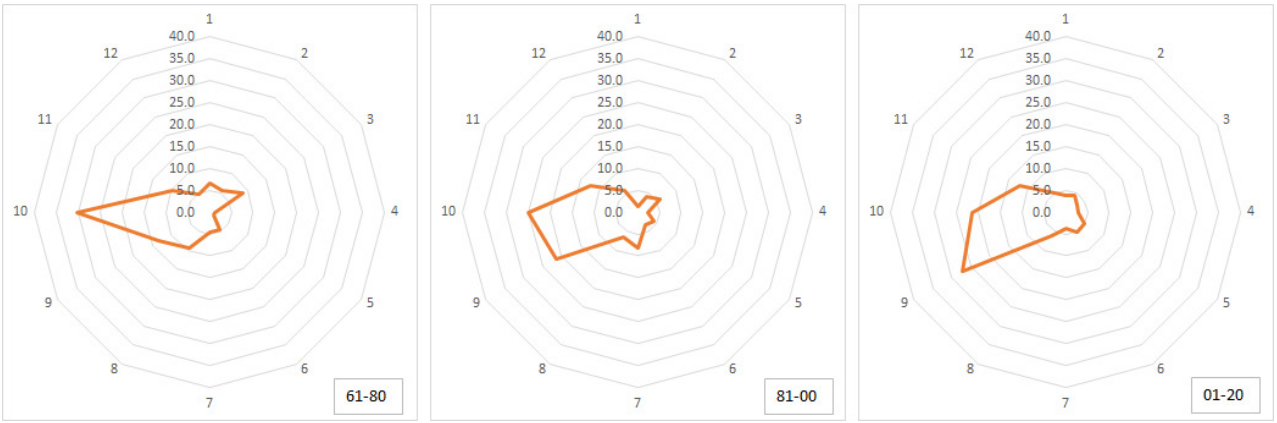

Figure 2. Monthly distribution of occurrences of 1-hour maximum rainfall values for the three periods.

References

Dutra E, Muñoz-Sabater J, Boussetta S, Komori T, Hirahara S, Balsamo G (2020) Environmental Lapse Rate for High-Resolution Land Surface Downscaling: An Application to ERA5. Earth and Space Science 7(5): e2019EA000984. https://doi.org/10.1029/2019EA000984

Hersbach H, Bell B, Berrisford P et al. (2020) The ERA5 global reanalysis. Quarterly Journal of the Royal Meteorological Society 146(730): 1999-2049. https://doi.org/10.1002/qj.v146.73010.1002/qj.3803

Kendall MG (1962) Rank Correlation Methods. Hafner Publishing Company, New York

Mann HB (1945) Nonparametric tests against trend. Econometrica 13(3): 245–259

Muñoz-Sabater J, Dutra E, Agustí-Panareda A et al. (2021) ERA5-Land: A state-of-the-art global reanalysis dataset for land applications. Earth System Science Data 13(9): 4349-4383. https://doi.org/10.5194/essd-13-4349-2021

Sen PK (1968) Estimates of the regression coefficient based on Kendall's tau. Journal of the American Statistical Association 63(324): 1379–1389. https://doi.org/10.1080/01621459.1968.10480934

Investigating alternative approaches to drought visualisation

H. Vangelis[1*], V. Krassanakis[2], I. Kourtis[1], D. Tigkas[1]
[1] Laboratory of Reclamation Works and Water Resources Management, School of Rural, Surveying and Geoinformatics Engineering, National Technical University of Athens, Athens, Greece
[2] Department of Surveying & Geoinformatics Engineering, University of West Attica, Egaleo (Athens), Greece
* e-mail: harrivag@central.ntua.gr

Introduction

Drought mapping is the most popular way to illustrate drought conditions. Conventionally, drought maps visualise drought severity through a predefined colour pallet, corresponding to drought severity classes and following the typical "alert conditions" colour classification, therefore spanning from blue shades for humid conditions to red shades for drought representation. In this way, drought maps achieve the simultaneous presentation of two dimensions of drought, the severity and the areal extent, overcoming the major obstacles of other graphical representations, which can only present point results. The temporal dimension is usually covered by creating a set of maps, each corresponding to a different time period.

Could drought maps become more informative? The paper investigates alternative approaches to drought visualisation, which may change the perspective of the usual drought mapping. Techniques used in cartography are utilised to explore the possibility to present more information on drought maps (e.g., three dimensions of drought) or at least make drought maps more comprehensive.

Materials and methods

The concept was applied in the island of Rhodes, located in the South Aegean region of Greece. The island is the ninth largest island in the overall Mediterranean Sea (about 1,400 km^2) and is considered to have a shape of a spearhead. The climate of the island is typical Mediterranean with hot summers and mild winters. The daily mean temperature is about 19 °C, with the highest temperature recorded 41.2 °C and the average annual rainfall depth does not exceed 700 mm.

Meteorological data for the entire Rhodes island (temperature, precipitation, etc.) were downloaded using the Data Extraction Application for Regional Climate (DEAR-Clima) platform (http://meteo3.geo .auth.gr:3838/). The platform provides various climate variables, from different General Circulation Models (GCM) dynamically downscaled using different Regional Climate Models (RCM), based on the simulations of the CORDEX (Coordinated Regional Downscaling Experiment; http://www.euro-cordex.net/060378 /index.php.en) research program. The temporal resolution of the utilised data is monthly and the spatial resolution is 0.11° covering the historical period 1950 to 2005.

Drought severity was calculated using DrinC software, based on the Agricultural Standardised Precipitation Index (aSPI), a modification of the well-known SPI, that uses the parameter of effective precipitation for improving the accuracy of agricultural drought identification (Tigkas et al. 2022).

Four different visualisation techniques were utilised: (a) The 'conventional' method; (b) the construction of contiguous irregular cartograms; (c) a three-dimensional (3D) perspective map; and (d) the dot map method.

Results and concluding remarks

Drought visualisation (Figure 1) is based on the implementation of four different techniques which consider as input the aSPI values. Specifically, the indicative implemented visualisations involve: (a) The 'conventional' method, where aSPI point values are translated into cells according to drought classification for the hydrological year 1968-69; (b) The construction of contiguous irregular cartograms (e.g., Markowska 2019), in which the area of each cell is recalculated according to the aSPI values, and then, each cell is spatially transformed based on the (re)calculated area values, considering 1000 iterations and 10% average

error; (c) A three-dimensional (3D) perspective map (e.g., Kraak 1994), where the third dimension corresponds to the absolute aSPI values. In case both negative and positive values should be presented simultaneously, visualisation (d), the dot map method (e.g., Hey 2012), is considered. As an example, the value of 0.005 is assigned to each dot for the hydrological year 1998-99. Based on this value, the total number of dots per visualization unit (i.e., cells) is calculated and dots are randomly allocated within the unit, while positive and negative values are separated using different colour hues.

The QGIS software with "cartogram3" and "Qgis2threejs" plugins were utilised for the implementation of methods a, b and c, while the method d was performed in ArcGIS (ESRI®).

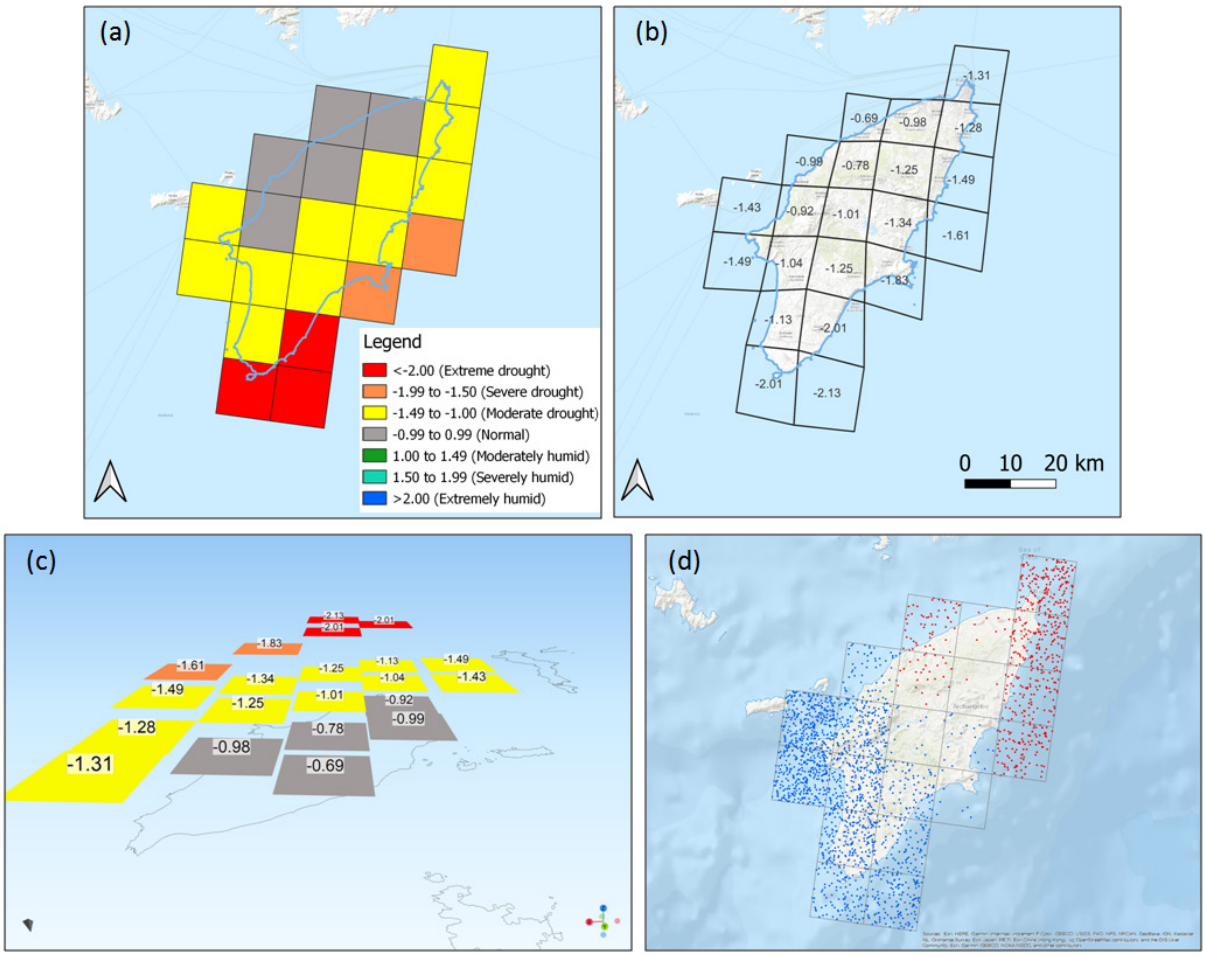

Figure 1. Alternative drought visualisation methods.

Alternative approaches definitely provide a new perspective in drought mapping. In case d, for example, humid and drought conditions are represented only by one colour each, and the density of dots represent the difference in severity.

The main enhancement, however, is the more detailed presentation of drought severity within a predefined drought class. The specific perception is presented in the 3D map (case c), where the differences in severity of each area cluster within the same drought class are presented through the different elevation of each cluster. This is definitely an additional information and an added value in drought mapping.

References

Hey A (2012) Automated dot mapping: How to dot the dot map. Cartography and Geographic Information Science 39(1): 17-29

Kraak MJ (1994) Interactive modelling environment for three-dimensional maps: Functionality and interface issues. Visualization in Modern Cartography 2: 269-279

Markowska A (2019) Cartograms–classification and terminology. Polish Cartographical Review 51(2): 51-65

Tigkas D, Vangelis H, Proutsos N, Tsakiris G (2022) Incorporating aSPI and eRDI in Drought Indices Calculator (DrinC) software for agricultural drought characterisation and monitoring. Hydrology 9(6): 100

Temporal variability of annual daily extreme minimum flows in southern Quebec (1930-2020)

A.A. Assani
Department of Environmental Sciences and Research Centre for Watershed-Aquatic Ecosystem Interactions (RIVE, UQTR), University of Quebec at Trois-Rivières, 3351 Boulevard des Forges, Trois-Rivières, QC G9A 5H7, Canada
** e-mail: Ali.Assani@uqtr.ca*

Introduction

Climate change is increasingly reflected in the amplification of extreme hydrological events in particular. Thus, in 2022, most countries in Western Europe in particular have just been confronted with one of the worst episodes of hydrological drought rarely recorded on the continent. This extreme drought has thus transformed the hydrological regimes of many streams and rivers. Despite the reputedly humid climatic character of Western Europe, many rivers have however seen their permanent hydrological regimes transformed into intermittent hydrological regimes due to the total drying up of their flows, even for some large rivers of the continent. This change in hydrological regime is also affecting many streams in many regions of the world, which are considered naturally humid. The North American continent is no exception to this trend (https://www.carbonbrief.org/climate-change-made-2022s-northern-hemisphere-droughts-at-least-20-times-more-likely/; https://www.bbc.com/news/62751110; Toreti et al. 2022).

In Quebec, the hydrological regimes of all streams larger than 100 km² are characterized by a permanent flow throughout the year due to the humid nature of the region. However, due to the significant drop in the amount of snow, which is the main source of aquifer recharge that influences low water flows (Lavigne et al. 2010), the risk of transformation of this permanent regime into an intermittent regime is becoming increasingly high. To assess this drought trend, this study aims to analyze the temporal variability of extreme minimum flows over a very long period (1930-2020) in order to determine if this variability results in a tendency to decrease these flows on the one hand, and to determine the factors which influence this variability, on the other hand.

Materials and methods

This study is based on the analysis of 17 natural rivers grouped into three homogeneous hydroclimatic regions (Assani et al. 2011). Five rivers are located on the north shore of the St. Lawrence River, a region (southwest hydroclimatic region) characterized by a temperate continental climate. Six rivers are located on the south shore north of 47°N, a region (eastern hydroclimatic region) characterized by a temperate maritime-type climate. The last six rivers, whose watersheds are the most agricultural in the province, are located south of this parallel (southeast hydroclimatic region) and their climate is of the mixed temperate type (continental and maritime). Snow is the main source of flows for all these rivers. For each river, a series of annual daily minimum flows (the lowest flows measured during a hydrological year from October to September) measured during the period from 1930 to 2020 was compiled.

To analyze the temporal variability of these hydrological series, we applied the following three statistical tests: the first two tests are Mann-Kendall trend tests modified to eliminate the effects of short-term persistence (MK-STP) and long-term persistence respectively (MK-LTP) (Dinpashoh et al. 2014), and the last (Lombard test, LT), to detect the dates of gradual or abrupt breaks in the means in the event of non-stationarity of the series (Lombard 1995).

Results and concluding remarks

The results of the application of these three tests are summarized in Table 1. This Table shows that the flows increase significantly in a generalized manner in the hydroclimatic region of the southeast, the most agricultural region of Quebec. On the other hand, it decreases in an almost general way in the

hydroclimatic region of the East located to the north of the first region. No significant change in flows was observed on the north shore. The increase in flows in the first hydroclimatic region is explained by the increase in infiltration following the increase in rainfall and the significant reduction in agricultural areas since 1950. This increase occurred before 1980. As for the drop in flows, it is associated with the decrease in the amount of snow and occurred after 1980. The presence of more extensive wetlands on the north shore than on the south shore would have significantly reduced the impacts of this decrease in the snowfall on flows.

Thus, changes in land use (reduction of agricultural areas) and soil cover (areas of wetlands) have significantly attenuated the effects of the decrease in the amount of snow on the temporal variability of annual daily extreme minimum flows in southern Quebec in the two regions located south of 47°N on either side of the St. Lawrence River, preserving a permanent hydrological regime there.

Table 1. Results of the modified Mann-Kendall and Lombard tests applied to the series of daily minimum annual discharges during the period 1930-2020.

Rivers	Drainage area (km²)	MK-SLP (Z-Value)	MK-LSP (Z-value)	LT (T1-T2)
Southwestern Hydroclimatic Region (south of 47°N on the north shore: the least agricultural watersheds)				
Petite Nation	1331	-0.167	0.149	-
Du Nord	1163	**-4.011***	**-2.459***	**1980-81**
L'Assomption	1286	-1.053	-0.630	-
Matawin	1387	-0.947	-0.781	-
Vermillon	2662	0.918	0.680	-
Southeastern Hydroclimatic Region (south of 47°N on the south shore: the most agricultural watershed)				
Chateaugay	2492	***2.491****	***2.515****	***1984-85***
Eaton	646	***2.346****	1.276	***1959-60***
Nicolet SW	562	***4.915****	***3.188****	***1965-66***
Etchemin	708	***2.718****	***1.889****	***1965-67***
Beaurivage	1152	***6.177****	***6.092****	***1964-68***
Du Sud	821	***2.562****	***1.958****	***1952-53***
Eastern Hydroclimatic Region (north of 47°N on the south shore)				
Ouelle	796	**-1.690***	-1.209	-
Du Loup	1042	**-2.562***	0.397	**2002-03**
Trois-Pistoles	930	**-1.910***	-1.612	**1992-94**
Rimouski	1615	**-3.562***	**-3.444***	**1985-86**
Matane	1655	***2.250****	1.329	***1966-67***
Blanche	223	1.454	***1.828***	-

* statistically significant Z value at the < 10% threshold; italics: significantly positive trend; underlined: significantly negative trend; T1 = year of the start of the shift in the mean; T2 = year of the end of the shift in mean.

References

Assani AA, Chalifour A, Légaré G, Manouane C-S, Leroux D (2011) Temporal regionalization of 7-day low flows in the St. Lawrence watershed in Quebec (Canada). Water Resources Management 25: 3559-3574. https://doi.org /10.1007/s11269-011-9870-6

Dinpashoh Y, Mirabbasi R, Jhajharia D, Abianeh HZ, Mostafaeipour A (2014) Effect of short-term and long-term persistence on identification of temporal trends. Journal of Hydrologic Enginnering-ASCE 19: 617-625

Lavigne M-A, Nastev M, Lefebvre R (2010) Numerical simulation of groundwater flow in the Chateaugay River aquifer. Canadian Water Resources Journal 35: 469-486

Lombard F (1995) Rank tests for changepoint problems. Biometrika 74: 615-624

Toreti A, Bavera D, Acosta Navarro J, Cammalleri C, de Jager A, Di Ciollo C, Hrast Essenfelder A, Maetens W, Magni D, Masante D, Mazzeschi M, Niemeyer S, Spinoni J (2022) Drought in Europe August 2022. Publications Office of the European Union, JRC130493, Luxembourg, https://doi.org/10.2760/264241

A novel flow-based multi-model ensemble for runoff simulation using CMIP6 GCMs

S.T. Chae, E.S. Chung*, J.H. Kim
Faculty of Civil Engineering, Seoul National University of Science and Technology, 232 Gongneung-ro, Nowon-gu, Seoul 01811, Korea
** e-mail: eschung@seoultech.ac.kr*

Introduction

General circulation models (GCMs) to quantify the impacts of climate change have been improved in output as the coupled model intercomparison project (CMIP) phase has progressed. Although studies on runoff simulation using GCM climate variables have been conducted, the abrupt increasing number of GCMs and insufficient knowledge about the physical climate simulation process have reduced the accuracy of historical runoff simulation result and increased uncertainty of future runoff simulation runoff simulation result. The multi-model ensemble (MME) method was able to improve historical runoff simulation performance and lower uncertainty of future runoff simulation results using GCMs climate variables, and the use of efficient GCM subsets and various GCMs weighting methods were considered when generating MME runoff.

When simulating runoff based on GCMs climate variables, the MME method, which aggregates GCMs climate variables and then simulates runoff (climate-based MME), has been traditionally used in many studies. However, there was an opinion that the climate-based MME method may not be appropriate because the effect of climate variables on the hydrological impact is non-linear (Wang et al. 2019). Accordingly, a flow-based MME method that aggregates runoff simulation results by GCMs climate variables was proposed (Dong et al. 2021). Therefore, this study compares the historical runoff simulation performance of climate-based and flow-based MME methods according to the GCM selection method and weighting method. Furthermore, this study proposes a novel flow-based MME method to increase the accuracy and lower the uncertainty of historical and future runoff simulation results.

Materials and methods

Evaluation metrics: The four-evaluation metrics (normalized Nash-Sutcliffe, NNSE; root mean square error, RMSE; Kling-Gupta efficiency, KGE; modified index of agreement, MD) were used to evaluate the performance of GCMs climate and runoff simulations and runoff simulations result of MME methods.

Uncertainty analysis: The reliability ensemble averaging (REA) method can analyse uncertainty through two criteria (model performance, RB,i; model convergence, RD,i). In this study, it used to analyse the uncertainty of runoff simulation results according to climate-based and flow-based MME.

$$R_i=[(R_{B,i})^m(R_{D,i})^n]^{[1/(mn)]} \quad (1)$$

GCM ranking and weight: The Technique for order of preference by similarity to ideal solution (TOPSIS) method was used to rank GCMs according to their performance in climate and runoff simulations. The TOPSIS ranking is derived from the relative closeness coefficient (Ci) value calculated by di+ and di-, which represent the distance between the positive ideal solution (PIS) and the negative ideal solution (NIS) for each alternative.

$$Ci=d_i^-/(d_i^++d_i^-) \quad (2)$$

The weight of each GCM is calculated through the ranking sum weight method based on the TOPSIS ranking.

$$Wi=(n-r_i+1)/\sum(n-r_k+1) \quad (3)$$

Results and concluding remarks

The historical runoff simulations results of climate-based and flow-based MME were evaluated using 4 evaluation metrics. The runoff simulation performance of climate-based and flow-based MME was divided into two GCMs selection methods (When all GCMs are used and when a subset of GCMs with good simulation performance is used) and two weighting methods (When using the equal weight and when using the unequal weight according to the simulation performance) as shown in Table 1.

As a result, in all GCMs selection and weighting cases, the flow-based MME showed improved runoff simulation performance than the climate-based MME. Specially, the difference in simulation performance became larger when efficient GCMs subsets and unequal weight were used based on the GCMs runoff simulation performance.

Through the results of this study, the importance of flow-based MME was confirmed, and this study proposes a novel flow-based MME method that can improve the historical runoff simulation performance and lower the uncertainty of future runoff simulation results.

Table 1. Comparison of historical runoff simulation performance according to climate-based and flow-based multi-model ensemble.

MME approach		Evaluation metric			
		NNSE	**RMSE**	**KGE**	**MD**
GCM all & equal weight	Climate-MME	0.722	3.384	0.758	0.723
	Flow-MME	0.722	3.384	0.758	0.723
GCM all & unequal weight	Climate-MME	0.727	3.34	0.765	0.724
	Flow-MME	0.738	3.251	0.775	0.725
GCM subset & equal weight	Climate-MME	0.734	3.279	0.772	0.725
	Flow-MME	0.754	3.116	0.786	0.728
GCM subset & unequal weight	Climate-MME	0.736	3.266	0.775	0.726
	Flow-MME	0.757	3.087	0.788	0.729

Acknowledgments: This research was supported by the National Research Foundation of Korea (2021R1A2C200569912).

References

Wang HM, Chen J, Xu CY, Chen H, Guo S, Xie P, Li X (2019) Does the weighting of climate simulations result in a better quantification of hydrological impacts? Hydrology and Earth System Sciences 23: 4033-4050. https://doi.org/10.5194/hess-23-4033-2019

Dong F, Javed A, Saber A, Neumann A, Arnillas CA, Kaltenecker G, Arhonditsis G (2021) A flow-weighted ensemble strategy to assess the impacts of climate change on watershed hydrology. Journal of Hydrology 594: 125898. https://doi.org/10.1016/j.jhydrol.2020.125898

Evaluation of climate change impacts on the hydrometeorological variables of the Ceira river basin in Portugal

M. Costa[1,2*], J. Mendes[1,2], R. Maia[1,2]
[1] FEUP – Faculty of Engineering of the University of Porto, Department of Civil Engineering / Hydraulics, Water Resources and Environment Division, Porto, Portugal
[2] Interdisciplinary Centre of Marine and Environmental Research (CIIMAR), University of Porto, Terminal de Cruzeiros do Porto de Leixões, Matosinhos, Portugal
* e-mail: mapcosta@fe.up.pt

Introduction

In the last years, the centre of Portugal has been devastated by extreme climate phenomena, with floods (namely in the Coimbra region), droughts and wildfires becoming more recurrent. Moreover, in Portugal, the recent climate change projections show that these events will be more frequent and more intense (do Ó and Seiz 2021). In this regard, to better cope and adapt to the upcoming impacts, it is crucial to quantify the expected magnitude change of future meteorological variables and how these changes will impact the different components of the hydrological cycle (Ramos et al. 2014). This type of assessment must be, preferably, carried out at the regional level, since it is where the effects will be more noticeable and adaptation and mitigation measures will need to be applied (New et al. 2022).

In this context, the main purpose of the present work was the development of climate change scenarios of precipitation and temperature, for the Ceira river basin (total area of 737 km^2), located in the centre of Portugal, through the application of a methodology adapted to Portuguese river basins. With the definition of these scenarios, an evaluation of the climate change impacts in the basin will be assessed, namely regarding the occurrence of extreme drought and water scarcity events, as well as the impact on the basin´s streamflow. The results obtained will help to define concrete adaptation measures, aiming to improve the resilience and responsiveness of the basin to climate change. This work is being developed in close collaboration with the Portuguese Mondego RBD authority (APA - Agência Portuguesa do Ambiente) and municipalities, under the scope of the Rio Ceira project (EEA Grants 2022), still ongoing during 2023.

Materials and methods

The definition of climate change scenarios in this study is based on precipitation (P) and temperature (T) through the application of a methodology developed for application to Portuguese river basins (Ramos et al. 2014).

Firstly, it was necessary to define the climate projections of the basin. For this, the historical period selected was 1971 – 2015, with daily P and T data collected from IBERIA01 (Herrera et al. 2019). The climate projections were obtained from 13 regional climate models (RCM) of the EURO-CORDEX project, with resolution of 0.11°, considering two Representative Concentration Pathways (RCP), namely RCP4.5 and RCP8.5, and three future periods: 2011-2040 (near future), 2041-2070 (mid future), 2071-2100 (far future). After, the climate projections were bias-corrected through the Quantile Mapping technique. In this study, the "qmap" R package (Gudmundsson et al. 2012) was used, with the application of the most adequate quantile mapping method for each RCM, selected based on a statistical analysis.

Once bias-corrected, the period-change approach (future change in period mean-annual relative to historical) is applied in each P and T climate projection, originating the expected future modifications (signal and magnitude). Based on these, five climate change scenarios (Figure 1) are defined for each future period. To do this, three climate change metrics are calculated, both for P and T: 50th percentile or median (central tendency); 25th and 75th percentiles, which correspond to the range of modification variability (spread). With the intersection of these metrics, five scenarios are obtained, with the most appropriate climate change projections for each scenario selected based on the Euclidean distance to the scenario.

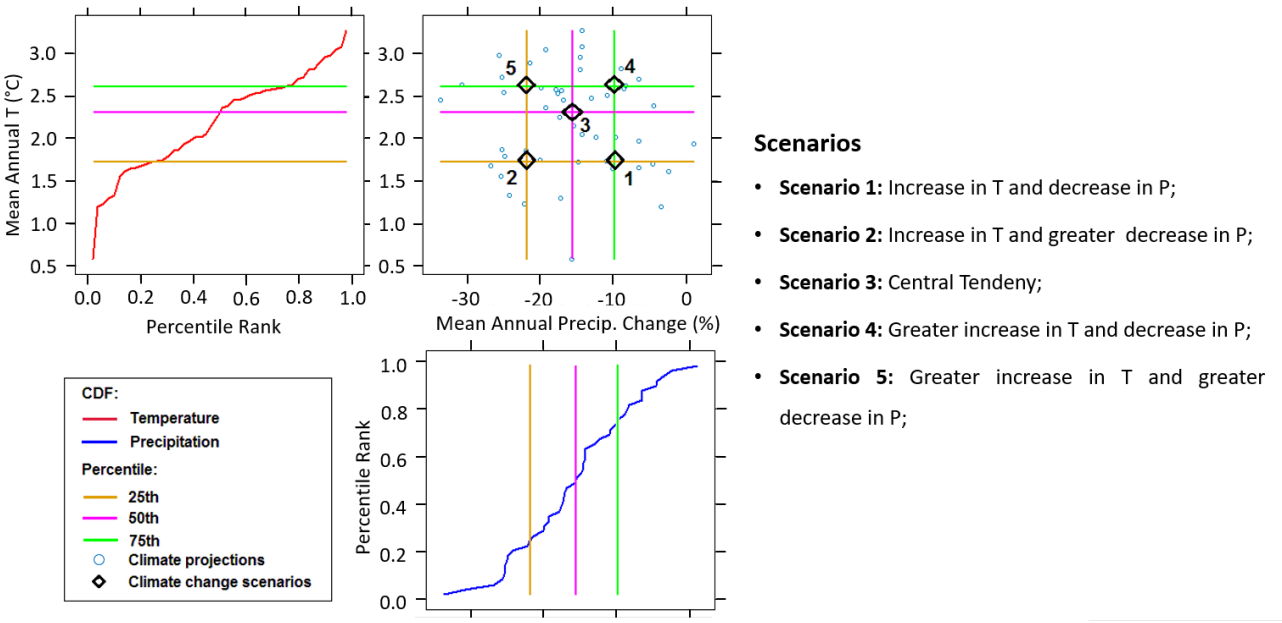

Scenarios

- **Scenario 1:** Increase in T and decrease in P;
- **Scenario 2:** Increase in T and greater decrease in P;
- **Scenario 3:** Central Tendeny;
- **Scenario 4:** Greater increase in T and decrease in P;
- **Scenario 5:** Greater increase in T and greater decrease in P;

Figure 1. Definition of climate change scenarios.

Results and concluding remarks

The definition of the climate change scenarios in the Ceira river basin was concluded. A downward trend on P was verified in the historical period, more accentuated from 2000 onwards, resulting in the general occurrence of dry years after 2005 (intense drought event). In reverse, as expected, an upward trend of T and evapotranspiration was verified.

With the obtained climate change scenarios, an assessment of the expected occurrence and intensity of future drought and water scarcity event will be performed through the evaluation of indices (e.g., common ones as SPI, and specific indices, as defined for Iberian transboundary river basins (Maia et al. 2022)). The scenarios will also be used to simulate the expected future streamflows in the basin, through application of a continuous hydrologic model. These analyses are expected to be done shortly.

Acknowledgments: EEA Grants Portugal 2014-2021 (through the Pre-defined Project 3 “Management of the Ceira river basin adapted to a changing climate”, of the Environment Programme)

References

Do Ó A, Seiz R (2021) Impacts of Climate Change in Iberia. Less rain and more uncertainty in Iberian Rivers. NP WWF & WWF España. https://www.natureza-portugal.org/conteudos2/biblioteca_/

EEA Grants (2022) PDP#3 – Gestão da Bacia Hidrográfica do Rio Ceira face às Alterações Climáticas. https://www.eeagrants.gov.pt/pt/programas/ambiente/projetos/projetos-pre-definidos/pdp3-gestao-da-bacia-hidrografica-do-rio-ceira-face-as-alteracoes-climaticas/

Gudmundsson L et al. (2012) Technical Note: Downscaling RCM precipitation to the station scale using statistical transformations - a comparison of methods. Hydrology and Earth System Sciences 16: 3383-3390. https://doi.org/10.5194/hess-16-3383-2012

Herrera S et al. (2019) Iberia01: a new gridded dataset of daily precipitation and temperatures over Iberia. Earth System Science Data 11(4): 1947-1956. https://doi.org/10.5194/essd-11-1947-2019

Maia R et al. (2022) Improving Transboundary Drought and Scarcity Management in the Iberian Peninsula through the Definition of Common Indicators: The Case of the Minho-Lima River Basin District. Water 14(3): 425. https://doi.org/10.3390/w14030425

New M et al. (2022) Decision Making Options for Managing Risk. In Pörtner H et al. Climate Change 2022: Impacts, Adaptation, and Vulnerability. Contribution of Working Group II to the Sixth Assessment Report of the Intergovernmental Panel on Climate Change, Cambridge University Press, Cambridge, UK and New York, NY, USA, pp 2539-2654. https://doi.org/10.1017/9781009325844.026

Ramos V et al. (2014) Methodology for the Development of Climate Change Scenarios and Climate Inputs to Run Impacts Models. Application to the Guadiana River Basin. In: Proceedings of the 3rd IAHR Europe Congress, Porto, Portugal

Extreme hydrometeorological events and the role of reclamation works and irrigation - drainage systems in the era of climate crisis

D. Tigkas[1,2*], N. Proutsos[3], G. Sofou[1], D. Papalexis[1], A. Kitsos[1], H. Vangelis[2], G. Tsakiris[2], E. Papadiamantopoulou[1], K. Stournaras[1]

[1] *Directorate of Land Reclamation and Soil-Water Resources, Ministry of Rural Development and Food, Athens, Greece*
[2] *Centre for the Assessment of Natural Hazards and Proactive Planning & Lab. of Reclamation Works and Water Resources Management, School of Rural and Surveying Engineering, National Technical University of Athens, Greece*
[3] *Institute of Mediterranean & Forest Ecosystems, Hellenic Agricultural Organization "DEMETER", Athens, Greece*
** e-mail: ditigas@mail.ntua.gr*

Introduction

Nowadays, there is prevalent concern regarding recorded and further expected climate changes, referred to as climate emergency or climate crisis (UN 2019), considering that adaptation measures need to be taken to mitigate the consequences of adverse climate conditions and extreme events (floods, droughts, heatwaves, etc.). Such events used to be typically perceived as a main problem of developing countries, due to climatic causes (e.g., arid or semi-arid environments) coupled with limited resources (economic, social and political) for reducing system vulnerability and combating the impacts. Nonetheless, during the last years there is strong evidence that extreme events are also an active and major issue for developed regions, as well, requiring close attention.

The field of water and food security is particularly sensitive to the above matters, while extensive supply deficits may occur (Fraser et al. 2013). Thus, proper management including proactive and structural measures are essential for decreasing the vulnerability of the systems to extreme events (Tigkas et al. 2020). To this end, reclamation works and irrigation – drainage systems may play key role for enhancing the water-land-food nexus under a climate change perspective (Iglesias et al. 2019). In this paper, the aforementioned role is examined towards managing insecurities and strengthening the interrelated systems against the anticipated impacts of hydro-meteorological extremes, taking into account potential conflicts between water uses and other limitations and factors related to sustainability goals.

Materials and methods

The positive aspects of reclamation works including irrigation and drainage systems for mitigating the impacts of extreme hydro-meteorological events are examined considering the anticipated adverse effects of such events due to climate change on the design principles of structural and institutional matters. Further, the contradictory issues that may arise among different sectors (agricultural production, urban water supply, environment, etc.) are also investigated based on international cases and paradigms.

Results and concluding remarks

There are several indications that the frequency and the severity of extreme events have increased during the last years. In Europe, severe and prolonged droughts and heatwaves occurred during the past decade in several regions, causing significant losses of crop yields with consequent widespread economic impacts. Also, intense storm events and cyclones leading to floods have caused damages in the agricultural sector, either directly (crop damages, yield reduction, etc.) or indirectly (damages on irrigation and drainage networks, etc.). Due to the above, increasingly more international policies lean towards measures in various sectors for adapting to climate crisis. For instance, the European Union has declared adaptation as a clear objective of the common agricultural policy for 2021-2027, providing opportunities for implementing a variety of measures to enhance water security and improve resilience against climate extremes (EEA 2019).

It is a fact that adequate infrastructure for water storage, management and distribution of irrigation

water is critical for reducing the vulnerability of agricultural systems to water scarcity due to drought, that may include design and construction of new projects, as well as proper operation and maintenance of existing networks. Also, well designed and properly maintained drainage systems, apart from retaining suitable soil conditions for crop development, can also contribute to reducing the damages of flood events.

Planning decisions upon the above are not straightforward, e.g. based mainly on financial criteria, but a complex task that should be carefully prepared and follow an established driver-pressure-state-impact-response (DPSIR) framework (Hettelingh et al. 2001). Indicatively, the common belief, that modern irrigation systems certainly lead to a more sustainable use of water, has been questioned by several studies (Perry et al. 2017). It is important to carefully define the objectives of any intervention, whereas understanding and considering the underlying hydrological and biophysical principles and mechanisms, in connection to socio-economic and environmental factors, can clearly point up the pros and cons of each project.

Recent cases in various areas of the globe show that, despite infrastructural improvements in the agricultural - water sector, unfavourable effects may come of, if adequate policy measures are not envisaged for maintaining proper management. Such adverse outcomes may include the deterioration of water quality, the misapprehension of the "lost" water concept leading to environmental impacts, conflicts between water users, etc. (e.g., Al-Faraj et al. 2016; Berbel et al. 2019; Nyam et al. 2020; Van der Kooij et al. 2017). To this end, water utilities supported by users' participation can play critical role for applying the appropriate measures and maintaining optimal operational schemes, while sufficient and well-informed personnel should be available to supervise and put into practise scientific and technological advancements.

Based on the above, it can be argued that infrastructural development is a major asset, though not panacea for water and food security. It is important to keep up sustainable solutions and integrated planning, balanced with the social, economic, cultural and environmental conditions of a region, while adopting appropriate strategic and institutional measures. The development schemes of a region, including the construction and operation of agricultural and water-related infrastructure, need to be carefully prepared, considering cost-benefit analyses according to established socio-economic and environmental criteria and follow a DPSIR framework. Such an approach ensures the creation of robust and sustainable systems, smoothly fitted within the existing and anticipated conditions of the region. Additionally, public participation in decision making is crucial for addressing issues raised by all interested parties and enhancing collective understanding and acceptance of the implemented measures.

References

Al-Faraj FAM, Tigkas D, Scholz M (2016) Irrigation efficiency improvement for sustainable agriculture in changing climate: A transboundary watershed between Iraq and Iran. Environmental Processes 3: 603–616

Berbel J, Expósito A, Gutiérrez-Martín C, Mateos L (2019) Effects of the irrigation modernization in Spain 2002–2015. Water Resources Management 33: 1835-1849. https://doi.org/10.1007/s11269-019-02215-w

EEA (European Environment Agency) (2019) Climate change adaptation in the agriculture sector in Europe. EEA report No 4/2019, ISSN 1977-8449

Fraser ED, Simelton E, Termansen M, Gosling SN, South A (2013) "Vulnerability hotspots": Integrating socio-economic and hydrological models to identify where cereal production may decline in the future due to climate change induced drought. Agricultural and Forest Meteorology 170: 195-205

Iglesias A, Garrote L, Granados A (2019) On the institutional framework for drought planning and early action. In: Iglesias A et al. (eds), Drought: Science And Policy, J. Wiley & Sons, https://doi.org/10.1002/9781119017073.ch5

Hettelingh JP, Pearce D, Kapros P, Cofala J, Amann M (2001) European Environmental Priorities: An Integrated Economic and Environmental Assessment. RIVM report 481505010, National Institute of Public Health and the Environment, Bilthoven, The Netherlands

Nyam YS, Kotir JH, Jordaan AJ, Ogundeji AA, Turton AR (2020) Drivers of change in sustainable water management and agricultural development in South Africa: A participatory approach. Sustainable Water Resources Management 6(4): 62. https://doi.org/10.1007/s40899-020-00420-9

Tigkas D, Vangelis H, Tsakiris G (2020) Implementing crop evapotranspiration in RDI for farm-level drought evaluation and adaptation under climate change conditions. Water Resources Management 34: 4329-4343

Van der Kooij S, Kuper M, de Fraiture C, Lankford B, Zuarteveen M (2017) Re-allocating yet-to-be-saved water in irrigation modernization projects. The case of the Bittit irrigation system, Morocco. In: Venot J-P et al. (eds) Drip irrigation for agriculture: Untold stories of efficiency, innovation and development. Routledge, Abingdon

UN (United Nations) (2019) The Climate Crisis – A race we can win. Available online: https://www.un.org/sites /un2.un.org/files/2020/01/un75_climate_crisis.pdf

Coupling machine learning algorithms with the tunable q-factor wavelet transform in forecasting the SPEI at the Bogra station in Bangladesh

S.A. Osmani[1], R. Narimani[2], J. Baik[2], J. Lee[2], C. Jun[1,2*]
[1] Department of Smart Cities, Chung-Ang University, Seoul, Republic of Korea
[2] Department of Civil and Environmental Engineering, Chung-Ang University, Seoul, Republic of Korea
* e-mail: cjun@cau.ac.kr

Introduction

Drought forecasting has an important role in reducing devastating agricultural and social impacts. Due to its nonlinear trends and random behaviour, drought forecasting has been established as one of most stochastic and uncertain approaches. In particular, there were severe drought events with reduced or no rainfall in Bangladesh for the years of 1973, 1978, 1979, 1981, 1982, 1984, 1989, 1992, 1994, and 1995 (Paul 1998; Shahid and Behrawan 2008) which had resulted huge losses in agricultural production (Mondal 2010). It is also known that western and central regions of the country are more vulnerable to drought (Kamruzzaman et al. 2019). There are several studies on analysis of rainfall shortage issues with a concept of meteorological drought in Bangladesh (Mondol et al. 2021; Mortuza et al. 2019). In particular, the standardized precipitation evapotranspiration index (SPEI) has been considered as a representative indicator to depict drought scenarios across the globe.

It is known that use of wavelet decomposition on pre-processing of input data can be useful for drought forecasting with high accuracy (Özger et al. 2020). However, there are limited researches on development of an ensemble model from machine learning algorithms with wavelet decomposition methods for the SPEI's prediction in Bangladesh. The main objective of this study is to suggest a new approach on drought forecasting with machine learning algorithms, focusing on the SPEI. Here, the tunable q-factor wavelet transform (TQWT) is considered for a wavelet decomposition method (Selesnick 2011) with different lead times such as 6, 12, 18, and 24 months.

Materials and methods

A flowchart for the proposed approach is described in Figure 1. At first, monthly data on precipitation, maximum temperature, and minimum temperature are collected from 1964 to 2019 at the Bogra station (24° 51′ N and 89° 22′ E) in Bangladesh. SPEI12 (i.e., SPEI in 12-month scale) is calculated from monthly precipitation, maximum and minimum temperature using the *SPEI* tool in R-studio.

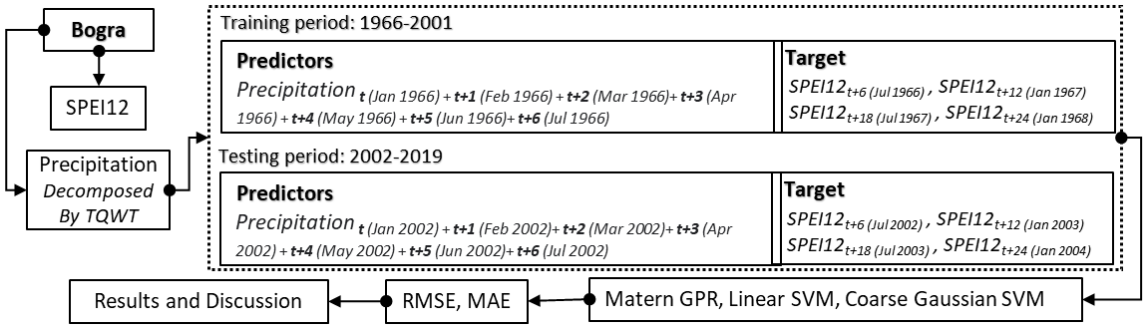

Figure 1. A flowchart for the proposed approach in this study.

By using the TQWT, monthly precipitation data is decomposed with one of the q-factor with 7 levels of decomposition. Three machine learning algorithms of Matern GPR (MGPR), linear SVM (LSVM), and coarse Gaussian SVM (CGSVM) are incorporated with decomposed data for forecasting SPEI12 in 6, 12, 18, and 24 months of lead times. Each model's performance is evaluated from root mean squared error (*RMSE*) and mean absolute error (*MAE*), dependent upon different lead times.

Results and concluding remarks

Figure 2 represents comparison results of *MAE* and *RMSE* for the forecasted SPEI12 in three machine learning algorithms with four lead times such as 6, 12, 18, and 24 months. It indicated that performance levels of machine learning models getting deviated as lead time goes higher. The results from the MGPR, compared to other two models, were consistent in producing minimum *MAE* and *RMSE* for all lead times in both training and testing periods.

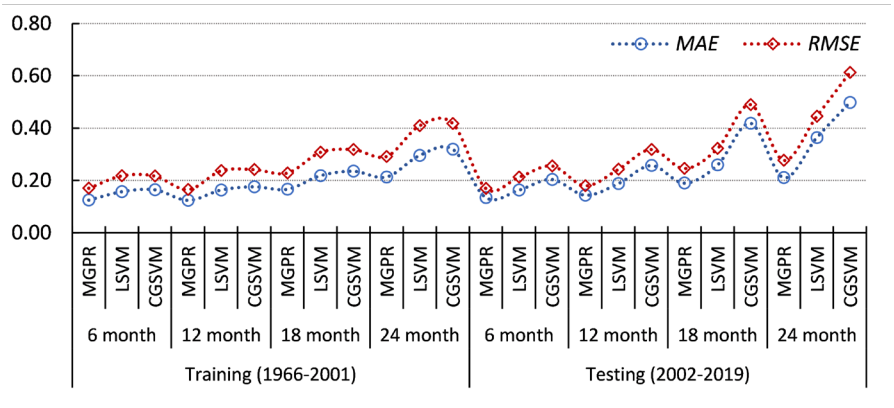

Figure 2. Comparison results of MAE and RMSE for the predicted SPEI12 in three machine learning algorithms with four lead times.

This study proposed a new approach for forecasting SPEI12 from decomposed times series of precipitation using the TQWT with specific subsequent lags. Our results showed a possibility of considering the TQWT in time series analysis for drought forecasting with machine learning algorithms. For better results in further studies, they require more wavelets with different lag combinations to compare and validate several execution levels of the TQWT in drought forecasting at various study areas under different climate conditions.

Acknowledgments: This research was supported by Korea Environment Industry & Technology Institute (KEITI) through Water Management Innovation Program for Drought (No. 2022003610001) funded by Korea Ministry of Environment.

References

Kamruzzaman M, Hwang S, Cho J, Jang MW, Jeong H (2019) Evaluating the spatiotemporal characteristics of agricultural drought in Bangladesh using effective drought index. Water 11(12): 2437

Mondal MH (2010) Crop agriculture of Bangladesh: Challenges and opportunities. Bangladesh Journal of Agricultural Research 35(2): 235-245

Mondol MAH, Zhu X, Dunkerley D, Henley BJ (2021) Observed meteorological drought trends in Bangladesh identified with the Effective Drought Index (EDI). Agricultural Water Management 255: 107001

Mortuza MR, Moges E, Demissie Y, Li HY (2019) Historical and future drought in Bangladesh using copula-based bivariate regional frequency analysis. Theoretical and Applied Climatology 135: 855-871

Özger M, Başakın EE, Ekmekcioğlu Ö, Hacısüleyman V (2020) Comparison of wavelet and empirical mode decomposition hybrid models in drought prediction. Computers and Electronics in Agriculture 179: 105851

Paul BK (1998) Coping mechanisms practised by drought victims (1994/5) in North Bengal, Bangladesh. Applied Geography 18(4): 355-373

Selesnick IW (2011) Wavelet transform with tunable Q-factor. IEEE Transactions on Signal Processing 59(8): 3560-3575

Shahid S, Behrawan H (2008) Drought risk assessment in the western part of Bangladesh. Natural Hazards 46: 391-413

The potential of nowcasting floods at street-level detail

V. Bellos[1*], C. Costanzo[2], J. Kalogiros[3], P. Costabile[2]
[1] Department of Environmental Engineering, Democritus University of Thrace, Xanthi, Greece
[2] Department of Environmental Engineering, University of Calabria, Rende (CS), Italy
[3] Institute of Environmental Research and Sustaibale Development, National Observatory of Athens, Greece
* e-mail: vbellos@env.duth.gr

Introduction

The increase of urbanization seems to be the most crucial component in order to investigate the trend in flood impacts. The concentration of socio-economic life in large metropolitan areas, which are characterized by the absence of urban planning, make the single use of structural measures for the flood defence a piecemeal strategy. In our era, the flood nowcasting and the installation of an early warning system based on this prediction is a substantial non-structural measure. However, until now, all the approaches towards on this direction are rather rough, whilst the information is provided in coarse resolutions. The latter had as a consequence that the system was either overestimating or underestimating the flood danger, whereas citizens start not to trust the alarms, reminding the liar shepherd Aesop's ancient story.

In this paper, we present a full paradigm coupling cutting-edge technologies which can potentially allow us to develop an accurate, fast and reliable flood nowcasting system at detailed scales (even in the street-level of a city). The three pillars of the proposed methodology are: a) Integrated mechanistic algorithms written in parallel for the simulation of a flood at the catchment scale; b) High Performance Computing (HPC) facilities in order to perform fast runs with the latter simulators; c) Weather radars which can provide a reliable rainfall grid forecasting with a considerable time horizon (namely, a couple of hours) with a significant level of detail both in space and time.

Materials and methods

The paradigm is based on the flood of Mandra (western Athens, Greece) occurred in November, 2017 and destroyed the city, while it caused 24 fatalities (Bellos et al. 2020; Bellos et al. 2022). The city is built in the outlet of two medium-sized catchments, named Soures and Agia Aikaterini (about 20-25 km^2). The catastrophic event was part of the medicane Numa-Zenon. Specifically, a local horographic phenomenon was observed in small scale which had as a consequence that the accumulated rainfall depth reached over than 300 mm in few hours at the half part of the catchments. Then, two flood waves propagated towards the city (the peak of both hydrographs was more than 100 m^3/s). The time response of the catchments was few hours which led us to characterize this event as a flash flood.

The mobile X-band dual-polarization Doppler weather radar (XPOL) radar of the National Observatory of Athens (Kalogiros et al. 2013) recorded this event with a significant level of detail. Specifically, the spatial resolution was 200 m, while the temporal resolution 2 min. This detail is of great importance in order to nowcast flash floods in complex urban environments, especially at the ephemeral rivers of Mediterranean region. Radar rainfall measurements when assimilated in weather forecast models can also produce sufficiently accurate rainfall nowcasting 1 to 3 hours in advance (Wang et al. 2013).

For the simulation, the in-house, UniCal software (Costabile et al. 2013) was used, which is based on the 2D Shallow Water Equations (2D-SWE). The solver is integrated, which means that simulates all the processes related to the water cycle in the catchment scale, with a great level of detail (the cell size ranges from 9 m^2 at the area of the city until 65 m^2 at the upstream hillslopes). Finally, the simulations were performed at the GALILEO 100 supercomputer of the Italian Cineca computing centre, in order to take the advantage of parallel writing of the UniCal code and fasten the simulations. Specifically, it was required 30 min of computational time for a 15 h event.

Results and concluding remarks

Floods are one of the most complex natural phenomena. First, the rainfall forecast is always a question regarding if is trustworthy. Second, even the most sophisticated algorithm which can describe the fluid behaviour in very small scales is unable to capture all the flow patterns observed in nature. Finally, the real-world events are characterized by great randomness as far as the input data is concerned: topography is changing all the time (both the landscape and the built environment) in all the time scales while there is no way to predict the behaviour of moving obstacles such as cars or trees which are drifted by the water.

Therefore, even with the proposed approach we do not recommend to produce flood hazard maps in their raw form, namely water depth and flow velocity, but in the form of flood hazard indices, which are a function of the natural hydraulic variables. In this paradigm, we used the flood hazard index used by the Australian Institute of Disaster Resilience (AIDR) for the output form of the maps. According to AIDR (2017), there are six hazard zones as a function water depth and flow velocity. In every zone, a qualitative description is given. Figure 1 depicts an example of the potential output if a flood nowcasting system is installed.

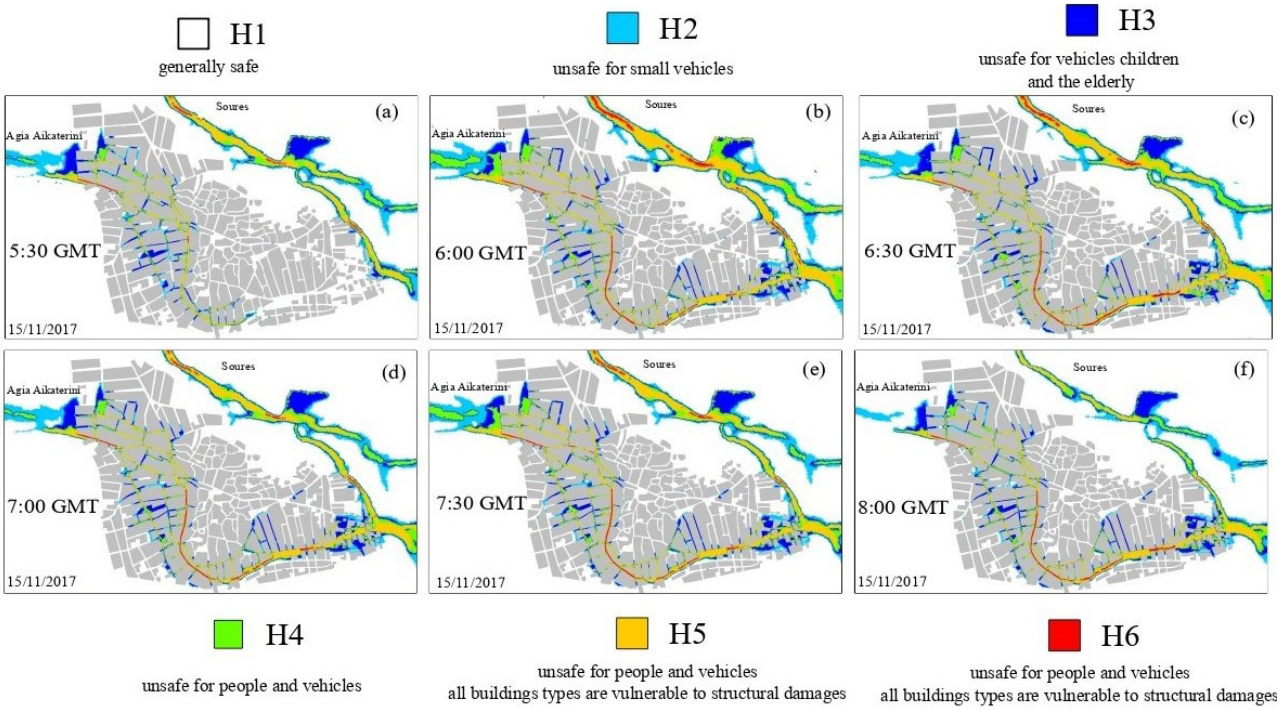

Figure 1. Flood hazard maps derived every 30 min in Mandra city.

References

AIDR (2017) Flood Hazard. Australian Disaster Resilience Handbook Collection. Guideline 7-3. Retrieved from https://knowledge.aidr.org.au/media/3521/adr-handbook-7.pdf

Bellos V, Kourtis I, Raptaki E, Handrinos S, Sibetheros I., Tsihrintzis VA (2022) Identifying modelling issues through the use of an open real-world flood dataset. Hydrology 9: 194. https://doi.org/10.3390/hydrology9110194

Bellos V, Papageorgaki I, Kourtis I, Vangelis H, Kalogiros I, Tsakiris G (2020) Reconstruction of a flash flood event using a 2D hydrodynamic model under spatial and temporal variability of storm. Natural Hazards 101: 711–726. https://doi.org/10.1007/s11069-020-03891-3

Costabile P, Costanzo C, Macchione F (2013) A storm event watershed model for surface runoff based on 2D fully dynamic wave equations. Hydrological Processes 27(4): 554-569. https://doi.org/10.1002/hyp.9237

Kalogiros J, Anagnostou, MN, Anagnostou EN, Montopoli M, Picciotti E, Marzano FS (2013) Correction of polarimetric radar reflectivity measurements and rainfall estimates for apparent vertical profile in stratiform rain. Journal of Applied Meteorology and Climatology 52(5): 1170-1186. https://doi.org/10.1175/JAMC-D-12-0140.1

Wang H, Sun J, Zhang X, Huang X-Y, Auligné T (2013) Radar data assimilation with WRF 4D-Var. Part I: System development and preliminary testing. Monthly Weather Review 141(7): 2224–2244. https://doi.org /10.1175/MWR-D-12-00168.1

Non-stationary frequency analysis of annual maximum standard duration precipitation

A. Yarci, T. Baran*
Civil Engineering Department, Dokuz Eylul University, Izmir, Turkey
** e-mail: turkay.baran@deu.edu.tr*

Introduction

The construction of water structures is a high-cost and long-lasting laborious process. Frequency analysis of extreme hydrological events should be taken into account during the design and planning of these structures. Precipitation has become irregular as a result of global warming, the effect of which has been increasing due to climate change in recent years. Aşıkoğlu and Çiftlik (2015), applied various trend tests to observed precipitation data in the Aegean Region and detected a decreasing trend in the annual precipitation data of 47 stations. In the presented study the decreasing trend has been detected in the data series. Since the trends have observed, it can be assumed that the stationary properties of precipitation have been disrupted. Therefore, models containing non-stationary parameters should be used instead of stationary parameters when modelling extreme precipitation.

Materials and methods

In the presented study, the time series consisting of observed annual standard-duration maximum precipitation data, which have been obtained from the central meteorological stations from the Aegean Region were first investigated in terms of trend. Parametric trend tests can give better results in detecting trends in variables that fit the normal distribution compared to non-parametric tests. But, hydrometeorological data usually show a tendency to not to comply with the normal distribution (Onyutha, 2016). Also, the Mann-Kendall test showed the best performance in data which fit the Generalized Extreme Value (GEV) distribution. Therefore, in the presented study, in order to detect trends in time series, the Mann Kendall test was used.

The GEV cumulative distribution function (shown in Equation 1) was used to model the maximum precipitation.

$$if\ \xi \neq 0,\ \mathrm{F}_{\xi}(x) = \exp - (1+(\ \xi\ (x-\mu)\ /\sigma\ ))^{-1/\xi} \quad (1)$$

where μ is the location, σ is the shape and ξ is the scale parameter.

The GEV models with stationary and non-stationary parameters used in the study are shown in Table 1.

Table 1. Stationary and non-stationary GEV models.

Model	Parameters		
GEV	μ =constant	σ =constant	ξ =constant
GEV1	μ (t)= μ_0+ μ_1t	σ =constant	ξ =constant
GEV2	μ =constant	σ (t)= σ_0+ σ_1t	ξ =constant
GEV3	μ (t)= μ_0+ μ_1t	σ (t)= σ_0+ σ_1t	ξ =constant

It is also necessary to conduct tests for choosing the most suitable one among the models. Akaike Information Criterion (AIC) and Bayesian Information Criterion (BIC) were used to decide the choice of the model that would best represent the process and give the future forecast in the most realistic way.

Results and concluding remarks

Within the scope of the study, the results of trend tests and the most suitable models selected for trend-observed stations according to AIC and BIC are summarized in Table 2. In the Table, upward pointing

arrows represent increasing trends and downward pointing arrows represent decreasing trends.

Table 2. The most suitable distribution models for precipitation periods with a trend.

Station	Trend observed precipitation periods	Mann Kendall test	Most suitable distribution
Aydın	30 Minutes to 12 hours	↑	GEV3
Balıkesir	5 Minutes	↓	GEV2
İzmir	30 Minutes to 24 hours	↑	GEV3
Kütahya	12 hours to 18 hours	↓	GEV3
Muğla	8 hours to 18 hours	↓	GEV3

For precipitation periods with no trend, GEV distribution with stationary parameters is more successful in representing the hydrological process. For precipitation periods with trend, GEV distribution with non-stationary parameters (GEV2 and GEV3) are more acceptable according to AIC and BIC. Therefore, it was concluded that at the design stage, it would be more appropriate to use non-stationary GEV distributions with two or mostly three parameters for those stations.

Considering an upward trend, especially seen in Aydin and Izmir stations, the observed and design precipitations are distinctively different. When considering flood modelling the risks will be critical. In this context, it is recommended to review the existing risks with non-stationary frequency analyses.

References

Aşıkoğlu OL, Çiftlik D (2015) Recent rainfall trends in the Aegean region of Turkey. Journal of Hydrometeorolgy 16(4): 1873-1885. https://doi.org/10.1175/JHM-D-15-0001.1

Onyutha C (2016) Statistical uncertainty in hydrometeorological trend analysis. Advances in Meteorology 2016: 8701617. http://doi.org/10.1155/2016/8701617

Trend analysis of gridded daily rainfall indices in Savitri River basin, India

E.S. Namitha*, V. Jothiprakash, B. Sivakumar
Indian Institute of Technology, Bombay, India
** e-mail: namithaelza@gmail.com*

Introduction

Understanding the temporal and spatial variation of rainfall is a prerequisite for modeling and forecasting extreme hydrologic events like floods and droughts. Many studies have carried out trend analysis on observed as well as gridded rainfall data over several river basins in India (Pattanaika and Rajeevan, 2010; Chandniha et al. 2017). Few studies have reported the trend of certain indices developed for the extreme conditions of rainfall events (Sharma et al. 2018; Ali et al. 2014; Deshpande et al. 2016). These studies found that the rainfall over Indian basins are showing a decreasing trend except during monsoon season. The importance of temporal analysis of extreme rainfall events is increasingly realized at the current time, because of climate change and its effect on water availability.

In this study, the temporal variation of daily gridded rainfall events from the Savitri River basin, India is analyzed using indices proposed by the Expert Team on Climate Change Detection Monitoring Indices (ETCCDI). The daily gridded rainfall observed over a period of 40 years from 1980 to 2020 is used for the temporal analysis. The temporal variation is examined using trend analysis. The commonly used Mann-Kendall and Sen's slope tests are used for trend analysis.

Materials and methods

Trend analysis shows the general nature of the variation of the variable under consideration. In this study, the commonly used MK test and Sen's slope test are used to analyse the trend. The trend analysis is performed on the ETCCDI indices at a significance level of 5%. There are 9 indices in total; definition of each index is presented in Table 1. The indices are developed from daily data for annual and seasonal time scales. The four seasons in India are the Summer (March-May), south-east monsoon season (June–September), North-east monsoon (October – November), and winter (December – February).

Table 1. List and definitions of indices used.

Indicator	Indicator name	Description	Unit
PRCPTOT	Total rainfall	Annual/seasonal total rainfall from days ≥ 2.5mm	mm
RD	Rainy days	Annual/seasonal number of days when rainfall ≥ 2.5mm	days
SDII	Simple daily intensity index	The ratio of annual/seasonal total rainfall to the number of rainy days	mm/day
R1DAY	Maximum 1-day rainfall amount	Annual/seasonal maximum 1-day rainfall	mm
R99P	Extremely wet rainfall	Annual/seasonal total rainfall from days > 99th percentile	mm
R95P	Very wet rainfall	Annual/seasonal total rainfall from days > 95th percentile	mm
RLOW	Number of low rainfall days	Number of days when annual/seasonal rainfall ≤ 64.4 mm	days
RMED	Number of medium rainfall days	Number of days when annual/seasonal rainfall > 64.4 mm and ≤ 124.4 mm	days
REXT	Number of extreme rainfall days	Number of days when annual/seasonal rainfall > 124.4 mm	days

The MK test gives the significance of the trend by checking the null hypothesis that there is no trend in the series and the alternate hypothesis is taken as there is a trend in the series (Kendall 1975). As a prerequisite for the MK test, the series should be checked for the independency of values. Therefore, the serial correlation of each series is checked, and if it is correlated, pre-whitening needs to be carried out. Here, the pre-whitening for the MK test is done by following the procedure suggested by Yue and Wang (2004) by using effective sample size (ESS) approach. The Sen's slope test gives the direction of the trend. It

identifies the direction of the trend by using the slope of all the data point pairs in the time series (Sen 1968).

Results and concluding remarks

This study performed a trend analysis of the gridded daily rainfall for 16 grid points in and around the Savitri river basin which is having a total area of 2262.42 km^2. The results show an increase in the total rainfall, rainy days, and intense rainfall during the pre-monsoon, monsoon, and post-monsoon seasons. During the winter season, the amount of rainfall received is decreasing. Therefore, good irrigation practice is needed in the region during the winter season for rabi crops. The extreme rainfall events are increasing during monsoon. During pre-monsoon and winter season, the extreme rainfall events are not occurring. Thereby more chance for flooding during monsoon season. These results are very much useful for the planning and management of water resource related problems in the area, such as irrigation, water distribution, water storage by dams, and disaster management, among others.

Table 2. Summary of trend analysis results.

Indicator	Trend (%area)				
	Annual	Pre monsoon	Monsoon	Post monsoon	Winter
PRCPTOT	Increase (91%)	Increase (91%)	Increase (91%)	Increase (91%)	Decrease (63%)
RD	Increase (91%)	Increase (91%)	Increase (82%)	Increase (91%)	Decrease (73%)
SDII	Increase (91%)	Increase (100%)	Increase (91%)	Increase (73%)	Decrease (64%)
R1DAY	Increase (54%)	Increase (100%)	Increase (64%)	Increase (73%)	Increase (55%)
R99P	Increase (81%)	No values	Increase (82%)	Decrease (36%)	No values
R95P	Increase (91%)	Decrease (55%)	Increase (91%)	Increase (54%)	No values
RLOW	Increase (91%)	Increase (91%)	Increase (54%)	Increase (91%)	Decrease (54%)
RMED	Increase (91%)	No values	Increase (91%)	Decrease (55%)	No values
REXT	Increase (91%)	No values	Increase (91%)	Decrease (64%)	No values

References

Ali H, Mishra V, Pai DS (2014) Observed and projected urban extreme rainfall events in India. Journal of Geophysical Research: Atmospheres 119: 12621–12641. https://doi.org/10.1002/2014JD022264

Chandniha SK, Meshram SG, Adamowski JF, Meshram C (2017) Trend analysis of precipitation in Jharkhand state, India: investigating precipitation variability in Jharkhand state. Theoretical and Applied Climatology 130: 261–274. https://doi.org/10.1007/s00704-016-1875-x

Deshpande NR, Kothawaleb DR, Kulkarnic A (2016) Changes in climate extremes over major river basins of India. International Journal of Climatology 36: 4548–4559

Kendall MG (1975) Rank Correlation Methods. 4th edition. Charles Griffin, London

Pattanaika DR, Rajeevan M (2010) Variability of extreme rainfall events over India during southwest monsoon season. Meteorological Applications 17: 88–104. https://doi.org/10.1002/met.164

Sen PK (1968) Estimation of regression coefficient based on Kendall's test. Journal of American Statistical Association 63(324): 1379–1389

Sharma PJ, Loliyana VD, Resmi SR, Timbadiya PV, Patel PL (2018) Spatiotemporal trends in extreme rainfall and temperature indices over Upper Tapi Basin, India. Theoretical and Applied Climatology 134: 1329–1354

Yue S, Wang CY (2004) The Mann-Kendall Test Modified by Effective Sample Size to Detect Trend in Serially Correlated Hydrological Series. Water Resources Management 18: 201–218

The increasing frequency of heatwaves and extreme droughts in the Lisbon area, Portugal

M.M. Portela[1*], L.A. Espinosa[2]
[1] IST, University of Lisbon, Civil Engineering Research and Innovation for Sustainability (CERIS), Portugal
[2] IST-ID, University of Lisbon, Civil Engineering Research and Innovation for Sustainability (CERIS), Portugal
* e-mail: maria.manuela.portela@tecnico.ulisboa.pt

Introduction

The paper presents some of the results from a recent research aiming to develop a comprehensive and able of being spatially extrapolated methodology to address changes in the behaviour of some of the hydrological variables more closely related to the extreme hydrological events (Espinosa et al. 2022). The purpose is to conclude whether those changes can be explained by the natural variability of the historical samples or, on the contrary, they are not encompassed by such variability, denoting signs likely to be attributed to climate change. To develop and test the models to be integrated into the methodology and to systematize the presentation of the respective results, a specific location in Lisbon coastal metropolitan area (mainland Portugal) was selected. From the results so far achieved, those related to the frequency of the heatwaves and droughts of are briefly presented herein. In fact, severe droughts and heatwaves have already affected Portugal and will continue to do so, expectedly with increasing frequency and intensity.

Materials and methods

To create a comprehensive picture of the climate and its changes in a region long and quasi continuous data series at short timescales are required. In the case study of Lisbon coastal metropolitan area, the Lisboa-Geofísico weather station (29U 487481.65 m E 4287553.88 m N, 77 m height) was selected due to its location inside the study area and the availability of long and high quality records of other variables besides rainfall. The results mentioned herein utilized daily values of precipitation and mean (Tmean), maximum (Tmax) and minimum (Tmin) temperatures, for the period of 157 hydrological years, between Oct/1864 and Sep/2021 (records were made available by the Portuguese Institute for the Ocean and Atmosphere, IPMA).

The extreme temperature events were analysed based on the heatwave periods, i.e., the periods of 3 or more consecutive days with Tmax above the daily threshold defined as the 90th percentile of daily Tmax, centred on a 31-day window (Russo et al. 2014). For a given day *d*, the threshold series A_d of the dataset is given by:

$$A_d = \bigcup_{y=1864}^{2021} \bigcup_{i=d-15}^{d+15} Tmax_{y,i} \quad (1)$$

where U denotes the union of sets and $T_{y,i}$ is the Tmax of the day i in the year y. The frequency of the heatwaves utilized the kernel occurrence rate estimator (KORE) applied to time data, i.e., to the days belonging to heat waves, according to the stepwise approach developed by Silva et al. (2012).

Given the critical role of temperature and hence evapotranspiration on drought development, the Standardized Precipitation Evapotranspiration Index (SPEI), an extension of the more common Standardized Precipitation Index (SPI), was used for drought detection. The SPEI accounts for both rainfall and potential evapotranspiration (PET), thus capturing the main impact of temperature changes on water availability. For the sake of simplicity, the PET was estimated based on the Thornthwaite method applied to Tmean (Beguería et al. 2014). The analysis of the frequency of the droughts utilized an approach similar to the one applied to the heatwaves, but considering as time data the periods under extreme drought conditions.

Results and concluding remarks

Figure 1 shows the results from the heatwaves frequency analysis. In the figure, the red curve represents the number of heatwaves days per year, λ(t); the blue lines the daily values of Tmax; and the

yellow curve the heatwave daily threshold. A point-wise bootstrap confidence band was constructed around λ(t) for a more accurate interpretation of the results. The confidence band quantifies the uncertainties associated with the occurrence rate estimates: the narrower the band is, the less uncertainty.

The results related to the drought frequency are exemplified in Figure 2 for the time scales of 6 and 12 months and extreme droughts (threshold of -1.65).

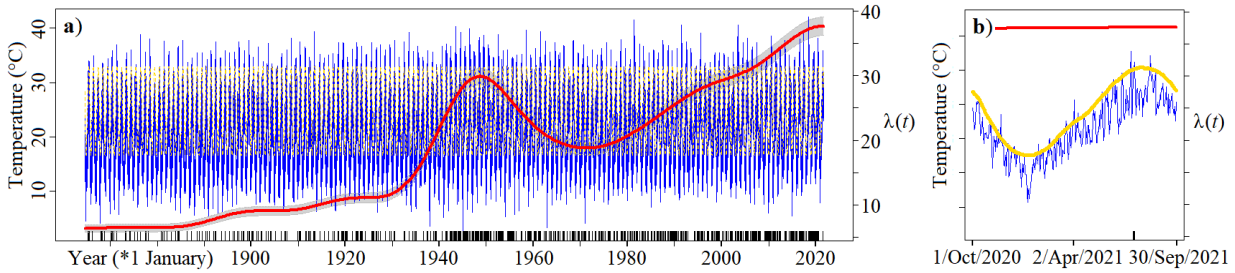

Figure 1. Time-dependent occurrence rate of heatwave days at Lisboa Geofísico weather station (1864-2021). a) Vertical left axis: daily Tmax in blue, and heatwave magnitude index threshold series, Ad, in gold; vertical right axis: number of heatwave days per year, λ(t), red line; and confidence band, grey area. b) Detail based on one hydrological year (the confidence band is omitted). The vertical ticks are the dates of ≥3 consecutive days with Tmax above Ad.

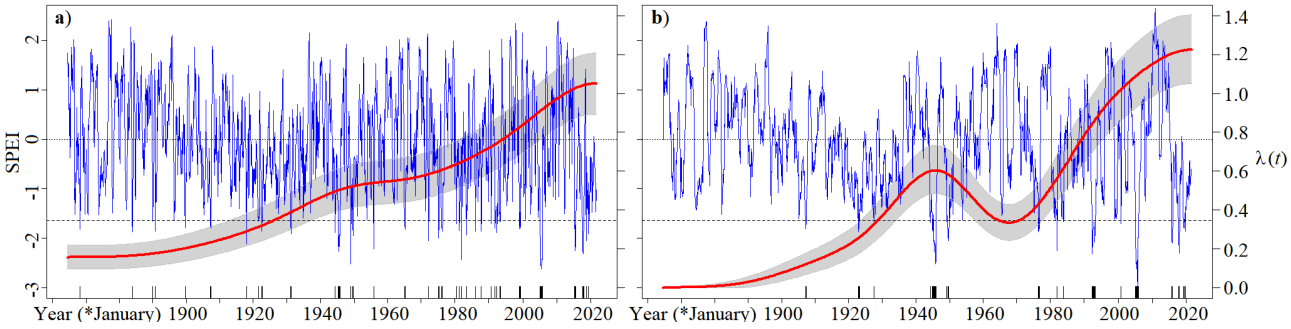

Figure 2. Time-dependent occurrence rate of periods under extreme drought conditions at Lisboa Geofísico weather station (1864-2021) for a) SPEI6, and b) SPEI12. Vertical left axes: SPEI series in blue, and drought thresholds by horizontal dashed lines at -1.65. Vertical right axes: the number of periods under drought conditions per year, λ(t), depicted by a red line, and the confidence band by a grey area. The vertical ticks are the dates of the drought periods.

The previous figures show anomalies that clearly deviate from their long-term natural variability, evidencing that Lisbon area is warming and suffering more frequent heatwaves and droughts. Although not shown here, the analysis of the frequency of the heatwaves applied to Tmin also denoted a pronounced frequency increase of the corresponding heatwave days. Having in mind that Lisbon is a coastal urban environment particularly stressed by human activity, including tourism, makes it unavoidable to raise awareness towards the expected adverse climate impacts and the urge of adaptation measures.

Acknowledgments: Research carried out at the Civil Engineering Research and Innovation for Sustainability (CERIS), a registered research unit in the Fundação para a Ciência e a Tecnologia (FCT), UIDB/04625/2020; and supported by the European Union's Horizon 2020 via the SCORE project, grant No. 101003534.

References

Beguería S, Vicente-Serrano SM, Reig F, Latorre B (2014) Standardized precipitation evapotranspiration index (SPEI) revisited: parameter fitting, evapotranspiration models, tools, datasets and drought monitoring. Int. J. Climatol., 34: 3001–3023. https://doi.org/10.1002/joc.3887

Espinosa LA, Portela MM, Matos JP, Gharbia S (2022) Climate change trends in a European Coastal Metropolitan Area: rainfall, temperature, and extreme events (1864-2021). Atmos 13(12): 1995. https://doi.org/10.3390/atmos13121995

Russo S et al. (2014) Magnitude of extreme heat waves in present climate and their projection in a warming world. JGR Atmos 119: 12500–12512. https://doi.org/10.1002/2014JD022098

Silva AT, Portela MM, Naghettini M (2012) Nonstationarities in the occurrence rates of flood events in Portuguese watersheds. Hydrol Earth Syst Sci 16: 241–254. https://doi.org/10.5194/hess-16-241-2012

Quantifying uncertainty in future runoff estimation based on SSP scenarios

J.H. Kim, S.T. Chae, J.Y. Song, Y.H. Song, E.S. Chung*
Department of Civil Engineering, Seoul National University of Science and Technology, 232 Gongneung-ro, Nowon-gu, Seoul, 01811, Korea
** e-mail: eschung@seoultech.ac.kr*

Introduction

Global climate change affects the patterns in climate variables and causes severe and frequent water-related disasters, such as droughts and floods (IPCC 2014). Future changes in the water cycle will make water resource management and planning more challenging over the world, especially in East Asia which have four distinct seasons (Song et al. 2022). Regional runoff is the most basic and important data for establishing a water resource management plan. Observed runoff data are uncertain due to sparsely located observatories, thus the runoff outputs from hydrological model simulation can be used to estimate hydrological factors. General circulation models (GCM) are widely used by researchers to assess the effect of climate change in water related studies for the future. Due to the differences in the physical climate simulation process of climate models, the scenarios considered, and the initial conditions, GCMs are inherently includes uncertainty. The identification of major uncertainty components and quantification of uncertainty contributions of different sources may help to reduce potential uncertainty in assessing the hydroclimatic impact (Wang et al. 2020). Therefore, the objective of this study is to quantify the uncertainties of future runoff estimations resulted by GCMs according to SSP scenarios.

Materials and methods

Soil & Water Assessment Tool (SWAT) model: The SWAT model is a physically based, semi-distributed, and process based river basin model which is mainly used in hydrological studies to evaluate stream flow. It has the advantage of simulating the hydrological cycle processes in watersheds using relatively simple input data. The hydrological cycle of the SWAT model is interpreted as Eq. (1):

$$SW_t = SW_0 + \sum_{i=0}^{t} (R_{day} - Q_{surf} - E_a - w_{seed} - Q_{gw}) \quad (1)$$

where SW_0 is the initial soil moisture content (mm), SW_t is the total soil moisture per day (mm), R_{day} is precipitation (mm), Q_{surf} is surface runoff (mm), E_a is evapotranspiration (mm), w_{seed} is penetration, Q_{gw} is groundwater runoff (mm), and t is time (day).

Jensen–Shannon divergence (JS-D): JS-D can measure the similarity between two distributions. The uncertainty in the estimated future runoff and observed runoff was evaluated using JS-D. JS-D formula for the two distributions P and Q is shown in Eq(2):

$$JSD(P,Q) = 1/2D(P \| M) + 1/2D(Q \| M) \quad (2)$$

where $M = 1/2(P+Q)$.

Interprets of how much the selection of GCMs data affect future runoff uncertainty was conducted using Bayesian model averaging (BMA). The BMA method is a statistical approach for combining predictions obtained from different GCMs.

Results and concluding remarks

The uncertainty in future runoff estimates according to GCMs are calculated using BMA. All of the indices for evaluation were set to have higher uncertainty when the value increases. The values for both

Near future (NF) and Far future (FF) of SSP2-4.5 and SSP5-8.5 were evaluated. INM-CM4-8 among GCMs was found to have the highest uncertainty, while IPSL-CM6A-LR was the lowest. The sum of all evaluation indices presented that SSP5-8.5 has a higher uncertainty than SSP2-4.5. In SSP2-4.5, uncertainty in NF is higher than FF, on the other hand, SSP5-8.5 was found to have a higher uncertainty in FF than NF.

Table 1. Uncertainty in estimated future runoff for SSP2-4.5 scenarios, two future periods and eleven GCMs.

GCMs	RMSE	1-NSE	RSR	1-KGE	Average	Rank	RMSE	1-NSE	RSR	1-KGE	Average	Rank
	Near future (2021-2060)						Far future (2061-2100)					
ACCESSESM1-5	11.73	0.02	0.14	0.02	11.91	5	11.74	0.02	0.13	0.01	11.9	4
CanESM5	12	0.02	0.14	0.02	12.18	4	11.74	0.02	0.13	0.01	11.9	5
INM-CM4-8	25.39	0.09	0.3	0.07	25.85	1	25.36	0.08	0.29	0.06	25.79	1
INM-CM5-0	7.19	0.01	0.09	0.01	7.3	10	7.22	0.01	0.08	0.01	7.32	10
IPSL-CM6A-LR	5.7	0	0.07	0.01	5.78	11	5.36	0	0.06	0	5.42	11
MIROC6	9.64	0.01	0.12	0.01	9.78	8	9.2	0.01	0.1	0.01	9.32	8
MPI-ESM1-2-HR	10.08	0.02	0.12	0.01	10.23	7	8.8	0.01	0.1	0.01	8.92	9
MPI-ESM1-2-LR	19.97	0.06	0.24	0.04	20.31	2	19.73	0.05	0.22	0.04	20.04	2
MRI-ESM2-0	18.69	0.05	0.22	0.04	19	3	18.18	0.04	0.2	0.03	18.45	3
NorESM2-LM	11.23	0.02	0.13	0.01	11.39	6	11.11	0.02	0.12	0.01	11.26	6
NorESM2-MM	9.57	0.01	0.11	0.01	9.7	9	9.64	0.01	0.11	0.01	9.77	7

Table 2. Uncertainty in estimated future runoff for SSP5-8.5 scenarios, two future periods and eleven GCMs.

GCMs	RMSE	1-NSE	RSR	1-KGE	Average	Rank	RMSE	1-NSE	RSR	1-KGE	Average	Rank
	Near future (2021-2060)						Far future (2061-2100)					
ACCESSESM1-5	11.48	0.02	0.14	0.02	11.66	5	12.37	0.02	0.13	0.01	12.53	5
CanESM5	11.19	0.02	0.14	0.01	11.36	4	13.01	0.02	0.14	0.01	13.18	4
INM-CM4-8	24.67	0.09	0.3	0.07	25.13	1	25.79	0.07	0.27	0.05	26.18	1
INM-CM5-0	7.13	0.01	0.09	0.01	7.24	10	7.66	0.01	0.08	0.01	7.76	10
IPSL-CM6A-LR	5.19	0	0.07	0	5.26	11	7.52	0.01	0.08	0.01	7.62	11
MIROC6	8.53	0.01	0.12	0.01	8.67	8	9.8	0.01	0.1	0.01	9.92	8
MPI-ESM1-2-HR	8.92	0.01	0.12	0.01	9.06	7	9	0.01	0.09	0.01	9.11	9
MPI-ESM1-2-LR	18.73	0.05	0.24	0.04	19.06	2	21.08	0.05	0.22	0.04	21.39	2
MRI-ESM2-0	18.2	0.05	0.22	0.04	18.51	3	19.3	0.04	0.2	0.03	19.57	3
NorESM2-LM	10.82	0.02	0.13	0.01	10.98	6	11.58	0.02	0.12	0.01	11.73	6
NorESM2-MM	9.3	0.01	0.11	0.01	9.43	9	10.17	0.01	0.11	0.01	10.3	7

Acknowledgments: This research was supported by the National Research Foundation of Korea (2021R1A2C200569912).

References

IPCC (2014) IPCC Climate Change 2014: Synthesis Report. Contribution of Working Groups I, II and III to the Fifth Assessment Report of the Intergovernmental Panel on Climate Change. IPCC, Geneva, Switzerland. https://doi.org/10.1017/cbo9781107415324.004

Song YH, Chung ES, Shahid S (2022) Differences in extremes and uncertainties in future runoff simulations using SWAT and LSTM for SSP scenarios. Science of The Total Environment 838: 156162. https://doi.org/10.1016/j.scitotenv.2022.156162

Wang HM, Chen J, Xu CY, Zhang J, Chen H (2020) A framework to quantify the uncertainty contribution of GCMs over multiple sources in hydrological impacts of climate change. Earth's Future 8(8): e2020EF001602. https://doi.org/10.1029/2020ef001602

Preliminary analyses of changes in intense precipitation in FVG, northeastern Italy

E. Arnone[1*], D. Treppiedi[2], V. Zoratti[1], L.V. Noto[2]
[1] Dipartimento Politecnico di Ingegneria e Architettura, Università degli Studi di Udine, Udine, Italy
[2] Dipartimento di Ingegneria, Università degli Studi di Palermo, Palermo, Italy
* e-mail: elisa.arnone@uniud.it

Introduction

Changes in extreme precipitation and precipitation properties have been widely assessed over the Mediterranean area and, in particular, Italy (Libertino et al. 2019; Treppiedi et al. 2021; Caporali et al. 2021). Libertino et al. (2019) provides a comprehensive evaluation of the regional trend in the magnitude and frequency of annual rainfall maxima over the entire Italy, analysing trends for sub-daily precipitation at 1,3,6,12, and 24 hours by means of the Mann-Kendall test (MK). According to the study, significant trends emerge mainly in small domains (compared to the whole-country scale) with homogeneous geographical characteristics. Specifically, an increase of rainfall severity for all the durations has been observed in the northeastern part of the country.

In the present study we focus on a region of northeastern Italy, i.e. the Friuli Venezia Giulia (FVG), to carry out more local analyses, as suggested by Libertino et al. (2019), in order to assess changes in sub-hourly precipitation. The adopted method is based on the Quantile Regression method, which allows to screen continuous time-series exceeding selected quantiles. Analyses of the continuous database of high-resolution records for the region have been described by Arnone et al. (2023), where preliminary results of statistical changes are presented for selected locations. In this study the assessment is extended to the entire region.

Materials and methods

The analysed dataset is a subset of the ground rain-gauges network of the FVG region, which consists of more than 200 ground stations managed by the regional Civil Protection Agency (Arnone et al. 2023). Specifically, the entire network is composed mainly by two different series of rain gauges, i.e. the network originally managed by the Hydrographic Operative Unit that is now based on CAE technology, and the network built with the SIAP+Micros hardware technology, which is directly managed by the agency OSMER ARPA-FVG (*OSservatorio MEteorologico Regionale-Agenzia Regionale per la Protezione dell'Ambiente*), hereinafter SIAP+Micros network. In this study, we analysed the time series of rain gauges controlled by the agency OSMER, which are shown in Figure 1 and belong to the SIAP+Micros network.

The SIAP-Micros rain-gauges have been installed starting from the 1990s at an initial recording frequency of 1 h (Arnone et al. 2023). The resolution has been increased up initially to 5 min (around the 1997) and more recently (from 2018) to 1 min. The continuous series with longest recording length is at a rate of 5 min, with an average of 22 years for the oldest rain-gauges (30% of the network, Arnone et al. 2023).

The continuous series are checked and cleaned up by means of a very simple method presented in Arnone et al. (2023), which allows to remove suspicious outliers and recurring values. It is worth noting that the method was appositely developed for obtaining series suitable for the extreme trend analyses. The Quantile Regression (QR) method (Koenker 2005; Treppiedi et al. 2021) has been applied to the corrected series to assess eventual trends in sub-hourly data. The QR is an extension of the standard linear regression model that allows to perform a regression on different quantiles instead of only on the mean, by inspecting at different the tail of the rainfall distribution. Here the values of 0.90, 0.95 and .099 quantiles have been considered.

Results and concluding remarks

This study provides the preliminary results of the regional analyses applied to the rain gauge network shown in Figure 1. Obtaining reliable continuous time series at very high resolution, i.e. 5 minutes, represents the main challenge of the work, given that official validation is not provided, to our knowledge.

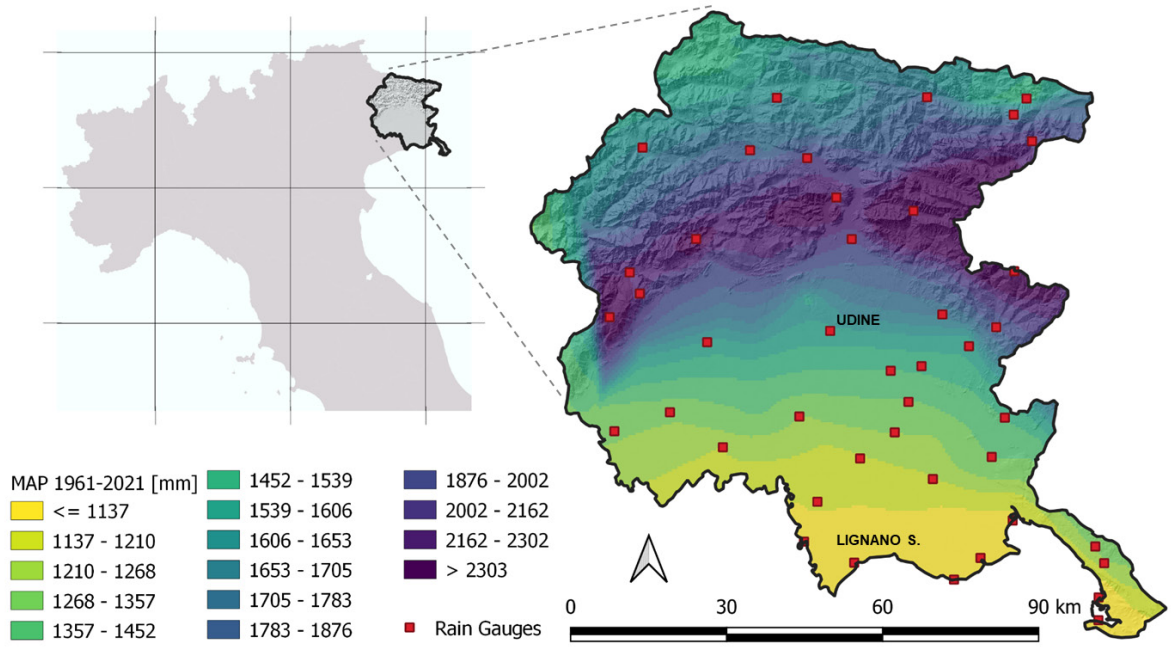

Figure 1. Map of Mean Annual Precipitation (MAP) of Friuli Venezia Giulia (FVG) region and location of the analysed rain gauges.

The results of some selected stations showed that significant trends, either increasing or decreasing, are not homogenous across the region and they depend on the location and selected duration. Specifically, significantly increasing trends (5% significant level) have been observed at Lignano Sabbiadoro, which is close to the sea (Figure 1), for different durations (e.g. from 20 minutes to 24 hour). Whereas, decreasing trends were observed at Udine, located in the in the middle of the plain area (Figure 1), only for the very short durations, i.e. 5 and 10 minutes.

A comprehensive spatial analysis of the obtained trend will be provided in the next steps of the work.

Acknowledgments: This study has been supported by the inter-departmental project *ESPeRT (Energia, Sostenibilità dei Processi produttivi e Resilienza Territoriale per la Transizione ecologica), "Piano strategico Università degli Studi di Udine 2022-2025".*

References

Arnone A, Treppiedi D, Noto LV (2023) Analysis of high-resolution rain analysis in FVG, northeastern Italy. In "IAHS2022 – Hydrological sciences in the Anthropocene: Variability and change across space, time, extremes, and interfaces", XIth Scientific Assembly of the International Association of Hydrological Sciences (IAHS 2022), 29 May-3 June 2022, Montpelier, France (in press)

Caporali E, Lompi M, Pacetti T, Chiarello V, Fatichi S (2021) A review of studies on observed precipitation trends in Italy. Int J Climatol 41: E1–25, TS7. https://doi.org/10.1002/joc.6741

Koenker R (2005) Quantile Regression. Cambridge University Press, Cambridge. https://doi.org/10.1017/CBO9780511754098

Libertino A, Ganora D, Claps P (2019). Evidence for increasing rainfall extremes remains elusive at large spatial scales: The case of Italy. Geophysical Research Letters 46: 7437– 7446. https://doi.org/10.1029/2019GL083371

Treppiedi D, Cipolla G, Francipane A, and Noto LV (2021) Detecting precipitation trend using a multiscale approach based on quantile regression over a Mediterranean area. Int J Climatol 35 (41): 5938–5955. https://doi.org/10.1002/joc.7161

Generalised increasing frequency and intensity of Tmax heatwaves in Portugal in the last four decades (1980-2021)

L.A. Espinosa[1*], M.M. Portela[2]
[1] IST-ID, University of Lisbon, Civil Engineering Research and Innovation for Sustainability (CERIS), Portugal
[2] IST, University of Lisbon, Civil Engineering Research and Innovation for Sustainability (CERIS), Portugal
* e-mail: luis.espinosa@tecnico.ulisboa.pt

Introduction

The climate of Portugal is highly affected by extreme weather events, including heatwaves and warm spells. Since the mid-twentieth century, many regions have experienced an increase in the frequency and duration of these extreme events, which have had a profound impact on the country. Heatwaves are a major concern due to their link to significant increases in mortality rates both in Portugal and globally, with notable examples in Portugal including those of the years 1981, 2003, and 2018. The effects of heatwaves on surface water security, wildfires, and public health are also of great concern. The year 2020 saw an exacerbation of this relationship, with several warm episodes and significant mortality excess during one of the hottest periods on record (Sousa et al. 2022). In addition, Portugal experienced its highest-ever July temperature of 47°C in 2022, although the data is still considered preliminary. Despite these alarming trends, comprehensive assessments of the impact of temperature trends — mostly in daily maximum temperature (Tmax) — on heatwaves in the country using detailed spatiotemporal data have yet to be undertaken. Thus, this research aims to address this gap by analysing relevant changes in (i) Tmax, (ii) heatwave days, and (iii) associated temperature trends in representative locations in mainland Portugal.

Materials and methods

The daily maximum temperature (Tmax) data used in this study covers the period from 1 October 1980 to 30 September 2021. The data was obtained from ERA5-Land, which is the fifth-generation reanalysis dataset developed by the European Centre for Medium-Range Weather Forecasts (ECMWF). This dataset provides high-resolution (0.1° x 0.1°) gridded temperature data for the past 4 to 7 decades. In this study, data from eight ERA5-Land grid-points (Figure 1a) was used to analyse the temperature trends. Although not shown here, the ERA5-Land dataset has been validated by comparing it with temperature records obtained from the national met office's (IPMA) stations located within 2.3 to 4.6 km of the grid-points.

The extreme temperature events were analysed based on the heatwave periods described by Russo *et al*. (2014), which are defined as periods of 3 consecutive days with Tmax above a daily threshold. The threshold is defined as the 90th percentile of daily Tmax, centred on a 31-day window. For a given day *d*, the threshold series, A_d,of the dataset is:

$$A_d = \bigcup_{y=1980}^{2021} \bigcup_{i=d-15}^{d+15} Tmax_{y,i} \quad (1)$$

where U denotes the union of sets and $Tmax_{y,i}$ is the Tmax of the day i in the year y. Furthermore, non-parametric trend test methods, as reviewed by Mudelsee (2019), including Sen's slope and sequential Mann-Kendall (SQMK) tests (Kendall and Gibbons 1990), were employed to detect monotonic trends and sequential shifts in the annual Tmax time series (averaged from daily Tmax data), the number of heatwave days per year, and the yearly average temperature of the identified heatwave days.

Results and concluding remarks

Figure 1b displays the annual Tmax derived from ERA5 observations, revealing two distinct patterns. The southern region (grid-points 515, 636, 761, 911, and 1062) is warmer than the northern region (grid-points 30, 70, and 384). Statistically significant increases in annual Tmax were observed in all locations over the 41-year period, ranging from 0.74°C (grid-point 1062, near Faro airport) to 1.13°C (grid-point 761, located in

Lisbon). Daily thresholds for heatwave identification (A_d) during the 1980/81–2020/21 reference period (41 hydrological years) were obtained using Equation 1, as shown in Figure 1c. Southern locations exhibited higher thresholds, consistent with their corresponding annual Tmax series. Approximately 800 Tmax heatwave days were identified in each of the eight locations, with varying trends in occurrence and average temperature. Heatwave days have steadily increased since the hydrological year 2010/11 (Figure 1d), with the grid-point 1062 experiencing the highest increase (approximately 16 heatwave days in 41 years). Moreover, heatwave days have become hotter in all locations, except for the grid-point 59 (Figure 1e), with the grid-point 911 (Beja city) showing the highest temperature increase (approximately 4.5°C in total).

These findings highlight the need for risk-mitigation procedures to address the increasing threat of heatwaves and their negative impacts in Portugal.

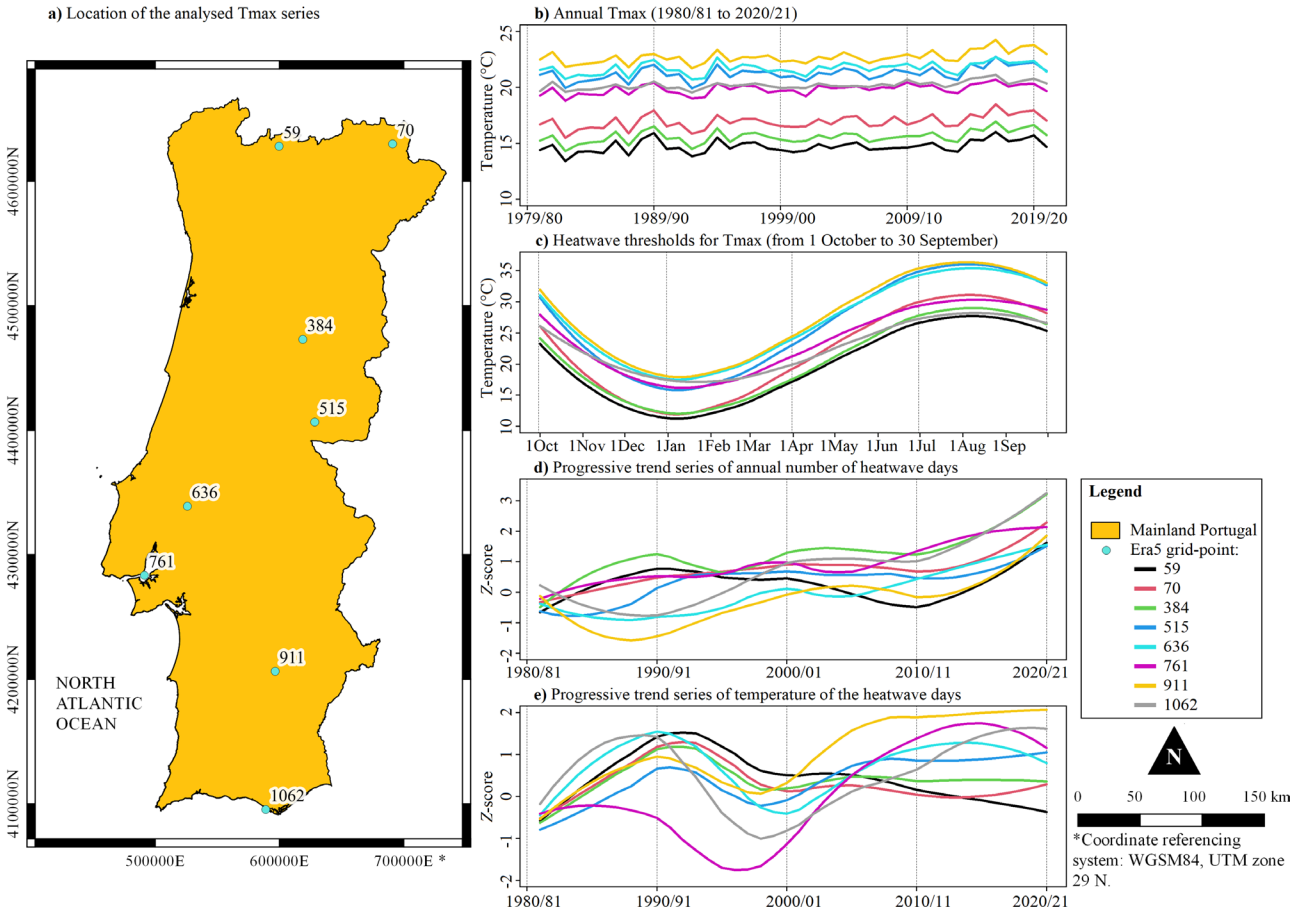

Figure 1. a) Location of the eight selected ERA5-Land grid-points with daily Tmax data; b) annual Tmax. c) Heatwave thresholds of daily Tmax for each of the grid-points in a given year — applicable in the analysed 41hyrological years. SQMK results, progressive trend series of: d) Heatwave days per year, and e) temperature of the heatwave days.

Acknowledgments: Research carried out at the Civil Engineering Research and Innovation for Sustainability (CERIS), a registered research unit in the Fundação para a Ciência e a Tecnologia (FCT), UIDB/04625/2020; and supported by the European Union's Horizon 2020 via the SCORE project, grant No. 101003534.

References

Kendall M, Gibbons J (1990) Rank correlation methods. On statistical analysis of series of observations. Technical Note No 143. World Meteorological Society, Geneva, Switzerland

Mudelsee M (2019) Trend analysis of climate time series: A review of methods. Earth-Science Reviews 190: 310-322

Russo S, Dosio A, Graversen RG, Sillmann J, Carrao H, Dunbar MB, Vogt JV (2014) Magnitude of extreme heat waves in present climate and their projection in a warming world. Journal of Geophysical Research: Atmospheres 119(22): 12-500

Sousa PM, Trigo RM, Russo A, Geirinhas JL, Rodrigues A, Silva S, Torres A (2022) Heat-related mortality amplified during the COVID-19 pandemic. International Journal of Biometeorology 66(3): 457-468

Assessing the impacts of potential climate change on watershed hydrologic response using FDCs

A. Manekar*, M. Ramadas
Research Scholar, School of Infrastructure, IIT Bhubaneswar, Khordha-752050, Odisha, India
** e-mail: am54@iitbbs.ac.in*

Introduction

It is observed that the local and regional hydroclimatic variables such as rainfall and temperature drive different processes of the hydrological cycle (infiltration, evapotranspiration, groundwater storage, surface runoff, baseflow), and changes in these variables influence the streamflow response of watersheds. The hydrological impacts of natural and anthropogenic climate change can be determined by combining simulations of hydrological models with future climate change projections. After downscaling and bias correction (Mohan and Bhaskaran 2019), future climate data from general circulation models (GCMs) can be input to hydrological models to quantify the possible changes in future water balance at local scales. Additionally, changes in hydrological regime of streamflow due to future climate change can be accomplished by using flow duration curve (FDC) analysis that highlights the changes in the magnitude of low and high range daily streamflows (Cigizoglu and Bayazit 2000). FDCs are popular for hydrologic design and management actions concerning water supply, hydropower generation, irrigation, and hydrologic extreme events.

The objective of the present study is to assess the impacts of potential climate change on hydrologic response of an agricultural watershed in Eastern India using the popular hydrological model -Soil and Water Assessment Tool (SWAT). Future climate projections simulated by the popular GCMs are downscaled and bias corrected before utilizing them for water balance modeling. Then, the FDC analysis is performed to quantify the likely impacts of climate change on flow regime in this watershed.

Materials and methods

The study area Govindapur watershed lies in the eastern part of India between 21°30' N to 22°38' N latitudes and 86°28' E to 86°94' E longitudes. We extracted daily streamflow data for the outlet of this tropical watershed from the India-Water Resources Information System (WRIS) web portal for the 1990-2014 (baseline) period. In this study, 0.12° spatial and daily temporal resolution gridded data of precipitation, and maximum and minimum temperature for the baseline period, required for hydrological model development were obtained from the Indian Monsoon Data Assimilation and Analysis (IMDAA; Ashrit et al. 2020) project. We used the freely available coupled multi-model inter-comparison project phase 6 (CMIP6; Eyring et al. 2016) downscaled GCM data of daily precipitation, and maximum and minimum temperatures at 0.25° spatial resolution prepared by Mishra et al. (2020) for the baseline and two future periods, 2041-2070 (near future) and 2071-2100 (far future), in this study. We utilized downscaled future climate projections from 3 GCMs (BCC-CSM2-MR, EC-Earth3-Veg and MPI-ESM1-2-HR) corresponding to an extreme climate change scenario - shared socioeconomic pathway SSP585, in this study. The datasets were regridded to 0.12° resolution using bilinear interpolation method, and bias corrected using power transformation and CDF matching techniques utilizing IMDAA data.

We calibrated and validated SWAT model with streamflow data and IMDAA climate inputs. Once the model performance was found satisfactory, it is used for simulating hydrologic response of the watershed using corrected climate model projections of the baseline and the future periods. We computed the likely changes in temperature, rainfall and streamflow in the future periods, and assessed the changes in flow regime at the watershed outlet by comparing the baseline and future period FDCs.

Results and concluding remarks

As shown in Figure 1(a), increase in maximum temperature is projected to vary between 0.5% to 3.5% by the MPI-ESM1-2-HR model under SSP585 scenario, whereas the other models projected increase in the range 3% to 5.8%. It is found that the average rainfall in the study watershed is likely to increase during the future periods according to BCC-CSM2-MR and EC-Earth3-Veg models, but a decrease is projected by MPI-ESM1-2-HR (see Table 1). With the help of SWAT model, we also evaluated the performance of the corrected data from the 3 GCMs for simulating baseline streamflows. Future streamflows simulated using different GCMs are compared with baseline flows. While the models could capture the overall streamflow variability, in some cases, flows are overestimated, especially by the EC-Earth3-Veg model simulations. Comparing FDCs shown in Figure 1(b), it is seen that high flows (10% exceedance probability) are likely to increase slightly (by 2%) in the far future as per BCC-CSM2-MR, while MPI-ESM1-2-HR projects a large increase (67%). In fact, about 6% to 47% reduction of the low flows (90% exceedance probability) is projected in the future, implying scarcity of water resources in this region for meeting various demands during the non-rainy periods. The study emphasizes the need for conservation of water resources in the region during dry season and flood management techniques to cope with rising rainfall and streamflows in rainy periods, as potential steps to be taken for future climate change adaptation and mitigation with regard to water resources management.

Table 1. Percentage change in the precipitation and streamflow for the near and far future time period under SSP585 scenario.

	Rainfall		Streamflow	
	Near future (2041-2070)	Far future (2071-2100)	Near future (2041-2070)	Far future (2071-2100)
BCC-CSM2-MR	0.66	7.26	7.20	-5.42
EC-Earth3-Veg	53.69	73.76	11.08	36.34
MPI-ESM1-2-HR	-14.55	-13.23	-15.57	-8.29

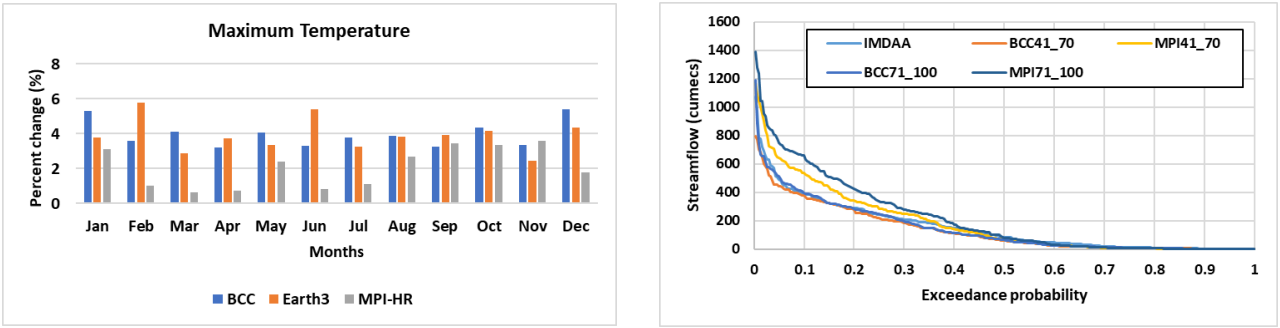

(a) *(b)*

Figure 1. (a) Changes in maximum temperature under SSP585 scenario in near future (2041-2070) projected by the GCMs, and (b) comparison of FDCs of the baseline period with future projections from GCMs.

References

Ashrit R, Rani SI, Kumar, S, Karunasagar S, Arulalan T (2020) IMDAA Regional Reanalysis: Performance Evaluation During Indian Summer Monsoon Season. Journal of Geophysical Research: Atmospheres 125: 1–26. https://doi.org/10.1029/2019JD030973

Cigizoglu HK, Bayazit M (2000) A generalized seasonal model for flow duration curve. Hydrol Processes 14: 1053–1067. https://doi.org/10.1002/(SICI)1099-1085(20000430)14:6<1053::AID-HYP996>3.0.CO;2-B

Eyring V, Bony S, Meehl GA, Senior CA, Stevens B, Stouffer RJ, Taylor KE (2016) Overview of the Coupled Model Intercomparison Project Phase 6 (CMIP6) experimental design and organization. Geoscientific Model Development 9(5): 1937-1958. https://doi.org/10.5194/gmd-9-1937-2016, 2016

Mishra V, Bhatia U, Tiwari AD (2020) Bias-corrected climate projections for South Asia from Coupled Model Intercomparison Project-6. Scientific Data 7(1): 1–14. https://doi.org/10.1038/s41597-020-00681-1

Mohan S, Bhaskaran PK (2019) Evaluation and bias correction of global climate models in the CMIP5 over the Indian Ocean region. Environmental Monitoring and Assessment 191: 806. https://doi.org/10.1007/s10661-019-7700-0

Cost-benefit analysis and prescriptive decision tree model for planning flood risk mitigation measures

J. Napolitano[1*], M. Di Francesco[2], G.M. Sechi[1]
[1] Department of Civil and Environmental Engineering, University of Cagliari, Cagliari, Italy
[2] Department of Mathematics and Computer Science, University of Cagliari, Cagliari, Italy
* e-mail: jacopo.napolitano@unica.it

Introduction

Planning of infrastructures for flood mitigation must now take up these numerous challenges also increasing the attention towards economic sustainability of the proposed flood mitigation solutions (Poljanš ek et al . 2017). Trends in hydrological extremes occurrences and extensions in urbanization generated flood disasters worldwide and motivated the need to set up adequate flood risk management plans (Price and Vojinovic 2008). In the context of flood risk, the European Commission Flood Directive 2007/60 (2007) requires preliminary damage evaluations to estimate flood impact on the territories and recommends policy-makers to decide upon flood mitigation work construction and mitigation strategies implementation via a Cost-Benefit Approach (CBA).

Flood damage assessment and loss estimation forecasts are then essential for planning flood mitigation actions since decisions should be based on CBA. Costs are related to each mitigation infrastructure and its maintenance over their life cycle. Benefits can be evaluated in terms of expected damage reductions (Ramirez et al. 1988; Jongman et al. 2012). Damages can be avoided by the realization of scenario mitigation works and the proper management of flood-risk occurrences (Sulis et al. 2020). To perform a coherent comparison, the expected damages can be evaluated both in the current scenario (actual configuration) and in future scenarios after building mitigation works (Pistrika et al. 2014; Napolitano et al. 2022). Once estimated costs for realization of mitigation works and the expected benefits, using CBA the decision maker could opt for the best mitigation alternative, maximizing benefits while preserving savings (Nas 1996).

Materials and methods

This research integrates CBA with Prescriptive Decision Trees (PTDs) to optimize planning measures for a flood-mitigation problem. PTDs (Bertsimas and Freund 2004) are logical and systematic ways to address a variety of problems involving decision making with a single criterion in an uncertain environment. Since CBA is based on a single objective criterion (in this study we consider the actual value of the net benefit (NPV) of each possible implemented mitigation measure), it is of interest to build a prescriptive decision tree with this criterion.

The proposed methodology estimates the expected damage when works are not present and when the works are in place and identifies benefits with the difference between damage "without" and damage "with" the mitigation infrastructure. Benefits related to each configuration are estimated from the reduction of expected damages for different categories of land use which characterized this area. Damage function definition has been made by a flood damages assessment according to the evaluation of water depth resulting from the hydraulic simulation models (Sulis et al. 2020). Expected benefits of each alternative are computed comparing each proposed Configuration of mitigation measures with Configuration 0 (not-intervention option). Once benefits are assessed, the CBA will allow comparison between the costs of the hydraulic works supported over their life cycle and the generated expected benefits. In this study we assume that the only criterion on which to differentiate between policies is the NPV of benefits and one obviously prefers a higher net benefit to a lower net benefit. This NPV is computed as the difference between benefits and costs, which account for construction costs, operation, maintenance and replacement costs, as well as additional penalties. These penalties are paid if the budget

for a more expensive configuration is available and works construction is not made.

The construction of the PDT starts from the list of possible decisions and the list of possible outcomes. Each decision step is represented by a decision or event node interconnected by arcs. The procedure for solving a decision tree is called backwards induction or folding back. It starts from the final branches of the decision tree and moves toward the starting node. When an event node is visited, one computes the average value of criterion from all possible outcomes. In a CBA analysis, this means to convert the distribution of possible net benefits to a single numerical value using the average, which weights all possible outcomes by their probability. When a decision node is visited, one chooses the branch emanating from this node with the best value of the criterion. In a CBA analysis, this means to cross off the branches emanating from a node with worse value of the NPV of benefits. The prescriptive decision tree is solved after the evaluation of the root node after all other nodes.

Results and concluding remarks

The proposed methodology has been tested on a real case study of the Coghinas river flood plain, located in the north Sardinia (Italy). This valley had a long history of floods causing significant damages to civil properties, crops, infrastructures and environment. Therefore, the Sardinia Region Administration defined some strategic solutions such as critical bridges demolition, levees and channel improvements and new constructions. These mitigation actions can be clustered into five main configurations by merging different single works protecting different floodplain areas form upstream to downstream along the Coghinas river (Napolitano et al. 2022).

In this study we applied the CBA methodology integrated with PDT model for planning possible mitigation measures in the Coghinas floodplain with a fixed planning horizon of 100 years.

The optimal solution has been achieved by folding back the decision tree, identifying the best value of the selected criterion (net benefit). By applying the proposed methodology we can identify among all the different scenarios the optimal decision strategy according to the chosen economical criterion. This solution allows us to provide Sardinian Authorities with a strategical information about which flood mitigation measure to realize.

Acknowledgments: This study has been supported by the Italian Ministry of the Environment and Protection of the Territory and the Sea, Project RIDES-IDRO.

References

ARDIS (2014) Piano di Gestione del rischio alluvioni, Hydrographic District - Regional Board of Sardinia, Cagliari

Bertsimas D, Freund RM (2004) Data, Models and Decisions. Dynamic ideas

Jongman B, Kreibich H, Apel H, Barredo JI, Bates PD, Feyen L, Gericke A, Neal J, Aerts JCJH, Ward PJ (2012) Comparative flood damage model assessment: towards a European approach. Natural Hazards and Earth System Sciences 12: 3733–3752. https://doi.org/10.5194/nhess-12-3733-2012

Napolitano J, Di Francesco M, Sechi GM (2022) Integrated Cost-Benefit Analysis and Perscriptive Decision Tree Model for a Flood Risk Management Problem. 39th IAHR World Congress. https://doi.org/10.3850/IAHR-39WC2521716X20221755

Nas TF (1996) Cost-Benefit Analysis: Theory and Application. Sage, Thousand Oaks

Poljanš ek K et al . (2019) Science for disaster risk management 2017: knowing better and losing less. European Commission, Joint Research Centre, Publications Office. https://data.europa.eu/doi/10.2788/842809

Pistrika A, Tsakiris G, Nalbantis I (2014) Flood depth-damage functions for built environment. Environmental Processes 1(4): 553–572. https://doi.org/10.1007/s40710-014-0038-2

Ramirez J, Adamowicz WL, Easter KW, Graham-Tomasi T (1988) Ex post analysis of flood control: benefit–cost analysis and the value of information. Water Resources Research 24(8): 1397–1405. https://doi.org/10.1029/WR024i008p01397

Sulis A, Frongia S, Liberatore S, Zucca R, Sechi GM (2020) Combining water supply and flood control purposes in Coghinas Basin (Sardinia, Italy). International Journal of River Basin Management 18(1): 13-22. https://doi.org/10.1080/15715124.2018.1476366

Runoff study of the upper Torysa sub-basin

P. Nagy, M. Hlinková, M. Dobranský*
Department of Environmental Engineering, Faculty of Civil Engineering, Technical University of Košice, Slovak Republic
** e-mail: marian.dobransky.2@tuke.sk*

Introduction

The intensity, length, frequency, and phase of rain are just as significant from a sociological, meteorological, and climatic standpoint as the overall amount of rain because they affect how the rain is distributed and how much runs off once it reaches the ground. Extreme rainfall events are what lead to floods and droughts, and variations in their frequency and intensity have a significant effect on the environment and society. Therefore, it is crucial to increase our understanding of how to forecast and predict rainfall yet doing so calls for innovative ways to look at data and models (Trenberth et al. 2003).

The demand for precise data on the geographical and temporal variations in precipitation on the Earth's surface has increased due to worries about anthropogenic climate change. Surface gauges or satellite remote sensing can be used to estimate large-scale precipitation (New et al. 2001). Precipitation is directly impacted by global warming. Droughts become more severe and last longer as a result of increased evaporation and surface drying brought on by increased temperature. As a result, storms, whether they be single storms, extratropical rain or snowstorms, or tropical cyclones, deliver more intense precipitation thanks to the additional moisture. Even in areas where overall rainfall totals are declining, such events frequently take place. Flooding becomes more likely as a result. The hydrological cycle and the slower rate of change that occurs with total precipitation than with the total water vapour column are both impacted by the atmospheric and surface energy budget. Although precipitation patterns are not significantly altered by minor variations in winds, dry areas become drier and wet areas become wetter, especially at mid- and high latitudes (Trenberth 2011). The pattern of rainfall, the hydraulic conductivity of the soil, the topography, and the state of the soil surface all affect the amount and intensity of infiltration and runoff on sloping ground. These factors are interconnected and present at the same time and depending on the rainfall event or the scale of the landscape, they may contribute differently (Joel et al. 2002). The issue of surface runoff is solved zonally according to basin or partial sub-basins.

Materials and methods

The studied area is focused on the part of the Torysa river basin, also known as the upper Torysa, situated in Slovakian region Šariš. The sub-basin is defined by river station 65,000 km to 130,000 km for the Torysa river and river station 0,000 km to 13,000 for the Slavkovský stream as shown in the Figure 1.

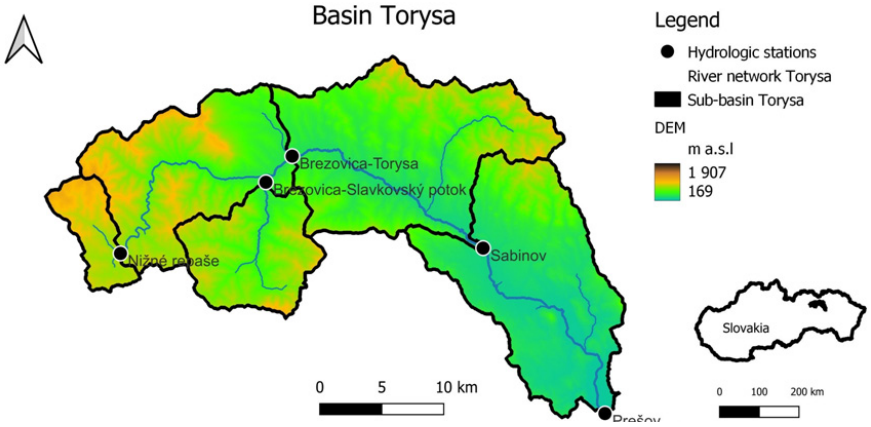

Figure 1. Schematic map of the study area.

According to important cities where hydrological stations are located, the basin was divided into smaller sub-regions. Table 1 shows the catchment areas (*S*) for sub-regions and its name according to the station.

Table 1. Average runoff values per time intervals and catchment areas for sub-regions.

Hydrological station	River	Catchment area (km^2)	Average Runoff (mm) 1980 - 2000	Average Runoff (mm) 2000 - 2020	Average Runoff (mm) 1980 - 2020
Prešov	Torysa	667.34	46,96	52,09	49,29
Sabinov	Torysa	476.19	50,63	56,74	53,42
Brezovica	Torysa	263.50	42,82	52,40	47,52
Brezovica	Slávkovský stream	83.08	38,18	42,02	40,04
Nižné Repaše	Torysa	32.79	60,09	75,11	66,92

The mathematical model was based on *Q* - daily average flows (m^3s^{-1}), that were measured in hydrological stations in the mentioned cities. The database of these values from stations were provided to us by the Slovak Hydrometeorological Institute. The next step was the calculation of *R* - the runoff (mm) according to daily discharge and catchment areas of the sub-regions per *t* - day (s).

$$R = Q \cdot t / S \text{ (mm)} \quad (1)$$

Then a seasonal summary for each year from 1979 to 2020 was calculated. Seasons were divided as winter: December to February, spring: March to May, summer: June to August and autumn: September to November.

Results and concluding remarks

The targeted data was divided into two time-identical stages. Before and after year 2000 and then compared with the total time interval from 1980 to 2020. The aim was to compare the average runoff between periods and what changes occurred from an overall point of view. In Figure 2 and Table 1, we can trace the changes and development of how runoff from the study area has increased over the last 20 years.

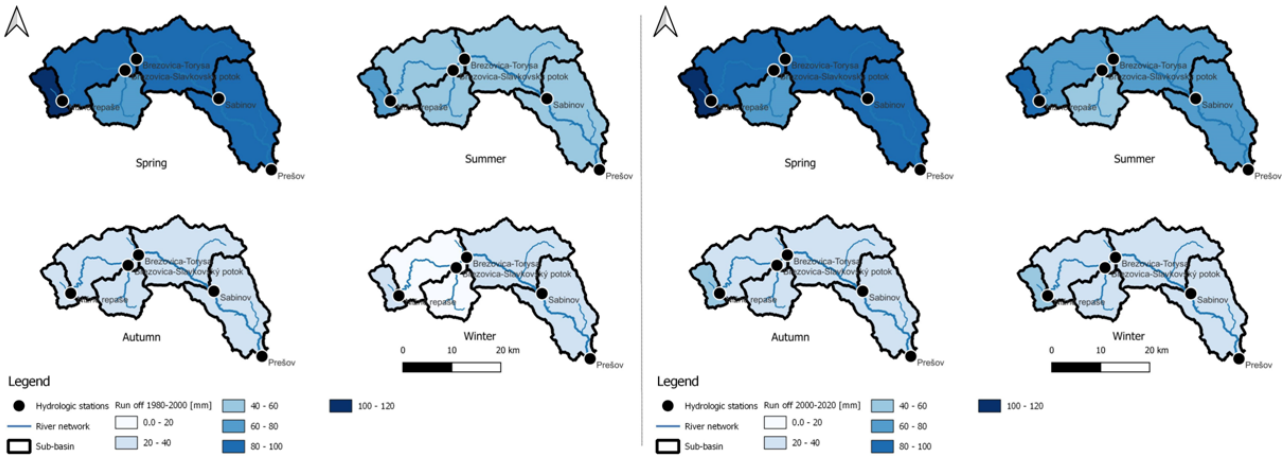

Figure 2. Schematic map of result divided into time intervals.

Acknowledgments: This work has been supported by Slovak Research and Development Agency under the Contract no. APVV-20-0281.

References

Trenberth KE, Dai A, Rasmussen RM, Parsons DB (2003) The changing character of precipitation. Bulletin of the American Meteorological Society 84(9): 1205-1218

New M, Todd M, Hulme M, Jones P (2001) Precipitation measurements and trends in the twentieth century. International Journal of Climatology 21(15): 1889-1922

Trenberth KE (2011) Changes in precipitation with climate change. Climate Research 47(1-2): 123-138

Joel A, Messing I, Seguel O, Casanova M (2002) Measurement of surface water runoff from plots of two different sizes. Hydrological Processes 16(7): 1467-1478

Links between GRACE water storage and NAO-EA-SCAND climate patterns in Iberia

M.C. Neves[1,2*], R.G.M. Neves[3,4]
[1] Universidade do Algarve, FCT, Campus de Gambelas, 8005-139, Faro, Portugal
[2] Instituto Dom Luiz (IDL), Universidade de Lisboa, 1749-016, Lisboa, Portugal
[3] Universidade Autónoma de Lisboa, DCEE, 1150-293, Lisboa, Portugal
[4] CICEE - Centro de Ciências Económicas e Empresariais, 1150-293, Lisboa, Portugal
* e-mail: mcneves@ualg.pt

Introduction

Groundwater drought develops as a smoothed and delayed response to persistent or frequent deficits in rainfall, or as result of a continued negative balance between recharge and extraction. Although not as accurate as in-situ observations, remote sensing has the advantage of providing near real-time and spatially continuous data. GRACE satellite data has been used to show evidence of groundwater depletion in aquifers all over the world (Rodel et al. 2018), and NASA currently generates weakly groundwater and soil moisture drought indicators based on GRACE-FO as part of the United States drought monitoring program. In Europe the Copernicus Global Drought Observatory also uses GRACE total water storage (TWS) anomalies as a proxy of groundwater drought. The use of GRACE satellite data for water resources management, particularly for groundwater systems in the Iberia Peninsula, looks promising (Neves et al. 2020), but its suitability to monitor drought requires further research.

On the other hand, large scale atmospheric circulation patterns also known as teleconnections control the interannual to interdecadal natural variability of the climate system. In the Iberian Peninsula, the North Atlantic oscillation (NAO), the East Atlantic (EA) and the Scandinavian (SCAND) patterns are the three main modes of variability driving winter precipitation, river flow and therefore surface and subsurface water storage. These patterns or modes of variability are characterized by indices which measure the strength of atmospheric pressure anomalies. Positive and negative phases of the indices, defined by values above or below given thresholds (e.g. NAO+ is defined for aggregates of winter month indices above 0.5), are generally associated with either wet or dry conditions. Previous studies have shown that wintertime NAO+ and EA- phases potentiate droughts in Iberia, the opposite occurring for NAO- and EA+ phases. However, few studies have recognized the importance of interactions amongst climate patterns and only recently did we become aware that their combinations or superpositions, as well as the temporal shifts in their synchronization, may lead to major anomalies in groundwater storage (Neves et al. 2019).

The purpose of the present study is to address the question: Do combined NAO-EA-SCAND phases also produce noticeable extremes in GRACE TWS observations? This question is relevant for two main reasons. First, GRACE offers a unique opportunity of fast and reliable large-scale monitorization of groundwater and can be used as an early warning system for groundwater drought or aquifer depletion. Second, the NAO-EA-SCAND indices provide a potential source of seasonal forecast since their wintertime value determines the availability of water in the following summer. Teleconnections may also be a source of long-term forecasting as they exert periodic controls on groundwater level and are linked to recurrent droughts.

Materials and methods

Monthly data from GRACE and GRACE-FO missions and ancillary datasets of precipitation, runoff and soil moisture were obtained from publicly available models and datasets (E-OBS, GLEAM, GRUN and ERA5) as referenced in Neves et al. (2020). The GRACE TWS anomalies in Iberia were downscaled using a multivariate regression model as proposed by Vishwakarma et al. (2021). The Standardized Groundwater Index (SGI) (Bloomfield and Marchant 2013) was then computed from GRACE TWS anomaly. The NAO, EA and SCAND climate indices were retrieved from the NOAA Climate Prediction Center. The links between

TWS anomalies and the coupled phases of the climate indices has been evaluated using wavelet transform methods and singular spectral analysis as explained in Neves et al. (2019).

Results and concluding remarks

The analysis of GRACE TWS time-series was performed over the five larger rivers basins in Iberia (Douro, Tagus, Guadiana, Guadalquivir and Ebro). The results showed distinct seasonal and annual water storage characteristics over these river basins. Overall, TWS showed a downward trend between 2003 and 2022 over all regions. The temporal evolution of SGI also exhibited specific characteristics over each river basin, but an overall common feature is that droughts became more frequent in recent years. Good correlations between time-series of TWS anomalies and climate indices confirms the influence of teleconnections in each of the river basins.

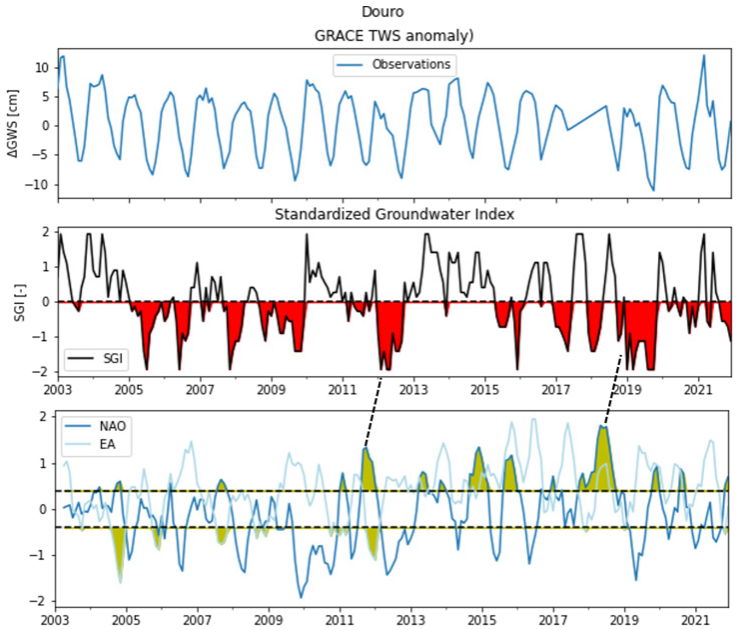

Figure 1. Example of the relationships between GRACE TWS anomaly in the Douro basin, episodes of groundwater drought denoted by negative values of SGI and the positive and negative phases of NAO and EA. Major droughts occurred for combined NAO+EA- phases in 2012 and 2018.

Specific phase combinations enhance the possibility of extreme hydrologic events particularly droughts (NAO+ EA–) as shown in Figure 1 for the Douro Basin. In response to the initial research question posed in the introduction, extremes in GRACE TWS can indeed be linked with combined phases of climate patterns. Although extremely challenging the prospective forecasting of climate pattens, months or even one year ahead, can be used to improve the design and implementation of management measures such as adaptive planning and flexible water allocation to reduce the impact of future droughts.

Acknowledgments: The authors would like to acknowledge the financial support of Fundação para a Ciência e a Tecnologia (FCT), I.P./MCTES, through national funds (PIDDAC) –UIDB/50019/2020

References

Bloomfield JP, Marchant BP (2013) Analysis of groundwater drought building on the standardised precipitation index approach. Hydrol. Earth Syst Sci 17: 4769–4787. https://doi.org/10.5194/hess-17-4769-2013

Neves MC, Jerez S, Trigo R (2019) The response of piezometric levels in Portugal to NAO, EA, and SCAND climate patterns. J Hydrol 568: 1105–1117. https://doi. org/10.1016/j.jhydrol.2018.11.054

Neves MC, Nunes LM, Monteiro JP (2020) Evaluation of GRACE data for water resource management in Iberia: a case study of groundwater storage monitoring in the Algarve region. J Hydrol Reg Stud 32: 107734. https://doi.org/10.1016/j. ejrh.2020.100734

Rodell, M, Famiglietti JS, Wiese DN, Reager JT, Beaudoing HK, Landerer FW, Lo MH (2018) Emerging trends in global freshwater availability. Nature 557: 651–659. https://doi.org/10.1038/s41586-018-0123-1

Vishwakarma, BD, Zhang J, Sneeuw N (2021) Downscaling GRACE Total Water Storage Change using Partial Least Squares Regression. Sci Data 8: 95. https://doi.org/10.1038/s41597-021-00862-6

Propagation of meteorological to hydrological drought: An example of the Middle Struma Valley, Bulgaria

N. Nikolova, R. Stoyanova, K. Radeva*
Sofia University "St. Kliment Ohridski", Faculty of Geography and Geology, Sofia, Bulgaria
** e-mail: kradeva@gea.uni-sofia.bg*

Introduction

Drought is a recurring and complex phenomenon characterized by slow onset. However, its nature is dynamic, with a specific development cycle manifested by a variable increase in the difference between available water resources and the needs of society, the environment and the economy. The beginning of drought is associated with a long-term lack of precipitation or deficiency and the accompanying high air temperature. Frequently, negative anomalies in precipitation propagate slowly through the hydrological cycle, giving rise to hydrological drought. This process is denoted as drought propagation (Eltahir and Yeh 1999). Drought propagation depends on the climate, biophysical and geographic properties of the region, as well as anthropogenic influences such as land cover change, dams, irrigation, and urbanization (Van Loon et al. 2016). Bulgaria belongs to countries with limited water resources; their high variability in time and space necessitates rational water management. Recognition of the phenomenon of drought as well as the development of methods to counteract its effects should be part of national strategies, plans, programs and concepts, and a detailed discussion of the problem should already take place at the local level.

The purpose of this study is to establish the propagation time of meteorological to hydrological droughts in the investigated region – the middle part of the Struma River valley. The Struma River is a transboundary river flowing from Bulgaria to Greece and its waters are used for water supply, power generation and irrigation in both countries. The present analysis extends the previous research of the authors on drought occurrence, river runoff and precipitation characteristics in Southwest Bulgaria (Nikolova et al. 2017; Nikolova and Radeva 2019; Stoyanova and Nikolova 2023).

Materials and methods

The study is based on monthly precipitation data observed in meteorological stations Boboshevo and Blagoevgrad and monthly stream flow data registered in two closely located hydrometric stations. The investigated period is 1961-2020. Meteorological drought was evaluated by Standardized Precipitation Index (SPI) calculated on a timescale from 1 to 12 (SPI-x, where x is from 1 to 12) using the SPI Generator; Version 1.7.5 (National Drought Mitigation Center, 2018). The occurrence and intensity of hydrological drought were determined by Streamflow Drought Index (SDI) at timescale 1 (SDI-1), He et al. (2022), calculated in the same way as SPI-1 but instead of precipitation data runoff data were used in SPI Generator. In the years with negative precipitation/streamflow anomalies, the values of drought indices are negative. When the drought indices have values between 0.99 and -0.99 the conditions are close to normal. Based on Svoboda et al. (2012) we consider that drought occurs when SPI/ SDI is -1 or less. The drought continues until drought indices become 0 or higher. In order to determine the propagation time of meteorological to hydrological drought the correlation coefficients between SPI-x and SDI-1 are calculated. The timescale with the highest correlation coefficient is the time for the propagation of meteorological to hydrological drought (He et al. 2022).

Results and concluding remarks

According to the SPI-1 and SDI-1, during the investigated period, 76 and 89 drought events occurred in the regions of the meteorological stations while hydrological events were 20-24 (Table 1). The maximal duration was observed in the 90s with a longer period for the hydrological drought. The average duration was 2 months for meteorological and 8 months for hydrological drought.

Table 1. Characteristics of meteorological and hydrological droughts.

	Meteorological		Hydrological	
	Boboshevo	**Blagoevgrad**	**Boboshevo**	**Blagoevgrad**
Number of drought events	89	76	24	20
Maximal duration (months)	8 / Apr 1994-Nov 1993	20 / Aug 1992-Mar 1994	32 / Jan 1994-Aug 1996	32 / Jan 1994-Aug 1996
Average duration (months)	2	2	8	8
Peak	-2.97	-3.66	-2.19	-2.18
ADI	-1.27	-1.35	-1.02	-0.97

The correlation analysis confirms the impact of meteorological on hydrological drought in the study area. The Pearson correlation coefficients are the highest for SPI-4 and SPI-5 at the region of Boboshevo and for SPI-3 and SPI-4 for Blagoevgrad (Table 2). These indicate that the propagation time from meteorological to hydrological drought is between 3 and 5 months depending on the geographical and climate conditions. Boboshevo is in the region with a moderate continental climate while the region of Blagoevgrad is characterized by the Mediterranean accidence and the precipitation regime probably influences the occurrence of drought. A more detailed analysis will be done in future studies to understand the drivers of drought propagation in the Struma River basin.

Table 2. Correlation coefficients between meteorological (SPI) and hydrological (SDI) drought.

	SPI 1	**SPI 2**	**SPI 3**	**SPI 4**	**SPI 5**	**SPI 6**	**SPI 7**	**SPI 8**	**SPI 9**	**SPI 10**	**SPI 11**	**SPI 12**
SDI-1 (Boboshevo)	0.467	0.624	0.648	**0.657**	0.654	0.648	0.629	0.622	0.622	0.616	0.615	0.615
SDI-1 (Blagoevgrad)	0.456	0.602	**0.638**	0.637	0.636	0.628	0.615	0.609	0.605	0.596	0.591	0.589

The highest coefficients are marked in bold

The spatio-temporal variability of the obtained results shows the need to develop adaptation solutions and rational planning and management of water resources in the Struma River basin to deal with drought in the future.

Acknowledgments: This work has been carried out in the framework of the National Science Program "Environmental Protection and Reduction of Risks of Adverse Events and Natural Disasters", approved by the Resolution of the Council of Ministers № 577/17.08.2018 and supported by the Ministry of Education and Science (MES) of Bulgaria (Agreement № Д01-271/09.12.2022).

References

Eltahir E, Yeh P (1999) On the Asymmetric Response of Aquifer Water Level to Droughts and Floods in Illinois. Water Resources Research 35(4): 1199-1217

He S, Zhang E, Huo J, Yang M (2022) Characteristics of Propagation of Meteorological to Hydrological Drought for Lake Baiyangdian in a Changing Environment. Atmosphere 13: 1531. https://doi.org/10.3390/ atmos13091531

National Drought Mitigation Center (2018) SPI Program (SPI Generator; Version, 1.7.5) [Computer software]

Nikolova N, Radeva K (2019) Data Processing for Assessment of Meteorological and Hydrological Drought. In: Information Technology in Disaster Risk Reduction. IFIP Advances in Information and Communication Technology, vol 516. Springer, Cham, pp 145–160

Nikolova N, Radeva K, Nikolova V (2017) Variability of River Runoff in the Bulgarian Part of Struma River Catchment and its Relation to Precipitation. International Conference Landscape Dimensions of Sustainable Development. Tbilisi, Georgia

Stoyanova R, Nikolova N (2022) Meteorological Drought in Southwest Bulgaria during the Period 1961-2020. J Geogr Inst Cvijic 72(3): 243–255

Svoboda M, Hayes M, Wood D (2012) Standardized Precipitation Index: User Guide (WMO-No. 1090). World Meteorological Organization. https://library.wmo.int/doc_num.php?explnum_id=7768

Van Loon AF (2016) Drought in the Anthropocene. Nature Geoscience 9: 89–91. https://doi.org/10.1038/ngeo2646

Land use and climate change impacts on streamflow and droughts in Küçük Menderes Basin, Türkiye

G. Onuşluel Gül[1*], A. Kuzucu[2], M. Najar[3], M. Günaçtı[1], A. Gül[1]
[1] Civil Engineering Department, Dokuz Eylül University, Izmir, Turkey
[2] Grad. School of Natural and Applied Sciences, Dokuz Eylül University, Izmir, Turkey
[3] GIS Department, Islamic University of Gaza, Gaza, Palestine
* e-mail: gulay.onusluel@deu.edu.tr

Introduction

This study focuses on the effects of land use and climate change on streamflow and hydrological droughts in Küçük Menderes Basin in western Turkey. Küçük Menderes Basin has fertile lands with a wide variety of crops and intensive agricultural activities. In addition to agricultural products with high economic value in the basin; silage crops such as barley, corn, etc., which have importance for the continuation of large-scale livestock activities are also planted. Being located in a semi-arid region, the basin began to be affected by negative consequences of climate change regarding soil moisture and water resources availability. In addition; land use changes, greatly from agriculture to industrial or residential, are another point that significantly affects the basin. For all these reasons, it has been a priority to examine the basin as a hot-spot with intensive agricultural activities risked under emerging climatic and land-use related instabilities.

Materials and methods

In the study, the Soil and Water Assessment Tool (SWAT) developed by Arnold et al. (1998) was centrally applied to Küçük Menderes Basin for assessing land use and climate change impacts on streamflow quantities and associated drought appearances. The SWAT model basically requires topography (DEM), land use, soil map, and climate data which includes precipitation, maximum and minimum air temperatures, wind speed, solar radiation, and relative humidity.

The input data for the modeling phase of the reference period were obtained from the records of meteorological and stream flow observations recorded in the basin. Future meteorological data, which originated from the RegCM 4.4 version regional model to downscale the global climate data to 1 km resolution through the double nesting method, was prepared by compiling the global outputs of the MPI-ESM-MR model with the RCP8.5 scenario. Future changes in climate variables were calculated for future periods accordingly. The land use maps of the years 2035, 2065 and 2085 were predicted through the land use change modeling efforts that were conducted by a neural network and Markov chain-Cellular Automata based built-in module of TerrSet software called Land Change Modeler (LCM). Land use and climate change patterns were assessed toward three subsequent horizons: (a) Short term (2025-2050), (b) Medium term (2050-2075) and (c) Long term (2075-2100) periods. The Standardized Streamflow Index (SSFI), which is based on the same calculation steps as the Standardized Precipitation Index (SPI) presented by Mckee et al. (1993), was used to examine hydrological droughts emerge, develop, and further intensify under climate and land use change impacts. In doing so, climate and land use-driven enhancing impacts were examined both separately and through an integrated consideration.

Results and concluding remarks

Figure 1 shows the calibration and validation results of the SWAT model after sensitivity analysis. Having achieved a sufficient degree of consistency between the observed and simulated streamflow time series, land use and climate change scenarios were then applied. Figure 2 reveals, on the other hand, the SSFI values that were calculated via 3-monthly spanning windows (i.e., SSFI-3) over the simulation outputs under (1) land use change, (2) climate change, and (3) combined land use and climate change scenario

impacts.

SWAT simulations provided informative outputs that distinguish between the impacts solely resulting from hydro climatic impacts, those that are contributed by the driven land use patterns and the total patterns that consider integrated impacts. Always with respect to the conditions of the reference period, the model outputs reveal reductions in the projected monthly average stream flows in quantities varying between 15% and 90% when only the changing climatic conditions are taken into consideration.

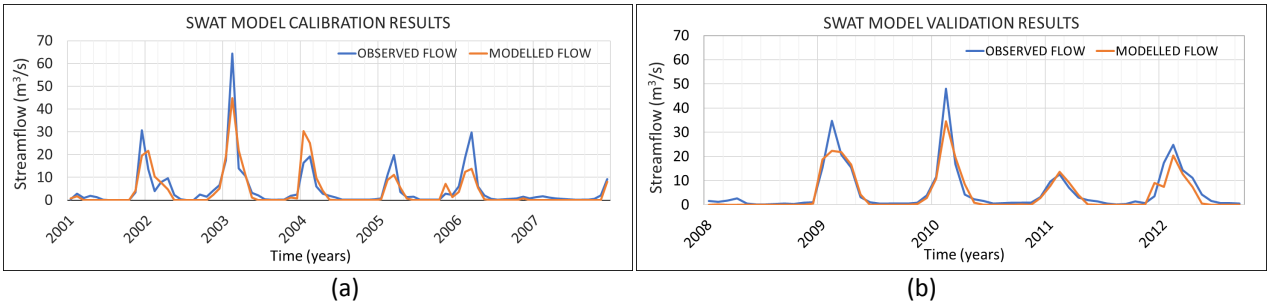

(a) (b)

Figure 1. Calibration (a) (NSE=0.8 and R^2=0.81) and validation results (b) (NSE= 0.89 R^2=0.90) of the SWAT model for Küçük Menderes River basin outlet.

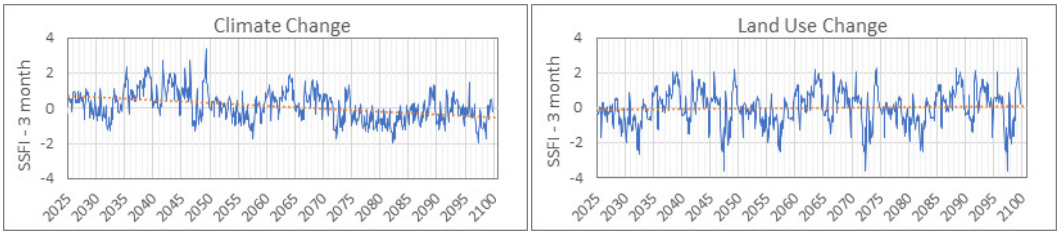

(a) (b)

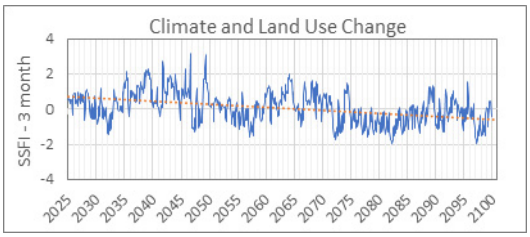

(c)

Figure 2. SSFI-3 series for the conditions under: (a) Climate change, (b) Land use change, (c) Both climate and land use change (Küçük Menderes River basin outlet).

The study mainly assessed the integrated impacts of climate and land use change and predicted decreases in surface water quantities in the basin in levels ranging from only 2% in the short-term period to more remarkable rates by 80% in the longest period toward the horizon 2100 (see Figure 1). By applying Mann-Kendall test to the SSFI values given in Figure 2, an increasing trend in drought is revealed both under the isolated impacts of climate change and in the case when the integrated impacts of climate and land use changes are counted. For the sole consideration of the land use change aspect (Figure 2b), it is seen that the SSFI drought index holds much lower values when compared to the results obtained from other scenarios, even though there happens to be a decreasing trend appearance in drought emergence.

References

Arnold JG, Srinivasan R, Muttiah RS, Williams JR (1998) Large-area hydrologic modeling and assessment: Part I. Model development. J American Water Resour Assoc 34(1): 73-89. https://doi.org/10.1111/j.1752-1688.1998.tb05961.x

McKee TB, Doesken NJ, Kleist J (1993) The relationship of drought frequency and duration to time scales. Preprints, Eighth Conf. on Applied Climatology, Anaheim, CA, Amer Meteor Soc 179- 184

Climate change impact on reservoir inflows using Arc-SWAT MODEL

M.M. Mushtaq, M.U. Rashid*, M. Zia, A.N. Nadeem, T. Ashfaq, R. Ahmad
Department of Civil Engineering, University of Management and Technology, Lahore, Pakistan
** e-mail: usman.rashid@umt.edu.pk*

Introduction

The increase in surface temperatures, frequent floods and droughts, extensive icing and snow cover have been reported to be major hydrological changes associated with global climatic change. River systems have been affected significantly by climate change in the recent decades. The rapidly melting glaciers in the rocky and Himalayan ranges of the world have made rivers volatile. As ocean temperatures rise, the hydroelectric infrastructure is at danger, and whole areas may be inundated (Adnan and Atkinson 2011). Pakistan is one of the most affected country of the world due to climate change and has faced the severe floods, droughts and storms in the last few decades. The increase in population, urbanization and change in the land use has enhance the impacts of climate change (Hassan et al. 2016). Inflows projections of Tarbela Reservoir on Indus River were determined by hydrological model using regional climate model. The rise in temperature and precipitation were envisaged 2.64^{o}C and 6% due to climate change in the region (Khan et al. 2015).

Tarbela is one of the largest Reservoir of Pakistan available on Indus River. It is a multipurpose dam provides water for irrigation, hydropower, and control floods. Tarbela is also one of the largest earth fill dam of the world. The mean annual inflows of Indus River are 79 Billion m^3 and its catchment area is 169,000 km^2. Climate change has great impact on Tarbela Reservoirs inflows. It is imperative to compute the impact of climate change on Tarbela Reservoir catchment and inflows to ascertain the performance and safety of the reservoir. The main objectives of the study were to carry out Tarbela Reservoir catchment modelling using Arc-SWAT for characterization and analysis of the features after calibration and validation. The impact of climate change on the Tarbela Reservoirs inflows were also examined in the study.

Materials and methods

The methodology flowchart of the study is provided as Figure 1.

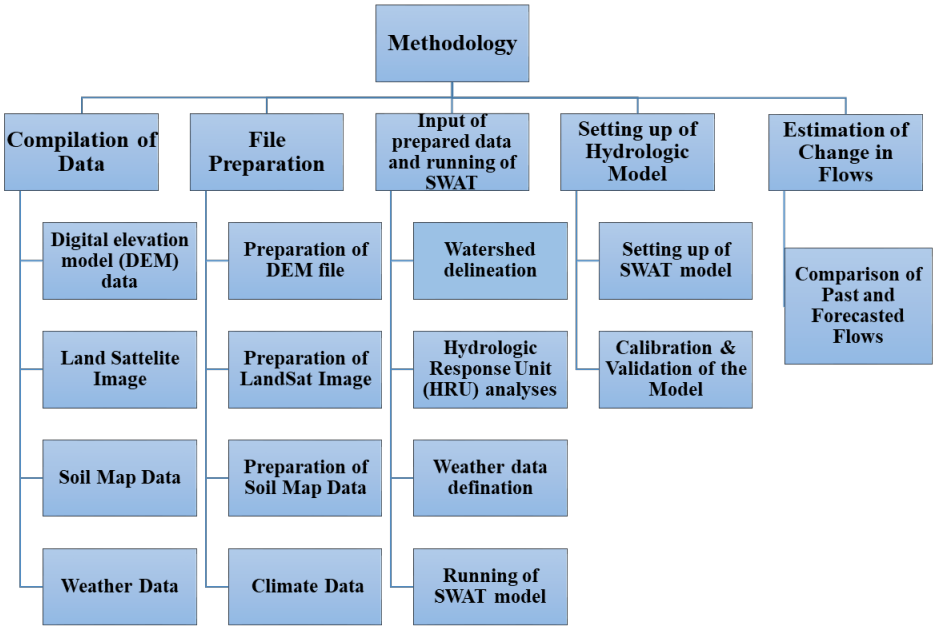

Figure 1. Methodology flowchart.

The data used in the study was collected from various sources. The DEM data with 30m resolution and soil map were obtained from Shuttle Radar Topographic Mission (SRTM) and Food and Agriculture Organization (FAO) respectively. The meteorological data including rainfall and temperature data was taken from Water and Power Development Authority (WAPDA) Pakistan and Global Weather Data. The land satellite images for the tiles were obtained from the United States Geographical Survey (USGS), and the tiles were then mosaicked. The Tarbela dam catchment area clipped for further analysis. The trimmed off data was then subjected to supervised classification. After successfully completing supervised classification on the data, the file was utilized in the Arc-SWAT for Hydrologic Response Unit (HRU) analysis as land use.

Results and concluding remarks

The watershed delineation of Tarbela Catchment in the SWAT model was done for characterization and analysis of the features. The SWAT model was successfully run for 22 years i.e., 1994-2015. The delineated Tarbela Reservoir watershed was found 169289.2 km^2. The detailed characterization results are shown in Table 1.

Table 1. Tarbela reservoir catchment characterization results for year 2015.

Land use classes	Area (km^2)	Percentage of the total area
Mountainous and Barren Area	117492.92	69.4%
Urban Area	5551.88	3.27%
Forestation Area	14859.72	8.77%
Water Body	31385.28	18.5%
Total Area	**169289.80**	

The SWAT model was subsequently successfully calibrated and validated by SWAT CUP software through comparison of observed flows and simulated flows. The yearly (1994-2015), monthly (2010) and daily (2010) calibration coefficient R2 and Nash Sutcliffe coefficient (NES) values were found greater than 0.5 for successful calibration. The SWAT model was then validated for the year 2013.

The biased corrected MIROC-ESM model data of climatic parameters of the Indus River catchment obtained from NASA Earth Exchange Global Daily Downscaled Projection (NEX GDDP) for emission scenario RCP 4.5 was used. MIROC-ESM model was used for the projecting climate data and climate change of the area was predicted using regional climate models (RCMs). The RCMs predicted an increase in precipitation by 20% (0.5 to 0.6 mm/day) and temperature enhancement of 6.5% (3.1^{o}C to 3.3^{o}C) as per RCP 4.5 by middle of century. By using this change in precipitation and temperature the available rainfall and temperature data was interpolated and employed as the input in SWAT model. i.e. 0.1mm/day and 0.015 ^{o}C for the emission scenario RCP 4.5 in the current study (Nauman et al. 2019).

Tarbela Reservoir catchment Image classification was accomplished successfully in the study comprising of mountainous and barren area (69.4%), urban area (3.27%), forestation area (8.77%) and water body (18.5%). The study indicated that with the increase in temperature, the precipitation has increased which will enhance the Indus River flows with maximum flows during the summer season. Over the period of 2015-2037, due to climate change Tarbela inflows will increase from 2444.2 to 2562.2 m^3/s with 4.84% enhancement. The effect of reservoir sedimentation should also be considered for assessing the climate change impact on the Tarbela Reservoir inflows. The construction of new reservoirs should be completed on priority to minimize the impact of climate change. The capacity of spillways also need to be checked by adding the impact of climate change.

References

Adnan NA, Atkinson PM (2011) Exploring the impact of climate and land use changes on stream flow trends in a monsoon catchment. International Journal of Climatology 31(6):815-831

Hassan Z, Shabbir R, Ahmad SS, Malik AH, Aziz N, Butt A, Erum S (2016) Dynamics of land use and land cover change (LULCC) using geospatial techniques: A case study of Islamabad Pakistan. SpringerPlus 5:812

Khan F, Pilz J, Amjad M, Wiberg DA (2015) Climate variability and its impacts on water resources in the Upper Indus Basin under IPCC climate change scenarios. International Journal of Global Warming 8(1):46-69

Nauman S, Zulkafi Z, Ghazali BHA, Yousuf B (2019) Impact of Future Climate Change on Stream flows Upstream of Khanpur Dam, Pakistan using Soil and Water Assessment Tool. Water 11(5): 1090

Multivariate analysis of meteorological drought using the D-vine copula in western Iran

N. Jahannemaei[1], P. Khosravinia[1], H. Sanikhani[1*], R. Mirabbasi[2]
[1] Water Science and Engineering Department, Faculty of Agriculture, University of Kurdistan, Sanandaj, Iran
[2] Water Engineering Department, Faculty of Agriculture, Shahrekord University, Shahrekord, Iran
* e-mail: h.sanikhani@uok.ac.ir

Introduction

Hydrological phenomena such as floods and droughts are associated with several dependent characteristics, but most of previous researches have been considered the univariate analysis because of its simplicity (Hao and Singh, 2016). In order to understand the phenomenon of drought more accurately, multivariate analysis of its characteristics seems necessary. Sklar (1959) first proposed the theory of copula functions, which makes multivariate analysis easier than the previous methods.

In recent years, multivariate analysis of drought has attracted the attention of researchers (Ni et al. 2020; Hui-Mean et al. 2019). Multivariate analysis of drought, especially by the vine copula functions, is relatively new both globally and in Iran. Therefore, lack of applied researches in the field of multivariate regional modeling of drought was the main motivation for the present study. Our aim in this study is to use the D-vine copula function to model the dependency structure of drought characteristics.

Materials and methods

Study area: Western Iran comprises an area extending from about 26–39◦ N to 45–51◦ E. The region is mostly occupied by Zagros Mountain systems. The amount of precipitation varies significantly over the region because of the latitudinal range and its intricate terrain structure. During the last 30 years, the annual precipitation varied between 212 and 425 mm, and the rate of evapotranspiration in the region has varied between 1054 and 2017 mm per year. In this study, Firstly, the standardized precipitation evapotranspiration index (SPEI) was calculated for all stations using monthly precipitation values and evapotranspiration estimated by Penman-Monteith FAO method. Then, four drought characteristics (i.e., severity (S), duration (D), inter-arrival time (L), and peak of the SPEI (M)) were extracted from the SPEI time series (Vicente-Serrano et al. 2010). In the next step, the common two-parameter and three-parameter distributions were fitted to the drought variables and the best fitted univariate distribution was selected for each drought characteristics. The maximum likelihood method is used to estimate the parameters of the marginal distribution functions.

Model: Bedford and Cooke (2002) have proposed the vine structure to create the multivariate distributions with higher dimensions. The class of regular vines (R-vine) is also very general and includes a vast number of possible pair-copula decompositions. In this study, to simulate the characteristics of drought in western part of Iran, the D-vine structures have been used. The four-dimensional density function of random variables in the structure of the D-vine structure is defined as follow:

$$f(x_1,x_2,...,x_d)=f(x_d)f(x_{d-1}|x_d)...f(x_1|x_2,...,x_d) \quad (1)$$

that T_1 (first tree) includes four characteristics of the drought, including (x_1,x_2,x_3,x_4) and three copulas, including (C_{12},C_{23},C_{34}). Joint return periods can be used as hydraulic design criteria in the water resources planning and management. The joint return period can be defined in two states (And state & OR state). For bivariate case, the joint return period is defined as follow:

$$T'_{XY}=\frac{E(L)}{P(X>x \quad \text{or} \quad Y>y)}=\frac{E(L)}{1-C(F_X(x),F_Y(y))} \quad (2)$$

$$T_{XY}=\frac{E(L)}{PX>x \quad and \quad Y>y}=\frac{E(L)}{1-F_X(x)-F_Y(y)+C(F_X(x),F_Y(y))} \quad (3)$$

Results and concluding remarks

During the 30-year study period, 865 drought events were detected for all of the 13 stations.

The correlation between drought variables was calculated using the Kendall's correlation coefficient. The results showed that the correlation between D-L, S-L, and M-L is poor, while the correlation between other drought variables is relatively high and positive.

Twenty-four different D-vine structures can permute the four variables, but only 12 of them give different decompositions. Table 1 showed the best D-vine structures, the estimated parameters, the maximum value of the log-likelihood function and the values of the AIC and BIC. It should be notated; the Archimedean copulas were fitted to pair-copula. Around 60 percent of the best fitted copula functions were Frank. The findings showed that the strongest correlations in the first tree in Dehloran, Kermanshah, Ravansar, Saqez, Sanandaj, and Hamedan had led to the most accurate D-vine structure. At the same time, the strongest correlation in the first tree did not lead to the best structure in other stations. The results indicate that the best structure cannot be determined either by linear or nonlinear correlation coefficient values and that other variables also play a role in constructing an accurate structure.

Finally, the results showed that the joint return period of severity and peak SPEI is about 201 years. The joint return period of droughts in the central, eastern, and western regions was short.

Table 1. D-vine structures for studied station in western Iran.

Station	Structure	*BIC*	*AIC*	*Loglik*	$\theta_{14\|23}$	$\theta_{24\|3}$	$\theta_{13\|2}$	θ_{34}	θ_{23}	θ_{12}
Bijar	DSLM	-58.66	-71.89	124.48	F(-0.31)	F(-0.64)	C(0.08)	C(0.11)	J(1.14)	G(2.93)
Dehloran	MSDL	-60.76	-72.11	97.10	C(0.15)	F(-0.12)	F(3.88)	F(-1.50)	F(12.06)	F(12.58)
Eslamabad garb	DLMS	-158.98	-172.03	136.57	F(-0.02)	F(0.10)	F (0.90)	C(7.13)	F(-1.12)	F(-1.66)
Hamedan	SLDM	-23.21	-10.18	107.66	G(1.04)	C(0.26)	F (-1.27)	C(2.02)	C(0.21)	C(0.29)
Ilam	MSDL	-132.33	1450.06	118.63	C(0.27)	F(0.31)	F(3.42)	F(-0.44)	J(4.37)	F(14.44)
Kangavar	DMLS	-18.30	-31.69	136.23	C(0.0002)	C(0.11)	F(0.04)	F(-0.66)	F(-0.55)	C(1.25)
Kermanshah	SMDL	-52.94	-65.89	132.20	J(1.00)	F(-0.53)	F(-4.76)	F(-0.38)	G(1.95)	C(6.24)
Qorveh	DMSL	-155.53	-169.82	167.07	F(0.10)	F(-1.82)	F(-2.27)	F(0.10)	C(8.30)	F(5.01)
Ravansar	DSML	-167.53	-180.57	117.27	F(-0.42)	F(-0.39)	F(3.04)	J(1.13)	F(19.55)	G(2.70)
Sanandaj	DSML	-145.93	-158.88	125.63	F(-0.30)	F(-0.45)	F(3.93)	J(1.16)	C(7.18)	J(3.25)
Saqez	DMSL	-95.60	-109.42	141.29	C(0.0001)	F(-0.49)	F(-2.68)	F(0.16)	C(5.92)	F(3.99)
Sarpolzahab	DSLM	-89.87	-102.73	130.63	F(0.04)	G(1.17)	F(-0.10)	F(-1.50)	F(-1.66)	J(3.33)
Zarrineh	DMSL	-112.98	-127.10	158.25	C(0.05)	F(-0.99)	F(-2.30)	C(0.17)	C(6.15)	F(4.55)

F, C, J, and G are the copula functions of Frank, Clayton, Joe, and Gumbel, respectively.

References

Bedford T, Cooke RM (2002) Vines: A new graphical model for dependent random variables. Annals of Statistics 30(4): 1031-1068

Hao Z, Singh VP (2016) Review of dependence modeling in hydrology and water resources. Progress in Physical Geography 40(4): 549-578

Hui-Mean F, Yusof F, Yusop Z, Suhaila J (2019) Trivariate copula in drought analysis: a case study in peninsular Malaysia. Theoretical and Applied Climatology 138(1-2): 657-671

Ni L, Wang D, Wu J, Wang Y, Tao Y, Zhang J, Liu J, Xie F (2020) Vine copula selection using mutual information for hydrological dependence modeling. Environmental Research 186: 109604

Sklar A (1959) Fonctions de répartition à n dimensions et leurs marges. Publ Inst Statist Univ Paris 8: 229–231

Vicente-Serrano SM, Beguería S, López-Moreno J I (2010) A multiscalar drought index sensitive to global warming: the standardized precipitation evapotranspiration index. Journal of Climate 23(7): 1696-1718

Forecasting drought based on projected climate change scenarios

H. Vangelis*, I.M. Kourtis, D. Tigkas, I. Nalbantis, V.A. Tsihrintzis
Center for the Assessment of Natural Hazards and Proactive Planning & Laboratory of Reclamation Works and Water Resources Management, School of Rural, Surveying and Geoinformatics Engineering, National Technical University of Athens, Athens, Greece
** e-mail: harrivag@central.mail.ntua.gr*

Introduction

Drought is among the most common and disastrous natural hazards, with direct and/or indirect economic, social and environmental impacts. Climate change and the projected global warming are foreseen to impact natural hazards and extreme events (floods, droughts, etc.), thus, posing an additional risk for economy, health and life (Kourtis and Tsihrintzis 2021). In the literature, several researchers have assessed the impacts of climate change on different regions around the globe, concluding that both drought hazard and risk will intensify as a result of the projected climate change (e.g., Cheng et al. 2015). Consequently, in order to develop holistic and robust climate change adaptation strategies, it is essential to study and understand drought hazard under different future climate scenarios.

The overarching goal of the present work is to assess climate change impacts on drought hazard for the island of Rhodes, Greece under different Representative Concentration Pathways (RCPs). Future drought assessment took place utilizing different climate variables (i.e., precipitation and temperature) under two future climate change scenarios (i.e., RCPs 4.5 and 8.5) developed using different General Circulation Models (GCMs) dynamically downscaled using Regional Climate Models (RCMs). Drought was assessed by means of two indices, i.e., the Reconnaissance Drought Index (RDI) and the Standardised Precipitation Index (SPI), calculated at the 12-month time scale based on the hydrological year (October to September). Finally, annual trends of the two aforementioned indices were estimated based on the widely used Mann–Kendall trend test and Sen's Slope method, using a Matlab code developed by Kourtis et al. (2022).

Materials and methods

Drought assessment took place for the island of Rhodes, Greece. Rhodes, the fourth largest island of Greece, has an area of approximately 1,400 km^2 and a population of about 115,000 inhabitants. The climate of Rhodes is typical Mediterranean (warm and temperate) with dry summers and mild winters. Mean monthly temperature ranges from 12.2 °C to 27.3 °C and mean monthly precipitation ranges from 0.2 mm to 152.8 mm (HNMS 2023).

Future climate projections for the entire Rhodes island were acquired using the DEAR–Clima (Data Extraction Application for Regional Climate, 2023) web application tool. DEAR–Clima provides several climate variables for selected temporal resolutions (daily, monthly and annual) produced by the Coordinated Regional Downscaling Experiment (CORDEX) research program. In the present work, we utilised monthly precipitation and temperature data under two RCPs (4.5 and 8.5) covering the future period 2025 to 2100. The spatial resolution of the entire dataset was 0.11°, resulting in 21 pixels needed to cover the entire area. Drought hazard for the future period was evaluated using the standardised RDI and SPI indices, calculated using DrinC software (Tigkas et al. 2015). Trend analysis was conducted employing the non-parametric Mann–Kendall test and the Sen's Slope estimator. Trend tests were applied on the timeseries of both drought indices, for all pixels representing our study area, and on the mean annual value.

Results and concluding remarks

Figure presents the future drought hazard, for the 75 hydrological years 2025–2026 to 2099–2100, assessed using RDI and SPI indices under both future climate scenarios. It can be observed that, under the

same climate scenario, the two indices are comparable, presenting, however, a slight difference. Based on the Mann–Kendall trend test and the Sen's slope, trends were assessed at the 1%, 5% and 10% significance levels. Significant trends are detected, depending on the examined scenario and the pixel examined. For instance, at the 10% significance level, an increasing trend, for the entire study area, was detected for RDI (mean Sen's slope = 0.09) and SPI (mean Sen's slope = 0.011) under RCP4.5 (Figure 1a), while a decreasing trend was detected for RDI (mean Sen's slope = -0.010) and SPI (mean Sen's slope = -0.005) under RCP8.5 (Figure 1b).

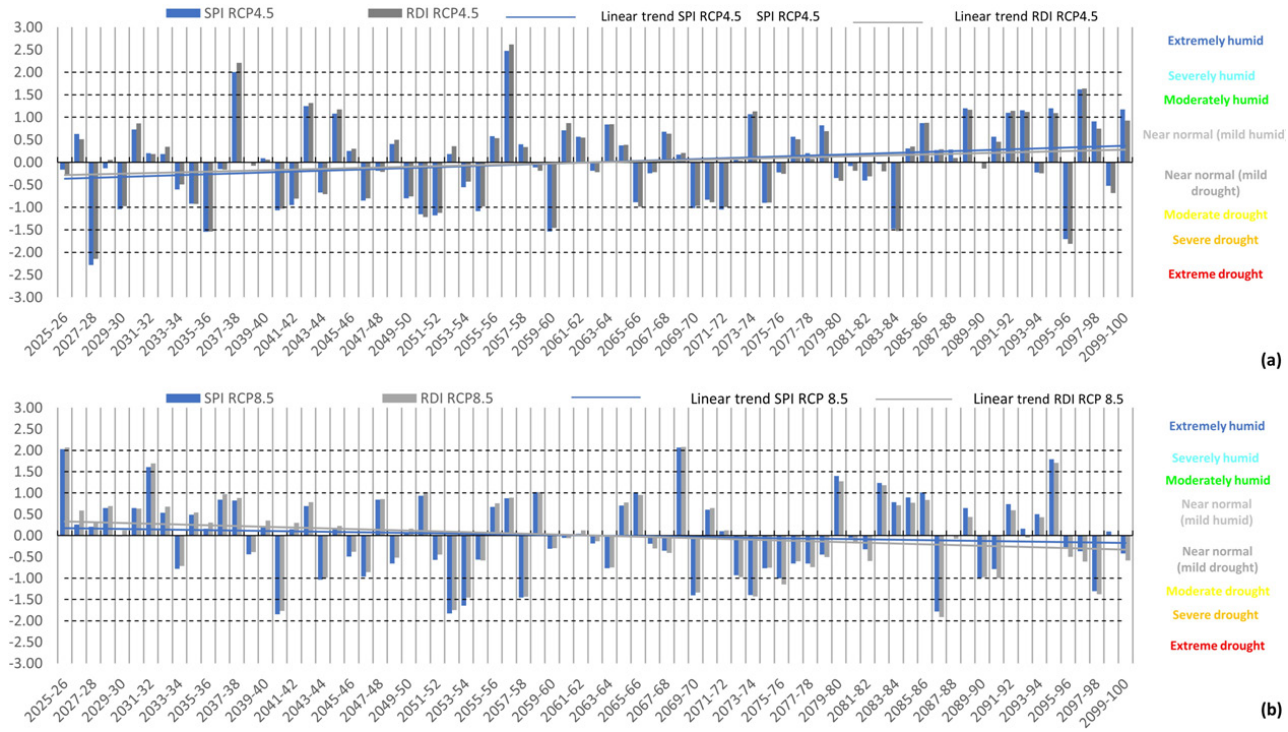

Figure 1. Future drought hazard for the island of Rhodes (a) under RCP4.5; and (b) under RCP8.5.

It can be argued that the future climate scenarios used, can affect the assessment of future drought and the associated uncertainties. Therefore, the corresponding scenario should be carefully selected and/or a multi-model multi-member ensemble should be used. For operation purposes, it is safer to assess future drought based on the climate scenario RCP 8.5, as more intense droughts are predicted. Although the differences between SPI and RDI are rather small, the outcomes of RDI in the long run produce more robust predictions because RDI includes evapotranspiration and, therefore, it also incorporates anticipated temperature changes in the future horizons.

References

Cheng L, Hoerling M, AghaKouchak A, Livneh B, Quan XW, Eischeid J (2016) How has human-induced climate change affected California drought risk? Journal of Climate 29(1): 111-120. https://doi.org/10.1175/JCLI-D-15-0260.1

Data Extraction Application for Regional Climate (2023) Data Extraction Application for Regional Climate (DEAR-Clima) web application tool. http://meteo3.geo.auth.gr:3838/ (accessed on 9/03/2023)

HNMS (Hellenic National Meteorological Service) (2023) Climatic Data for selected stations in Greece. http://www.emy.gr /emy/en/climatology/climatology_city?perifereia=South%20Aegean&poli=Rodos (accessed on 17/03/2022)

Kourtis IM, Bellos V, Kopsiaftis G, Psiloglou B, Tsihrintzis VA (2021) Methodology for holistic assessment of grey-green flood mitigation measures for climate change adaptation in urban basins. Journal of Hydrology 603: 126885. https://doi.org/10.1016/j.jhydrol.2021.126885

Kourtis IM, Tsihrintzis VA (2021) Adaptation of urban drainage networks to climate change: A review. Science of the Total Environment 771: 145431. https://doi.org/10.1016/j.scitotenv.2021.145431

Tigkas D, Vangelis H, Tsakiris G (2015) DrinC: a software for drought analysis based on drought indices. Earth Science Informatics 8(3): 697-709. http://doi.org/10.1007/s12145-014-0178-y

Precipitation estimation using weather radar data in Thessaly, Greece during medicane Ianos

G. Karoutsos[1*], N. Tzonichakis[1], N. Rammos[1], E. Chrisovergis[1], P. Sidiropoulos[2], N. Dalezios[2]
[1] General Aviation Applications S.A. "3D", Thessaloniki, Greece
[2] Department of Civil Engineering, University of Thessaly, Volos, Greece
* e-mail: karougeo@3dsa.gr

Introduction

On 15th September 2020, a low-pressure system formed in the Gulf of Sidra. In the next days this system intensified and moved north-northeast towards the Ionion sea. It exhibits characteristics like tropical cyclones, acquiring an eye-like feature and was named Medicane Ianos by the National Observatory of Athens. Ianos medicane impacted Greece in the period from 17 to 20 September 2020. It made landfall on Greece at peak intensity during the night on 18th September with storm surges accompanied by high coastal waves, heavy rainfall and very strong winds. Four people were killed, cities such as Karditsa and Mouzaki were flooded for several days and extended damages in the infrastructure were reported in the Ionian islands and in the Central part of the country (Zekkos et al. 2020).

In this study an estimation of the precipitation amount is attempted for the Region of Thessaly using a network of two C-Band radars located in Filiro, Thessaloniki and Liopraso, Trikala. The goal is to create a system that can monitor the region and issue alerts in case of extreme amounts of precipitation.

Materials and methods

The radar data consist of radar reflectivity values in a 750x750x750m grid. The time resolution of the data is 3.5 minutes approximately. To estimate the precipitation amount for the Region of Thessaly the TITAN (Thunderstorm identification, Tracking, Analysis and Nowcasting) (Dixon and Wiener 1993) software was used to process the data. Five applications of the Marshall-Palmer equation $Z=aR^b$ (Marshall and Palmer 1948) were made with the following parameters: a=200 & b =1.6, a=200 & b=1.3, a=150 & b=1.6, a=200 & b=1.25 and a=285 & b=1.42. Precipitation data from weather stations of the National Observatory of Athens network (Karditsa, Trikala, Larissa, Agia, Pertouli, Mouzaki) and of the Hellenic National Meteorological Service (Nea Anchialos) were also used (Mamara et al. 2020). To compare the estimated precipitation from the radar data with the measured one from the stations, the maximum value of the grid points on a radius of 2km around the station was used for all stations except Mouzaki, where a radius of 4 km was used, because between the radar of Liopraso and the city of Mouzaki the existence of an antenna bloackage makes the radar blind in this direction. The best fitted equation was then used to calculate the area with more than 100mm and 200mm of accumulated precipitation per day for each one of the four regional units that of the Region of Thessaly. On the other hand, the Drainage District of Thessaly (GR-08) is combined by two drainage basins (Pinios & Almyros-Pilio) and the same equation was used to calculate the area of each drainage basin with more than 100mm and 200mm of accumulated precipitation per day.

Results and concluding remarks

The results showed that the best fitted parameters for the Marshall-Palmer equation were for a=200 and b=1.25. Using them, a small underestimation of the actual amount of precipitation is observed (Table 1). The weather station network of NOA was able to record the extreme amounts of precipitation in the western part of Thessaly mainly in Pertouli, Mouzaki and Karditsa and using standard interpolation techniques an estimation of the amount of precipitation in the space between two stations can be achieved (Lagouvardos et al. 2021). On the contrary the lack of weather stations near Almyros made this method unable to monitor the large amounts of water that fell there causing huge damages in the area. Using the radar data, it is clear why there were flooded incidents in the Almyros area, which in addition belongs in a

different drainage basin than the western part of Thessaly (Figure 1). Almost 40% of the area of the regional unit of Karditsa had over 100mm on 18th September 2020. More than 20% of the Almyros-Pilio drainage basin had over 100 mm on the same day.

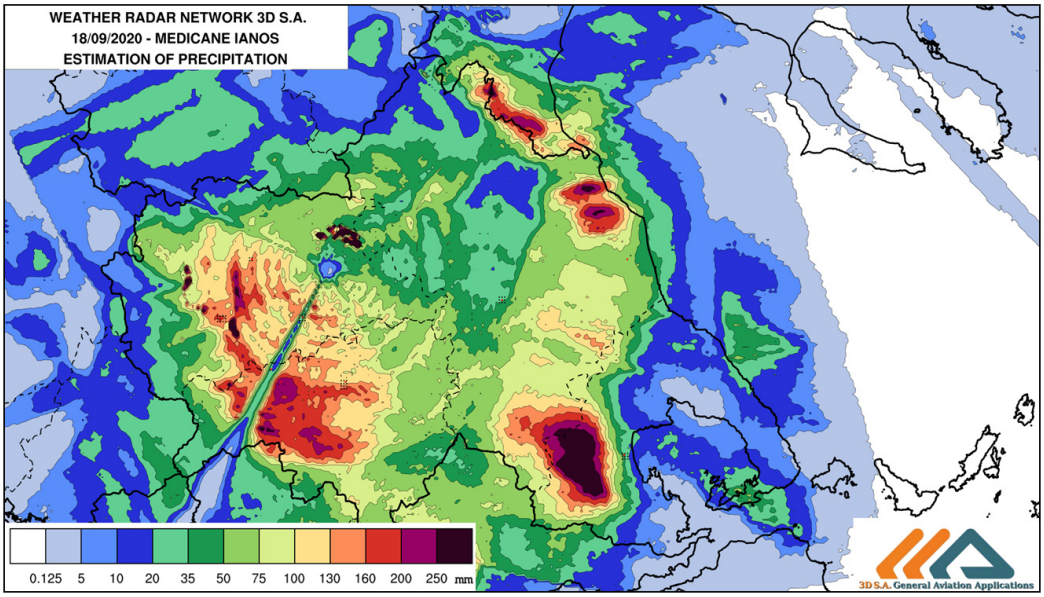

Figure 1. Estimation of Precipitation using the weather radar network data of 3DSA for 18/09/2020. Region of Thessaly, Greece.

Table 1. On the left, 24-h accumulated precipitation data from the Weather Stations and from the radar data estimation (a=200, b=1.25). On the right, the total area with 24-h accumulated precipitation above 100mm for each regional unit and for each drainage basin. (18/09/2020).

	Precipitation (mm)	
	Weather Station	Radar Data
Karditsa	190.6	171.0
Mouzaki	254.2	252.1
Pertouli	238.8	170.2
Trikala	103.8	108.3
Larissa	54.0	41.8
Nea Anchialos	44.0	56.4
Agia	38.6	56.0

	Area with Precipitation 100mm <= P < 200mm		Area with Precipitation 200mm < P	
Regional Unit	**km^2**	**%**	**km^2**	**%**
Larissa	660.9	12.3	69.2	1.3
Trikala	903.9	26.7	35.4	1.0
Karditsa	943.9	35.8	96.8	3.7
Magnesia	213.8	9.0	213.8	9.0
Drainage Basin	**km^2**	**%**	**km^2**	**%**
Pinios	2288.3	20.9	179.4	1.6
Almyros-Pilio	234.6	11.3	208.7	10.0

Acknowledgments: This research has been co-financed by the European Regional Development Fund of the European Union and Greek national funds through the Operational Program Competitiveness, Entrepreneurship and Innovation, under the call RESEARCH – CREATE – INNOVATE (project code: T2EDK-05354 - "EXTREMES").

References

Dixon M, Wiener G (1993) TITAN: Thunderstorm identification, Tracking, Analysis. and Nowcasting-A Radar-based Methodology. Journal of Atmospheric and Oceanic Technology 10:785-797

Lagouvardos K, Karagiannidis A, Dafis S, Kalimeris A, Kotroni V (2022) Ianos – A Hurricane in the Mediterranean. American Meteorological Society 103(6): E1621–E1636. https://doi.org/10.1175/BAMS-D-20-0274.1

Mamara A, Chatziapostolou E, Karatarakis N (2021) Annual Report for Climate in Greece 2020. HNMS, Athens

Marshall JS, Palmer WMK (1948) The Distribution of Raindrops with Size. Journal of Meteorology 5: 165-166. http://doi.org/10.1175/1520-0469(1948)005<0165:TDORWS>2.0.CO;2

Zekkos D, Zalachoris G, Alvertos AE, (2020) The September 18-20 2020 Medicane Ianos Impact on Greece - Phase I Reconnaissance Report. Geotechnical Extreme Events Reconnaissance Report, GEER-068, https://doi.org/10.18118/G6MT1T

Sequential meteorological-hydrological-hydraulic modeling as a flash flood forecasting tool: The January 2023 flooding incident in Evrotas river

G. Papaioannou[1*], G. Varlas[2], A. Papadopoulos[2], V. Markogianni[2], L. Vardakas[2], E. Dimitriou[2]
[1] *Department of Forestry and Management of the Environment and Natural Resources (FMENR), Democritus University of Thrace (DUTH), 68200 Orestiada, Greece*
[2] *Institute of Marine Biological Resources and Inland Waters (IMBRIW), Hellenic Centre for Marine Research (HCMR), 46.7 km of Athens-Sounio Ave., 19013 Anavissos, Attica, Greece*
** e-mail: gpapaio@fmenr.duth.gr*

Introduction

Flash flooding is one of the most severe natural hazards in terms of people affected and fatalities worldwide. However, precise flash flood forecasting remains a challenging task that demands a comprehensive approach encompassing hydrometeorological and hydraulic components. In this line, the objective of this study is to assess the capabilities of an integrated forecasting tool designed explicitly for flash floods using as a case study the recent flash flood event in Evrotas river that occurred on 26 January 2023. The forecasting tool structure is based on the three main modeling components: meteorological, hydrological and hydraulic.

Materials and methods

The structure of the flash flood forecasting system is based on the Advanced Weather Research and Forecasting (WRF-ARW) model, the WRF-Hydro hydrological model, and the HEC-RAS hydraulic–hydrodynamic model. Several studies have indicated that WRF-ARW and WRF-Hydro are capable of providing accurate precipitation and flood hydrograph forecasts while HEC-RAS can provide reliable estimations of flood characteristics such as water depth, flood extent, etc. (Kaffas et al. 2022; Papaioannou et al. 2019, 2021; Varlas et al. 2019, 2021). In this study, the WRF-ARW was configured with four nested domains covering the entire Mediterranean basin with a horizontal grid spacing of 36 km, the eastern Mediterranean with 12 km, Greece with 4 km, and finally the Evrotas river basin (ERB) with 1-km horizontal grid spacing. WRF-Hydro was set up in the ERB (100 m resolution) to estimate the flood hydrograph using forcing meteorological data provided by the WRF-ARW model. The 2D-flood inundation modeling configuration was based on the usage of high-resolution river geometry data (Unmanned Aerial Vehicle derived DEM) to minimize the uncertainty induced by the topographical accuracy, while other parameters were set based on the user manual guides. The geometry of the bridge was obtained from the topographical survey that was conducted for the eastern Peloponnese flood management risk plans. More details on the models' configuration can be found in a recent paper (Varlas et al. 2021). The proposed methodological framework was implemented for the flash flood event in Evrotas river that occurred on 26 January 2023 and caused extensive damages in agricultural and rural areas. Vehicle passing through the bridge located in the town of Skala was prohibited due to the high-water depth. According to the collected non-conventional flood data (i.e., photographs, videos, and mass media reports), the maximum water depth at the Skala's bridge location was estimated to be close to 6 m, thus approximately reaching the bridge.

Results and concluding remarks

The WRF-ARW results show that it can reasonably simulate the storm that caused the flash flood. As demonstrated in Figure 1a, despite a small spatial deviation, daily precipitation forecasts for 26 January 2023 agree with measurements provided by stations of the IMBRIW-HCMR, the National Observatory of Athens and the Harokopio University of Athens. Subsequently, as shown in Figure 1b, the WRF-Hydro model accurately captured the features of the river flash flooding, with a simulated peak streamflow of 769

$m^3 s^{-1}$ at 10:00 UTC (12:00 local time, LT). The generated flood hydrograph from WRF-Hydro, in combination with the 2D HEC-RAS modeling application, provided the maximum water depth at Skalas' bridge (Figure 1c). According to the collected non-conventional flood data, the simulated maximum water depth is very close to the observed one. Finally, similar results are observed in Figure 1d, where the water depth time series upstream of the validation (bridge) location at Skala town are presented. The total wall time to run the entire process (i.e., retrieval of global atmospheric data for 25 January at 12:00 UTC, preprocessing, 36-h simulations from all 3 models, postprocessing) on the HCMR's computing resources was about 3 hours. Specifically, it started on 25 January at 20:30 LT and ended at 23:30 LT, giving more than 12 hours of warning lead time for the flood. Therefore, the findings of this study indicate that the integrated flash flood forecasting system can timely provide skillful forecasts, which are validated using precipitation measurements and non-conventional flood data (observed water depth). In conclusion, the proposed methodological framework can be applied as a flood warning tool for emergency responses.

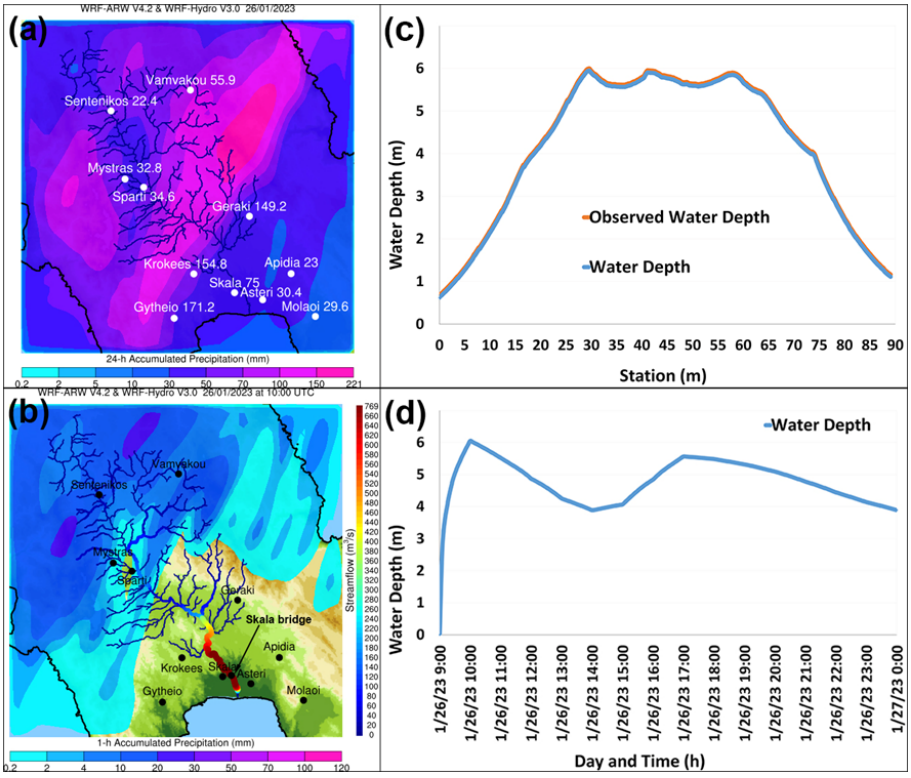

Figure 1. (a) 24-h accumulated precipitation (mm) for 26 January 2023 spatially distributed from the 1-km WRF-ARW forecasts, and point measurements from meteorological stations; (b) Forecasts of spatially distributed 1-h accumulated precipitation and Evrotas river streamflow (m3 s-1) on 26 January at 10:00 UTC (12:00 LT); (c) Simulated and observed maximum water depth and (d) water depth time series at location upstream of the Skala's bridge.

References

Kaffas K, Papaioannou G, Varlas G, Sayah MJ, Papadopoulos A, Dimitriou E, Katsafados P, Righetti M (2022) Forecasting soil erosion and sediment yields during flash floods: The disastrous case of Mandra, Greece, 2017. Earth Surface Processes and Landforms. https://doi.org/10.1002/esp.5344

Papaioannou G, Varlas G, Papadopoulos A, Loukas A, Katsafados P, Dimitriou E (2021) Investigating soil state effects on flash flood hydrograph and inundation forecasting. Hydrological Processes 35(4): 1–20. https://doi.org/10.1002/hyp.14151

Papaioannou G, Varlas G, Terti G, Papadopoulos A, Loukas A, Panagopoulos Y, Dimitriou E (2019) Flood inundation mapping at ungauged basins using coupled hydrometeorological-hydraulic modelling: The catastrophic case of the 2006 Flash Flood in Volos City, Greece. Water 11(11): 2328. https://doi.org/10.3390/w11112328

Varlas G, Anagnostou MN, Spyrou C, Papadopoulos A, Kalogiros J, et al. (2019) A multi-platform hydrometeorological analysis of the flash flood event of 15 November 2017 in Attica, Greece. Remote Sensing, 11(1): 45. https://doi.org/10.3390/rs11010045

Varlas G, Papadopoulos A, Papaioannou G, Dimitriou E (2021) Evaluating the forecast skill of a hydrometeorological modelling system in Greece. Atmosphere 12(7): 902. https://doi.org/10.3390/atmos12070902

Evaluation of climate change impacts on a basin in northern Greece

I.M. Kourtis[1*], C-A. Papadopoulou[2], M. Papadopoulou[2], N. Melios[3], C. Laspidou[3], V.A. Tsihrintzis[1]
[1] *Center for the Assessment of Natural Hazards and Proactive Planning & Laboratory of Reclamation Works and Water Resources Management, School of Rural, Surveying and Geoinformatics Engineering, National Technical University of Athens, Greece*
[2] *Laboratory of Natural Geography and Environmental Impact, School of Rural, Surveying and Geoinformatics Engineering, National Technical University of Athens, Greece*
[3] *Department of Civil Engineering, University of Thessaly, Volos, Greece*
** e-mail: gkourtis@mail.ntua.gr*

Introduction

Climate change is to impact the hydrological cycle and as a result extreme storm events are projected to become more frequent and more devastating in the future (Kourtis et al. 2021). Consequently, the regional impacts of climate change on water resources are of paramount importance from the social, economic and environmental perspectives. The use of hydrological and/or hydrodynamic models to assess the impacts of climate change has become a standard approach (e.g., Kourtis et al. 2021). The key concept is that changes in climatic drivers, e.g., precipitation, temperature, etc., can result in significant changes in the hydrological cycle of a basin. Climate change scenarios for meteorological variables are developed based on the results of General Circulation Models (GCMs) and/or Regional Climate models (RCMs) or from empirical approaches (Kourtis and Tsihrintzis 2021).

The goal of the present work is to assess climate change impacts on Platanovrisi basin, located in Northern Greece. To this end, the hydrological model of the basin was developed using the HEC-HMS software (e.g., Vangelis et al. 2022). An approach similar to the one proposed by Mimikou and Kouvopoulos (1991) was adopted. More specifically, historical temperature was assumed to uniformly increase by 1.5 °C and 2 °C, while historical precipitation was assumed to increase by 10% and 20% and decrease -10% and -20%. Thus, eight future climate scenarios (i.e., 2 temperature scenarios × 4 precipitation scenarios) were developed and were used as inputs to the hydrological model.

Materials and methods

The study area is the Platanovrisi basin, upstream the Platanovrisi dam. It covers an area of approximately 396 km^2. The altitude of the basin ranges from 220 m a.s.l. to about 1952 m a.s.l. with the mean altitude estimated at about 421 m a.s.l. The time of concentration was estimated employing the Giandotti empirical Equation at 4.36 h. Losses were estimated using the Soil Conservation Service (SCS) Curve Number (CN) empirical approach, based on the land use/land cover data from 2018 Corine Land Cover and the soil data for our basin.

All hydrological simulations were undertaken employing the widely used HEC-HMS software (Vangelis et al. 2022) developed by the United States Army Corps of Engineers Hydrologic Engineering Center. HEC-HMS is able to simulate all hydrological processes (e.g., Theodosopoulou et al. 2022). Daily rainfall was obtained from the Special Secretariat for Water (http://kyy.hydroscope.gr/) for the Skaloti station for the period 01/09/1950 to 30/11/2019. In addition, daily discharge for the Platanovrisi basin was obtained from the Public Power Corporation (PPC) for the period 01/09/2018 to 31/12/2021. Calibration was undertaken for the period 01/12/2008 to 31/12/2010 and validation was undertaken for the period 01/04/2017 to 30/04/2018.

Results and concluding remarks

The calibration of HEC-HMS model was conducted for peak discharge, time to peak, and total runoff volume using data from one station. Agreement between the simulated and the observed data of flow for

both periods, calibration and validation, is considered acceptable, as all the calibration criteria examined were within acceptable limits (Table 1).

Table 1. Calibration-validation results.

Criteria	Calibration	Validation
Nash-Sutcliffe	0.73	0.64
RMSE	0.27	0.54
KGE	0.73	0.66

Eight climate change scenarios (Figure 1) were tested with the historical period (calibration period). Comparison took place for precipitation volume and losses at the outlet of the Platanovrisi basin. Results presented significant variations according to the scenario examined. For instance, for scenarios (1, 2, 5 and 6) results showed an increase of precipitation volume ranging from 9% to 37% (Figure 1). On the other hand, under scenarios (3, 4, 7 and 8) results showed an increase of loss volume (decrease of precipitation volume) ranging from 3% to 14% (Figure 1).

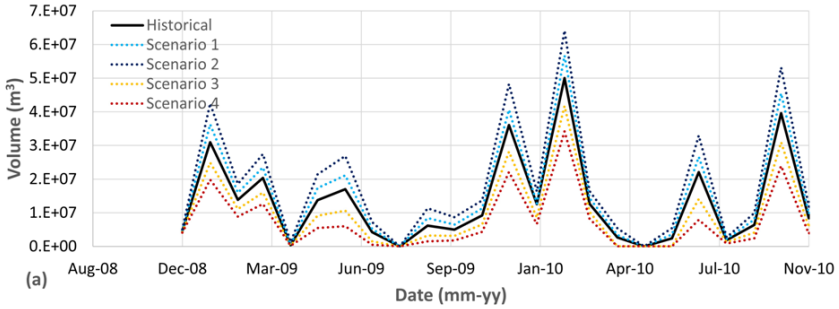

Scenario	Rainfall	Temperature
Scenario 1	10%	+ 1.5 °C
Scenario 2	20%	+ 1.5 °C
Scenario 3	-10%	+ 1.5 °C
Scenario 4	-20%	+ 1.5 °C
Scenario 5	10%	+ 2.0 °C
Scenario 6	20%	+ 2.0 °C
Scenario 7	-10%	+ 2.0 °C
Scenario 8	-20%	+ 2.0 °C

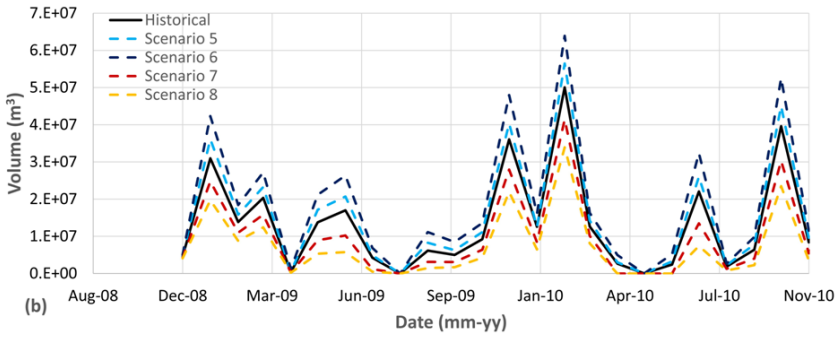

Difference (%)	Precipitation volume (mm)	Loss volume (mm)	Excess volume (mm)
Scenario 1	10	6	18
Scenario 2	9	3	20
Scenario 3	-25	-10	-47
Scenario 4	-11	-5	-25
Scenario 5	37	14	110
Scenario 6	9	3	20
Scenario 7	-25	-10	-47
Scenario 8	-11	-5	-26

Figure 1. Comparison of the historical results with the eight scenarios.

Overall, results present significant sensitivity of rainfall and runoff characteristics to climate change, thus, it is proposed to include assessment of climate change impacts in the design procedure. In addition, the effect of land use – land cover changes must be also studied.

Acknowledgments: Part of the work described in this paper has been conducted within the NEXOGENESIS project. This project has received funding from the European Union's Horizon 2020 research and innovation programme under Grant Agreement No. 101003881.

References

Kourtis IM, Bellos V, Kopsiaftis G, Psiloglou B, Tsihrintzis VA (2021) Methodology for holistic assessment of grey-green flood mitigation measures for climate change adaptation in urban basins. Journal of Hydrology 603: 126885. https://doi.org/10.1016/j.jhydrol.2021.126885

Kourtis IM, Tsihrintzis VA (2021) Adaptation of urban drainage networks to climate change: A review. Science of the Total Environment 771: 145431. https://doi.org/10.1016/j.scitotenv.2021.145431

Mimikou MA, Kouvopoulos YS (1991) Regional climate change impacts: I. Impacts on water resources. Hydrological Sciences Journal 36(3): 247-258. https://doi.org/10.1080/02626669109492507

Theodosopoulou Z, Kourtis IM, Bellos V, Apostolopoulos K, Potsiou C, Tsihrintzis VA (2022) A Fast Data-Driven Tool for Flood Risk Assessment in Urban Areas. Hydrology 9(8): 147. https://doi.org/10.3390/hydrology9080147

Vangelis H, Zotou I, Kourtis IM, Bellos V, Tsihrintzis VA (2022) Relationship of Rainfall and Flood Return Periods through Hydrologic and Hydraulic Modeling. Water 14(22): 3618. https://doi.org/10.3390/w14223618

Controls of preferential flow along hillslopes: A case study in a small forested Mediterranean catchment

K. Kaffas[1*], M. Verdone[1], F.S. Manca di Villahermosa[1], A. Dani[1], J. Klaus[2], C. Segura[3], M. Macchioli Grande[4], C. Massari[5], D. Penna[1]

[1] *Department of Agriculture, Food, Environment and Forestry, University of Florence, Italy*
[2] *Department of Geography, University of Bonn, Germany*
[3] *Oregon State University, College of Forestry, Corvallis, USA*
[4] *Department of Geology, Faculty of Physical and Mathematical Sciences, University of Chile*
[5] *Research Institute of the Geo–Hydrological Protection, National Research Council, Italy*
** e-mail: konstantinos.kaffas@unifi.it*

Introduction

The occurrence of preferential flow (PF) is a key factor for understanding the dynamics of runoff generation. Preferential flow is important because the rapid vertical movement of rain into the soil and its subsequent transit downslope through the subsurface lateral flow can control rapid hydrograph response (Weiler and McDonnell 2007). However, PF remains largely unexplored in forested catchments. PF pathways can be identified through geophysical methods, such as Ground Penetrating Radar (GPR) or electrical resistivity tomography (ERT) surveys (Guo et al. 2014), experimental observations (dye staining method, Grant et al. 2019), or through analysis of soil moisture (SM) data, where non-sequential (non-SEQ) SM responses (a first response in the deeper soil layer) are commonly treated as an indication of PF (Grant et al. 2019). The type of subsurface flow response depends on different factors, such as the meteorological forcings, antecedent wetness conditions, soil texture and presence of rocks, land cover, and topography. Yet, the exact conditions that favor the occurrence of PF remain elusive (e.g., Liu and Lin 2015; Wiekenkamp et al. 2016). In this work, we use SM and precipitation data to study the occurrence of PF (by identifying non-SEQ SM responses) in a small mountain forested catchment in central Italy. Our objective is to identify controlling factors among precipitation characteristics and antecedent wetness conditions.

Materials and methods

The Re della Pietra experimental catchment is a 2 km^2 mountain forested catchment in the Tuscan Apennines. The catchment has a steep topography, a wide elevations range (650–1280 m), a mean annual precipitation of 1,300 mm, and is covered almost entirely by beech and oak trees, with a smaller portion of conifers species.

Two sets of six SM sensors were installed along two hillslope transects, one at the outlet of the Lecciona headwater sub-catchment (0.3 km^2) and one at the Re della Pietra catchment outlet (C4). Each set of SM probes was placed in pairs, at 15 cm and 35 cm depths, at three locations at the riparian, lower-hillslope, and mid-hillslope zones. The probes recorded the volumetric SM at a 10-min time step from August 2020 onwards at the outlet of the Lecciona sub-catchment and from December 2021 onwards at the outlet of the Re della Pietra catchment. A 1% increase in SM was registered as response (Tang et al. 2020). The antecedent wetness conditions were assessed in terms of the Antecedent SM Index (ASI):

$$ASI = \theta \times D \quad (1)$$

where θ is the volumetric soil moisture content (m^3/m^3) and D is the installation depth (m).

Precipitation events were defined with at least one mm of precipitation and a minimum inter-event time (MIT) of four hours. Precipitation and catchment characteristics such as precipitation depth (P), duration, average intensity, and maximum intensity, as well as ASI, ASI+P, and peak SM response (SM_{peak}) were investigated as possible controls.

Results and concluding remarks

Figure 1 displays the control of ASI over the type of SM response by depth and zone for Lecciona and C4. At 15 cm, SM peaks faster than at 35 cm and for lower ASI values. ASI's as low as 6 mm, at 15 cm depth in Lecciona, are able to trigger responses at the lower hillslope while at 35 cm, SM does not respond below 36 mm. Though this is also a depth-dependent index, it is obvious that considerably higher antecedent SM (ASM) conditions are required to trigger a response in the deeper soil layer. In all cases, most non-sequential responses occur at the higher range of ASI, which means that higher ASM is likely to prompt irregularities in the subsurface flow response. It seems that more solid conclusions can be drawn for the upper soil layer at C4, which presents the most consistent behavior as to the SM response at all zones.

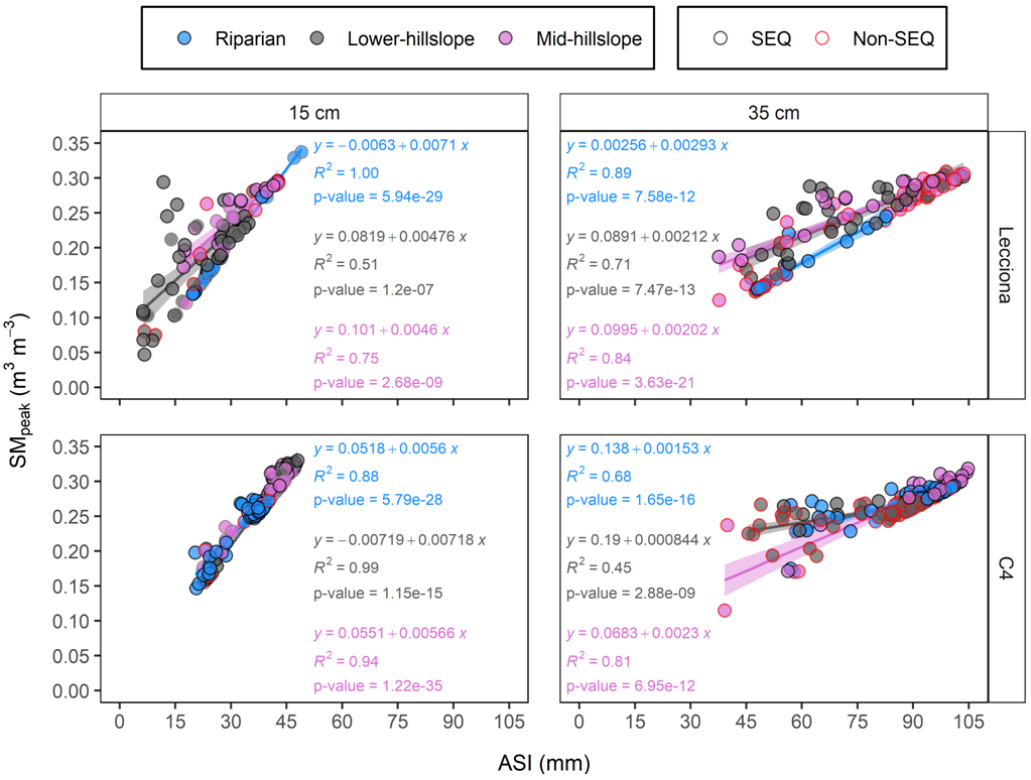

Figure 1. Control of ASI over the type of soil moisture response by depth and by zone for Lecciona and for C4.

These preliminary results contribute to the current knowledge regarding the occurrence of preferential subsurface flow in forested Mediterranean catchments, but further investigation is needed to better unravel the interplay of different driving factors.

Acknowledgments: WATERSTEM project (call PRIN 2017, code: 20202WF53Z), funded by the Italian Ministry of University and Research (MIUR).

References

Grant KN, Macrae ML, Ali GA (2019) Differences in preferential flow with antecedent moisture conditions and soil texture: Implications for subsurface P transport. Hydrological Processes 33(15): 2068-2079. 10.1002/hyp.13454

Guo L, Chen J, Lin H (2014) Subsurface lateral preferential flow network revealed by time-lapse ground-penetrating radar in a hillslope. Water Resources Research 50(12): 9127-9147. 10.1002/2013WR014603

Liu H, Lin H (2015) Frequency and control of subsurface preferential flow: From pedon to catchment scales. Soil Science Society of America Journal 79(2): 362-377. 10.2136/sssaj2014.08.0330

Tang Q, Duncan JM, Guo L, Lin H, Xiao D, Eissenstat DM (2020) On the controls of preferential flow in soils of different hillslope position and lithological origin. Hydrological Processes 34(22): 4295-4306. 10.1002/hyp.13883

Weiler M, McDonnell JJ (2007) Conceptualizing lateral preferential flow and flow networks and simulating the effects on gauged and ungauged hillslopes. Water Resources Research 43(3): 1-13. 10.1029/2006WR004867

Wiekenkamp I, Huisman JA, Bogena HR, Lin HS, Vereecken H (2016) Spatial and temporal occurrence of preferential flow in a forested headwater catchment. Journal of Hydrology 534: 139-149. 10.1016/j.jhydrol.2015.12.050

II. Water Related Hazards and Risks

Strategic assessment of causal and preference relations between criteria in water management using the DEMATEL methodology

B. Srdjevic*, Z. Srdjevic
University of Novi Sad, Faculty of Agriculture, Trg Dositeja Obradovića 8, Novi Sad 21000, Serbia
** e-mail: bojan.srdjevic@polj.uns.ac.rs*

Introduction

In this paper, the authors utilize the commonly used DEMATEL (Decision Making Trial and Evaluation Laboratory) methodology to evaluate the criteria relevant to water management. By establishing a suitable decision-making framework and employing DEMATEL, a strategic perspective can be obtained on the causal relationships between criteria, and a rough estimate of the relative importance (weights) of each criterion can be derived.

In contrast to standard MCDM (Multi-criteria decision-making) methodologies, such as TOPSIS, PROMETHEE, Compromise Programming, VIKOR, or AHP, DEMATEL does not primarily focus on criterion preferences. Instead, the method indirectly determines relative importance and is not methodologically validated for this purpose. The main objective of DEMATEL is to identify cause-effect relationships between criteria, based on the original works of Gabus (1973) and Fontela (1974), which investigated the factors influencing the performance of social systems. Similarly, in this study, the multi-criteria decision-making process is viewed as a system, where criteria are the factors that impact system behavior. The study focuses on commonly used criteria for evaluating alternative water management plans at the basin scale and selecting the most desirable one (Srdjevic and Srdjevic, 2022).

Materials and methods

In the context of water resources planning and management, where multiple stakeholders with differing strategic interests are involved, and where the factors governing the process are highly complex, it is crucial to recognize the causal relationships between criteria. This is because straightforward applications of MCDM models may produce misleading results. MCDM models assume that criteria are independent, but in reality, they are often interdependent. Identifying potential dependencies between criteria early on is strategically important for later evaluations of alternatives and deriving final decisions. DEMATEL is based on pair-wise comparisons of influential factors in a system and identifying their inter-relationships described in the causes-effects setting (Si et al. 2018; Han and Deng, 2018). By mapping these relationships, DEMATEL enables the identification of internal dependencies between factors and makes them understandable (Feng and Ma, 2020).

This study employs the DEMATEL method in both individual and group settings. Theoretical and practical issues related to the method are extensively discussed in scientific papers (e.g. Lakicevic and Srdjevic, 2022). DEMATEL has different versions in crisp, fuzzy, and rough methodological settings, and it has been widely applied in managing insufficient or unreliable information. Researchers generally agree on the high potential of the method in supporting strategic and tactical decision-making processes, including the ability to extend its results to other methods and methodologies positioned at higher levels of water and other resources planning and management.

In this study, the DEMATEL method is used to identify the cause-effect status of five key criteria for evaluating alternative water management plans in a river basin in Serbia. The criteria assessed include political impacts, economic issues, social issues, environmental issues, and technical criteria. The initial step of the DEMATEL is conducted individually by the authors, creating two direct relation matrices for criteria that are then aggregated into a single group matrix. Using a computed total relation matrix, criteria are mapped onto a cause-effect diagram for each individual and group, enabling the derivation of conclusions about causal and importance relations between criteria. Moreover, two possible approaches relying on the

total relation matrix of DEMATEL are used to determine the preferences or weights of criteria, which can be used in standard MCDM applications.

Results and concluding remarks

In this study, the DEMATEL method is used first individually and then by a two-member group to evaluate criteria for water resources management in a river basin. The study discusses the DEMATEL results from a strategic perspective, highlighting the causalities and importance of criteria to develop a proper development strategy for the basin. Individual and aggregated results are compared and recommendations are given on how to combine DEMATEL and MCDM methods for water resources planning and operational management. Overall, the study aims to contribute to the effective management and sustainable use of water resources in the given river basin.

Acknowledgments: This work was partially funded by the Ministry of Education, Science, and Technological Development of Serbia (Grant No. 451-03-68/2022-14/200117).

References

Gabus A (1973) Communicating with those bearing collective responsibility. Battelle Geneva Research Centre, Geneva

Feng C, Ma R (2020) Identification of the factors that influence service innovation in manufacturing enterprises by using the fuzzy DEMATEL method. Journal of Cleaner Production 253: 120002. https://doi.org/10.1016/j.jclepro.2020.120002

Fontela EG (1974) Structural analysis of the world problematique. Battelle Geneva Research Centre, Geneva.

Han Y, Deng Y (2018) An Enhanced fuzzy evidential DEMATEL method with its application to identify critical success factors. Soft Computing 22(15):5073–5090. https://doi.org/10.1007/s00500-018-3311-x

Lakicevic M, Srdjevic B (2022) An approach to developing the multicriteria optimal forest management plan: The "Fruska Gora" national park case study. Land 11(10): 1671. https://doi.org/10.3390/land11101671

Si SL, You XY, Liu HC, Zhang P (2018) DEMATEL technique: A systematic review of the state-of-the-art literature on methodologies and applications. Mathematical Problems in Engineering 2018: 1–33. https://doi.org/10.1155/2018/3696457

Srdjevic Z, Srdjevic B (2022) Use of DEMATEL and AHP in analysing causality and preferences of criteria in water management related decision-making. Vodoprivreda 54(3):69-78 (in Serbian)

Estimating flood damage to crops and implications for flood risk assessment

A.R. Scorzini*, C. D'Eramo, M. Di Bacco
Department of Civil, Environmental and Architectural Engineering, University of L'Aquila, L'Aquila, Italy
** e-mail: annarita.scorzini@univaq.it*

Introduction

Damage models are a key element for quantitative (i.e., economic) flood risk assessments, as they relate information on flood hazard and vulnerability features of exposed items to express expected losses (Merz et al. 2010). While more advanced modelling tools exist for estimating direct damage to residential properties, only recently the agricultural sector has started to receive increasing attention from researchers. In this context, Molinari et al. (2019) developed AGRIDE-c, a synthetic, expert-based model relying on a coupled approach considering the physical damage to crops (i.e., yield reduction as a function of hazard and vulnerability features) and its economic effects in terms of loss of revenue and variation in production costs for farmers. The model, after adaptation to the context of implementation ("regional model", as shown in Scorzini et al. 2021), allows estimating, for each crop type, the economic damage caused by a flood event of certain hazard characteristics. Differently from other sectors, crop damage depends on many hazards parameters beyond traditional variables reported in flood hazard maps, as water depth and flow velocity; indeed, other important influencing factors include inundation duration, water salinity, yield of sediments and/or contaminants, as well as the month of flood occurrence, due to the seasonality of crop production and changing plant vulnerability over the different phenological phases. In particular, the last factor would imply a shift from the traditional representation of inundation scenarios based on annual probability (i.e., return period), as requested for instance by the Floods Directive ("very rare/rare/frequent flood scenario"), to monthly-based risk estimations.

By means of an example of application for the system of Panaro and Reno river basins in northern Italy, this study aims at showing the usefulness of a model like AGRIDE-c for supporting informed decisions on flood risk management.

Materials and methods

Agricultural flood risk assessment with the regional analytical model of AGRIDE-c for cereal crops (maize, wheat, barley, grassland), developed in the framework of the MOVIDA project (https://sites.google.com/view/movida-project), requires the combination of hazard data with information on exposure in flood affected areas. In this study, the available inundation maps produced by the Po River Basin Authority for three synthetic flood events with return period of 25, 100 and 500 years were the main hazard input data; these consisted of raster files depicting inundation features in terms of water depth and flow velocity, at a resolution of 10 m and 5 m for the Reno and Panaro River, respectively. For the sake of conciseness, inundation duration was assumed to be fixed and shorter than 5 days, as typical for the region. The four considered crop types, which extended over an area of about 286 km^2 for the 100-year flood, were identified by using the agricultural parcel dataset of the Emilia Romagna Region.

With the total losses obtained with the application of AGRIDE-c for each flood scenario, it was possible to determine the expected annual agricultural damage (EAD), as follows:

$$EAD = \sum_{j=1}^{N} \Delta P_j \cdot D_j \quad (1)$$

where ΔP_j and D_j are respectively the exceedance probability increment and average damage of two events with exceedance probabilities (P_j) and (P_{j+1}). However, the seasonal varying susceptibility of agricultural crops would affect the estimation of flood damage D_j. To evaluate the influence of accounting for this variability on an ex-ante flood risk assessment, the EAD was calculated in two different ways: the first

considering D_j as the weighted average of possible losses occurring in the different months of the year (D_{ave}), with weights given by the probability of flooding in each specific month, and the second simply assuming for D_j the maximum value of the monthly expected losses (D_{max}). In the first case, monthly maximum flow timeseries available for river gauges in the areas were considered for deriving monthly flood probabilities. The implications of the method selected for calculating D_j on the results of decisional processes for the identification of risk reduction measures are here exemplified by considering a possible scenario concerning the calculation of the maximum cost for economically efficient structural mitigation measures in the area (under the assumption of totally avoiding agricultural damages). The benefit-cost ratio (BCR), defined as the ratio between discounted benefits (i.e., avoided damages) and costs over the lifetime of the intervention, is considered as an indicator for evaluating the cost-effectiveness.

Results and concluding remarks

The results of monthly damage calculations are reported in Figure 1 (left panel), which indicates the largest losses to be expected for an event occurring between May and July, with D_{max} ranging from about 1.7 M€ for the 25-y flood (July) to 29.4 (April-May) and 40.5 M€ (July) for the 100-y and 500-y flood, respectively. However, the combination of monthly losses with the related flooding probability would lead to a weighted average annual damage (D_{ave}) for the Panaro-Reno river system of about 1.2, 17.8 and 23.5 M€ for the 25-y, 100-y and 500-y event, respectively. These differences have clearly an impact on the calculation of the EAD and, consequently, on the results of the cost-benefit analysis (right panel of Figure 1), which would indicate economically feasible mitigation measures with costs lower than 7-12 M€ or 13-20 M€ (depending on the discount rate, t) when using D_{ave} or D_{max} for the assessment.

Overall, these results indicate the advantages of flood damage models, like AGRIDE-c, considering the effect of seasonal varying susceptibility of the exposed asset for a more informed flood risk management.

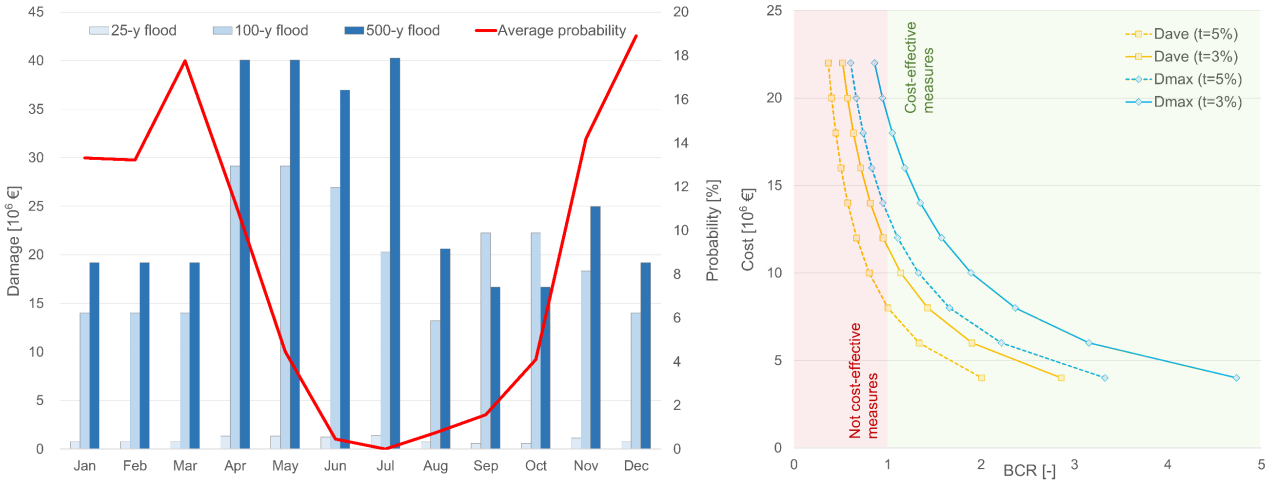

Figure 1. Left: monthly flood probability for the Panaro and Reno river and expected losses for the considered synthetic flood scenarios. Right: influence of the method for damage calculation on the results of the cost-benefit analysis.

References

Bremond P, Grelot F, Agenais AL (2013) Economic evaluation of flood damage to agriculture-review and analysis of existing methods. Natural Hazards and Earth System Sciences 13(10): 2493-2512. doi:10.5194/nhess-13-2493-2013

Merz B, Kreibich H, Schwarze R, Thieken A (2010) Assessment of economic flood damage. Natural Hazards and Earth System Sciences 10(8): 1697-1724. doi: 10.5194/nhess-10-1697-2010.

Molinari D, Scorzini AR, Gallazzi A, Ballio F (2019) AGRIDE-c, a conceptual model for the estimation of flood damage to crops: development and implementation. Natural Hazards and Earth System Sciences 19(11): 2565-2582. doi: 10.5194/nhess-19-2565-2019

Scorzini AR, Di Bacco M, Manella G (2021) Regional flood risk analysis for agricultural crops: Insights from the implementation of AGRIDE-c in central Italy. International Journal of Disaster Risk Reduction 53: 101999. doi: 10.1016/j.ijdrr.2020.101999

Fluctuation of bacterial indicators in coastal water at Durrës and Jala beaches

M. Bakalli[1*], I. Malollari [2], J. Selamaj[3]
[1] *Department of Apllied Natural Siences, University of Aleksandër Moisiu, Durrës, Albania*
[2] *Department of Chemistry, University of Tirana, Tirana, Albania*
[3] *Microbiology Laboratory, Central Laboratory of Armed Forces, Tirana, Albania*
** e-mail: bakallim@gmail.com*

Introduction

The urban development during the last decade in Albania has affected the coast line. The Adriatic and Ionian Seas during these years have become hosts for urban and industrial discharges. Inhabitants have increased in coastline areas, and the level of contamination is much higher. Another source of pollution is from rivers that contain wastes. Most reports emphasize that the main source of pollution in Albania is urban solid waste and most of this waste ends in the Adriatic and Ionian Seas. Urban waste can pollute the beaches and the marine environment. On the other side, untreated wastewater discharge into sea water is a major problem for seawater contamination. Untreated wastewater can cause high health risk to humans due to microbial and chemical pollution, particularly those who use these beaches during the tourist season. Also, microbial contamination is a serious problem for the aquatic ecosystem. Faecal coliforms are indicators of enteric pathogens that can cause water borne diseases (Steward et al. 2008; Halpern et al. 2008; Karbasdehi et al. 2017). Based on some studies (e.g., Bakalli et al. 2021; Bakaj et al. 2016) the seawater in some beaches in Albania has high level of microbial indicators. Microbial pressure increases during the summer period because of anthropogenic activities and the influx of tourists.

The aim of our study is to evaluate and to compare the changes of microbial indicators in relation to the location and different years in three areas (Plepa, Currila and Jala) of Albania coastline during the touristic season. The quality of coastal water is based on two microbiological parameters (*Escherichia coli* and Intestinal enterococci) defined in the bathing water Directive 2006/7/EC, because these microorganisms are considered as microbial contamination indicators.

Materials and methods

During the study of 5 years we conducted analyses at the Central of Laboratory of Armed Forces, the sea water collected at three points located in Currila, Plepa and Jala beaches in Albania. We collected five samples from each beach during July and August. Samples were taken near the coastline and up to 200 m seaward, and at about 0.5 m below the water surface. All samples were mixed and transported in refrigerator box to the laboratory within 1 to 3 hours and analyzed during the same day. Each sample was analyzed for *E. coli* and intestinal enterococci. For determination of *E. coli* (through the membrane filtration method), we used C-EC agar incubated at 37 ^{o}C for 24 h. Intestinal enteroccoci content was determined with E.C.O.A agar (membrane filtration method) incubation at 37 ^{o}C for 24 h.

Results and concluding remarks

The 5-year concentrations of *E. coli* and Intestinal enterococci are presented in Figs. 1 and 2. Bacterial indicators indicate decreasing microbial contamination. We notice a trend of improving sea water quality during the monitoring period. The average concentration of *E. coli* ranges from 250 to 650 colonies per 100 mL and of Intestinal enterococci from 190 to 285 colonies per 100 mL. During these years, the higher concentration of *E. coli* was observed in 2017 in Plepa beach, while the lowest concentration is 2021 in Jala beach. Higher concentration of intestinal enterococci was observed in 2019 at Plepa beach, and the lowest concentration was in 2021 and 2022 at Jala beach.

According the directive 2006/7/EC concerning the concentration of *E. coli* in Currila and Plepa beaches

seawater may be classified as “sufficient” bathing water. Colonies ranged from 630 colonies per 100mL in 2019 to 520 colonies per 100mL in 2021 in Currila beach, whereas in Plepa beach colonies ranged from 650 colonies per 100mL in 2017 to 520 colonies per 100mL. At Jala beach the concentration of *E. coli* ranged from 317 colonies per 100 mL in 2019 to 250 in 2021 and sea water can be classified as good to excellent quality for bathing. The concentration of intestinal enterococci in samples at Currila ranged from 255 colonies per 100 mL in 2017 to 205 in 2022; at Plepa beach it ranged from 285 in 2019 to 245 in 2022 and at Jala from 225 in 2019 to 190 in 2021 and 2022. Sea water in July and August at Currila, Plepa and Jala can be classified as of good quality. These data show the trend of improving sea water quality during the monitoring years. The results of our study concern to the seasonal changes in the respective years. Sewage treatment plant operation seems to have had a positive effect on sea water quality mainly in Currila and Plepa beaches. In Jala beach the high concentrations of bacterial indicators is related to the large number of tourists during the summer months, and the poor management of urban waste.

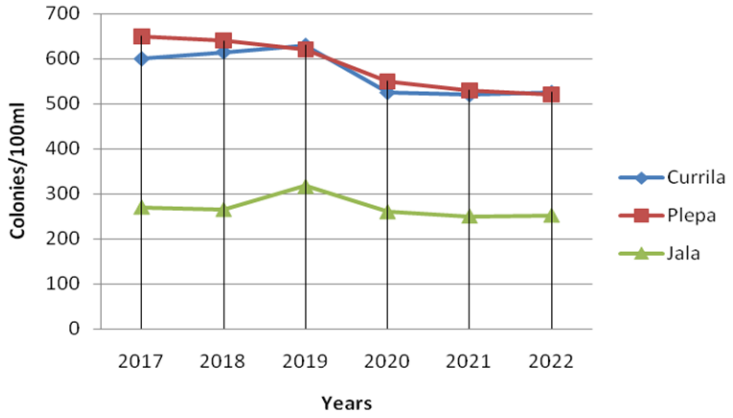

Figure 1. Average concentration of E. coli.

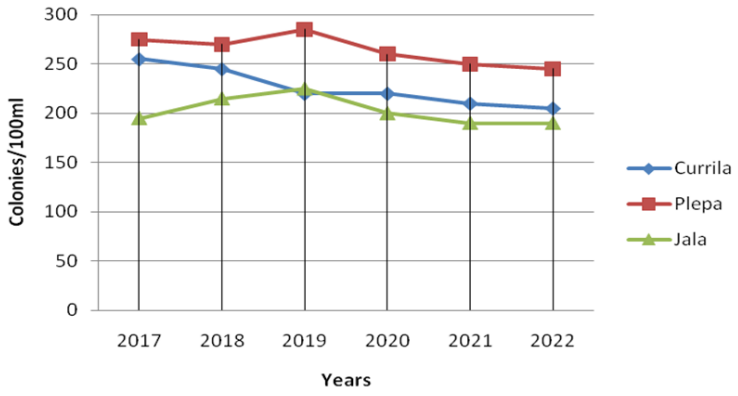

Figure 2. Average concentration of intestinal enterococci.

References

Bakalli M, Malollari I, Selamj J (2021) Microbial indicator of coastal water in Albania. Wseas Transaction on Environment and Development 17(23): 232-236. http://doi.org/10.37394/232015.2021.17.23

Halpern BS, Walbridge SH, Selkoe KA et al. (2008) A global map of human impact on marine ecosystems. Science 319(5865): 948-952. http://doi.org/10.1126/science.1149345

Bakaj A, Ruci E, Kalaja J (2017) Monitoring of microbiological parameters on the coast of Durres, Albania. Albanian J.Agric.Sci 16(sp): 95-101.

Steward JR, Gast RJ, Fujioka RS et al. (2008) The coastal environment and human health microbial indicators, pathogens, sentinels and reservoirs. Environ Health 7 (suppl 2):S3 1-14. http://doi.org/101186/1476-069X-7-S2-S3

Karbasdehi VN, Dobaradaran S, Nabipou I et al. (2017) Indicator bacteria community in seawater and coastal sediments: the Persian Gulf as a case. J Environ Health Sci Eng 15 (6): 1-15. http://doi.org/101186/s40201-017-0266-2

Outlining a master plan framework for the design and assessment of flood mitigation infrastructures across large-scale watersheds

P. Dimas[1*], G.K. Sakki[1], P. Kossieris[1], I. Tsoukalas[1], A. Efstratiadis[1], C. Makropoulos[1], N. Mamassis[1], K. Pipili[2]
[1] Dept. of Water Resources and Environmental Engineering, School of Civil Engineering, NTUA, Athens, Greece
[2] ANODOS S.A., Athens, Greece
* e-mail: pdimas@mail.ntua.gr

Introduction

On September 16, 2020, the Hellenic Ministry of Infrastructure assigned to the concessionaire of the Central Greece Motorway E65 the design and construction of supplemental works for the urgent flood protection of areas along the motorway alignment, including the Western Thessaly region (Greece). Considering the damages and losses induced by the Medicane Ianos over the greater Thessaly region the concessionaire, on its own initiative, proclaimed the need for developing a Master Plan for the West Thessaly flood protection. The final area of interest, herein referred to as Western Peneios watershed, occupies approximately 6400 km^2, thus constituting a mega-scale hydrological, hydraulic and water management study that poses multiple conceptual and computational challenges (Papaioannou et al. 2021). The overall question of the Master Plan is to provide a synthesis of already proposed as well as new projects (dams, embankments, ditches), and prioritize them under a multipurpose prism. The methodological framework is comprised of three axes: (i) a preliminary assessment of specific areas where high risk is expected due to flood phenomena, by utilizing a GIS-based multi-criteria decision analysis approach, (ii) a semi-distributed representation of the rainfall-runoff transformations and the flood routing processes across the entire watershed, and (iii) a coupled 1D/2D hydrodynamic simulation of the flood prone riverine system, also including a highly complex system of artificial channels. The final planning prioritizes the strengthening of flood protection in the study area through the combined influence of a set of large-scale projects, i.e., dikes, multi-purpose dams (permanent reservoirs) and retention basins of controlled inundation (temporary reservoirs). The objective is to sketch a framework for facing similar studies in a holistic manner, while maintaining a high level of computational efficiency and explainability.

Materials and methods

The first pillar of the methodology consists of an efficient way to make a preliminary assessment of the areas where a high flood risk is expected utilizing simple geospatial criteria, by following Allafta and Opp (2021). In this vein, we first compile eight thematic layers, i.e.: (i) mean annual rainfall, (ii) distance from river network, (iii) elevation, (iv) terrain slope, (v) land use/land cover, (vi) drainage network density, (vii) soil permeability, and (viii) hydrolithology. Based on experts' knowledge, the highly heterogeneous information of these layers (either quantitative or qualitative) is "translated" into flood susceptibility scores, from 1 (very low) to 5 (very high). Eventually, we produce an overall flood susceptibility map, as a weighted overlay of individual layers, which is the guide for employing the detailed hydrodynamic analysis. Characteristic snapshots are shown in Figure 1.

The hydrodynamic analysis across the flood prone areas is driven by design flood hydrographs that are produced through a hydrological simulation model (2nd methodological pillar) that runs over the entire watershed. The representation of the generation and routing mechanisms of flood flows is based on a semi-distributed discretization of the hydrological system, by formulating a network-type model consisting of nodes, stream/river branches, and sub-basins. The configuration of the complete rainfall-runoff system includes 212 nodes, 210 branches and 306 sub-basins, thus composing a mega-scale case study. The event-based approach, following the combined NRCS-CN and synthetic unit hydrograph methods is applied: the first implements the transformation of the design storm event over each sub-basin into flood runoff, while

the second implements its routing to the corresponding outlet node. Next, the point hydrographs through all sub-basins are synthesized and propagated along the hydrographic network by applying a novel conceptual approach that allows assigning travel time parameters on the basis of macroscopic properties of the river system (Efstratiadis et al. 2022). The computational implementation is employed through HEC-HMS software, allowing the representation of major hydraulic structures (i.e., reservoirs, spillways, gates).

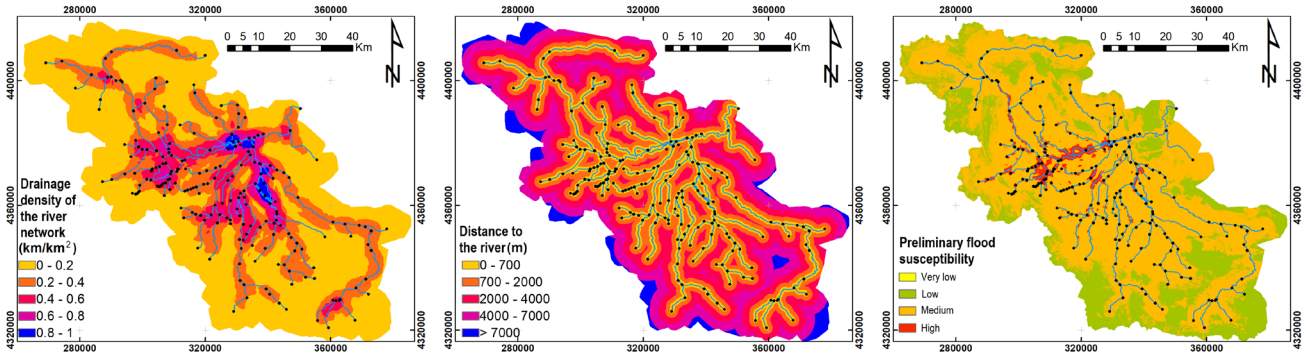

Figure 1. Two out of eight thematic layers used in assessing the flood prone areas in Western Thessaly (left: drainage density, middle: distance from river network) and final map of preliminary flood susceptibility (right).

The final pillar of the methodology aims at disclosing the inundation mechanisms in the areas of interest through hydrodynamic analysis. In this context, we use the HEC-RAS software, by performing coupled 1D-2D simulations (Brunner et al. 2015). Emphasis is given on representing the flow exchange mechanisms from the main river channels (within the banks and/or dikes) to the broader floodplains and vice versa. This is employed using lateral structures that control the overflow dynamics. Automated procedures and interfaces of HMS and RAS with the data processing system HEC-DSS are developed in R environment.

Results and concluding remarks

The simulations through the combined hydrological-hydrodynamic modelling scheme are performed by considering a set of storm events for a return period of 100 years. Initially, this scheme is used to represent the current status of the system. Next, we inspect several planning scenarios, involving the development of three types of flood mitigation works, namely: (a) dikes, along parts of the lower channel network, (b) six new multi-purpose reservoirs in the upstream, mountainous, parts of the watershed, and (c) nine retention basins in the middle and downstream parts, extending over 390 km^2 of agrarian land. Regarding the operation of reservoirs (existing and planned), a critical assumption is their storage conditions at the beginning of the flood event. In this vein, we examine two sub-scenarios, i.e., considering them full or assuming a buffer storage equal to 15% of their capacity.

Our analyses reveal the effectiveness of the combined scheme of the different flood mitigation works, and particularly the role of good management practices of reservoirs. The full development scenario ensures significant retention of the flood volumes and attenuation of flood peaks, as well. In particular, the reservoirs can store 65 out of 150 hm^3 produced in their upstream sub-basins, and the larger ones decrease flood peaks up to 75-95%. An important amount of about 56 hm^3 can also be temporarily retained in the closed basins, most of which is diverted from the adjacent channel network. Their performance may also be further improved by installing control structures along the dikes (e.g., lateral gates), to better manage the arriving flood flows.

References

Allafta, H. and Opp, C. (2021) 'GIS-based multi-criteria analysis for flood prone areas mapping in the trans-boundary Shatt Al-Arab basin, Iraq-Iran'. Geomatics, Natural Hazards and Risk 12(1):2087–2116

Brunner GW et al. (2015) Combined 1D and 2D Hydraulic Modeling within HEC-RAS. World Environmental and Water Resources Congress, May 17–21, 2015, Austin, TX, pp 1432–1443

Efstratiadis A et al. (2022) Revisiting Flood Hazard Assessment Practices under a Hybrid Stochastic Simulation Framework. Water 14(3):457

Papaioannou G et al. (2021) A Flood Inundation Modeling Approach for Urban and Rural Areas in Lake and Large-Scale River Basins. Water 13(9): 1264

Evaluation of drought risk mapping by Kaplan-Meier method

C.P. Cetinkaya*, M.C. Gunacti
Dokuz Eylül University, Faculty of Engineering, Department of Civil Engineering, Izmir, Turkey
** e-mail: cem.cetinkaya@deu.edu.tr*

Introduction

Dry periods and droughts are natural phenomena yet with the climate change pressures ever so intensified, they occur at a much more often and severe rate worldwide (Tramblay et al. 2020). These phenomena can be traced with various indicators and related indices (Mukherjee, Mishra, and Trenberth 2018; Liu et al. 2020). Generally, drought risk assessment is done by modeling these indicators and determining the drought occurrence probabilities (Hervás-Gámez and Delgado-Ramos 2019). The suggested adaptation incorporates the "Kaplan-Meier Estimator", which is a non-parametric statistic utilized to estimate the survival function from lifetime data. Kaplan-Meier Estimator is often used on medical patients to evaluate their survivability, evaluating their deaths as "events". The adapted method evaluates the Standardized Precipitation Index (SPI) scaled wet and dry state, considering drought as the "event".

Suggested method results indicate the non-occurrence probability, so inverted results are considered as the occurrence probability of the events namely, the droughts. Plotted drought risk maps hold value for easy interpretation and implementation decision-making tools for decision-makers. As the case study, the method implemented to the SPI values at various time steps (3, 6, and 12 months) calculated from 27 meteorological stations in Gediz River Basin located in Western Turkey, in the Mediterranean region, that is expected to be one of the most climate changes affected areas worldwide.

Materials and methods

Gediz River Basin is located in the West of Turkey. The basin substantially changed in the 90s era due to anthropogenic activities and climate change related pressures. Thus, the declining water resources and increasing urban and industrial demands raise concerns about water quality and quantity (Harmancioglu et al. 2020). Determining and projecting possible future droughts is a valuable tool in decision-making and planning for the basin.

27 meteorological stations were selected according to their data availability and spatial location aiming for homogeny as data representation. Data records are from between the years 1924 and 2013 but most of the data is available between the 1960s and late 1990s. The missing data among selected stations were imputed by the R project software according to linear regression. The package "MICE" was utilized in the process. After data imputation, SPI (3, 6, and 12 monthly) values were calculated for the selected stations. While shorter timescales are generally used as indicators for reduced soil moisture and flow in small reaches, longer timescales are commonly used as indicators for reduced streamflow and reservoir storage.

Determined SPI values are classified as wet (positive values) and dry (negative values) states. The transitioning of wet state to dry state, or drought occurrence, indicate the "events" described by Kaplan-Meier (1958). The study is based on this synergy where the drought occurrences are named "events". Thus, applying Kaplan-Meier or "Product-Limit" estimator would produce the product limit or the survivability of the wet periods (in a monthly timescale).

$$\hat{S}(t) = \Pi_{i:t,i\leq t}(1-(d_i/n_i)) \quad (1)$$

where t_i is the time at which a dry state occurs; n_i is the number of wet states still running at the time t_i and di is the number of dry states that occurred at time t_i.

Since dry states can occur consecutively, the adapted method also includes the following dry state occurrences in the same wet period. This provides extra knowledge about the occurrence probabilities of the follow-up dry states, not just the initial one, e.g., Ahmetli station has 32 wet but 44 dry periods

recorded. Including every dry state into the equation requires an update on the description of n_i, which now can be explained as "number of dry states has not happened yet at the time t_i" or "number of unrealized dry states". The result $S(t_i)$ indicates the probability of a wet period lasting longer than t_i or the "event" not taking place at the time t_i, on a drought risk perceptive 1-S(t) would describe the probability of "event" taking place or the drought occurrence risk, DR(t).

$$DR(t) = 1-\hat{S}(t) = 1- (\Pi_{i:t,i\leq t}(1-(d_i/n_i))) \quad (2)$$

Results and concluding remarks

Adapting the Kaplan-Meier Estimator method into the presented study and defining the drought risk, DR(t), provides faster results to be utilized as tools in water resources management. Calculated local drought risk values have been plotted as a drought risk map by using ArcGIS software, where point values are extrapolated via the "SPLINE" tool.

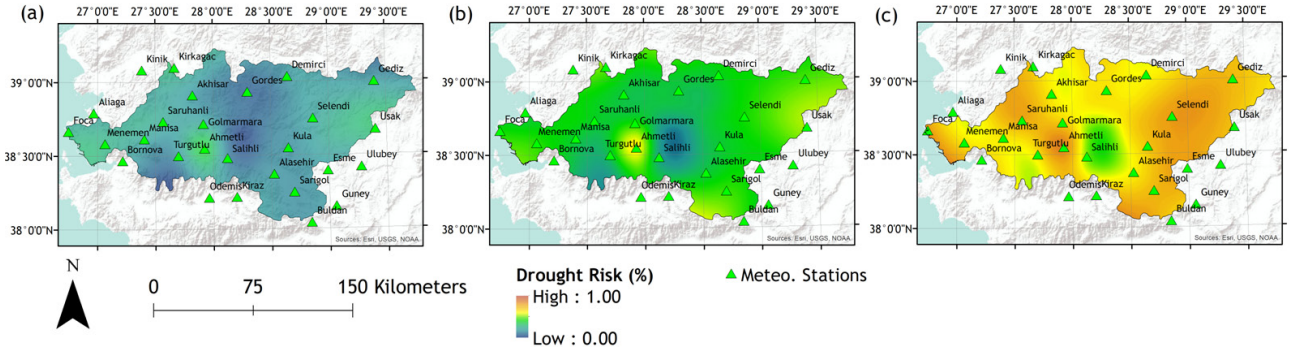

Figure 1. Drought risk maps of; (a) 3-month, (b) 6-month, and (c) 12-month periods according to SPI-3.

Drought risks escalate while the examined period expands, which is natural because the possibility of observing an event increases while the observation time expands. Figure 1 shows only the results of the Drought Risks according to SPI-3, whereas calculations have been carried out for SPI-6 and SPI-12 as well. In the case of the Gediz River Basin, drought can be expected near Lake Marmara and in the upstream regions more intensely relative to the rest of the basin on shorter periods (3 – 6 months), such as Usak and Gediz. While on the longer periods (12 months), the whole basin would likely suffer droughts, specifically Saruhanli, Ahmetli, and again upstream regions. Yet around the Salihli region, relatively lower risks of drought can be expected.

Acknowledgments: The MARA-MEDITERRA project (2121 Call 2021 Section 1 Water RIA) is funded by the Horizon 2020 European Union Funding for Research & Innovation under the Partnership for Research and Innovation in the Mediterranean Area Programme (PRIMA).

References

Harmancıoglu HN, Cetinkaya CP, Barbaros F (2020) Sustainability Issues in Water Management in the Context of Water Security. In: Harmancıoglu HN, Altinbilek D (eds) Water Resources of Turkey, 1st ed, Springer International, Cham, pp 517-533

Hervás-Gámez C, Delgado-Ramos F (2019) Drought Management Planning Policy: From Europe to Spain. Sustainability 11(7): 1862. https://doi.org/10.3390/su11071862

Kaplan EL, Meier P (1958) Nonparametric estimation from incomplete observations. Journal of the American Statistical Association 53(282): 457–481. https://doi.org/10.2307/2281868

Liu Q, Zhang S, Zhang H, Bai Y, Zhang J (2020) Monitoring drought using composite drought indices based on remote sensing. Science of The Total Environment 711: 134585. https://doi.org/10.1016/j.scitotenv.2019.134585

Mukherjee S, Mishra A, Trenberth KE (2018) Climate Change and Drought: a Perspective on Drought Indices. Curr Clim Change Rep 4: 145–163. https://doi.org/10.1007/s40641-018-0098-x

Tramblay Y, Koutroulis A, Samaniego L, Vicente-Serrano SM, et al. (2020) Challenges for drought assessment in the Mediterranean region under future climate scenarios. Earth-Science Reviews 210: 103348. https://doi.org/10.1016/j.earscirev.2020.103348

Evaluation of precipitation variability with an entropy-based approach

F. Barbaros*, T. Baran
Department of Civil Engineering, Faculty of Engineering, Dokuz Eylül University, Izmir, Turkey
** e-mail: filiz.barbaros@deu.edu.tr*

Introduction

Investigation of long-term time series of hydro-meteorological variables is vital for assessing potential water resources and examining environmental changes (Gu et al. 2020). Analysis of long-term hydro-meteorological variables plays an important role in water resource planning and climate change impact studies (Mishra et al. 2009). In general, global warming intensifies the hydrological cycle and thus increases the global average precipitation, evaporation, and runoff (Clark et al. 1999).

It is essential to measure the spatial and temporal characteristics of precipitation to assess the regional effects of climate change and water resource management (Zhang et al. 2016). Understanding the spatial and temporal differences in precipitation regimes is important for studying the response of the hydrological cycle to climate change and its impact on the variability and availability of water resources on a regional and global scale (Cleridou et al. 2014).

The method mentioned in the presented study was applied in 11 meteorological observation stations in the Eastern Black Sea basin, especially for the precipitations observed between 1975 and 2012. Spatial and temporal variability of long-term precipitation data were evaluated with entropy-based methods.

Materials and methods

Entropy-based variability is defined by the Index of Variability (*IV*) and is calculated by Eq. 1 as the difference between the maximum possible entropy (*max H*) and the entropy calculated from a single time series.

$$IV = (\max H) - H \quad (1)$$

If the variable has a uniform distribution, Shannon entropy reaches its maximum value. Therefore, the range of variation of *H* ranges from [0, log R]. Here, *R* is the difference between the lowest and the highest value taken by the random variable in the current data set and is expressed by Eq. 2 (Xiong et al. 2018).

$$maxH = \log (R) \quad (2)$$

When *IV* is calculated from the intensity entropy, it is called the Intensity Variability Index (*IVI*), and the higher the *IV* value (hence the *IVI* value), the higher the variability is defined.

The presented study is carried out on the existing long-term daily precipitation data of the Eastern Black Sea region, having extreme precipitation. The Eastern Black Sea Basin is located in the northeastern part of Turkey between 40^{o} $15^{'}$ - 41^{o} $34^{'}$ north latitudes and 36^{o} $43^{'}$ - 41^{o} $35^{'}$ east longitudes, constituting 2.92% of Turkey with a total area of 2,284,439 ha.

In general, when the whole basin is analyzed annually, it is determined that the western part of the basin has high *IVI* values and therefore high uncertainty. The spatial distribution of *IVI* values of long-term annual precipitation data is shown in Figure 1. When analyzed seasonally, it is observed that *IVI* values had the lowest values in the spring season and the highest values in the summer season as seen in Figure 2. It is stated that the precipitation variability varies according to each season. It is also seen from the annual and summer spatial distribution maps, that the most active season in the annual evaluation of the basin is summer. Similarly, when the *IVI* values of the seasons are evaluated, it is observed that the entropy-based variability of each month in that season is not exactly the same as the value of the season it belongs to. This situation can be explained mainly by the irregular nature of precipitation.

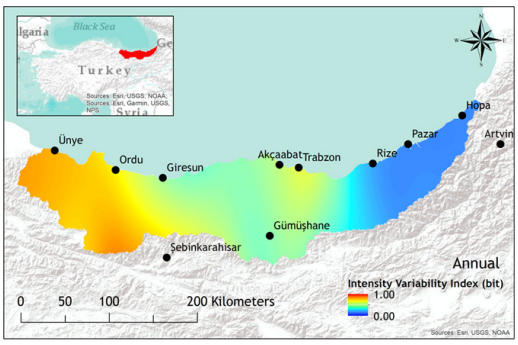

Figure 1. Annual spatial distribution of IVI of precipitation time series in the Eastern Black Sea Basin.

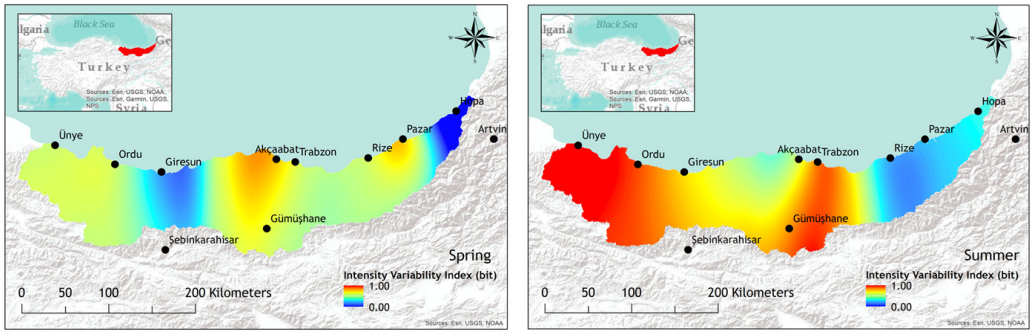

Figure 2. Spatial distribution of IVI of precipitation time series in the Eastern Black Sea Basin for seasons, spring, and summer.

Results and concluding remarks

With the method used in the presented study, using the calculated entropy values, a regional analysis is made to create risk maps throughout the basin. As a result, regional risks are visualized both annually, seasonally, and optionally divided periods through index-based maps created for the Eastern Black Sea region.

By the risk maps, it has been determined that the risks related to precipitation are found in the western part of the Eastern Black Sea Basin, especially in the areas where Ünye and Ordu stations are located. In the annual and seasonal evaluations, it is determined that each season has not the same distributions as the annual ones and the importance of considering the issue seasonally in the evaluation of a precipitation risk throughout the basin has been revealed. By the presented study, areas with high precipitation variability can be determined and timely actions can be taken in areas with disaster risk. The precipitation variability profile in the region will play an active role in current and future management decisions and evaluation stages for the river basins as a whole. Obtained entropy-based maps will be an effective tool for researchers and decision-makers to overcome climate change and flood risk.

Acknowledgments: Authors would like to acknowledge to M.Sc. Mert Can GÜNAÇTI for his great contribution to the mapping process of the manuscript.

References

Clark PU, Alley RB, Pollard D (1999) Northern hemisphere ice-sheet influences on global climate change. Science, 286(5442): 1104–1111. https://doi.org/10.1126/science.286.5442.1104

Cleridou N, Benas N, Matsoukas C, Croke B, Vardavas I (2014) Water resources of Cyprus under changing climatic conditions: modelling approach, validation and limitations. Environ. Model. Softw. 60:202–218. https://doi.org/10.1016/j.envsoft.2014.06.008

Gu H, Yu Z, Li G, Luo J, Ju Q, Huang Y, Fu X (2020) Entropy-Based Research on Precipitation Variability in the Source Region of China's Yellow River. Water 12:2486. https://doi.org/10.3390/w12092486

Mishra AK, Özger M, Singh VP (2009) An entropy-based investigation into the variability of precipitation. Journal of Hydrology 370(1–4): 139-154. https://doi.org/10.1016/j.jhydrol.2009.03.006

Xiong F, Guo S, Chen L, Chang F, Zhong Y, Liu P (2018) Identification of flood seasonality using an entropy-based method. Stochastic Environmental Research and Risk Assessment, 32: 3021–3035. https://doi.org/10.1007/s00477-018-1614-1

Zhang Q, Zheng Y, Singh VP, Xiao M, Liu L (2016) Entropy-based spatiotemporal patterns of precipitation regimes in the Huai River basin, China, International Journal of Climatology, 36:2335–2344. https://doi.org/10.1002/joc.4498

Implementation of nature-based solutions (NBS) for flood protection in Naxos island

S.M. Kapiris, A.P. Theochari*, E. Baltas
Department of Water Resources and Environmental Engineering, School of Civil Engineering, National Technical University of Athens, 5 Iroon Polytechniou, 157 80 Athens, Greece
** e-mail: atheochari@chi.civil.ntua.gr*

Introduction

Natural disasters are becoming more severe over the years, having a terrible influence on communities, the economy and the environment. Floods are a major concern in Europe that urgently needs to be managed. In this context, the European Commission has paid special attention to Nature-Based Solutions (NBS), which are cost-effective, decreasing the flood risks and simultaneously providing environmental sustainability. In the literature, various studies have examined the NBS for flood protection (e.g. Spyrou et al. 2021; Potočki et al. 2021).

In this paper two NBS are proposed and applied at basin scale, which covers an area of 44 km^2, located at Naxos Island, Greece. The specific basin is chosen for study as it is vulnerable to floods with a large volume of runoff at the outlet, putting the downstream settlement at high risk of flooding. The aim of this study is to highlight the contribution of NBS to peak discharge and flood volume decrease and simultaneously time to peak increase of a flood hydrograph in the outlet of a basin, reducing the downstream communities flood risk. The NBS applied concern the land cover change and the construction of retention pods along the hydrographic network. The output of such implementation provides valuable findings for a more efficient way of sustainability promotion in terms of a greener environment and economy, flood risk prevention and local biodiversity enhancement.

Materials and methods

The calculation of flood hydrographs in the outlet of the basin both prior to and after the NBS application within it, is conducted performing a hydrological analysis based on the time-area diagram method for the determination of a Unit Hydrograph through the Hydrological Engineering Canter's Hydrological Modelling System (HEC-HMS) model. For the computation of precipitation losses, the Soil Conservation Service (SCS) curve number (CN) method is selected. The CN distribution is calculated based on the land cover and soil type of the basin and the mean value found to be 75.

Regarding the application of the land cover change, the parts of land within basin where they are not exploited by humans are identified using the Corine Land Cover (2018) and the surface is covered by a denser forest than the existing one. The replacement with a denser vegetation changes the CN value and thus a new mean CN value calculated at about 70. In addition to the CN parameter, the k100 parameter, which is used in time-area diagram method, is also changed depending on the land cover, and is related to the speed of movement of water on the ground. Subsequently, new UH is determined, which together with the new value of CN, are inserted to HEC-HMS in order to calculate a new flood hydrograph.

The other proposed possible solution involves the utilization of retention ponds. The logic behind this NBS of choice is as follows: a series of small ponds and depressions are designed in a geographic information system (GIS) environment, by identifying suitable areas. The latter are located along the greater course of the riverine system, in regions where water is staying stagnant during storms, and occupy land that is not exploited by human activity and, hence, can be modified accordingly to accommodate this artificial infrastructure. More specifically, twenty ellipse-shaped lakes that cover an area of approximately 5000 m^2 are designed in the greater floodplain areas of the hydrographic network. Since their accompanying construction costs are significant, a typical depth of 2 m is chosen according to good engineering practices. Therefore, the resulting total volume stored is 0.2 hm^3. The latter is subtracted from

the calculated volume prior to the NBS (2.7 hm^3), leading to a post-NBS volume equal to 2.5 hm^3. This is accomplished by modifying the individual values of the pre-NBS hydrograph rising limb after its third quartile and up until the total hydrograph volume meets the post-NBS one. In this way, the flow velocity is reduced as the concentrated time is increased, the time to peak at the outlet of the basin is increased, and most importantly, the flood volume at the outlet is significantly reduced.

Results and concluding remarks

The methodology presented in this paper concerns the implementation of two NBS in a basin at Naxos Island for flood protection to the downstream community. In the following Figure 1, for the purpose of comparing the benefits and evaluating the effectiveness of the NBS, the flood hydrograph curves before (Total Flow) and after the application of NBS (New Total Flow) are depicted. From this comparison, it is evident that after land cover change the peak discharge has decreased to 69.1 m^3/s and the flood volume to 2.28 hm^3 against the initial values of 90 m^3/s (30% reduction) and 2.7 hm^3 (16% reduction) respectively. Furthermore, regarding the results of UH calculation, it is observed that the peak discharge decreased from 15.3 m^3/s to 14 m^3/s after the land cover change, while the time to peak increased by two hours. It can be concluded that this NBS seems to greatly influence the results of the hydrological analysis, and hence is of great importance in terms of flood risk management. The construction of retention ponds through earthworks also has a positive impact on reducing both the flood volume and the peak discharge. More specifically, the twenty lakes proposed, covering an approximate area of 5000 m^3, reduced the peak flow to 81 m^3/s when its initial value was 90 m^3/s and the flood volume from 2.7 hm^3 to 2.5 hm^3. In conclusion, the NBS constitute an effective means for the management and control of flood water movement and volume, reducing the risk to people and property, and achieving environmental sustainability. In the framework of future research, it is suggested to investigate the influence of soil erosion on the retention ponds effectiveness. Additionally, the implementation of combined NBS would be of interest.

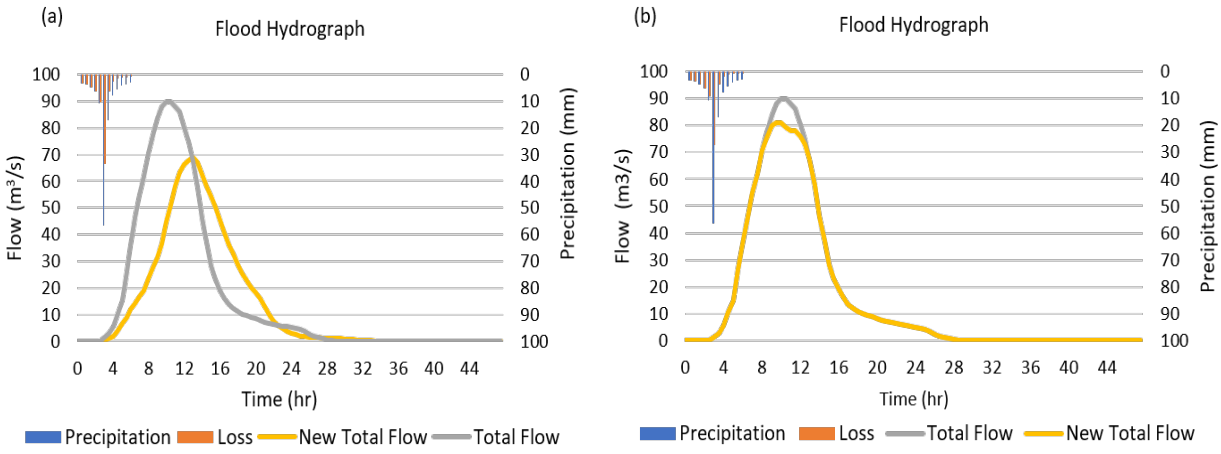

Figure 1. Flood hydrographs at the outlet of the basin before (Total Flow) and after (New Total Flow) land cover change (a), and construction of retention pods (b).

References

Spyrou C, Loupis M, Charizopoulos N, Apostolidou I, Mentzafou A, Varlas G, et al. (2021) Evaluating nature-based solution for flood reduction in spercheios river basin under current and future climate conditions. Sustainability, 13(7): 3885. https://doi.org/10.3390/su13073885

Potočki K, Bekić D, Bonacci O, Kulić T (2021) Hydrological aspects of nature-based solutions in flood mitigation in the Danube River Basin in Croatia: green vs. grey approach. In: Nature-Based Solutions for Flood Mitigation: Environmental and Socio-Economic Aspects. Cham: Springer International Publishing, 263-288. https://doi.org/10.1007/698_2021_770

CORINE Land Cover (2018) Land cover dataset for 2012. https://land.coper nicus.eu/pan-european/corine-land-cover/clc-2012/ (accessed 28 August 2021)

Retain for resilience: Natural water retention measures contribution to hydro-meteorological hazards risk reduction at the river basin level

B.B. Matić[1], B. Karleuša[2*]
[1] *Educons University, Sremska Kamenica, 21208, Serbia*
[2] *Faculty of Civil Engineering University of Rijeka, Rijeka, 51 000, Croatia*
** e-mail: barbara.karleusa@uniri.hr*

Introduction

Runoff generation primarily depends on the intensity of precipitation and its time distribution. When the rainfall intensity exceeds the basin/catchment/drainage area water retention capacity, a series of events follows that lead to surface runoff (Srebrenović 1986). Due to the capacity of the river basin to retain precipitation the difference between the discontinuity of precipitation and the continuity of runoff is increasing (Jevđević 1956) and a more uniform surface water runoff regime (quantity and speed) is generated.

Hydro-meteorological risks due to natural hazards such as severe floods, storm surges, landslides and droughts are causing impacts on different sectors of society (Ruangpan et al. 2020). This paper summarizes the overlapping and differences between two ecosystem-based concepts applied in river basin management and disaster risk reduction planning processes and the contribution of natural water retention measures identified for the Danube River Basin in hydrometeorological risk reduction.

Materials and methods

Ecosystem-based disaster risk reduction (Eco-DRR) is the sustainable management, conservation and restoration of ecosystems to reduce disaster risk, with the aim of achieving sustainable and resilient development (Estrella and Saalismaa 2013).

Natural Water Retention Measures (NWRM) are multifunctional measures that aim to protect and manage water resources and address water–related challenges by restoring or maintaining ecosystems as well as natural features and processes (EC DGE 2015).

Given the multifunctional benefits of NWRMs, these measures are identified in the Danube River Basin Flood Risk Management Plan (DFRMP) Update 2021 (ICPDR).

Based on previous research (Matić and Karleuša 2022) Figure 1 is prepared and it clearly indicates that NWRM implementation within the Danube River basin supports resilience to hydrometeorological hazards and Ecosystem-based disaster risk reduction (Eco-DRR) approach integration in the disaster risk reduction plans.

Results and concluding remarks

The interactions of two concepts presented in this paper manifest the significance of the NWRMs application to increase the resilience to hydro-meteorological hazards at the river basin level. In addition to multifunctional benefits, their integration into planning processes should be based on cooperation among various sectors and stakeholders from local to transboundary scale.

Due to increased interest in ecosystem-based approaches within scientific and professional communities, different sectors and organizations developed definitions that might decrease acceptance of concepts and their integration into national policies and strategies action plans.

Although the benefits they provide are numerous, the constraints associated with low-probability events, land ownership, potential space limits in urban areas, etc., should be underlined and mentioned in the planning documents. In addition, their integration with the existing grey infrastructure has to be elaborated comprehensively.

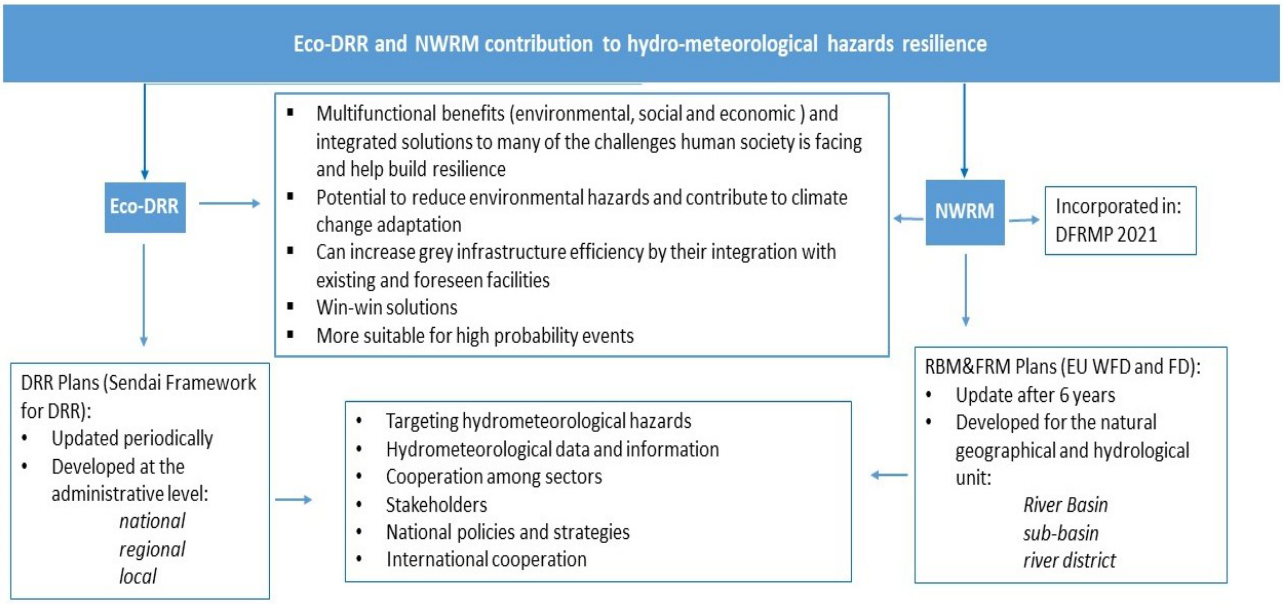

Figure 1. Eco-DRR and NWRM interactions and application (prepared by authors).

Given the nature of hydrometeorological hazards, the level of river basin, sub-basin, and river district - the natural geographical and hydrological unit - instead of administrative or political boundaries should be comprehensively elaborated in disaster risk reduction plans development. Very likely, this will increase full integration and efficiency of the measures.

Acknowledgements: This research and publication of this article is funded by the University of Rijeka within projects “Implementation of Innovative Methodologies, Approaches and Tools for Sustainable River Basin Management” (UNIRI-TEHNIC-18-129) and “Hydrology of Water Resources and Identification of Flood and Mudflow Risk in Karst” (UNIRI-TEHNIC-18-54).

References

Danube River Basin Flood Risk Management Plan (DFRMP) Update 2021, ICPDR, http://icpdr.org/main/publications/danube-flood-risk-management-plan-dfrmp-update-2021

Estrella M, Saalismaa N (2013) Ecosystem-based disaster risk reduction (Eco-DRR): An overview. In: Renaud F G et al. (eds) The role of ecosystems in disaster risk reduction, UNU Press, Tokyo, 26-54

European Commission, Directorate-General for Environment (2015) EU policy document on natural water retention measures: by the drafting team of the WFD CIS Working Group Programme of Measures (WG PoM), Publications Office, https://data.europa.eu/doi/10.2779/396202

Jevđević V (1956) Hidrologija I Deo. special ed, book 4, Hidrotehnički institut “Ing. Jaroslav Černi”, Beograd

Matić BB, Karleuša B (2022) Ecosystem-Based Disaster Risk Reduction Framework as a Tool for Improved River Basin Natural Water Retention Capacity and Environmental Hazard Resilience. Environmental Sciences Proceedings 21(1): 40. https://doi.org/10.3390/environsciproc2022021040

Ruangpan L et al. (2020) Nature-based solutions for hydro-meteorological risk reduction: a state-of-the-art review of the research area. Natural Hazards and Earth System Sciences 20: 243–270. https://doi.org/10.5194/nhess-20-243-2020

Srebrenović D (1986) Primjenjena hidrologija. Tehnička knjiga, Zagreb

Resilience optimization of water quality sensor designs in water distribution networks against cyber-physical attacks

D. Nikolopoulos*, G. Moraitis, G. Karavokiros, D. Bouziotas, C. Makropoulos
Department of Water Resources and Environmental Engineering, National Technical University of Athens, Zografou, Athens, Greece
** e-mail: nikolopoulosdio@central.ntua.gr*

Introduction

Water distribution networks (WDNs) are critical infrastructure for the society, supplying water safe for consumption. Due to their spatially large and disperse nature, there are multiple accessible entry points for malicious contamination actions with biological or chemical agents. Thus, there are ever-growing concerns about the security of WDNs (Nikolopoulos et al. 2021), especially in view of the severe consequences (fatalities, illnesses, monetary and reputational losses) from historical accidental contamination incidents, like the Milwaukee cryptosporidium outbreak in 1993. Water utilities typically employ contamination warning systems (CWS) to secure WDNs via the timely detection of contaminants through a water quality sensor network, and the activation of response and mitigation measures (public warnings, supply cut-off, flushing contaminants etc.). The design problem of optimal placement of water quality sensors has been extensively investigated in the literature, with various different approaches and optimization schemes emerging, although it remains an open problem for practical applications. A CWS is essentially a component of the SCADA (system control and data acquisition) system installed, which typically connects to the main business/corporate network and to the Internet for remote control and monitoring; thus, it is exposed to cyber-attacks, digital threats recently gaining attention in the water sector. An increasing number of cyber-attack incidents targeting water infrastructure have been recorded (Tuptuk et al. 2021). Particularly threatening attack scenarios comprise cyber-attacks on the CWS (e.g., manipulating water quality readings of sensors, or making them go offline), complementing physical ones on the WDN, like backflow contaminant injection, with the intent to mask the event (Nikolopoulos and Makropoulos 2022). We argue that such scenarios should be incorporated into the formulation of sensor design strategies with the intent to maximize the WDN's resilience against cyber-physical attacks. In this work, we present a cyber-physical resilience optimization framework as formulated by Nikolopoulos and Makropoulos (2023), expanded by the inclusion of more performance metrics for the objective function evaluation.

Methodology

For the definition of resilience in the context of CWS performance under cyber-physical attacks, we rely on the modification of the resilience assessment framework by Makropoulos et al. (2018) as described in Nikolopoulos and Makropoulos (2023). Resilience is "the degree to which the water quality sensor design continues to perform under progressively increasing disturbance". Performance is measured through the expected value of a typical metric for sensor placement (expanded in this work to include population affected, contamination extent, time to detection and mass consumed), whereas disturbance is introduced though a series of scenario ensembles. Each ensemble describes individual combinations of sensor failures because of cyber-attacks (e.g., 1, 2, ..., X sensors failing from the installed pool), combined with backflow injection attacks on all possible locations in the WDN. Simulation results from stress-testing the system against these scenarios constitute a "resilience profile graph", where on the x-axis are the cyber-physical attack scenarios and on the y-axis the performance metric's value. Resilience is communicated as the area under the performance curve, scaled from 0 to 1 by comparing with the ideal system's performance curve area, as shown in Figure 1. A more resilient sensor design can resist more disturbance (number of sensors failing) from cyber-attacks, retaining the capacity to operate and identify contamination events (which constitute the physical part of the attacks). A complex resilience evaluation routine leverages results from

hydraulic and quality simulations of the WDN for the placement of *N* number of new water quality sensors in a pool of preinstalled *R* sensors. The routine works with different performance metrics for evaluation and calculates the expected performance in the cases of $k=\{0,1,2,\ldots,N+R-1\}$ sensors failing, and includes a Monte Carlo scheme for the evaluations if the number $N+R$ is high, leading to numerous combinations for scenarios. The resilience evaluation routine is combined with an optimization scheme, where the control variable is the list of new sensor locations, allowing the following optimization problems to be expressed: a) the generation of an entirely new sensor design that maximizes resilience in terms of the performance metric selected, and b) the upgrade of an existing sensor design with more sensors, aiming to maximize the resilience in terms of the performance metric selected.

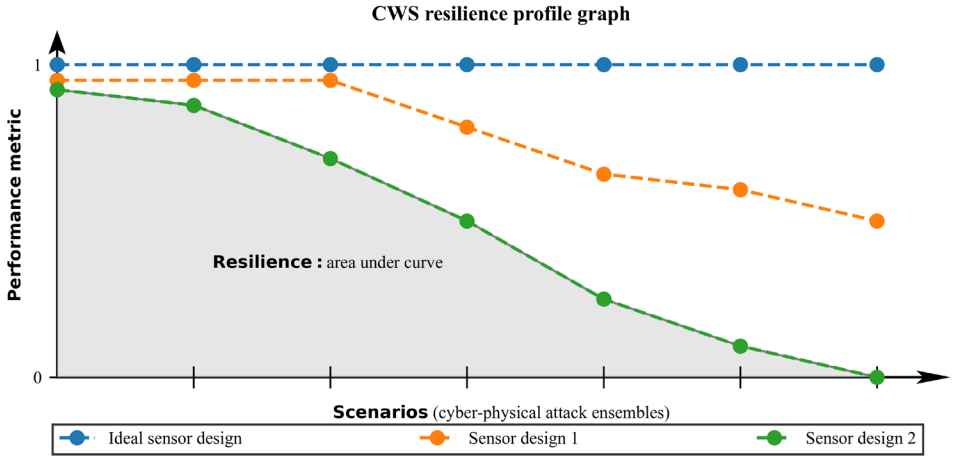

Figure 1. Resilience profile graphs for two sensor designs, compared to the ideal sensor design.

Results and concluding remarks.

The cyber-physical resilience optimization framework is used to generate sensor designs for a variety of different real-world systems and is compared with designs generated conventionally with widely used performance metrics, against scenarios of cyber-physical attacks and under the benchmark "nominal" case of only physical attacks. Results show that resilient designs perform significantly better under cyber-physical attacks, while there are minimal performance losses in the nominal cases, across all different systems. As such, the described resilience optimization framework can be a useful tool for designing safe water quality sensor layouts for systems where cyber-physical concerns are critical.

Acknowledgments: The research work was supported by the project PROCRUSTES which is funded by the Hellenic Foundation for Research and Innovation (H.F.R.I.) under the "First Call for H.F.R.I. Research Projects to support Faculty members and Researchers and the procurement of high-cost research equipment grant" (Project Number: HFRI-FM17-2918).

References

Giudicianni C, Herrera M, Di Nardo A, Creaco E, Greco R (2022) Multi-Criteria Method for the Realistic Placement of Water Quality Sensors on Pipes of Water Distribution Systems. Environmental Modelling and Software 152: 105405. https://doi.org/10.1016/j.envsoft.2022.105405

Nikolopoulos D, Makropoulos C (2022) Stress-Testing Water Distribution Networks for Cyber-Physical Attacks on Water Quality. Urban Water Journal 19(3): 256–70. https://doi.org/10.1080/1573062X.2021.1995446

Nikolopoulos D, Makropoulos C (2023) A Novel Cyber-Physical Resilience-Based Strategy for Water Quality Sensor Placement in Water Distribution Networks. Urban Water Journal 20(3):278-297. https://doi.org/10.1080/1573062X.2023.2174032

Nikolopoulos D, Ostfeld A, Salomons E, Makropoulos C (2021) Resilience Assessment of Water Quality Sensor Designs under Cyber-Physical Attacks. Water 13(5): 647. https://doi.org/10.3390/w13050647

Tuptuk N, Hazell P, Watson J, Hailes S (2021) A Systematic Review of the State of Cyber-Security in Water Systems. Water 13(1): 81. https://doi.org/10.3390/w13010081

A study on the reservoir system operation to reduce flood discharge at a downstream junction

Y. Choi[1], S. Yoon[1], H. Shin[2], M. Park[1*]
[1] Korea Institute of Civil Engineering and Building Technology, Goyang, Republic of Korea
[2] Korea Hydro & Nuclear Power Co. Ltd, Gapyeong, Republic of Korea
* e-mail: moon@kict.re.kr

Introduction

A reservoir is an artificial facility that is used to manage water resources. Reservoirs can serve various purposes, including flood control, water supply, and power generation. In the context of flood control, reservoirs are designed to store excess water during flood season, which can help prevent downstream flooding. To design the flood control volume of a reservoir, engineers must determine its design flood volume calculated statistically by the historical flood or rainfall data (Han et al. 2022). However, over time, changes in precipitation patterns, land use, and other environmental factors can alter the hydrological regime of a watershed, which may impact the design flood of a reservoir. In this study, the design flood volume of two reservoirs connected in parallel was recalculated, and the flood control volume of the reservoirs and the flood volume at the downstream junction were evaluated. These reservoirs, the Hwacheon and Soyanggang Reservoirs, built in 1944 and 1973, have never been re-evaluated for their flood volume at the confluence considering the operations of these reservoirs. As a result of the analysis, when a 200-year frequency flood flowed into the reservoirs, it was found that each dam could control the floods safely using existing flood control volume and operating rules. However, the peak discharge at the downstream junction exceeded the designed flood discharge. New operation rules for each reservoir were analysed to reduce the peak flood volume at the junction. As a result, it was proposed to increase the flood control volume of the Hwacheon Reservoir by lowering the initial water level through pre-release before the flood flow-in and to reduce the maximum release amount of the existing operation rule for the Soyanggang Reservoir. It was confirmed that the peak discharge at the junction could be lowered below the design flood volume when the two reservoirs are operated with these new operating methods.

Materials and methods

The Hwacheon and Soyanggang Reservoirs are located in the North-Han River basin in South Korea, and their basin areas are 3,901 km^2 and 2,703 km^2, respectively (Figure 1). The frequency analysis must use long-term flow data to calculate the design flood volume. However, if there is no long-term flow data, the design flood volume can be calculated through rainfall-runoff analysis with frequency analysis results using historical rainfall data. Although the historical flow data for the reservoirs in this study area is long-term (over 30 years), it is unsuitable for frequency analysis due to many missing periods and outliers. Therefore, in this study, the 200-year flood was calculated based on the rainfall-runoff analysis using the 200-year rainfall data estimated through the frequency analysis with the rainfall data until 2021. These reservoirs' recalculated 200-year peak floods were 7,780 m^3/s and 12,349 m^3/s, respectively.

The HEC-ResSim was used to simulate the reservoir system in this study (Klipsch et al. 2021). It is suitable for simulating and analyzing the operation of single reservoirs and tandem or parallel reservoir systems. A reservoir system simulation model was constructed using these inflow data. The operation rule consisted of a total of 6 cases in consideration of the situation of each reservoir. Case 1 was a model that applied the existing operation rules of each reservoir, and cases 2 and 3 were models that applied the existing rule to the Soyanggang Reservoir and utilized an emergency spillway and an additional flood control volume (3 m) below the flood-restricted water level to Hwacheon Reservoir, respectively. Case 4 was a model that applied a new rule that reduced the maximum discharge (5,500 m^3/s) from the existing Soyanggang Reservoir operation rule to 5,000 m^3/s, while the existing operation rule was applied to

Hwacheon Reservoir. Case 5 and 6 were models that applied the new operation rule (maximum release 5,000 m^3/s) to Soyanggang Reservoir and utilized an emergency spillway and an additional flood control volume (3 m) below the flood-restricted water level to Hwacheon Reservoir, respectively.

Figure 1. Study reservoirs.

Results and concluding remarks

Table 1 shows the reservoir system simulation results. The flood rate at the junction was higher than the sum of the releases of the two dams, as the tributary flow between each dam and the junction was considered. As a result of the analysis, in Case 1, where the existing operation rules were applied to each dam, the peak flow (16,828 m^3/s) exceeded the design flood discharge (16,440 m^3/s) at the junction. In Case 2, the peak flow was 16,813 m^3/s, which was decreased compared to Case 1 but exceeded the design flood discharge. The peak flow was not exceeded the design flood discharge in Cases 3 – 6. The rule applied to Case 6 was the most effective operation rule regarding reducing peak flood at the junction. This rule reduced the maximum release from the Soyanggang Reservoir to 5,000 m^3/s and secured an additional flood control volume at the Hwacheon Reservoir.

Table 1. Reservoir system simulation results by each case.

	Case 1	Case 2	Case 3	Case 4	Case 5	Case 6
Maximum release from HC Reservoir (m^3/s)	7,579	7,574	7,569	7,579	7,574	7,569
Maximum release from SYG Reservoir (m^3/s)	5,500	5,500	5,500	5,000	5,000	5,000
Peak flow at the junction (m^3/s)	16,828	16,813	16,013	15,997	16,004	15,749

In many regions of the world, changes in the amount and pattern of rainfall due to climate change are occurring, and there are also many changes in the flow rate. Since many water resource facilities have been designed using the historical data at the design time, the design flood must be checked periodically and applied to analyze the impact on the reservoir and downstream. Also, to reduce flood damage downstream of the reservoir, it is necessary to analyze the operating rules of the parallel reservoir system in consideration of each reservoir's existing operating rules and physical specifications.

Acknowledgments: This work was supported by KOREA HYDRO & NUCLEAR POWER CO., LTD (No. 2018-Tech-20)

References

Han. H, Kwak. J, Kim. D, Jung. J, Joo. H, Kim. H.S. (2022) Development of Simple Method for Flood Control Capacity Estimation of Dam in South Korea. Water 14(9): 1366. https://doi.org/10.3390/w14091366

Klipsch. J. D., Hurst. M. B., Modini. G. C., Black. D. L., O'connell. S. M. (2021) HEC-ResSim Reservoir System Simulation User's Manual Ver.3.3, Davis, CA

The role of meteorological factors in recent advances on drought identification in agricultural and forest ecosystems: A short review

N. Proutsos[1], D. Tigkas[2*], H. Vangelis[2], G. Tsakiris[2]
[1] Institute of Mediterranean & Forest Ecosystems, Hellenic Agricultural Organization "DEMETER", Athens, Greece
[2] Centre for the Assessment of Natural Hazards and Proactive Planning & Lab. of Reclamation Works and Water Resources Management, School of Rural and Surveying Engineering, National Technical University of Athens, Greece
* e-mail: ditigas@mail.ntua.gr

Introduction

Vegetation is particularly vulnerable to extreme events, such as droughts. Several studies indicate that drought events are anticipated to be more frequent and severe in many parts of the globe due to climate change that, in turn, may jeopardise the survival and growth of agricultural and forest ecosystems. Accurate drought characterisation and monitoring is a valuable process for timely evaluation of the risk and responding appropriately for mitigating foreseen damages (yield loss, forest fires, etc.).

Recently, two specialised drought indices were developed, namely the Agricultural Standardised Precipitation Index (aSPI) and the Effective Reconnaissance Drought Index (eRDI), for enhancing the accuracy of well-established drought indices for characterising vegetation-agricultural drought. These indices aim at maintaining the drought characterisation process within a prompt framework through a straightforward and non data-demanding approach. To this end, parameters based on easily accessible meteorological data were used. In this paper, the role of these parameters in characterising drought using the aforementioned indices is examined through a review of recent drought studies in agricultural and forest ecosystems.

Materials and methods

The developed indices focusing on vegetation-agricultural drought are modifications of the broadly used Standardised Precipitation Index (SPI) and Reconnaissance Drought Index (RDI). These indices are relying only on common meteorological parameters (precipitation for both indices and, additionally, potential evapotranspiration for RDI). The aSPI and the eRDI retain the basic structure of the corresponding original index. However, substitute precipitation with effective precipitation (EP), i.e., the portion of the total precipitation that can be used productively by the plants. Data requirements remain the same, since EP is assessed with empirical precipitation-based methods. The concept of EP considers and incorporates additional factors, apart from precipitation, such as evapotranspiration, soil infiltration, runoff, etc. Detailed information on these indices can be found in Tigkas et al. (2017; 2019; 2022).

The performed review analyses studies published within the last 5 years, available in academic databases (Scopus, Google Scholar), using as keywords the names of the indices and similar phrases (e.g. drought, standardised indices). Main criteria for selecting the studies for further evaluation were to include in their objectives the characterisation of drought through these indices and/or the analysis of their outcomes in comparison with the original (SPI, RDI) or other similar drought indices.

Results and concluding remarks

Based on the aforementioned approach, a total of 178 studies were initially collected and, among them, 29 that met the criteria were finally evaluated. The analysis focused on identifying whether the EP parameter used in the modified indices, can enhance the accuracy of vegetation-agricultural drought assessment and/or reduce data demand, having similar performance compared with indices with additional data requirements. An indicative list of selected studies with their main objectives and findings is presented in Table 1.

Table 1. Indicative list of studies with their main objectives and findings.

Study	Main objectives and findings
Nguyen et al. (2023)	Drought impacts on maize and soybean yields in the U.S. during 1979–2019 were assessed. The outcomes showed that the aSPI (using only EP – CropWat method) has similar performance with SPEI (using both P and PET) in assessing drought impacts on crop production.
Teutschbein et al. (2023)	The eRDI was used along with a set of standardized drought indices to represent different nexus sectors (water-energy-food-ecosystem; WEFE) in Sweden. The results examine the propagation of drought through the WEFE nexus, with eRDI indicating the sort of response of the agricultural sector to precipitation deficits in cold climates.
Zarei et al. (2023)	Ten ground-based and remote sensing drought indices have been compared for agricultural drought identification, based on winter wheat yield in Iran. The outcomes indicate that aSPI and eRDI were among the three drought indices that provided the most accurate agricultural drought assessment.
Llanes-Cárdenas et al. (2022)	The sensitivity of SPI, RDI, aSPI and eRDI for the prediction of rainfed maize yield has been evaluated in the region of Sinaloa (Mexico). The outcomes show that aSPI and eRDI for specific reference periods provided the most significant associations, with improved performance compared to the original indices.
Vishwakarma et al. (2022)	Three drought indices (SPI, aSPI, SPEI) have been used to examine their accuracy of representing agricultural drought over Bundelkhand region (India). All indices had similar response, though aSPI appeared to have better performance, also considering the fact that it is using only the EP parameter.
Javed et al. (2021)	The aSPI and the Standardized Vegetation Supply Water Index (SVSWI) were used for agricultural drought characterisation in four regions of China. The results of aSPI, mainly in 3-month timescale which provide similar correlations with SVSWI, revealed the drought effects on winter wheat and corn yield, based on consistent spatiotemporal patterns in the areas of the study region.
Proutsos and Tigkas (2020)	The effect of drought episodes on black pine tree growth is assessed based on SPI, RDI, aSPI and eRDI. The results illustrate that aSPI and eRDI are more sensitive in this task compared to the original indices, indicating their accuracy on drought characterisation in the forest environment.

The analysis of the studies reveals that the use of EP enhances, indeed, the ability of aSPI and eRDI to characterise vegetation-agricultural drought, compared to the corresponding original indices. Regarding aSPI, it seems that the use of only one parameter facilitates the assessment of vegetation-agricultural drought, provided that it has similar performance with indices using additional parameters (e.g. SPEI). Furthermore, it is shown that the selection of the most suitable method for estimating the EP in each region may have a significant role in increasing the accuracy of the utilised index. Overall, based on the analysed studies, both aSPI and eRDI appear to have a satisfactory performance in characterising drought in agricultural and forest environments.

References

Javed T, Zhang J, Bhattarai N, Sha Z et al. (2021) Drought characterization across agricultural regions of China using standardized precipitation and vegetation water supply indices. Journal of Cleaner Production 313: 127866

Llanes-Cárdenas O, Norzagaray-Campos M, Gaxiola A et al. (2022) Sensitivity of four indices of meteorological drought for rainfed maize yield prediction in the state of Sinaloa, Mexico. Agriculture 12(4): 525

Nguyen H, Thompson A, Costello C (2023) Impacts of historical droughts on maize and soybean production in the southeastern United States. Agricultural Water Management 281: 108237

Proutsos N, Tigkas D (2020) Growth response of endemic black pine trees to meteorological variations and drought episodes in a Mediterranean region. Atmosphere 11(6): 554. http://doi.org/10.3390/atmos11060554

Teutschbein C, Jonsson E, Todorović A, Tootoonchi F, Stenfors E, Grabs T (2023) Future drought propagation through the water-energy-food-ecosystem nexus–A Nordic perspective. Journal of Hydrology 617: 128963

Tigkas D, Vangelis H, Proutsos N, Tsakiris G (2022) Incorporating aSPI and eRDI in Drought Indices Calculator (DrinC) Software for Agricultural Drought Characterisation and Monitoring. Hydrology 9: 100. https://doi.org/10.3390/hydrology9060100

Tigkas D, Vangelis H, Tsakiris G (2017) An Enhanced Effective Reconnaissance Drought Index for the characterisation of agricultural drought. Environmental Processes 4(suppl 1): 137-148. http://doi.org/10.1007/s40710-017-0219-x

Tigkas D, Vangelis H, Tsakiris G (2019) Drought characterisation based on an agriculture-oriented standardised precipitation index. Theoretical and Applied Climatology 135: 1435-1447. http://doi.org/10.1007/s00704-018-2451-3

Vishwakarma A, Choudhary MK, Chauhan MS (2022) Non-parametric trend and the validity of a newly developed drought indicator for agricultural application over the central India region. Arabian Journal of Geosciences 15(4): 365

Zarei AR, Mokarram M, Mahmoudi MR (2023) Comparison of the capability of the Meteorological and Remote Sensing Drought Indices. Water Resources Management 37: 769–796

Large river diversion effects on downstream sediment transport and channel dynamics: A case from the lowermost Mississippi River

Y.J. Xu[1,2]
[1] School of Renewable Natural Resources, Louisiana State University, Baton Rouge, United States
[2] Coastal Studies Institute, Louisiana State University, Baton Rouge, United States
* e-mail: yjxu@lsu.edu

Introduction

Large rivers in the world are often engineered to meet societal needs for a variety of purposes including navigation, flood control, and water supply. One of the engineering practices is river diversion, which can strongly alter natural processes of sediment transport and channel dynamics. Diverting a river can change downstream sediment load and distribution over time, making the diversion unstable and potentially leading to a complete river avulsion (Kleinhans et al. 2013). Such avulsion of large lowland alluvial rivers could be catastrophic for their densely-populated delta, for instance, the Mississippi River Delta (Wang and Xu, 2018). In this paper, we synthesize the findings from our recent studies on the long-term sediment transport and riverbed deformation within and downstream of the Mississippi-Atchafalaya River diversion, also famously known as the Old River Control Structure (ORCS). We focus on two critical questions: 1) How the river channel beds within and downstream of the ORCS have changed over the past three decades, and 2) if the river diversion has maintained a proportionate water-sediment diversion. Answers to these questions provide insights into sediment transport in the backwater zone of one of the world's largest and most engineered alluvial rivers.

Materials and methods

The Mississippi River (MR) enters the Northern Gulf of Mexico through its main channel extending southeasterly and its distributary - the Atchafalaya River (AR) - located to the west on the Louisiana central coast (Figure 1). Since the early 20th century, the flow from the MR into the AR kept increasing, raising the concern that the AR would soon capture the entire MR flow. To prevent such an avulsion from happening, the US Army Corps of Engineers completed a river diversion structure, the ORCS. The ORCS was designed to maintain a 24% water diversion (Horowitz 2010; Xu et al. 2021) but a 30-60% sediment diversion (Mossa and Roberts, 1990) from the MR into the AR under normal flow conditions.

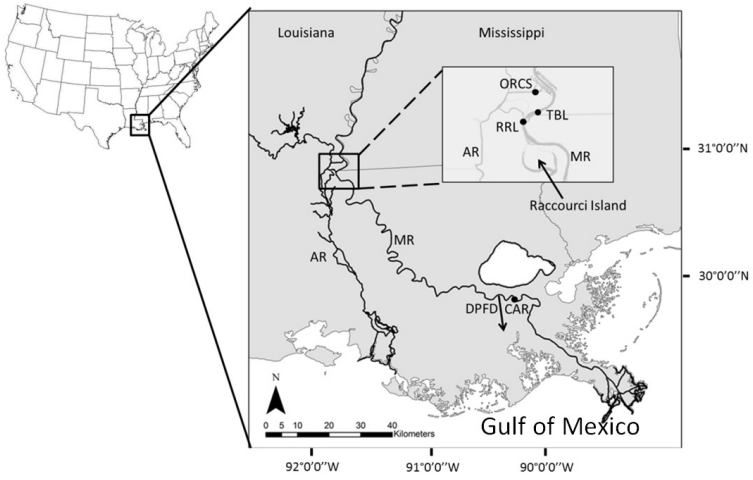

Figure 1. Geographical locations of the MR, AR and ORCS in Southern United States.

A series of large data sets were used in the assessments presented in this paper including, among

others:

- channel bathymetric surveys and navigation charts from 1967 to 2013, which were used to assess riverbed elevation and volume changes;
- long-term records on river discharge, stage and sediment concentration at several locations along the MR and AR, which were utilized to estimate riverbed material and suspended sediment loads;
- multi-year remote sensing data, which were employed to determine changes in channel form and bar over the past three decades.

Results and concluding remarks

Over the past several decades, the Mississippi River mainstem downstream of the ORCS experienced considerable channel aggradation, while the Atchafalaya River downstream of the ORCS showed large channel erosion (Figure 2). From 2004 to 2013, approximately 24% of the MR flow was diverted into the AR, but only about 17% of riverbed material load passed through the diversion channel to the AR.

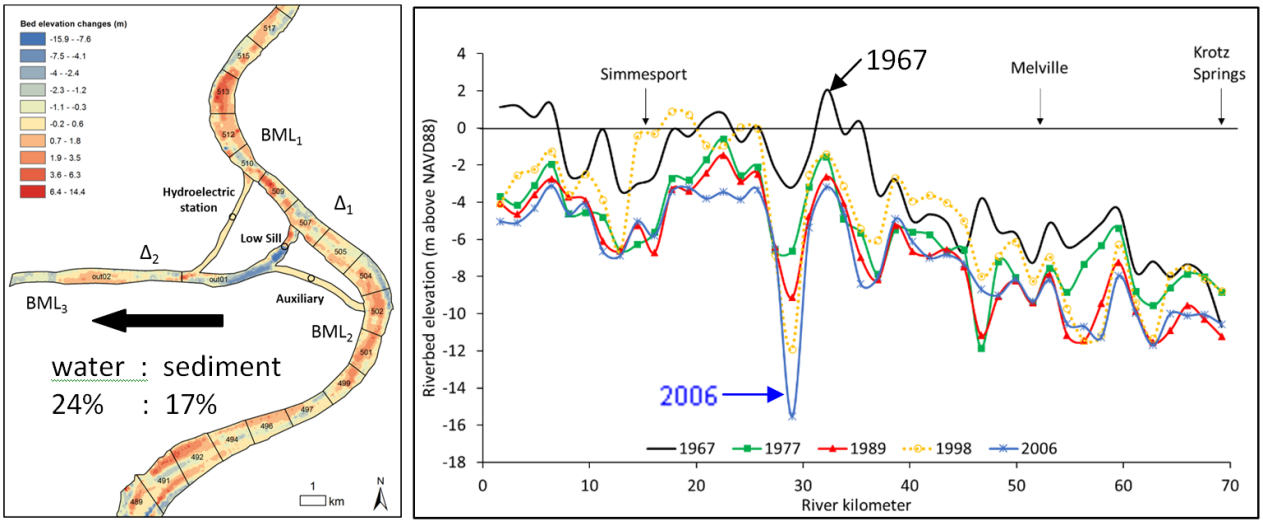

Figure 2. Left: bed elevation change in the MR and diversion channels; Right: bed elevation change in the AR. Figures are modified from Wang and Xu (2020) and Xu et al. (2021).

The sediment diversion from the MR to the AR was far less than the designed sediment diversion ratio (i.e., 30-60%). This disproportionate flow/sediment ratio (24%/17%, Figure 2) has caused the MR mainstem channel to aggrade and the AR channel to degrade. The aggradation has reduced channel flow capacity, and the degradation has increased the channel hydraulic gradient between the AR and MR. These findings imply a potential risk of having high backwater on the MR mainstem during mega floods and a tendency of the backwater overpowering the diversion control structure. This highlights the important role that flow/sediment ratio can play in maintaining the long-term stability of a river diversion.

Acknowledgments: This research received funding support from NSF, NFWF, and USDA. The author is grateful to the USGS and USACE for making river discharge, bathymetry and sediment data available.

References

Kleinhans MG, Ferguson RI, Lane SN, Hardy RJ (2013) Splitting rivers at their seams: Bifurcations and avulsion. Earth Surface Processes and Landforms, 38(1), 47–61. https://doi.org/10.1002/esp

Mossa J, Roberts HH (1990) Synergism of riverine and winter storm-related sediment transport processes in Louisiana's coastal wetlands. Transactions Gulf Coast Association of Geological Societies, 40, 635–642

Wang, B, Xu, YJ (2018) Decadal-scale riverbed deformation and sand budget of the last 500 km of the Mississippi River: Insights into natural and river engineering effects on a large alluvial river. Journal of Geophysical Research: Earth Surface, 123. https://doi.org/10.1029/2017JF004542

Wang B, Xu YJ (2020) Estimation of bedload sediment fluxes upstream and downstream of a controlled bifurcation node - the Mississippi-Atchafalaya river diversion. Hydrological Processes, https://doi.org/10.1002/hyp.13771

Xu YJ, Wang B, Xu W, Tang M, Tsai FTC, Smith LCS (2021) Four-decades of bed elevation changes in the heavily regulated upper Atchafalaya River, Louisiana, USA. Geomorphology. doi: 10.1016/j.geomorph.2021.107748

Flood mapping using remote sensing and geographical information systems in Karditsa region, Greece

G. Karoni, E. Tzimika, L. Vasiliades*, M. Spiliotopoulos, N. Mylopoulos
Department of Civil Engineering, School of Engineering, University of Thessaly, Pedion Areos 38334 Volos, Greece
** e-mail: lvassil@civ.uth.gr*

Introduction

Floods are a common natural disaster that can cause significant damage to communities and their infrastructure. In order to mitigate the impact of floods, effective flood risk assessment and management strategies are required. This is where the combination of Remote Sensing and Geographical Information Systems (GIS) can play a crucial role. Flood mapping with GIS and remote sensing is a useful tool for detecting flood risk zones and developing flood susceptibility maps (Wang and Xie 2018). Remote sensing images are used as base maps for flooded areas since they can be acquired in all weather conditions and at any time. The analysis of remote sensing data through GIS techniques allows the gathering of different datasets to reveal high-risk areas and generate flood hazard maps (Munawar et al. 2022). Flood-inundated areas have been mapped using a combination of geographical information systems, remote sensing, and multi-criteria decision analyses (Abdullah et al. 2021; Albertini et al. 2022).

By integrating satellite data with other updated spatial and non-spatial data, potential flood mapping areas can be estimated (Papaioannou et al. 2015). The objective of this study is to estimate potential flood zones for the Prefecture of Karditsa, Thessaly, Greece and to compare the accuracy of the derived zones with an observed flood event caused by the Medicane (Mediterranean Hurricane) "*Ianos*" on September 18th, 2020. Medicane "*Ianos*" affected Thessaly and had produced substantial structural damages, including flash flood associated consequences that led in four deaths and extended infrastructure losses and landslides mainly in the Prefecture of Karditsa (Lagouvardos et al. 2021).

Materials and methods

In this study, Sentinel 2 images acquired from the *Copernicus Open Access Hub* for the 20th and 25th of September 2020 and used for observed flood extent modelling. Two remote sensing indices were used to estimate observed flooded areas of the "*Ianos*" flood event: the Normalized Different Water Index (NDWI) of Gao (Gao 1996) and the NDWI of McFeeters (McFeeters 1996). It should be mentioned that the NDWI takes values between -1 and +1, and the potential water bodies have values above zero (0) and dry areas below zero (0). After the estimation process of the two (2) indices, the distinction between the water bodies and non-water areas was performed using sensitivity analysis. Several thresholds were investigated covering a wide range of index values such us 0.1, 0.2, 0.3, 0.5, etc. Subsequently, the study presents the statistical analysis of the affected land uses / land covers on the 20th of September 2020.

In the second part, the flood hazard map is assessed and estimated using topographic and geomorphological indices using the Analytical Hierarchy Process (AHP) (Saaty 1987). Regarding to the Flood Hazard Index map, a Digital Elevation Model (DEM) with pixel size 20x20 is selected to produce the Dem derivatives and Aspect, Slope, Flow Direction, Flow Accumulation, Stream Power Index, Topographic Position Index, Topographic Wetness Index, Horizontal Overland Flow Distance and Vertical Overland Flow Distance maps are estimated. Furthermore, Curve Number of the SCS method and Rainfall maps are produced using the available information. Cross-correlation analysis identified the most important geomorphological parameters, and these parameters are selected for mapping potential flooded areas. In order to apply the AHP method, all the parameters were normalized in the scale 1-10 using the appropriate functions for each parameter and the flood indices are estimated and evaluated. Three (3) scenarios are examined: the 1st one using eight (8) indices, the 2nd using seven (7) and the 3rd using six (6) indices, respectively. Furthermore, they were formed three eigenvector matrixes from which the weights of every

index were calculated. The consistency of the matrixes has been done calculating the Consistency Ratio (CR) which should be lower than 0.1. Completing the evaluation of each AHP scenario, three Flood Hazard Index maps were produced using the type of the Flood Hazard Index (FHI, Equation 1):

$$FHI = \sum_{i=1}^{n} r_i * w_i \quad (1)$$

Results and concluding remarks

In the Prefecture of Karditsa, the integration of GIS and remote sensing technologies demonstrate the potential to provide valuable information for flood mapping, which can be used to support decision-making processes and enhance flood preparedness and response efforts. The results from the two remote sensing NDWI indices were evaluated and validated and with the observed flooded area estimated from Sentinel images by the Copernicus Emergency Management Service (EMSR465: Floods in Thessaly Region, Greece). Hence, using the sensitivity analysis the best fitted threshold value was the NDWI value of 0.3 (=index threshold) for date 20th of September. Similar results are also obtained for the date 25th of September 2020. According to the statistical analysis using Corine Land Cover 2018 data, the most affected land uses areas on the 20th of September were agricultural areas with a percentage of 81%, following by the forest and seminatural areas with 16%, artificial surfaces and water bodies with 1% flood areas, and wetland areas with less than 1% flooded areas.

Application of the AHP method estimated the FHI for the three examined scenarios. Comparison of the derived three (3) FHI maps with the NDWI showed that the 2nd scenario with the seven (7) indices seems to be the more reliable and capable in in flood prone area mapping. Furthermore, the selected map was evaluated according to the physical (slope, average latitude etc.) and hydrogeological features of the sub basins. As a result, it was produced a final flood prone map categorized in three groups of high flood risk, relatively high flood risk and moderate flood risk.

In conclusion, the integration of remote sensing and GIS has the potential to play a crucial role in flood risk assessment and management. This study evaluated potential flood prone areas in the Prefecture of Karditsa, Thessaly Greece, using remote sensing and gis data and analysis techniques, thus improving the ability to respond to future flood events. By providing valuable information for flood mapping and a comprehensive understanding of the spatial distribution of flood risk, this technology can support decision-making processes and enhance flood preparedness and response efforts.

References

Abdullah MF, Siraj S, Hodgett RE (2021) An Overview of Multi-Criteria Decision Analysis (MCDA) Application in Managing Water-Related Disaster Events: Analyzing 20 Years of Literature for Flood and Drought Events. Water 13: 1358. https://doi.org/10.3390/w13101358

Albertini C, Gioia A, Iacobellis V, Manfreda S (2022) Detection of Surface Water and Floods with Multispectral Satellites. Remote Sensing 14:6005. https://doi.org/10.3390/rs14236005

Gao B (1996) NDWI—A normalized difference water index for remote sensing of vegetation liquid water from space. Remote Sensing of Environment 58:257–266. https://doi.org/10.1016/S0034-4257(96)00067-3

Lagouvardos K, Karagiannidis A, Dafis S, et al. (2021) Ianos - A hurricane in the Mediterranean. Bulletin of the American Meteorological Society 1–31. https://doi.org/10.1175/BAMS-D-20-0274.1

McFeeters SK (1996) The use of the Normalized Difference Water Index (NDWI) in the delineation of open water features. International Journal of Remote Sensing 17: 1425–1432. https://doi.org/10.1080/01431169608948714

Munawar HS, Hammad AWA, Waller ST (2022) Remote Sensing Methods for Flood Prediction: A Review. Sensors 22:960. https://doi.org/10.3390/s22030960

Papaioannou G, Vasiliades L, Loukas A (2015) Multi-criteria analysis framework for potential flood prone areas mapping. Water resources management 29:399–418

Saaty RW (1987) The analytic hierarchy process—what it is and how it is used. Mathematical Modelling 9: 161–176. https://doi.org/10.1016/0270-0255(87)90473-8

Wang X, Xie H (2018) A Review on Applications of Remote Sensing and Geographic Information Systems (GIS) in Water Resources and Flood Risk Management. Water 10:608. https://doi.org/10.3390/w10050608

Agricultural drought risk and vulnerability assessment in Maharashtra, India

G. Ganjir[1*], M.J. Reddy[1,2], S. Karmakar[1,3]
[1] IDP in Climate Studies, IIT Bombay, Mumbai, India
[2] Department of Civil Engineering, IIT Bombay, Mumbai, India
[3] Centre for Environmental Science and Engineering, IIT Bombay, Mumbai, India
* e-mail: 214406001@iitb.ac.in

Introduction

In recent times, there is substantial increase in drought events across the globe under the changing climate, which has very adverse effect on humans, animals, and vegetation. In India, most of the population depend on agriculture for their livelihood. Hence, it is crucial to have a drought assessment for every location because the repercussions of this cause migration of people and animals, leaving behind barren land. According to the Fifth Assessment Report (AR5) of the Intergovernmental Panel on Climate Change (IPCC) (IPCC 2014), the risk of an extreme event can be calculated as a function of hazard, vulnerability, and exposure. Vittal et al. (2020) have included exposure to be an integral part of the vulnerability, since such a definition does not alter the overall conclusions of risk assessment. In order to conduct a thorough study of the drought risk, it is necessary to choose the right drought indicators for hazard analysis and the right drought vulnerability indicators and appropriate aggregation method for vulnerability analysis (Sahana et al. 2021). Due to sensitive demography in the study region, areas with typical hazard circumstances became hotspots of drought risk, emphasising the significance of socioeconomic characteristics (Singh et al. 2019). The present study aims to develop district-level agriculture drought risk map using the IPCC risk framework, accomplished by agricultural drought hazard map and vulnerability map.

Materials and methods

In order to assess the agricultural drought hazard, the root zone soil moisture data from the Global Land Evaporation Amsterdam Model (GLEAM) available at 0.25° for the period 1980-2021 was used. The data was processed to get the area averaged soil moisture at district level and computed the standardised soil moisture index (SSMI) (Han et al. 2021) using Eq. 1.

$$SSMI_{ij} = (SM_{ij} - \mu_{SMi}) / \sigma_{SMi} \quad (1)$$

where $SSMI_{ij}$ is the SSMI for month *i* and year *j*, SM_{ij} is the mean soil moisture values, μ_{SMi} *and* σ_{SMi} are the mean and standard deviations of soil moisture of month *i* across all years.

The drought properties, duration and severity, are calculated using the run theory. The hazard is computed by adding normalised maximum duration, maximum severity, and total number of drought events. The vulnerability map is generated by considering eight indicators, namely total working population, population density, population SC and ST, literacy rate, total number of wells and tube wells, ground water level, net irrigated area and this data was obtained from census 2011 at district level. These indicators were classified as exposure, sensitivity, and adaptive capacity. The literacy rate, net irrigated area and total number of wells and tube wells falls under the adaptive capacity which means the higher the values, the lower will the vulnerability. The TOPSIS tool (Technique for Order Preference by Similarity to Ideal Solution) (Hwang and Yoon 1981), a technique useful in dealing with multi-attribute or multi-criteria decision making was used to rank the various indicators of vulnerability, and it does not have subjectivity as in Analytical Hierarchy Process. This study defined the risk as the function of vulnerability and hazard. Further, to have a better understanding of drought risk in the region, bivariate choropleth risk map was created (Figure 1). Such maps can clearly depict the hazard-driven and vulnerability-driven risk.

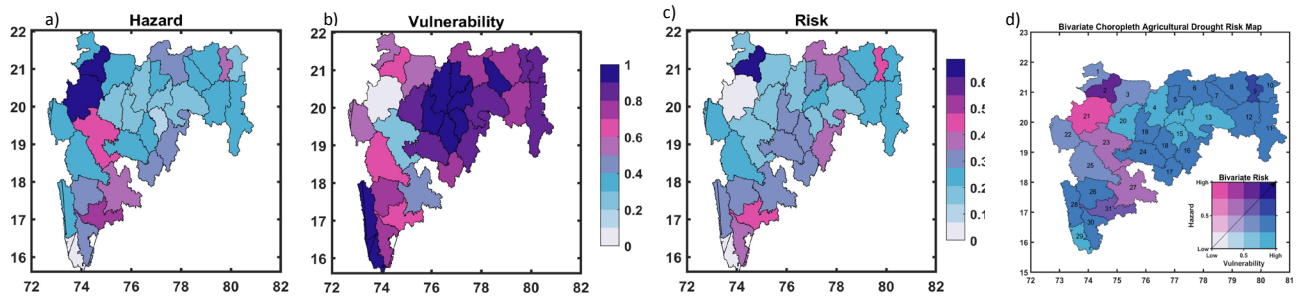

Figure 1. Spatial variation of agricultural drought hazard (a), vulnerability (b), risk (c), and bivariate choropleth risk map of Maharashtra (d); the districts are represented with numbers.

Results and concluding remarks

The study assessed the drought risk in Maharashtra state of India by combining drought hazard and drought vulnerability in the region. The maps clearly show the districts with high hazard and vulnerability. The highest drought hazard can be seen in Dhule (2) and Nashik (21). The Ahmadnagar (23), Sangli (31) and Bhandara (9) districts falls under moderate drought hazard and least hazard is seen in Sindhudurg (29) district. The drought properties box plot analysis was performed and the 75 percentile values of duration and severity for all districts falls below 5 months and 8 respectively, whereas maximum drought of 16 months and maximum severity of 28 was noted for Nashik (21). The vulnerability map shows the western district and central Maharashtra is the most vulnerable, whereas Nashik (21) is the least vulnerable. This is reflected in the risk map as high vulnerability and least hazard and vice versa results in the least risk; hence the Nashik and Sindhudurg districts shows the least risk, the highest risk is seen in Dhule (2), south-eastern districts have high risk. The bivariate risk map shows Bhandara (9) district has equally high hazard and high vulnerability Also, the districts with high hazard are less vulnerable which reduces the risk. The bivariate choropleth analysis demonstrates that in south-eastern districts, susceptibility brought on by socio-economic factors greatly influences drought risk rather than variations in hazard due to the climate change. Consequently, improving socioeconomic circumstances must be a part of future efforts to increase drought resilience in Maharashtra. The results have great potential and can be used by the policy makers and government agencies for managing agricultural droughts in Maharashtra.

Acknowledgments: The research work is financially supported by the Department of Science and Technology DST - Centre of Excellence in Climate Studies IIT Bombay DST/CCP/CoE/140/2018 (G) Code (RD/0117-DST0000-038).

References

Han Z, Huang Q, Huang S, Leng G, Bai Q, Liang H, Wang L, Zhao J, Fang W (2021) Spatial-temporal dynamics of agricultural drought in the Loess Plateau under a changing environment: Characteristics and potential influencing factors. Agricultural Water Management 244: 106540. https://doi.org/10.1016/j.agwat.2020.106540

Hwang C L, Yoon K (1981) Methods for Multiple Attribute Decision Making. In: Multiple Attribute Decision Making. Lecture Notes in Economics and Mathematical Systems, Vol. 186, Springer, Berlin, Heidelberg. https://doi.org/10.1007/978-3-642- 48318-9_3

IPCC: Climate Change (2014) Impacts, Adaptation and Vulnerability. Contribution of Working Group II to the Fifth Assessment Report of the Intergovernmental Panel on Climate Change. Cambridge University Press, Cambridge and New York, ISBN 978-1- 107-05807-1

Sahana V, Mondal A, Sreekumar P (2021) Drought vulnerability and risk assessment in India: Sensitivity analysis and comparison of aggregation techniques. Journal of Environmental Management 299: 113689. https://doi.org /10.1016/j.jenvman.2021.113689

Singh G R, Jain M K, Gupta V (2019) Spatiotemporal assessment of drought hazard, vulnerability and risk in the Krishna River basin, India. Natural Hazards, 99, 611-635

Vittal H, Karmakar S, Ghosh S, Murtugudde R G (2020) A comprehensive India-wide social vulnerability analysis: highlighting its influence on hydro-climatic risk. Environmental Research Letters 15: 014005, https://doi.org/10.1088/1748-9326/ab6499

Is ERA5 able to reproduce flood inundation at the regional scale? A systematic analysis using LISFLOOD-FP

H. Singh, M.P. Mohanty*
Department of Water Resources Development and Management, Indian Institute of Technology Roorkee, Uttarakhand
** e-mail: mohit.mohanty@wr.iitr.ac.in*

Introduction

Reanalysis datasets are collections of weather and climate data that have been reconstructed using modern data assimilation techniques to create a consistent, gridded record of the Earth's atmosphere and surface. These datasets are used by scientists and researchers to study the Earth's climate system, monitor weather patterns, and make weather and climate predictions. ERA5 (ECMWF Reanalysis 5) is a recently released high-resolution global atmospheric reanalysis dataset (Hersbach et al. 2020). Although a few studies have compared the reliability of ERA5 with other reanalyses products and ground truth, its efficacy in reproducing inundation over large regions has not been explored much. The study aims to quantify flood inundation and hazards while considering ERA5 over the severely flood-prone Mahanadi River Basin (geographical area - 1.41 million sq. km) located in the Eastern part of India. To reproduce flood patterns, LISFLOOD-FP, a two-dimensional computationally efficient hydrodynamic model is considered. The study addresses the efficacy of ERA5 as a reliable product to quantify flood hazards at a regional scale, which forms the basis for identifying flood risks to vulnerable communities and assets.

Materials and methods

In the present study, discharge forcing from ERA5 available at a daily-time step and spatial resolution of 0.1° x 0.1° from 1 January 1979 to near real-time is considered. To reproduce the flood inundation over the study region, LISFLOOD-FP, a well-known global hydrodynamic model that simulates the hydrological cycle and water flow in river basins is considered. In addition to the discharge, LISFLOOD-FP requires various other ancillary datasets, such as Digital Elevation Model (DEM), river network, river width, bank and bed elevation etc. The proposed schematic framework for floodplain mapping for the Mahanadi basin is illustrated in Figure 1. The time series discharge values are extracted for the Mahanadi basin for 14 to 18 September 2008 flooding event, and provided as input to LISFLOOD-FP to determine the flood inundation.

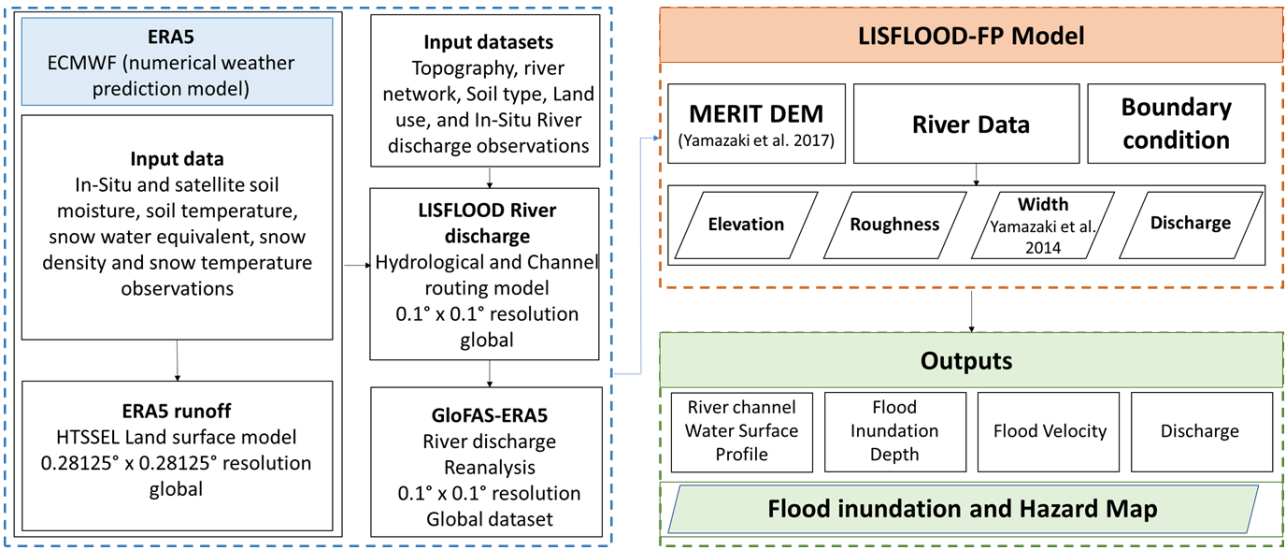

Figure 1. The proposed framework of flood inundation and hazard modelling over Mahanadi river basin.

Results and concluding remarks

The present study quantifies inundation and hazard at a high resolution for major flood events over the Mahanadi river basin, while utilizing the latest ERA5 reanalysis product. It was noticed that ERA5 is competent in capturing the flooding hotspots over the region as compared with the reports of flooding for the taken flooding event. The inundation patterns, especially in areas such as Nayagarh (marked in Section 1 of Figure 2) and Cuttack(Section 2 of Figure 2) which are at the lower floodplains reported to be high flooding inundation in some regions and coastal stretches of entire Jagatsinghpur and Puri (Figure 2, Section 3) which were reported to be entirely flooded with medium inundation was precisely captured, thereby establishing it as a reliable input for flood modelling over large regions. Overall, analysing flood inundation using ERA5 can provide valuable information for flood risk assessment, disaster planning, and management, and can help to improve our understanding of the impacts of climate change on flooding.

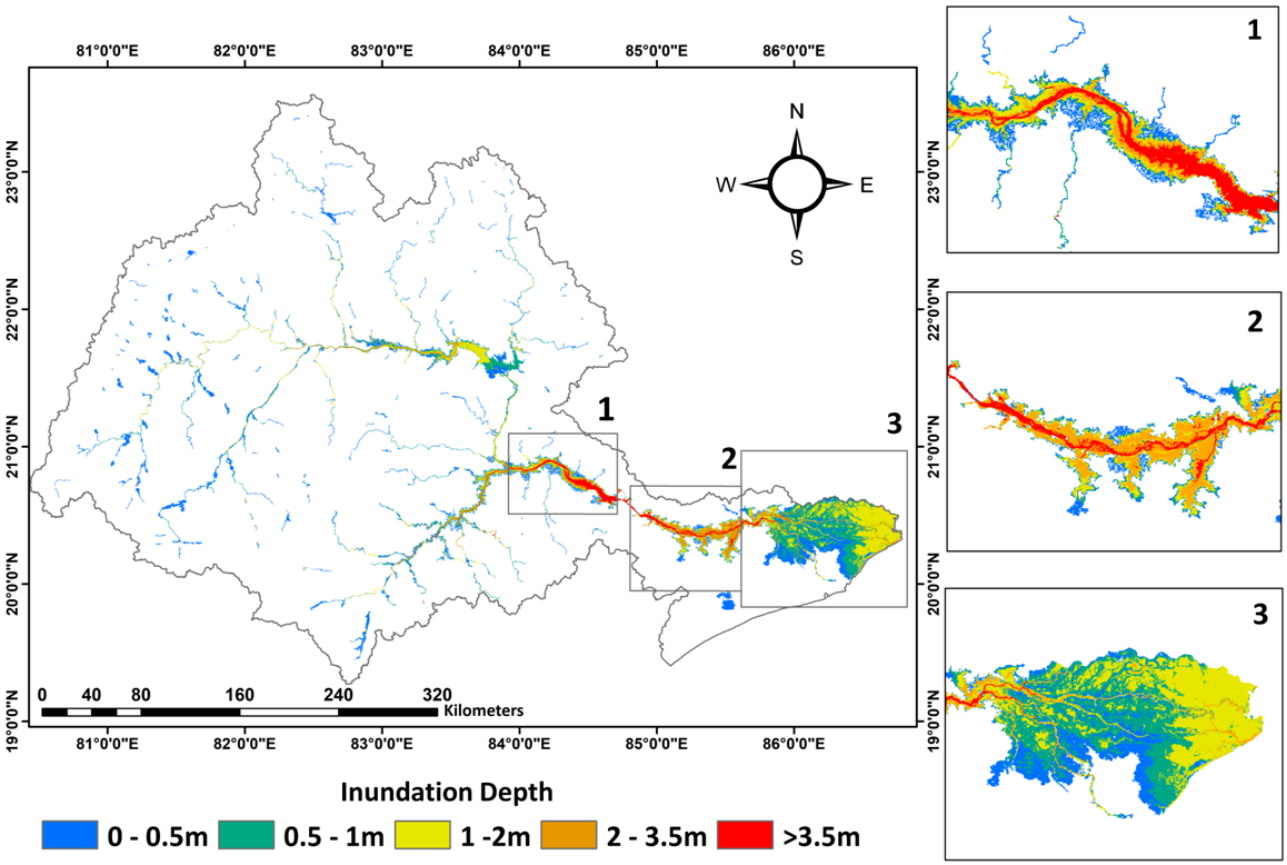

Figure 2. Lisflood-FP Simulation Results obtained using ERA5 Discharge data over Mahanadi River Basin

References

Bates PD, De Roo APJ (2000) A simple raster-based model for flood inundation simulation. Journal of Hydrology 236(1-2): 54-77. https://doi.org/10.1016/S0022-1694(00)00278-X

Harrigan S, Zsoter E, Alfieri L, Prudhomme C, Salamon P, Wetterhall F, Barnard C, Cloke H, Pappenberger F (2020) GloFAS-ERA5 operational global river discharge reanalysis 1979–present, Earth Syst. Sci. Data, 12:2043–2060. https://doi.org/10.5194/essd-12-2043-2020

Hersbach H, Bell B, Berrisford P, Hirahara S, Horányi A, Muñoz-Sabater J, et al. (2020) The ERA5 global reanalysis. Quarterly Journal of the Royal Meteorological Society, 146(730), 1999-2049. https://doi.org/10.1002/qj.3803

Yamazaki D, Ikeshima D, Tawatari R, Yamaguchi T, O'Loughlin F, Neal JC, et al. (2017) A high-accuracy map of global terrain elevations. Geophysical Research Letters 44(11): 5844-5853. https://doi.org/10.1002/2017GL072874

Yamazaki D, O'Loughlin F, Trigg MA, Miller ZF, Pavelsky TM, Bates PD (2014) Development of the global width database for large rivers. Water Resources Research 50(4): 3467-3480. https://doi.org/10.1002/2013WR014664

Fidelity of machine learning models in capturing flood inundation through geomorphic descriptors over Ganga sub-basin, India

V. Tripathi, M.P. Mohanty*, H. Singh
Department of Water Resources Develeopment and Management, IIT Roorkee, Roorkee, Uttarakhand, India
** e-mail: mohit.mohanty@wr.iitr.ac.in*

Introduction

Floods are the most cataclysmic natural hazards worldwide associated with significant economic damage and lives. In such a disaster-looming situation, flood risk assessment is indispensable for ensuring appropriate resilience to vulnerable communities. The first step of flood risk assessment is the identification of flood-prone regions within a watershed. Hydraulic-cum-Hydrodynamic modeling often requires multidimensional inputs and computational resources, which may not be feasible for low, and middle-income nations as they are associated with a significant cost. The fidelity of Geomorphic Flood descriptors (GFDs) for flood inundation mapping has been recognized in recent times. Based on the characteristics of the river basin, GFDs indicate the probability and severity of flooding. The incorporation of Machine Learning (ML) models to flood inundation mapping is widely regarded, however, their application to GFDs is still at a nascent stage (Deroliya et al. 2022). The present study determines the fidelity of various ML models in flood inundation mapping over the severely flood-prone Ganga sub-basin (geographical area of 93,854 km^2). The central aim of the study is to identify the best classification model, which can be employed for accurate flood inundation mapping while incorporating various GFDs. The outcomes from the study suggest a careful selection of an ML model for identifying flood-prone areas, which will further necessitate in the least errors during flood risk mapping.

Materials and methods

In the present study, four well-known machine learning (ML) models: logistic regression (LR), random forest (RF), AdaBoost and K-nearest neighbor (KNN) were employed to classify flooded and non-flooded pixels. The input parameters to these ML models were the GFDs derived from CartoDEM (resolution~1 arc-second). A suite of 15 GFDs was developed: slope (S_l), plan curvature (K_h), profile curvature (K_p), tangential curvature (K_t), topographic wetness index (TWI), downslope index (DI), multi bottom valley flatness index (MRVBF), elevation difference from nearest drainage (H), distance from nearest stream (D), elevation, flow accumulation (A_r), convergence index (CI), geomorphons, stream power index (SPI) and geomorphic flood index (GFI), as represented in Figure 1. S_l, K_h, K_p, K_t and CI captures the local flow behavior, while TWI, DI, H and D captures the global behavior of the flow. MRVBF captures the lowness and flatness of the terrain. Geomorphons represent the landforms of the terrain, while SPI indicates the erosive power of flowing water.

This study essentially considers flood hazard as a binary classification problem, i.e., the classification of a location as either "flooded" or "non-flooded" (Samela et al. 2017). The standard flood hazard map developed by the European Commission, Joint Research Centre (JRC) was considered as the ground truth (Dottori et al. 2016). A tabular dataset was created by generating random points and the values of GFDs at various locations were calculated based on their information of being "flooded" or "non-flooded". This dataset was segregated into "training" and "testing" in a ratio of 70:30. A grid search approach was adopted to estimate the best hyperparameter of these classification models, and hence testing results were calculated at these values so as to identify the best classifier. The performance of these classifiers was calculated using the area under the receiver operating characteristics curve (AUC), which is a threshold-independent metric that is widely used in flood susceptibility mapping.

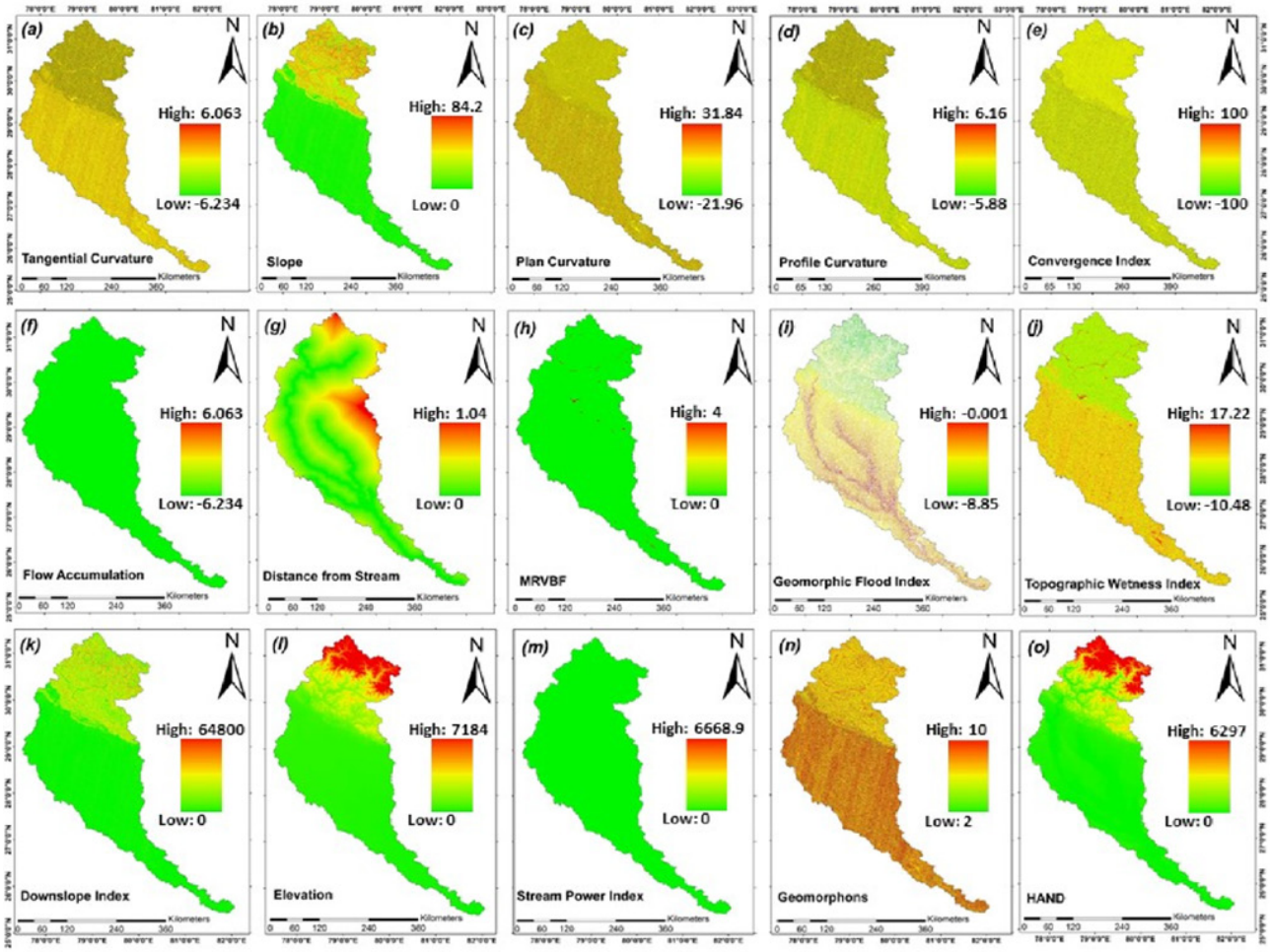

Figure 1. Geomorphic flood descriptors- (a) tangential curvature, (b) slope, (c) plan curvature, (d) profile curvature, (e) convergence index, (f) flow accumulation, (g) distance from stream, (h) multi resolution valley bottom flatness, (i) geomorphic flood index, (j) topographic wetness index, (k) downslope index, (l) elevation, (m) stream power index, (n) geomorphons, and (o) height above nearest drainage.

Results and concluding remarks

The present study evaluates the fidelity of Machine Learning models based on the values of different GFDs. Area under ROC represents the model performance and how exactly a trained model can classify between flooded and non-flooded locations. Random Forest performed better in the training phase (AUC = 0.98) as compared to other models, but in the testing phase, AdaBoost was found slightly better than the rest of the models (AUC=0.95), followed by Random Forest (AUC=0.94), Logistic Regression (AUC=0.89) and K-nearest neighbor (AUC=0.70). Our study suggests a superior performance of Random Forest over other ML models, which may be considered further for deriving flood inundation maps. The study recommends avoiding the copious usage of ML models for flood inundation mapping, especially for large regions where hydrodynamic modelling of floods is a challenging task. This will ensure minimal generation of uncertainties in the flood hazard and flood risk dimensions.

References

Deroliya P, Ghosh M, Mohanty MP, Ghosh S, Rao KD, Karmakar S (2022) A novel flood risk mapping approach with machine learning considering geomorphic and socio-economic vulnerability dimensions. Science of The Total Environment, 851, p.158002. https://doi.org/10.1016/j.scitotenv.2022.158002

Dottori F, Alfieri L, Salamon P, Bianchi A, Feyen L, Hirpa F (2016). Flood hazard map of the World–100-year return period, European Commission, Joint Research Centre (JRC) [data set]. http://data.europa.eu/89h/jrc-floods-floodmapgl_rp100y-tif

Samela C, Troy TJ and Manfreda S (2017) Geomorphic classifiers for flood-prone areas delineation for data-scarce environments. Advances in Water Resources, 102, pp.13-28. https://doi.org/10.1016/j.advwatres.2017.01.007

12th World Congress on Water Resources and Environment (EWRA 2023)
"Managing Water-Energy-Land-Food under Climatic, Environmental and Social Instability"
Thessaloniki, Greece, 27 June - 1 July 2023

Extreme rainfall and 2D flood modelling in urban catchments to assess flood exposure of buildings: A case study in Thessaloniki city, Greece

C. Iliadis[1*], P. Galiatsatou[2], V. Glenis[1], P. Prinos[2], C.G. Kilsby[1,3]
[1] School of Engineering, Newcastle University, Newcastle Upon Tyne, NE1 7RU, UK
[2] School of Civil Engineering, Aristotle University of Thessaloniki (AUTh), 54124 Thessaloniki, Greece
[3] Willis Research Network, 51 Lime St., London, EC3M 7DQ, UK
* e-mail: c.iliadis2@newcastle.ac.uk

Introduction

Urban floods are amongst the most widely distributed natural hazards, endangering lives and causing damage to properties worldwide. The extent and severity of the damage caused by urban floods is a product of both intensity and duration of an extreme rainfall event, and its interaction with the complex flowpaths in a city on the ground surface and below it. Therefore, there is a great need to combine hydrological with hydrodynamic modelling to understand the impacts of urban floods, the water flowpaths in a city, and the urban features exposed at high flood risk. A detailed and contemporary analysis and modelling of extreme rainfall events in an urban area combined with an advanced hydrodynamic model to simulate pluvial flooding, can significantly assist a reliable assessment of infrastructure exposure to flooding, as well as contribute to flood damage mitigation and flood risk reduction.

Materials and methods

The study area of the present work is the historic centre of Thessaloniki city in Greece. Dailly rainfall data at AUTh station consist of 64 years (1958-2021) of measurements, obtained from the database of the School of Geology, AUTh. There also exist short-duration rainfall measurements at Mikra station for a shorter period of 25 years (1963-1987), made available from the National Meteorological Service of Greece. This dataset includes annual maximum rainfall intensities and depths for time periods of 5min, 10min, 15min, 30min, 1h, 2h, 6h, 12h and 24h. The latter are used to construct idf and ddf (intensity/depth-duration-frequency) curves and extract rainfall return levels for different durations and return periods.

Rainfall features of different temporal scales can be linked using scaling models, mainly based on the multifractal behaviour of rainfall. A scaling procedure is applied here to rainfall intensity quantiles corresponding to different durations, considering that their cumulative distribution function has a standardized form independent of the rainfall duration (Galiatsatou and Iliadis, 2022). The scaling laws are assessed for all return periods for rainfall durations from 5min to 30min and from 30min to 24h. Two modern threshold detection methods proposed by Bader et al. (2018) and Silva Lomba and Fraga Alves (2020) are used, to assist a less ambiguous selection of daily extreme rainfall events. The Generalised Pareto distribution is then fitted to daily rainfall excesses and 24h-rainfall levels are assessed for the selected return periods. The scaling laws extracted from the short-duration measurements are then applied to extracted 24h-quantiles to estimate rainfall levels corresponding to hourly and sub-hourly durations.

An advanced and fully featured hydrodynamic model, CityCAT-City Catchment Analysis Tool (Glenis et al. 2018) developed at Newcastle University, is then utilised to assess the flooding hazard. CityCAT is a fully coupled 1D/2D hydrodynamic model, able to simulate fully coupled surface and pipe network flows. The model can represent natural drainage systems and built-up areas, and also explicitly represent buildings, as well as different types of Blue-Green Infrastructure (Glenis et al. 2018; Kilsby et al. 2020). The required inputs of the model include storm profiles, a high-resolution Digital Terrain Model (DTM), the buildings' footprint, and the green spaces. An algorithm was developed here to extract the DTM of the study area with a 2m resolution of computational grid squares and a physical slope of about 15%. The buildings' footprint was extracted from the ONEGEO Data (https://onegeo.co/data), while the permeable spaces were designed manually. Flood exposure of buildings (low, medium or high) is assessed using simulated

flood depths in a 3m buffer zone around each building's perimeter, where the mean and the 90th percentile values are calculated (Bertsch et al. 2022). A simple assumption that 20% of the rainfall enters the drainage system is utilised.

Results and concluding remarks

The 100-years rainfall depth is assessed here about 70% higher for durations of 1h and 2h, compared to the respective quantiles of the ddf curves extracted from the short-duration 25-years dataset. CityCAT model is used to simulate the two storm events (100-year events with duration 1h and 2h). Figure 1 presents flood depths, velocity, and flood exposure of buildings in a selected area of the historic centre (Pavlou Mela, Tsimiski, Palaion Patron streets) at the middle of each storm event, with red, orange and grey colours defining buildings at high, medium and low risk, respectively. Table 1 presents the total number of inundated buildings per scenario.

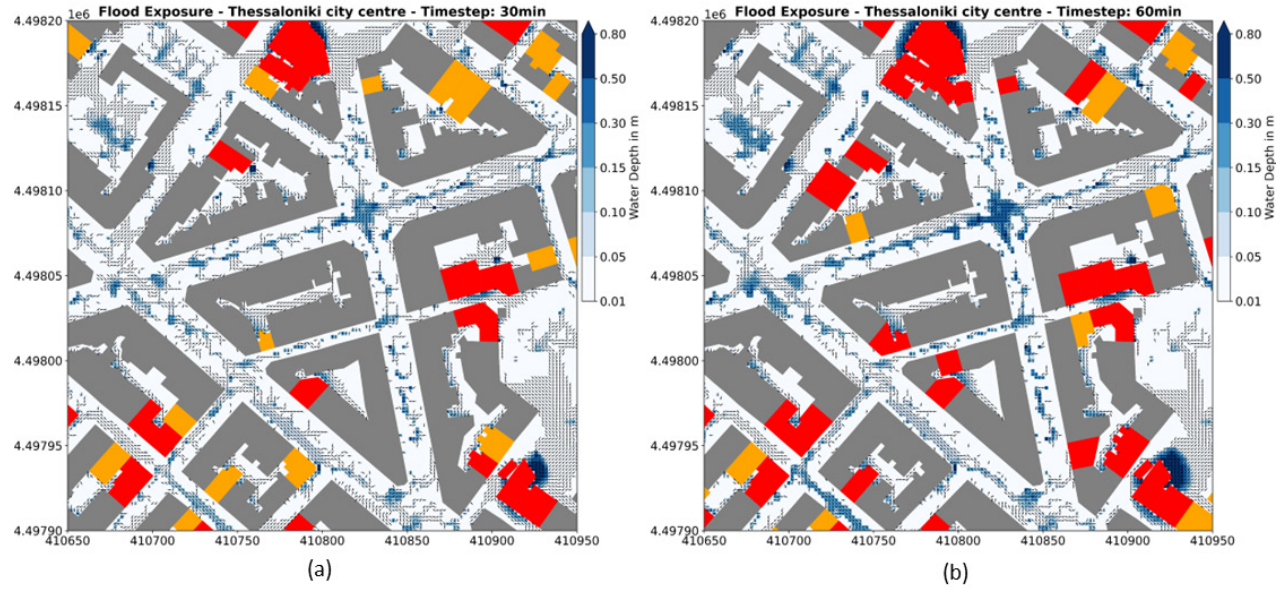

Figure 1. Flood depths, velocity (arrows) and flood exposure of buildings for a 100-years storm event of: (a) 1h, (b) 2h.

Table 1. Total number of inundated buildings per scenario.

	Medium	High
100-years event of 1h	15	14
100-years event of 2h	11	25

Acknowledgments: This work has been funded by the Engineering and Physical Science Research Council as part of the Centre for Doctoral Training in Water Infrastructure and Resilience (WIRe, EP/S023666/1).

References

Bader B, Yan J, Zhang X (2018) Automated threshold selection for extreme value analysis via ordered goodness-of-fit tests with adjustment for false discovery rate. Ann Appl Stat. 12(1): 310-329. doi: 10.1214/17-AOAS1092

Bertsch R, Glenis V, Kilsby C (2022) Building level flood exposure analysis using a hydrodynamic model. Environ. Model. Softw. 156, 105490. https://doi.org/https://doi.org/10.1016/j.envsoft.2022.105490

Galiatsatou P, Iliadis C (2022) Intensity-Duration-Frequency Curves at Ungauged Sites in a Changing Climate for Sustainable Stormwater Networks. Sustainability 14(3), 1229. https://doi.org/10.3390/su14031229

Glenis V, Kutija V, Kilsby CG (2018) A fully hydrodynamic urban flood modelling system representing buildings, green space and interventions. Environ. Model. Softw. 109: 272-292. https://doi.org/10.1016/j.envsoft.2018.07.018

Kilsby C, Glenis V, Bertsch R (2020) Coupled surface/sub-surface modelling to investigate the potential for blue-green infrastructure to deliver urban flood risk reduction benefits. In: Thorne C (eds) Blue-Green Cities: Integrating urban flood risk management with green infrastructure, ICE Publishing, London, pp. 37-50

Silva Lomba J, Fraga Alves MI (2020) L-moments for automatic threshold selection in extreme value analysis. Stoch. Environ. Res. Risk Assess. 34(3): 465-491. https://doi.org/10.1007/s00477-020-01789-x

Climate change related risks on agricultural water availability in Turkiye

T. Pilevneli[1], G. Capar[1*], C. S. Cerda[2]
[1] Water Management Institute, Ankara University, 06135 Ankara, Turkey
[2] Department of Biology, Healthcare, and the Environment, Barcelona University, 08007 Barcelona, Spain
* e-mail: gcapar@ankara.edu.tr

Introduction

Agriculture is an important sector in the Turkish economy, representing 27-100% of the total labor force. Agriculture heavily depends on water, which is provided either from the precipitation alone (rain-fed) or coupled with irrigation, where the latter accounts for over 70% of the country's annual water potential (MoAF 2021). Although seasonal and regional differences are present, a general decreasing precipitation pattern exists throughout the country. In parallel, decreasing streamflow patterns are observed in the western, central, and southern parts. For example, the annual surface runoff of the Euphrates-Tigris river basin is expected to decrease significantly by up to 55% by 2100 (Bozkurt and Sen 2013). These figures show that the impacts of climate change on the water resources of Turkiye may possess high risks to food security. Therefore, it is essential to identify the expected adverse impacts on water availability.

This study estimates the irrigation water demand in 25 river basins, covering the whole country with all agricultural products taken into account. The water footprint (WF) approach was integrated to water budget analysis at the river basin scale. The water adequacies of river basins were assessed for current conditions and three projected periods until 2100 under the RCP 4.5 and RCP 8.5 scenarios. The water availability was compared to sectoral water demand (household, industry, and agriculture), where green water footprint (GWF) and blue water footprint (BWF) data were used for estimating irrigation water demand (IWD).

Materials and methods

Data from several sources were used and processed to obtain river basin scale results. The details of all calculations, data sources, temporal and spatial resolutions, and methods to convert to a basin resolution are provided elsewhere (Pilevneli et al. 2023). First, the annual blue water availability for irrigation was estimated. Second, the annual production of agricultural products in each river basin was calculated. The IWD was calculated using a volumetric WF approach based on annual agricultural productions (Figure 1). In the third step, these findings were combined with climate projections to estimate the water budget in the reference year (2015) and three projected periods (2015–2040, 2041–2070, and 2071–2100).

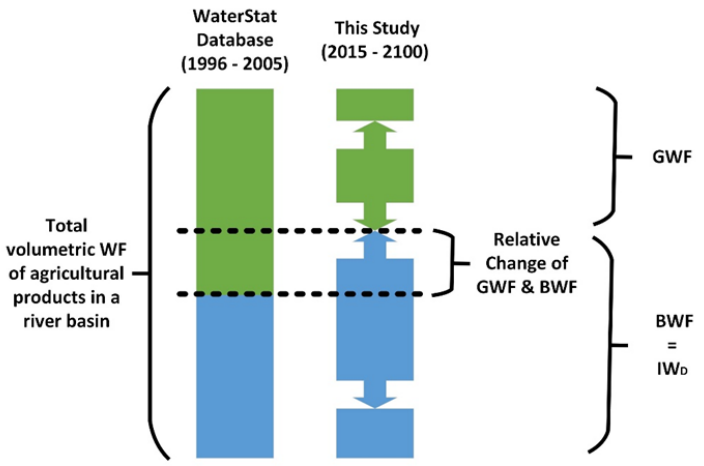

Figure 1. Methodology for the estimation of irrigation water demand (IWD).

The incomes were estimated based on production estimations and market prices of agricultural products. Then, key agricultural products were identified and water use efficiency, water productivity, and yield were evaluated. Finally, the results of this study were compared to the outputs of WaterGAP v2.2d, which is a global water use and availability model (Müller Schmied et al. 2021).

Results and concluding remarks

The study showed that the highest impact of climate change on water availability is expected to be observed during the 2015–2040 period. The irrigation water availability in river basins is depicted in Figure 2. The irrigation water demands show the risk of water deficiency with a possible decrease from a surplus of 14.6 km^3 per year to a deficit of 57.3 km^3 under the RCP8.5 scenario for the 2071–2100 period. Both the total production and income in the Aegean region might decrease drastically up to 100%.

The estimated cost of climate change is between €14.15 and €18.01 Billion per year if no action is taken. Therefore, there is an urgent need to increase water use efficiency and productivity in 15 river basins. The median income per water used was found to be 2.24 €/m^3.

The ranking of agricultural products according to their annual production, income, and blue water footprints revealed that among the 12 priority key products, maize and wheat are highly vulnerable to drought as a consequence of climate change.

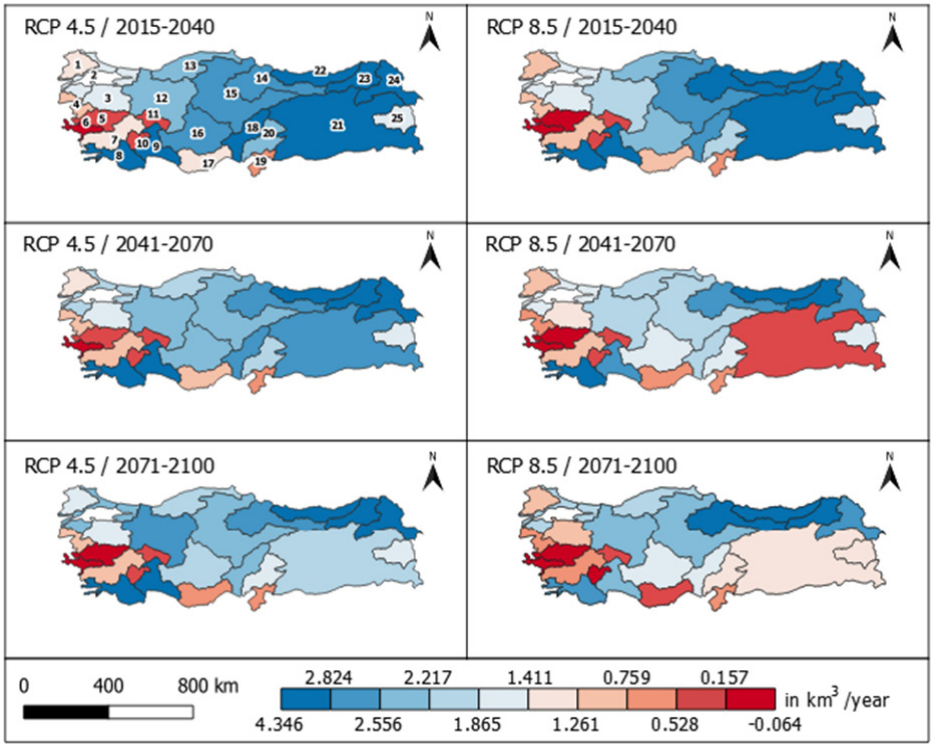

Figure 2. Projections of irrigation water availability in river basins

References

Bozkurt D, Sen OL (2013) Climate change impacts in the Euphrates-Tigris Basin based on different model and scenario simulations. J Hydrol (Amst) 480, 149–161. https://doi.org/10.1016/j.jhydrol.2012.12.021

MoAF (2021) Toprak Su Kaynakları (in Turkish), Ministry of Agriculture and Forestry - General Directorate of State Hydraulic Works. URL https://www.dsi.gov.tr/Sayfa/Detay/754 (accessed 1.11.22)

Pilevneli T, Capar G, Sanchez CC (2023) Investigation of climate change impacts on agricultural production in Turkey using volumetric water footprint approach. Sustainable Production and Consumption 35: 605-623. https://doi.org/10.1016/j.spc.2022.12.013

Schmied M, Caceres H, Eisner D, Flörke S, Herbert M, et al. (2021) The global water resources and use model WaterGAP v2.2d: model description and evaluation. Geoscientific Model Development 14: 1037–1079. https://doi.org/10.5194/GMD-14-1037-2021

Estimation of non-stationary flood frequencies for coastal-fluvial flooding of west-flowing rivers in Kerala, India

S. Bhere[1*], M.J. Reddy[1,2]
[1] Department of Civil Engineering, Indian Institute of Technology Bombay, Mumbai- 4000076, India
[2] Interdisciplinary Program (IDP) in Climate Studies, Indian Institute of Technology Bombay, Mumbai- 4000076, India
* email: sachinbhere.iitbcivil@gmail.com

Introduction

To quantify the impact of the flood, various methods are used, and flood frequency analysis is one of the most popular ones. The flood frequency analysis determines the probability of the occurrence of extreme events which is based on stationary assumptions in most cases i.e., distribution parameters are assumed to be constant (Machado et al. 2015; Seidou et al. 2012). However, due to changes in the climate and anthropogenic conditions, the assumption of stationarity may not stand true. Therefore, in the recent past, various studies have come up proposing the non-stationary approach for flood frequency analysis, in which the distribution parameters are assumed to be changing with time or other physical covariates like climate indices, land use changes, rainfall, etc. (Condon et al. 2015; Debele et al. 2017; Singh and Chinnasamy, 2021). In this study, the stationary and non-stationary flood frequencies are compared for various hydro-meteorological stations of the west-flowing rivers of Kerala state of India along with the frequencies of the maximum wave height to understand the changes in the coastal-fluvial flood risk with changing environment. The section below discusses the data and methodology for the objective to determine the best-fit model and understand the changes in flood frequencies for stationary and non-stationary conditions.

Materials and Method

The coastal-fluvial flood frequency models are developed for stationary and non-stationary conditions based on the assumption that the distribution parameters are constant (stationary condition) and distribution parameters are changing with time (non-stationary condition) to determine the best-fit models for flood frequency. Figure 1 shows the methodology used for the flood frequency analysis in the study. The study also calculates the changes in the return periods of extremes for both (stationary and non-stationary) conditions. For coastal-fluvial flooding, the significant wave height and discharge data of the west-flowing river of Kerala are considered due to its history of large-scale flood damages in the region. The frequency models are fitted using the annual maximum values of the hourly wave height from ERA5 data and the daily discharge values of the 18 stations which are acquired from the India water resources information system (India-WRIS).

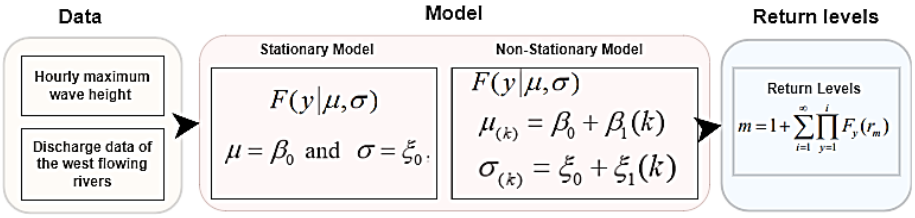

Figure 1. Flowchart of the methodology for stationary and non-stationary flood frequency analysis.

Six two-parameter distributions are used to fit the models, and the best-fit models are then determined using the Akaike Information Criterion (AIC) (defined as $AIC = [2k - 2\log(L)]$). For non-stationary models, the time is considered as a covariate with which we are assuming the parameters are changing. The probability distribution models are developed for the wave height as well as discharge data of the west-flowing rivers of Kerala.

Results and concluding remarks

Before discussing the flood frequencies, the trend is determined to understand the changes in the annual maximum values of the wave heights. Figure 2a shows trends in wave heights for each grid, indicating a significant increasing trend in the magnitude of the maximum wave heights, proving non-stationarity in the wave heights. The coastal and fluvial flood frequencies are dependent on the sea surge along with the discharge of the rivers near the coast and therefore the west-flowing river discharges are used along with the wave heights for the Kerala state.

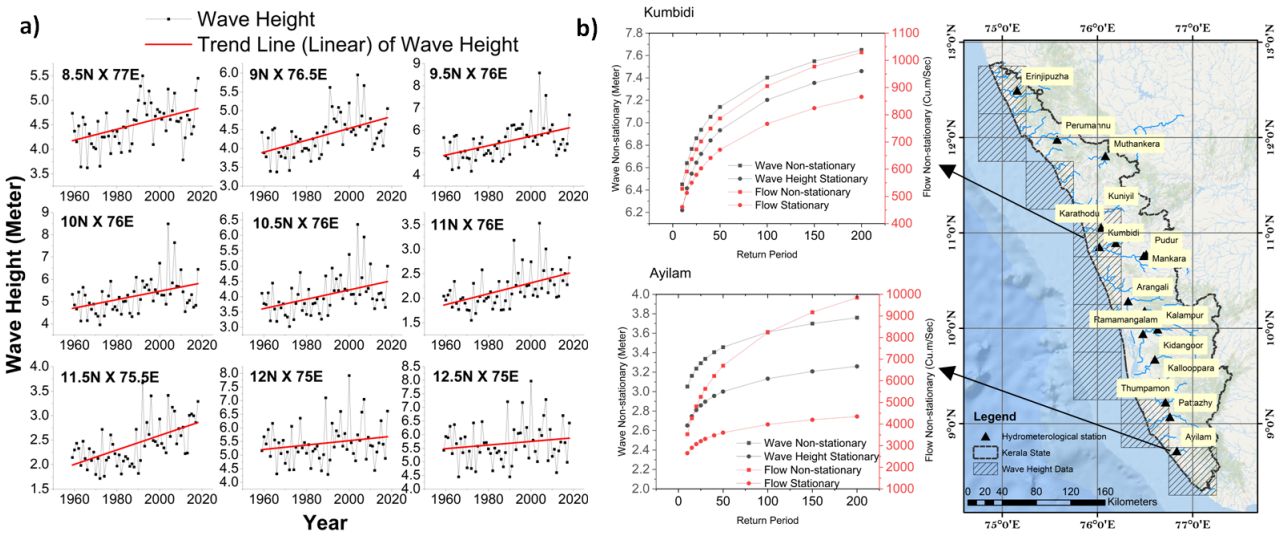

Figure 2. a) Trend of the wave heights for the coast of Kerala state b) The comparison of the stationary and non-stationary return levels for wave height (m) and flows (m^3/s) for two hydrometeorological stations (Kumbidi and Ayilam)

The AIC values for the non-stationary model at all locations are less than the stationary models, indicating that the non-stationary models are better fitted for both wave heights and river flows. This shows that there is non-stationarity in flow and wave height. The AIC value for the best-fit stationary model and non-stationary model for wave height (flow) were 72.91(120.17) and 62.25(109.94), respectively. The study determined the changes in the flood return levels for both coastal and fluvial parameters. Figure 2b shows the return levels for wave height and flows for Kumbidi and Ayilam which are hydrometeorological stations near the coast of Kerala. The wave height return levels are higher for non-stationary than stationary conditions. For example, at Kumbidi, the stationary wave height corresponding to 100 years is the same as that of the 60-year wave height of non-stationary conditions. Similarly, the discharge return levels are higher for non-stationary conditions than the stationary conditions at all locations. The study concludes that the non-stationary models give better estimates of flood return levels than the stationary models. The increase in the return levels of both discharge and the sea surge in terms of wave height can be observed, proving the increasing risk of flooding in the coastal regions of Kerala.

References

Condon LE, Gangopadhyay S, Pruitt T (2015) Climate change and non-stationary flood risk for the upper Truckee River basin. Hydrology and Earth System Sciences 19(1): 159–175. https://doi.org/10.5194/hess-19-159-2015

Debele SE, Strupczewski WG, Bogdanowicz E (2017) A comparison of three approaches to non-stationary flood frequency analysis. Acta Geophysica 65(4): 863–883. https://doi.org/10.1007/s11600-017-0071-4

Machado MJ, Botero BA, López J, Francés F, Díez-Herrero A, Benito G (2015) Flood frequency analysis of historical flood data under stationary and non-stationary modelling. Hydrology and Earth System Sciences, 19(6), 2561–2576. https://doi.org/10.5194/hess-19-2561-2015

Seidou O, Ramsay A, Nistor I (2012) Climate change impacts on extreme floods II: Improving flood future peaks simulation using non-stationary frequency analysis. Natural Hazards 60(2):715–726. https://doi.org/10.1007/s11069-011-0047-7

Singh N, Chinnasamy P (2021) Non-stationary flood frequency analysis and attribution of streamflow series: a case study of Periyar River, India. Hydrological Sciences Journal 66(13): 1866–1881. https://doi.org/10.1080/02626667.2021.1968406

Drought analysis using SPI under climate change conditions: Application in Chalkidiki Region (Greece)

S. Zacharoudi*, D.K. Karpouzos, P.E. Georgiou
School of Agriculture, Aristotle University of Thessaloniki, Thessaloniki, Greece
** e-mail: stavroulazachar@gmail.com*

Introduction

Drought is a major challenge for water resource management and agriculture in many parts of the world. The ongoing climate crisis has raised global concern about its negative effects on available water resources and rising temperatures. This study aims to perform a local drought analysis using the RCA4 Regional Climate Model (RCM) with output data from three different Global Climate Models (GCMs), the ICHEC-EC-EARTH, the MPI-M-MPI-ESM-LR, and the HadGEM2-ES, under the climate change scenario RCP 4.5. As a drought indicator, the monthly Standardized Precipitation Index (SPI) was selected (McKee et al. 1995). The SPI is a widely used tool for drought analysis, providing a standardized measure of precipitation anomalies over different time scales. The evaluation period of climate change is 2030–2050, and the precipitation data for the historical reference period (1976–2005) refers to seven meteorological stations (Agios Mamas, Agios Prodromos, Arnaia, Megali Panagia, Ormylia, Plana, and Taxiarchis) located in the Chalkidiki Region (Greece).

Materials and methods

The analysis is based on the RCA4 Regional Climate Model with output data from three different Global Climate Models (GCMs), the EC-EARTH (Hazeleger et al. 2012), the MPI-ESM-LR (Giorgetta et al. 2013), and the HadGEM2-ES (Martin et al. 2011), and under the climate change scenario RCP 4.5. The Linear Scaling (LS) bias correction approach (Lenderink et al. 2007) was applied to adjust the models' data to the historical data from the stations (Shrestha 2015). LS is a method of bias-correcting regional climate model simulations using a constant correction factor estimated from the difference between the original RCM simulations and monthly observations (Teutschbein and Seibert 2012). The monthly Standardized Precipitation Index (SPI) (McKee et al. 1995) was calculated using the adjusted data from the climate models. The drought classification according to the monthly SPI values is shown in Table 1.

Table 1. Classification of drought according to the SPI values.

SPI value	Drought classes
2 or more	Extremely wet
1.5 to 1.99	Very wet
1 to 1.49	Moderately wet
0.99 to 0.0	Normal
0.0 to −0.99	Near normal
−1 to −1.49	Moderately dry
−1.5 to −1.99	Severely dry
−2 and less	Extremely dry

Based on the above table, for analysis purposes, two major categories of drought classes are adopted: (a) the significant drought, which is considered the sum of the severely and extremely dry classes, and (b) the total drought, which comprises the moderately, severely, and extremely dry classes.

Results and concluding remarks

In Figures 1 and 2, the results of the drought analysis for all stations and models are presented with regard to two drought categories (significant and total drought, respectively). For the future period (2030–

2050), there is a predicted small increase in total drought for almost all stations (except Ormylia Station). Specifically, at four stations, this increase was indicated by all climate models. The most noticeable increase occurs at Taxiarchis Station, where the percentage of months that belong to the total drought category ranges from 16% to 18% compared to 15%, which corresponds to the historical data. Concerning the significant drought, there is a clear increase in four stations (Agios Mamas, Arnaia, Agios Prodromos, and Ormylia), as predicted by all models. Comparing the three climate models, there is a slight variation in the predicted outputs, highlighting the need to use an ensemble of models in drought analysis to enhance the reliability and address the uncertainty of the results.

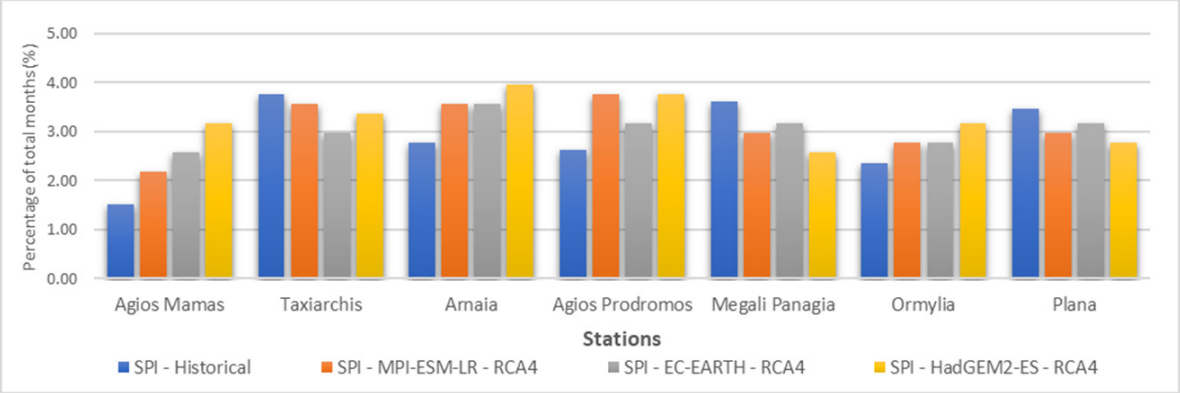

Figure 1. Significant drought for monthly SPI at the meteorological stations of the study area.

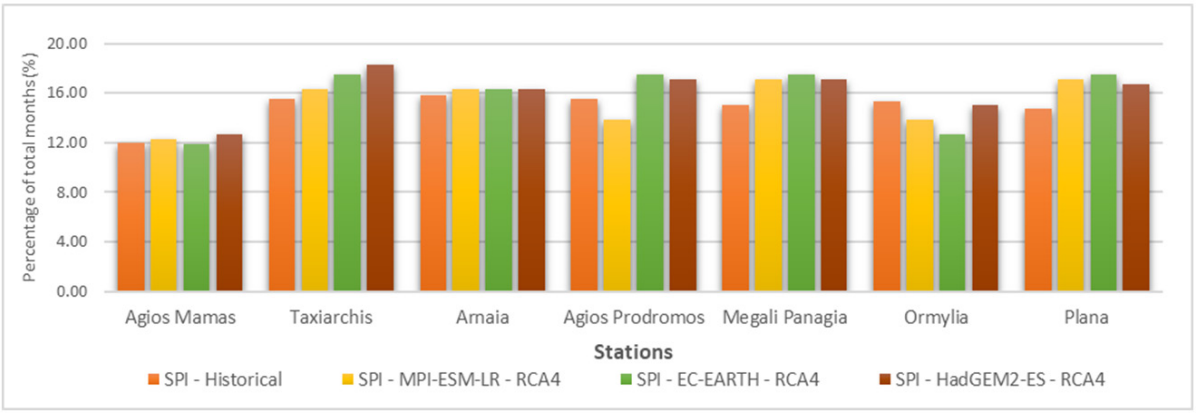

Figure 2. Total drought for monthly SPI at the meteorological stations of the study area.

References

Hazeleger W, Wang X, Severijns C et al. (2012) EC-Earth V2.2: description and validation of a new seamless earth system prediction model. Climate Dynamics 39(11): 2611–2629. https://doi.org/10.1007/s00382-011-1228-5

Giorgetta MA et al. (2013) Climate and carbon cycle changes from 1850 to 2100 in MPI-ESM simulations for the Coupled Model Intercomparison Project phase 5. Journal of Advances in Modeling Earth Systems 5: 572–597. https://doi.org/10.1002/jame.20038

Lenderink G, Buishand A, Van Deursen W (2007) Estimates of future discharges of the river Rhine using two scenario methodologies: direct versus delta approach. Hydrol Earth Syst Sci 11(3): 1145–1159

Martin GM et al. (2011) The HadGEM2 family of Met Office Unified Model climate configurations, Geoscientific Model Development 4(3): 723–757. https://doi.org/10.5194/gmd-4-723-2011

McKee TB, Doesken NJ, Kleist J (1995) The relationship of drought frequency and duration to time scales. In: Proceedings of the 9th Conference on Applied Climatology, AMS, Boston, pp 233–236

Shrestha M (2015) Data analysis relied on Linear Scaling bias correction (V.1.0) Microsoft Excel file

Teutschbein C, Seibert J (2012) Bias correction of regional climate model simulations for hydrological climate-change impact studies: Review and evaluation of different methods. Journal of Hydrology 456–457: 12–29. https://doi.org/10.1016/j.jhydrol.2012.05.052

III. Water Quality and Advanced Water Treatment

12th World Congress on Water Resources and Environment (EWRA 2023)
"Managing Water-Energy-Land-Food under Climatic, Environmental and Social Instability"
Thessaloniki, Greece, 27 June - 1 July 2023

Architecting Fe^0/Fe_3C with Fe_3O_4 redox sites for electrochemical detection of 4-nitrophenol in environmental water

A.F. Baye, H. Kim*
Department of Energy Science and Technology, Environmental Waste Recycle Institute, Myongji University, Yongin, Gyeonggi-do 17058, Republic of Korea
** e-mail: hernkim@mju.ac.kr*

Introduction

4-nitrophenol (4-NP) is a water-miscible and highly toxic contaminant which is commonly found in industrial effluents, pesticide run-offs, and explosive residues. It is reported to be carcinogenic, mutagenic, and damaging to the central nervous system, liver, kidney, and blood, even in trace amounts, and has high bioavailability. Due to these factors, 4-NP is categorized as a main pollutant by the US Environmental Protection Agency (EPA) with only 60 ppb (0.43 μM) allowed in drinking water. To guarantee perfect compliance, a highly efficient and robust 4-NP sensing, and detection protocol is needed at drinking water and waste treatment facilities. Unlike other detection methods, electrochemical sensing offers more in terms of sensitivity, cost-effectiveness, portability, and simplicity; hence, it has gained focus for its betterment. Amongst the transition metals, Fe-based electrocatalysts are extensively employed for electrochemical sensing due to their Fe^{2+}/Fe^{3+} redox couple, low toxicity, and abundance. Numerous high-performing Fe_3O_4-Carbon electrodes have been effectively used for the electrochemical detection of glucose, dopamine, uric acid, and ascorbic acid with an extremely low limit of detection (LOD) and high sensitivity. However, Fe-based 4-NP electrodes have been shown poor electrochemical sensing performance (Cheng 2017; Sarno and Ponticorvo 2020). This is because the electroreduction capability of Fe_3O_4 redox sites is poor. Therefore, the electroreduction capability of Fe_3O_4 in the carbon matrix must be improved for sensitivity sensing of 4-NP.

Both Fe^{2+} and Fe^0 are excellent reducing agents, according to corrosion chemistry and electrolytic-induced reduction, especially when combined with Fe_3C because oxide formation is constrained, which increases electron transport (Baye et al. 2021; 2023; Li et al. 2019). With the use of Fe^0/Fe_3C/carbon composite, chromium (IV) was successfully reduced to chromium (III). Due to its remarkable capacity to donate electrons, zero-valent iron (Fe^0) contained in mesoporous carbon was also employed to effectively reduce nitrate (Teng et al. 2018). It makes sense that linking Fe_3O_4 to Fe^0/Fe_3C may enhance 4-NP electroreduction and enhance the efficacy of electrochemical sensing. Here, we show how this constraint can be overcome by hybridizing Fe_3O_4 with Fe^0/Fe_3C, which results in remarkable 4-NP detection. The heterostructure comprising Fe_3O_4, ZnO, Fe^0, Fe_3C, and g-C is created by the carbothermal reduction of ZnFe-LDH@carbon under N_2 atmosphere. In $Fe_3O_4/ZnO/Fe^0/Fe_3C$/g-C heterostructure, ZnO and g-C produce structural porosity by preventing Fe_3O_4 particle aggregation, which results in high electrochemical surface area (ECSA) and mass transfer. In the meantime, a high temperature (900 °C) is necessary to completely change ZnFe-LDH@carbon into $Fe_3O_4/ZnO/Fe^0/Fe_3C$/g-C (ZnFe@C-900) and prevent the inactive $ZnFe_2O_4$ phase. Fe_3C serves as a conductive channel for quick electron transport at Fe^{2+}/Fe^{3+} redox couple sites in Fe_3O_4 where 4-NP electroreduction takes place while the Fe^0 site promotes 4-NP adsorption. These characteristics combine to deliver high sensitivity, low LOD and selectivity in PBS as well as tap and river water. Additionally, a $Fe_3O_4/ZnO/Fe^0/Fe_3C$/g-C was used for Fenton degradation of organic pollutants, such as methylene blue, by producing enough free •OH to oxidize and breakdown organic dyes, diversifying its range of application in water treatment.

Materials and methods

Firstly, carbon sphere (C) was obtained by hydrothermal method (4 h at 180 °C) using dextrose as a precursor. In a hydrothermal reactor, 100 mg of C, 63 mg of $ZnCl_2$, 375 mg of Fe (NO_3) $9H_2O$, 750 mg of

urea, 375 mg of NH_4F, and 60 mL of DI-water were added and mixed for 4 h. The solution was heated at 120 °C for 17 hours. A precipitate product (ZnFe-LDH@C) was collected and dried at 60 °C under vacuum after being washed with DI water. Then, ZnFe-LDH@C was heated in a furnace at different temperatures (700-900 °C) for 1 h under N_2 using 1 °C/min and the produced materials were designated as ZnFe@C-700, ZnFe@C-800, and ZnFe@C-900. Figure 1 describes the entire synthesis process. The prepared samples were modified on a glassy carbon electrode (GCE) to fabricate the sensing electrode (i.e., ZnFe@C-900/GCE).

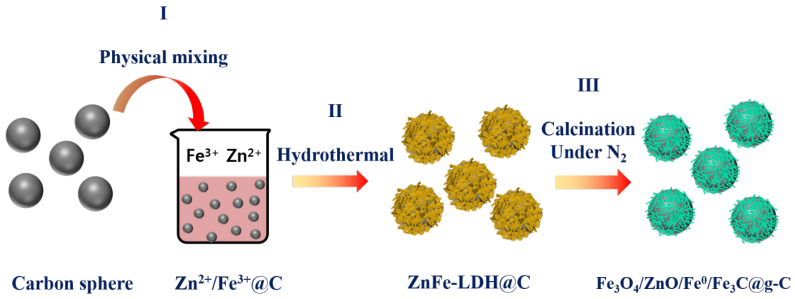

Figure 1. A schematic illustration of the method used to prepare Fe_3O_4/ZnO/Fe^0/Fe_3C@g-C.

Results and concluding remarks

In conclusion, the carbothermal reduction of ZnFe-LDH@carbon under N_2 at 900 °C (ZnFe@C-900) is the sole method that can produce Fe_3O_4/ZnO/Fe^0/Fe_3C/g-C. To maintain a porous structure, boost ECSA, and promote ion diffusion of ZnFe@C-900, ZnO and g-C are essential. The synergy of Fe_3O_4 and Fe^0/Fe_3C leads to ultra-low LOD (3.61 nM), high sensitivity, and selectivity over metal salts and 4-NP analogous compounds. To demonstrate the real-life practicality, 4-NP concentrations in tap water and river water were measured using ZnFe@C-900/GCE. The calculated 4-NP recovery values are summarized in Table 1 with a range from 96.8-103.8% and have a low RSD (below ~ 4%) which indicates that ZnFe@C-900/GCE can effectively detect 4-NP in real samples. Furthermore, efficient Fenton degradation of methylene blue was achieved over ZnFe@C-900.

Table 1. Determination of 4-NP in tap and river water samples using ZnFe@C-900/GCE.

Sample	4-NP added (μM)	4-NP found (μM)	RSD	Recovery (%)
Tap water	10	10.08	1.87	100.8
	60	58.10	1.51	96.8
	100	99.70	1.83	99.7
River water	10	9.95	2.94	99.5
	60	62.30	3.07	103.8
	100	100.10	1.14	100.1

References

Baye AF, Nguyen HT, Kim H (2023) Fe^0/Fe_3C-Assisted Fe_3O_4 Redox Sites as Robust Peroxidase Mimics for Pico-Molar H2O2 Colorimetric Response. Sensors and Actuators B: Chemical 377: 133097. http://doi.org/10.1016/j.snb.2022.133097

Baye AF, Han DH, Kassahun SK, Appiah-Ntiamoah R, Kim H (2021) Improving the reduction and sensing capability of Fe_3O_4 towards 4-nitrophenol by coupling with ZnO/Fe0/Fe_3C/graphitic carbon using ZnFe-LDH@carbon as a template. Electrochimica Acta 398: 139343. https://doi.org/10.1016/j.electacta.2021.139343

Cheng Y (2017) A Sensor for Detection of 4-nitrophenol Based on a Glassy Carbon Electrode Modified with a Reduced Graphene Oxide/Fe3O4 Nanoparticle Composite. Int J Electrochem Sci 12:7754–7764. https://doi.org/10.20964/2017.08.08

Li J, Lan H, Liu H, et al. (2019) Intercalation of Nanosized Fe3C in Iron/Carbon To Construct Multifunctional Interface with Reduction, Catalysis, Corrosion Resistance, and Immobilization Capabilities. ACS Appl Mater Interfaces 11: 15709–15717. https://doi.org/10.1021/acsami.9b03409

Sarno M, Ponticorvo E (2020) Fe3O4/graphene electrode for the electrochemical detection of 4-ntrophenol. Chem Eng Trans 79:427–432. https://doi.org/10.3303/CET2079072

Teng W, Bai N, Liu Y, et al. (2018) Selective Nitrate Reduction to Dinitrogen by Electrocatalysis on Nanoscale Iron Encapsulated in Mesoporous Carbon. Environ Sci Technol 52:230–236. https://doi.org/10.1021/acs.est.7b04775

Current state and physic-chemical characterization of the waters of Oued Gueridjima: Drain of domestic liquid effluents (NE Algeria)

N. Bougherira[1*], D. Nechem[2], H. Bouguerra[1], L. Djabri[1], H. Chaffai[1], A. Hani[1], N. Sedrati[1]
[1] Laboratory Water Resources and Sustainble Development (REDD), Department of Geology, Faculty of Earth Sciences, University Badji Mokhtar-Annaba, Algeria
[2] Laboratory of Geology, Department of Geology, Faculty of Earth Sciences, University Badji Mokhtar-Annaba, Algeria
* e-mail: nabil.bougherira@univ-annaba.dz

Introduction

In general, gray water, whose total fraction estimated at 75% of residential drainage (Hansen and Kjellerup 1994; Eriksson et al. 2002), contains low levels of organic matter compared to black water (ordinary wastewater), in which are included urine, faeces, toilet paper, etc.

In this article, we are interested in the evaluation of the current state of urban waste water (black or gray) that come from the places of residence of the new city Benmostefa Benaouda. The use of watercourses Gueridjima for the evacuation of liquid waste of the city 712 dwellings and the first cause of the deterioration of water quality. This problem remains entirely because of the lack of any urban wastewater treatment plant.

The analysis campaign includes analysis of surface water (Wadis waters: O.Gueridjima and O.El Aneb) and groundwater represented by surface (01 wells), a few meters far from the Gueridjima wadi. The physical measurements and chemical parameters carried out are: pH, temperature, EC, biological oxygen demand BOD_5. And the undesirable substances are: nitrates (NO_3^-), nitrites (NO_2^-), phosphates (PO_4^-), and orthophosphates. The aim is to predict chemical reactivity in water.

Materials and methods

The main parameters measure pollutants in domestic wastewater:

- The physical parameters such as conductivity, temperature, pH and dissolved oxygen and T° were measured on site using a multi-parameter, WTW brand,
- The samples were taken until they overflowed in vials (PET bottle), then corked and immediately placed in a cooler bag.

The BOD 5 measured using an Oxitop at the laboratory level of the Department of Geology.

Results and concluding remarks

The distribution of oxygen (5.2 mg/l), nitrate (7 mg/l), and PO_4^- values (less than 0.07) in the well indicates an oxidizing phase throughout the year (recharge and renewal of water by pumping) means that the nitrite (NO_2^-) levels remain very low, even zero.

According to Table 1, it is observed that the values of nitrates (NO_3^-), follow an increase in the discharges at the level of the Wadi, with the consumption of oxidizing species, and a joint decrease in nitrites (NO_2^-), and phosphates (PO_4^-). The fluctuations of the BOD_5 contents are also remarkable since they go from nearly 48.5 $mg.L^{-1}$ to the discharge R1 in the direction of the flow.

In conditions where the water table is only a few meters from the surface of the ground, there is the phenomenon of denitrification with the appearance of high levels of NO_3, O_2 and high values of BOD_5, in the waters of the Wadi, Between the two a transition zone is developing which deserves monitoring to protect the groundwater.

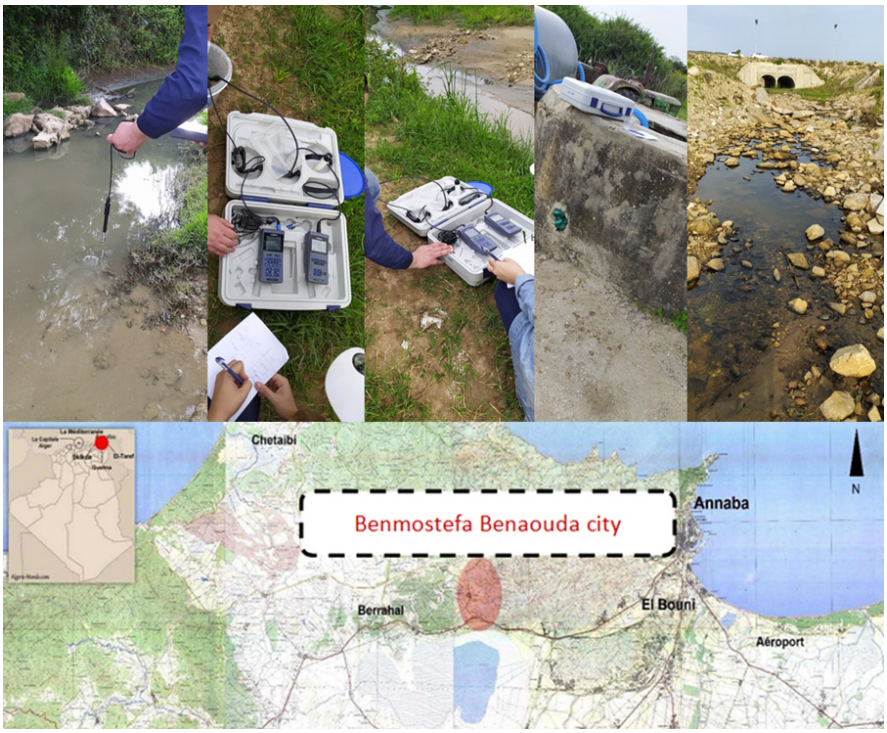

Figure 1. Measurements at the study site.

Table 1. Average variation of physic-chemical parameters.

	A-R	Well	R1	R2	R3	Standard
pH	8.43	7.58	7.68	7.65	7.53	-
T°C	18.6	18.25	20.7	18.75	20.15	**30**
CE (µS/cm)	790	1462	1653	976	1002	**1200**
Dissolved O_2 ($mg.L^{-1}$)	8.07	5.20	7.02	7.03	7.67	**7**
BOD_5	8.0	13.3	48.5	14.5	9.5	**30**
NO_3^- ($mg.L^{-1}$)	2	7	15	29	33	**10**
NO_2^- ($mg.L^{-1}$)	0.001	-	2.40	2.04	1.10	**10**
PO_4^- ($mg.L^{-1}$)	0.07	0.07	0.1	0.1	0.07	**3**

Acknowledgments: I warmly thank all the authors for their collaboration, their help, and their patience, especially the support given by Professor Djabri Larbi, Professor Hani Azzedine & Professor Chaffai Hicham of the laboratory of Water Resources and Sustainable Development of Badji-Mokhtar Annaba University.

References

Djabri L (1996) Mécanismes de la pollution et vulnérabilité des eaux de la Seybouse. Origines géologique industrielle, agricole et urbaine. Th. Doct. Es-Sciences, Univ Annaba, 261 p

Eriksson O (2002) Ontogenetic niche shifts and their implications for recruitment in three clonal Vaccinium shrubs: Vaccinium myrtillus, Vaccinium vitis-idaea, and Vaccinium oxycoccos. Canadian Journal of Botany 80(6): 635-641

Hani A (2003) Annalyse méthodologiques de la structure et des processus anthropiques : application aux ressources en eau d'un bassin côtier méditerranéen. Th. Doct. Es-Sciences, Univ Annaba, 214 p

Hansen JF, Kjellerup V (1994) The nutritional effect of phosphorus and sodium in sewage sludge and straw ash; Micro plot experiment. Goedningsvirkning af fosfor og kalium i slam og halmaske; Rammeforsoeg SP Rapport, 2(14), Denmark

Yahiatene S, Tahirim T (2010) Réflexion sur la caractérisation physico-chimique des effluents liquides rejetés dans la grande sebkha d'Oran. Université d'Oran-Licence Bâtiment

Wastewater recycling for industrial applications using membrane technology: Case study, Bandar Abbas wastewater treatment

S. Shojaie[1], V. Alipour[2*], S. Binaei[1]
[1] Persian Gulf Infrastructure Supply and Development Company, Bandar Abbas, Iran
[2] Environmental Health Engineering Dept., Hormozgan University of Medical Sciences, Bandar Abbas, Iran
* e-mail: v_alip@yahoo.com

Introduction

The volume of water consumption in 2000 was equal to 4430 km^3, while a significant increase in water demand equivalent to 5240 km^3 y until 2025 is predicted (Lazarova and Asano 2013). Compared to this increase in water demand, the total volume of recycled water is relatively small; approximately 5% of the wastewater si collected and treated throughout the world (Lazarova and Asano 2013). Municipal wastewater is increasingly recognized as a valuable source of water, nutrients, and energy. It is estimated that 380 km^3 of wastewater si produced worldwide annually, which is more than 5 times the annual volume of water from Niagara Falls. The large investment required to manage the human water cycle can be easily recovered by benefiting from the recycling of treated water (Lazarova et al. 2012). Water reclamation for industries is mostly done due to a lack of local water resources, either due to limited water resources or intense competition for energy supply. The ratio of industrial water to total water demand in developed and developing countries si 41%, and 3%, respectively (World Bank 2014). Although industrial harvest tends to increase, it is estimated that $1.9\times10^9 m^3.d^{-1}$ in 1995 will reach about $3.2\times10^9 m^3.d^{-1}$ by 2025 (Holden 2019; Gulamussen et al. 2019). The regional difference in water reclamation for industrial applications projects shows that most of them are concentrated in developed countries, where the amount of water consumption for industries is higher than in developing countries. In developing countries, there are a number of conditions that affect water reuse potential, including a lack of wastewater collection and inadequate treatment systems (Gulamussen et al. 2019). The purpose of compiling this article is to inform the world about the useful and effective results of recycling 100% of the wastewater of a city in Iran and turning it into industrial water to preserve the environment and achieve economic benefits.

Materials and methods

Bandar Abbas (BA) is a coastal city in the south of Iran, where due to the high level of underground water, there is significant penetration of salty underground water into the sewage collection network. These conditions have caused disturbances in the wastewater treatment operation, and therefore the treated wastewater of (BA) is not effective for the usual use of treated wastewater. So, this wastewater is discharged to the sea and thus creating a huge challenge to ehtPersian Gulf environment in ehtcoast of BA. For this reason, a mega project was planned, designed, and implemented to convert this poor-quality wastewater into valuable recycled water. This Megaproject is located in (BA) (Figure 1), where many various industries such as oil and gas refineries, aluminium and steel production, and shipbuilding are located. Industrial water supply is one of the obstacles to the development of these industries.
Construction of operation and process units based on a reverse osmosis desalination process, side structures and buildings, and electrical, mechanical, and precision equipment. During the implementation of this mega project, the facilities are being built as follows:

a. Reconstruction, development, and upgrading of the existing wastewater treatment plant in order to increase the capacity of the treatment plant from 64,000 to 100,000 m^3/d in BA city.
b. An 85,000 m^3/d capacity desalination plant with an (85% recovery) in BA city.
c. A 10,000 m^3 tank and a pumping station to store and transfer reclaimed water in BA city.
d. 22 km long reclaimed water transmission line with 900 mm diameter steel pipe.
e. 40,000 m^3 storage tank to store recycled water in the Persian Gulf Special Economic Zone.

f. 21 km long distribution network to distribute reclaimed water in the industrial zone of the Persian Gulf.

Figure 1. The location of the industrial water recycling project from the urban sewage in the south of Iran.

Results and concluding remarks

Water reclamation opportunities should be identified and cost-effectiveness optimized with the participation of stakeholders through the development of synergies and the exploration of production opportunities. This project, which was accompanied by the participation of the industry sector and the public water supply authorities, as well as the local authorities, was one of the important indicators that can show the role of inter-sectoral cooperation in the success of such projects. As the development of wastewater reclamation and reuse can lead to environmental and economic benefits, such as reducing water scarcity, reducing pollution emissions, improving soil quality, and saving production costs; therefore, the project aimed to achieve the following goals; (a) Solve the environmental challenge of BA city, (B) Sanitizing the ecosystem of the Persian Gulf shores, and (C) Creating a single structure for 85,000 m^3/d sustainable water supply for BA industries. As the feed water is brackish, the environmental problems related to rejected brine are excluded; and, the cost of desalinated water is more than half that of water produced from the sea (US$0.55 compared to US$1-1.1). This means the environmental benefits, preserving water resources, and rich economic benefits can be achieved through the reuse of wastewater.

Acknowledgments: The authors of the article thank the Persian Gulf Infrastructure Supply and Development Company for cooperation in data preparation.

References

Gulamussen NJ, Arsénio AM, Matsinhe NP, Rietveld LC (2019) Water reclamation for industrial use in sub-Saharan Africa–a critical review. Drinking Water Engineering and Science 12(2): 45-58

Holden J (2019) Water resources: an integrated approach. Routledge

Lazarova V, Asano T (2013) Milestones in water reuse. IWA Publishing

Lazarova V, Choo KH, Cornel P (2012) Water-energy interactions in water reuse. IWA Publishing

World Bank (2014) World development report 2015: Mind, society, and behavior. The World Bank

Origins of water mineralization in a coastal area: The case of Annaba-Echatt-El Hadjar region (NE Algeria)

L. Djabri[1*], H. Bouguerre[1], C.E. Fehdi[2], S. Bouhsina[3], N. Boughuerira[1], H. Chaffai[1], A. Hani[1]
[1] *Laboratory Water Resources and Sustainable Development (REDD), Department of Geology, Faculty of Earth Sciences, University Badji Mokhtar-Annaba, Algeria*
[2] *Laboratoire Eau et Environnement, Université Larbi Tebessi, Tebessa, Algeria*
[3] *Université du Littoral, Avenue Maurice Schumann, ULCO, Dunkerque, France*
** e-mail: djabri_larbi@yahoo.fr*

Introduction

In Algeria, the littoral zone occupies 5% of the total surface of the country and contains 95% of the population, which implies a significant demand for water locally, hence a significant solicitation of the aquifers This situation has led to an imbalance of the water interface fresh-salt water, causing seawater intrusion resulting in increased water salinity. This tendency towards imbalance is accelerated by the harmful effects of climate change. Many researchers have dealt with the issue as Djabri et al. (2014) demonstrated that the geological structure favors marine intrusion.

Geographical location and geological aspect: The study area is located in the northern part of Algeria (Figure 1a). It is bordered to the north by the Mediterranean, to the south by the highlands and Wilaya of Constantine, to the east by Wilaya of El Tarf, and to the west by Wilaya of Skikda. The geology of this area is characterized by the outcrop of Quaternary age formations with good permeability.

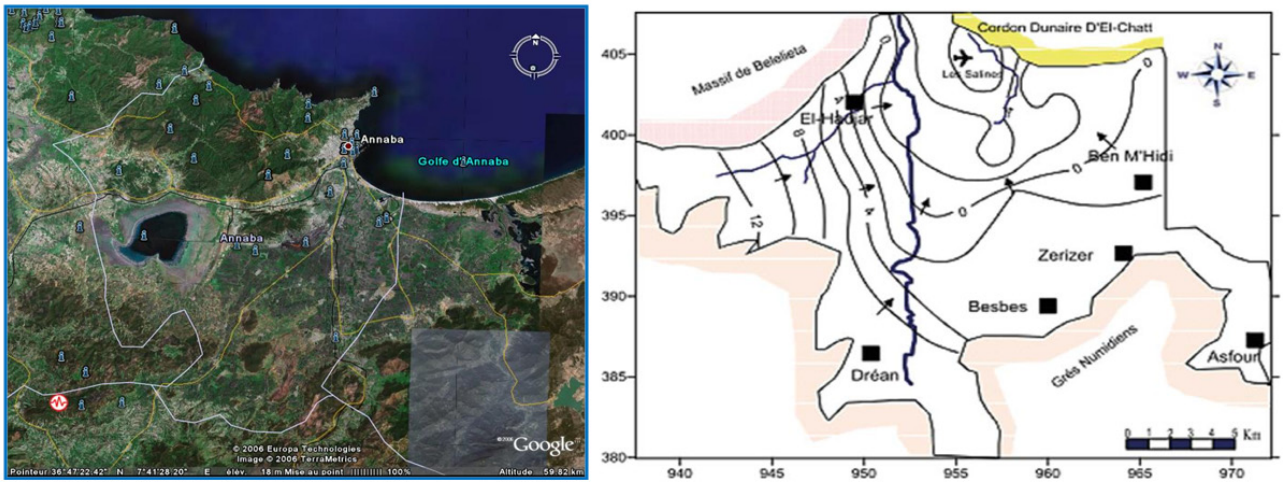

(a) *(b)*

Figure 1. a) Geographical map; b) piezometric map of the aquifers studied.

Climatic and hydrogeological characteristics of the study area: The climate is of Mediterranean type The wet season lasts on average seven months. During the wet season the maximum rainfall is recorded and there is a recharge of the aquifers, but in the summer season the groundwater overexploitation increases the risk of seawater intrusion.

Materials and methods

This work was carried out on three coastal aquifers in Algeria. Firstly, to carry out our research, we considered the piezometric state of the studied aquifers. The piezometric map (Figure 1b) indicates an aquifer-sea exchange. The second part of the study deals with the hydrochemical tools which give a good vision on the seawater intrusion.

Results and concluding remarks

The Piper diagram (Figure 2a) shows that the waters analyzed are rich in chlorides for the anions, and in sodium for the cations. By observing the figure, we notice that samples are located above the mixing line. The majority of the samples are in the following areas:

- mixed (mixture), with a maximum of samples, we find all types of water,
- slight intrusion, the samples characterizing this family are numerous,
- seawater intrusion, consisting of a significant number of samples, highlighting a sea-groundwater relationship
- freshwater, consisting of about fifteen samples showing that the waters of the study area are mineralized
- slightly soft water, characterized by about fifteen samples.

We notice that the waters indicating a completed seawater intrusion or a slight seawater intrusion, are located in the extension (above) of the sea waters. The rest of the samples are located in the center of the figure constituting the mixed domain.

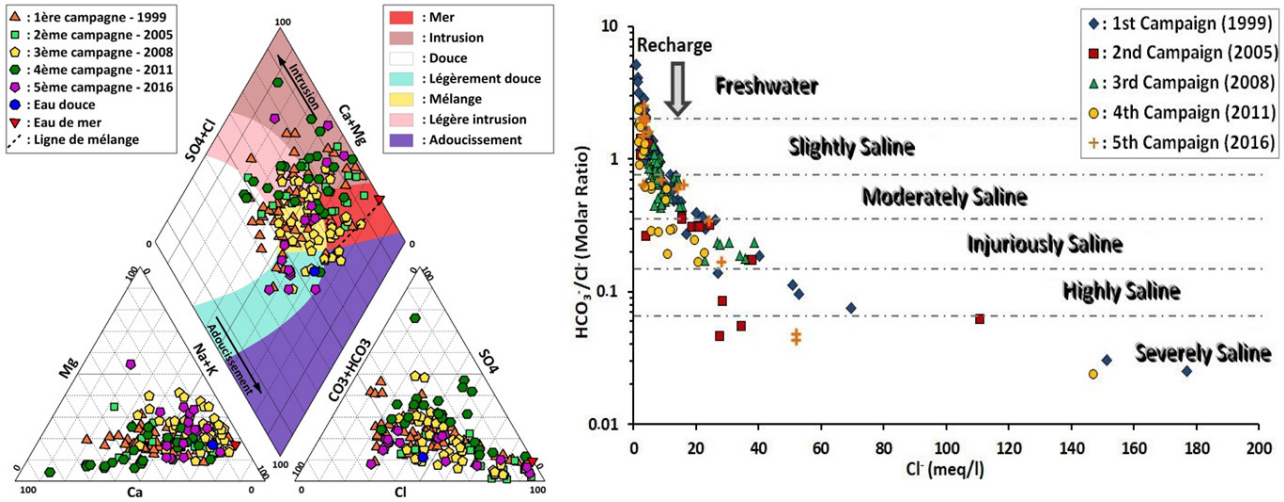

(a) *(b)*

Figure 2. (a) The water distribution in the Piper diagram; (b) distribution of samples to their salinity

Classification of the waters of the Annaba aquifer according to their mineralization: Looking at the water classification diagram (Figure 2b), we find various classes of mineralization thus demonstrating the impact of factors such as the sea, the geology and the climatic variations on the analyzed waters.The results obtained from the compilation of two methods (piezometry and hydrochemistry) indicate a clear exchange between the aquifers and the sea. The two approaches used remain sufficient to highlight the phenomenon of seawater intrusion caused by groundwater overexploitation and climatic variations as a result of the decrease in precipitation.

Acknowledgments: This work was carried out with the help of the engineers of our laboratory help of engineers from our laboratory, particularly Mrs. Djamila Khader and Mr. Hichem Sedairia.

References

Benchaib A (2021) Utilisation d'une approche multicritère pour l'analyse de l'eau dans le Golf d'Annaba. Thèse de doctorat de L'Université d'Annaba, 210 p

Djabri L, Ghrieb L, Guezgouz N, Hani A, Bouhsina S (2014) Impacts of morphological factors on the marine intrusion in Annaba region (east of Algeria). Desalination and Water Treatment 52(10-12): 2151-2156. http://doi.org/10.1080/19443994.2013.808585

Djoudar Dahbia (2006) Etat actuel de l'invasion marine dans la baie d'Alger. Rapport interne, 10 p

Mazouzi C, Tioumassi M (2022) Origines de la minéralisation des eaux de la région Annaba-Echatt-El Hadjar (N.E. Algérien). Master en Hydrogéologie, Université Badji Mokhtar Annaba, 75 p

Mastrocicco M, Colombani N (2020) The Issue of Groundwater Salinization in Coastal Areas of the Mediterranean Region: A Review. Water 13(1): 90. https://doi.org/10.3390/w13010090

Preliminary data on antibiotic resistant bacteria in surface waters in Albania

E. Hamzaraj[1*], B. Parllaku[1], S. Zhubi[2]
[1] Department of Biology, Faculty of Natural Sciences, University of Tirana, Tirana, Albania
[2] Intermedica Diagnostic Center, Tirana, Albania
* e-mail: etleva.hamzaraj@fshn.edu.al

Introduction

The emergence of antibiotic-resistant bacteria and antibiotic resistance genes in aquatic environments is a growing concern worldwide. Since antibiotic contamination is not regulated either globally or locally, their amount in terrestrial, freshwater and marine environments is ever increasing. The antibiotics are typically received by surface water via urban wastewater discharge and animal waste (Qiao M et al. 2018). Among the receiving water environment, surface waters, especially rivers, appear to play an important role in the spread of antibiotic-resistant bacteria because they serve as habitats and as a transport medium for microorganisms (Allocati et al. 2013).

In Albania, many studies have been conducted regarding the quality of surface water, as well as the resistance of bacteria to antibiotics. But there are no studies on antibiotic-resistant bacteria in the environment and on the role of surface water in their spread. The objective of our study was to evaluate the water pollution level and the antibiotic resistance of bacteria isolated from two rivers in Albania: Ishmi and Vjosa. Ishmi River, flowing through central Albania, has a length of 74 km and is formed by the merging of Tirana River, with Terkuze and Zeze streams. Before joining Terkuze stream, Tirana River also takes waters of the Lana River, that passes through Tirana. Vjosa is a transboundary river, shared between Greece and Albania, whose spring is in Pindi Mountains. Its total length is about 272 kilometres, of which the first 80 kilometres are in Greece, and the remaining 192 kilometres are in Albania, where it passes through many urban and rural areas.

Materials and methods

Sterile glass bottles are used to take water samples for microbiological analysis. Samples are taken at a depth of 30-50 cm from the water surface, at a distance of 30 - 100 cm from the river bank and in accordance with all standards for sampling for microbiological analysis (ISO 19458). The Most Probable Number method (ISO 9308-2, ISO 7899-2) is used to determine the concentration of fecal coliforms, *E. coli* and *Enterococcus faecalis*. For the determination of heterotrophs, PCA medium, pour plating method and incubation at 22°C in a biological thermostat for 48 hours are used. Kirby-Bauer test is used for determination of antibiotic sensibility of *E. coli* isolated from river water (Hudzicki 2009).

Results and concluding remarks

Our data on microbial indicators of water pollution (fecal coliforms and fecal enterococci) clearly show the difference in water quality of Ishmi and Vjosa. During the period of investigation (Spring-Autumn 2022) we analysed 15 samples from three sampling sites in Ishmi River and 38 samples from 19 stations along the Vjosa River. We found a very high load of Ishmi River water with fecal coliforms (min. 2100 cfu/100 ml, max. 1.5×10^6 cfu/100 ml) and fecal enterococci (min. 700 cfu/100ml, max. 2.1×10^5 cfu/100 ml). This could be due to wastewater discharges and agricultural runoff since the river section monitored passes through a rural area with high agricultural activity and through many urban areas. Based on the classification system of water quality according to fecal pollution by Kavka et al. (2006) and Kirschner et al. (2009) critical to excessive pollution is observed in Ishmi River (Table 1). According to the same classification system, *E. coli* concentration in 11 out of 19 sampling sites in Vjosa River show little or moderate pollution, with a minimum of 30 cfu/100ml and a maximum of 930 cfu/100ml. A strong (class IV) to excessive (class V)

pollution is observed only in three sampling sites near urban areas. The difference in water quality between the two rivers has also been noted by other studies in Albania (Keci et al. 2018; Hamzaraj et al. 2014).

Table 1. Microbiologically based classification system of water quality according to faecal pollution (Kavka et al. 2006; Kirschner et al. 2009).

Classification of faecal pollution		Class				
		I	**II**	**III**	**IV**	**V**
Parameter	Faecal pollution	**little**	**moderate**	**critical**	**strong**	**excessive**
Escherichia coli	In 100 ml water	≤100	> 100 - 1000	>1000 - 10000	> 10000 - 100000	> 100000

Thirty-two *E. coli* isolates from Ishmi and Vjosa are analysed with the disc diffusion method for their antimicrobial resistance to 22 antibiotics. In general, 20 of all isolates were resistant to one or two antibiotics and the rest (12 isolates) were resistant to three or more antibiotics. The antibiotics with the highest resistance rate were Clindamycin and Augmentin. Because of a relatively small number of *E. coli* isolates form each river we cannot make any statistically based comparison regarding the antimicrobial resistance between the two rivers. But in this phase of our study, we can say that antimicrobial resistant *E. coli* can be isolated from river water despite the level of fecal pollution. This is a first step of the study in Albania of the contribution of surface waters to the spread of antimicrobial resistant bacteria.

References

Qiao M, Ying GG, Singer AC, Zhu YG (2018) Review of antibiotic resistance in China and its environment. Environment International 110: 160-72.

Allocati N, Masulli M, Alexeyev MF, Di Ilio C (2013) Escherichia coli in Europe: an overview. Int J Environ Res Public Health 10: 6235–54

Hudzicki J (2009) Kirby-Bauer Disk Diffusion Susceptibility Test Protocol, American Society for Microbiology. https://asm.org/getattachment/2594ce26-bd44-47f6-8287-0657aa9185ad/Kirby-Bauer-Disk-Diffusion-Susceptibility-Test-Protocol-pdf.pdf.

Kavka G, Kasimir G, Farnleitner A (2006) Microbiological water quality of the River Danube (km 2581 - km 15): Longitudinal variation of pollution as determined by standard parameters. In: Proceedings of 36th International Conference of IAD. Austrian Committee Danube Research/ IAD, Vienna: 415–421

Kirschner AKT, Kavka GG, Velimirov B, Mach RL, Sommer R, Farnleitner AH (2009) Microbiological Water Quality along the Danube River: Integrating Data from Two Whole-River Surveys and a Transnational Monitoring Network. Water Res. 43 (15): 3673–3684. http://doi.org/10.1016/j.watres.2009. 05.034

Keci E, Pepa B, Paparisto A, Duka S (2018) Biodiversity indices and nutrient load assessment in Ishmi River, Albania during 2012 – 2013. European Water 58: 245–250

Hamzaraj E, Lazo P, Paparisto A, Duka S, Mavromati J, Halimi E, Topoviti D (2014) An overview of water quality of Vjosa river in Albania based on biological and chemical parameters. International Journal of Advances in Engineering & Technology 7(5): 1359-1374

Treatment of contaminated water containing two triazole fungicides in pilot-scale horizontal subsurface flow constructed wetlands

P. Parlakidis[1], I. Gounari[2], A. Georgiou[2], G. Adamidis[1], Z. Vryzas[1*], G.D. Gikas[2]
[1] Laboratory of Agricultural Pharmacology and Ecotoxicology, Department of Agricultural Development, Democritus University of Thrace, 68200 Orestias, Greece
[2] Laboratory of Ecological Engineering and Technology, Department of Environmental Engineering, School of Engineering, Democritus University of Thrace, 67100 Xanthi, Greece
* e-mail: zvryzas@agro.duth.gr

Introduction

Pesticides are applied to crops to control weeds, diseases, and pests. However, pesticides can easily enter natural water reservoirs due to incorrect handling of tank-mix leftovers, accidents, direct application, or other point and nonpoint pollution sources, raising concerns about their impact on the environment and human health (Sahin and Karpuzcu 2020). Myclobutanil is a systemic fungicide used against a broad spectrum of diseases in cereals, fruits, and vegetables. Its high chemical, biological, and photochemical persistence with a high half-life value in water and soils raise concerns about a potential contamination in water bodies (Wang et al. 2011). Triticonazole is used to control soil and seed-borne diseases, primarily in cereals. It has a field half-life of over 100 days on average, with a strong potential for accumulation in soil and other matrices. This fungicide can enter water bodies through runoff after use in farms (García-Valcárcel and Tadeo 2011).

Constructed wetlands (CW) are artificial systems created to take advantage of various physicochemical and biological processes of pollutants dissipated under regulated settings, and can treat agricultural runoff. Treatment in CWs involves biological, chemical, and physical processes such as biodegradation, plant uptake, adsorption, retention, and settling (Gikas et al. 2018). Therefore, the purpose of the present study was to optimize the effectiveness of mature pilot-scale CWs to remediate water polluted by persistent fungicides. Such polluted water is usually spraying equipment rinsing water or seed-coating industry wastewater.

Materials and methods

The four pilot-scale HSF CWs used in this investigation were named WMG-C, WMG-R, WMG-U, and WFG-R. Medium gravel (MG) was used as the porous media in the WMG-C, WMG-R, and WMG-U units. In the WFG-R unit, the porous media was fine gravel (FG). The plant species used were common reed (R, *Phragmites australis*) in WMG-R and WFG-R, and cattail (C, *Typha latifolia*) in WMG-C. The WMG-U unit was not planted (U) and was used as a control unit. From March 2022 to July 2022, water enriched with commercial formulations of myclobutanil and triticonazole at a concentration of about 1.9 mg/L was loaded to the pilot-scale CWs. During the spring, an 8-day hydraulic residence time (HRT) was employed while an HRT of 6 days was applied in June and July. With this configuration, it was possible to evaluate the phytoaccumulation capacity of common reed and cattail, and the effect of porous media and HRT on the removal of the two fungicides.

Weekly water samples from the influent and effluent of each CW were taken for analysis and processed to determine the CW unit performance. Simultaneously with the sampling, physicochemical parameters in the water such as dissolved oxygen (DO), pH, electrical conductivity (EC), and temperature (T) were measured in situ by a portable device. To determine the concentration of the two fungicides in the substrate, 500 g samples of substrate were collected from the inlet and outlet of each CW unit using a soil sampling auger. Additionally, the role of the plant in fungicides removal was evaluated by collecting plants from each CW unit at random in triplicate and the roots, stems, and leaves of the plants were separately analyzed to determine the myclobutanil and triticonazole concentrations. The determination of fungicide

residues in water, plants and substrate was conducted using a GC-MS/MS system. To evaluate the differences in the fungicide removal efficiency of the CW units, nonparametric tests such as Kruskal–Wallis and Mann–Whitney U were used.

Results and concluding remarks

The water temperature in the CW units followed the seasonal variation and varied from 8.0 to 32.5 °C The pH values throughout the measurement period varied between acidic (6.66) and alkaline values (7.73). The mean pH values of all pilot-scale CWs were in the alkaline range with no significant variation among them. The influent EC value was lower than the mean effluent EC values for all CWs. The results also indicated that the mean effluent EC value of the planted units was higher than that of the WMG-U unit. The mean DO concentration in the influent was 7.37 mg/L and in the effluent was 4.01, 5.66, 5.12, and 4.57 mg/L for WMG-C, WMG-R, WMG-U, and WFG-R, respectively.

The effluent concentrations of the four CW units were lower than those of the influent, confirming myclobutanil and triticonazole removal. Myclobutanil mean influent concentration was 1.79 mg/L, while the WMG-C, WMG-R, WMG-U, and WFG-R had respective mean effluent concentrations of 0.71, 0.29, 1.12, and 0.20 mg/L for the entire operation period (EP). The mean percentage removals of myclobutanil were 59.3%, 83.4%, 36.6%, and 88.4% for the WMG-C, WMG-R, WMG-U, and WFG-R, respectively. Triticonazole had an average influent concentration of 1.92 mg/L, while the EP mean effluent values for the WMG-C, WMG-R, WMG-U, and WFG-R were 0.55, 0.55, 0.97, and 0.22 mg/L, respectively. The mean removal efficiencies of triticonazole were 71.02%, 70.87%, 49.21, and 88.5% for the WMG-C, WMG-R, WMG-U, and WFG-R units, respectively.

For the three units with the same porous material (i.e., WMG-C, WMG-R, and WMG-U), a comparison was conducted to determine plants contribution. The WMG-R and WMG-C displayed the highest myclobutanil and triticonazole removal efficiencies, with mean removal rates of 83.4% and 71.0%, respectively. Myclobutanil removal in the WMG-C and WMG-R were statistically significantly higher than that in the WMG-U, and the removal in the WMG-C unit was statistically significantly higher than that in the WMG-R unit. The removal of triticonazole in the WMG-U was statistically significantly lower than that in the WMG-C and WMG-R, and there was no statistically significant difference of triticonazole removal between the WMG-C and WMG-R. The WMG-R and WFG-R units, which contained different porous media, and were planted with common reed, were compared, to determine the impact of the two porous media on the fungicides removals. The mean percentage removals of myclobutanil were 83.4% and 88.4%, and of triticonazole were 79.9% and 88.5%, for the WMG-R and WFG-R (statistically significant difference), respectively. Furthermore, the four units showed higher mean removal values of myclobutanil and triticonazole at the HRT of 8 days.

The results of this study indicate that the plants and their ability to uptake fungicides, HRT, and the type and gradation of porous media are the most crucial parameters determining the CW capability for the removal of myclobutanil and triticonazole, while hydrolysis, photodegradation, and volatilization are negligible. Also, the different physicochemical properties (i.e., lipophilicity) of the two fungicides determine their fate within CW systems.

Acknowledgments: This work was supported by the Hellenic Foundation for Research and Innovation (HFRI) under the HFRI PhD Fellowship grant (Fellowship Number: 353).

References

García-Valcárcel AI, Tadeo JL (2011) Determination of azoles in sewage sludge from Spanish wastewater treatment plants by liquid chromatography-tandem mass spectrometry. Journal of Separation Science 34(11): 1228–1235. https://doi.org/10.1002/jssc.201000814

Gikas GD, Vryzas Z, Tsihrintzis VA (2018) S-metolachlor herbicide removal in pilot-scale horizontal subsurface flow constructed wetlands. Chemical Engineering Journal 339: 108–116. https://doi.org/10.1016/j.cej.2018.01.056

Sahin C, Karpuzcu ME (2020) Mitigation of organophosphate pesticide pollution in agricultural watersheds. Science of the Total Environment, 710: 136261. https://doi.org/10.1016/j.scitotenv.2019.136261

Wang C., Wu Q, Wu C, Wang Z (2011) Application of dispersion-solidification liquid-liquid microextraction for the determination of triazole fungicides in environmental water samples by high-performance liquid chromatography. Journal of Hazardous Materials 185(1): 71–76. https://doi.org/10.1016/j.jhazmat.2010.08.124

12th World Congress on Water Resources and Environment (EWRA 2023)
"Managing Water-Energy-Land-Food under Climatic, Environmental and Social Instability"
Thessaloniki, Greece, 27 June - 1 July 2023

Residues of polycyclic aromatic hydrocarbons (PAHs) in waters of the Ili-Balkhash Basin, arid Central Asia

B. Shen[1], J. Wu[2*]
[1] College of Environmental Science and Engineering, Yangzhou University, Yangzhou, 225127, China
[2.] State Key Laboratory of Lake Science and Environment, Nanjing Institute of Geography and Limnology, Chinese Academy of Sciences, Nanjing 210008, China
* e-mail: w.jinglu@niglas.ac.cn

Introduction

Polycyclic aromatic hydrocarbons (PAHs) are emitted mainly from anthropogenic sources, and some of them with four or more rings are carcinogenic and mutagenic (Sarria-Villa et al. 2016). They are persistent, semi-volatile chemicals that can move from their source area via long-range transport, and have become widespread across the globe, even high-altitude zones far from sources (e.g., the Tianshan Mountains and Tibetan Plateau) (Wania and Mackay 1996; Wang et al. 2016).

In Central Asia, precipitation and glacial meltwater from the Tianshan Mountains play a vital role in supplying water to the extensive surrounding lowlands. The area is home to several major river and lake basins, including the Syr Darya-Aral Sea Basin, the Chu River-Lake Issyk-Kul Basin and the Ili-Balkhash Basin. There has, however, been little research on PAHs in the aquatic environments of the Ili-Balkhash Basin. The basin is characterized by a suite of distinct altitudinal climatic zones that extend from the Tianshan Mountains to the China-Kazakhstan border region and Lake Balkhash, the lowest point in the basin. Precipitation and glacial meltwaters from the Tianshan Mountains are the main hydrologic sources for the basin's lowlands and the lake. Human activities in the region have increased to the point that water quality in downstream parts is impaired by pollutants (Krupa et al. 2020; Shen et al. 2022). This raised concerns that surface waters in the region might have been negatively affected by anthropogenic organic pollutants, given increasing agricultural activities and industrialization along the rivers and lake. Additionally, mountainous areas and the region along the China-Kazakhstan border are relatively remote; and, less attention has been paid to chemical contamination of aquatic environments. Studies on the concentrations of PAHs in this basin should provide information about pollution that affects the aquatic environment, as well as be useful to understand the global distribution behaviours of these pollutants.

In this study, we determined the residual concentrations and spatial distributions of OCPs and PAHs in waters of the Ili-Balkhash Basin, investigated their potential sources, and evaluated the consequent biological and human health risks.

Materials and methods

According to the topographic and hydrological characteristics of the basin, as well as population distribution, we collected 16 water samples from input rivers and two water samples from Lake Balkhash in 2018 to evaluate PAH concentrations.

PAHs in water were extracted by the method of solid-phase extraction (SPE) (Busetti et al. 2006). First, the cartridges were preconditioned by successive elution with 10 mL methanol and 10 mL ultrapure water. Second, 2 L of filtered water was passed through the cartridges, under vacuum. Finally, after eluting subsequently with 10 mL hexane and twice with 20 mL dichloromethane, the latter extracts containing PAHs were dewatered with anhydrous sodium sulphate, and then rota-evaporated and solvent-exchanged to hexane. They were then concentrated to 1 mL under nitrogen flow and stored at -20 °C until analysis. PAHs were analyzed using a high performance liquid chromatograph (Agilent 1200) with diode array detection (238 nm) and a fluorescence detector, according to ISO 1799 standard (ISO 1799 2002; Wolska 2008).

Results and concluding remarks

ΣPAH concentrations in waters of the Ili-Balkhash Basin were between 7.58 and 70.98 ng L^{-1}, with a mean of 32.33 ng L^{-1}. Compared to concentrations reported for global surface water systems, the concentrations are lower than values in water samples from large rivers or downstream of highly populated urban or industrialized areas, but higher than nonurban sites.

The dominant detected pollutants in waters were Nap, Ace, Phe and Pyr. With respect to aromatic ring numbers, the 2- and 3-ring PAHs (low-molecular-weight PAHs, LMW PAHs) were abundant at all sampling sites. Together with molecular ratios of Ant/(Ant + Phe), Flu/(Flu + Pyr) and BaA/(BaA + Chr), PAH contamination of these areas originated from petroleum and combustion processes. Furthermore, the primary sources of PAHs at different sites were identified using a Positive Matrix Factorization model: 1) oil leakage (33.9%), 2) biomass burning (29.5%), 3) coal combustion (22.6%), and 4) petroleum-powered vehicles (14.1%).

Overall, PAH concentrations in the basin were relatively low, with only a few exceptions. The highest concentration was observed near the capital of Almaty Oblast, Taldyqorghan City. Municipal wastewater discharge and vehicular emissions from the densely populated urban area, as well as industrial activities in the upstream, therefore, are responsible for PAH contamination in the area. On the other hand, as the city is surrounded by one of the largest rice-producing regions in Kazakhstan, fossil fuel from farm vehicles or generators, open burning of biomass, and combustion of agricultural residue for cooking are important sources of PAHs. Higher PAH concentrations with the greater proportional contributions of more volatile LMW constituents were measured in waters from relatively undisturbed sites, i.e., Tianshan Mountains and in the vicinity of the China-Kazakhstan border, where there are no pollutant sources. It is possible that long-range transport and meltwater sources has become a non-negligible mechanism for pollutant distribution.

To obtain an overall view on the possible toxic effects of PAHs in waters of the Ili-Balkhash basin, risk quotient (RQ) was calculated for the aquatic biota, and carcinogenic risk (R) and hazard quotient (HQ) were evaluated for the carcinogenic potential and hazard to human health. Results of RQs indicated low to moderate toxicity for aquatic organisms. HQs of all compounds were <1, and Rs were lower than the 10^{-6} threshold, meaning that these pollutants probably have no negative health effects.

Acknowledgments: We thank the CAS Research Center for Ecology and Environment of Central Asia for assistance with this work and Yuqing Wu for data processes assistances. The study was supported by the National Natural Science Foundation of China (U2003202, 41671200), the Strategic Priority Research Program of Chinese Academy of Sciences, Pan-Third Pole Environment Study for a Green Silk Road (XDA2006030101).

References

Busetti F, Heitz A, Cuomo M, et al. (2006) Determination of sixteen polycyclic aromatic hydrocarbons in aqueous and solid samples from an Italian wastewater treatment plant. Journal of Chromatography A 1102: 104-115. https://doi.org/10.1016/j.chroma.2005.10.013

Krupa E, Barinova S, Aubakirova M (2020) Tracking pollution and its sources in the catchment-lake system of major waterbodies in Kazakhstan. Lakes and Reservoirs: Research and Management 25(1): 18-30. https://doi.org/10.1111/lre.12302

Sarria-Villa R, Ocampo-Duque W, Páez M, et al. (2016) Presence of PAHs in water and sediments of the Colombian Cauca River during heavy rain episodes, and implications for risk assessment. Science of the Total Environment. 540, 455–465. https://doi.org/10.1016/j.scitotenv.2015.07.020

Shen B, Wu J, Zhan S, et al. (2022) Spatial Distributions, Sources and Risk Assessment of Toxic Elements in Waters of a Central Asian Basin. Water Resources Management 2022: 1-17. https://doi.org/10.1007/s11269-022-03348-1

Wania F, Mackay D (1996) Peer reviewed: tracking the distribution of persistent organic pollutants. Environmental Science and Technology 30: 390A-396A. https://doi.org/10.1021/es962399q

Wang X, Gong, P, Wang C, et al. (2016) A review of current knowledge and future prospects regarding persistent organic pollutants over the Tibetan Plateau. Science of the Total Environment 573: 139-154. https://doi.org/10.1016/j.scitotenv.2016.08.107

ISO procedure 1799 (2002) Water quality—determination of 15 PAHs in water by HPLC with fluorescence detection

Wolska L (2008) Determination (monitoring) of PAHs in surface waters: why an operationally defined procedure is needed. Analytical and Bioanalytical Chemistry 391: 2647-2652. https://doi.org/10.1007/s00216-008-2173-y

Evaluation of microplastic pollution from treated wastewaters in terrestrial inland waters: A case study from Nif river

N.Baycan[1], N.Alyürük[1], N.Kara[1], C.Alpergün[1], Y. Kazancı[2*], O. Gündüz[2]
[1] Environmental Engineering Department, Dokuz Eylul University, Izmir, Turkey
[2] Environmental Engineering Department, Izmir Institute of Technology, Izmir, Turkey
* e-mail: yigithankazanci@iyte.edu.tr

Introduction

Microplastics (MPs) are defined as polymeric particles less than 5 mm in size (GESAMP 2015). MP sources are divided into two main groups "primary sources" formed by plastic particles that are shredded by grinding or extrusion for direct use, and "secondary sources" formed by the fragmentation of larger-sized plastic material into smaller pieces in the environment (Tunçelli and Erkan, 2021). Primary sourced MPs can also originate from large plastic objects during manufacture, use, or maintenance stages, such as the wear of vehicle tires or the appearance of synthetic textiles during laundry. MPs can be found in many shapes and colors. The form of a microplastic is often used to assign a common category that helps inform the source (Helm 2017). They can then be transported via rivers to seas and oceans, creating a widespread distribution and leading to potential harm to marine and freshwater wildlife. Microplastics can also act as a vector for toxic chemicals, posing a threat to human health throughout the food chain. Thus, it is crucial to understand the pathways and transport of microplastics in the environment and act to mitigate their impacts. Based on this premise, this study aims to evaluate the presence of MPs in the Nif Creek and Gediz River in Western Anatolia, which receive numerous domestic and industrial treated wastewater discharges.

Materials and methods

In this study, 11 sampling stations (3 wastewater discharges and 8 river sampling points) were used to analyze the presence of microplastics in wastewater treatment plants discharges and along the river. The field campaign conducted in this study included in-situ measurements and sample collection activities for laboratory analysis. Field measurements of pH (SM 4500 H^+ B), temperature (SM 2550 B), dissolved oxygen (SM 4500-O C), and electrical conductivity (SM 2510 B) were performed by portable probes (Multi 340i WTV). Then, 2L samples were collected from the field for chemical oxygen demand (COD), heavy metals and trace elements, and microplastics analysis. Samples collected from the field were taken to the laboratory under temperature-controlled conditions and were analyzed at the earliest possible time slot. Samples were stored at 4°C until laboratory analysis. Chemical Oxygen Demand and heavy metal and trace elements (Ag, Al, As, B, Cd, Co, Cr, Cu, Fe, Li, Mg, Mn, Mo, Ni, Pb, Sb, Se, Sr, V, Zn, Hg) were measured in the laboratory according to the standard COD analysis method (SM 5220 B) and inductively coupled plasma mass spectroscopy (SM 3030 K, SM 3120 B, EPA 6010 D), respectively.

For microplastic analysis, samples were filtered by using 4 different steel sieve sets of 500, 250, 100, and 25-micron pore sizes. Each of the steel sieves was washed with distilled water, and the particles on it were transferred to the beaker. Approximately 100 ml of the filtrate obtained from each steel sieve was divided into 3 equal volumes to work with different molars and dried in an oven at 60°C for 24 hours. Then, for each sieve size, 20 ml of H_2O_2 was added to the samples dried in the oven, and they were studied in 3 different molars 1M, 5M, and 10M. The dry samples to which H_2O_2 were added were then mixed in the heater with a magnetic stirrer for 60 minutes at 40°C to totally destruct the organic matter in the sample. Samples were then filtered through a 10 cm diameter steel sieve with a pore size of 25 microns and left to dry in the oven at 40°C for microscope analysis. A three-dimensional stereomicroscope (Leica S Apo) was used to analyze the amount, size, color, and shape of microplastics in the samples. After quantifying the microplastics remaining on the steel sieve with the stereomicroscope, further analysis was performed with an attenuated total reflection Fourier transform infrared (ATR-FT-IR) spectroscope (Perkin Elmer Frontier)

to determine the type of plastic material detected under the microscope. Since sub-samples were formed in the analyses, the data of the species were recorded as percentages. The raw data obtained from microscopic and spectroscopic analysis were later analyzed using JASP statistical software (Version 0.16.4). ANOVA was performed to compare the microplastic counts obtained at 11 different points on the same day. The relationship between the abundance of microplastics in water samples and other environmental factors such as COD, TSS, pH, dissolved oxygen, conductivity, temperature, and heavy metals was evaluated using Spearman correlation. The results were considered statistically significant if the p-value was less than 0.05.

Results and concluding remarks

The results of the sampling campaign from the river and wastewater discharges are given in Table 1. Based on surface morphological characteristics, MPs found in this study were divided into seven colors (black, blue, green, red, yellow, transparent), five size categories (<0.1 mm, 0.5-0.1 mm, 1–0.5 mm, 5-1 mm, >5mm), and four shapes (fiber, film, foam, particle). The major shapes observed in surface water samples were fibers (mean value: 59 particle/L) and particles (mean value: 51 particle/L), with films (mean value: 14 particle/L) and foam (mean value: 1 particle/L) having a comparably lower presence. The high abundance of small-sized MPs were attributed to the fragmentation of larger plastic particles due to the effects of physical variables (salinity, light, and temperature) and bacterial degradation. The majority of particles found in the environment are considered secondary MPs, which typically make up over 80% of all MPs, and result from the breakdown of larger plastic objects. In addition, the number of MPs in river water samples was found to be higher than in wastewater discharges. Among the 11 stations, the maximum fiber abundances were observed at the most upstream stations 1 and 1A. MPs are evenly scattered on both banks of the river and its basin in urban areas. Since most of the stations sampled were under road bridges, it was likely that a large number of MPs were transferred from the road to the river. Accordingly, the total number of MPs found in surface water and wastewater discharges differed significantly in this study with lower occurrences of MPs in treated wastewater discharges.

Table 1. Characterization of Surface Water (River) and Wastewater Discharges (WWD).

Sta.	Group	pH	Temp. (°C)	D.O. (mg/L)	Elec. Cond. (µS/cm)	COD (mg/L)	TSS (mg/L)	∑MP (part./L)
1	River	7.57	25.0	0.32	1760	180	40	3812
1A	River	7.44	25.0	5.35	2820	136	29	4926
2	WWD	7.89	25.7	5.30	5350	64	26	2740
3	WWD	7.62	22.4	5.75	1266	<6.07	<2.95	824
4	River	8.05	25.0	9.05	3380	28	5	4092
5	River	7.61	16.7	5.01	2520	24	13	5824
6	River	7.70	16.3	0.12	3380	80	268	6264
7	River	8.12	17.2	3.74	3780	60	29	2992
8	WWD	7.13	27.3	4.87	3490	108	46	4016
9	River	7.85	25.0	5.45	2310	12	13	4014
10	River	8.15	19.4	10.6	2390	44	11	3220

Acknowledgments: This study was supported by the Scientific and Technological Research Council of Turkey (TÜBİTAK) with project number 121Y460.

References

GESAMP (2015) Sources, fate and effects of MP in the marine environment: A Global Assessment. In Joint Group of Experts on the Scientific Aspects of Marine Environmental Protection; GESAMP No. 93, pp 1-220. ISSN 1020-4873

Helm PA (2017) Improving microplastics source apportionment: A role for microplastic morphology and taxonomy? Analysis Methods 9: 1328-1331. https://doi.org/10.1039/C7AY90016C

Tuncelli C, Erkan N (2021) Gıda güvenliği açısından su ürünlerinde mikroplastik riski ve araştırma yöntemleri. Aquatic Research 4(1): 73-87. https://doi.org/10.3153/AR21007

Evaluation of human health (neurodegenerative) risks in rice cultivation based on heavy metal and pesticide load in water

F. Dökmen[1*], Y. Ahi[2], T.T. Dündar[3], İ. Doğan[4], Z. Vryzas[5]
[1] Kocaeli University, Vocational School of İzmit, Department of Crop and Animal Production, Kocaeli, Turkey
[2] Ankara University, Water Management Institute, Ankara, Turkey
[3] Bezm-i Alem Vakıf University, Faculty of Medicine, Department of Neurosurgery, Istanbul, Turkey
[4] Ankara University, Faculty of Medicine, Department of Neurosurgery, Ankara, Turkey
[5] Democritus University, Department of Agricultural Development, Orestiada, Greece
* e-mail: funda.dokmen@kocaeli.edu.tr

Introduction

Paddy is cultivated on an area of approximately 162.5 million hectares in the world, and the amount of rice obtained is approximately 497 million tons. While India ranks first in paddy cultivation areas with 44.2 million hectares, China ranks second in production with 148.5 million tons (MAF 2020; TEPGE 2020). In the summer months, which is critical in paddy production in the northern hemisphere, there are increased needs for clean irrigation water. In Asian and African continents, there are area-oriented increases (FAO 2018). The highest yield in paddy can be obtained in temperate climate conditions. Turkey's share in world rice production is approximately 450.00 tons per year. Although it is above the world average production, 20-25% of the need is imported as production is not enough to meet consumption (MAF 2023).

The pressure on water resources and therefore on safe food supply has increased due to the growing industrialization in parallel with the increase in population and excessive consumption and pollution as a result of these. For this reason, it is urgently necessary to define the effects of pollutants in water resources on food and human health and to develop solutions for their removal.

Heavy metals and pesticide residues have different origin but both can be accumulated in agroecosystems through irrigation with polluted water. Heavy metals and certain pesticide residues negatively affect plant physiology of and through the food chain can affect human health and non -target organism. In this study, the effect of heavy metals and pesticides on the physiology of the rice crop and yield quality, the tolerance mechanisms against heavy metals and pesticides and their effects on human health are discussed. In this regard, a holistic methodology was established.

Materials and methods

Turkey has suitable climatic conditions in terms of paddy production. Paddy production is carried out in 31 provinces in Turkey (Figure 1). Meriç-Ergene River basin of Thrace region is in the first place in production. Although it varies according to years, irrigation water problems pose a great problem for rice producers and become the most important factor limiting rice farming. Insufficient rainfall, especially in winter, can cause shrinkage in paddy cultivation areas. One of the other important reasons is the insufficient supply of clean irrigation water. In the Thrace Region, which has the highest cultivation and productivity in paddy production, it has become impossible to use qualified and clean water resources with the desired irrigation water quality in paddy production due to the intense pollution level of the water resources.

In this study, we aim to develop a methodology based on a literature review to determine the effects of heavy metals and pesticide residues in water resources on rice crops and human health. Many studies reviewed (Bowman et al. 2011; Abedin et al. 2020; Yerli et al. 2020) include physical, chemical and biological detection of water resources based on irrigation water quality regulations, monitoring the effects of pollutants in water resources on crop production according to food legislation, and also on human health with mouse experiments in medicine and MRI examinations.

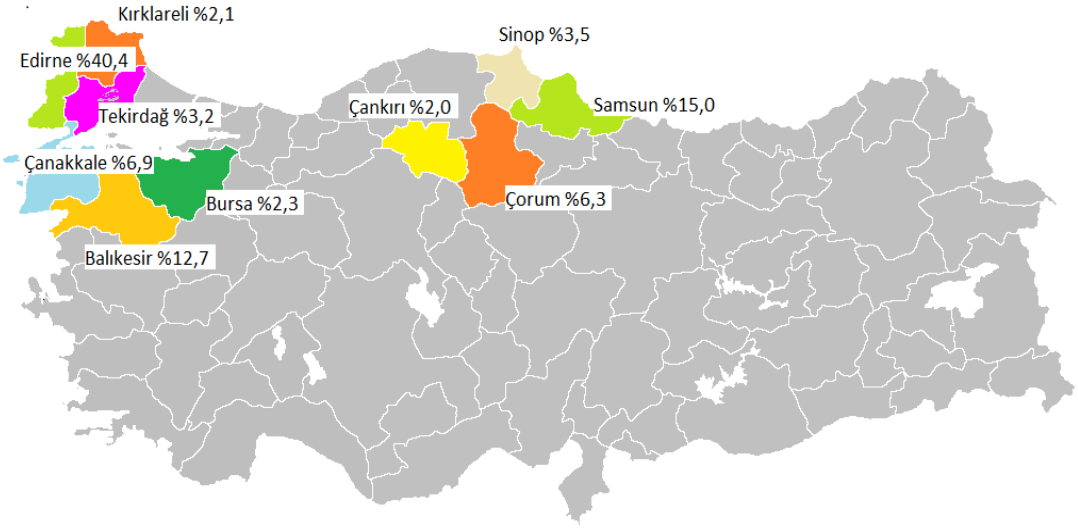

Figure 1. Provinces that are at the forefront of paddy cultivation in Turkey (%).

Results and concluding remarks

Environmental pollution caused by heavy metals and pesticide residues can easily reach water resources through runoff, leaching and other processes. As a result, heavy metals and pesticide residues pass from soils to plants and from there to agricultural food production. It can pass into the human body and cause accumulation here.

Since paddy is a plant usually cultivated with border irrigation, water with heavy metal load heavily affects the rice plant, which is exposed to more water during the growing period. Toxic heavy metals such as Cd (cadmium), Cr (chromium), Ni (nickel), Pb (lead), Hg (mercury), Al (aluminum) and As (arsenic), which are found in large amounts in industrial wastewater, and pesticide residues or metabolites of persistant compounds are mainly detected. The long-term persistence of these inorganic factors in their environment creates toxic effects on living organisms and creates risks for human health by accumulating in food chains. For this reason, the heavy metal bioaccumulation levels in the paddy grown and thus in the rice increase to levels that will adversely affect human health.

Most heavy metals and insecticides are characterized as neurotoxic compounds that can harm nervous system and cause chronic diseases. Our brain and nervous system control fine motor skills. Since heavy metals are known to kill healthy nerve cells, it is a scientific fact that heavy metals negatively affect fine motor skills. Most of the time, symptoms occur with weakening memory, language skills and thinking skills (MH 2022).

The relationship between irrigation water quality and heavy metals of the paddy/rice plant, which has an important agricultural production potential in the world and in our country, and, accordingly, important neurodegenerative disorders in human health have been discussed.

References

Abedin MJ, Cotter-Howells J, Meharg AA (2020) Arsenic uptake and accumulation in rice (Oryza sativa L.) irrigated with contaminated water. Plant and Soil 240(2): 311-319

Bowman AB, Kwakye GF, Hernandez EH, Aschner M (2011) Role of manganese in neurodegenerative diseases. Journal of Trace Elements in Medicine and Biology 25(4): 191-203

FAO (2018) Global Information and Early Warning System (GIEWS) (Food Outlook-July), Rome, Italy

MAF (2020) Status and Forecast Rice. T.C. Ministry of Agriculture and Forestry Institute of Agricultural Economy and Policy Development, Ankara, Türkiye

MAF (2023) T.C. Ministry of Agriculture and Forestry Reports. Ankara, Türkiye

MH (2022) T.C. Ministry of Health Reports. Ankara, Türkiye

TEPGE (2020) Institute of Agricultural Economy and Policies Development Directorate, Agricultural Products Markets Paddy Report, Ankara, Türkiye.

Yerli C, Çakmakçı T, Şahin Ü, Tüfenkçi Ş (2020) Ağır metallerin toprak, bitki, su ve insan sağlığına etkileri, Türk Doğa ve Fen Dergisi (Turkish Journal of Nature and Science) 9: 103-114

Treatment of table olive processing wastewater by means of electrocoagulation: Effect of key operating parameters

K. Davididou[1], A.G. Kapagiannidis[1*], D. Gkelezis[1], A. Chatzimpaliotis[2], E. Amanatidou[2]
[1] Alphabio Ltd, Thessaloniki, Greece
[2] Department of Chemical Engineering, University of Western Macedonia, Kozani, Greece
* e-mail: tasos.kapagiannidis@alpha-bioenergy.com

Introduction

Table olive worldwide production reached more than 3.4 million tons in the 2021/22 crop year, with nearly 30% produced in Europe (IOC 2023). The olive industry, which is of special economic importance to the Mediterranean countries, is heavily dependent on natural resources (water, air, soil, etc.), making the efficient management of inputs (energy, water, etc.) and outputs (by-products, effluents, waste products) vital for business sustainability. Regarding water use, table olive processing is a water-intensive operation generating up to 7.5 m^3 wastewater per ton of olives processed (Kopsidas 1992). Table olive processing wastewater (TOPW) is commonly characterised by high conductivity, increased COD, and poor biodegradability. Disposal of untreated or partially treated TOPW poses significant threats to the receiving environment, including, but not limited to, toxicity, oxygen depletion/imbalance, and eutrophication.

Up to date, several treatment methods have been reported for TOPW treatment, including aerobic/anaerobic biological systems, as well as advanced oxidation processes, however a highly efficient, sustainable, and simple method has yet to be identified (Ayed et al. 2017). Electrocoagulation (EC) constitutes an attractive treatment alternative for agro-industrial effluents owing to the process's well-proved high efficiency, ease of operation, short treatment residence time and no chemical addition (Benekos et al. 2019). In the present study, the efficiency of EC for the treatment of real TOPW is investigated. In this direction, the effect of key operating parameters (i.e., electrode material, pH, and current density) on process efficiency is assessed, while the coherent treatment cost is estimated.

Materials and methods

TOPW was obtained from a green olive processing plant, located in the Chalkidiki region (northern Greece), and used throughout the experiments without any prior treatment (Table 1).

Table 1. Main physico-chemical characteristics of TOPW.

Parameter	Unit	Value
pH		8.3 ± 0.3
electrical conductivity	mS/cm	22.3 ± 2.8
chemical oxygen demand, COD	mg/L	2730 ± 328
biochemical oxygen demand, BOD_5	mg/L	205 ± 29
total suspended solids, TSS	mg/L	430 ± 85
total nitrogen, TN	mg/L	46.3 ± 8.4
NH_4^+-N	mg/L	4.5 ± 1.1
NO_3^--N	mg/L	2.7 ± 0.5
NO_2^--N	mg/L	0.19 ± 0.07
total phosphorus, TP	mg/L	15.8 ± 2.2

Experiments were carried out in a lab-scale electrolytic cell with 6 monopolar electrode plates (15 x 8 x 0.5 cm) connected in parallel, with inter-electrode gaps of 1 cm. The electrodes used were made of either aluminum (Al) or iron (Fe). The pH of TOPW was adjusted by adding diluted sulfuric acid prior to each test commencement. The reactor (4 L effective volume) was operated in batch mode, applying a treatment time of 60 min. During the EC experiments, samples were withdrawn at regular intervals and filtered through 0.45 μm syringe filters to remove suspended material. Samples were further analyzed regarding their pH,

electrical conductivity, color, and COD, TN, and TP concentration. In order to assess the treatment cost, electrode consumption was determined by recording the weight of each electrode before and after treatment.

Conductivity and pH measurements were performed by using a WTW 3620 IDS multiparameter portable meter. COD, TP, TN, and nitrogen ions were determined according to the Standard Methods (APHA 2012) and color was evaluated spectrophotometrically at 400 nm, as reported elsewhere (Benekos et al. 2019).

Results and concluding remarks

In order to investigate the effect of pH on process efficiency, experiments were carried out at pH 5, 7, and 8, using three different material configurations for anodic and cathodic electrode plates, namely Al-Al, Al-Fe, Fe-Fe, in a triple plate couples' cascade. In all cases, color removal efficiency was higher than 85% and it was found to descend in the following order: Al-Al > Al-Fe > Fe-Fe. In terms of COD removal efficiency, EC resulted in percentages over 80%, under all the conditions applied, with Al-Fe combination demonstrating the highest performance. Furthermore, the process led to complete removal of phosphorus, while nitrogen was removed by more than 65%, in any case. According to the obtained results, pH had no significant impact on TOPW treatment by means of EC. However, it is worth mentioning that pH tended to increase with treatment time; the pH of the TOPW after 60 min of treatment was invariably higher, by at least 2.5 units, compared to the initial value. This should be taken into consideration if the effluent is to be discharged into the municipal sewer network or to be further treated by biological means. Having this in mind, subsequent experimental tests were carried out at initial pH of 5, in order to obviate the need for pH adjustment after EC, using Al-Al and Al-Fe electrode configurations since those led to the highest pollutants removal efficiencies.

Furthermore, the effect of the applied current density (i.e., 4.17, 5.55, 6.94 mA/cm^2) on EC performance was assessed. For this purpose, the electric current was appropriately regulated through the power supply unit. The results showed that color and TN removal are decreased with decreasing current density for both Al-Al and Al-Fe configurations. On the other hand, COD removal remains constant when Al-Fe scheme is used and, interestingly, it is increased with decreasing current density for the Al-Al combination.

A cost analysis of TOPW treatment by EC was then performed for every experimental run, considering (a) electrode material consumption, (b) energy consumption, and (c) chemicals for pH adjustment. It was found that material consumption increases with current density and, also, when Fe-Fe combination is used. On the other hand, it was found that aluminum electrodes consume more energy compared to iron, for the same current density applied. Overall, considering the current Greek market prices, the use of the Al-Al combination at the lowest current density applied, results in a total operational cost lower than 2.5 €/m^3 for the treatment of TOPW by means of EC.

Conclusively, the EC process has proven its high performance for the removal of color, organics and nutrients from TOPW with a fairly reasonable operational cost. The effluent produced after EC treatment meets the basic requirements for being discharged in municipal sewer networks or further being carried through a final polishing treatment step.

References

APHA (2012) Standard Methods for the Examination of Water and Wastewater, 22nd edn. American Public Health Association, Washington DC

Ayed L., Asses N, Chammem N, Ben Othman N, Hamdi M (2017) Advanced oxidation process and biological treatments for table olive processing wastewaters: constraints and a novel approach to integrated recycling process: a review. Biodegradation 28: 125–138. http://dx.doi.org/10.1007/s10532-017-9782-0

Benekos AK, Zampeta C, Argyriou R, Economou CN, Triantaphyllidou IE, Tatoulis TI, Terlekopoulou AG, Vayenas DV (2019) Treatment of table olive processing wastewaters using electrocoagulation in laboratory and pilot-scale reactors. Process Safety and Environmental Protection 131: 38-47. https://doi.org/10.1016/j.psep.2019.08.036

IOC, The world of table olives. Available from: https://www.internationaloliveoil.org/the-world-of-table-olives/ (accessed: 24 February 2023)

Kopsidas GC (1992) Wastewater from the preparation of table olives. Water Research 26(5): 629-631. https://doi.org/10.1016/0043-1354(92)90237-X

Optimizing the wastewater treatment method for industrial use: A case study of Bandar Abbas city

S. Shojaie[1], S.A. Sajadi[2,3*], M. Mollaei[3], H. Amiri[3]
[1] Persian Gulf Infrastructure Supply and Development Co, Bandar Abbas, Iran
[2] Department of Irrigation & Reclamation Engineering, University of Tehran, Karaj, Iran
[3] Sadrab niroo Consulting Engineers Co, Urmia, Iran
*e-mail: S_ahmadsajadi@ut.ac.ir

Introduction

Iran is situated within the arid belt of the world. Climatic shifts attributable to global warming over the past few decades and the indiscriminate utilization of available water resources have put Iran at a high risk of experiencing severe water shortages (Zarepour Moshizi et al. 2022). According to recent surveys, the impacts of climate change and drought have been more pronounced in the south of Iran than in other regions of the country (Mansouri Daneshvar et al. 2019). As a result, water consumption management and wastewater use in industries have become imperative, particularly in these areas (Charkhestani et al. 2016). Discharging wastewater from urban and industrial activities leads to the destruction of biological environments and ecological changes. Consequently, water reuse, an old practice but a novel approach, has become the focus of all governmental and non-governmental. Therefore, to preserve water reserves and promote the development of industry and agriculture, it is necessary to utilize the full potential of sewage effluents in accordance with all environmental standards, particularly given the impact of drought and water scarcity on water resources in the Bandar Abbas city (located south of Iran) in recent years. This study examines the feasibility of using Bandar Abbas wastewater treatment effluents in industries located to the west of the city. Three different wastewater treatment and reuse methods have been assessed in this study, and the optimal option has been selected based on technical, environmental, economic, and operational considerations.

Materials and methods

The proposed supplementary treatment unit will be situated within the Bandar Abbas wastewater treatment plant. It is noteworthy that the treatment plant was designed to handle a flow rate of 64 thousand cubic meters per day. However, the current flow rate of incoming wastewater to the plant has exceeded its capacity, with 100 thousand cubic meters per day, leading to the discharge of untreated wastewater into the sea. As such, the primary aim of this project is to reuse wastewater and prevent environmental pollution. Based on the investigations carried out, three different options have been suggested for the additional treatment of Bandar Abbas wastewater. These options are outlined as follows:

- Option 1: This method involves chemical precipitation, double layer filtration, ozonation, activated carbon, ultrafiltration, filter cartridge, reverse osmosis, and final purification.
- Option 2: This method includes chemical precipitation, double layer filtration, ultrafiltration, advanced oxidation, filter cartridge, reverse osmosis, and final purification.
- Option 3: This method involves chemical precipitation, double layer filtration, advanced oxidation, ultrafiltration, filter cartridge, reverse osmosis, and final purification.

Results and concluding remarks

Based on the information provided, it appears that all three options have several stages of treatment including chemical precipitation, double-layer filtration, and reverse osmosis. However, the main difference lies in the additional treatment steps such as ozonation and activated carbon in option 1, advanced oxidation in option 2, and dissolved air flotation in option 3. Option 1 has a comprehensive treatment plan

that includes ozonation and activated carbon to remove the remaining organic matter. However, the high-dose chlorine injection may raise environmental concerns. Option 2 has a similar treatment process to option 1 but with the addition of advanced oxidation to remove organic matter, reducing the amount of ozone needed for the ozonation process. It also includes a UV disinfection system to reduce microbial burden. Option 3 has the most complex treatment plan with dissolved air flotation added to the chemical precipitation process, followed by advanced oxidation and ultrafiltration. This may result in higher costs and greater technical challenges. In terms of economic factors, option 2 may be the most cost-effective due to the reduced ozone usage and simpler treatment process. However, the advanced oxidation unit and UV disinfection system may add to the capital and operational costs. From an environmental perspective, option 2 may also be preferable as it reduces the amount of ozone required for treatment, reducing the potential for harmful by-products. From a technical perspective, option 1 may be the most reliable as it includes multiple treatment stages to ensure high-quality effluent, but the high-dose chlorine injection may pose technical challenges. Therefore, based on the given information, option 2 may be the most favourable choice, as it offers a good balance between economic, environmental, and technical factors.

The economic and technical advantages of the third option for the additional treatment of Bandar Abbas wastewater treatment plant are highlighted in the evaluation matrix (Tables 1 and 2). The low initial investment cost and the low cost of treating each cubic meter of wastewater make this option economically favourable. Additionally, the less energy consumption compared to the first option is a technical advantage that can reduce operational costs over time. Moreover, the ease of operation of the system due to the units considered for desalination water pre-treatment is another significant technical advantage of the third option. The speed and ease of system implementation according to the type of units considered can also reduce the downtime of the plant during the construction phase. Another technical advantage of the third option is less water wastage due to the absence of active carbon filters, which can result in lower operational costs. Overall, the third option offers a balanced approach, making it the best option for the additional treatment of Bandar Abbas wastewater treatment plant.

Table 1. Economical evaluation matrix of different options.

Alternative	Treatment cost per m^3		Initial investment cost		Operation cost		Total
A1	73	7.3 10	68.8	8.6 8	72	9 8	213.8
A2	100	10 10	80	10 8	80	10 8	260
A3	100	10 10	80	10 8	80	10 8	260

Table 2. Technical and operational evaluation matrix of different options.

Alternative	Amount of energy consumption		Ease of use		Speed and ease of implementation		Executive records and operation inside the country		Amount of water wastage		Ensuring the quality of outgoing water		Total
A1	80	10 8	63	7 9	49	7 7	63	9 7	54	9 6	56	7 8	365
A2	61.6	7.7 8	72	8 9	70	10 7	42	6 7	60	10 6	64	8 8	369.6
A3	61.6	7.7 8	81	9 9	70	10 7	42	6 7	60	10 6	72	9 8	386.6

References

Zarepour Moshizi M, Yousefi A, Amini AM, Shojaei P (2022) Rural vulnerability to water scarcity in Iran: an integrative methodology for evaluating exposure, sensitivity and adaptive capacity. GeoJournal 88: 2121–2136. https://doi.org/10.1007/s10708-022-10726-0

Mansouri Daneshvar MR, Ebrahimi M, Nejadsoleymani H (2019) An overview of climate change in Iran: facts and statistics. Environmental Systems Research 8: 7. https://doi.org/10.1186/s40068-019-0135-3

Charkhestani A, Salehi Ziri M, Amini Rad H (2016) Wastewater reuse: potential for expanding Iran's water supply to survive from absolute scarcity in future. Journal of Water Reuse and Desalination 6(3): 437-44. https://doi.org/10.2166/wrd.2015.210

Estimating water quality index of effluent water with artificial neural network

H.T. Gültaş[1*], Ç. Coşkun Dilcan[2], D.D. Köksal[2], Y. Ahi[2]
[1] Department of Biosystems, Faculty of Agricultural and Natural Sci., University of Bilecik Şeyh Edebali, Bilecik, Turkey
[2] Water Management Institute, Ankara University, Ankara, Turkey
* e-mail: huseyin.gultas@bilecik.edu.tr

Introduction

As it is known, water resources are a very critical material for life and today they are under many negative effects by various factors. In order for water resources to be used for a specific purpose (for example, domestic use or irrigation) they need to be classified in some way. Conditions of use can be evaluated by taking into account the characteristics and criteria that water must provide, which are announced by various organizations in the world. As a result of analyses and measurements made in water, data are obtained that can be used to classify water use individually or when evaluated together. Some of these data are; It can be specified as pH, electrical conductivity, salt content, dissolved oxygen amount, chemical oxygen demand, suspended solids, and the like. By evaluating these data under various methods, it can be concluded whether the use of water for the determined purpose is appropriate. The electrical conductivity of the water, the pH and the amount of anion cation it contains are used to determine whether it can be used for irrigation or not. In addition to these values, it is possible to conclude whether it can be used as drinking and utility water by using values such as the salts it contains, the amount of dissolved oxygen, the chemical oxygen demand, the number of suspended solids and fecal coliform.

One of the methods by which we can decide on the use of water for a specific purpose by evaluating the data in question is the water quality index. By evaluating the parameters exemplified above or more parameters together, it is possible to determine for which purpose the water is suitable for use. The data obtained as a result of measurements and analyses made in a long-term or a certain time interval provide a decision that is not too difficult. There are many water quality index determination methods created by many researchers and organizations, and the calculation methods and the parameters they use differ. Bascaron index, NSF index, British Colombia index, CCME index, Hanh index, Almeida index are among the most well-known water quality indexes in use (Uddin et al. 2021).

In the study, the water quality index results obtained using the National Sanitation Foundation Index (NSFI) will be compared with the results obtained using artificial intelligence applications. According to the results of the evaluation, when artificial intelligence applications provide the necessary learning with historical data sets, if there is less data available to determine the water quality index, it will be revealed how the results are obtained. It will be evaluated whether reliable and usable index results can be obtained when less data sets are used.

Materials and methods

The study was created by using the effluent data of Kırklareli Domestic Wastewater Treatment Plant in 2018 and 2019. Kırklareli Domestic Wastewater Treatment Plant is seen as a medium-sized urban wastewater treatment plant, considering the Thrace Region. In order to keep the operation of the facility under control and to operate it in a healthy way, the data are examined by sampling at certain times. In case of any problem, necessary intervention is made and the facility is brought back to its normal conditions. There are 192 lines in the data set containing pH, conductivity (EC, mg/L), salinity (TDS, mg/L), dissolved oxygen (DO, mg/L), chemical oxygen demand (COD, mg/L), total nitrogen (N, mg/L), ammonium (NH_4, mg/L), nitrate (NO_3, mg/L), total phosphorus (P, mg/L) and total suspended solid (TSS, mg/L) data.

Using the aforementioned data, the water quality index (WQI) was found according to the National Sanitation Foundation (NSF) water quality index method (Brown et al. 1972). Artificial intelligence is

applications that are applied in today's conditions in different work areas and whose reliability is constantly tested and discussed. The WQI data were evaluated by the use of raw data gathered from the study of Köksal (2020) and compared with the artificial intelligence application results. The reliefF algorithm was used to filter and rank the input parameters according to their properties (Budak 2018) and to create the scenarios. The results were also analysed statistically and the usability of the results was discussed.

Results and concluding remarks

Descriptive statistics of input and output data and the weights of input data are given in Table 1. According to the results of the reliefF algorithm, ten scenarios were obtained with ten input parameters. The first scenario was created by ordering all parameters according to reliefF weight factor, and the next scenarios were created by eliminating the parameters with the lowest weight factor one by one. The output parameter, WQI, varied between 62.3 and 682.1 throughout 2017, 2018 and 2019 years. This result is described as "very poor water (76-100)" and "water unsuitable for the intended use (>100)" according to the classification ranges announced by İbrahim (2019). The scenarios created based on these results were run with the ANN model with different training functions and testing-training-validation rates, and the model that produces the most statistically strong prediction were selected. Thus, the applicability of artificial intelligence was evaluated in terms of ease of implementation.

Table 1. Descriptive statistics and reliefF results of data set.

Parameters	Inputs										Output
	Total N	*Total P*	*TSS*	*COD*	*NH4*	*TDS*	*EC*	*DO*	*NO3*	*pH*	*WQI*
Mean	79.6	8.9	98.5	286.3	38.6	5215.5	1046.6	2.0	2.6	7.4	157.4
Standard error	4.1	3.0	5.8	7.6	1.5	59.4	11.4	0.3	1.3	0.0	5.6
Median	59.8	5.4	68.0	282.0	36.5	5100.0	1022.0	1.2	0.7	7.5	136.9
Standard deviation	57.1	41.2	80.0	105.8	21.5	825.5	158.8	4.8	18.7	0.4	78.2
Variance	3265.9	1700.8	6401.2	11188.6	461.2	681423.8	25224.0	23.3	348.5	0.2	6114.8
Kuortosis	2.3	191.8	7.0	1.1	99.8	9.4	9.4	152.6	191.2	5.9	10.3
Skewness	1.8	13.8	2.2	0.7	8.6	2.3	2.3	11.7	13.8	0.1	2.5
Range	266.2	576.2	496.0	623.0	281.4	6600.0	1273.0	65.0	259.7	3.8	619.8
Min	2.8	1.8	6.0	71.0	9.6	3200.0	659.0	0.0	0.3	5.8	62.3
Max	269.0	578.0	502.0	694.0	291.0	9800.0	1932.0	65.0	260.0	9.7	682.1
Count	193.0	193.0	193.0	193.0	193.0	193.0	193.0	193.0	193.0	193.0	193.0
Weights of ReliefF	0.1476	0.0765	0.0403	0.0302	0.0180	0.0131	0.0126	0.0085	0.0029	0.0008	

References

Anonymous (2010) Atıksu arıtma tesisleri teknik usüller tebliği (in Turkish). Official newspaper, 27527

Brown RM, McClelland NI, Deininger RA, O'Connor MF (1972) A Water Quality Index — Crashing the Psychological Barrier. In: Thomas, W.A. (eds) Indicators of Environmental Quality. Environmental Science Research, vol 1. Springer, Boston, MA. https://doi.org/10.1007/978-1-4684-2856-8_15

Budak H (2018) Feature selection methods and a new approach. SDU J Nat Appl Sci 22(SI):21–31

FAO (1992) Wastewater Treatment and Use in Agriculture, FAO. Irrigation and Drainage Paper 47, Rome

Ibrahim MN (2019) Effluent Quality Assessment of Selected Wastewater Treatment Plant in Jordan for Irrigation Purposes: Water Quality Index Approach. Journal of Ecological Engineering 20(10): 206-216. http://doi.org/ 10.12911/22998993/112491

Köksal DD (2020) Evaluation of treated domestic wastewater reuse for agriculture using artificial intelligence methods. Master Thesis of International Centre for Advanced Mediterranean Agronomic Studies (CIHEAM) of Bari

Uddin Md G, Nash S, Olbert AI (2021) A review of water quality index models and their use for assessing surface water quality. Ecological Indicators 122: 107218

12th World Congress on Water Resources and Environment (EWRA 2023)
"Managing Water-Energy-Land-Food under Climatic, Environmental and Social Instability"
Thessaloniki, Greece, 27 June - 1 July 2023

Assessment of a Hybrid Renewable Energy System to meet water and energy demands in Serifos island

C. Lagaros[1*], A.-F. Papathanasiou[2], E. Baltas[2]
[1] School of Rural and Surveying Engineering, National Technical University of Athens, Greece
[2] School of Civil Engineering, National Technical University of Athens, Greece
* e-mail: ch_lagaros@mail.ntua.gr

Introduction

Greek Islands suffer water and energy shortages, the scale of which depends on the island's size. In the past years, technology and innovation in the fields of renewable energy sources has made possible the development of sophisticated hybrid systems to cover such shortages. Taking into consideration the extreme temperatures and physical phenomena that are already happening and will continue to occur even more frequently due to the climate crisis, it is important that islands become water and energy independent. Almost every Greek island depends solely on fossil fuels, for coverage of energy demand. For the supply of potable water most islands don't even have a functioning refinery and distribution system, therefore bottled water is needed (Bertsiou et al. 2017). As for the energy provided for homes and other residential uses, it can be inadequate especially in summer months i.e. tourism season (Skroufouta and Baltas 2021), one of the basic industries of Greek islands. The aim of this study is the evaluation of a Hybrid Renewable Energy System (HRES), to meet water and electricity demand on Serifos island.

Materials and methods

Serifos island is located in the South Aegean and is part of the Cyclades island complex. The permanent population according to the 2021 census, is 1,400 people (Hellenic Statistical Authority 2021). That number during summer climbs up to about 9,000 due to tourists. The electrical energy of the island is produced through an Autonomous Power Station (APS), based on fossil fuels. Such a system is subject to many glitches such as a failure of the APS which would mean a total blackout of the island until the damage can be restored, with further impacts on potable water production and distribution, transportation and other important aspects (Bertsiou and Baltas 2022). Finally, a system that depends solely on fossil fuel consumption is not environmentally friendly.

The proposal of this paper is the installation of an HRES, to render the island independent on energy and potable water as well as lowering the environmental impact of using fossil fuels. Essentially, it is a system in which wind turbines and photovoltaic panels (PV) harness the energy of wind and sun, to cover household demand, use it for desalination to produce clean water and equally important, reduce the emission of pollutants into the atmosphere. The excess energy is stored using the method of pumped water. The island setting is ideal for wind turbines, with excess winds coming from the upper Aegean Sea. Also, they can be efficiently combined with desalination and water pump storage, which acts as a backup power supply when dropped into a water turbine. Water pumped and stored in higher altitudes serves as a great equalizer for possible energy excess coming from wind turbines and PV. Therefore, it can be used for energy production and water desalination, in extreme situations of excessive summer heat and high tourism season. With the proposed HRES, two scenarios were put under the scope, of which the first prioritizes the energy grid supply and the second the clean water supply. Two wind turbines of 2 MW power each and a photovoltaic station of 1 MW power for energy production, a desalination plant, able to process 3,000 m^3 of water per day with an adjacent 20,000 m^3 water storage tank. Also, two 700,000 m^3 reservoirs (of which the lower altitude one already exists but is not used) are used to store water. Pumping of the water in the upper reservoir is carried out by 12 pumps of 100 kW each, and a 3 MW water turbine is used for energy production.

Results and concluding remarks

The results of the HRES simulation run show that the installation of wind turbines combined with PV can meet the needs of the island even in peak tourism season.

Both scenarios supply 30% of the produced energy directly to the electrical grid of the island. After that, the first scenario assumes as most basic the need for coverage, with the remaining 70%, of all energy demands that haven't been covered by the first 30% and then prioritizes desalination and clean water supply. Finally, any energy excess is used for pumping water in the upper reservoir. The results concluded 83% coverage of electrical energy demand and 96% coverage of potable water demand.

After the first 30% is used by the local grid, the second scenario assumes as a priority the desalination and supply of potable water. If there is any energy excess it is used to cover any shortages of energy supply. Finally, if there is still excess energy after that it is used for pumping water in the upper reservoir. The results from the second scenario show 85% coverage of electrical energy demand and 99% coverage of potable water demand.

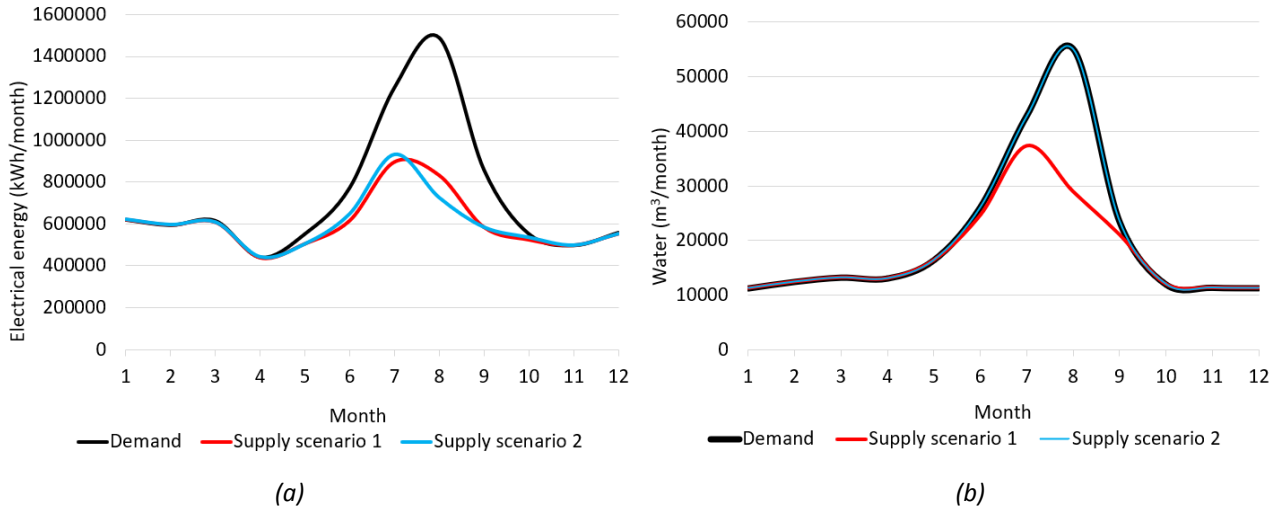

Figure 1. Electrical energy (a) and clean water (b) demand and coverage for scenario 1 and 2.

Figure 1 presents monthly data on average electrical energy and clean water demand and its coverage by the HRES in scenarios 1 and 2, for the years 2010-2022. As expected, summer poses a great challenge when it comes to covering the demand for both water and electricity demand, of the tourists who flood the island and multiply the population even by 6 times compared to winter. In spite of that, the percentages described above point out the great efficiency of the HRES.

References

Bertsiou M, Baltas E (2022) Management of energy and water resources by minimizing the rejected renewable energy. Sustainable Energy Technologies and Assessments 52 Part A: 102002. http://doi.org/10.1016/j.seta.2022.10200

Bertsiou M, Feloni D, Karpouzos D, Baltas E (2017) Water management and electricity output of a Hybrid Renewable Energy System (HRES) in Fournoi Island in Aegean Sea. Renewable Energy 118: 790-798. http://doi.org/10.1016/j.renene.2017.11.078

Development Program of Non-interconnected Island Systems (Directory of Island Management, March 2021), Available at: http://www.rae.gr/ (accessed 21 November 2022)

Hellenic Statistical Authority (2021) 2021 Population-Housing Census. http://www.statistics.gr/ (accessed 21 November 2022)

Skroufouta S, Baltas E (2021) Investigation of hybrid renewable energy system (HRES) for covering energy and water needs on the Island of Karpathos in the Aegean Sea. Renewable Energy 173: 141-150. http://doi.org/10.1016/j.renene.2021.03.113

12th World Congress on Water Resources and Environment (EWRA 2023)
"Managing Water-Energy-Land-Food under Climatic, Environmental and Social Instability"
Thessaloniki, Greece, 27 June - 1 July 2023

Evaluating the metal removal efficiency of coal mine water treatment schemes across the UK

O. Okeleji[1], V.G. Ioannidou[2*]
[1] *School of Engineering and the Built Environment, Birmingham City University, Birmingham B4 7XG, UK*
[2] *School of Engineering and Built Environment, Leeds Beckett University, Leeds, LS2 8AG, UK*
** e-mail: v.ioannidou@leedsbeckett.ac.uk*

Introduction

Coal mining is one of the major industries that contributes to the economy of a country, but it also causes noticeable deterioration to the environment (Gombert et al. 2019; Rinder et al. 2020). Discharging coal mine wastewater into waterways is frequently associated with unnatural alterations to water quality, manifesting as elevated salt levels, higher amounts of heavy metals, like nickel and zinc, and modifications to pH and ionic balance (Fleming et al. 2021). If not properly treated before discharge, mine drainage can have a serious impact on the environment, aquatic ecosystems, water quality and drinking water resources. Therefore, understanding the physicochemical properties of mine drainage will help evaluate the impact of mine water on the environment and identify the major controlling factors of the treatment process which will aid in improving the treatment performance of water treatment systems.

The aim of this paper is to evaluate the metal removal efficiency of a number of mine water treatment schemes across the UK and to investigate and validate which parameters/features of the treatment schemes contribute to the removal of metals, so as to enhance and/or optimise their treatment efficiency. In addition, the work intends to contribute as a useful guide to inform stakeholders on the best decision making for the design of new schemes or for the retrofitting of existing schemes.

Materials and methods

The study was undertaken at 5 full-scale passive mine water treatment schemes (MWTS), located at the Northwest of England and consisting of settlement lagoons and wetlands. The datasets spanned over a period of 12 years (i.e. January 2007-September 2018), and contained monthly records of physicochemical parameters, including Conductivity, pH, Suspended Solids (SS), alkalinity as $CaCO_3$; Fe^{3+}, Fe^{2+}, Mn and SO_4^{2-}. Design aspects, including shape, surface area, aspect ratio, volume, position of inlet and outlets, number of inlets and outlets, were also obtained from topographic maps of the MWTS. The measured sites were assessed for their treatment performance using removal efficiency (R.E). The influence of design aspects and seasonal variation on the treatment performances of the MWTS were explored through statistical analyses. Correlation analysis was conducted among design aspects, seasons, and discharge concentrations to obtain the Pearson correlation coefficient and the degrees of significance among any pair of indices (i.e. design aspects, seasons, and removal efficiencies). The level of significance was set to 0.05 in all tests. All statistical analyses were performed with Python 3.6.8.

Results and concluding remarks

A summary of the performance of the MWTS with respect to their physicochemical parameters is presented in Table 1, presenting the mean influent and effluent concentrations and standard deviation (s.d).

Overall, the pH increased as the mine water flowed through all the respective studied schemes from slightly acidic to neutral. The pH values in the effluent were in the neutral range (6.93-7.97), specific conductivity between 951.16 to 2037.97 µS/cm, SS between 5.64 and 13.39 mg/L and alkalinity as $CaCO_3$ between 81.33 – 571.80 mg/L. The discharge concentrations of Fe^{3+} in all schemes ranged from 0.25 to 8.12 mg/L, Fe^{2+} ranged from 0.11 to 5.98 mg/L, Mn from 0.38 to 2.14 mg/L and SO_4^{2-} from 221.70 to 768.78 mg/L.

An increase in pH can be observed across all schemes, with an associated reduction in Fe^{3+} and Fe^{2+} concentrations. Compared to Fe^{3+} and Fe^{2+}, the reduction of Mn, SO_4^{2-}, $CaCO_3$, and SS were considerably lower. This could be due to the fact that passive MWTS are focused on iron removal and less on the other contaminants, since iron is the primary metal of concern in mine drainage (Persson et al. 1999; Kusin et al. 2014). Fe^{2+} effluent concentrations were consistently lower than the corresponding influent, which shows that Fe^{2+} is being oxidised to Fe^{3+} as the mine water flows. Fe^{3+} then begins to settle, resulting in the decrease of Fe^{3+} concentration in the flow. This indicates that both Fe^{2+} oxidation rate and particulate Fe^{3+} settling rate are important in the overall treatability of the mine drainage (Skousen et al. 2019).

Table 1. Influent and Effluent concentrations of each Scheme (± s.d).

Site	In/Out	pH	Conductivity (µS/cm)	SS (mg/L)	Fe^{3+} (mg/L)	Fe^{2+} (mg/L)	CaCO3 (mg/L)	Mn^{2+} (mg/L)	SO_4^{2-} (mg/L)
Strafford	C_{in}	7.35 ± 0.37	2056.77 ± 175.34	14.93 ± 3.49	7.18 ± 1.17	6.81 ± 1.29	590.46 ± 28.19	1.03 ± 0.11	482.82 ± 72.17
	C_{out}	7.80 ± 0.27	2037.97 ± 162.76	8.47 ± 3.94	1.36 ± 0.82	0.44 ± 0.49	571.80 ± 34.93	0.53 ± 0.35	491.15 ± 65.50
Sheephouse Wood	C_{in}	6.48 ± 0.42	1069.25 ± 78.12	47.81 ± 16.91	31.64 ± 10.51	30.17 ± 10.10	92.97 ± 36.33	1.96 ± 0.44	468.30 ± 41.77
	C_{out}	7.33 ± 0.45	991.24 ± 102.22	9.54 ± 3.99	0.62 ± 0.35	0.26 ± 0.25	81.33 ± 35.02	0.51 ± 0.46	439.87 ± 42.49
Aspull	C_{in}	6.61 ± 0.42	1685.33 ± 173.53	35.63 ± 13.08	29.52 ± 4.22	26.30 ± 3.59	198.83 ± 18.24	2.84 ± 0.22	778.17 ± 94.27
	C_{out}	7.75 ± 0.24	1646.59 ± 168.26	5.64 ± 0.74	0.25 ± 0.17	0.11 ± 0.08	186.62 ± 18.26	0.38 ± 0.37	768.78 ± 93.79
Bridgewater	C_{in}	7.11 ± 0.38	1407.99 ± 111.33	24.27 ± 9.65	12.28 ± 1.99	9.55 ± 1.34	321.94 ± 17.91	2.71 ± 0.26	451.87 ± 58.01
	C_{out}	7.97 ± 023	1360.34 ± 117.30	7.63 ± 2.86	0.51 ± 0.27	0.16 ± 0.10	298.56 ± 24.99	0.40 ± 0.29	443.58 ± 59.15
Silkstone	C_{in}	6.47 ± 0.31	959.51 ± 47.94	20.45 ± 7.68	15.61 ± 1.56	13.52 ± 2.17	196.13 ± 15.73	2.35 ± 0.31	219.14 ± 26.85
	C_{out}	6.93 ± 0.43	951.16 ± 51.27	13.39 ± 5.48	8.12 ± 3.50	5.98 ± 2.96	193.32 ± 12.30	2.14 ± 0.28	221.70 ± 25.60

Shape, aspect ratio and number of inlets-outlets has been observed to have an effect on the Fe^{3+} concentration, as there was a significant difference among the respective categories investigated. For shape, lagoons with oval shape appeared to have a higher Fe^{3+} R.E range than Rectangle shape. In addition, lagoons with higher aspect ratio have demonstrated better performance in removing Fe^{3+}. Inlet-outlet configuration, was found to have less effect of Fe^{3+} removal compared to the shape and aspect ratio design features, with Mid-Corner configuration indicating the highest Fe^{3+} R.E.

Further analyses are being conducted on other contaminants (e.g. Calcium, Magnesium, Sodium) as well as investigation of possible affiliations between design features, seasons and removal efficiencies.

References

Fleming C, Morrison K, Robba L, et al. (2021) 4-Month Water Quality Investigation of Coal Mine Discharge on Two Rivers in NSW, Australia: Implications for Environmental Regulation. Water Air Soil Pollut 232: 90. https://doi.org/10.1007/s11270-021-05020-7

Gombert P, Sracek O, Koukouzas N, et al. (2019) An Overview of Priority Pollutants in Selected Coal Mine Discharges in Europe. Mine Water Environ 38: 16–23. https://doi.org/10.1007/s10230-018-0547-8

Kusin FM, Jarvis AP, Gandy CJ (2014) Hydraulic performance and iron removal in wetlands and lagoons treating ferruginous coal mine waters. Wetlands 34: 555–564. https://doi.org/10.1007/s13157-014-0523-4

Persson J, Somes NLG, Wong THF (1999) Hydraulics efficiency of constructed wetlands and ponds. Water Sci Technol 40: 291–300. https://doi.org/10.1016/S0273-1223(99)00448-5

Rinder T, Dietzel M, Stammeier JA, et al. (2020) Geochemistry of coal mine drainage, groundwater, and brines from the Ibbenbüren mine, Germany: A coupled elemental-isotopic approach. Appl Geochemistry 121: 104693. https://doi.org/10.1016/J.APGEOCHEM.2020.104693

Skousen JG, Ziemkiewicz PF, McDonald LM (2019) Acid mine drainage formation, control and treatment: Approaches and strategies. Extr Ind Soc 6: 241–249

Sustainable decentralized domestic wastewater treatment unit using hybrid treatment system

M.K. Younes[1*], A.S. Alshdiefat[2], I. Al-Smadi[2]
[1] Department of Civil Engineering, Applied Science Private University, Amman, Jordan
[2] Department of Civil Engineering, Philadelphia University, Amman, Jordan
* e-mail: m_younes@asu.edu.jo

Introduction

Proper management of decentralized wastewater treatment systems is essential to protect the environment. However, these systems need regular inspection, maintenance as well as an financial resources for operation (Younes 2020). Traditionally, wastewater (WW) is treated using aerobic biological processes, such as activated sludge process (Aiyuk et al. 2010). However, it stills favourable option for low strength WW and efficiently removes soluble biodegradable organic materials as well as generates well flocculated solids (Stazi et al. 2022). Anaerobic WW Treatment (WWT) requires no aeration; produces much less sludge, allows fertilizing nutrients recovery, energy saving and production. Thus, it became an attractive WWT technology. Sustainable decentralized WWT focuses on simplicity, on-site treatment and recycling of local resources contained in the WW, low investment and operation costs. But it needs professional workers and deep knowledge that is lack especially in developing countries. This study aims to develop a sustainable WWT unit to be used in rural area in Jordan. The proposed system is hybrid (anaerobic-aerobic) and self-powered using the solar system to minimize the operation and construction costs. Moreover, the operation is based on intermittent base to mimic the wastewater flow at small scale.

Materials and methods

A comprehensive literatures and researches were reviewed to determine the best treatment techniques of the domestic wastewater as well as fulfil the local regulation requirements. Moreover, the impacts of the WW treatment facility, that are likely to be created, were considered. However, the proposed hybrid treatment system will consist from receiving tank, anaerobic reactor, aerobic reactor and storage tank as shown in Figure (1). The study will analyze implementation of hybrid treatment technique; as well as self-powered system using the solar energy. Furthermore, a local materials were used during the construction in order to minimize the cost. Finally, the built decentralized unit will be used to evaluate the efficiency of the treatment by measuring the quality of influent and reclaimed water. Moreover, a field survey will be implemented in order to properly locate the plant. Initial seeding of some well digested anaerobic sludge could be used with a minimum seeding is 10% of total anaerobic reactor volume.

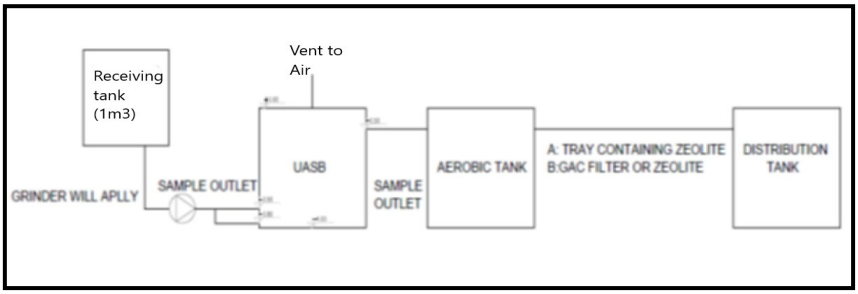

Figure 1. Schematic diagram of the proposed WWTU.

Results and concluding remarks

The selected system integrates the anaerobic treatment using Up-flow Anaerobic Sludge Blanket (UASB) with aerobic treatment using a tank equipped with air diffuser. Such sequence aims to improve the quality

of reclaimed water as well as reduces the sludge generation. Moreover, the unit is closed to minimize the maintenance and powered by solar energy. The expected WW amount to be treated is about 0.6-1 m^3 daily. The receiving tank volume is 1m^3 ; it is equipped with submersible pump that is used to pump the WW into the UASB reactor. The expected working head is about 5.7m with a flow rate equal to 50 L/min. The designed anaerobic reactor is circular with a diameter about 1.2 m. The UASB has a total volume about 4.2 m^3 and working volume is about 3.2 m^3. It has been build underground from precast cement.

The aeration tank is made from plastic and available at local market; its size is about 2 m^3. It has been equipped with an air diffuser. While the storage tank is also made form plastic and has a volume of 2 m^3. However, it is equipped with a pump for distributing the reclaimed water to a proposed agricultural zone. Table (1) shows the results of initial samples that have been collected after one month of operation. However, more samples are advised to generalize the results and conclusions.

Table 1. Results of collected reclaimed and wastewater samples.

Sample ID	Tests				
	BOD_3/($BOD_{5)}$ (ppm)	COD (ppm)	TDS (ppm)	pH	Turbidity (NTU)
Effluent from the unit	155	818	2,352	7.7	20
Inlet to the unit	910*	1,944	2,401	8.2	117
Out flow of UASB	962*	2,535	2,422	7.0	53
Treatment (removal) efficiency	83%	58%	2%	-	83%

Acknowledgments: The authors are grateful to the National Centre for Research and Development –Jordan for financial assistance and Water Research Institute –Italy for their support.

References

Younes M (2020) Integration of mathematical median ranked set sample and decision making AHP tools to enhance decentralized wastewater treatment system. Journal of Water Chemistry and Technology 42: 472-479

Aiyuk S, Odonkor P, Theko N, van Haandel A, Verstraete W (2010) Technical Problems Ensuing From UASBReactor Application in Domestic WastewaterTreatment without Pre-Treatment. International Journal of Environmental Science and Development 1(5): 392

Stazi V, Annesini MC, Tomei MC (2022) Anaerobic domestic wastewater treatment in a sequencing granular UASB bioreactor: Feasibility study of the temperature effect on the process performance. Journal of Environmental Chemical Engineering 10(5): 108512

IV. Hydrological Modelling of Complex River Basins

12th World Congress on Water Resources and Environment (EWRA 2023)
"Managing Water-Energy-Land-Food under Climatic, Environmental and Social Instability"
Thessaloniki, Greece, 27 June - 1 July 2023

Comprehensive hydrologic modeling of a watershed with managed reservoirs for assessing water availability

E. Getahun*, A.F. Prada, Z. Zhang, L. Keefer , G. Qie
Prairie Research Institute, University of Illinois, Champaign, Illinois, USA
** e-mail: egetahun@illinois.edu*

Introduction

Water availability in a watershed mainly depends on its climate conditions, water demands and water quality. Global climate change could cause alterations of precipitation patterns and surface air temperatures, which in turn could impact regional hydrologic cycles and river flows (Ehsani et al. 2017). Based on increased water demand for food and energy production resulting from global population growth, patterns of future water use could deviate from past trends (Cosgrove and Loucks 2015). Anthropogenic activities in a watershed can affect the water quality in streams and rivers, impacting water availability for various uses. For example, actively managed agricultural landscapes release nutrients to downstream water bodies, impacting the availability of clean water (Getahun and Keefer 2016). Thus, proper accounting of factors affecting water availability facilitates its effective management through prioritization of water allocation.

In this study, comprehensive hydrologic modeling of the Kaskaskia River watershed located in Illinois, USA has been completed to assess water availability under changing climate and water use conditions. The Kaskaskia River is the second largest river in Illinois with total length and drainage area of approximately 515 km and 15,022 sq. km, respectively, flowing southwest to its confluence with the Mississippi River. The Shelbyville and Carlyle dams were both built on the main stem of the Kaskaskia River in 1969 and 1967, respectively, serving as primary sources of water supply in the Kaskaskia River watershed region. The two federal reservoirs (i.e., Lake Shelbyville and Carlyle Lake) are being operated and managed by the United States Army Corps of Engineers (USACE) to meet water demand in the watershed including water supply, flood control, navigation, and recreational needs. The reservoirs' water has been fully allocated for their intended uses. Climate change and future water demand are expected to affect water availability in the watershed, in addition to storage reduction due to sediment deposition in the reservoirs. The hydrologic model of the Kaskaskia River watershed was developed using the Soil and Water Assessment Tool (SWAT) with several code modifications to its reservoir and water use routines that allowed incorporating the reservoirs' operating rules and water uses from different sources, respectively. To account for the spatial heterogeneity in the watershed characteristics, four standalone subwatershed models were setup and distributed parameter calibration using observed data at several gages was implemented. This paper discusses hydrologic modeling of the Kaskaskia River watershed.

Materials and methods

The SWAT model, which is a physically based, semi-distributed hydrologic and water quality model (Neitsch et al. 2011), was used to develop the complete Kaskaskia River watershed model (CKRWM). The watershed is divided into 239 HUC12-based subbasins and 836 hydrologic response units (HRUs). Based on the CKRWM segmentation, four standalone subwatershed models were set up. These models cover the following drainage areas: upstream of Kaskaskia River near Shelbyville (05592000), between downstream of 05592000 and upstream of Kaskaskia River near Carlyle (05593000), Shoal Creek watershed, and downstream of both 05593000 and Shoal Creek watershed outlet.

Modifications to SWAT were made to incorporate reservoir operating rules and water uses from surface water (i.e., from river reaches and reservoirs) and groundwater. Modified target release method was implemented at daily time-step using long-term observed outflow data and storage volumes derived from pool elevation data based on each reservoir's storage-elevation relationship. Annual water use data was

obtained for 37 groundwater and 29 surface water withdrawal locations, of which one is direct withdrawal from Carlyle Lake. Using typical water use variability in the region, monthly water use data was generated and incorporated into the watershed simulation. For accurate simulation of all water uses from different sources, the water withdrawal locations were mapped into the CKRWM configuration and the reaches, subbasins and reservoirs of water withdrawal were identified in the model. In addition, effluent discharges, which affect low flow conditions particularly in the tributaries, were obtained for 116 locations in the watershed and were mapped into 93 reaches of the CKRWM and were included as constant average daily discharges at the reaches.

Multi-objective evolutionary algorithm was used for automatic model calibration through optimization of Nash-Sutcliffe efficiency (NSE) and percent bias (PBIAS) of the hydrologic variables, simultaneously. Daily flows at four USGS gaging stations and reservoir storage volumes of the two lakes were calibrated and validated for 1990-2009 and 2010-2019 periods, respectively.

Results and concluding remarks

Comprehensive hydrologic modeling of the Kaskaskia River watershed resulted in the development of a robust model for simulating flows, reservoir storage volumes and outflows. Performance statistics for model calibration and validation periods are presented in Table 1, indicating close matches between observed and simulated hydrologic variables. The multi-objective automatic calibration allowed exploring the model parameters extensively and providing optimal trade-off between the NSE and PBIAS for each hydrologic variable. The daily target release rate method employed resulted in better simulation of the reservoirs' water balance and thus provided good hydrologic model performance. Incorporating the water withdrawals and effluent discharges reduced the model biases.

Table 1. Performance statistics for calibration and validation of flows and reservoir storage volumes.

Hydrologic variable	**Calibration period (1990-2009)**				**Validation period (2010-2019)**			
Flows at USGS gages	*NSE*	*PBIAS*	*Obs. (m^3/s)*	*Sim. (m^3/s)*	*NSE*	*PBIAS*	*Obs. (m3/s)*	*Sim. (m^3/s)*
05592000	0.7	-1.5	27.2	27.6	0.6	-11.2	29.7	26.7
05593000	0.7	-15.9	66.0	76.5	0.7	-18.0	94.2	79.8
05594000	0.5	-11.8	17.5	19.6	0.6	-12.5	25.0	22.3
05594100	0.8	-16.1	110.1	127.9	0.7	-19.7	158.7	132.5
Reservoir volume	*NSE*	*PBIAS*	*Obs. ($x10^8$ m^3)*	*Sim. ($x10^8$ m^3)*	*NSE*	*PBIAS*	*Obs. ($x10^8$ m^3)*	*Sim. ($x10^8$ m^3)*
Lake Shelbyville	0.7	0.2	2.8	2.8	0.4	-4.1	2.8	2.7
Carlyle Lake	0.7	-2.6	3.7	3.8	0.7	-3.3	3.7	3.8

The hydrologic model developed for the Kaskaskia River watershed has been used to investigate water availability in the watershed through simulation of ranges of climate change and projected water demand scenarios. Such investigations could inform decision making towards effective water management, which is particularly critical for future coal-fired power plant developments in the watershed. The model can further be developed to simulate the river's water quality and evaluate the impact of selected agricultural best management practices on reducing nonpoint source pollution in the watershed.

References

Cosgrove WJ, Loucks DP (2015) Water management: Current and future challenges and research directions. Water Resources Research 51: 4823–4839. http://doi.org/10.1002/2014WR016869.

Ehsani N, Vorosmarty CJ, Fekete BM, Stakhiv, EZ (2017) Reservoir operations under climate change: Storage capacity options to mitigate risk. Journal of Hydrology 555: 435–446. http//doi.org/10.1016/j.jhydrol.2017.09.008.

Getahun E, Keefer L (2016) Integrated modeling system for evaluating water quality benefits of agricultural watershed management practices: Case study in the Midwest. Sustainability of Water Quality and Ecology 8: 14–29. http//doi.org/10.1016/j.swaqe.2016.06.002.

Neitsch SL, Arnold JG, Kiniry JR, Williams JR (2011) Soil and Water Assessment Tool Theoretical Documentation Version 2009. Texas Water Resources Institute. https://hdl.handle.net/1969.1 /128050.

Hydrological modelling for flood forecasting in the Douro river basin

M. Ferreira*, J. Mendes, R. Maia
FEUP – Faculty of Engeneering of the University of Porto/Hydraulics Water Resorces and Enviroment Division, Portugal
** e-mail: mafalda.araujo.ferreira@gmail.com*

Introduction

The incidence of extreme floods has been increasing and the need to predict those is nowadays of great interest. The Douro River basin is the largest river basin in Portugal, so its analysis has significant value in the study of the consequences of extreme floods.

This study proposes the construction of a hydrological model of precipitation runoff in the Douro River basin, its calibration and validation to verify the methodologies used in the modelling and subsequent confirmation of its accuracy for future application in flood event forecasting. The hydrological model was implemented in the Portuguese part of the Douro River basin, with a contribution area of approximately 15,128 km^2, considering inflows to the Pocinho reservoir, to represent the flow originating in Spain. It should be noted that the hydroelectric plants present in the Portuguese portion of the Douro River are run-of-river plants, and therefore the simulated flows are in natural regime. Figure 1 represents the study area.

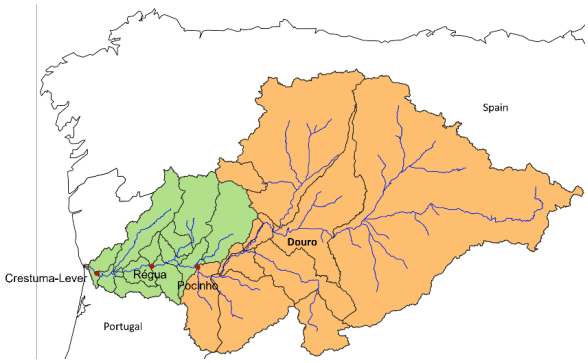

Figure 1. Study area and important section in the Douro River basin.

Materials and methods

The construction of the hydrological model relied on the HEC-HMS software and requires the definition of the river sections characteristics, as well as of the sub-basins, which were obtained through the MDT processing, with a resolution of 25x25 m. Other preliminary data, such as the initial flow and the precipitation values in the chosen periods for modelling, were taken from a national public portal, SNIRH, (SNIRH, 2021). The present study used the simulation method of the soil conservation service, SCS, in order to simulate the total runoff volume, according to which, the precipitation-runoff process in the developed model is mainly influenced by the values of the curve number, CN, and therefore the model calibration was mainly focused on it. For Portugal there is a public database containing CN numbers for the whole territory (SNIAmb 2017), assuming an average moisture condition, AMC-II. Another important parameter for SCS is the recession constant, R, defined as the exponential rate of decrease of the baseflow, which was adopted a value of 0.9 for all sub-basins, considering the analysis of the HEC-HMS program manual (Feldman 2000).

Crestuma and Régua dams were chosen as reference sections to assess the similarity of simulated and observed flows, taking advantage of the hydrometric stations associated to the corresponding reservoirs and of their location immediately upstream of the flood zones of the Areas of Significant Flood Risk (ARPSI), respectively, of Porto and Régua. The evaluation of the hydrological model performance on those two sections was carried out through evaluating three performance indicators, Nash-Sutcliffe Efficiency Indicator, NSE, and Bias Percentage, PBIAS and PBIAS$_{peak}$, which evaluates the difference between maximum flow values. Table 1 summarises the reference values of the parameters mentioned for the evaluation of model performance. The analysis was made on daily basis.

Three simulation periods were set for calibration and validation of the model: 14 to 24 December 2019 for the calibration and 01 to 11 March 2001 and 20 to 30 November 2006 for the validation periods.

Table 1. Reference values of the parameters mentioned for the evaluation of model performance.

Performance	|PBIAS|	NSE	$\|PBIAS_{peak}\|$
Very Good	PBIAS<10%	0,75<NSE≤1,0	$PBIAS_{peak}$<10%
Good	10%≤PBIAS<15%	0,65<NSE≤0,75	10%≤$PBIAS_{peak}$<15%
Satisfactory	15%≤PBIAS<25%	0,5<NSE≤65	15%≤$PBIAS_{peak}$<25%
Unsatisfactory	PBIAS≥25%	NSE≤0,5	$PBIAS_{peak}$≥25%

Results and concluding remarks

After running the simulation for the calibration period, the results of flow are presented in Figure 2 and it is find that the simulated flow is overestimated comparing with observed values, so the calibration was supported by implementing a 15% decrease in the initial values of CN in order to also decrease the simulated values of flow and keep the initial values of R, 0.9. The results of the calibration are presented in Table 2, and by their analysis, they classify the model as very good, which concludes that the model was calibrated for the flood event of 14-24 December 2019.

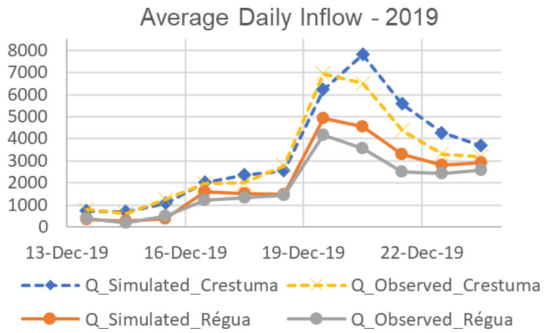

Figure 2. Average daily inflow, m^3/s, without calibration, for the period considered of 2019.

Table 2. Summary of statistic results after calibration, for the three considered periods.

	2019				2001				2006			
	Q_{peak} (m^3/s)	|PBIAS|	NSE	$\|PBIAS_{peak}\|$	Q_{peak} (m^3/s)	|PBIAS|	NSE	$\|PBIAS_{peak}\|$	Q_{peak} (m^3/s)	|PBIAS|	NSE	$\|PBIAS_{peak}\|$
Crestuma	6937	2.89%	0.905	0.35%	8834	8.97%	0.854	16,75%	7791	4.49%	0.762	33.76%
Régua	4155	6.49%	0.958	3.35%	6206	0.59%	0.957	4,70%	6122	7.54%	0.862	28.53%

The model was then validated by applying the calibrated CN values to the two validation periods, and the results presented in Table 2 were obtained. According the statistic parameters, the calibration carried out presents itself adjusted for the flood event of 2001. For the period of 2006, the model had a very good behaviour according to NSE and PBIAS in Crestuma and Régua, contrary to the $PBIAS_{peak}$ that evaluates the model as unsatisfactory in both sections. Although the poor evaluation of the $PBIAS_{peak}$, the model is, in its generality, adjusted for the flood event of 2006. The results obtained for the 2006 peak flow raised concerns but could not be justified by the increase in CN values as it impairs the model performance on the remaining simulation days. The analysis of the quality of the daily precipitation values could not be performed due to the lack of available hourly precipitation data for the period in question. Additionally, the model had a better behaviour in the Régua section in all three periods, something that may be related to its proximity to the model inlet and have a smaller drainage area.

Thus, we conclude that decreasing the CN values by 15% for the December 2019 calibration period led to a more reliable approximation of the flow simulation that was validated in 2001 and 2006 periods. The study developed allowed the construction of a suitable model for the simulation of flood events and possibly application in their forecasting.

References

Feldman AD (2000) Hydrologic Modeling System HEC-HMS Technical Reference Manual. https://www.hec.usace.army.mil/software/hec-hms/documentation.aspx

SNIAmb. (2017). Número de Escoamento, CN. https://sniambgeoportal.apambiente.pt/geoportal/catalog/search/resource/details.page?uuid={93B1694F-502B-4A53-9F61-2DB5FC97218D}

SNIRH. (2021). SNIRH - Monitorização. https://snirh.apambiente.pt/index.php?idMain=2&idItem=1&objCover=920123704&objSite=920685506

Future space-temporal and seasonal changes of mean monthly discharges in selected basins of Slovakia

Z. Sabová*, A. Liová, Z. Németová, S. Kohnová
Department of Land and Water Resources Management, Faculty of Civil Engineering, Slovak University of Technology in Bratislava, Bratislava, Slovak Republic
** e-mail: zuzana.sabova@stuba.sk*

Introduction

Projections of climate models in combination with hydrological models are most often used to assess future runoff conditions. Climate models can provide different predictions of the future climate; therefore, evaluating several climate models is essential (Kling et al. 2012).

Several authors studied climate and anthropogenic changes in the hydrological regime (Wood et al. 2022; Alsilibe and Bene, 2022). On the territory of Slovakia, in the Danube basin, some authors focused on identifying long-term changes in the hydrological regime using spatial and temporal changes, duration, and frequency of high discharges (see, e.g., Pekárová et al. 2016). Pramuk et al. (2016) analysed long-term discharge changes in the hydrological characteristics of mean annual discharges and the rate of rise and fall of discharge waves in selected Slovak basins. Halmová et al. (2022) evaluated long-term changes in the water balance in the Krupinica basin.

This study deals with the evaluation of the spatial-temporal changes in mean monthly discharges in selected basins throughout Slovakia using the KNMI and MPI climate scenarios from 1981 until 2100. The mean monthly discharges are divided into two seasonal groups, the summer half-year (from April to September) and the winter half-year (from October to March). From the results, it is possible to detect changes in discharge conditions, especially in the future summer season.

Materials and methods

The studied area is the territory of Slovakia, within are selected the Myjava – Jablonica, Nitra – Nitrianska Streda, Turiec – Martin, Váh – Liptovský Mikuláš, Hron – Banská Bystrica, Poprad – Chmeľnica, Topľa – Hanušovce and Topľou, Laborec – Humenné gauging stations.

The input data consist of daily mean discharge series of observed data from 1981 to 2010, which were provided for the study by the Slovak Hydrometeorological Institute. A conceptual the TUW rainfall-runoff model, based on the HBV type, was used to model runoff for future periods in selected catchments. The model requires rainfall in the basin, atmospheric temperatures, and potential evaporation as input data. The TUW model operates on a daily time stage and was calibrated on data from the period 1981 to 2010 (Sleziak et al. 2018). Using this model, the input was used to simulate the mean daily discharge at 2100.

The model outputs of the mean monthly discharges were divided into two groups of long-term seasonal discharges. The first group consists of the mean monthly flows of the summer half-year, and the second group consists of the mean monthly discharges of the winter half-year. To better represent future changes in long-term seasonal discharges, the results of modelled long-term seasonal discharges from the reference period (1981-2010) and the results of long-term seasonal discharges from the KNMI and MPI climate scenario from the period 2071 -2100 were compared. The results are presented as a percentage change in the future according to the relative deviation, calculated between the simulated long-term seasonal discharges according to the KNMI and MPI climate scenarios from the period 2071-2100 and modelled long-term seasonal discharges using the HBV model from the period 1981-2010.

Results and concluding remarks

The study focused on evaluating future spatial-temporal and seasonal changes in mean monthly

discharges in selected River basins in Slovakia. The results are divided into two time periods, the summer half-year, which includes the months from April to September, and the winter half-year, which includes the months from October to March.

The study results pointed to the highest decrease in long-term seasonal discharges in the summer half-year in the eastern part of Slovakia (the Laborec – Humenné gauging station), where according to the simulated long-term seasonal discharges from the KNMI climate scenarios, the value of the long-term seasonal discharges will decrease by 37%. The long-term seasonal discharges simulated according to the KNMI climate scenario (Figure 1) also assume the highest increase in the values of long-term seasonal discharges by 26% in the mountainous central part of Slovakia (the Turiec – Martin gauging station) by the year 2100. A decrease and an increase in the values of the long-term seasonal discharges characterise the summer half-year. On the contrary, only an increase in long-term seasonal discharges is visible in the winter half-year. The highest increase in these values is recorded in the western lowlands of Slovakia, especially at the Nitra – Nitrianska Streda gauging station, up to 85%.

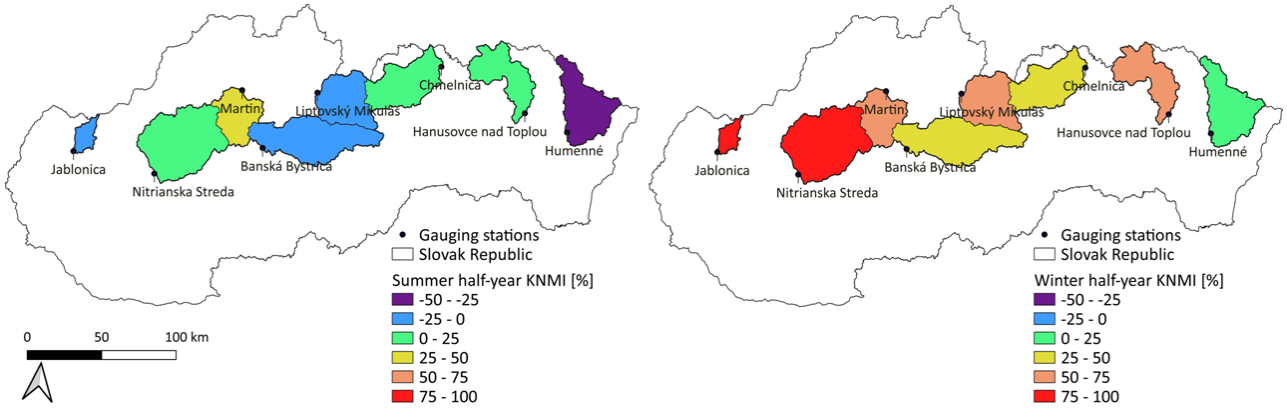

Figure 1. Future changes in mean monthly discharges according to the simulated mean daily discharges from the KNMI climate scenario.

In general, in the summer half-year, there is a higher probability of the occurrence of dry periods, which can reduce the flow conditions in the basins. The increase in air temperature in the winter months may affect future forms of precipitation that may not be in a solid state. This fact can significantly affect snow cover and associated snow melting, unfrozen soil soaked in water, and increased discharges in basins in the winter season.

Acknowledgements: This study was supported by the Slovak Research and Development Agency under Contract No. APVV-20-0374. The study was also supported by the VEGA Grant Agency under Project No. 1/0632/19. The authors are very grateful for their research support.

References

Alsilibe F, Bene K (2022) Watershed subdivision and weather input effect on streamflow simulation using SWAT model. Pollack Periodica 17(1): 88-93. https://doi.org/10.1556/606.2021.00349

Halmová D, Pekárová P, Podolinská J, Jeneiová K (2022) The assessment of changes in the long-term water balance in the Krupinica River basin for the period 1931–2020. Acta Hydrologica Slovaca 23(1): 21-31

Kling H, Fuchs M, Paulin M (2012) Runoff conditions in the upper Danube basin under an ensemble of climate change scenarios. Journal of Hydrology 424-425: 264-277. https://doi.org/10.1016/j.jhydrol.2012.01.011

Pekárová P, Halmová D, Mitková VB (2016) Analysis of changes in the characteristics of maximum Danube floods in Bratislava station. Acta Hydrologica Slovaca 17(2):215-223

Pramuk B, Pekárová P, Škoda P, Halmová D, Mitková VB (2016) Identification of the Slovak rivers daily discharge regime changes. Acta Hydrologica Slovaca 17(1): 65-77

Sleziak P, Szolgay J, Hlavčová K, Parajka J, Kubáň M (2018) Impact of the spatial conceptualization of a hydrological model on the accuracy of flow simulations. Acta Hydrologica Slovaca 19(1): 60-68

Wood AW, Mauer EP, Kumar A, Lettenmaier P (2002) Long-range experimental hydrologic forecasting for the eastern United States. Journal of Geophysical Research: Atmospheres 107(D20): 4429. https://doi.org/10.1029/2001JD000659

Methodology for flood forecasting and management in a regularized river basin: The case of the Mondego river

J. Mendes[1,2*], R. Maia[1,2]
[1] Civil Engineering Department, Faculty of Engineering of the University of Porto (FEUP), Porto, Portugal
[2] Interdisciplinary Centre of Marine and Environmental Research (CIIMAR), University of Porto, Matosinhos, Portugal
* e-mail: juliana@fe.up.pt

Introduction

Operational flood monitoring, forecasting and alert systems, based on integrated models which encompass hydrological and meteorological forecasting components, have been developed worldwide. Due to the need for improvement of the systems' reliability and the extension of the forecasting lead time, the use of a probabilistic approach has become the norm, through the use of Ensemble Forecasting Systems. In Portugal, like many other countries, this type of approach is still not yet properly implemented; flood forecasting continues to be undertaken merely over a short term horizon.

In this context, the present work aimed at the development and application of a methodology for flood forecasting and management in a regularized river basin, which can be continuously used over time and which enables the timely and accurate prediction of flood occurrence, so that, in due time, adequate reservoir management measures can be taken to dampen the impacts from such events, through more efficient management of stored volumes.

Materials and methods

The flood forecasting and management methodology was developed and applied to the Mondego River basin (Mendes 2017), located in the centre of Portugal, which has two large reservoirs (Aguieira and Fronhas). Together, they ensure the regularization of the streamflow generated in about 75% of the watershed area upstream of Coimbra - the city in this basin most often impacted by river floods. The effective management of these reservoirs is very important to minimize the occurrence of floods in Coimbra, but it is not always enough to avoid these scenarios. The Ceira River, a tributary of its left bank, is not regularized and, particularly in flood situations, contributes significantly to the streamflows in Coimbra.

In brief, the methodology hereby presented is based on: i) ensemble precipitation forecasts obtained from global circulation models, with a lead time of 10 days and a 3 hour time step, generated and disclosed by the ECMWF; and ii) the use of a semi-distributed hydrologic model, which is automatically calibrated, in a continuous manner, as a function of the variation in the hydrological state of the basin through time, and applied on a daily basis, for each of the members of the precipitation forecasts (Mendes and Maia 2016). An ensemble forecast– with a 10 day horizon and a timeframe of 3 hours - for each of the spatial units (sub-basins) defined in the model is thus obtained and evaluated in terms of its quality and consistency (Mendes and Maia 2023). Subsequently, an operational management model for the reservoirs in flooding situations was developed, based on runoff predictions as well as on the characteristics of the hydraulic structures in the basin which hold a flood cushioning capacity. This model enables the optimization of the flow amount to be discharged daily by each of the reservoirs in the system in order to: 1) avoid or minimize river flooding downstream; and ii) maintain the reservoir water levels as high as possible, without compromising the safety conditions in their structures (dam and discharge elements) (Mendes and Maia 2022).

In the application to this case study, hydrological simulations were performed in order to obtain the corresponding forecasts for the sections of Aguieira, Fronhas and Coimbra. Six wet periods (ranging from 12 to 28 days), linked with the occurrence of floods in Coimbra, were selected to perform the testing of the entire methodology, including the final stage of reservoirs' management. Two of these periods were to ensure the calibration and verification of the reservoir management model, while the 4 remaining periods were used to conduct the evaluation of its performance.

Results and concluding remarks

The flood forecasting methodology developed in this work consists of the scheme summarized in Figure 1.

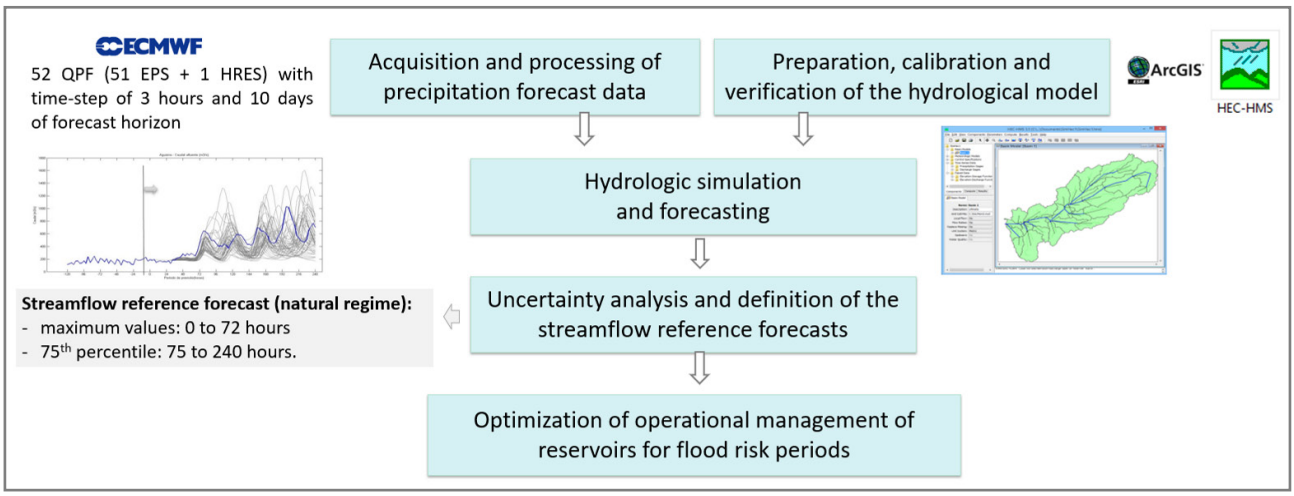

Figure 1. Scheme of the methodology developed for flood forecasting and management in a regularized river basin.

The ensemble streamflow forecasts obtained through the application of this methodology showed, in general terms, good quality to predict the occurrence of flood flows.

Considering the results thus obtained, and the conclusions derived from the statistical / uncertainty analysis of the streamflow ensemble forecasts, the reference forecast to take into account for optimal reservoir operation in the case of floods was defined as: i) the maximum values of the ensemble, in the first 72 hours and ii) the values corresponding to the 75th percentile of the ensemble, in the following hours.

The results obtained for the six wet/flood periods under analysis enable the conclusion that the methodology applied in this work is suitable for forecasting and managing various flood scenarios, encompassing very different flow magnitudes. The results also show that, in flood situations, the reservoir management model thus developed enables a better management of the reservoirs of Aguieira and Fronhas, than the rules currently in operation, which do not incorporate the hydrological forecast data. This could have made it possible to reduce the occurrence and impacts of floods in Coimbra. In addition, it enables high water levels to be maintained in the reservoirs during periods in which no significant inflows are forecasted, which is beneficial for other uses, in particular energy production. The integration of inflow forecasts thus proved to have effective added value for the operational management of the reservoirs.

The application of this methodology represents progress with regard to the framework currently in force at national level for the prediction and warning of floods in regularized basins, as well as triggering response actions to these situations, through the operational management of reservoirs.

Acknowledgments: The authors are grateful to the Portuguese Foundation for Science and Technology (PhD grant reference SFRH/BD/65905/2009, supported by POPH/FSE funding) and the EEA Grants Portugal 2014-2021 (through the Pre-defined Project 3 “Management of the Ceira River basin adapted to a changing climate”, of the Environment Programme) for funding for the development and dissemination of this work. Moreover, the authors also thank APA, EDP-Produção and ECMWF for providing the data used in this study.

References

Mendes J (2017) Previsão e Alerta de Cheia em bacias regularizadas. Aplicação ao caso de uma bacia portuguesa. Doctoral dissertation. Faculty of Engineering of University of Porto.

Mendes J, Maia R (2016) Hydrologic Modelling Calibration for Operational Flood Forecasting. Water Resources Management 30(15): 5671–5685. https://doi.org/10.1007/s11269-016-1509-1

Mendes J, Maia R (2022) Reservoir management model optimized for flood risk periods. A Portuguese case. 6th International Dam Safety Conference 2022, 10 to 12 October 2022, India.

Mendes J, Maia R (2023) Evaluation of Ensemble Inflow Forecasts for Reservoir Management in Flood Situations. Hydrology, 10(2): 28. https://doi.org/10.3390/hydrology10020028

Environmental assessment of Nif Creek in terms of microplastics: A mathematical modeling approach

Y. Kazancı[1*], O. Gündüz[1], N. Baycan[2]
[1] Environmental Engineering Department, Izmir Institute of Technology, Izmir, Turkey
[2] Environmental Engineering Department, Dokuz Eylul University, Izmir, Turkey
* e-mail: yigithankazanci@iyte.edu.tr

Introduction

Microplastics are small plastic particles, less than 5mm in size, that have become a major environmental concern due to their widespread presence in the world's oceans and freshwater systems. They are generated from a variety of sources including the breakdown of larger plastic items, microbeads from personal care products, and fibers from synthetic clothing. Microplastics can enter the environment through wastewater discharge, stormwater runoff, and the release of air-borne fibers. They can then be transported via rivers to seas and oceans, creating to a widespread distribution and leading to potential harm to marine and freshwater wildlife. Microplastics can also act as a vector for toxic chemicals, posing a threat to human health through the food chain. Unfortunately, the potential consequences of microplastics on human health are yet to be discovered. Thus, it is crucial to understand the pathways and transport of microplastics in the environment and take action to mitigate their impacts.

The limited number of studies (Whitehead et al. 2021; He et al. 2021; Bondelind et al. 2020) on microplastic fate and transport in freshwater, particularly in rivers, is the driving force behind this study. The scarcity of research in this area highlights the need for more comprehensive assessment and modeling of microplastics in fresh waterbodies.

Materials and methods

In this study, a well-known and one of the most used commonly used water quality models, QUAL2K (Chapra et al. 2003), is used for simulating the steady-state transport of microplastics along Nif Creek and adjacent Gediz River and understanding the waterbody response in terms of microplastics. The QUAL2K solves physical, chemical, and biological processes, which are based on a combination of empirical data and theoretical models such as mass balance equations and biogeochemical cycles. The study is conducted in Nif Creek of the Gediz River Basin situated in Western Anatolia, Turkey. The river system is schematized using 28 segments and 168 reaches. The Nif Creek is surrounded by the factories of Kemalpaşa Organized Industrial Zone that contain numerous establishments processing plastic as raw material. The treated effluent discharges from this zone as well as numerous tributary inputs were also taken into account in this modeling application (Figure 1).

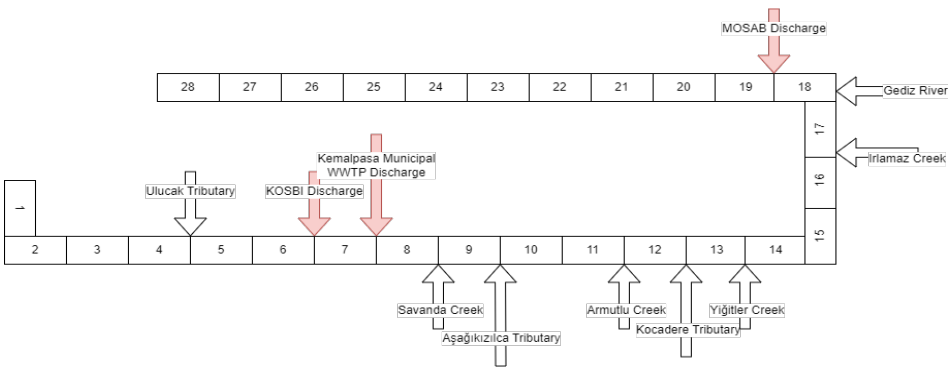

Figure 1. Model segmentation.

In order to verify the model, a total of 11 samples, 3 of which represented the treated industry

wastewater effluents, one represented the upstream boundary condition, and the remaining 7 corresponded to in-stream samples from the creek, were taken along the river in November 2022 (Figure 2). The monthly average flow for November were used in simulations.

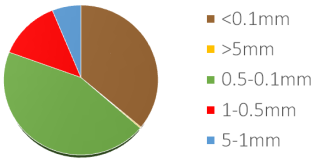

Figure 2. The distribution of microplastics for 11 sampling stations.

Results and concluding remarks

The results for flow (Figure 3) and microplastic concentrations (Figure 4) revealed that the developed model adequately represented the conditions in the river. With the help of the model, for the first time in this basin a rough estimate of the contribution of the tributaries were determined. Based on the deductions made from the model results, it was concluded that about 33.3 million microplastic particles reached the Aegean Sea in every second for the month of November (Q=10.20 m^3/s at the last reach). Finally, it can be concluded that despite the settling mechanism used in the simulations (V_s=13.85 m/day) (Elagami et al. 2023), no major reduction was observed in microplastic concentration due to the fairly small diameter of the particles as well as the relatively high water velocity in the system.

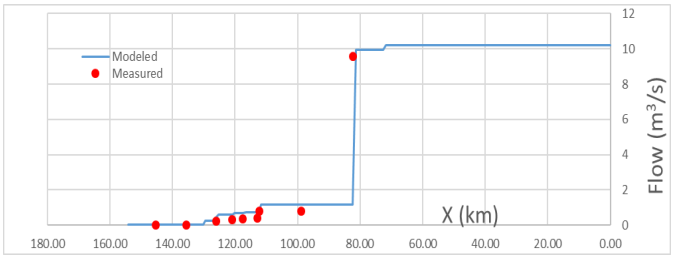

Figure 3. Hydraulic Result of Nif Creek for the month of November.

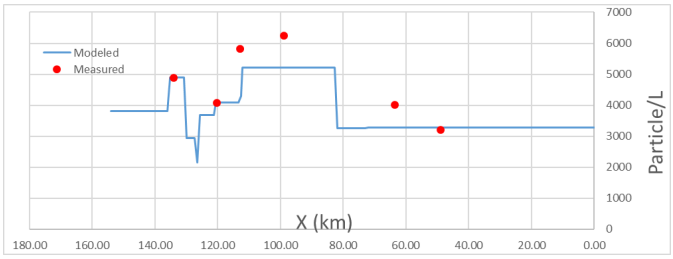

Figure 4. Hydraulic Result of Nif Creek for the month of November.

Acknowledgments: This study was supported by Scientific and Technological Research Council of Turkey (TÜBİTAK) with project number of 121Y460.

References

Whitehead PG, Bussi G, Hughes JMR, Castro-Castellon AT, Norling MD, Jeffers ES, Rampley CPN, Read DS, Horton, AA (2021) Modelling Microplastics in the River Thames: Sources, Sinks and Policy Implications. Water 13(6): 861. https://doi.org/10.3390/w13060861

He B, Smith M, Egodawatta P, Ayoko GA, Rintoul L, Goonetilleke A (2021) Dispersal and transport of microplastics in river sediments. Environmental Pollution 279: 116884. https://doi.org/10.1016/j.envpol.2021.116884

Bondelind M, Sokolova E, Nguyen A, Karlsson D, Karlsson A, Björklund K (2020) Hydrodynamic modelling of traffic-related microplastics discharged with stormwater into the Göta River in Sweden. Environmental Science and Pollution Research 27(19): 24218–24230. https://doi.org/10.1007/s11356-020-08637-z

Chapra SC, Pelletier GJ, Tao H (2003) Qual2K. Civil and Environmental Engineering Department, Medford, Tufts University

Elagami H, Frei S, Boos JP, Trommer G, Gilfedder BS (2023) Quantifying microplastic residence times in lakes using mesocosm experiments and transport modelling. Water Research 229: 119463. https://doi.org/10.1016/j.watres.2022.119463

Turbidity source analysis of the urban lakeside river network

R. Yan, J. Gao*
Key Laboratory of Watershed Geographic Sciences, Nanjing Institute of Geography & Limnology, Chinese Academy of Sciences, Nanjing 210008, P.R. China
** e-mail: gaojunf@niglas.ac.cn*

Introduction

With the rapid economic growth and land use/cove change, turbidity impairment of water bodies has increasingly become a global concern (Alcântara et al. 2009; Bowie et al. 1985; Chao et al. 2022; Chen et al. 2011, 2021). The first step to addressing the turbidity problem is pollutant source tracking and analysis of key driving forces that affect the spatio-temporal distribution of turbidity (Cham berlain and Ioannou 2019; Lizotte and Locke 2018; Ljunggren and Sandström 2007). However, less effort has been implemented to analyze the urban river network areas neighboring the large lake. They are vulnerable to turbidity impairment due to fragile aquatic systems, complex but gentle flow, and intensified human interference (Xiao et al. 2016). Quantifying turbidity source is essential but complex for precise environmental rehabilitation of worldwide urban lakeside river networks impaired by turbidity.

In response to this demand, the objectives of the present study are as follows: (1) to develop a method for quantitative analysis of the turbidity source for an extremely turbid river network of urban lakeside with reverse flow and shipping; (2) to assess the major turbidity sources of Huzhou urban lakeside river networks.

Materials and methods

The Huzhou urban river network lies in the southwest of the Lake Taihu (E: 119°10′- 120°11′; N: 30°04′- 30°58′), which is China's third largest freshwater lake. Turbidity in the concerned Huancheng River located in an urban core area, was mainly due to integration effect of SIM, algae, and other SOM. Based on the field investigation, the shipping, Tiaoxi River, Lake Taihu, and urban non-point source pollution were identified as four major TSS sources that caused turbidity. The field campaign, remote sensing (RS), and scenario simulation of MIKE 11-based TSS model served the quantification of TSS source. The RS imageries of Sentinel-2 taken from January 24, March 20, April 9, May 24, August 17, October 31, November 15, November 20, and December 10, 2019, were interpreted using the relationship model between the TSS and RS reflectance. 14 TSS sampling sites were assigned along the river network to collect water samplers and water parameters in situ. Water samples at 14 sites were mostly collected twice a day in summer and autumn, 2019, when high turbidity in the rivers was most likely to occur.

The hydrodynamic (HD), advection-dispersion (AD), and sediment transport modules in the MIKE 11 model were used for river hydrodynamic and TSS modelling. The manning roughness coefficient of the HD module and diffusion coefficient of AD module were calibrated with the observed daily flows or water level and TSS concentration in the year 2019.

Results and concluding remarks

The calibration and validation results showed that MIKE 11-based TSS model can accurately reflect the TSS process of urban lakeside river network. Huancheng River has an annual total TSS load of 209846 tonnes.The Huzhou turbidity problem was largely SIM-driven, which constituted 58% of the average turbidity at the Huancheng River, the remaining 42% included SOM (19%) and dissolved colored organic compounds and colloid (23%). Tiaoxi River and busy shipping were the two largest contributors to the total TSS load of Huancheng River, with the same percentage of 34%. The TSS load by Lake Taihu in the autumn and winter months accounted for 79.7% of the annual TSS load by Lake Taihu, while those in the spring and summer month were less. The large water volume of reverse flow and high TSS concentration of Lake Taihu

in the autumn and winter months are two factors accounting for the seasonal change in Lake Taihu's TSS load.

Acknowledgments: We are grateful for the grant supports from the National Natural Science Foundation of China (42071052), Science and Technology Planning Project of NIGLAS (NIGLAS2022GS10), and Young Science and Technology Talents Lifting Project of Jiangsu Association for Science and Technology (2021–2023). We specifically thank Huzhou Water Resources Department for its help on the sampling during the COVID-19 lockdown period.

References

Alcântara E, Barbosa C, Stech J, Novo E, Shimabukuro Y, (2009) Improving the spectral unmixing algorithm to map water turbidity Distributions. Environmental Modelling & Software 24(9): 1051-1061

Bowie GL et al. (1985) Rates, constants, and kinetics formulations in surface water quality modeling. Epa, 600: 3-85.

Chamberlain AC, Ioannou CC (2019) Turbidity increases risk perception but constrains collective behaviour during foraging by fish shoals. Animal Behaviour 156: 129-138

Chao C et al. (2022) The spatiotemporal characteristics of water quality and phytoplankton community in a shallow eutrophic lake: Implications for submerged vegetation restoration. Science of The Total Environment, 821: 153460

Chen C-Y, Fytanidis DK, García MH (2021) Entrainment, Transport, and Fate of Sediments during Storm Events in Urban Canals and Rivers: Case Study on Bubbly Creek, Chicago. Journal of Hydraulic Engineering 147(8): 05021005

Chen S, Huang W, Chen W, Chen X, (2011) An enhanced MODIS remote sensing model for detecting rainfall effects on sediment plume in the coastal waters of Apalachicola Bay. Marine Environmental Research 72(5): 265-272

Lizotte R, Locke M (2018) Assessment of runoff water quality for an integrated best management practice system in an agricultural watershed. Journal of Soil and Water Conservation 73(3): 247-256

Ljunggren L, Sandström A, (2007) Influence of visual conditions on foraging and growth of juvenile fishes with dissimilar sensory physiology. Journal of Fish Biology 70(5): 1319-1334

Xiao R, Wang G, Zhang Q, Zhang Z (2016) Multi-scale analysis of relationship between landscape pattern and urban river water quality in different seasons. Scientific Reports 6(1): 25250

Incorporating uncertainties in streamflow estimation using two monthly rainfall-runoff models

L. Vasiliades*, I. Mastraftsis
Department of Civil Engineering, School of Engineering, University of Thessaly, Pedion Areos 38334 Volos, Greece
** e-mail: lvassil@civ.uth.gr*

Introduction

Rainfall-runoff models are used to estimate runoff generation and water balance components. Calibrating model parameters often leads to a match between observed and simulated outputs, but results are uncertain due to aleatory and epistemic uncertainty. Input data inaccuracies and calibration data inaccuracies, along with model parameters and mathematical model structure errors, are the main causes of epistemic uncertainty. Therefore, uncertainty estimation is crucial in hydrological and water resources management studies.

This study aims to evaluate uncertainties in streamflow using two monthly water balance models (WBMs): the 6-parameter UTHBAL model (Loukas et al. 2007), and the 2-parameter GR2M (Mouelhi et al. 2006) in Portaikos river catchment in Thessaly, Greece. Three types of uncertainty are examined: input data, model structure and model parameters. The uncertainties are estimated using the "hydroPSO" R-package, a global Particle Swarm Optimisation (PSO) algorithm (Zambrano-Bigiarini and Rojas 2013). The two water balance models are integrated with hydroPSO and sensitivity, optimization and uncertainty analyses, with user-friendly evaluation plots are provided for interpretation of results.

Materials and methods

The study focuses on the Portaikos River watershed located in the Thessaly Region with a total area of 133 km^2. The watershed, a forested mountainous area, is a tributary of the Pinios River and streamflow data was collected from Oct. 1990 to Sep 1993 at Pyli hydrometric station. Meteorological data for the same period were used to estimate areal data inputs (precipitation and mean temperature) using typical engineering methods and potential evapotranspiration was calculated using the Thornthwaite method based on monthly temperature.

The UTHBAL and GR2M models are selected and redesigned in R-Project due to their previous successful water balance applications. The models utilize monthly time series of precipitation, mean temperature, and potential evapotranspiration as input datasets. To discover important model parameters and the necessary mathematical model structure, the Latin-Hypercube One-factor-At-a-Time technique established by van Griensven et al. (2006) is initially employed. Then, using the temporal split-sample test, the skill and robustness of the two water balance models to make consistent streamflow predictions were evaluated. Several objective functions (Root Mean Square Error, Nash-Sutcliffe Efficiency and two variations or adaptations of the Kling-Gupta efficiency formulations) are used to assess model parameter uncertainty and model structure. The hydroPSO method was used to determine the confidence intervals in the simulated runoff due to input data uncertainty, parameter uncertainty, and total uncertainty. To accomplish specific user demands, hydroPSO applies various state-of-the-art improvements and fine-tuning options to the Particle Swarm Optimization (PSO) algorithm. Through simple ASCII files and/or R wrapper functions, hydroPSO connects the calibration engine to several model codes for easy calibration parameter exchange. Then, until a certain number of iterations or a convergence threshold are reached, optimizes a user-defined goodness-of-fit measure. Finally, enhanced charting features make it easier to understand and evaluate the calibration findings.

Results and concluding remarks

Application of sensitivity analysis revealed that all model parameters should be included in the mathematical model structure. Hence the R-based water balance GR2M and UTHBAL models have been calibrated with the hydroPSO algorithm. Using the temporal split-sample test between 1st (Oct1960-Sep1977) and 2nd period (Oct1977-Sep1993) the models have been calibrated for half of the years during both 1st and 2nd periods leaving the rest half of the years for validation and using a warm-up period of one (1) year. The KGE2 values of the optimisation process were 0.79 and 0.87 for the 1st and 2nd period, respectively for 2000 model realisations for the UTHBAL. Similarly, the KGE2 values for GR2M were 0.75 and 0.86 for the two periods, respectively. Based on the above calibration and verification/validation results, using several statistical performance indicators and Taylor diagrams the two models show similar capabilities to simulate the observed patterns of monthly streamflows.

Finally, based on a selected threshold of KGE2>0.3 as behavioural threshold, all parameter values above the threshold were selected and weighted quantiles of model parameters were calculated to provide an estimate of the uncertainty in each model parameter. Using the P-factor, which represents the percent of observations that are within the user-defined uncertainty bounds and the R-factor that represents the average width of the user-defined uncertainty bounds divided by the standard deviation of the observations a quantification of the uncertainty was estimated (Abbaspour et al. 2007). Figure 1 presents the results of the uncertainty analysis for the verification period and shows the best simulated streamflows along with the 95 Percent (%) Prediction Uncertainty (95 PPU) for GR2M (similar plots are also produced for UTHBAL model). These results show that the uncertainty in streamflow estimation should always be accounted for and evaluated in operational water resources management projects.

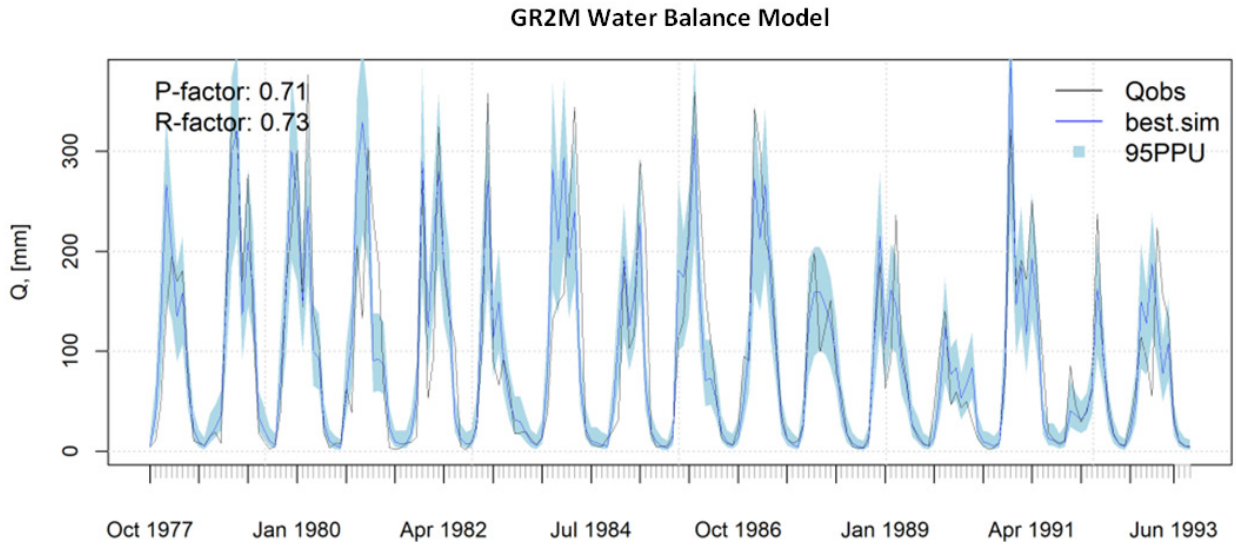

Figure 1. 95 Percent Prediction Uncertainty (95 PPU) for GR2M model simulations during the 2nd period (Oct 1977 –Sep 1993).

References

Abbaspour KC, Yang J, Maximov I et al. (2007) Modelling hydrology and water quality in the pre-alpine/alpine Thur watershed using SWAT. Journal of Hydrology 333: 413–430. https://doi.org/10.1016/j.jhydrol.2006.09.014

Loukas A, Mylopoulos N, Vasiliades L (2007) A Modeling System for the Evaluation of Water Resources Management Strategies in Thessaly, Greece. Water Resour Manage 21: 1673–1702. https://doi.org/10.1007/s11269-006-9120-5

Mouelhi S, Michel C, Perrin C, Andréassian V (2006) Stepwise development of a two-parameter monthly water balance model. Journal of Hydrology 318: 200–214. https://doi.org/10.1016/j.jhydrol.2005.06.014

van Griensven A, Meixner T, Grunwald S et al. (2006) A global sensitivity analysis tool for the parameters of multi-variable catchment models. Journal of Hydrology 324: 10–23. https://doi.org/10.1016/j.jhydrol.2005.09.008

Zambrano-Bigiarini M, Rojas R (2013) A model-independent Particle Swarm Optimisation software for model calibration. Environmental Modelling & Software 43: 5–25. https://doi.org/10.1016/j.envsoft.2013.01.004

Developing and stabilizing a multivariate mutual information estimator to compute the available information of hydrological datasets

E. Findanis*, A. Loukas
Department of Rural and Surveying Engineering, Faculty of Engineering, Aristotle University of Thessaloniki, Greece
** e-mail: findanis@topo.auth.gr*

Introduction

The Available Information (AvInf) contained in a hydro-meteorological dataset is defined as the beneficial information measured in bits per timestep which is inputted into a model to produce runoff prediction. The concept of AvInf is limited to gauged watersheds, for which a model can be calibrated. It has been shown that, for two gauged sub-basins located in Thessaly Greece, the performance of five lumped models was improved when the AvInf of the dataset exploited by the models was increased (Findanis and Loukas 2022). An accurate estimation of AvInf is imperative to examine its relationship with model performance and to evaluate a model's parametric and structural uncertainty, but computing AvInf is unstable, since multiple evaluations of AvInf may lead to slightly different results.

This is because, to estimate the AvInf of dataset {X} containing N observed time series (precipitation, temperature, runoff, etc), Independent Component Analysis (ICA) must be performed aiming to find n independent source signals which can be mixed to retrieve the original dataset {X}. These source signals are formulated by maximizing their Non-Gaussianity, implying that optimization is performed each time the ICA is used, which can lead to equivalent but different sets of source signals. Moreover, the source signals are not always truly independent, as they should be, but they share mutual information (MI). Thus, by evaluating the total pairwise mutual information contained in these signals, false solutions of the ICA technique can be eliminated, potentially improving the stability while calculating AvInf.

Materials and methods

A routine for calculating the AvInf of an observed dataset was developed in Python 3.11 and it consists of six main sub-routines. Three of them estimate univariate and bivariate differential entropies by dividing the 1D or 2D domain into equiprobable portions (Gupta et al. 2021). The fourth sub-routine computes multivariate (nD) differential entropy by utilizing the FastICA function of Python Package Scikit-Learn. The fifth and sixth routines calculate the bivariate (2D) and multivariate (nD) mutual information between hydrological time series. The number of equiprobable 2D portions is specified by an additional secondary routine, which calibrates the 2D mutual information function against a bivariate normal distribution.

More precisely, two bivariate entropy routines were developed (Hoshen et al. 2013). The first routine employs an Adaptive Grid (AG) to divide the 2D domain into equiprobable bins. The second one divides the domain into approximately equiprobable bins utilizing a Joint Probability Matrix (JPM) and then applies bin counting to estimate the exact probability of each bin. The former routine is more precise but less stable than the latter. A criterion of uniformity was formulated to indicate when the 2D bins can be considered exactly equiprobable or not, and thus this criterion indicates when the AG routine cannot be applied.

The computational procedure to estimate AvInf is the following: Initially, the available data are log-transformed, and a small amount of Gaussian noise is added to them. Then, the bivariate mutual information routine is calibrated to find the optimum number of 1D and 2D bins. The mutual information MI(X,Y) between two variables X and Y is given by the equation,

$$MI(X,Y) = h(X) + h(Y) - h(X,Y) \quad (1)$$

where h(X) is univariate differential entropy of X and h(X,Y) is the bivariate differential entropy of X and Y. As a result, the 2D mutual information routine depends on the 1D and 2D differential entropy routines. In addition, the 2D MI routine is used inside the nD differential entropy routine (figure 1), which performs

multiple ICA runs to find the set of independent source signals S sharing the less unwanted mutual information. The total shared information ε between a set of n source signals is given by the equation,

$$\varepsilon = \sqrt{\sum_{i=1}^{N-1}\sum_{j=i}^{N} MI^2(S_i, S_j)} \quad (2)$$

The multivariate mutual information between the set {X} of input observed time series and the observed output Y is defined as,

$$MI(\{X\},Y) = h\{X\} + h(Y) - h(\{X\},Y) \quad (3)$$

Hence, the nD MI routine requires multiple runs of the nD differential entropy routine to estimate h{X} and h({X},Y). Finally, the AvInf of dataset {{X},Y} is the average value of multiple nD MI routine runs.

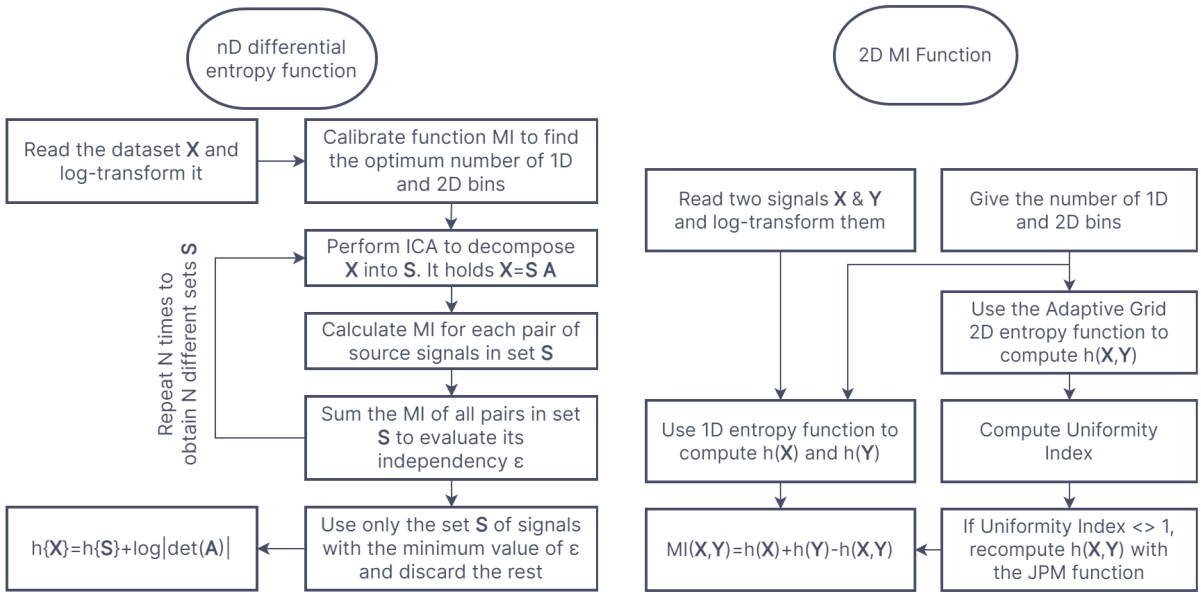

Figure 1. Flowcharts showing the operations inside nD differential entropy and 2D Mutual Information functions.

Results and concluding remarks

The available information of the observed data recorded in five sub-basins of Pinios River, Thessaly Greece, was estimated using two different variations of the same nD mutual information routine. In the first variation, the set of source signals, sharing the minimum amount of mutual information, was selected to estimate the nD differential entropies involved in equation (3). In the second variation, each nD differential entropy of equation (3) was considered as the simple average of multiple ICA runs. Similar values of nD MI occurred from the two variations. The computational burden of the first variation was significantly higher due to several evaluations of the 2D MI routine. Hence, computing the total pairwise mutual information between the source signals does not necessarily improve the stability of the nD MI routine by eliminating invalid sets of non-independent source signals. Future research will be focused on estimating the AvInf of datasets inputted in semi-distributed and distributed hydrological models.

References

Findanis E, Loukas A (2022) The implicit information nature of hydrological uncertainty: estimating and detangling components of uncertainty, 7th IAHR Europe Congress, Book of Abstracts, 273-274, https://www.erasmus.gr/microsites/1227/book-of-abstracts

Gupta HV, Ehsani MR, Roy T, Sans-Fuentes MA, Ehret U, Behrangi A (2021) Computing Accurate Probabilistic Estimates of One-D Entropy from Equiprobable Random Samples. Entropy 23(6): 740, https://doi.org/10.3390/e23060740

Hoshen Y, Arora C, Poleg Y, Peleg S (2013) Efficient representation of distributions for background subtraction, 10th IEEE International Conference on Advanced Video and Signal Based Surveillance 276-281, doi: 10.1109/AVSS.2013.6636652

The decadal changes in climate and streamflow in the Balkhash Lake basin

G. Gan, J. Wu*
Nanjing Institute of Geography and Limnology, Chinese Academy of Sciences, Nanjing 210008, China
** e-mail: w.jinglu@niglas.ac.cn*

Introduction

As the climate continues to warm, the water cycle in High Mountain Asia (HMA) has been intensively altered. Glaciers in the HMA are accelerating to melt, posing serious challenges for water resources management. Also, it is anticipated that an increase in air temperature will induce a shift of precipitation from snow towards rain, which will alter the partitioning of precipitation into runoff and evapotranspiration.

The Balkhash Lake Basin (BLB), which covers 41.3×10^4 km^2, is one of the largest internal drainage areas in Central Asia. Discharge in all five rivers showed decreasing trends from 1949 to 1986 (Kezer and Matsuyama, 2006). However, at a longer time scale, the streamflow of the Ili River is increasing due to the increase in precipitation from 1929-2014 (Thevs et al. 2017). However, how the climate changes and how such changes induce hydrological changes in different sub-basins of the BLB still needs to be analyzed.

Materials and methods

Five major rivers (Ili, Kartaral, Aksu, Lepsy, and Ayaguz) that originated from the Tienshan Mountains are the main tributaries to the lake Balkhash. After the drastic shrinkage of the Aral Sea, Lake Balkhash has been the largest lake (1.7×10^4 km^2) in Central Asia, with a mean depth of 8 m. We derived gridded meteorological forcing data from the hourly ERA5-Land dataset, at the spatial resolution of 0.1°. We acquired gauge runoff data from 13 stations in all five rivers in the BLB (Figure 1) from the hydrological yearbook and literature. Because most of the runoff gauges (1949-1986) did not cover the whole study period (1949-2014), we used two monthly gridded discharge datasets to extend the runoff time series from the gauges, i.e., the GLDAS and ERA5-Land data.

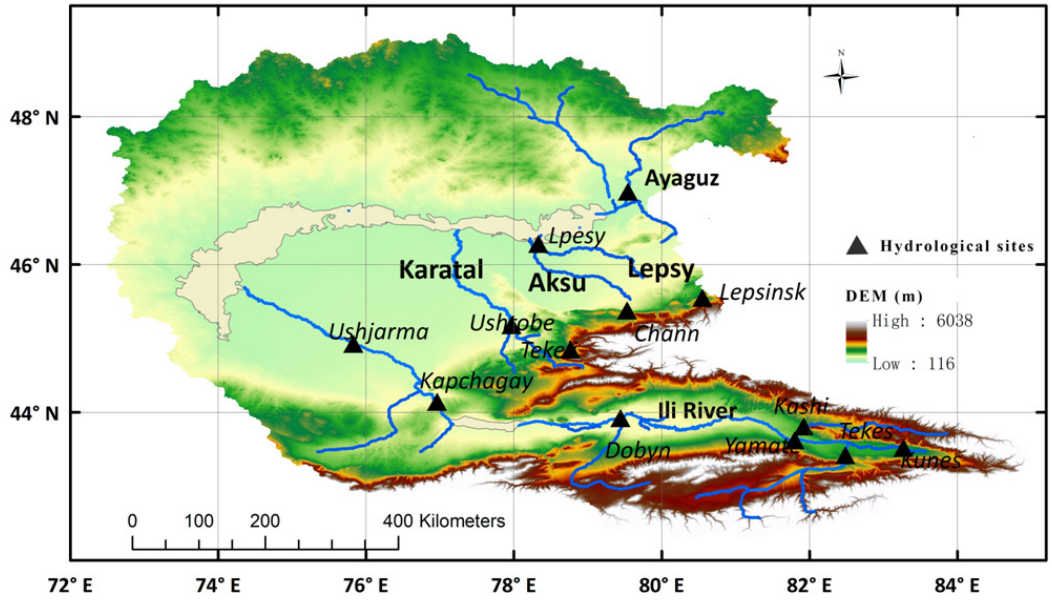

Figure 1. Elevation in the BLB and river networks.

Results and concluding remarks

The multi-year air temperature and precipitation of the BLB are 6.75°C and 342.2 mm, with 27.9% precipitation falling as snow. Air temperature increases at a rate of 0.01-0.03 °C /yr across the BLB, where increasing rates are higher in the lower elevation regions. Precipitation changes in a more heterogenous way, where increasing trend and decrease trend were mostly found in the high and low elevation regions, respectively. However, precipitation showed an increasing trend in all catchments except in the Ayaguz catchment. Snow ratio over precipitation (f_s) showed an overall decreasing trend as the air temperature increases, indicating that more precipitation falls as rain instead of snow.

Streamflow in the Ili river and the Lepsy river showed an overall significant increasing trend, with the Z values in the MK test larger than 1.28 at the Kashi and Tekes sites in the upper reaches and Dobyn site in the mainstream of the Ili river and both the Lepsinsk and Lepsy sites in the Lepsy river (Figure 2). Streamflow in other rivers showed no overall trends. However, streamflow in the 1950-1982 period showed different trends compared to those in the 1983-2014 period. Most of the sites showed stable or decreasing trends during the 1950-1982 period, in contrast, streamflow was increasing at most of the sites in the 1983-2014 period.

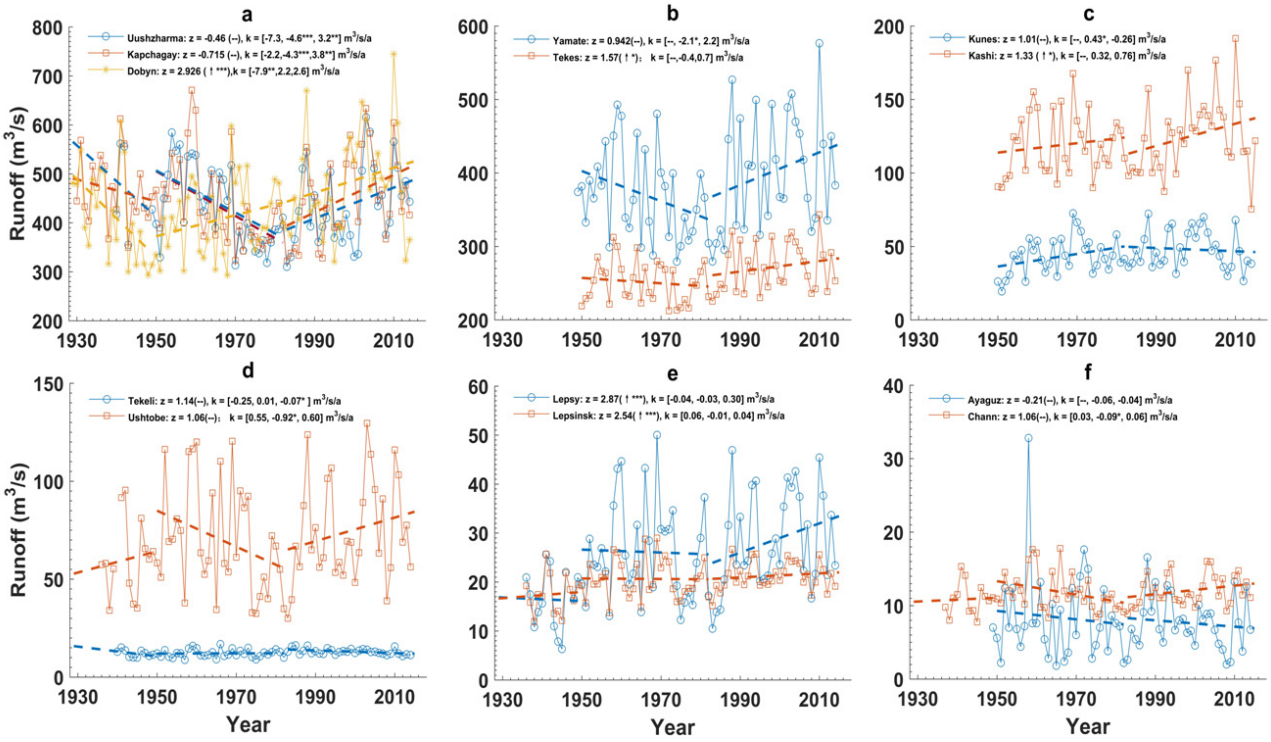

Figure 2. Annual runoff at 13 stations in the BLB in 1929-2014.

Our study demonstrated that although streamflow in the BLB was decreasing before the 1980s, streamflow showed an increasing trend since 1982. The overall increase in the streamflow was mainly due to the increase in precipitation and the accelerated melting of glaciers. However, whether such an increasing trend will be lasting needs further study under a warming environment in which the glaciers will be finally depleted.

Acknowledgments: Our research is jointly funded by the National Natural Science Foundation of China (U2003202, 42071054).

References

Kezer K, Matsuyama H (2006) Decrease of river runoff in the Lake Balkhash basin in Central Asia. Hydrol Process 20(6): 1407-1423. https://doi.org/10.1002/hyp.6097

Thevs N, Nurtazin S, Beckmann V, Salmyrzauli R, Khalil A (2017) Water Consumption of Agriculture and Natural Ecosystems along the Ili River in China and Kazakhstan. Water 9(3): 207. https://doi.org/10.3390/w9030207

Setting for long-term analysis of the hydrological water budget components in a north-eastern Italian basin

V. Zoratti[1*], G. Formetta[2], E. Arnone[1]
[1] Polytechnic Department of Engineering and Architecture (DPIA), University of Udine, Udine, Italy
[2] Department of Civil, Environmental and Mechanical Engineering, University of Trento, Trento, Italy
* e-mail: veronica.zoratti@uniud.it

Introduction

Climate change directly affects the components of the hydrological water balance and several authors have investigated potential changes and future scenarios in the catchment water budget by means of hydrological models (e.g. Roati et al. 2022; Pumo et al. 2017; Kour et al. 2016; Brêda et al. 2020). North Italy and Europe at large have been recently hit by prolonged and intense droughts that are causing dramatic water shortages. The Friuli-Venezia Giulia (FVG) region, located in north-eastern Italy, is one of the areas that is experiencing unprecedented changes in climate variables, especially in terms of maximum temperature values in spring and summer (ARPA-Osmer, FVG 2022). Significant variations in the precipitation extremes have been also observed in specific areas of the region (e.g. Arnone et al. 2022). Such changes may significantly affect the water budget components and, ultimately, the water availability. Potential impacts on water quantity, in terms of groundwater level variation, have been analysed by Baruffi et al. (2012) in the upper Veneto and FVG plains by using climate model projections.

In this context, this contribution aims at setting the work for investigating the long-term behaviour of the water budget components of a specific study area of the FVG region, by using a semi-distributed hydrological model to simulate the hydrological processes over the last decades.

Materials and methods

The work analyses the Fella basin, which extends in the Alpine territory of the FVG for 710 km^2 with a main stream of 54 km approximately and it is characterized by a humid continental climate. The FVG region counts on two main meteorological networks, based on CAE and Micros+SIAP technology, respectively, that measure all the required hydro-meteorological variables. 37 out of all gauges fall within or are in proximity of the analysed basin, with 28 meteorological gauges (which measure both rainfall and temperature), and 9 water level gauges (Figure 1a).

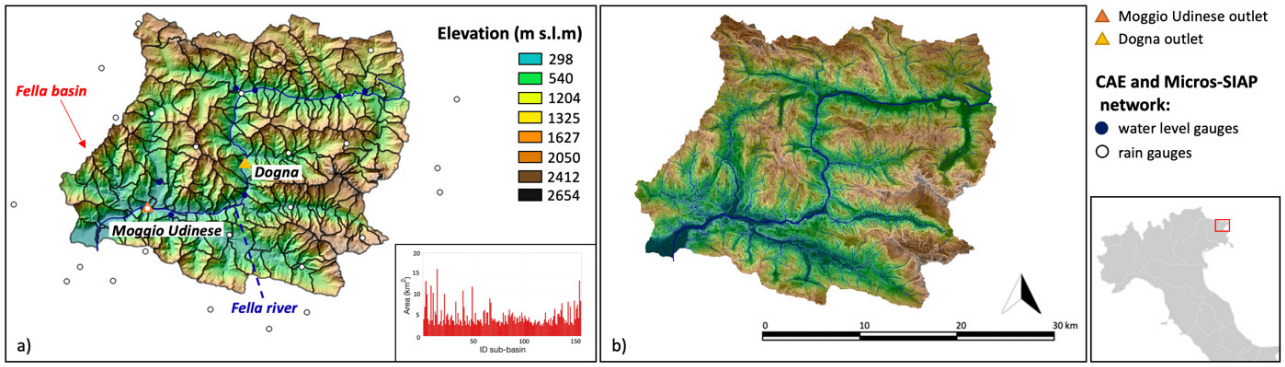

Figure 1. a) The Fella basin discretization into 153 HRUs and the hydrometeorological network therein; b) the slope map of the Fella basin.

The hydrological modelling is being conducting by using the GEOframe-NewAge semi-distributed component-based model, suitable for the modelling in alpine environment (Formetta et al. 2014; Bancheri et al. 2020). GEOframe-NewAge is able to simulate the entire hydrological cycle providing as output the

hydrograph at the outlet and in each inner outlet; moreover, as a result of the geomorphological analysis it is possible to discretize the basin in more Hydrological Response Units (HRUs).

Results and concluding remarks

At this stage of the work, preliminary results regard the geomorphological analysis of the GEOframe-NewAge using a 10-meters resolution DTM. Specifically, the Fella basin has been discretized in 153 HRUs (Figure 1a), with an average area of the sub-basins of about 5 km^2 and standard deviation of 2.4 km^2. Figure 1a also shows the statistics of the HRUs area and the slope map of the basin is reported in Figure 1b.

In order to calibrate and validate the model, the longest available water level series have been retrieved. Specifically, 21 years of water level data (2002-2023) are available for Moggio Udinese outlet (Figure 2a) and 19 years (2004-2023) for Dogna outlet (Figure 2b), both with a time-step of 30 minutes. The availability of multiple water level gauges will give us the possibility to carry out a calibration of the hydrological model at Moggio Udinese with an independent validation at the inner upstream sub-basins (including Dogna). Figure 2 shows the observed series at 30 minutes. The hydrological model allows to reproduce the main components of the hydrological budget, i.e. runoff, evapotranspiration, snow coverage, interception and groundwater level (Bancheri et al. 2020). The temporal dynamic of the simulated water budget components over the analysed period (2002-2023) will be further verified by exploiting by remote sensing data such as MODIS for snow cover or GLEAM for evapotranspiration fluxes.

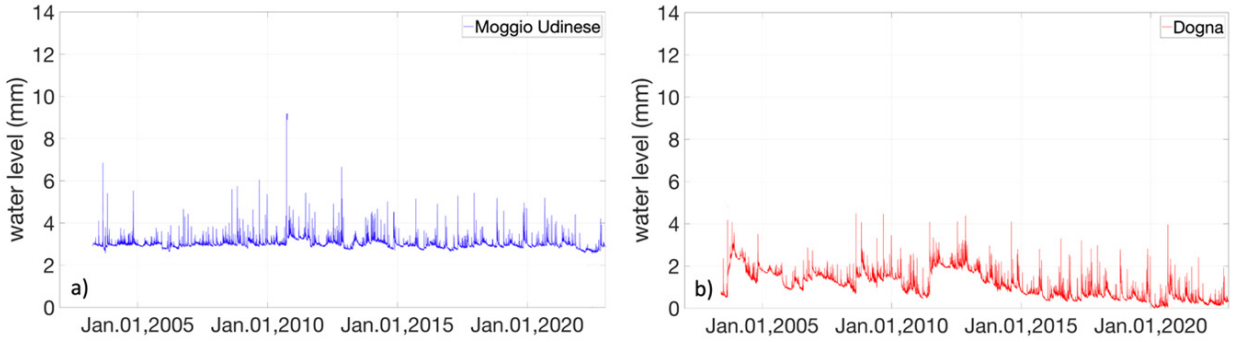

Figure 2. Observed water level at Moggio Udinese (a) and Dogna outlet (b).

References

Agenzia Regionale per la Protezione e per l'Ambiente del Friuli Venezia Giulia, ARPA-FVG (2022) Meteo. FVG report: Mensile

Arnone E, Treppiedi D, Noto LV (2022) High-resolution rain analysis in FVG, Northeastern Italy. Proceeding of XIth Scientific Assembly of the International Association of Hydrological Sciences (IAHS 2022), Montpellier, France, 35, 29 May–3 June 2022. IAHS2022-177, https://doi.org/10.5194/iahs2022-177

Bancheri M, Rigon R, Manfreda S (2020) The GEOframe-NewAge modelling system applied in a data scarce environment. Water 12(1): 86. https://doi.org/10.3390/w12010086

Baruffi F, Cisotto A, Cimolino A, Ferri M, Monego M et al. (2012) Climate change impact assessment on Veneto and Friuli plain groundwater. Part I: An integrated modeling approach for hazard scenario construction. Science of the Total Environment 440: 154-166. https://doi.org/10.1016 /j.scitotenv.2012.07.070

Brêda JPLF, de Paiva RCD, Collischon W, Bravo JM, Siqueira VA, Steinke EB (2020) Climate change impacts on South American water balance from a continental-scale hydrological model driven by CMIP5 projections. Climatic Change, 159(4): 503-522. https://doi.org/10.1007/s10584-020-02667-9

Formetta G, Kampf SK, David O, Rigon R (2014) Snow water equivalent modeling components in NewAge-JGrass. Geoscientific Model Development 7(3): 725-736. https://doi.org/10.5194/gmd-7-725-2014

Kour R, Patel N, Krishna AP (2016) Climate and hydrological models to assess the impact of climate change on hydrological regime: a review. Arabian Journal of Geosciences 9: 544. https://doi.org/10.1007/s12517-016-2561-0

Pumo D, Arnone E, Francipane A, Caracciolo D, Noto LV (2017) Potential implications of climate change and urbanization on watershed.Journal of Hydrology 554: 80–99. https://doi.org/10.1016/j.jhydrol.2017.09.002

Roati G, Formetta G, Pecora S, Brian M, Rigon R, Stevenin H (2022) Hydrological modeling and water budget quantification of the Po river basin through the GEOframe system. In EGU General Assembly Conference Abstracts (pp. EGU22-12562). https://doi.org/10.5194/egusphere-egu22-12562

12th World Congress on Water Resources and Environment (EWRA 2023)
"Managing Water-Energy-Land-Food under Climatic, Environmental and Social Instability"
Thessaloniki, Greece, 27 June - 1 July 2023

Systematic parameterization of a trans-Himalayan river basin using SUFI-2 and Particle Swarm Optimization algorithms

B. Kalita[1*], S. Barman[1], W. R. Singh[1], R. Kumar Bhattacharjya[2], M. Kumar Dutta[3]
[1] North Eastern Regional Center-National Institute of Hydrology, Roorkee, Assam, India
[2] Indian Institute of Technology, Guwahati, Assam, India
[3] Jorhat Engineering College, Assam, India
* e-mail: bimankalita@gmail.com

Introduction

The Majuli River island, which is considered the cultural capital of the Indian state of Assam, has lost approximately 70% of its land since 1950 due to continuous erosion and flooding of the Brahmaputra River (Sankhua et al. 2005). For this reason, several studies about the geomorphological changes of the island have been conducted over the years. Most of them employ remote sensing techniques to quantify erosion rates and identify vulnerable areas. Additionally, some studies were performed using artificial neural networks (ANN) and reduced complexity models (RCM) to analyze erosion and deposition patterns (Prasujya and Nayan 2021; Sankhua et al. 2005). However, very few studies related to the hydrology and hydrodynamics of the region are available, despite their usefulness in providing information for making sound management policies and regulatory decisions.

The present study attempts to address this issue by developing a hydrological model of the Brahmaputra watershed with its outlet placed near the upstream region of Majuli. The model parameters are calibrated with observed streamflow data at four locations in the watershed using the Sequential Uncertainty Fitting version 2 (SUFI-2) algorithm and then further optimized using the Particle Swarm Optimization (PSO) algorithm for a better representation of the watershed (Hui et al. 2020). The daily spatiotemporal streamflow obtained from this process can be used to study the hydrodynamics of the Brahmaputra River along Majuli and the other subbasin outlets. Moreover, the optimized model can be used to study the potential impact of climate change on the island using future-projected meteorological conditions. Such assessments are particularly beneficial as several developmental works, including bank protection measures and bridges, are taking place in the vicinity of Majuli. Furthermore, the model-sensitive parameters obtained in this study can be a valuable resource for future studies in similar catchments.

Materials and methods

The hydrological model was developed using the Soil and Water Analysis Tool (SWAT) through the ArcSWAT interface in ArcGIS 10.2 using free and globally available datasets. SWAT simulates water flow in a catchment through input parameters like topography, land use, soil properties, and climate. Table 1 lists the various input data sources for the current study and their respective spatial resolutions.

The model performed simulation from 1970 to 2014 at the daily scale with a warmup period of 2 years. Following the simulation, the model parameters were calibrated and validated in SWAT-CUP (Abbaspour et al. 2017). The Central Water Commission (CWC), New Delhi, and the Water Resources Department of Assam (AWRD) provided daily observed discharge data at four locations on the Brahmaputra River, i.e., Passighat, Sivsagar, Chenimari, and Bessamora (outlet). Thirty parameters were identified for calibration from hydrological models of similar watersheds (Chiphang et al. 2020). For SUFI-2 calibration, the parameters were sorted into sub-groups based on their behaviour on the catchment's water balance, and each group was calibrated separately. Sensitive parameters were calibrated multiple times to reduce uncertainty. The model was calibrated against observed streamflow at Passighat, Sivsagar, and Chenimari. All the parameters were first optimized for the entire watershed and then at subbasin scales. After reaching satisfactory values for calibration metrics such as the Nash Sutcliffe Efficiency (NSE), coefficient of

determination (R^2), and Percent Bias (PBIAS) from the calibration process, the optimized model was validated against the observed discharge at Bessamora. Following SUFI-2 calibration, the parameters were further calibrated at the three locations using the PSO algorithm to reduce model uncertainties.

Table 1. Sources and spatial resolutions of the SWAT model inputs.

Data	Source	Spatial Resolution
Land Use/Land Cover	MODIS Land Cover (2010)	0.5 km
Soils Data	FAO Soil Map	1:5000000
Digital Elevation Model	GMTED 2010	30 arc seconds
Rainfall	APHRODITE + IMD	0.25 X 0.25 degree
Temperature	ERA5	0.25 X 0.25 degree
Relative Humidity Solar Radiation Wind Speed	NCEP CFSR Global Weather Data for SWAT (https://globalweather.tamu.edu/)	38 km

Results and concluding remarks

Table 2 shows the values of the criteria used for assessing the goodness-of-fit and the associated uncertainties between observed and simulated streamflow at all locations from different stages of the calibration process. The final NSE and PBIAS values obtained after the SUFI-2 calibrations can be classified as satisfactory according to the guidelines provided in ASABE (2005). A significant improvement in the goodness-of-fit criteria is seen after initial calibration by the SUFI-2 algorithm. However, only a slight improvement over the SUFI-2 calibration results could be made by further calibrating with the PSO algorithm.

Table 2. Statistics of the calibration and validation process.*

Gauging Station	Uncalibrated			SUFI-2			PSO		
	R^2	NSE	PBIAS	R^2	NSE	PBIAS	R^2	NSE	PBIAS
Passighat	0.64	0.45	47.8	0.79	0.70	22.6	0.79	0.71	18.2
Chenimari	0.44	0.41	386.7	0.68	0.67	-1.0	0.69	0.68	-0.8
Sivsagar	0.32	-0.24	723.9	0.64	0.54	-24.9	0.63	0.57	-17.7
* Bessamora	0.56	0.37	46.4	0.74	0.63	28.2	0.78	0.67	19.4

After fitting the best parameter values to the model, a daily flow hydrograph from 1972 to 2014 was obtained at the outlet. The simulated streamflow average is found to be 9% less than the observed flow average. Nevertheless, it can be used to conduct hydrodynamic studies in the region by taking this difference into consideration. Moreover, the satisfactory calibration statistics demonstrate the reliability of the model, which, thus, can be used to carry out future studies.

Acknowledgments: The authors thank the Department of Science and Technology, India, CWC, AWRD, and the Director, National Insititute of Hydrology, Roorkee, for funding and facilitating this study.

References

Abbaspour KC, Vaghefi SA, Srinivasan R (2017) A guideline for successful calibration and uncertainty analysis for soil and water assessment: A review of papers from the 2016 international SWAT conference. Water 10(1): 6. https://doi.org/10.3390/w10010006

ASABE (2005) Guidelines for Calibrating , Validating and Evaluating Hydrologic and Water Quality (H / WQ) Models.

Chiphang N, Bandyopadhyay A, Bhadra A (2020) Assessing the Effects of Snowmelt Dynamics on Streamflow and Water Balance Components in an Eastern Himalayan River Basin Using SWAT Model. Environmental Modeling and Assessment 25(6): 861–883. https://doi.org/10.1007/s10666-020-09716-8

Hui J, Wu Y, Zhao F, Lei X, Sun P, Singh SK, Liao W, Qiu L, Li J (2020) Parameter optimization for uncertainty reduction and simulation improvement of hydrological modeling. Remote Sensing 12(24): 4069. https://doi.org/10.3390/rs12244069

Prasujya G, Nayan S (2021) Spatio-temporal study of morpho-dynamics of the Brahmaputra River along its Majuli Island reach. Environmental Challenges 5: 100217. https://doi.org/10.1016/j.envc.2021.100217

Sankhua RN, Sharma N, Garg PK, Pandey AD (2005) Use of remote sensing and ANN in assessment of erosion activities in Majuli, the world's largest river island. International Journal of Remote Sensing 26(20): 4445–4454. https://doi.org/10.1080/01431160500185474

Assessment of Porsuk river basin by using the DPSIR approach

H.C. Çetin*, Y. Şahin
General Directorate of State Hydraulic Works 2nd Region, Izmir, Turkey
** e-mail: hccetin@gmail.com*

Introduction

Management of water resources in an effective and efficient way in respect of sustainable development goals requires the application of sound methods for integrated river basin management, like the DPSIR approach. In this study, the DPSIR approach is applied to the case of the Porsuk which is a problematic river basin. D (driving forces), P (pressures) and S (state) components of the methodology are identified and alternative scenarios are generated to reveal, I (impacts) and R (responses) of the study area. The case is comprehensively investigated from water pollution and water scarcity perspectives. The results reveal that the recent condition of water quality in the river is not within acceptable boundaries according to various water pollution criteria. The basin is investigated under three different scenarios: baseline, optimistic and pessimistic. According to these scenarios, most of the demand sites do not receive sufficient supply of water. Furthermore, none of the scenarios, even the optimistic one, can effectively solve the water pollution problem.

Materials and methods

DPSIR is an approach that defines the impacts and pressures on a watershed system and presents the status and consequences of the system under these impacts. In spite of there is no universal measurement system that can fully measure sustainable development. The DPSIR approach is preferred in the analysis of environmental problems and in finding cause-effect relationships (Langeweg 1998). Integrated watershed management evaluates the basin as a whole and consider solutions in the light of various scenarios and different models in evaluation. In this study, WEAP (Water Evaluation and Planning System) used as a water budget model. The model evaluates irrigation systems in terms of demand, supply, reclamation, pollution, and pricing in light of various scenarios and policies. The most important advantage of the models, especially the WEAP model, is that can easily enable create multiple scenarios according to different variables. Porsuk river basin is a branch of the Sakarya river, the length is 460 km. The drinking and utility water demand of Kütahya and Eskişehir cities are supplied from the Porsuk river.

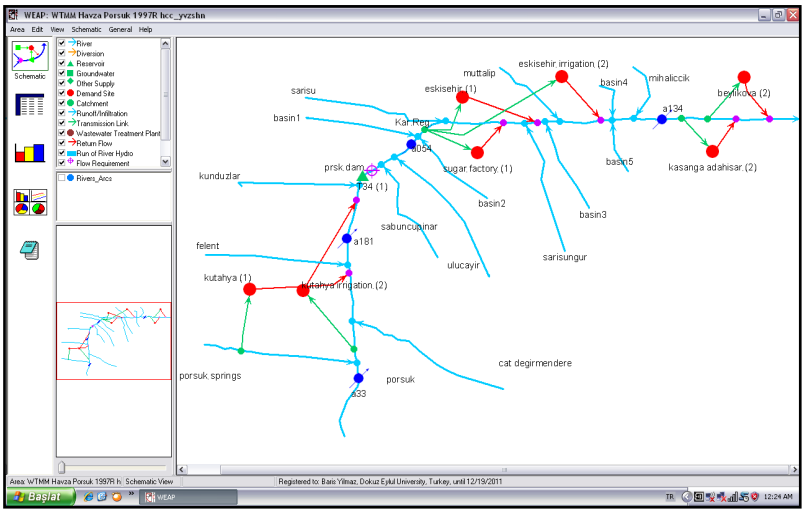

Figure 1. Display of the WEAP modelling.

Results and concluding remarks

In coming years, the increasing drinking and utility water demands of the province in the region, the new irrigation areas to be opened, the increase in the water usage rates in the existing irrigations, etc. These reasons increase the need for water and pollution discharges, along with the inability to meet the demands and the risk of water quality problems. By evaluating the basin with DPSIR method, various scanarios for the future (2050) were produced and the situation of the basin was examined. In the evaluation of the basin in terms of water scarcity, three different scenarios were considered in order to make predictions about the future. These are: i) Present Situation Scenario, ii) Optimistic Scenario and iii) Pesimistic Scenario (Table 1).

Table 1. The results of WEAP model according to water budget in the Porsuk River Basin.

Demand Region	Annual Water Demand (million m^3)				Annual Water Requirement (inc. losses) (million m^3)				Unmet Water Requirement (million m^3)			
	Present	BAU	OPT	PES	Present	BAU	OPT	PES	Present	BAU	OPT	PES
	1997		2050		1997		2050		1997		2050	
Kütahya Irrigation Area	2.0	2.0	1.8	3.7	5.2	5.2	2.6	9.6	0	4.9	0	9.6
Kütahya Domestic Water	5.0	22.7	18.5	35.3	12.4	56.8	26.4	88.3	0	23.3	0	54.7
Eskişehir Irrigation Area	35.8	35.8	39.4	46.3	79.6	79.6	56.3	103.0	0	51.2	0	101.5
Eskişehir Domestic Water	14.7	44.4	35.0	104.6	43.2	130.6	50.1	307.7	0	6.1	0	148.3
Sugar Factory	15.6	15.6	15.6	15.6	15.6	15.6	15.6	15.6	0	0.8	0	7.1
Beylikova Irrigation Area	0	30.4	27.4	38.2	0	46.8	36.5	76.4	0	0	0	4.5
Kaşanga Irrigation Area	0	8.6	7.8	10.9	0	13.3	10.4	21.7	0	0	0	1.3

In present situation, when the Porsuk river basin examined in terms of water amount, it seems that there is not a critical region where water scarcity is encountered, the application year was chosen as a dry year though. Table 1 shows that expect for the optimistic scenario (OPT) in 2050, there is a risky situation where demands not able to meet demanding region. Especially, Demand of drinking and utility water is encountered scarcity problem for Kütahya and Eskişehir provinces. The rehabilitation in irrigation has a crucial factor to encounter demands in case of present and pessimistic scenarios. The results show that tributary of the Porsuk River will be insufficient in the future. Also, reducing the losses of approximately 60% in drinking and utility water transmission and distribution lines through rehabilitation and renewal works will ensure that resources such as Porsuk springs are used for a longer period of time with lower operating costs than treated water.

References

Çetin HC, Harmancıoğlu N (2007) Implementation of DPSIR approach in integrated management of the Porsuk Basin.

Langeweg F (1998) The implementation of Agenda 21 'our common failure'? Science of the Total Environment 218: 227-238. https://doi.org/10.1016/S0048-9697(98)00210-1

A novel framework for Low Impact Development (LID) planning and runoff control in urban watersheds

A. Roozbahani[1*], A.H. Nazari [2] , S.M. Hashemy Shahdany[2]
[1] Faculty of Science and Technology, Norwegian University of Life Sciences (NMBU), Ås, Norway
[2] Faculty of Agricultural Technology, College of Agriculture and Natural Resources, University of Tehran, Tehran, Iran
* e-mail: abbas.roozbahani@nmbu.no

Introduction

The lack of sustainable development in numerous cities has altered watersheds' permeability characteristics, leading to a higher risk of urban flooding (Yao et al. 2016). Besides, traditional grey urban drainage networks have been shown to be inefficient in terms of environmental protection and technical performance. Low Impact Development (LID) practices have been proposed by many researchers as a substitute, however, restoring urbanized watersheds to the desired hydrological conditions may impose excessive costs on decision-making organizations (Kim et al. 2017; Rezazadeh Helmi et al. 2019). Hence, the selection of LID combinations should be based on criteria such as cost-effectiveness and adaptation to the urban context.

Numerous studies have been conducted on optimizing and planning schemes for LID combinations to mitigate urban runoff and several models coupled with other tools have been investigated (Taghizadeh et al. 2021; Hassani et al. 2023). Some of the most popular LID types include green roofs, rain barrels, bio-retention cells, porous pavements, and vegetated swales (Liu et al. 2021). In this study, an integrated framework based on modeling, multi objective optimization and decision support tools have been proposed through a dynamic interaction between Storm Water Management Model (SWMM), System for Urban Stormwater Treatment and Integration (SUSTAIN), and Multi-Criteria Decision Making (MCDM) models. This method is capable of not only determining cost-effective solutions for a single scenario, but also prioritizing scenarios of various LID types based on technical and economic criteria that could help decision makers to select most suitable LID schemes for stormwater systems in urban watersheds.

Materials and methods

The proposed method was applied in a stormwater system located in the northern part of district 11, Tehran, Iran occupying a total area of 2.7 km^2. Six diverse LID schemes were defined as stormwater control scenarios considering land use and spatial limitations (Table 1). SWMM was used for rainfall-runoff modelling as well as simulating the hydrological processes of the drainage network during a 10-year return period storm event (USEPA, 2015). The SWMM output was imported to SUSTAIN model and cost-effectiveness analysis was conducted using the SUSTAIN built-in optimization module for each scenario (USEPA, 2009). In the next step, the optimized LID schemes were simulated through the SWMM LID module to analyze the stormwater system's performance under LID and Non-LID scenarios.

Table 1. LID scenarios for runoff mitigation.

Scenario 1	Scenario 2	Scenario 3	Scenario 4	Scenario 5	Scenario 6
Green Roof Bioretention Vegetated Swale	Rain Barrel Bioretention Vegetated Swale	Green Roof Porous Pavement Vegetated Swale	Rain Barrel Porous Pavement Vegetated Swale	Green Roof + Rain Barrel Bioretention + Porous Pavement Vegetated Swale	Scenario 5 + Dry Pond

The most superior solution of each scenario were investigated and ranked using TOPSIS multi-criteria decision making model based on four criteria including: 1) Runoff Volume Reduction, 2) Peak Discharge Reduction, 3) Reduction of Surcharged Conduits, and 4) Implementation Costs. The weights for each criterion were determined using AHP, Entropy and combined AHP-Entropy methods to make robust weightings. The flow chart for the proposed methodology has been demonstrated in Figure 1.

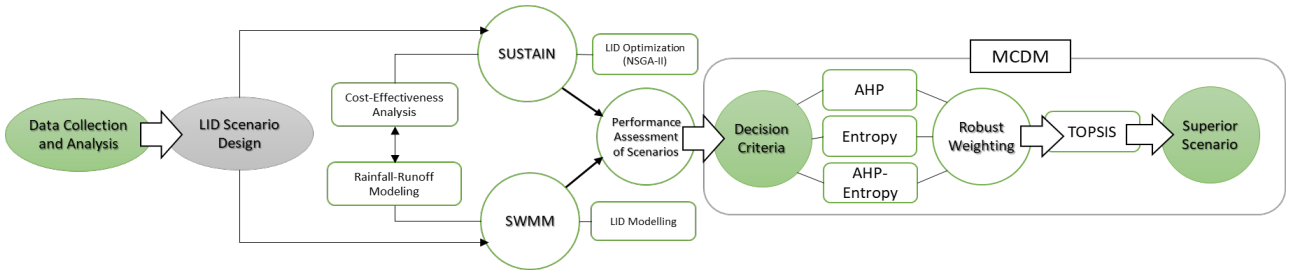

Figure 1. Research flowchart.

Results and concluding remarks

According to the summarized results in Table 2, the performance of each scenario has been shown based on four pre-defined criteria. All weighting methods including AHP, Entropy and AHP-Entropy represented the cost factor as the most contributing criterion in ranking the scenarios. Using TOPSIS method, Scenario 4 consisting of Rain Barrels, Porous Pavements, and Vegetated Swales was selected as the ideal scenario with 7.68 million dollars, reducing runoff volume, peak discharge, and the lengths of surcharged conduits by 20.77%, 19.2%, and 26.4%, respectively. Scenario 3 with a combination of Green Roofs, Porous Pavements, and Vegetated Swales ranked sixth despite the best performance comparing other scenarios due to the high implementation costs.

The proposed approach can help decision-makers and urban planners to determine the most suitable LID schemes, taking into account LID modelling, multi-objective optimization, and experts' attitudes through multi-criteria decision making. However, it is suggested that other criteria such as stormwater quality, social and aesthetics aspects be considered for future studies.

Table 2. Summarized results for the performance and ranking of LID scenarios.

Scenario	LID Coverage (m^2)	Total Cost (million $)	Peak Flow Reduction (%)	Runoff Reduction (%)	Reduction of Surcharged Conduits (%)	TOPSIS (Ranking)
Scenario 1	951354	196	51.3	59.44	52.8	5
Scenario 2	21160	3.25	4.3	15	5.1	2
Scenario 3	1147329	234.6	61.3	68.96	58.4	6
Scenario 4	*39699*	*7.68*	*19.2*	*20.77*	*26.4*	*1*
Scenario 5	630938	135.4	38.2	43.38	45.6	4
Scenario 6	626707	136.3	40.6	44.25	46.9	3

References

Hassani MR, Niksokhan MH, Mousavi Janbehsarayi SF, Nikoo MR (2023) Multi-Objective Robust Decision-Making for LIDs Implementation under Climatic Change. Journal of Hydrology 617: 128954

Kim JH, Kim HY, Demarie F (2017) Facilitators and barriers of applying low impact development practices in urban development. Water Resources Management 31: 3795-3808

Liu T, Lawluvy Y, Shi Y, Yap PS (2021) Low impact development (LID) practices: a review on recent developments, challenges and prospects. Water, Air, & Soil Pollution 232: 344

Rezazadeh Helmi N, Verbeiren B, Mijic A, Van Griensven A, Bauwens W (2019) Developing a modeling tool to allocate low impact development practices in a cost-optimized method. Journal of Hydrology 573: 98-108

Taghizadeh S, Khani S, Rajaee T (2021) Hybrid SWMM and particle swarm optimization model for urban runoff water quality control by using green infrastructures (LID-BMPs). Urban Forestry and Urban Greening 60: 127032

U.S Environmental Protection Agency (2009) SUSTAIN - A framework for placement of best management practices urban watersheds to protect water quality. Tetra Tech, Fairfax, Virginia

U.S Environmental Protection Agency (2015) Storm Water Management Model User's Manual Version 5.1. National Risk Management Research Laboratory, Office of Research and Development, 26 Martin Luther King Drive, Cincinnati, OH 45268

Yao L, Chen L, Wei W (2016) Assessing the effectiveness of imperviousness on stormwater runoff in micro urban catchments by model simulation. Hydrological Processes 30: 1836-1848

V. Urban and Agricultural Water Systems

Treated wastewater in precision agriculture: Performance evaluation of AUGEIAS ecosystem

M. Louta[1*], F. Papathanasiou[2], C. Papadopoulos[2,3], T. Kyriakidis[1], K. Banti[1], I. Karampelia[1], D. Theodorou[1], V. Lazaridis[1], D. Pantelakis[2], S. Lappos[3], E. Bagkavou[3], T. Adamidis[3], I. Ganatsa[3]
[1] *Department of Electrical and Computer Engineering, University of Western Macedonia, Kozani, Greece*
[2] *Department of Agriculture, School of Agricultural Sciences, University of Western Macedonia, Florina, Greece*
[3] *Municipal Enterprise for Water Supply and Sewerage Kozani (DEYAK), Kozani, Greece*
** e-mail: louta@uowm.gr*

Introduction

Water is a prerequisite for protecting human health, being also essential for industrial and domestic use, energy production, and agriculture. Agriculture is the most water-demanding sector, consuming over 85% of freshwater withdrawals (D'Odorico et al. 2020). Considering climate change and towards sustainable development, the exploitation of non-conventional water resources (e.g., treated wastewater) is constituted of paramount importance to minimize freshwater demands. In the light of the aforementioned, we propose AUGEIAS, an intelligent ecosystem that exploits in a safe way treated wastewater for irrigation in precision agriculture, improving crop production and reducing fertilizers and freshwater usage, while incentivizing farmers for its use through an intelligent dynamic pricing system. AUGEIAS consists of an easy-to-install low-power wide area network (LPWAN) and Internet of Things (IoT) devices that provide real-time measurements from agricultural fields and wastewater treatment plants (WWTP). AUGEIAS also utilizes data analysis and artificial intelligence mechanisms to assess the crop water needs, the risk of using treated wastewater for irrigation based on its quality characteristics and its effect on the crop production. A mixing ratio of treated wastewater with conventional water to optimize production will be defined and optimized irrigation doses will be scheduled considering soil moisture and weather forecasting data to reduce over-irrigation application. In this paper we present the results of the first version of AUGEIAS ecosystem application in the pilot sunflower field.

Materials and methods

A pilot study was implemented in a field located in north-western Greece, near the city of Kozani and its WWTP. An area of 0.128 ha with a loam-clay texture, organic matter between 3 and 3.4% and pH 7.7 was sown on the start of April 2022 with a sunflower hybrid at distances of 0.75 x 0.22 m between and within rows respectively. The experimental plot was divided in three areas that received the same fertilization and cultural practices but different irrigation treatments. An area of 0.045 ha, received no irrigation (rainfed), a second area of 0.061 ha was irrigated with treated wastewater and a third area of 0.022 ha was irrigated using conventional water from the town's supply system using drip irrigation systems. Two agrometeorological stations were deployed in the experimental area, as well as soil sensors to monitor soil status (i.e., temperature, moisture, salinity and conductivity at different depths). A water quality monitoring station has been installed to measure the quality characteristics of the treated wastewater (biophysical, biochemical and biological parameters, such as temperature, pH, oxidation-reduction potential (ORP), conductivity, dissolved oxygen, turbidity, total suspended solids (TSS), chemical oxygen demand (COD), and biochemical oxygen demand (BOD), coliforms. An intelligent engine that defines the appropriate mixing ratio of conventional water with treated wastewater, was developed in case the WWTP water didn't meet certain irrigation and quality standards that are specified from the relevant legislation. However, this was not necessary during the experimental period since the treated wastewater met the enforced limits and recommended guidelines for agricultural wastewater reuse. In addition, an intelligent irrigation algorithm has been developed, estimating daily the millimetres of water required, taking into

account soil moisture data from the sensors and automatically turning on and off water supply to each part of the field.

During the crop's growing period, from germination to physiological maturity, the rainfed treatment received a total of 190 mm precipitation whereas the other two treatments received the same water quantity (320 mm from irrigation according to the water needs of the crop plus 190 mm from precipitation). Within each treatment and before the start of irrigation, at 65 Days After Emergence (DAE), four plots of 15 m^2 were marked. Ten plants at random in each plot were selected to record plant height, number of leaves per plant and head diameter. Harvest was performed manually at individual plants at each plot and seed yield per plant and 1000 seed weight were recorded. Statistical analysis was performed with Analysis of Variance (ANOVA) while comparison of means was conducted by Least Significant Difference (LSD) at significance level $p \leq 0.05$. Finally, a drone equipped with a multispectral camera was exploited to extract useful vegetation indices, including NDVI (normalized difference vegetation index).

Results and concluding remarks

A statistical different response of the sunflower crop at the three irrigation treatments was shown on all the agronomic characteristics recorded (Table 1). Water stress at the rainfed treatment, especially during the flowering period, reduced plant growth and plant seed yield compared to the two irrigation treatments. Plants irrigated with treated wastewater showed a significant increase on plant height, leaf number per plant and head diameter compared to the plants irrigated with conventional water. An increased 1000-seed weight of 86.8 g was observed in the wastewater water source compared to the conventional water with 75.9 g. Similarly, achene yield per plant was significantly different between the two irrigation treatments with 26.6% higher yield in the plants irrigated with treated wastewater compared to the yield of the plants irrigated with conventional water.

Table 1. Effect of different irrigation treatments on agronomic and yield parameters of a sunflower crop.

Irrigation Treatments	**Plant height (cm)**	**Leaves /plant**	**Head diameter (cm)**	**1000 seed weight (g)**	**Achene yield/plant (g)**	**HI**
Rainfed	136.3a*	22.5a	14.9a	60.9a	54.3a	28.3a
Conventional water	132.1a	23.8b	16.3b	75.9b	63.5b	29.8a
Treated wastewater	146.4b	25.7c	17.5c	86.8c	80.4c	33.7b
LSD ($p \leq 0.05$)	4.26	0.79	0.89	4.03	7.54	2.10

*Means followed by the same letter within a column are not significantly different (LSD at $p \leq 0.05$)

Similar results have been reported in other studies (Dantas et al. 2019; Sher et al. 2022) attributed to the increase in nutrient accessibility which is the case also in our study. Analyses on seed protein and oil content, and the concentration of nutrients and heavy metals in soil, plant biomass and seeds are underway. Finally, machine learning algorithms that can adapt estimated irrigation dose to be applied and forecast crop yield will be developed, taking into account open weather forecasting data, irrigation treatment and vegetation indices obtained (e.g. NDVI).

Acknowledgments: This research has been co-financed by the European Regional Development Fund of the European Union and Greek national funds through the Operational Program Competitiveness, Entrepreneurship and Innovation, under the call RESEARCH – CREATE – INNOVATE (project code: T2EDK-04211).

References

D'Odorico P, Chiarelli D. D, Rosa L, Bini A, Zilberman D, Rulli MC (2020) The global value of water in agriculture. Proceedings of the National Academy of Sciences 117(36): 21985-21993. https://doi.org/10.1073/pnas.2005835117

Dantas DDC, Silva ÊFDF, Rolim MM, Silva MMD, Morais JEFD, Lira RM (2019) Production components of sunflower plants irrigated with treated domestic wastewater and drinking water in semiarid region. Revista Ceres 66:34-40. https://doi.org/10.1590/0034-737X201966010005

Sher A, Suleman M, Sattar A, Qayyum A, Ijaz M, Allah SU, Al-Yahyai R, Al-Hashimi A, Elshikh, M. S. (2022) Achene yield and oil quality of diverse sunflower (Helianthus annuus L.) hybrids are affected by different irrigation sources. Journal of King Saud University-Science 34(4): 102016. https://doi.org/10.1016/j.jksus.2022.102016

12th World Congress on Water Resources and Environment (EWRA 2023)
"Managing Water-Energy-Land-Food under Climatic, Environmental and Social Instability"
Thessaloniki, Greece, 27 June - 1 July 2023

Analysis of risks related to transients in water distribution systems

M. Ferrante*, F. Casinini
Department of Civil and Environmental Engineering, University of Perugia, Perugia, Italy
** e-mail: marco.ferrante@unipg.it*

Introduction

Most models for the analysis of the functioning conditions of water distribution systems (WDS) are based on a steady-state hypothesis. Even demand variations in the so-called extended period simulations are assumed to cause a transition through a sequence of steady states. Accordingly, water distribution managers monitor pressures and discharges with a sample rate that rarely reaches 1 sample per minute, a duration corresponding to up to 60 km travelled by a pressure wave. One of the consequences of this practice is that the effects of transients in WDS are often neglected. On the contrary, measurements at a high frequency of pressures in water distribution systems, with data acquired at more than 100 Hz, revealed that the assumption of steady-state conditions is wrong. For example, Ferrante et al. (2022), by synchronous 1 kHz pressure measurements at three measurement sections in the water distribution network of Milan, Italy, have shown that noticeable pressure variations can be explained by waves traveling in the systems. Consequently, transients can affect the integrity of the pipes and increase the number of failures in WDS, at least due to fatigue, especially for specific combinations of amplitudes and frequency of the pressure variation components.

Two main issues arise to explain the measured pressure variations: the causes that originate the pressure waves and the modifications introduced by the propagation in the network, i.e., the stimulus and the response of the system. Both aspects are also relevant to determining the risk related to transient effects and defining possible remedies to reduce it.

The main objective of this study is to present field and laboratory evidence of the causes and effects of transients in water distribution systems as a preliminary step toward risk assessment.

Materials and methods

Two sets of data are considered and used. The field data were acquired during tests in the WDS of Milan. As shown in (Ferrante, 2022), the WDS, managed by Metropolitana Milanese s.p.a. (MM), supplies 220 million cubic meters of water annually to about 50,000 connections, which often represent an aggregation of individual demands. The WDS is made of steel and cast-iron pipes for a total length of about 2280 km. About 28 pumping systems supply water and control the pressure in the interconnected system.

Pressure variations were measured during normal functioning conditions and transient tests induced by valve manoeuvres. Three acquisition systems were used and synchronized by GPS.

A laboratory setup has been used to simulate the effects of the demand variation in a system with a simple topology, controlling valve openings and closures at different locations and measuring pressures at several sections. The experimental set-up consisted of two DN 110 polymeric pipes, i.e., an upstream Oriented Polyvinyl Chloride (PVC-O) and a downstream High-Density Polyethylene (HDPE) pipe. The PVC-O upstream pipe, with an internal diameter of 103.0 mm and a wall thickness of 2.7 mm, had a total length of 99.18 m. The HDPE downstream pipe, with an internal diameter of 96.8 mm and a wall thickness of 6.6 mm, had a total length of 92.79 m. The setup, the instruments, and the acquisition system are also described in (Ferrante, 2021).

Results

The field data acquired during tests in Milan are analyzed to point out the amplitudes and frequencies of the most relevant component of the pressure variations. The presence of pressure waves traveling between measurement sections is pointed out, and the relevance of their effects on the systems they are

propagating in is explored.

The laboratory data are used to investigate how demand variations and system characteristics can give rise to pressure oscillations with different amplitudes and frequencies. During tests, valves are opened and closed, simulating the variation of the demands, and the pressure is acquired at several measurement sections. Compared to the field, laboratory tests can help reveal the effects of the parameters that govern the transformation of demands in pressure variations.

Conclusions

The normal management approach to water distribution systems, considering functioning conditions as a steady-state sequence on extended periods, can be useful in reducing symptoms such as leakage. Field data show that a complete risk assessment must also consider causes of failures, such as transients. This implies that measurement frequency and numerical modeling must also consider unsteady-state conditions.

Laboratory data show that impulsive discharge variations, such as those caused by user demands, can be transformed into pressure variations with different amplitudes and frequencies along the simple pipe system.

The shown results can be considered a first and necessary step toward elaborating more complex models for assessing risk related to transients.

References

Ferrante M (2021) Transients in a series of two polymeric pipes of different materials [Article]. Journal of Hydraulic Research 59(5): 810-819. https://doi.org/10.1080/00221686.2020.1844811

Ferrante M (2022) The Use of Hydrants for Transient Test-Based Diagnosis of the Water Distribution Systems of Milan, Italy. Journal of Pipeline Systems Engineering and Practice 13(3). https://doi.org/10.1061/(asce)ps.1949-1204.0000655

Ferrante M, Bartocci D, Busti B, Fracchia S, Gentile MT, Marelli F, Vidiri M (2022) Diagnosis of Water Distribution Systems through Transient Tests: The Pilot Study of Milan. Journal of Water Resources Planning and Management, 148(6). https://doi.org/10.1061/(asce)wr.1943-5452.0001565

12th World Congress on Water Resources and Environment (EWRA 2023)
"Managing Water-Energy-Land-Food under Climatic, Environmental and Social Instability"
Thessaloniki, Greece, 27 June - 1 July 2023

An investigation by laboratory experiments of the impact of intermittent water supply

M. Ferrante[1*], D. Rogers[2], J. Mugabi[3], F. Casinini[1]
[1] Department of Civil and Environmental Engineering, University of Perugia, Perugia, Italy
[2] DEWI s.r.l., Perugia, Italy
[3] World Bank, Nairobi, Kenya
* e-mail: marco.ferrante@unipg.it

Introduction

The interruption of supply in water distribution systems is a common occurrence, particularly in developing countries. This is due to the imbalance between water supply (production) and the demand (customer consumption and leakage) (Fan et al. 2014; Kumpel et al. 2017; Taylor 2018). Intermittent water supply (IWS) has many undesirable consequences, including water quality, supply equity, and the structural integrity of the pipes (Agathokleous and Christodoulou 2016; Gullotta et al. 2021; Kumpel and Nelson 2013; Simukonda et al. 2022). Furthermore, IWS increases leakage and reduces water meter reliability and accuracy. Transitioning from IWS to continuous water supply by eliminating leaks is traditionally considered the solution. However, in many cases, it is neither cost-effective nor practical, particularly in utilities with a large, unserved customer base and a rapidly growing population. For this reason, it is likely that interrupting the supply, however undesirable, is something that, at least in the short, has to be accepted. It follows, therefore, that remedies for reducing the impacts of IWS are needed to preserve water distribution systems. This paper presents the studies undertaken to understand in detail the impacts and solutions.

Water distribution systems are not generally designed for IWS and require safeguarding interventions. The management of system filling and emptying requires attention to the alternating flows of the two phases, air and water, governing inputs and outputs. Air release valves can be used for this aim.

Evaluating the impact of IWS on water distribution systems is a complex task. Laboratory tests in controlled conditions with virtually no constraints on the instrument and device location allow the analysis of the effects of single parameter variations on pressures and flows. Within the framework of a research consultancy commissioned by the World Bank, the test network at the Water Engineering Laboratory of the University of Perugia, Italy, was modified to assess pipe filling and emptying phenomena. Preliminary results of the experimental activity are shown in (Ferrante et al. 2022a,b). The effects of air valve locations and dimensions to reduce the effects of filling and emptying are considered here.

Materials and methods

The experimental set-up consisted in a series of two DN110 polymeric pipes, comprising an upstream polyvinyl chloride pipe and a downstream high-density polyethylene pipe, with a total length of 194 m. The system was fed directly by the pumping system.

Different pressure transducers were used during the tests, including GE UNIK 5000 pressure sensors with different full scale, f.s., and accuracy of 0.10% f.s. Air release valves were connected at different locations with the aim of discharging air during the pipe filling and enabling the air ingress during the emptying. An ISOIL electromagnetic flow meter was used to measure the discharge in steady-state conditions, having an accuracy of 0.2% of the measured value.

At the downstream end, valves with different dimensions were used. A water meter was also connected, simulating the user connection.

Several tests were undertaken on varying air release valve dimensions and locations, and downstream valve sizes. Water meter measurements during air and water flow were also acquired.

Tests started with an empty system, and the pipe filled by switching on the upstream pump. After filling the pipe, the steady-state conditions were reached and maintained for a few minutes. Then, the pump was

switched off to begin the pipe emptying, and the drains opened a few minutes later to allow the complete emptying of the pipes before beginning a new test.

Results and concluding remarks

The test identified three main phases: pipe filling before the waterfront arrival at the downstream valve, pressure increase and oscillation typical of water hammer phenomena after the arrival, and pipe emptying with low and even negative pressures. Severe overpressures were measured during the water hammer phase.

Unexpectedly, the rapid expulsion of the air using large air valves is not the answer to limit the overpressures. Instead, it is necessary to use a combination of slow-opening valves (or pumps) coupled to specifically designed air valves. It was clear too, that although air release valves can effectively reduce the impacts of IWS, traditional air valve design is not ideal, as they can in some cases increase overpressures instead of limiting them.

Simulations with numerical models coupled with laboratory measurements can be of great help in the design of the optimum mitigating solutions.

Customer water meters tended to over-read during the discharging of the air and suffered reliability issues as a result of the excessive velocities the meter was subjected to in dry conditions

References

Agathokleous A, Christodoulou S (2016) Vulnerability of Urban Water Distribution Networks under Intermittent Water Supply Operations. Water Resources Management 30(13): 4731-4750. https://doi.org/10.1007/s11269-016-1450-3

Fan L, Liu G, Wang F, Ritsema CJ, Geissen V (2014) Domestic Water Consumption under Intermittent and Continuous Modes of Water Supply. Water Resources Management 28(3): 853-865. https://doi.org/10.1007/s11269-014-0520-7

Ferrante M, Rogers D, Casinini F, Mugabi J (2022a) A Laboratory Set-Up for the Analysis of Intermittent Water Supply: First Results. Water 14(6): 936. https://doi.org/10.3390/w14060936

Ferrante M, Rogers D, Mugabi J, Casinini F (2022b) Impact of intermittent supply on water meter accuracy. Journal of Water Supply: Research and Technology-Aqua 71(11): 1241–1250. https://doi.org/10.2166/aqua.2022.091

Gullotta A, Campisano A, Creaco E, Modica C (2021) A Simplified Methodology for Optimal Location and Setting of Valves to Improve Equity in Intermittent Water Distribution Systems. Water Resources Management 35(13): 4477-4494. https://doi.org/10.1007/s11269-021-02962-9

Kumpel E, Nelson KL (2013) Comparing microbial water quality in an intermittent and continuous piped water supply. Water Res 47(14): 5176-5188. https://doi.org/10.1016/j.watres.2013.05.058

Kumpel E, Woelfle-Erskine C, Ray I, Nelson KL (2017) Measuring household consumption and waste in unmetered, intermittent piped water systems. Water Resources Research 53(1): 302-315. https://doi.org/10.1002/2016wr019702

Simukonda K, Farmani R, Butler D (2022) Development of scenarios for evaluating conversion from intermittent to continuous water supply strategies' sustainability implications. Urban Water Journal 19(4): 410-421. https://doi.org/10.1080/1573062x.2021.2024582

Taylor DDJ (2018) Tools for Managing Intermittent Water Supplies. PhD thesis, Massachusetts Institute of Technology, USA

A WebGIS-based decision support system for leakage control and water quality monitoring in the water supply system of Paramythia city in Greece

K. Panitsidis[1], S. Tsitsifli[1], N. Mantas[1], D. Theodorou[1], T. Kyriakidis[1], M. Louta[1*], A. Chasiotis[2]
[1] Department of Electrical and Computer Engineering - Telecommunication Networks and Advanced Services (TELNAS) Laboratory, University of Western Macedonia, Kozani, Greece
[2] Laboratory of Climatology and Atmospheric Environment, Faculty of Geology and Geoenvironment, National and Kapodistrian University of Athens, University Campus 15784, Zografou, Athens, Greece
* e-mail: louta@uowm.gr

Introduction

Globally, water leakage in drinking water distribution systems is a significant issue for many cities and a major concern for water utilities (Panitsidis et al. 2018). Non-Revenue Water (NRW), being the water volume not bringing revenues to the water utility (including water losses), threatens the financial viability of water utilities and the sustainable management of the natural water resources (Karamage et al. 2016). The average daily volume of NRW is estimated to 346 million m^3, and its annual cost and value are 39 billion USD (Liemberger and Wyatt 2019). As a result of the growing water demand and the effects of climate change, the preservation of water supply is already under stress, making the issue more urgent. Mediterranean countries are particularly vulnerable to water shortage. In some circumstances, in these countries NRW levels exceed 50% of water volumes entering the distribution system (Tsitsifli et al. 2017).

This work describes the development of a smart green decision support system (DSS) for leakage control and water quality monitoring in the water supply system of Paramythia city in Greece. The overall aim is to design and develop an effective tool (serving also as an early warning system) in the framework of a decision support process for leakage detection and optimal management of water supply system parameters in an automated manner.

Materials and methods

The first steps towards the final goal, as presented in this paper, are the development of the back-end solution of the decision support system (DSS) and its validation through simulation scenarios. The DSS architecture (Figure 1a) is comprised of four main subsystems: *language system*, *presentation system*, *knowledge system*, and *problem-processing system*. The development process of the DSS is decoupled into the front-end subsystem and the modelling framework in the back-end. Four subsystems comprise the proposed back-end architecture solution of the DSS, implemented to improve the decision-making usability: a) DSS Logic; b) Data Access Layer; c) Security/Authorizations Layer; and d) API Gateway. *DSS logic* includes all the tasks related to the basic workflow for managing the parameters of the water supply network, such as calculations of evaluation indicators and deviations, leak detection, what-if scenarios, etc. Specifically, data (i.e., water flow, pressure, temperature, pH, turbidity, residual chlorine, conductivity, and nitrates) from the IoT subsystem (comprising 3 local telemetry stations) is integrated with data retrieved from the water distribution network hydraulic simulation model, and from the virtual sensors' subsystem concerning water qualitative parameters. The data is compared and known performance indicators (such as the IWA ones) are calculated. Their values are used to calculate deviations between the current operational conditions and the normal ones (e.g., leakage free). When deviations exceed the threshold values set, which are based on historical data, various scenarios are set in place, feeding the hydraulic simulation model, subsequently providing their results (parameters' values) to the system. Indicators are then estimated and compared to the thresholds. Finally, the leakage is detected, and its wider area can be determined. To locate the exact location of the water leakage, the water utility should use leakage detection tools, such as correlators, acoustic devices, etc. *Data Access Layer* includes all the required communication functions with the database and *Security / Authorization Layer* secures identity and access

management process. Finally, all the required interactions with third-party systems (IoT subsystem, hydraulic simulation model and virtual sensors subsystem) are implemented in the *API Gateway*.

Results and concluding remarks

The implementation of this effort is based on System Development Life Cycle (SDLC) principles (Blanchard and Fabrycky 2006). The back-end is currently under development using ASP Net language (C#) and MySQL as relational database management system, while for the front-end, HTML, CSS, JavaScript and PHP language are exploited.

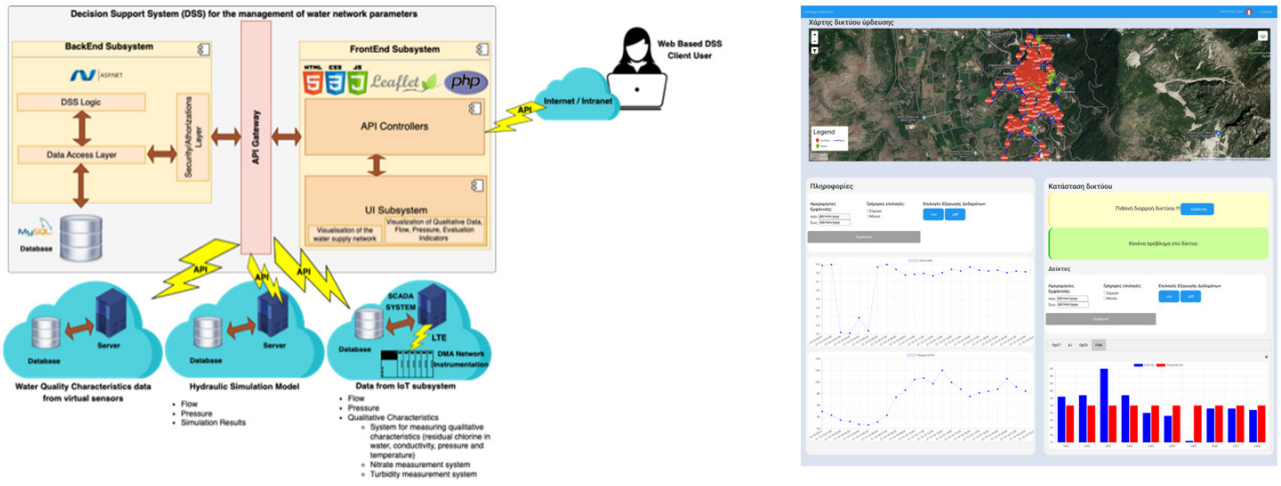

(a) ***(b)***

Figure 1. a) DSS architecture; b) DSS front-end screen.

A prototype application integrating the DSS structural components with an open-source Web-based Geographical Information Systems (Web GIS) tool and other open-source components and libraries is being built. It provides a visualization of the water distribution network using an interactive map where relevant information is displayed, such as, statistical values of water quantitative and qualitative parameters and real-time alarm events in case of leakage detection or exceedance of water quality parameters' thresholds (Figure 1b). The ability to examine different scenarios based on the conditions in real-time enables the decision-makers and operators to respond to promptly and efficiently to potential threats to the water supply system. The prototype application is currently being built and will be operational in the next 10 months. The prototype is custom-made for the water distribution network of Paramythia.

Acknowledgments: This work is co-financed by EEA Grants 2014 – 2021 and Greek Public Investments Program.

References

Blanchard BS, Fabrycky WJ (2006) Systems Engineering and Analysis, International Series in Systems Engineering. In Prentice-Hall International Series in Industrial and Systems Engineering.

Karamage F, Zhang C, Ndayisaba F, Nahayo L, Kayiranga A, Omifolaji JK, Shao H, Umuhoza A, Nsengiyumva JB, Liu T (2016) The Need for Awareness of Drinking Water Loss Reduction for Sustainable Water Resource Management in Rwanda. Journal of Geoscience and Environment Protection 4(10): 74-87. https://doi.org/10.4236/gep.2016.410005

Liemberger R, Wyatt A (2019) Quantifying the global non-revenue water problem. Water Science and Technology: Water Supply 19(3): 831–837. https://doi.org/10.2166/ws.2018.129

Panitsidis KG, Kokkinakis AK, Andreopoulou ZS (2018) Inland water fish management (iFM): A decision support system (DSS) for the management of inland water ecosystems. Journal of Environmental Protection and Ecology 19(3): 1270-1279

Tsitsifli S, Kanakoudis V, Kouziakis C, Demetriou G, Lappos S (2017) Reducing non-revenue water in urban water distribution networks using DSS tools. Water Utility Journal 16: 25-37

A new approach to find the economic pipe diameters in a pressurized irrigation network

A. Gravani, N. Samarinas*, C. Evangelides, A. Loukas
Department of Rural and Surveying Engineering, Aristotle University of Thessaloniki, 54124 Thessaloniki, Greece
** e-mail: smnikiforos@topo.auth.gr*

Introduction

Undoubtedly, to find the combination of the optimal pipe diameter, could reduce the overall required investment for a new irrigation network, acting as money saver, without affecting the overall network performance (Ma et al. 2019). The scientific community has given a lot of attention in this field starting with works related on the irrigation network design (Wang and Dal 2017), discharge estimation (Monserrat et al. 2021), as well as cost minimization through the use of Economic Series Method (Pauta et al. 2022), Genetic Algorithms (Pang et al. 2022), linear programming (Theocharis et al. 2010) and Jaya method (Gajghate and Mirajkar 2021).

Inspired of the above, the aim of this paper is the cost minimization of a collective irrigation sprinkler network by choosing the optimal combination of the pipe diameters. A new innovative approach is introduced, so called Combinational method, to find the economic pipe diameters, based on some already existing cost minimization methods, allowing the pipe splitting and strictly respecting the rules governing the pressurized pipelines (speed, losses, ect.) The results of the proposed Combinational method are compared with the corresponding results of the well-known Analytical method (Tzimopoulos 1982; Theocharis 2004), achieving remarkable outcomes. A practical application of both aforementioned methods was carried out on the existing open irrigation network of Limnochori, located in Northern Greece, which in this work was studied as a model pressurized irrigation network (Evangelides 2017). The findings of this work proved to be high reliable and are recommended to be used for both research applications and irrigation network construction purposes as well.

Materials and methods

In the existing Analytical continuous method (Tzimopoulos 1982) of network cost minimization, a system of nonlinear algebraic equations is solved by iterative methods, making use of the Lagrange multipliers. With the application of the Analytical method, it follows that for each pipeline of the network i, of a certain length L_i, an appropriate economic trade diameter $D_{itra.}$ is chosen, aiming at the minimum network cost.

The new proposed Combinational method is based on the extracted results of the above method and states that in the same pipeline i, two pipes of different diameters can be placed in a specific section of the pipeline, each one, with the aim of covering the allowable theoretical losses and, by extension, the further minimization of network cost.

The diameters of the pipes, to be placed in order, are: i) the already selected economic trade diameter $D_{itra.}$ of the Analytical method, ii) the immediately preceding smallest one $D_{(i-1)tra.}$, based on a selected trade table PN and will be applied respectively to suitable lengths L_{i1} and L_{i2} of the total length L_i of pipeline i, with the constraints that:

- the flow speeds, $V_{itra.}$ and $V_{(i-1)tra.}$, will vary between the values of 0.5-2 m/s and
- the sum of the real losses incurred, $Dh_{itra.} + Dh_{(i-1)tra.}$, has to be equal to the theoretical losses, Dh_i, calculated during the application of the existing Analytical method.

Considering the succession of pipe diameters from the largest to the smallest one, it should be noted that the diameter $D_{(i-1)tra.}$ selected as the second in line to be placed in a section of pipe i, should be strictly larger than the diameter of the next pipe i+1.

All the hydraulic calculations of this work were performed by the Excel add-in Solver tool.

Results and concluding remarks

Table 1 summarizes the pipelines costs of the network's main section, with the application of the Analytical and the proposed Combinational method respectively. As an example, for pipe G the initial D=302.80mm with L=303.15m calculated with Analytical method, corresponds to D=302.80mm for L=122.30m and for the rest L=180.85m of the pipe could be used D=268.60mm. It is observed that in all cases, in which the Combinational method can be applied, the costs of the pipelines show significant reduction. For the main section of the network this reduction corresponds to 6.41%, translated to 15355€.

Table 1. Main section pipelines costs by choosing appropriate trade diameters.

Main Section	**Analytical Method**			**Combinational Method**					**Reduction**	
Pipeline	Di(mm)	Li(m)	Pi(€)	Di(mm)		Li(m)		Pi(€)	Ri(€)	Ri(%)
A	426.40	357.89	73045		426.40		357.89	73045		
B	426.40	6.16	1257		426.40		6.16	1257		
C	383.80	314.48	54037	383.80	341.20	41.90	272.58	45841		
D	341.20	127.14	18023		341.20		127.14	18023		
E	341.20	188.90	26778	341.20	302.80	85.12	103.78	24169		
F	302.80	15.32	1787		302.80		15.32	1787		
G	302.80	303.15	35353	302.80	268.60	122.3	180.85	31601		
H	238.80	302.31	23913	238.80	213.20	258.1	44.19	23321		
I	170.60	118.42	5405	170.60	153.40	90.28	28.14	5200		
Total			239599					224244	15355	6.41%

Calculations were made with same approach for the remaining network branches, and it emerged that with the application of the Combinational method the total cost of the network was reduced by 4.87% (34237 €). This difference, considering that the studied network belongs to the medium-small size networks, is remarkable.

In conclusion, in the process of finding the economic diameters in the pipelines of a network, the application of the Combinational method, could be considered particularly remarkable and effective compared to the Analytical continuous method. Extension of this work could be the comparison of this new method with other advanced methods such as Linear or Dynamic programming.

References

Evangelides C (2017) Investigation of the replacement of the open irrigation Network of Limnochori. Research work. AUTh, Thessaloniki (in Greek)

Gajghate P, Mirajkar A. (2021) Irrigation pipe distribution network optimization with Jaya Algorithm: a hybrid approach. Water Supply 21(7): 3570-3583

Ma PH, Hu YJ, Liu HS, Li YN (2019) Simultaneous optimization of micro-irrigation subunit layout and pipe diameter and analysis of influencing factors. J. Hydraul. Eng. 50: 1350–1373

Monserrat J, Naghaee R, Cots L, Monem MJ, (2021) Application of Clément's First Formula to an Arranged-Schedule Secondary Canal. Journal of Irrigation and Drainage Engineering 147(2): 1-7

Pang Y, Li H, Tang P, Chen C (2022) Synchronization Optimization of Pipe Diameter and Operation Frequency in a Pressurized Irrigation Network Based on the Genetic Algorithm. Agriculture 12(5): 673

Pauta C, López-Armijos M, Martinez-Solano F, Aliod-Sebastián R (2022) Design Comparison between the Economic Series Method and the Heuristic Method in a Pressurized Irrigation Network. Chem. Proc. 10(1): 64

Theocharis M (2004) Irrigation networks optimization. Economic diameters selection. PhD thesis, Dep. of Rural and Surveying Engin. A.U.TH., Salonika (in Greek, with extended summary in English)

Theocharis ME, Tzimopoulos CD, Sakellariou-Makrantonaki MA, Yannopoulos SI, Meletiou IK (2010) Comparative calculation of irrigation networks using Labye's method, the linear programming method and a simplified no linear method. Elsevier 51(3-4): 286-299

Tzimopoulos C (1982) Agricultural Hydraulics, vol. II, Thessaloniki (in Greek)

Wang K, Dal M (2017) Optimization and Modelling of Pressurized Irrigation Networks. Turkish Journal of Water Science and Management 1(2): 62-80

12th World Congress on Water Resources and Environment (EWRA 2023)
"Managing Water-Energy-Land-Food under Climatic, Environmental and Social Instability"
Thessaloniki, Greece, 27 June - 1 July 2023

Multi-objective robust optimization design of water distribution networks under 'scenario uncertainty' of demand

R. Magini[1], M.C. Cunha[2*], J. Marques[2], E. Ridolfi[1]
[1] Sapienza, University of Rome, DICEA, Rome, Italy
[2] University of Coimbra, CEMMPRE, Department of Civil Engineering, Coimbra, Portugal
* e-mail: mccunha@dec.uc.pt

Introduction

Residential water demand, which represents about 70% of total consumption is affected by large uncertainty mainly due to the "behavioral variability" of users which manifests itself on a daily and seasonal scale and remains valid in both todays and future scenarios (Walker et al. 2003). But, in dealing with future time horizons, we must also consider the uncertainty related to "social variability" which is due to the unpredictable nature of social, economic, and cultural dynamics. Thus, it is rather difficult to predict and model future water uses.

Behavioral uncertainty is classified as 'statistical uncertainty' and this represents just one level of knowledge above determinism (Walker et al. 2003). It can be described in statistical terms exploiting information from available data. A higher level of uncertainty is 'scenario uncertainty' (Walker et al. 2003), which is related to 'social variability' and whereby scenarios represent possible states of reality, i.e., likely assumptions about the future. Regarding water demand, hypotheses can concern the number of users, socio-economic situation, changes in technology, tariffs, and users' behavior. Scenarios do not describe 'what the future will be like' but rather 'what it could be like'.

Mulvey et al. (1995) introduced two basic concepts for Robust Optimization (RO) formulation. The first one is related to the idea of solution robustness with a term for modeling the uncertainty of the objective function, which drives the solution to be 'close' to the optimum for each scenario. The second concept relates to solutions 'almost' feasible for each of the scenarios and it is expressed with a term representing model robustness used to penalize violation of constraints, to model the uncertainty of the feasibility of the solution. Therefore, deriving a suitable 'set of uncertainty', i.e. a set of scenarios and their probabilities is a critical passage in developing a robust optimization model.

Materials and methods

This paper presents a new methodology for considering 'scenario uncertainty' in facing a multi-objective RO problem for the design of a Water Distribution Network (WDN). Future behavioural uncertainty of water users is addressed in statistical terms making likely assumptions about statistical parameters. Specifically, the water demand scaling laws proposed by Magini et al. (2008) are used. Plausible hypotheses on future demand changes in specific nodes of the WDN concern users' typology and the number of users in each node of the WDN, which can be proposed, for example, by a panel of experts assuming possible urban, economic, and social developments. To determine the most robust design solutions, changes in future demand are considered in critical nodes of the WDN, i.e., where these changes can produce the most relevant hydraulic effects. A new approach for selecting these nodes is employed which involves the transinformation index derived from the entropy theory (Krstanovic and Singh 1991). This parameter defines the amount of information that is redundant in two or more Random Variables (RVs), in this case, the nodes of the network. In the multivariate case, this index represents a measure of the redundancy of the information provided by the nodes, when the m-th node is added to the others. This selection method is easy to use and does not imply any *a priori* assumption for the data. The bottom-up procedure proposed by Magini et al. (2019) is employed to generate snapshots and estimate their probabilities while keeping the statistical information on nodal demand. The snapshots reduced in this way with their probability represent the scenarios that embody the demand spectrum of variation in the RO model, maintaining a level of computational tractability.

A two-objective RO model is solved in which WDN's pipes cost is minimized and the Generalized

Resilience and Failure index (GRF by Creaco et al. 2016) mean-variance is maximized. The mean-var GRF objective is obtained for all demand scenarios under analysis and their probability and tends to address risk averse behaviour by reducing the chance of solutions that are particularly weak in some scenarios to be selected.

Results and concluding remarks

The proposed methodology is applied to the benchmark network Fossolo (Bragalli et al. 2019). It is assumed that all users belong to the residential typology. The parameters of the scaling laws, describing today's demand, derive from the dataset analyzed by Magini et al. (2008). Three nodes of WDN are selected for changing their water demand in future scenarios. At this aim, using 10000 snapshots of nodal pressures, derived with a pressure-driven model from corresponding nodal demands, the transinformation index is computed by adding each node to all the others (m^{-1}), where m is the total number of nodes, to evaluate the one that provides the maximum transinformation value. Nodes 5, 28, and 30 are selected. These nodes are the most redundant with all the others, meaning that they influence the most the behavior of the network and show the highest variability in pressure values. To assess future scenarios and their effect on the network design, in these selected nodes water demand is modified, changing the number and type of users. The RO problem is solved for 9 future demand scenarios. Then 3 Pareto front solutions are selected (Figure 1) and compared with similar cost (CT) solutions obtained using a deterministic approach. These pairs of solutions are loaded with the same hydraulic demand conditions given by 9 future demand scenarios plus the base demand condition. The results attest to the advantages of robust design producing lower Sum of Pressure Deficits (PD) and Undelivered Demands (UD) values than a deterministic design for the same level of investment, considering all the 10 demand conditions and all network nodes. It is clear that scenario uncertainty embedded into robust optimization models leads to more sustainable infrastructures. This paper represents a significant step towards more informed decision-making processes. The trade-off between different objectives, as investments and social aspects related to unmet demands, will contribute to evaluate people's willingness to fund more durable solutions.

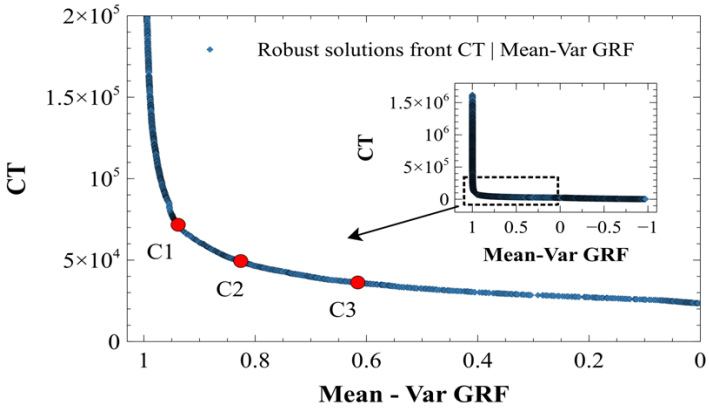

Three pairs of solutions

	CT (€)	Sum PD (m)	Sum UD (l/s)
C1 Robust	70 022	0	0
C1 Deterministic	70 028	119	9.9
C2 Robust	50 124	16	0.2
C2 Deterministic	50 124	394	34.4
C3 Robust	30 017	484	6.6
C3 Deterministic	30 023	926	88.3

Figure 1. Comparison of three pairs of robust and deterministic solutions with similar costs.

References

Bragalli C, D'Ambrosio C, Lee J, Lodi A, Toth P (2015) Optimizing the Design of Water Distribution Networks Using Mathematical Optimization. In: Murty K (eds) Case Studies in Operations Research. International Series in Operations Research & Management Science, 212, Springer, New York, NY

Creaco E, Franchini M, Todini E (2016) Generalized Resilience and Failure Indices for Use with Pressure-Driven Modeling and Leakage. J Water Resour Plann Manage 142(8): 872, 04016019.

Krstanovic PF, Singh VP (1991) A univariate model for long-term streamflow forecasting - 1. Development. Stoch Hydrol Hydraul 5(3): 173–188

Magini R, Boniforti MA, Guercio R (2019) Generating scenarios of cross-correlated demands for modelling water distribution networks. Water 11(3): 493

Magini R, Pallavicini I, Guercio R (2008) Spatial and Temporal Scaling Properties of Water Demand. J Water Resour Plan Manag 134(5): 276–284

Mulvey JM, Vanderbei RJ, Zenios S (1995) Robust Optimization of Large-Scale Systems. Oper Res 43(2): 264-281

Walker WE, Harremoes P, Rotmans J, van der Sluijs JP et al. (2003) Defining uncertainty: a conceptual basis for uncertainty management in model-based decision support. Integr Assess 4(1): 5e17

12th World Congress on Water Resources and Environment (EWRA 2023)
"Managing Water-Energy-Land-Food under Climatic, Environmental and Social Instability"
Thessaloniki, Greece, 27 June - 1 July 2023

Investigating vulnerability of urban drainage networks using novel network theory centrality metrics

N. Akbari, B. Omidvar*
Department of Environmental Engineering, School of Environment, College of Engineering, University of Tehran, Tehran, Iran
** e-mail: bomidvar@ut.ac.ir*

Introduction

Urban Drainage Networks (UDNs) are one of the crucial parts of the urban infrastructures that protects health and safety of the people by collecting and transferring sanitary sewage and stormwater runoff. In spite of considerable improvements in design and maintenance of UDNs, there exist several functional and structural problems such as climate change, urbanization, aging infrastructures, and so on that can influence UDNs' performance drastically. Therefore, vulnerability assessment of UDNs is of great importance. Numerous methodologies on evaluating vulnerability of UDNs has been proposed (Mugume et al. 2015). However, most of these studies need a huge amount of data and extensive numerical analysis to define hydraulic models to simulate the process. Unlike previous works, in this study we use network theory tools to analysis vulnerability of UDNs, which may be served as a complementary to hydraulic modelling approaches.

Network theory is expressed via a branch of mathematics called graph theory. It has been applied in a various subjects varying from modelling spread of diseases and social networks to electrical and transportation networks. Recently several authors began to use network theory tools in UDNs analysis. Metrics such as degree centrality, betweenness centrality, harmonic centrality has been utilized in their studied (Dastgir et al. 2023; Reyes-Silva et al. 2020; Simone et al. 2022). Unlike these studies we use eigenvector centrality and page rank centrality metrics to identify most critical nodes in UDNs.

Materials and methods

A graph is represented by $G = (V, E)$ where V denotes a set of nodes, i.e., $V = \{1, \dots, n\}$ and E represents a set of edges constructed by a pair of nodes. First a UDN should be projected onto a graph where the edges of the graph correspond to pipe sections and nodes are junctions between pipes which usually represented by manholes. Then we use eigenvector centrality and page rank centrality to identify the most vulnerable nodes in the network. Moreover, we propose a modified eigenvector centrality and page rank centrality measure which uses Horton's ranking law to obtain weights which are used to modify the original centrality definitions. For a graph with adjacency matrix of A, eigenvector centrality is defined as $C_E = \frac{1}{\lambda_{max}} Ax$, where λ_{max} is the largest eigenvalue of A, and x is its associated eigenvector. In addition, page rank centrality is defined as $C_P = D(D - \alpha A)^{-1}1$ with D being a diagonal matrix having degree of each ith node at D_{ii} element, $\alpha = 0.85$ and 1 is all-one vector, i.e., all elements of it is equal to 1. In modified eigenvector centrality, vector x is replaced with $x \circ w$, where w is relevant weights which here is obtained using Horton's law for the graph and $(\circ)$ is the element-wise multiplication operator. So modified eigenvector centrality is defined as $C_{EM} = \frac{1}{\lambda_{max}} A\, x \circ w$. In the same manner modified page rank centrality is defined as $C_{PM} = D(D - \alpha A)^{-1} w$. All the concepts and mathematical equations about graph theory and network theory can be found in (Newman 2010).

Results and concluding remarks

Consider a simple UDN shown in Figure 1. This graph has 9 nodes and 8 edges. We applied degree, eigenvector, page rank, modified eigenvector and modified page rank centralities to the graph of Figure 1.

Results are presented in Table 1. According to the degree centrality, nodes 5, 6 and 3 are most important nodes. Based on eigenvector centrality, node 5 is the most crucial node and nodes 6 and 3 are the next. Also when the modified eigenvector centrality is applied, the node 9 which is the outlet of the UDN, has more importance than other nodes with degree 1 (nodes 1, 2, 7 and 8) and even it is more critical than node 3. Similar pattern appears while applying modified page rank centrality.

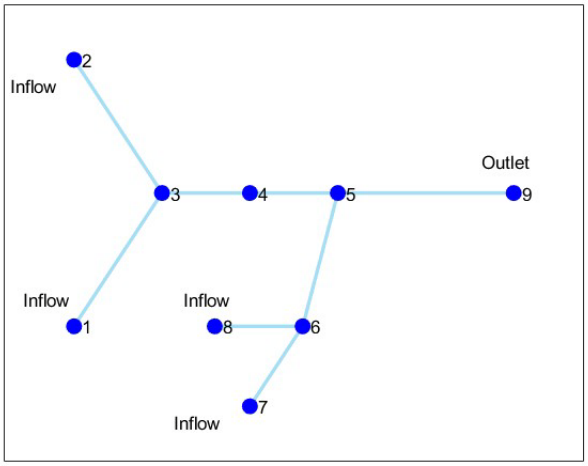

Figure 1. A UDN graph which is composed of 9 nodes and 8 edges.

As future works, we apply the presented schemes on real world UDNs along with hydraulic simulation to verify its efficacy considering flow risk and resilience. Furthermore, we incorporate hydraulic parameters in the UDN graph to assess the functional aspects of UDNS as well as their structural attributes.

Table 1. Results of different centrality metrics on graph of Figure 1.

Node number	Degree	Eigenvector (C_E)	Page rank (C_P)	Modified Eigenvector (C_{EM})	Modified Page rank (C_{PM})
1	1	0.36	4.13	0.36	6.12
2	1	0.36	4.13	0.36	6.12
3	3	0.76	11.02	1.51	18.06
4	2	0.89	7.10	1.78	13.32
5	3	1.12	10.50	3.37	21.90
6	3	0.96	10.95	1.91	19.11
7	1	0.45	4.10	0.45	6.41
8	1	0.45	4.10	0.45	6.41
9	1	0.53	3.97	1.59	9.21

References

Dastgir A, Hesarkazzazi S, Oberascher M, Hajibabaei M, Sitzenfrei R (2023) Graph method for critical pipe analysis of branched and looped drainage networks. Water Science and Technology 87(1): 157-173

Mugume SN, Gomez DE, Fu G, Farmani R, Butler D (2015) A global analysis approach for investigating structural resilience in urban drainage systems. Water Research 81: 15-26

Newman M (2010) Networks: an introduction. Oxford University Press

Reyes-Silva JD, Zischg J, Klinkhamer C, Rao PSC, Sitzenfrei R, Krebs P (2020) Centrality and shortest path length measures for the functional analysis of urban drainage networks. Applied Network Science 5(1): 1-14

Simone A, Cesaro A, Del Giudice G, Di Cristo C, Fecarotta O (2022) Potentialities of complex network theory tools for urban drainage networks analysis. Water Resources Research 58(8): e2022WR032277

An analysis of quality parameters changes in agricultural water systems with Wavelet Transform Model

O. Deniz[1], Y. Ahi[2*], Z. Aslan[3], A.H. Orta[4], F. Dökmen[5]
[1] Directorate of Climate Change and Zero Waste, Çorlu Municipality, Tekirdag, Turkey
[2] Water Management Institute, Ankara University, Ankara, Turkey
[3] Department of Computer, Faculty of Engineering, Istanbul Aydın University, Istanbul, Turkey
[4] Department of Biosystems, Faculty of Agriculture, University of Tekirdağ Namık Kemal, Tekirdag, Turkey
[5] Vocational School of Food & Agricultural, University of Kocaeli, Kocaeli, Turkey
* e-mail: ysmahi@ankara.edu.tr

Introduction

Continuous environmental impact assessment is essential for agricultural water management and for ensuring a healthy food supply. There is a growing need for big data techniques that integrate climate data, soil-water, crop quantity and quality data into a real-time model to increase the efficiency of water management systems. In this context, data science and artificial intelligence applications help to better understand agricultural management strategies and thus help stakeholders make more informed decisions. Additional benefits are also expected in other agricultural impact categories such as climate change, terrestrial acidification, toxicity related burdens, human health, terrestrial and freshwater ecosystems. Artificial intelligence models based on data science have the ability to produce output by learning the information entered into the model.

This study aims at investigating the positive/negative changes in the soil and water resources in an agricultural ırrigation area. The findings will be evaluated with one of the artificial intelligence models in terms of the effects of soil and water salinity parameters on the environment and agriculture and identify the potential risks from future irrigation projects. For this purpose, the data obtained from the soil and water in the basin were evaluated with the Wavelet Model (wavelet method). In essence of the method, both time and frequency information (in time dimension) are included in signal transmission, especially in non-stationary signals.

The model was developed by Grossman and Morlet in the 1980s (Furati et al. 2005), and modified and published by Hubbard (1996). Wavelets are mathematical functions that give a time-scale representation of time series and their relationships for analyzing non-stationary time series.

Examining the temporal patterns of hydrology and water quality contributes to understanding hydrological processes, improving hydrological modelling, monitoring water quality, and sustainability of ecosystem. Based on the results, further recommendations were developed and presented to the stakeholders.

Materials and methods

The Turkmenli Reservoir irrigation basin, which is located within the southeast of the Thrace Region of Turkey was chosen as the project area. The project site is irrigated by canals with a length of 7716 m from the right main canal, 9535 m from the left main canal and 4770 m from the auxiliary canal. The population in the irrigation area of the project is 3102 and the people are generally engaged in agriculture. Rain-fed and also irrigated farming was carried out in the field before the project, and crops such as cereals, sunflowers and watermelons are grown.

In order to evaluate the positive/negative changes in the water resources with the Wavelet model, water samples from the reservoir and the exit points of the irrigation canals and from 5 groundwater observation wells during the irrigation season of 2012 and 2013, were analysed in the laboratory. In the study, pH and salinity parameters of electrical conductivity (EC), sodium (Na^{+}), calcium (Ca^{+2}), magnesium (Mg^{+2}), chloride (cl^{-}), nitrate ($NO3^{-}$), nitrite (NO_2^{-2}) were investigated based on standard methods (Tüzüner,

1990). The wavelet method, which has the ability to analyze the changes and effects related to a certain time interval was used with the help of the Wavelet Analyzer module on the Matlab 2020Rb base.

Results and concluding remarks

In this section, Wavelet 1D, frequency, signal separation, continuous wavelet 1D, descriptive statistics, temporal changes and trend analysis of concentrations of all parameters are presented for water samples taken from 8 points. Only wavelet analysis results of EC parameter are presented in Figure 1.

When the EC values were examined, the water taken from the reservoir from which the irrigation water is supplied was class 2 (medium salty) according to the classification criteria, while the water samples taken from the right channel and left channel were class 3 (high salty) between 950 and 1375 micromhos/cm. The results obtained in the groundwater samples represent the 3rd class irrigation water. There was no significant variation between seasons in all water samples.

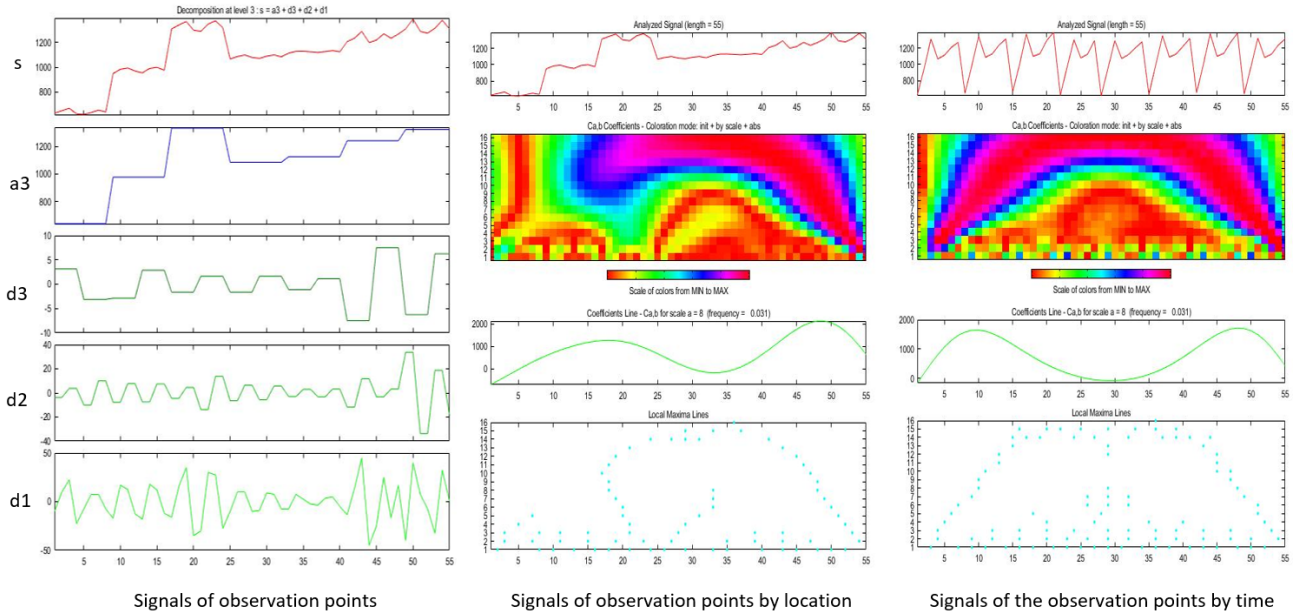

Figure 1. Analysis of salinity (EC) variation: 1D Continuous Wavelet Mexican Hat Results of EC (a; scaling (frequency) and translation (time) parameters, s; signal, d1, d2 and d3; small, medium and large scale effects, respectively).

Salinity results of the water samples show a significant decrease after the 25th value. In the irrigation area, macro and micro scale effects were observed in salinity parameters changes in water. Salinity parameters such as nitrate, nitrite, chlorine varied greatly with irrigation practices, drought and precipitation. The change in salinity over time shows continuity in small scale (Figure 1). While the 1st and 7th signal intervals in the time dimension represent the 2012 March period, the 1st and 4th signal intervals in the space dimension represent the pond. On a large scale, dry periods such as June and September salinity is high for all observation points but shows a minor deviation. If it is accepted that the major and minor events that will affect the salinity values in the study area do not change (except in extreme cases), no change is expected within a period of approximately 30 years from the time of sampling. According to Figure 1, it can be said that the sampling sites are under the influence of external and environmental factors, and this process is continuous in an average period of 10 to 20 years. It was determined that the irrigation project may pose danger to public health due to its proximity to the settlements and also as a result of fertilizers and industrial waste waters mixing with surface waters and aquifers.

References

Furati KM, Manchanda P, Ahmad MK, Siddiqi AH (2005) Trends in wavelet applications. In: Furati KM et al. (eds), Mathematical Models and Methods for Real World System, Chapman & Hall, CRC

Hubbard BB (1996) The world according to wavelets. A. K. Peters, Wellesley

Tüzüner A (1990) Soil and Water Analysis Laboratory Handbook. General Directorate of Rural Services Publications, Ankara

12th World Congress on Water Resources and Environment (EWRA 2023)
"Managing Water-Energy-Land-Food under Climatic, Environmental and Social Instability"
Thessaloniki, Greece, 27 June - 1 July 2023

Risk management of agricultural water supply and distribution systems using FDBN model and MULTIMOORA technique

A. Bozorgi[1], A. Roozbahani[2*], S.M. Hashemy Shahdany[3], R. Abbassi[1]
[1] School of Engineering, Faculty of Science and Engineering, Macquarie University, Sydney, NSW, Australia
[2] Faculty of Science and Technology, Norwegian University of Life Sciences (NMBU), Ås, Norway
[3] Faculty of Agricultural Technology, College of Agriculture and Natural Resources, University of Tehran, Tehran, Iran
* e-mail: abbas.roozbahani@nmbu.no

Introduction

Changes made to the environment by people or any shifts in climate patterns affect water volume demand in agricultural production and raise the risk of agricultural product failure. A risk assessment model is needed to improve the condition of agricultural water systems to use water resources during operation efficiently and to meet demands. In previous research, various models have been implemented to investigate the risk (Abedzadeh et al. 2020). Among them, Bayesian Networks have had effective results (Wang et al. 2022). Here, a Fuzzy Dynamic Bayesian Network (FDBN) as a superior version of BNs is used to model the risk assessment of agricultural water systems. FDBN is utilized to model causal and temporal relations between different system components and results obtained from FDBN are used to implement risk management approach.

Research on risk management in water systems has been conducted from different perspectives with different techniques (Orojloo et al. 2018; Roozbahani et al. 2012). In this study, various risk management scenarios of the Roodasht irrigation district, Esfahan, Iran, are defined. The capability of scenarios are assessed in multiple aspects of economic, social, environmental, and technical criteria. The applicable scenarios are selected with a MULTIMOORA as a multi-criteria decision making method and presented to the operators and network manager.

Materials and methods

Risk assessment is based on three main terms, which are defined due to hazards that threaten the system. These terms are the probability of hazard occurrences, systems' vulnerability against the hazard, and hazards' consequences. In this study, the Roodasht irrigation district was selected as a case study which is in Iran. This system is threatened by three hazards. These are Drought, Improper Performance of the Ditch-Riders (IPDRs) and Operational Losses (OL). The risk terms were calculated using hydraulic and hydrological indices based on the nature of the system and hazards (Bozorgi et al. 2021). The risk assessment was modelled by the FDBN method.

Risk management scenarios: In the next step, different risk management scenarios were identified by using expert opinion and historical case study research. These scenarios were classified into four types: non-structural, structural, automatic control, and integrated scenarios. Non-structural approaches improve network operation in water scarcity situations by using operational experience. The focus is to enhance the traditional way of manually or automatically adjusting water level structures. The four scenarios which were considered in this group are Scheduled water delivery (Scn.1), Operation method to reduce dewatering time (Scn.2), Inflow fluctuation prediction (Scn.3), Increasing the intake recharge and reducing the flow time in the irrigation canal (Scn.4). The Structural scenario (Scn.5) is the modernization or replacement of hydraulic structures. Integrated scenarios were made up of two structural and non-structural strategies. All necessary activities in non-structural scenarios (4 scenarios stated (Scn.6-9)) are performed in integrated scenarios, along with the required changes in catchment structures. In Automated control, the Model Predictive Control (MPC)(Scn.10) system and the decentralized automatic control system - Proportional-Integral Controller (PI) (Scn.11) are two selected scenarios in this group.

Criteria: In this step, criteria were defined to evaluate the performance of risk management scenarios.

These are the technical, economic, social, and environmental factors. The technical criterion is the potential of each scenario to reduce the system's risk. This is the difference between the average risk of the system in baseline (current situation) and the application of each scenario which was evaluated with the FDBN model. The economic criterion includes two sub-criteria: (a) the cost of implementing each scenario, (b) the agricultural benefits of modernizing the surface water distribution system. The next criterion is social, divided into two sub-criteria: (a) increased employment, which is considered by increasing the area under surface water irrigated, (b) equity of water delivery, a metric that measures the proportion of the amount delivered vs. required over time. The last one is environmental: (a) reduction of groundwater withdrawal, (b) saving energy by reducing groundwater withdrawal. These criteria were weighted through the AHP method. A questionnaire is designed and distributed among a few experts to collect their opinions. This questionnaire is made of the pairwise matrix, which is compared criteria two by two. Eventually, the best scenario(s) was selected by utilizing MULTIMOORA as a multi-criteria decision making method.

Results and concluding remarks

In this study, the risk management scenarios of the Roodasht irrigation district were evaluated according to different criteria. The best scenarios will be chosen with MULTIMOORA method. The accuracy of modelling risk assessment with the designed FDBN model is equal to 0.90. The results of applying risk management scenarios in the FDBN model show that the average risk of the system in the High category decreases by 13.36%. The decision matrix of different scenarios and criteria is illustrated in Table 1. The results show that PI and MPC as automated control scenarios are the best options, and then integrated scenarios (structural and scheduled water delivery, inflow fluctuation prediction, increasing the inlet recharge, and reducing the flow time in the irrigation canal) are the following options.

Table 1. Decision matrix.

Scn.	Tec.	Economic		Social		Environmental		Rank	Scn.	Tec.	Economic		Social		Environmental		Rank
	SubCrt:	a	b	a	b	a	b			SubCrt:	a	b	a	b	a	b	
W	0.43	0.08	0.09	0.13	0.10	0.12	0.03										
1	5.8	40.2	974.4	1832	8	7.30	3933.2	***6***	7	6.5	83.6	628.2	1181	9	4.70	2532.7	***9***
2	5.5	40.2	461.5	866	9	3.44	1851.1	***10***	8	7.9	84.6	864.1	1623	9	6.98	3759.4	***4***
3	5.6	41.1	633.3	1193	9	4.74	2554.4	***8***	9	6.1	83.7	1200.0	2257	9	9.05	4870.4	***5***
4	5.1	40.2	812.8	1528	9	6.11	3291.0	***7***	10	11.4	121.2	2869.2	5392	3	21.92	11802.7	***2***
5	4.7	43.5	297.4	561	10	2.28	1227.3	***11***	11	9.8	84.8	3092.3	5813	6	29.05	15640.1	***1***
6	6.8	83.6	1433.3	2693	8	10.76	5791.3	***3***									

The obtained results show that the top scenarios offer two categories of solutions to network managers. First is automated solution in which hydrodynamic flow simulators calculate the amount and duration of opening/closing hydraulic structures, and the motors adjust each structure. Hence, the operator's job is limited to monitoring the operation. Second, integrated solutions can be done by launching a simple telemetry system between the hydrometric station and the operation office, increasing the number of daily operations shifts and the inspection process. According to these results, decision-makers and network operators can use this model to clarify the conditions of the irrigation network when faced with various hazards that threaten the components of the system and make the best decision in risky situations.

References

Bozorgi A, Roozbahani A, Hashemy Shahdany SM, Abbassi R (2021) Development of multi-hazard risk assessment model for agricultural water supply and distribution systems using bayesian network. Water Resources Management 35(10): 3139-3159

Orojlo M, Hashemi Shahdani SM, Rouzbahani A (2017) Risk Assessment of main transmission line in Irrigation Networks with Application of Fuzzy Hierarchical method. Journal of Water and Soil Conservation 24(5): 25-47

Wang W, He X, Li Y, Shuai J (2022) Risk analysis on corrosion of submarine oil and gas pipelines based on hybrid Bayesian network. Ocean Engineering 260: 111957

Abedzadeh S, Roozbahani A, Heidari A (2020) Risk assessment of water resources development plans using fuzzy fault tree analysis. Water Resources Management 34(8): 2549-2569

Roozbahani A, Zahraie B, Tabesh M (2012) PROMETHEE with precedence order in the criteria (PPOC) as a new group decision making aid: an application in urban water supply management. Water Resources Management 26(12): 3581-3599

12th World Congress on Water Resources and Environment (EWRA 2023)
"Managing Water-Energy-Land-Food under Climatic, Environmental and Social Instability"
Thessaloniki, Greece, 27 June - 1 July 2023

Runoff prediction in a tropical agricultural watershed: A comparison between machine learning-based and conceptual hydrological models

S. Barbhuiya, M. Ramadas*, G.M. Kartick, S.S. Biswal
School of Infrastructure, Indian Institute of Technology Bhubaneswar, Khordha-752050, Odisha, India
** e-mail: meenu@iitbbs.ac.in*

Introduction

Hydrological modelling at watershed scale has numerous applications for regional water resources management. In developing countries such as India, for planning different watershed management plans and decision-making by stakeholders including farmers and engineers, water balance models have been useful. The advantage of using such models is that they simulate the complex rainfall-runoff relationships, that can be used to simulate the effects of different climatic perturbations and land use/land cover changes likely to occur at watershed-scale. The chosen model for streamflow prediction can be a distributed or lumped one, and it can be physically based, conceptual, machine learning-based or data-driven model for a particular study region, depending on the constraints posed by model complexity and data availability. In this context, owing to their simplicity and sparse data requirements, conceptual and data-driven hydrological models are relatively more popular.

Daily rainfall-runoff (RR) models and neural networks (NN)-based models have been used in numerous water balance studies (Anshuman at al. 2019; Gauch et al. 2021). In this study, we present a comparative assessment of the performance of two approaches: the conceptual Génie Rural à 4 Paramètres Journalie (GR4J) model and the data-driven long short-term memory (LSTM) network model, for hydrological modelling in a small tropical agricultural watershed in Eastern India. The present study attempts to address the following research questions: (i) What are the relative merits of a conceptual model or a state-of-the-art data-driven model for runoff prediction with fewer inputs? (ii) Can the LSTM model with a greater degree of parsimony be a better choice than the conceptual model for tropical agricultural watersheds?

Materials and methods

The study watershed lies in the Subarnarekha-Bahmani-Baitarani River Basin region in India and has its watershed outlet at Altuma, located at 20.93°N latitude and 85.52°E longitude, in Odisha State in India. The area of this tropical watershed is dominated by agricultural land use, and the agricultural activities are highly dependent on seasonal rainfall received during the monsoon months (June to September).

For this study, we used daily streamflow data recorded at the Altuma gauging site for the 1996–2016 period, available from the India Water Resources Information System (WRIS) web portal. For hydrological model development, daily climatic inputs—rainfall and maximum and minimum temperature data at 0.25° and 1° spatial resolution, available from the India Meteorological Department (IMD; Pai et al. 2014) were used. Potential evapotranspiration was then computed for the 1996–2016 period using the methodology outlined in Oudin et al. (2005).

In the GR4J model chosen in this study, only four model parameters are utilized to simulate processes of runoff modelling, groundwater flow and hydrologic routing, namely, the maximum capacity of the production store (X1, in mm), the water exchange coefficient (X2, in mm/day), the maximum capacity of the routing store (X3, in mm), and the time parameter for unit hydrographs (X4, in days). We encourage the readers to refer to Perrin et al. (2003) for details of the GR4J model. Though there are recent versions of this model with five (GR5J) and six parameters (GR6J), these could however increase the complexity of modelling when compared to the parsimonious GR4J model.

The LSTM model was used for hydrological modelling with fewer predictors such as rainfall and maximum and minimum temperatures averaged over the watershed area. The hydrological models for Altuma were calibrated and validated using the observed flow data for 1996–2007 and 2008–2015 periods,

respectively. A few years were left as a warm-up period in the GR4J model development and were not included in the model performance evaluation. The performance of the models during calibration and validation were evaluated using popular statistical measures: Nash-Sutcliffe efficiency (NSE) and correlation coefficient (R).

Results and concluding remarks

The Altuma-GR4J model parameters are: X1 = 140.88 mm, X2 = 12.54 mm/day, X3 = 196.59 mm, and X4 = 1.13 days, and were obtained by employing the Michel's (1991) algorithm for calibration. The conceptual RR model simulated runoff in the watershed reasonably well, as seen in the comparison plot in Figure 1. It could capture the monthly variability in runoff quite well and is found to be a suitable choice for hydrological modelling of watersheds with limited field data. The performance statistics for GR4J and LSTM models in terms of NSE and R are listed in Table 1. In comparison, the LSTM-based model performed less efficiently. As the tabulated results show, the parsimonious machine learning-based model is not a better alternative to the simpler conceptual model adopted in this study. Thus, the capabilities of data-driven hydrological models in simulating complex natural processes in agricultural watersheds may be limited.

Table 1. Performance evaluation of the hydrological models developed for Altuma watershed using Nash-Sutcliffe efficiency (NSE) and correlation coefficient (R).

	Calibration		Validation	
	NSE	**R**	**NSE**	**R**
GR4J conceptual model	0.68	0.69	0.77	0.88
LSTM network model	0.62	0.79	0.58	0.77

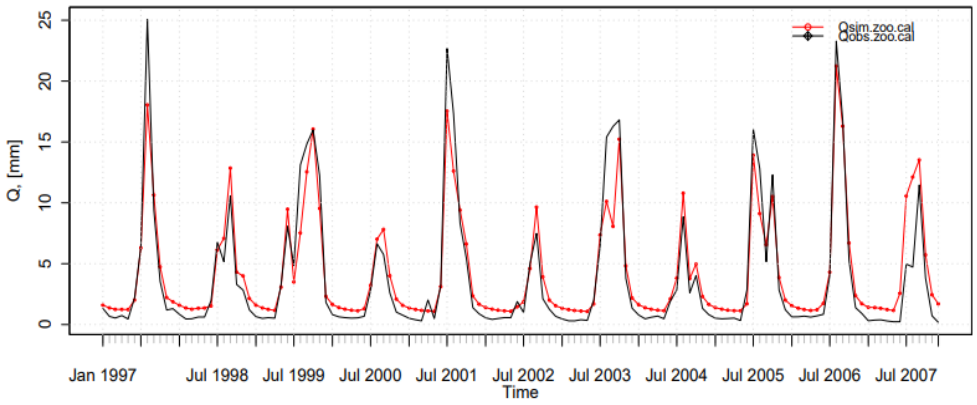

Figure 1. Comparison of observed monthly runoff (black line) and simulated monthly runoff from the conceptual model GR4J (red line) during the calibration period (1997-2007).

References

Anshuman A, Kunnath-Poovakka A, Eldho TI (2019) Towards the use of conceptual models for water resource assessment in Indian tropical watersheds under monsoon-driven climatic conditions. Environ Earth Sci 78: 282. https://doi.org/10.1007/s12665-019-8281-5

Gauch M, Kratzert F, Klotz D, Nearing G, Lin J, Hochreiter S (2021) Rainfall–runoff prediction at multiple timescales with a single Long Short-Term Memory network. Hydrol Earth Syst Sci 25(4): 2045-2062. https://doi.org/10.5194/hess-25-2045-2021

Michel C (1991) Hydrologie appliquée aux petits bassins ruraux. Cemagref, Antony, France

Oudin L, Hervieu F, Michel C, Perrin C, Andréassian V, Anctil F, Loumagne C (2005) Which potential evapotranspiration input for a lumped rainfall-runoff model? Part 2 - Towards a simple and efficient potential evapotranspiration model for rainfall-runoff modelling. J Hydrol 303(1-4): 290-306. https://doi.org/10.1016/j.jhydrol.2004.08.026

Pai DS, Sridhar L, Rajeevan M, Sreejith OP, Satbhai NS, Mukhopadhyay B (2014) Development of a new high spatial resolution (0.25° × 0.25°) long period (1901-2010) daily gridded rainfall data set over India and its comparison with existing data sets over the region. Mausam 65(1): 1–18. doi: https://doi.org/10.54302/mausam.v65i1.851

Perrin C, Michel C, Andréassian V (2003) Improvement of a parsimonious model for streamflow simulation. J Hydrol 279(1–4): 275–289. https://doi.org/10.1016/S0022-1694(03)00225-7

12th World Congress on Water Resources and Environment (EWRA 2023)
"Managing Water-Energy-Land-Food under Climatic, Environmental and Social Instability"
Thessaloniki, Greece, 27 June - 1 July 2023

Evolutionary, swarm-based, and hybrid metaheuristic algorithms for the optimal design of water distribution network: A comparative study

S.N. Poojitha*, V. Jothiprakash
Department of Civil Engineering, Indian Institute of Technology Bombay, Powai, Mumbai, India
** e-mail: poojitha@iitb.ac.in*

Introduction

The water distribution network (WDN) optimal design is often a challenging and enormously studied real-world problem in water resources engineering. For decades, formulating new optimization techniques or enhancing the existing models has become an active research area because of the nondeterministic polynomial-time hard nature of the WDN design problem (Moosavian and Lence 2019). Several modern stochastic metaheuristic algorithms have been proposed for the single-objective design of WDNs (Reca et al. 2008; Zheng et al. 2013; Poojitha and Jothiprakash 2022b). The present study provides a comparative computational analysis of an evolutionary algorithm (EA), the differential evolution (DE), a recent swarm-based innovation, the krill-herd algorithm (KHA), and a novel hybrid metaheuristic combining these two techniques, the DE-KHA model in optimally designing WDN. The major objective of the study is to demonstrate and compare the computational efficiency of these metaheuristic algorithms, highlighting their solution precision. The novelty of the study lies in extending these algorithms to design a real-scale, complex, large-size benchmark problem, the Balerma irrigation network (BIN). BIN is the adaptation of the existing irrigation WDN in the Sol-Poniente irrigation district, stationed in the Balerma province of Almería, Spain. It has 454 network pipes, each with ten commercially available diameter options, resulting in the vast solution search space size of 10^{454} possible solutions for its optimal design.

Materials and methods

DE, KHA, and DE-KHA are population-based metaheuristic algorithms, where the search for the optimal solution progresses by evolving the population members over iterations using their effective operators. The present study considers the fine-tuned KHA (FIT-KHA), an improvised version of KHA with better exploration properties. The detailed working mechanism of these optimization techniques is given in Poojitha and Jothiprakash (2022a). For the single-objective design of WDNs, with minimizing the capital investment of network pipes as the primary objective, the objective function is defined as the sum of pipe cost and penalty function. An additive static penalty function differentiates the feasible from infeasible solutions of the 10^{454} design options for BIN. The codes for the three algorithms are written in MATLAB 2015a and linked with EPANET 2.0 software for simulating the WDN hydraulic conditions.

Results and concluding remarks

The computational efficiency of the metaheuristic algorithm depends upon its control parameters, calibrated through sensitivity analysis. For DE, the control parameters ascertained are mutation factor, F_m=0.5, and crossover probability, P_c =0.3. Interestingly, for the FIT-KHA and DE-KHA models, the control parameters ascertained are the same as the ones found for the medium-sized network reported in Poojitha and Jothiprakash 2022(b) and (a), respectively, except for F_m = 0.3 and P_c = 0.5 for the DE-KHA model. With these optimal control parameter values, for BIN, the DE, FIT-KHA, and DE-KHA models converged to the optimal cost of 2,043,185 units, 3,954,023 units, and 1,926,779 units, respectively, as shown in Figure 1(a). The solutions located by the DE and DE-KHA models are improved costs over Reca and Martinez (2006), Reca et al. (2008), and Moosavian and Lence (2019). Notably, the DE-KHA model excels over many other single-objective optimization models reported by Geem (2009), Zheng et al. (2013), and Sheikholeslami et al. (2016). On the other hand, the optimal solution found by the FIT-KHA is greater than the maximum cost reported in the literature to date, 3.298 million by Reca et al. (2008).

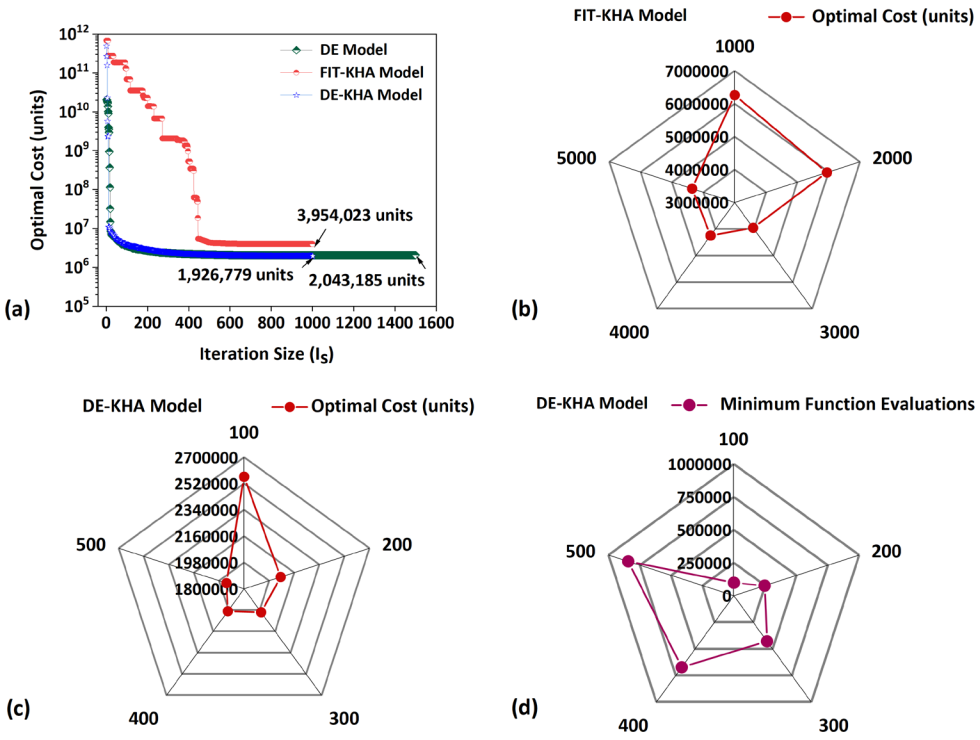

Figure 1. Computational results of DE, FIT-KHA and DE-KHA models.

To locate these optimal solutions, the DE model required population size, P_s of 500, and maximum iteration size, $I_{s,max}$ of 1,500. With a further increase in $I_{s,max}$, the saturation in the population members with no further improvement in convergence precision is noticed. Besides, for converging to 2,043,185 units, DE required a minimum function evaluation (MFEs) of 359,000. When FIT-KHA is considered, as test analysis, $I_{s,max}$ of 1,000 is used by varying P_s from 1,000 to 5,000. Figure 1(b) presents the variation in the optimal cost with the increase in P_s as a radar plot, with webs denoting the optimal cost and radii representing the P_s. Interestingly, the pipe investment cost followed a decreasing trend until P_s = 3,000, after which a sudden increase in the cost due to the saturation of the krill population is observed (Figure 1(b)). In contrast, with DE-KHA, even at P_s = {200, 300, 400}, a minimum cost solution than DE is obtained with $I_{s,max}$ of 1,000, as shown in Figure 1(c). The corresponding MFEs are shown in Figure 1(d), where the webs of the radar plots represent MFEs. From Figure 1(d), with P_s = 500, the DE-KHA required only 842,000 MFEs to converge to the optimal solution of 1,926,779 units, at least ten times less than the computational effort of the single-objective optimization models reported in literature solving BIN. Thus, compared to DE, and KHA, the hybrid model complementing the features of these two techniques, the DE-KHA outperforms in solving the real-scale BIN with solution precision and relatively less computation effort.

References

Geem ZW (2009) Particle-swarm harmony search for water network design. Engineering Optimization 41(4): 297-311

Moosavian N, Lence B (2019) Fittest individual referenced differential evolution algorithms for optimization of water distribution networks. Journal of Computing in Civil Engineering 33(6): 04019036

Poojitha SN, Jothiprakash V (2022a) Hybrid differential evolution and krill herd algorithm for the optimal design of water distribution networks. Journal of Computing in Civil Engineering 36(1): 04021032

Poojitha SN, Jothiprakash V (2022b) Application of fine-tuned krill herd algorithm in design of water distribution networks. Journal of Pipe Line Systems Engineering and Practice 13(4): 0402204

Reca J, Martinez J (2006) Genetic algorithms for the design of looped irrigation water distribution networks. Water Resources Research 42(5): W05416

Reca J, Martinez J, Banos R (2008) Application of several meta-heuristic techniques to the optimization of real looped water distribution networks. Water Resources Management, 22(2008): 1367-1379

Sheikholeslami R. Zecchin AR, Zheng F, Talatahari S (2016) A hybrid cuckoo-harmony search algorithm for optimal design of water distribution systems. Journal of Hydroinformatics 1893): 544-563

Zheng F, Zecchin AC, Simpson AR (2013) Self-adaptive differential evolution algorithm applied to water distribution system optimization. Journal of Computing in Civil Engineering 27(2): 148-158

12th World Congress on Water Resources and Environment (EWRA 2023)
"Managing Water-Energy-Land-Food under Climatic, Environmental and Social Instability"
Thessaloniki, Greece, 27 June - 1 July 2023

Modeling leakage and optimizing PRV settings for NRW reduction

N.P. Chela*, G. Moraitis, C. Makropoulos
Department of Water Resources and Environmental Engineering, School of Civil Engineering, National Technical University of Athens (NTUA), Athens, Greece
** e-mail: nataliachela@yahoo.com*

Introduction

One of the most pressing issues concerning water companies around the world is the reduction of Non-Revenue Water and especially of leakage in water distribution networks. Pressure management, paired with other techniques, has been proved to be one of the most effective methods battling this problem and there are many studies about optimizing the settings and locations of PRVs. An important constraint, though, in the efforts of finding the optimal pressure settings of the valves is the realistic interpretation, distribution and modelling of leakage in the network.

This study aims at developing an optimization framework for pressure management that acknowledges and addresses this constraint to create a more realistic model. This is achieved by incorporating a methodology for leakage modelling and its spatial distribution as well as preparing the network for the use of Pressure Driven Analysis. Then, there exist two scenarios that are implemented, that optimize the settings of the existing valves of the network: one using only fixed setting PRVs, and the other using only time-modulated PRVs.

Materials and methods

The KY11 demo model is based on a real water distribution network located in Kentucky, U.S.A and is comprised of 1 water source that supplies 802 nodes though approximately 447 km of pipes. The system operation is regulated by 28 tanks, 21 pumps and 14 active PRVs. The level of annual water losses is estimated at 21%, which, for the purposes of this study, are assumed to consist entirely of leakage.

The first step in the re-modelling of the WDN, to properly account for leakage, is to insert dummy emitter nodes in the middle of each pipe, assuming a uniform leakage profile along their length. This generated an additional set of 845 fictional nodes for the KY11 system, with zero water demand. Those nodes are used to mimic the outflow of a leaking pipe, following a power function of the pressure, an emitter coefficient and an exponent. For the exponent, studies indicate that the value ranges between 0.65 and 2.1, depending on the shape and size of the leaks, and suggest the value of 1.1 (Van Zyl et al. 2014) for WDNs with pipes of mixed materials, which is assumed in this case. The next step is the assignment of the emitter coefficients for each pipe which, in our study, indicates a leakage coefficient. Adhering to the study of Cobacho et al. (2015), we aim to assign such coefficients, that the total outflow of the fictional nodes will match the estimated leakage percentage of the network. The methodology suggests the association of each fictional node j with a weight parameter Γj, which in this study is defined by the length and the average operating pressure of the pipe. This may also account for other important factors of leakage, such as the material or the age of the pipe when known, yet any number and combination of characteristics can be used to form the weight parameter depending on each study's needs and the provided information.

Moving on to the assignment of leakage coefficient, associating the K_j to every j node is in reality an optimization problem with a large number of variables, even in skeletonized networks. Instead, an inverse approach was followed to solve the problem in a more direct manner. To do that, we used a pseudovariable (K_{net}), that represents the total losses of the network. By defining the leakage coefficient as $K_j = K_{net} * \Gamma_j$, we followed an iterative process for a range of K_{net} values. In each step, we spatially distributed the leakage coefficients based on the previous equation and simulated the WDN under DDA, to avoid imbalances in the losses ratio. This allows us to formulate a nomogram between the rate of leakage and the relevant leakage coefficients that characterize the network, from which every leakage ratio can be

associated with its respective leakage coefficient for modelling. In our case study, the average coefficient was approximately $2.83*10^{-4}$. The final step revolves around pressure driven analysis (PDA), which is essential when modelling leakage. The goal in this step is to estimate as closely as possible the range of pressure ($p_{min}<p< p_{req}$) where every WDN concerned delivers only a percentage of the demand depending on available pressure. This range and HFR are unique for each network, and they mostly depend on its operational regulations, infrastructure as well as the demand patterns. In the case of KY11, we consulted the regional water supply regulations to bound the search field according to the provisions regarding its acceptable and extreme pressure levels. The parameterization of the PDA was validated by the comparison of PDA and DDA results, both in terms of demand satisfaction and losses ratio. By utilizing the re-modelled network, the design and optimization of leakage reduction strategies can be based on more solid ground and yield more realistic results.

To explore the potential of the existing design, we proceeded with the examination of alternative settings for the PRVs under their current position, and implemented 2 optimization scenarios. The first one assumes fixed and the second one assumes time modulated PRVs. For KY11 a 24-hour PRV pattern was used for 3 periods, i.e. 01:00-09:00 (lowest demand), 09:00-19:00 and 19:00-01:00. Both optimization scenarios used Matlab's genetic algorithms, and a fitness function that minimizes total leakage while maintaining demand satisfaction at each node above 90%.

Results and concluding remarks

By optimizing the settings of the 14 existing PRVs of KY11 the reduction of leakage was accomplished by almost a full percentage unit (from 21 to 20.3%) based on spatially distributed leakage. The two valve types examined (fixed and time modulated) yielded similar results regarding losses reduction, although there were slight differences regarding the demand satisfaction ratio. Specifically, the time modulated PRVs performed better at satisfying the total demand in the network for the duration of the analysis.

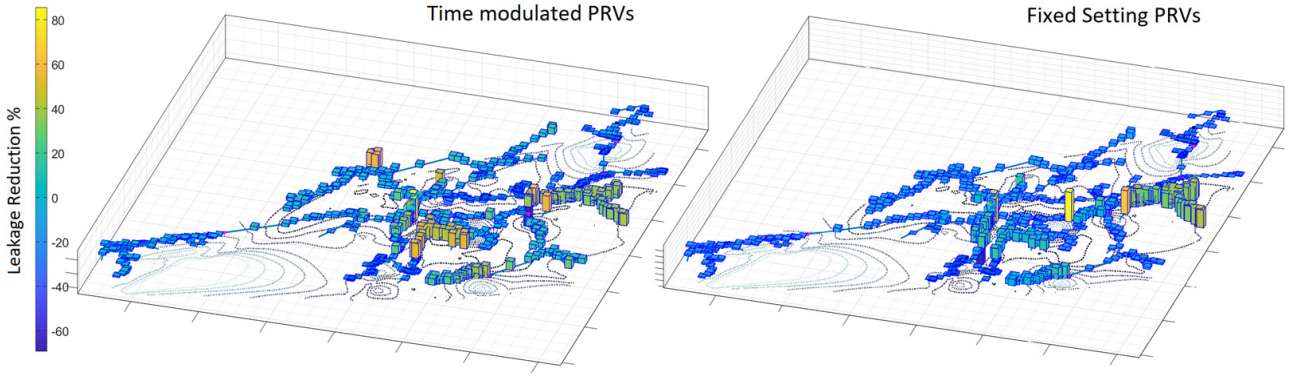

Figure 1. Spatial distribution of leakage reduction percentage for the fixed setting and time modulated settings PRVs.

The proposed framework can be implemented in any WDN with known losses and yield solutions to be instantly implemented with minimal cost to optimize operations using existing assets. The framework is adjustable to new data regarding total losses, changes in infrastructure (e.g. pipe replacement) or exploring different valve type combinations and demand patterns. Furthermore, it can work as a tool for evaluating different zones in the network and provide a starting point for other or more targeted leakage management methods.

References

Cobacho R, Arregui F, Soriano J, Cabrera Jr E (2015) Including leakage in network models: an application to calibrate leak valves in EPANET. Journal of Water Supply: Research and Technology—AQUA 64(2): 130-138. https://doi.org/10.2166/aqua.2014.197

Jolly MD, Lothes AD, Sebastian Bryson L, Ormsbee L (2014) Research database of water distribution system models. Journal of Water Resources Planning and Management 140(4): 410-416. https://doi.org/10.1061/(ASCE)WR.1943-5452.0000352

Van Zyl JE, Cassa AM (2014) Modeling elastically deforming leaks in water distribution pipes. Journal of Hydraulic Engineering 140(2): 182-189. https://doi.org/10.1061/(ASCE)HY.1943-7900.0000813

Estimation of storage capacity with the Gould-Dincer's normal approach using fuzzy and possibility theories

N. Mylonas[1], C. Tzimopoulos[2], G. Papaevangelou[2*], B. Papadopoulos[1]
[1] School of Engineering, Democritus University of Thrace, Xanthi 67100, Greece
[2] Department of Rural and Surveying Engineering, Aristotle University of Thessaloniki, 54124 Thessaloniki, Greece
* e-mail: geopapaevan@topo.auth.gr

Introduction

The determination of reservoir capacity to meet the demand with an acceptable level of reliability, is an age-old problem and there currently exist many techniques for accomplishing this task. Traditionally, water resources engineers have employed Rippl's mass curve method or the sequent peak algorithm in the design of water storage. According to McMahon et al. (2007), "*only one technique – Gould-Dincer (G-D) suite of equations - potentially can be applied using annual stream flows across the whole spectrum of global hydrology*". The Gould-Dincer suite of techniques is used to estimate the reservoir capacity and yield-reliability relationship based on annual streamflow statistics.

In the above technique one must handle measured data. Moreover, the Gould-Dincer formula is based on probability theory, resulting to a state of uncertainty. Zadeh (1965) has introduced the theory of fuzzy sets to measure and manage uncertainty problems that are due to vagueness. Although the theory of fuzzy sets was proven to handle a different type of uncertainty than the one modelled by probability theory, it did not reject its fundamental tenets. Dubois et al. (2004) gave the basis for a transformation of a probability distribution into a possibility distribution that generalises the notion of best interval substitute to a probability distribution with prescribed confidence. Mylonas (2022) extended this method for functions which do not have a probability distribution and constructed a fuzzy function for them. Consequently, using the possibility theory, he constructed an estimator for the fuzzy case with confidence intervals. In the present paper we present the construction of fuzzy estimators for the mean value, the variance, as well as for the autocorrelation coefficient, and introduce them in Gould-Dincer normal formula to construct a fuzzy function and consequently applying possibility theory to estimate the storage capacity of a water reservoir.

Materials and methods

Gould-Dincer's normal approach: Assuming normally distributed and independent annual flows with mean μ and standard deviation σ, the Gould-Dincer's normal approach for the reservoir capacity is:

$$C = \left[z_p^2/(4-4D)\right] C_v^2\, \mu \tag{1}$$

where Cv = σ/μ is the coefficient of variation of the annual inflows to the reservoir, D the constant draft as ratio of mean annual flow, p the annual probability of failure, which means that inflows into the reservoir will be just sufficient to allow the reservoir to meet the targeted draft with reliability 1 - p and $z_p = \Phi^{-1}(1-p)$ the standardized normal variate at $p(\Phi^{-1})$ of the standard normal distribution. To account for the auto-correlation effect on reservoir capacity, one can use a first-order autoregressive model and adjust the reservoir capacity computed from (1) by (1+ρ)/(1-ρ) as follows:

$$C = \left[z_p^2/(4-4D)\right] C_v^2\, \mu\, [(1+\rho)/(1-\rho)] \tag{2}$$

Fuzzy estimation: The fuzzification of equation (2) is obtained as follows (Mylonas 2022):

$$\tilde{C} = \left[z_p^2/(4-4D)\right] \tilde{C}_v^2\, \tilde{\mu}\, [(1+\tilde{\rho})/(1-\tilde{\rho})] \tag{3}$$

For equation (2) there is not a direct probability function. We can thus use the Mylonas (2022) theory in order to obtain a possibility distribution. According to Mylonas conjecture, the fuzzy number (3) has α-cuts

which are confidence intervals with a probability greater than 1-α. So, for α-cut value equal to 5%, the intervals of this α-cut are confidence intervals with a probability greater than 95%, and we can estimate the storage capacity included in the interval with a probability greater than 95%.

Results and concluding remarks

Application of Gould-Dincer's normal approach in the Crisp case: We have estimated the storage capacity required and the length of the critical drawdown period for the annual flows data for Mitta Mitta River at Tallandoon Victoria, Australia, for period 1936-1969 inclusive (Mylonas 2022):

$\bar{X} = 1674 * 10^6 m^3$, $\sigma = 731 * 10^6 m^3$, $C_v = 0.57$

So, for D = 0.75, p = 5%, we obtain: z_p = 1.65 and C = $1127 * 10^6 m^3$.

The annual serial correlation of these annual flows is found to be ρ=0.06, so the adjustment factor is (1+ρ)/(1-ρ) = 1.13. Therefore, the adjusted crisp estimation of the storage capacity is $1271 * 10^6 m^3$.

Application of Gould-Dincer's normal approach in the Fuzzy case: Applying Mylonas approach, we have constructed fuzzy estimators for the mean value, the coefficient of variation, the autoregressive model. This resulted in the fuzzy estimator of the storage capacity presented in Figure 1.

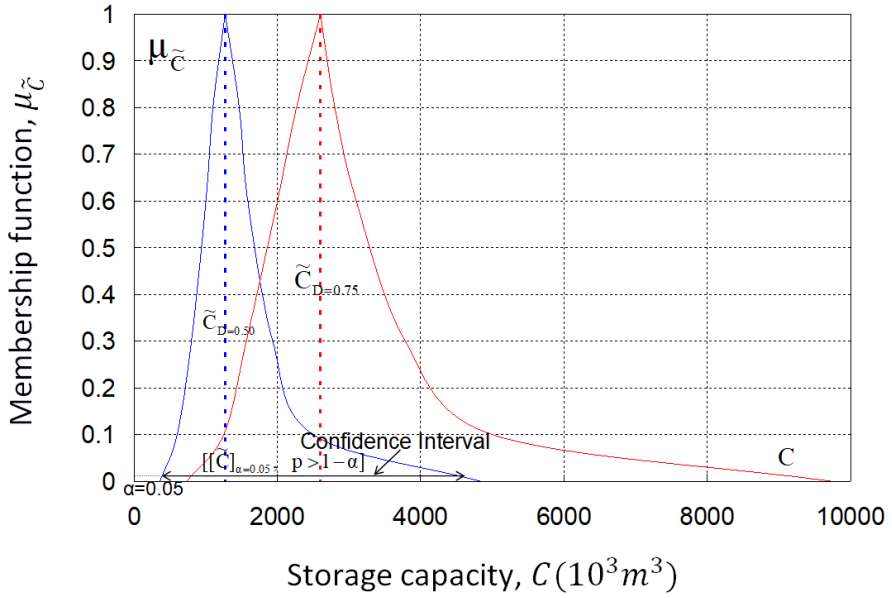

Figure 1. The possibility distribution of the fuzzy estimator of the storage capacity required for D=0.75 or D=0.5 and p=1%.

Using classical statistics we cannot infer confidence intervals for the reservoir capacity C, since we cannot derive their probability distribution. As shown here, using fuzzy logic and possibility theory, we can deduce confidence intervals within any given level of probability.

References

McMahon TA, Pegram GGS, Vogel RM, Peel MC (2007) Review of Gould-Dincer reservoir storage yield reliability estimates. Advances in Water Resources 30: 1873-1882. https://doi.org/10.1016/j.advwatres.2007.02.004

Zadeh LA (1965) Fuzzy Sets. Information and Control 8: 338-353. https://doi.org/10.1016/S0019-9958(65)90241-X

Dubois D, Foulloy L, Mauris G, Prade H (2004) Probability-Possibility Transformations, Triangular Fuzzy Sets, and Probabilistic Inequalities. Reliable Computing 10: 273–297. https://doi.org/10.1023/B:REOM.0000032115.22510.b5

Mylonas N (2022) Applications in fuzzy statistic and approximate reasoning. PhD thesis, Democritus University of Thrace-Greece, p 164 (in Greek)

Using Key Performance Indicators and benchmarking techniques to evaluate the use of reclaimed water in irrigation agriculture

M. Ballesteros-Olza[1*], A. Gómez-Ramos[2], I. Blanco-Gutiérrez[3], P. Saiz-Valle[3]
[1] CEIGRAM, Universidad Politécnica de Madrid, Senda del Rey 13, 28040 Madrid, Spain
[2] Dept. of Agricultural and Forestry Engineering, Universidad de Valladolid, Av. de Madrid 57, 34004 Palencia, Spain
[3] Dept. of Agricultural Economics, Statistics and Business Mgmt., UPM, Av. Puerta de Hierro 2-4, 28040 Madrid, Spain
* e-mail: mario.ballesteros@upm.es

Introduction

Water reuse is becoming more and more important in the recent years to tackle water scarcity, as it can enhance water management and address the global growing water demands (Qi et al. 2021). One of the most common uses for reclaimed water is agricultural irrigation, as it can contribute to improve production yields, reduce the ecological footprint, and promote several socio-economic benefits (Lu and Chen 2022). There are regions that have been gaining increasing experience on reusing water in agriculture, due to their structural water deficit problems (like the Region of Murcia in Spain). However, there are still many regions (particularly in developing countries) where its implementation is far below its potential.

The objective of this study is to evaluate the performance of different Irrigation Communities (ICs) using reclaimed water within the Region of Murcia (Segura River Basin District), which is pioneer in terms of treatment and water reuse. Using Key Performance Indicators (KPIs) and benchmarking techniques, the study evaluates which have been the key factors for implementing the use of reclaimed water in this region, which obstacles have been encountered during its adoption, and how could these be addressed. This benchmarking methodology has been previously applied to ICs (Arslan et al. 2022), even in the same region (Alcon et al. 2017), but with a more general approach, and less focus in the use of reclaimed water.

Materials and methods

The study analyzes 8 ICs of the Segura RBD in Murcia: Campo de Cartagena, Águilas, Puerto Lumbreras, Totana, Campotéjar, Jumilla-Miraflores, Yecla and Lorca. Besides, eleven KPIs were proposed, based on the guidelines for benchmarking performance in the irrigation and drainage sector from Malano and Burton (2001). These KPIs were divided into 4 dimensions as follows: 2 economic indicators (cost of reclaimed water and its cost difference with the most expensive source); 5 indicators related to production (reclaimed water per irrigator, reclaimed water concession per irrigable area, percentage of reclaimed water used, reclaimed water mixing and percentage of irrigated area with reclaimed water); 4 environmental indicators (days without reclaimed water, guarantee of supply, variation in fertilizer use, electrical conductivity); and 2 social indicators (general confidence and number of training courses). Face-to-face interviews were conducted with the managers of the ICs to gather these data.

Based on the results of the KPIs, a score from 1 (worst) to 3 (best) was awarded to each IC. These scores' thresholds were settled based on the literature and the insight from the interviewed irrigators. Thus, by averaging the performance score of each indicator (all of them were assumed to have equal weights), aggregated results were obtained for each IC, as well as for each of the four dimensions. Based on the final scores, a ranking was performed, to give an idea of the overall performance of the studied ICs.

Results and concluding remarks

Figure 1 shows the map of the municipalities where each IC belongs. Green areas indicate a better performance in terms of reclaimed water use, while red areas denote a worse one, based on the aggregated results. The results show that the performance of the ICs using reclaimed water is very heterogeneous. From the economic perspective, reclaimed water is more valued in those ICs where it does not compete with higher quality and lower cost resources such as surface water, despite its supply being

more uncertain. Environmental function is key in those seashore ICs with high risks of pollution from untreated discharges. Also, in inland communities, the maintenance of ecological flows limits further development. From the productive perspective, this water is well valued in areas where woody crops are present (due to a lower heath risk). Finally, the ICs that use a mix of water from different sources present lower health risks, although greater salinity. The overall valuation of reclaimed water is high in all ICs, although there are strengths and weaknesses depending on the location, configuration of the cost of the pool of water sources, and its proximity to areas of high environmental value.

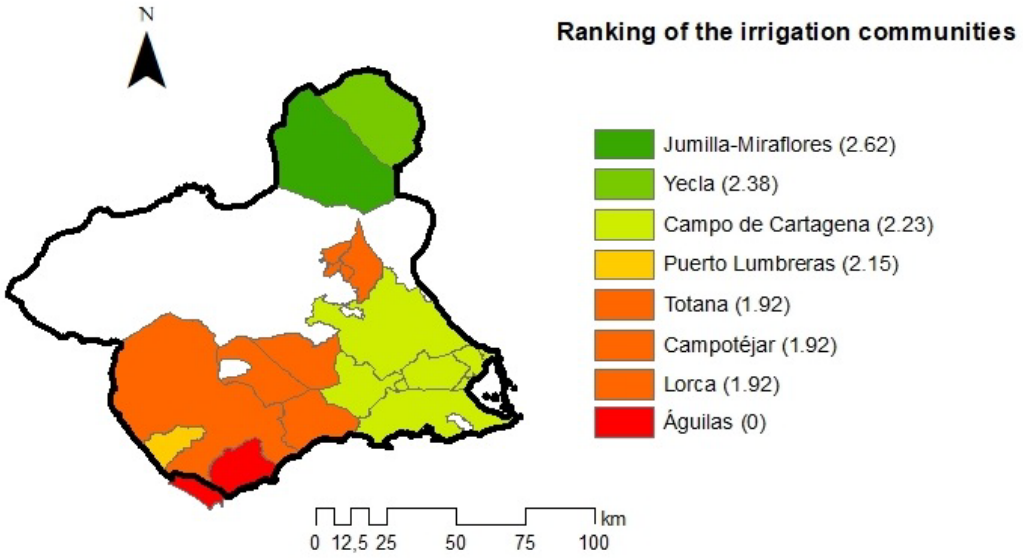

Figure 1. Ranking of the ICs, based on the KPIs aggregated results.

In general, it is necessary to have good infrastructures such as storage ponds or a good piping system to make a proper use of reclaimed water. Therefore, the quality and quantity of this resource would be better. Improving the acceptance of those consumers and irrigators that are still reluctant about the use of reclaimed water due to potential health risks is necessary to extend this practice. For this reason, it is essential to provide training courses so that farmers can manage the resource correctly and be sure of the benefits of irrigating with reclaimed water.

Acknowledgments: The research leading to these results has received funding from the RECLAMO project (Grant No. PID2019-104340RA-I00, funded by MCIN/AEI/10.13039/501100011033).

References

Alcon F, García-Bastida PA, Soto-García M, Martínez-Álvarez V, Martin-Gorriz B, Baille A (2017) Explaining the performance of irrigation communities in a water-scarce region. Irrig Sci 35: 193–203. https://doi.org/10.1007/s00271-016-0531-7

Arslan F, Córcoles JI, Rodríguez-Díaz JA, Zema DA (2023) Comparison of Irrigation Management in Water User Associations of Italy, Spain and Turkey Using Benchmarking Techniques. Water Resour Manage 37: 55–74. https://doi.org/10.1007/s11269-022-03355-2

Lu HL, Chen YH (2022) Reclaimed water reuse system on water quality, growth of irrigated crops, and impact of ecology: case study in Taiwan. Environmental Science and Pollution Research 1: 1–14. https://doi.org/10.1007/s11356-022-19872-x

Malano H, Burton M (2001) Guidelines for benchmarking performance in the irrigation and drainage sector. IPTRID Secretariat. Food and Agriculture Organization of the United Nations. Rome, Italy

Qi H, Zeng S, Shi L, Dong X (2021) What the reclaimed water use can change: From a perspective of inter-provincial virtual water network. Journal of Environmental Management 287: 112350. https://doi.org/10.1016/J.JENVMAN.2021.112350

A generic participatory decision support system for irrigation management for the case of cotton

A. Christofides[1,4*], I.L. Tsirogiannis[2,4], N. Malamos[3,4], C. Myriounis[4]
[1] Department of Water Resources & Environmental Engineering, National Technical University of Athens, 15780 Athens, Greece
[2] Department of Agriculture, University of Ioannina, Kostakii Campus, 47100 Arta, Greece
[3] Department of Agriculture, University of Patras, Nea Ktiria Campus, 30200 Messolonghi, Greece
[4] Efficient Water Resources Management P.C., Agios Georgios, 46100, Igoumenitsa, Greece
* e-mail: anthony@itia.ntua.gr

Introduction

Efficient soil water management is an important goal in cotton cultivation as it has significant impacts on the quantity and quality of yield (Koudahe et al. 2021). The present study concerns the evaluation for the case of cotton, of a generic web-based participatory decision support system for irrigation management, that does not require any specialized sensor to be installed in each field.

Materials and methods

The evaluation was carried out during the 2022 irrigation season (April–October) at the Local Land Reclamation Organisation (LLRO) of Kria Vrisi / General Land Reclamation Organisation (GLRO) of the plains of Thessaloniki-Lagadas (Arampatzis et al. 2011). Following the Greek legislation (GMA 1989), the generic limits for irrigation water usage for cotton at Central Macedonia, range between 499 and 608 mm (May 1st to August 31st, well maintained closed-pipes distribution system, use sprinkler irrigation). Two pilot fields (41: WGS 84: 40.654566° N, 22.301366° E, 1 ha, Clay soil and 111: WGS84: 40.650991° N, 22.306921° E, 1.98 ha, Clay soil) were used. They were planted with cotton (*Gossypium hirsutum* L.) var. Pionner 402 (seeded on April 23rd and harvested from September 22nd to October 16th) and irrigated using the same travelling gun sprinkler system. The growers were very experienced in cotton cultivation and irrigation management was performed following their experience. Water usage by the irrigation system was measured using a 100 mm volumetric dry dial water meters (accuracy 1L, type WT DN100, Madalena S.P.A., IT). Soil moisture was measured using a portable dielectric soil moisture sensor (accuracy 5% for the generic supplied soil calibration, type Thetaprobe ML2x, DT Devices Ltd, UK). Soil moisture measurement were performed four times during the irrigation period and each time, six measurements were made at a depth of 20 cm.

IRMA_SYS, a generic participatory decision support system for irrigation management (IRMASYS P.C., GR) (the DSS hereafter), was installed at the area in 2022, in collaboration with LLRO of Kria Vrisi and the GLRO of the plains of Thessaloniki-Lagadas (https://toebkb.irmasys.com/). This DSS does not require the installation of any special sensor at each field, provides real-time forecasts for soil moisture at the end of each day and generates recommendations for future irrigation applications, based on the outcomes of a daily ETo and water balance model that follows the principles of FAO's paper 56. It considers: (a) measurements from reference automatic agrometeorological stations for each area (for the case of the DSS of Kria Vrisi, data from two stations of the Directorate of Agricultural Economy and Husbandry (DAOK) of Pella were used: Kria Vrisi and Palaios Milotopos http://www.stravon.gr/stations); (b) field (soil, crop and irrigation system) parameters; (c) data from the actual irrigation applications and (d) weather forecasts. Irrigation is recommended when soil moisture reaches the lower level of the readily available water (RAW), while the irrigation dose is controlled by a refill factor (RF). Documentation and analytical flowcharts of the algorithm that is followed by the DSS is provided by Malamos et al. (2016).

The goal was to calibrate the field parameters of the DSS for cotton, aiming to match its estimation of soil moisture to the relevant measurements from the proximal sensors. MS-Excel (Microsoft Corp, USA) was

used for the processing and the statistical analysis of the data.

Results and concluding remarks

The total rainfall from 15/3/2022 up to 15/10/2022 was 257 mm (data from the agrometeorological station of Kria Vrisi, which was close to both fields). Four irrigations were applied by the grower for each field. For the field 41 they summed a total water height of 200 mm, while for the field 111, they summed a total water height of 229 mm. To model the fields at the DSS, the following parameters were concluded: irrigated area: 100% of the total area; soil moisture at saturation (S): 50% (m^3/m^3); field capacity (FC): 45% (m^3/m^3); permanent wilting point (PWP): 21% (m^3/m^3); maximum root depth: 0.50 m; maximum allowable depletion of the available soil moisture (MAD): 60%; length of growth stages (initial, crop-development, mid-season, late-season) starting from April 23th: 35, 48, 29 and 28 days; Kc for the growth stages (Kc_{ini}, Kc_{mid}, Kc_{end}): 0.3, 0.9 and 0.4; irrigation system efficiency: 75%; effective rain coefficient: 80%; RF: 80%. The DSS proposed three irrigations for both fields which summed 232 mm and 239 mm fields 41 and 111. The mean absolute difference between the estimations of soil moisture by the DSS and the measured values where found equal to 3.9% and 5.3% for the fields 41 and 111. Figure 1 synopsises the results.

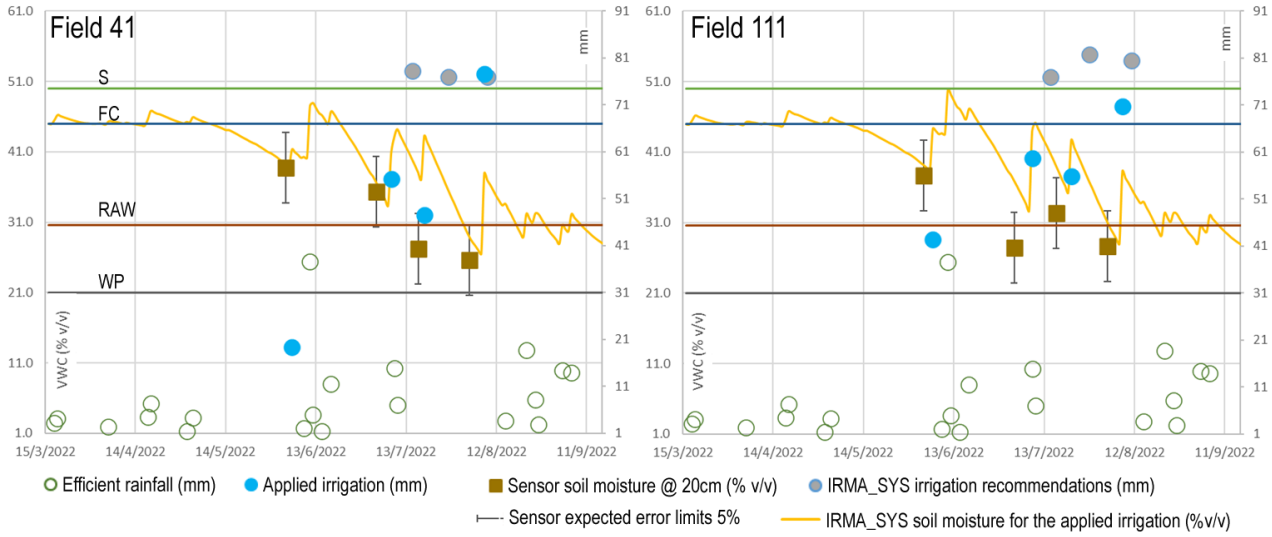

Figure 1. Synoptical presentation of the results for fields 41 and 111.

The results are very promising regarding the ability of the DSS to estimate soil moisture. Application of this kind of decision support systems could support extensive trials of special irrigation management approaches and help growers and agronomic consultants to document results, disseminate good practices and calculate environmental indices. In all cases, the operation of pilot evaluation fields is recommended for the development of proper sets of parameters for each crop and for demonstration purposes.

Acknowledgments: The authors would like to express their gratitude to the people of LLRO of Kria Vrisi, GLRO of the plains of Thessaloniki-Lagadas and DAOK of Pella for their support and collaboration.

References

Arampatzis G, Evangelides C, Hatzigiannakis E (2011) Crop requirements and water losses in collective pressurized irrigation networks in northern Greece Global Nest Journal 13: 11-17.

GMA-Greek Ministry of Agriculture. Determination of min and max limits of the necessary quantities for the sustainable use of water for irrigation. Govern. Gazette (GG) B' 42 2/6/1989 Ministerial Decision Φ.16/6631 1989

Koudahe K, Sheshukov AY, Aguilar J, Djaman K (2021) Irrigation-Water Management and Productivity of Cotton: A Review. Sustainability 13, 10070. https://doi.org/10.3390/su131810070

Malamos N, Tsirogiannis IL, Christofides, A (2016) Modelling irrigation management services: the IRMA_SYS case. International Journal of Sustainable Agricultural Management and Informatics 2(1): 1–18. https://doi.org/10.1504/IJSAMI.2016.077264

Agrometeorological simulation and Sentinel-2 images for monitoring maize water demands in Thessaly region (Central Greece)

G.A. Tziatzios[1], P. Sidiropoulos[1*], M. Spiliotopoulos[1], N. Alpanakis[1], I. Faraslis[2], S. Sakellariou[2], G. Karoutsos[3] , N.R. Dalezios[1], N. Dercas[4]
[1] *Laboratory of Hydrology and Aquatic Systems Analysis, Department of Civil Engineering, University of Thessaly, Volos, Greece*
[2] *Department of Environmental Sciences, University of Thessaly, Larisa, Greece*
[3] *General Aviation Applications "3D" S.A., 2 Skiathou str, 54646, Thessaloniki, Greece*
[4] *Department of Natural Resources Management and Agricultural Engineering, Agricultural University of Athens, Athens, Greece*
** e-mail: psidirop@civ.uth.gr*

Introduction

The accurate estimation as well as the future prediction of actual evapotranspiration is crucial for the proper planning of irrigation, the sustainable management of water resources, and consequently sustainable agriculture (Fu et al. 2021). This paper presents a combination of the use of remote sensing with the agrometeorological simulation to estimate and assess the actual evapotranspiration results. Remote sensing approach of estimating the actual evapotranspiration (ETa) is very important and displays great interest despite the challenges it may have such as for example the management of water resources and the understanding of the connection between ecosystem functions and climate feedbacks, and the limited availability of calibration. Nevertheless, it has the benefit of calculating the spatial variability of ETa, as compared to the other estimation methods, which do not provide such option (Bhattarai and Wagle 2021; Wanniarachchi and Sarukkalige 2022). The vulnerabilities are handled with the use of remote sensing SNAP – ET graphical user interface (Guzinski et al. 2020) with the sequence of the agrometerorological simulation. In this paper, the results from SNAP – ET are assessed through the FAO AquaCrop simulation tool (Steduto et al. 2009) for maize crop in the 2022 growing season.

Materials and methods

SNAP – ET plugin is a synergistic application of merging Sentinel 2 and Sentinel 3 to estimate actual evapotranspiration. SNAP employs geomorphological data, Weather Research and Forecasting (WRF) meteorological and land use data to calculate biophysical indicators on dynamics of the vegetation (estimate leaf reflectance and transmittance, estimate fraction of green vegetation, aero roughness), Earth's Energy balance (estimate longwave irradiance, estimate net shortwave radiation, estimate land surface energy fluxes) and finally estimating actual evapotranspiration, which is an important parameter of the water balance (Guzinski et al. 2020). AquaCrop calculates the soil water balance at field scale and estimates its components such as actual evapotranspiration, runoff, deep percolation, and hydraulic parameters, such as field capacity (FC), permanent wilting point (PWP), and saturation (SAT). The calibration of the AquaCrop for maize was carried out for the hydraulic conductivity (K_{sat}) of soil based on the soil moisture observed values and the final yield with the trial-and-error method (Sidiropoulos et al. 2022). In 2022, 11 cloud-free Sentinel-2 images were downloaded from the Copernicus Open Access Hub. Two irrigation practices for maize are evaluated: 1) the first one is the common irrigation practice that farmers apply based on their experience (farmer plot) and 2) the second one is irrigation strategies for water saving using precision agricultural tools (hubis plot). The total irrigation applied to the farmer plot was 640.31 mm, while in the hubis plot was 468.44 mm. This results in a reduction of water by 26,84% between the two plots.

Results and concluding remarks

The results of mean ETa produced from SNAP – ET and AquaCrop, respectively for the cultivation period of maize (from 28 of March to 2 of September) are presented in Figure 1. It's worth noting that SNAP - ET estimates the minimum, the mean, the median, and the maximum daily ETa. Two issues should be discussed regarding the results: 1) Important discrepancies are observed between these two methods at some days of the cultivation period. The satellite data overestimates the Eta, as compared to Aquacrop, a conclusion that many researchers have mentioned (Gonzalez-Dugo et al. 2009; Tasumi 2019; Musyimi et al. 2022); 2) The ETa timeseries of the two plots show a similarity without great differences and are very close to the maximum ETa. Since the farmer plot received more irrigation than the hubis one, greater volumes of water were drained out of the soil profile, a fact that highlights not only a waste of water but also of fertilization.

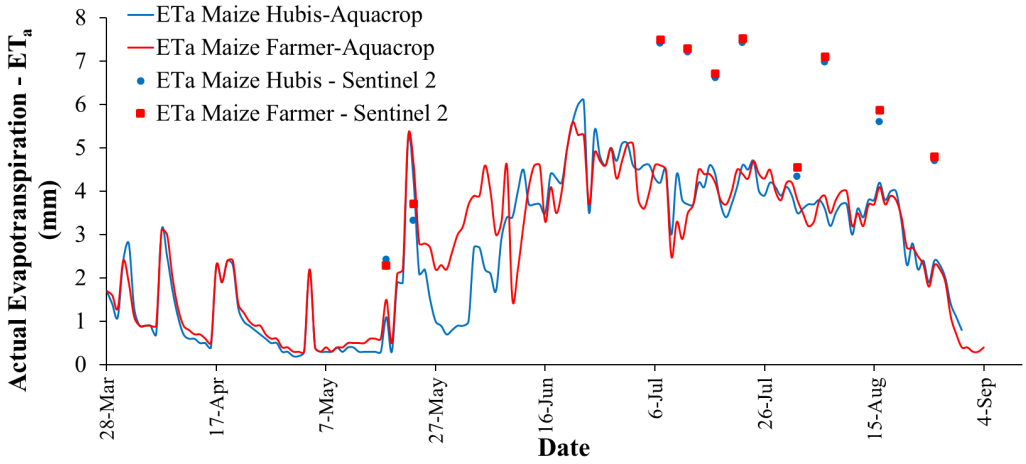

Figure 1. Actual Evapotranspiration results for SNAP -ET and AquaCrop.

Acknowledgments: The authors acknowledge the European Space Agency for the supported data and materials. The research was funded by «Open innovation Hub for Irrigation Systems in Mediterranean agriculture» with the acronym «Hubis» of PRIMA (Partnership for Research and Innovation in the Mediterranean Area) programme (Section 2 Call 2019 – multi-topic) supported under Horizon2020.

References

Bhattarai N, Wagle P (2021) Recent Advances in Remote Sensing of Evapotranspiration. Remote Sensing 13(21):4260. https://doi.org/10.3390/rs13214260

Fu T, Li X, Jia R, Feng L (2021) A novel integrated method based on a machine learning model for estimating evapotranspiration in dryland. Journal of Hydrology 603(A): 126881. https://doi.org/10.1016/j.jhydrol.2021.126881

Gonzalez-Dugo MP, Neale CMU, Mateos L, Kustas WP, Prueger JH, M.C. Anderson MC, Li F (2009) A comparison of operational remote sensing-based models for estimating crop evapotranspiration. Agricultural and Forest Meteorology 149(11): 1843-1853. https://doi.org/10.1016/j.agrformet.2009.06.012

Guzinski R, Nieto H, Sandholt I, Karamitilios G (2020) Modelling High-Resolution Actual Evapotranspiration through Sentinel-2 and Sentinel-3 Data Fusion. Remote Sensing 12(9): 1433. https://doi.org/10.3390/rs12091433

Musyimi PK, Sahbeni G, Timár G, Weidinger T, Székely B (2022) Actual Evapotranspiration Estimation Using Sentinel-1 SAR and Sentinel-3 SLSTR Data Combined with a Gradient Boosting Machine Model in Busia County, Western Kenya. Atmosphere 13(11): 1927. https://doi.org/10.3390/atmos13111927

Sidiropoulos P, Tziatzios G, Dercas N, Karoutsos G, Dalezios NR (2022) Comparative evaluation of irrigation practices for maize and cotton crops using the FAO Aquacrop model. Interregional Conference "Sustainable production in agroecosystems with water scarcity (SUPWAS)", 5-7 September 2022, Albacete, Spain

Steduto P, Hsiao TC, Raes D, Fereres E (2009) AquaCrop—the FAO crop model to simulate yield response to water: I. Concepts and underlying principles. Agronomy Journal 101(3):426–437. https://doi.org/10.2134/agronj2008.0139s

Tasumi M (2019) Estimating evapotranspiration using METRIC model and Landsat data for better understandings of regional hydrology in the western Urmia Lake Basin. Agricultural Water Management 226: 105805. https://doi.org/10.1016/j.agwat.2019.105805

Wanniarachchi S, Sarukkalige R (2022) A review on evapotranspiration estimation in agricultural water management: Past, present, and future. Hydrology 9(7): 123. https://doi.org/10.3390/hydrology9070123

Multi-criteria analysis in GIS environment to identify suitable areas for surface water storage in the Pinios river basin, Thessaly, Greece

E. Koutsimari[1*], A. Loukas[1], D. Fotakis[2]
[1] School of Rural and Surveying Engineering, Aristotle University of Thessaloniki, Thessaloniki, Greece
[2] Forest Research Institute, Hellenic Agricultural Organization – "DEMETER", Thessaloniki, Greece
* e-mail: koutsima@topo.auth.gr

Introduction

Unsustainable water resources management has been an ongoing, long-term problem for the agricultural sector in the Thessaly region of Greece. The uneven temporal and spatial distributions of precipitation and the insufficiency of surface water storage structures are some of the major factors that contribute to the problem and have led to unsustainable practices, such as groundwater overexploitation. The purpose of this study is to identify suitable areas for surface water storage in the Pinios River basin, by integrating Multi-Criteria Analysis (MCA) methods into a Geographic Information System (GIS) environment.

GIS-based MCA studies have been performed for decades now and the objective of finding potential sites for surface water storage has been particularly popular, in the last twenty years or so, in African and Middle Eastern countries, and India (e.g., Mbilinyi et al. 2007, Al-Ghobari and Dewidar 2021), where the climate is dry, and rainfalls are scarce. Greek literature on GIS-MCA studies consists of applications that have been implemented in a variety of scientific fields (e.g., Feloni et al. 2020, Demetsouka et al. 2013). In the present study, two (2) MCA methods were applied: a) the Analytical Hierarchy Process (AHP) and b) Compromise Programming (CP). Different criteria standardization techniques and rendering methods were tested as well as two (2) different sets of criteria.

Materials and methods

The first step of the MCA process was the selection of the criteria. Once the criteria were defined, then the necessary data was collected and processed to produce the criteria maps. The present study focuses on six (6) criteria, after analysis and evaluation: 1a) mean annual precipitation, 1b) rainfall with 70% probability of exceedance, 2) land slope, 3) Topographic Wetness Index (TWI), 4) stream order, 5) Relative Elevation Model (REM), and 6) Curve Number (CN). The analysis was performed to two (2) sets of criteria, to test the differences between the mean annual precipitation and the 70% exceedance rainfall. Criteria 1a), 2), 3), 4), 5), and 6) form the first set of criteria, and criteria 1b), 2), 3), 4), 5), and 6) form the second one. The relative importance weights (RIW) of the criteria were assessed using AHP.

It is crucial for the criteria to have a common scale before performing an MCA. For further testing, two (2) standardization methods were applied: the first was classifying the criteria maps into five suitability classes using the Natural Breaks by Jenks algorithm and the second was min-max scaling to transform the natural scales of the criteria into a [0,1] scale.

Two (2) MCA methods were applied to the standardized criteria maps, one being AHP and the second one being Compromise Programming. It is important to note that CP maps were tested each time for three values of p, a parameter that determines the degree of compromise between the criteria. When p=1 total compensation is assumed, whereas when p>10 a no compensatory situation is represented. Partial compensation happens when p=2.

The resulting maps were rendered using three (3) classification methods, namely: a) Natural Breaks, b) K-means, and c) Quantile, for further visualization of the results. A validation process was applied to the classified maps using existing and/or proposed surface reservoirs to ensure robustness.

The main steps and processes of the present study are shown in Figure 1.

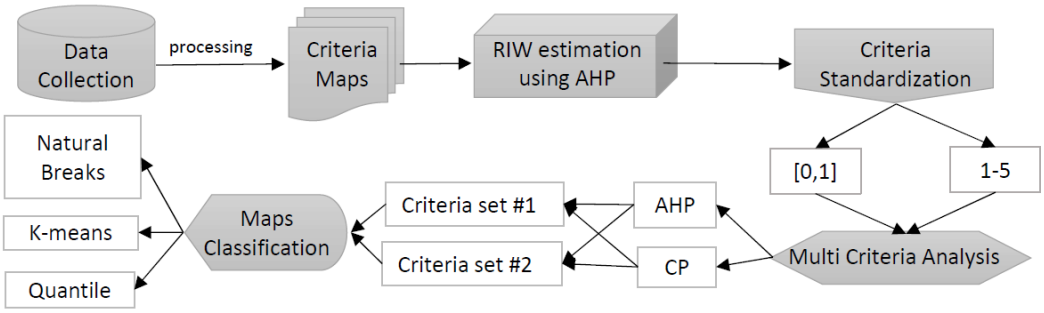

Figure 1. Methodology flowchart of the study's processes.

Results and concluding remarks

Combining different MCA methods, standardization techniques, sets of criteria, and rendering methods results in many maps, with some being more optimistic than others. In most cases, the maps produced using the [0,1] scaled criteria had higher suitability levels than the ones produced using the classified criteria. Similarly, AHP maps had similar results with the CP maps for p=1, which shows that AHP produced rather optimistic maps. The maps classified with the K-means and Quantile methods generally gave more optimistic maps than the ones classified with the Natural Breaks method. For the most part, there were no significant differences between the application of the two sets of criteria. The validation process against existing and/or proposed surface reservoirs further established the above findings. Figure 2 shows the CP map that was produced by the [0,1] criteria maps, using mean annual precipitation, for p=2 and Quantile classification and its visual validation for the proposed Pili reservoir.

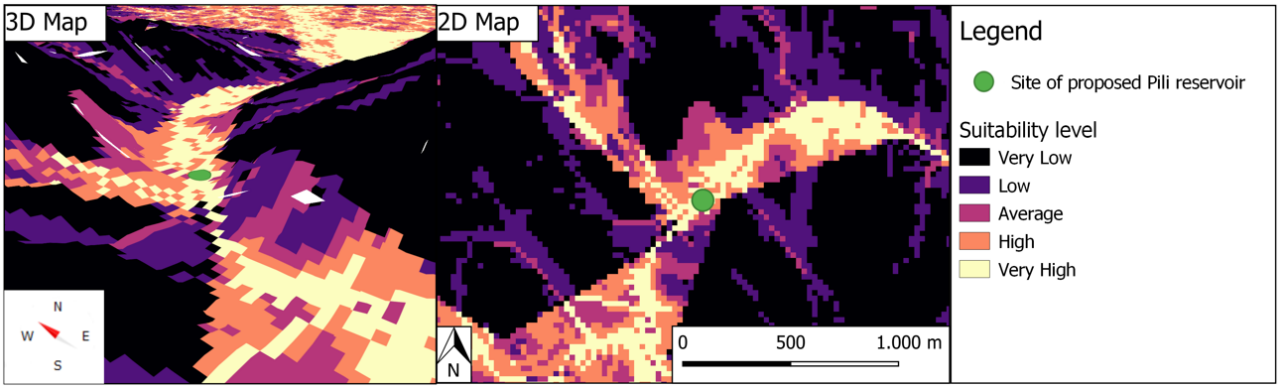

Figure 2. Results and visual validation for Pili reservoir of the [0,1], precipitation, Quantile rendered CP map for p=2.

References

Mbilinyi B, Tumbo S, Mahoo D, Mkiramwinyi FO (2007) GIS-based decision support system for identifying potential sites for rainwater harvesting. Physics and Chemistry of the Earth 32(15-18): 1074-1081. http://doi.org/10.1016/j.pce.2007.07.014

Al-Ghobari H, Dewidar AZ (2021) Integrating GIS-Based MCDA Techniques and the SCS-CN Method for Identifying Potential Zones for Rainwater Harvesting in a Semi-Arid Area. Water 13 (704): 1-16. https://doi.org/10.3390/w13050704

Feloni E, Mousadis I, Baltas E (2020) Flood vulnerability assessment using a GIS-based multi-criteria approach—The case of Attica region. Journal of Flood Risk Management 13(S1): 1-15. https://doi.org/10.1111/jfr3.12563

Demetsouka OE, Vavatsikos AP, Anagnostopoulos KP (2013) Suitability analysis for siting MSW landfills and its multicriteria spatial decision support system: Method, implementation and case study. Waste Management 33(5): 1190-1206. https://doi.org/10.1016/j.wasman.2013.01.030

VI. Water-Energy-Land-Food Nexus

12th World Congress on Water Resources and Environment (EWRA 2023)
"Managing Water-Energy-Land-Food under Climatic, Environmental and Social Instability"
Thessaloniki, Greece, 27 June - 1 July 2023

The use of non-conventional water resources for agricultural irrigation in the Segura basin in Spain

C. Villacorta[1*], I. Blanco[2], A. Gómez[3], P. Esteve[2]
[1] CEIGRAM, Universidad Politécnica de Madrid, Senda del Rey 13, 28040 Madrid, Spain
[2] Departemenr of Agricultural Economics, Statistics and Business Management, ETSIAAB, Universidad Politécnica de Madrid, Campus Ciudad Universitaria, Av. Puerta de Hierro 2-4, 28040 Madrid, Spain
[3] Department of Agricultural and Forestry Engineering, Universidad de Valladolid, Avda de Madrid 57, 34004, Spain
* e-mail: c.villacorta@upm.es

Introduction

Population growth and climate change are causing conventional resources to be unable to meet current and future water demands (Martínez-Álvarez et al. 2017). The Region of Murcia is characterized by a high plant production, representing 6.4% of the national total (del Villar et al. 2020), an arid climate and structural scarcity of water resources. The Tagus-Segura water transfer provides available resources to this region that suffers serious deficiencies (García-López et al. 2022), but after the approval of the new Tagus hydrological plan (PHT), there will be an increase in the ecological flows of this river, which will reduce by 17.5% the current maximum volume of the Tagus-Segura water Transfer.

The objective of this work is to study the impact of that reduction, and the contribution of unconventional resources, such as desalination and reclaimed water that represent a key tool to address water scarcity, adaptation to climate change and facilitate the implementation of a circular economy, since they reduce the exploitation of surface water resources and groundwater, achieving the improvement of ecosystems and pollution mitigation by discharging less wastewater into the environment (Navarro 2018).

Materials and methods

A farm-based mathematical programming model using positive mathematical programming (PMP) has been developed and calibrated to reproduce the situation observed in 2019, using the method of Blanco and Viladrich (2014). The model represents how the farm works technically and economically, which in this research will be taken by the Campo de Cartagena Irrigators Community (CRCC). The farmer is supposed to maximize a utility function (CRCC benefits) under area, labor, and water constraints. In this case, it should be noted that the CRCC has six water resources (surface water, Tagus-Segura water transfer, groundwater, seawater desalination, reclaimed water and brackish water desalination) with different supplies and prices.

The data were obtained from fieldwork carried out in mid-July 2022 and from the following databases: Area, yield, price, labor and costs of crops (del Villar et al. 2020), crop water needs (SIAR 2022), basic payment rights (MAPA 2022 and Order AAA/1747/2016), the availability and prices of water (Soto 2020) and groundwater (Custodio 2015).

Results and concluding remarks.

To study the impact of the reduction in Tagus-Segura water transfer on the use of the rest of the water sources and on the distribution of crops, three scenarios have been simulated. In scenario 1, the supply of the Tagus-Segura transfer has been reduced, due to the implementation of the new Tagus hydrological plan, as mentioned in the introduction, reducing it by 18.5%. When we compare it to the baseline situation, there is a decrease in margin of 11%, caused by the reduction of diversion and the increase in groundwater that is more expensive. If water use is reduced, crops with higher water needs are replaced by fallow and barley, such as melon and artichoke. When scenario 1 is already a reality, scenario 2 consists of replacing the reduction of the transfer with unconventional resources, increasing the supply equally between desalinated and reclaimed waters. In this case, the acreage of the crops is equal to that of the base scenario because the water use is the same. Despite the reduction of the transfer, unconventional sources increase

their use by 45% in the case of reclaimed water and 12% in desalinated water, another source that also increases is groundwater also increases with 14%. The greater growth of reclaimed water is due to the fact that its cost is lower than groundwater and desalinated water.

The increase in groundwater use is a problem, since it is a resource that is mostly deregulated, since it is managed by individual users without regulation by the hydraulic authorities, which causes the degradation of many aquifers (Calatrava et al. 2022). Therefore, as a solution, scenario 3 is proposed, which would be an evolution of the second, in which the cost of desalinated water would be reduced to 0.3828 €/m^3 VAT included, through the subsidy established in Royal Decree-Law 4/2022, of March 15. This would cause this resource to be used in front of the groundwater that would become the most expensive source of water.

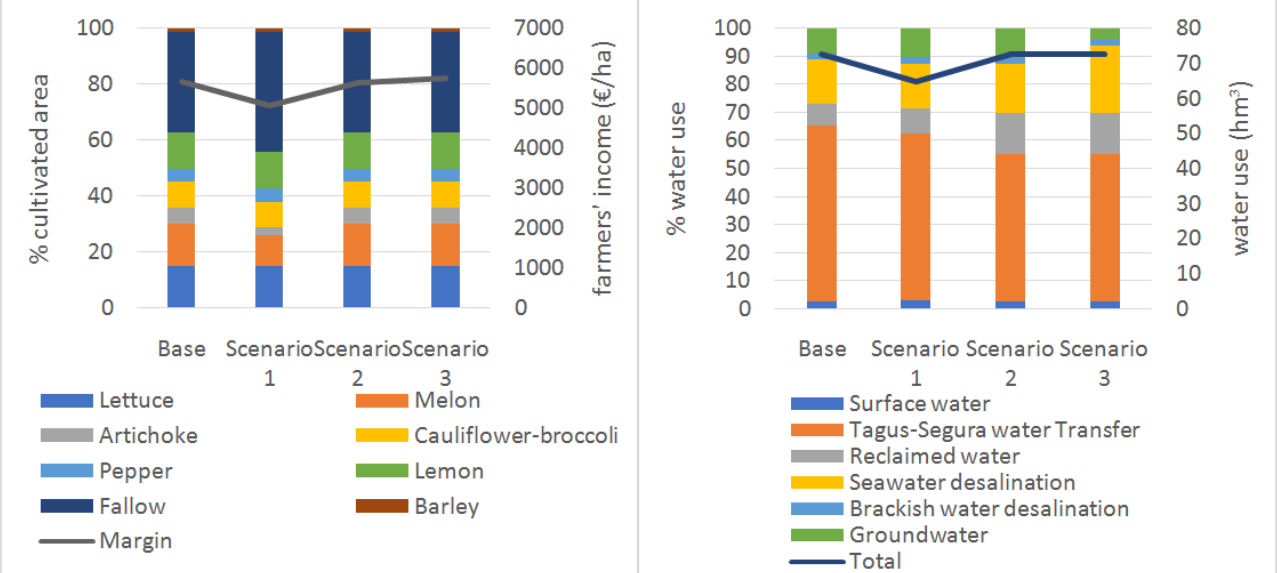

Figure 1. Cultivated area and farmers' income (left) and water use (right). Own elaboration.

In conclusion, non-conventional resources guarantee the availability of water when there is a reduction in conventional resources, therefore, it is necessary to bet on them, as the CRCC is doing, which has requested the processing of new desalinated water concessions, of which they have not yet received resolution as shown in their 2021/22 report. It has also carried out a study of alternatives for the construction of a new desalination plant. As for the reclaimed water, an improvement of the Torre-Pacheco WWTP is proposed, since currently its high salinity prevents its use, which could be achieved with the construction of a storm tank and a raft.

Acknowledgments: The research leading to these results has received funding from the Universidad Politécnica de Madrid (PhD grant in the context of the Own R+D+i Program) and the RECLAMO project (Grant No. PID2019-104340RA-I00, funded by MCIN/AEI/10.13039/501100011033)

References

Calatrava J, Martínez-Álvarez V, Martínez-Granados D (2022) Addressing aquifer overexploitation with desalinated seawater: an economic assessment of alternatives in south-eastern Spain. International Journal of Water Resources Development 38(2): 199-216. https://doi.org/10.1080/07900627.2021.1877635

García-López M, Montano B, Melgarejo J (2022) The Tariff Structure in the Tagus-Segura Water Transfer. Water 14(3): 413. https://doi.org/10.3390/w14030413

Martínez-Álvarez V, González-Ortega MJ, Martin-Gorriz B, Soto-García M, Maestre-Valero JF (2017) The use of desalinated seawater for crop irrigation in the Segura River Basin (south-eastern Spain). Desalination 422: 153-164. https://doi.org/10.1016/j.desal.2017.08.022

Navarro T (2018) Water reuse and desalination in Spain–challenges and opportunities. Journal of Water Reuse and Desalination 8(2): 153-168. https://doi.org/10.2166/wrd.2018.043

del Villar García A, Ortiz MIL, Moreno JM (2020) Valoración económica de las actividades agrarias en el Campo de Cartagena. Universidad de Alcalá e Instituto Universitario del Agua y las Ciencias Ambientales de la Universidad de Alicante, Alicante, Spain

The role of hydrogen in the storage of renewable energy sources for small non-interconnected islands

M. Bertsiou*, E. Baltas
Department of Water Resources and Environmental Engineering, School of Civil Engineering, NTUA, Athens, Greece
** e-mail: mbertsiou@chi.civil.ntua.gr*

Introduction

Climate change has highlighted the need for fossil fuel-free technologies, such as renewable energy sources (RES), to meet the world's electricity needs. Wind turbines can be applied to a wide range of applications. However, the increased proportion of RES in the power leads to the use of storage units to deal with the intermittent nature of wind and solar potential. In recent years, hydrogen has gained attention as a storage option in hybrid renewable energy systems (HRES). Hydrogen is produced locally and requires less space than other storage technologies (Yue et al. 2021). Conventional fuel-powered hydrogen production generates a large amount of carbon dioxide, however, green hydrogen, which uses RES for the electrolysis, is an environmentally friendly process (Yu et al. 2021). Recent publications on hydrogen storage focus on net present value (Hinokuma et al. 2021), cost of energy (Sultan et al. 2021; Phan and Lai 2019), consideration of the degradation of the components in the total performance (Ceran et al. 2021).

In this research work a Hybrid Renewable Energy System (HRES) in Fournoi island, Greece, is proposed for the energy and water demands of the island. The system is coupled with a desalination unit for the desalination of seawater for domestic and irrigation loads. An electrolyzer, a fuel cell and a hydrogen tank are used for the storage of excess energy. The novelty of this research study is summarized in the fulfilment of both water and energy demands using power to hydrogen technology. Results concerning the reliability of the system, and the environmental impact are presented.

Materials and methods

HRES consists of four wind turbines of 900 kW each. The produced energy from the wind turbines (WTs) is based on the wind potential and calculated according to the power curve, given by the manufacturer. Energy from WTs is calculated, and domestic water needs are met in priority, then the irrigation needs and finally the electrical needs. The time step is hourly ensuring the maximum reliability of the results. Excess of the energy produced by WTs is led to electrolysis. The electrolyzer should be able to convert RES into hydrogen and in this study is equal to 3.5 MW, while the fuel cell should be able to cover the uncovered load and is equal to 1.9 MW. The hydrogen tank is considered to provide an autonomy of two days and has been calculated equal to 1,860 kg. The mode of operation of the electrolyzer, the fuel cell and the hydrogen tank are presented in Bertsiou and Baltas (2022). Excess energy that is converted to hydrogen, through water electrolysis, is stored to the hydrogen tank. When there is a shortage of demand, this hydrogen in converted to energy through the fuel cell to cover the unmet loads. Demand that can be covered neither by the WTs nor by the fuel cell is covered by the local power system (LPS).

Loss of load probability (LOLP) refers to the probability that a power system is unable to meet the demand for electricity at a certain point in time. It is typically expressed as a percentage and calculated by taking the total number of hours in a given time period during which the demand for electricity exceeded the available supply, divided by the total number of hours in that time period. The resulting value is usually expressed as a percentage, with a lower value indicating a more reliable power supply. In this study, LOLP is estimated for each demand, domestic water, irrigation water, electric load and the entire operation of the HRES.

To calculate the eliminated CO_2 quantities in tons per year, by the integration of the HRES in the grid of the island, the following equation (1) is used.

$$EM_{CO2} = (E_{WT}(F_{GRID} - F_{WT}))/10^6 \quad (1)$$

where E_{WT} is the energy in kWh produced by the WTs, F_{WT} is the emission factor of wind technologies and is equal to 13.7 g CO_2/kWh (El-houari et al. 2021) and E_{GRID} is the emission factor of the grid, which is equal to 479.2 g CO_2/kWh for the year 2020, according to greenhouse gas emission intensity of electricity generation by the country datasheet.

Results and concluding remarks

Three different sources contribute to the energy mix of the island, the WTs, the hydrogen storage and the LPS. Results for one-year data show that energy from WTs contributes 54.8% to the total demand, while energy from the FC contributes 19.8%. The rest 25.4% of the total demand (desalinated water and electric load) is given by the LPS. The percentage of the fuel cell shows that without the hydrogen storage system, a large percentage of the energy from the wind turbines would be rejected and 20% of the total needs that are covered by the fuel cell would necessarily be covered by the LPS, which operates with conventional fuels. Therefore, in addition to WTs, this HRES contributes to the reduction of CO_2 further, by using the storage hydrogen system. Also, it appears that for two months of a year, September and October, HRES can fully cover the needs of the island without using the LPS.

Results about the loss of load probability show 14.67% for domestic water, 25.64% for irrigation water, 26.54% for electric load and 25.46 for the operation of the HRES. This means that this system can fulfill over 75% of the total demands. Especially concerning domestic water, this percentage is equal to 85%, which is quite satisfactory, especially for the case of the islands where the alternative supply of desalinated water is through the use of tankers which leads to a fairly high cost of cubic water.

By the integration of the HRES in the grid of the island, the eliminated CO_2 quantities in tons per year, show that 2,221 tn/year can be eliminated by the operation of this system in a Greek island. Considering the price of a ton of CO_2 in the market on 7 December 2022, this price is converted to 197,527 €.

References

Yue M, Lambert H, Pahon E, Roche R, Jemei S, Hissel D (2021) Hydrogen energy systems: A critical review of technologies, applications, trends and challenges. Renewable and Sustainable Energy Reviews 146: 111180. https://doi.org/10.1016/j.rser.2021.111180

Yu M, Wang K, Vredenburg H (2021) Insights into low-carbon hydrogen production methods: Green, blue and aqua hydrogen. International Journal of Hydrogen Energy 46(41):21261-21273. https://doi.org/10.1016/j.ijhydene.2021.04.016

Hinokuma T, Farzaneh H, Shaqour A (2021) Techno-economic analysis of a fuzzy logic control based hybrid renewable energy system to power a university campus in Japan. Energies 14: 1960. https://doi.org/10.3390/en14071960

Sultan HM, Menesy AS, Kamel S, Korashy A, Almohaimeed SA, Abdel-Akher M (2021) An improved artificial ecosystem optimization algorithm for optimal configuration of a hybrid PV/WT/FC energy system. Alexandria Engineering Journal 60(1): 1001-1025. https://doi.org/10.1016/j.aej.2020.10.027

Phan BC, Lai YC (2019) Control strategy of a hybrid renewable energy system based on reinforcement learning approach for an isolated microgrid. Applied Sciences 9(19):4001. https://doi.org/10.3390/app9194001

Ceran B, Mielcarek A, Hassan Q, Teneta J, Jaszczur M (2021) Aging effects on modelling and operation of a photovoltaic system with hydrogen storage. Applied Energy 297: 117161. https://doi.org/10.1016/j.apenergy.2021.117161

Bertsiou MM, Baltas E (2022) Power to Hydrogen and Power to Water Using Wind Energy. Wind 2(2):305-324. https://doi.org/10.3390/wind2020017

El-houari H, Allouhi A, Salameh T, Kousksou T, Jamil A, El Amrani B (2021) Energy, Economic, Environment (3E) Analysis of WT-PV-Battery Autonomous Hybrid Power Plants in Climatically Varying Regions. Sustainable Energy Technologies and Assessments 43: 100961. https:// doi. org/ 10. 1016/j. seta. 2020. 100961

12th World Congress on Water Resources and Environment (EWRA 2023)
"Managing Water-Energy-Land-Food under Climatic, Environmental and Social Instability"
Thessaloniki, Greece, 27 June - 1 July 2023

Discourse over the sustainability of irrigation with desalinated water in light of the water-energy-food nexus

B. Zolghadr-Asli[1,2*], N. McIntyre[1], S. Djordjevic[2], R. Farmani[2], L. Pagliero[1], D. Aitken[1]
[1] *Sustainable Minerals Institute, University of Queensland, Brisbane, Australia*
[2] *Centre for Water Systems, University of Exeter, Exeter, UK*
** e-mail: bz267@exeter.ac.uk; b.zolghadrasli@uq.net.au*

Introduction

Desalinated seawater has gained increasing popularity as an option for water-stressed regions worldwide to meet a general increase in water demand across most sectors. Considering current water and food crises that are exacerbating in many regions, desalination has gained traction as a suitable solution to alleviate these problems as a potentially limitless alternative water source. The agricultural industry is the largest global water consumer and the sector that is most likely to benefit from this technology to meet the increasing demand for irrigation. Despite the technology's considerable potential, there are numerous issues related the technology's sustainability that may prevent it from becoming a widely used solution for irrigation purposes. However, being affected by numerous interconnected factors, water resources problems are nuanced and multi-disciplinary. To account for these intricacies in the evaluation of the sustainability of this option for irrigation, the concept of the Water-Energy-Food (WEF) Security Nexus can be used. This paper provides a preliminary evaluation of the sustainability of the use of desalinated water for irrigation considering the WEF Security Nexus.

Materials and methods

Figure 1 depicts the general role of desalinated water in the WEF nexus. Though the impacts of irrigating with desalinated water are ideally determined on a case-by-case basis, there are general concerns that are similar across cases. From an agronomic perspective, these concerns are (I) a lack of essential nutrients; (II) phytotoxicity of chemical components such as Boron, Chloride, and Sodium; (III) risk of soil sodicity; and (IV) low alkalinity of desalinated water (Martin-Gorriz et al. 2021). These problems could, in turn, be manifested in reduced crop quality, crop yield, and disease resistance. Concerning environmental impacts, some of the most frequently cited issues are: (I) marine ecosystem impingement and entrainment; (II) visual and noise impacts; and (III) the overall greenhouse gas (GHG) emissions. GHG emissions are mostly related to the energy-intensive nature of this technology. The use of this technology, however, could also have some potential environmental benefits. Introducing desalinated water to a region for irrigation can be viewed as an additional component of the local hydrological cycle, which could help support the condition of the cycle at a regional scale (Pistocchi et al. 2020). This could also reduce the pressure on other exhausted water resources. The economic issues are another aspect that need to be addressed, as the overall cost of desalinated water is often high enough to leave little to no profit margin for most commercial crops. Figure 2 depicts a SWOT (strengths, weaknesses, opportunities, and threats) analysis for irrigation with desalinated water.

Experience has shown that while these issues can cause significant problems if not addressed correctly and promptly, they are manageable for the most part. Nevertheless, case-by-case evaluation is required to determine the applicability of these strategies. However, evaluating the effectiveness of such strategies comprehensively requires a perspective that goes beyond the conventional framework. The WEF Security Nexus is a relevant concept to shape such discourse regarding the sustainability of irrigation with desalinated water. Our studies show that based on the WEF-based paradigm of thinking, there are two main ideas to address the previously mentioned problems, namely, *prophylactic,* and *reactive* strategies. Prophylactic methods tend to address a problem before any significant impact appears. These strategies are based on regionally specific planning and management decisions that optimize the system for specific

conditions. These include creating a monitoring and regular maintenance plan, choosing an appropriate desalination technology or incorporating a cost-effective energy source. Socio-economic-oriented solutions can also be seen as prophylactic strategies. For instance, *water markets*, if put in place prior to operating the desalinated water supply, could be seen as a socio-economic strategy. Southeast Spain has temporarily exercised this strategy on a limited scale (Aznar-Sánchez et al. 2017). Planning renewable energy resources at the same time as planning the desalinated water supply is another prophylactic move that can mitigate the environmental impacts of desalination (Tubi and Williams 2021). Reactive strategies, on the other hand, aim to devise a procedure to address a specifically targeted issue. These are, for the most part, ad-hoc approaches that must be personalized to site-specific circumstances. Filtering sludge and brine, mixing different water resources to create a more suitable batch on farm sites, or installing energy recovery devices in the desalination units are some of the most known reactive strategies. In practice, a combination of prophylactic and reactive strategies is needed to address the potential impacts of desalination.

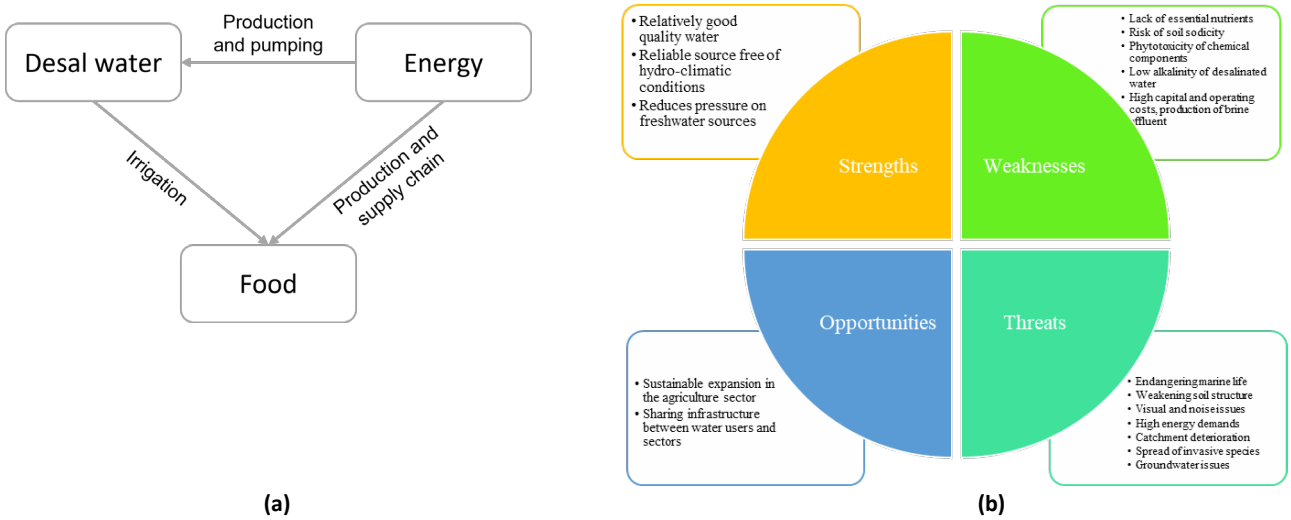

Figure 1. a) The general role of desalination in the WEF nexus; b) SWOT analysis for irrigating with desalinated water.

Concluding remarks

With the water and food crises exacerbating worldwide, it is essential to reconsider how water resources management must adapt to this new era. While the use of desalinated seawater looks to be an important part of the solution, there remain concerns regarding the sustainability of using desalinated water for irrigation. These concerns need to be investigated and understood to allow appropriate mitigation measures to be developed to avoid adverse impacts. Given the multi-faceted nature of the context and related issues, conventional assessment frameworks are not the ideal tool for sustainability analysis. Reinterpreting this issue within the context of the WEF Security Nexus may provide a more realistic and applicable understanding of the benefits and drawbacks of this technology. Overall, our findings suggest that, while there are problems with this practice in the context of the agriculture industry, these issues can be managed through the right strategic course of action on a case-by-case basis. A more comprehensive analysis that considers multiple case studies across different contexts will help develop the understanding of the sustainability of the use of desalinated seawater for irrigation and support the development of mitigation strategies.

References

Aznar-Sánchez JA, Belmonte-Ureña LJ, Valera DL (2017) Perceptions and acceptance of desalinated seawater for irrigation: A case study in the Níjar district (Southeast Spain). Water 9(6): 408

Martin-Gorriz B, Martínez-Alvarez V, Maestre-Valero JF, Gallego-Elvira B (2021) Influence of the water source on the carbon footprint of irrigated agriculture: A regional study in South-Eastern Spain. Agronomy 11(2): 351

Pistocchi A, Bleninger T, Breyer C, Caldera U, Dorati C et al. (2020) Can seawater desalination be a win-win fix to our water cycle? Water Research 182: 115906

Tubi A, Williams J (2021) Beyond binary outcomes in climate adaptation: The illustrative case of desalination. Wiley Interdisciplinary Reviews: Climate Change 12(2): e695

12th World Congress on Water Resources and Environment (EWRA 2023)
"Managing Water-Energy-Land-Food under Climatic, Environmental and Social Instability"
Thessaloniki, Greece, 27 June - 1 July 2023

A novel methodology to predict the thermal powerplants' water consumption in the context of water-electricity-climate nexus

C. Coskun Dilcan[1,2*], M. Aydinalp Koksal[1]
[1] Hacettepe University, Environmental Engineering Department, Ankara, Turkey
[2] Present address: Ankara University, Water Management Institute, Ankara, Turkey
* e-mail: coskunc@ankara.edu.tr

Introduction

Energy and water are the primary resources that have an interdependent relationship in the meaning of sustainability (Hadian and Madani 2013). This strong dependence on available water resources for electricity generation will further exacerbate existing vulnerabilities in the energy-water nexus context with climate change's negative impacts on water quality and quantity (Behrens et al. 2017). Some research about climate effects on the water-energy nexus, like Bogmans et al. (2017), indicated that heat waves, droughts, and low river flow might impact electricity generated by thermal power plants for decades. In the study of Petrakopoulou et al. (2020), the effect of rising ambient air temperatures and cooling water temperatures on power plant performance was investigated. The cooling water quantity of coal-fired plants was found to be sensitive to temperature differences compared to coal-to-natural gas plants. The efficiency of natural gas plants was more sensitive to temperature changes overall. But in the literature, there is a lack of studies including the nonlinear relationship with the artificial intelligence approach, which can interconnect the climate, electricity production, and the water consumption prediction of thermoelectric power plants. So, the main objective of this study is to determine the interaction between the water-electricity-climate of thermoelectric power plants with a new model approach via using ANFIS for sustainable resource management.

Materials and methods

The adaptive neuro-fuzzy inference system (ANFIS), proposed by Jang (1993) is a method for tuning the existing rule base of a fuzzy inference system (FIS) whose membership functions are adjusted using the adaptive learning capability of an artificial neural network (Jang 1993). MATLAB Neuro-Fuzzy Designer Toolbox was used as a modeling tool for model development which supports easy creation and modifying the ANFIS model properties. The input and output parameters of 70 thermoelectric plants above 100 MW installed capacity in Turkey were integrated into the study. Basin-based meteorological data, including global climate models (GFDL, HDGM, MPI) from the CMIP5 archive, was obtained from The Turkish State of Meteorological Service. The meteorological data as an annual average and maximum temperature (°C) between 1990 and 2000 were used to develop the ANFIS model to estimate the water consumption of thermoelectric power plants depending on their basins' location to be able to cover a large area depending on characteristic climatic features. The annual average electricity generation, fuel type, and cooling type parameters of 70 thermoelectric plants with installed capacity above 100 MWe were gathered from The Electricity Generation Corporation, Energy Exchange Istanbul (EXIST), and open sources. The water consumption (m^3) was the output, and the other parameters were input for developing ANFIS models. The cooling system and fuel types of plants were categorized from 1 to 3. and summarized in Table 1.

Descriptive statistics are used to describe the basic features of input parameters used in this study and are given in Table 2.

All data is divided into a training and testing dataset by the ratio of 65-35%, 70-30%, 80-20%, and 85-15% randomly for all average and maximum temperatures of Gfdl, Hdgm, and MPI climate reference data, respectively. The three most commonly used statistical measures to determine the model's prediction accuracy are root mean square error (RMSE), mean absolute percent error (MAPE), and coefficient of determination (R-square). In the following formulas, X_i is simulated, Y_i is the actual variable, and m is the

number of variables.

$$RMSE = \sqrt{(1/n * \sum (X_i - Y_i)^2)} \quad (1)$$

$$MAPE = (100\%/n * \sum |e_t - y_t|) \quad (2)$$

Table 1. Categorization of power plants depending on fuel and cooling system types.

Fuel Type	Category	Cooling System Type
Lignite	1	Wet cooling type
Imported Coal/ Hard Coal/ Asphaltite	2	Once-through type
Natural Gas	3	Dry cooling type

Table 2. Descriptive statistics of the input and output parameters.

Input & Output Parameters	Statistical data			
	Ranges	Mean	SD	Units
Annual Avg. Generation	147 – 17216	3060.51	2965.98	(GWh)
Annual Max Temperature	13.46 - 20.45	17.24	1.69	(^{0}C)
Annual Avg. Temperature	8.62 - 15.38	12.37	2.00	(^{0}C)
Fuel Type	1 - 3	-	-	-
Cooling system type	1 - 3	-	-	-
Annual Avg. Water Consumption	1,102.5 – 23,916,900	3,027,528.56	4,383,661.07	(Mm^3)

Results and concluding remarks

The ANFIS model, including average temperature input, resulted in 0.99%, 0.54%, and 0.53% MAPE of training data for Hdgm, MPI, and GFDL climate scenarios, respectively. The testing data results were about 4.73%, 4.63%, and 4.62% for Gfdl, Hdgm, and MPI, respectively (Table 3).

The ANFIS model with average temperature resulted better in MAPE % than the ANFIS model that was constructed with maximum temperature. The average temperature, electricity generation, fuel, and cooling system types could be used in ANFIS modeling as input parameters. At the same time, the water consumption is output one for estimating the thermal power plant's water consumption in the context of the water-electricity-climate nexus.

Table 3. Comparison of ANFIS models of thermal PPs with different temperature inputs.

MAPE %	Temp. °C	Data Splitting Percentage (Train-Test)														
		65-35%			70-30%			75-25%			80-20%			85-15%		
		Train	Test	All	Train	Test	All	Train	Test	All	Train	Test	All	Train	Test	All
GFDL	**Avg.**	0.48	13.56	4.96	0.20	7.15	2.29	1.49	11.17	3.84	0.44	5.67	1.48	0.55	**4.73**	1.15
	Max.	0.08	9.30	3.24	0.18	7.80	2.47	1.90	11.15	4.14	0.80	5.38	1.71	2.02	6.00	2.59
HDGM	**Avg.**	0.48	13.38	4.90	0.18	7.20	2.29	1.49	11.61	3.95	0.39	6.66	1.64	0.99	**4.63**	1.51
	Max.	0.47	13.44	4.92	0.19	7.92	2.51	1.93	12.06	4.39	0.65	6.16	1.75	2.09	5.19	2.54
MPI	**Avg.**	0.47	13.41	4.91	0.19	7.17	2.28	1.49	10.38	3.65	0.43	4.48	1.24	0.54	**4.62**	1.12
	Max.	0.09	9.10	3.18	0.20	7.46	2.38	2.09	10.09	4.03	0.70	6.17	1.79	2.01	6.13	2.59

Acknowledgments: The authors acknowledge the support of the Turkish State of Meteorological Service, The Electricity Generation Corporation (EUAS), and Energy Exchange Istanbul (EXIST).

References

Behrens P, van Vliet M, Nanninga T et al. (2017) Climate change and the vulnerability of electricity generation to water stress in the European Union. Nat Energy 2: 17114. https://doi.org/10.1038/nenergy.2017.114

Bogmans CW, Dijkema GP, van Vliet MT (2017) Adaptation of thermal power plants: The (ir)relevance of climate (change) information. Energy Economics 62: 1-18. https://doi.org/10.1016/j.eneco.2016.11.012

Hadian S, Madani K (2013) The water demand of energy: Implications for sustainable energy policy development. Sustainability 5: 4674-4687. https://doi.org/10.3390/su5114674

Jang JSR (1993) ANFIS: Adaptive-Network-Based Fuzzy Inference System. IEEE Trans. Syst. Man Cybern 23(3): 665–685

Petrakopoulou F, Robinson A, Olmeda-Delgado M (2020) Impact of climate change on fossil fuel power-plant efficiency and water use. Journal of Cleaner Production 273: 122816. https://doi.org/10.1016/j. jclepro.2020.122816

12th World Congress on Water Resources and Environment (EWRA 2023)
"Managing Water-Energy-Land-Food under Climatic, Environmental and Social Instability"
Thessaloniki, Greece, 27 June - 1 July 2023

Monitoring and modelling multilayer green roofs effectiveness for thermal insulation of buildings: The experimental blue-green roof of Palermo

D. Pumo*, G. Brucato, F. Alongi, L.V. Noto
Department of Engineering, University of Palermo, Palermo, Italy
** e-mail: dario.pumo@unipa.it*

Introduction

Several Nature Based Solutions (NBSs) have been proposed to improve cities resilience to climate change and have been widely recognized as sustainable and low-cost solutions, able to restore natural processes and mitigate the impact of pluvial floods and warming in urban areas (e.g., Seddon et al. 2021). Green Roofs (GRs) are among the most important NBSs to deal with urban challenges, since they provide several benefits such as contributing to the reduction of the Urban Heat Island (UHI) effect and providing greater thermal insulation to buildings. Moreover, GRs facilitate the increase of urban biodiversity, improve the buildings aesthetic value and favour human well-being. Multilayer GRs, or Blue-Green Roofs (BGRs), have an additional layer (Blue Layer–BL) to retain rainwater, usually equipped with a valve that allows for regulating water storage. BGRs are still scarcely explored in literature due to their recent development. An overview of the key constructive elements of BGRs and their hydrological and thermal benefits in Mediterranean urban areas is provided in Cristiano et al. (2022) where preliminary monitoring results from four different experimental sites in Italy have been discussed. The hydrological effectiveness of BGRs in term of retention function is deeply analyzed in Pumo et al. (2023) for a case study in Palermo city, Italy. Thermal advantages of GRs were widely studied in the past, while analogues analysis on BGRs are still lacking. What are the thermal benefits that a BGRs can provide compared to traditional GRs? How can we model the thermal response of BGRs to climatic forcings? This study tries to address such research questions through the analysis of an experimental BGR prototype installed on the Department of Engineering's roof at the University of Palermo, Italy. The specific aim of the present work is to focus on thermal system properties and analyze the results regarding a monitoring period of over two years, trying to infer the potential thermal advantages related to the use of BGRs in an urban Mediterranean context. Another specific objective of the research is to develop a model able to reproduce the thermal response of the system. More specifically, the suitability of two different models is analyzed and compared: a physically based model, implemented within the EnergyPlus building energy simulation program, and a data-driven soft computing-based model, i.e., a Multi-Layers Perceptron Artificial Neural Network. EnergyPlus (https://energyplus.net) is a free, open-source, and cross-platform, developed by the U.S. Department of Energy's (DOE) Building Technologies Office (BTO).

Materials and methods

The present work describes a technologically advanced BGR. The system has an extension of almost 33 m^2 and is made of two areas with different soil thickness having a substrate of a mixture of volcanic materials covered by different Mediterranean vegetation (e.g., *sedum album*, *trifolium angustifolium*, *rosmarinus officinalis*, *lavandula spica)*, with sedum and meadow species in the shallower region and perennial and aromatic species in the remaining region. A remotely controlled "smart" weir allows for regulating discharge outflow and water storage. An equal size "GREY" roof bordering the BGR is also monitored for comparison. A Polder Roof integrated monitoring system includes sensors for the real time observation of several variables such as precipitation, air temperature, wind speed, and water levels within the BL. Other data used in this study are collected by a pre-existing advanced weather monitoring system, located close to the experimental site, which includes three different sensors for rainfall monitoring and a meteorological weather station, equipped with a thermo-hygrometer sensor. Outflow water volumes from the GREY and the BGR are conveyed toward two external rain barrels and continuously measured by a

couple of pressure sensors. Finally, a network of four thermometers have been installed at different points of the experimental of both the BGR and GREY roof: a couple of sensors is installed at vertical corresponding positions in the upper (outdoor) and bottom (indoor) surfaces of the two roofs. The period considered in the present study covers about two years (from Dec. 2020 to Dec. 2022). The 30-min time series of temperature from the four sensors and air temperature are used to evaluate some typical GR's thermal indices, such as the surface temperature reduction, the external temperature ratio and the temperature excursion reduction (Bevilacqua et al. 2017; Cristiano et al. 2023).

Results and concluding remarks

This study contributed to the quantitative assessment of some potential benefits related to the use of BGRs in a Mediterranean context. The analysis of temperature over the monitoring period, shown in Figure 1, demonstrated that the BGRs in a semiarid environment are expected to further improve building thermal insulation compared to traditional GRs, especially during the hotter summer conditions. The system was able to reduce the external roof surface temperature, which is also reflected in a lowering of the temperature at the indoor roof surface, and attenuate the daily temperature excursion of both outdoor and indoor roof surfaces. Our outcomes provided clear insight of a higher thermal insulation capacity and thermal inertia of the vegetated roofs, with possible advantages in terms of reduction of the building's energy demand and attenuation of the well-known UHI effect. EnergyPlus simulation has provided satisfying performances in reproducing the thermal response of the system during the reference period, and it could allow for further specific investigations on the advantages of BGRs in terms of reduction of energy consumption for internal air conditioning. Comparable performances have been obtained using an ANN, which represents a much simpler approach than physically based ones, in terms of model parameterization. Both methods represent fundamental tools for evaluating the potentialities of BGRs under future scenarios impacted by climate change.

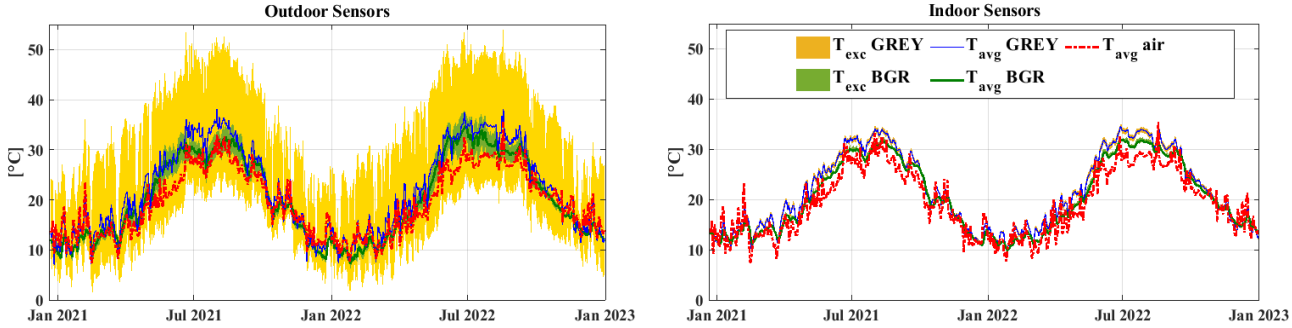

Figure 1. Outdoor (right panel) and indoor (left panel) roof surface average daily temperature (T_{avg}) and daily temperature excursions (T_{exc}) for both the BGR and the GREY rooftop and average air temperature (T_{avg} air, red lines).

Acknowledgments: The work was developed within the project "Multilayer Green Roofs: multipurpose nature-based solutions towards sustainable and resilient cities" (NextGenerationEU –MUR D.M. 737/2021).

References

Bevilacqua P, Mazzeo D, Bruno R, Arcuri N (2017) Surface temperature analysis of an extensive green roof for the mitigation of urban heat island in southern Mediterranean climate. Energy and Buildings 150: 318-327

Cristiano E, Annis A, Apollonio C, Pumo D, Urru S, Viola F et al. (2022) Multilayer blue-green roofs as nature-based solutions for water and thermal insulation management. Hydrology Research 53(9): 1129–1149. https://doi.org/10.2166/nh.2022.201

Pumo D, Francipane A, Alongi F, Noto LV (2023) The potential of multilayer green roofs for stormwater management in urban area under semi-arid Mediterranean climate conditions. Journal of Environmental Management 326: 116643. https://doi.org/10.1016/j.jenvman.2022.116643

Seddon N, Smith A, Smith P, Key I, Chausson A, Girardin C, House J, Srivastava S, Turner B (2021) Getting the message right on nature-based solutions to climate change. Glob. Change Biol. 27: 1518-1546. https://doi.org/10.1111/gcb.15513

Developing a smart integrated platform for leakage detection on water supply network of municipality of Argos, Greece

A. Chasiotis[1], S. Chasiotis[1], P.T. Nastos[1], E. Feloni[1], M. Bousdeki[1], T. Manthos[1], E. Minakaki[1], C. Theodorakis[1], K. Sakellariou[1], T. Kyriakidis[2], M. Louta[2]
[1] *Laboratory of Climatology and Atmospheric Environment, Faculty of Geology and Geoenvironment, National and Kapodistrian University of Athens, University Campus 15784, Zografou, Athens, Greece*
[2] *Telecommunication Networks and Advanced Services (TELNAS) Laboratory, Department of Electrical and Computer Engineering, University of Western Macedonia, Campus ZEP 50100, Kozani, Greece*
** e-mail: a.chasiotis@geol.uoa.gr*

Introduction

Non-revenue water (NRW) is the volume of water that participates in the urban water supply processes (i.e., water extraction, transport, treatment, storage, distribution, and consumption) but does not generate revenues for the water utility company (Janson 2017). NRW is divided into two main categories: water losses and unbilled consumption (Liemberger and Frauendorfer 2010). Pressure management, active leak control, speed and quality of repairs and asset management are the four strategies to reduce real losses (Kingdom et al. 2006).

Water leakages in the internal water supply networks of cities are the most common and, at the same time, the most important problem water utility companies face (Lechevallier 2014). Indicatively, the cost of leakages is estimated at 39 billion USD per year (Liemberger and Wyatt 2019), while, apart from this cost, the impact on potable water quality is also important, which monitoring is still not easy (Patelis et al. 2020). In Argos (Greece), according to the Municipal Enterprise for Water and Wastewater of Argos (DEYA.ARM), water leakage is estimated around 65%, an amount that cannot be accurately calculated, not even monitored. Trying to deal with this issue, one of the main purposes of the research project entitled "Smart integrated platform for Leakage Detection of water supply Network of Municipality of Argos" is to develop a smart monitoring system that is estimated to contribute to saving up to 1,200,000 cubic meters water per year in the internal water network of the city of Argos. This work presents the general framework of the project.

Materials and methods

The system is designed for the city of Argos, which is served by DEYA.ARM. Argos is the largest city in Argolis Prefecture with a total population of 26.361 habitants. It is one of the warmest Greek cities, with very high temperatures during summer months, when temperature often exceeds 40°C, and it often reaches 47°C during heatwaves. Winter is mild with low total precipitation depth.

According to DEYA.ARM, the water supply network of the Municipality is divided into two parts: (i) the main network that serves the city of Argos and the city's surrounding area, and (ii) local networks in other municipal areas. Regarding exploitation of local water resources, the city of Argos is supplied by the springs of Lerna and Amymone, located approximately 10 km to the South, in the coastal settlement of Mylon.

Regarding water requirements in this area, there is a seasonal fluctuation due to tourism, with an increased demand during summer months, which is difficult to be fully met. Particularly, Table 1 presents the estimated daily water needs per capita, which correspond to an annual water supply from the DEYA.ARM around 2,5 hm^3. Considering this situation and after taking into account the available data from the local system operation and water supply infrastructures, DEYA.ARM in collaboration with the Laboratory of Climatology and Atmospheric (LACAE), assessed the value of improving the water supply system operation, through setting as first priority the monitoring of quality and quantity-related parameters in combination with the development of a hydraulic model for the water supply network of Argos city.

Table 1. Daily water needs per person (data source: River Basin Management Plans, in the frame of Water Framework Directive 2000/60/EC).

Population class	Water needs (l/cap/d)
Permanent Population	250
Tourists	400
Residents in B' residence	250
Total	**900**

Expected results and contribution

In the frame of this project, DEYA.ARM will acquire a smart integrated platform for leakage detection on the water supply network, through utilizing modern digital telemetry, remote control and management, and through procuring the sensors required to record and monitor consumption.

The implementation of the project is estimated to upgrade and modernize the operation of the existing water supply network in the city of Argos, as parts of the existing network will be restored, and also an efficient system for monitoring and detecting water leakage will be installed. This modernization of the network will prevent further consumption of valuable local resources and will also contribute to diminishing NRW (Antzoulatos et al. 2020). In addition, in the frame of the smart integrated platform development, a water leakage monitoring system will be designed based on the minimum night flow analysis.

The optimization of operation and management regarding water resources distribution will be based on the installation of remote-control systems at specific points in the city of Argos, to actively control leakage and remotely monitor several critical parameters. Through the operation of automation systems with programmable logic controllers (PLC) and Data Logger, the sensors' installation and the water parameters' monitoring parameters will further provide valuable data for the rational management of water supply infrastructures and local water resources in the area. These improvements in the overall operation of the closed water supply zone of the city of Argos are estimated to contribute to saving up to 1,2 hm^3 of fresh water per year.

Acknowledgments: The research project entitled "Smart integrated platform for Leakage Detection of water supply Network of Municipality of Argos" is co-funded by the Program "Water management" of EEA Grants 2014-2021, with the contribution of Iceland, Liechtenstein and Norway, and the Greek Public Investments Program. Authors would like to thank the Municipal Enterprise for Water and Wastewater of Argos for the provision of available data regarding water consumption.

References

Antzoulatos G, Mourtzios C, Stournara P, Kouloglou I-O, Papadimitriou N, Spyrou D, Mentes A, Nikolaidis E, Karakostas A, Kourtesis D, Vrochidis S, Kompatsiaris I (2020) Making urban water smart: the SMART-WATER solution. Water Science & Technology 82(12): 2691–2710

Janson N (2017) Current governance and performance of the water supply and sanitation sector in the Caribbean. In: IDB/GOJ Conference: Financing Water Utilities of the Caribbean – Towards Efficient and Financially Sustainable Services, Kingston, Jamaica

Kingdom W, Liemberger R, Marin P (2006) The Challenge of Reducing Non-Revenue Water (NRW) in Developing Countries – How the Private Sector Can Help: A Look at Performance-Based Service Contracting, WSS Sector Board Discussion, World Bank, DC, USA

Lechevallier M (2014) The impact of climate change on water infrastructure. American Water 0.5942/jawwa.2014.106.0066

Liemberger R, Frauendorfer R (2010) The Issues and Challenges of Reducing Non-Revenue Water. Asian Development Bank, Mandaluyong, Philippines

Liemberger R, Wyatt A (2019) Quantifying the global non-revenue water problem. Water Supply 19(3): 831-837

Patelis M, Kanakoudis V, Kravvari A (2020) Pressure Regulation vs. Water Aging in Water Distribution Networks. Water 12(5): 1323

Understanding the impacts of droughts on winter wheat growth in the Po Valley (Italy) through vulnerability curves

I. Borzì[1*], B. Monteleone[2], M. Arosio[2], B. Bonaccorso[1], M. Martina[2]
[1] Department of Engineering, University of Messina, Italy
[2] IUSS University School for Advanced Studies–Pavia, Italy
* e-mail: iolanda.borzi@unime.it

Introduction

The Agricultural sector is responsible for 72% of water withdrawals worldwide (FAO 2021), and its water demand is expected to increase in the next years to meet the increasing need for food production without expanding harvested areas. Today 77% of croplands are rainfed; only 23% of crops are irrigated (Rosa et al. 2020). Thus, agriculture is highly affected by drought events.

The allocation of water resources has a crucial role to ensure the sustainability of agriculture and to meet the global food demand. As remarked by Rey (2017), the increased frequency of droughts will require in future more collaborative partnership-based approaches to water resources and drought management. Therefore, understanding drought impacts on agriculture is essential to ensure the sector's sustainability and to develop effective water allocation strategies.

This study examines the vulnerability of winter wheat to water stress due to drought by implementing crop-specific vulnerability curves which relate water stress with yield losses. The curves are developed for various crop growth stages and their combinations and indicate in which crop growth stage irrigation is required to avoid irreparable yield losses or crop failure.

The developed curves are tailored to the Po Valley, the selected case study area. The Po Valley represents the main Italian agricultural area accounting for 35% of the national agricultural production (Musolino et al. 2019). Cereals are the main crops.

The Po Valley has been usually characterized by an abundance of water resources. In the past, this abundance has often led to inefficient water use because farmers have preferred less expensive but inefficient irrigation methods, with serious consequences during drought events when irrigation is the main source of water for crops (Bozzola and Swanson 2014).

The Valley has been hit by multiple droughts over the past years, causing huge economic impacts on agriculture. The high losses were linked to inefficient water use by both farmers and governance authorities (Musolino et al. 2017).

Materials and methods

Three provinces in the Po Valley have been selected. The development of stage-specific vulnerability curves for winter wheat foresees four steps:

1. Identification of harvested areas and extraction of weather and physical variables over those areas (Precipitation, temperature, soil textures, etc);
2. Identification of winter wheat management practices (sowing date, sowing depth, fertilization, etc.);
3. Yield modelling;
4. Derivation of vulnerability functions.

The harvested area has been derived from the Corine Land Cover dataset, while weather variables over the Po Valley have been retrieved from the E-OBS dataset and the soil texture from the SoilGrids database. Soil texture is classified according to the USDA soil classification system. Winter wheat management practices are described in the Lombardy region guidelines.

Yield modelling has been performed using the Agricultural Production System sIMulator (APSIM), which is a tool to simulate the plant growth with daily steps.

At first reference yield (the yield in the absence of any water stress during the entire growing season) was computed for each growing season. Then, the reduced yield for the same season was derived by introducing water stress in each single growth stage (establishment, vegetative, flowering and yield formation) by progressively decreasing the precipitation amount during that growth stage. Finally, the yield losses for each growth stage and the combination of growth stages are computed. The water stress is plotted versus the corresponding yield losses and the obtained data points have been fitted to the most appropriate function.

Results and concluding remarks

Flowering is the most sensitive growth stage to water deficit in all the considered areas, followed by yield formation (Figure 1, province of Cremona). The establishment and the vegetative stages wwww lower sensitivity to water stress, coherently with the results of (Steduto et al. 2012). If the combination of multiple stages is considered, high water stress involving the establishment and vegetative phases prevent winter wheat development, while prolonged deficits during the vegetative and flowering or the flowering and yield formation result in high losses but not crop failure.

Overall, the chosen function fits the data points well, with R^2 ranging from 0.69 to 0.995.

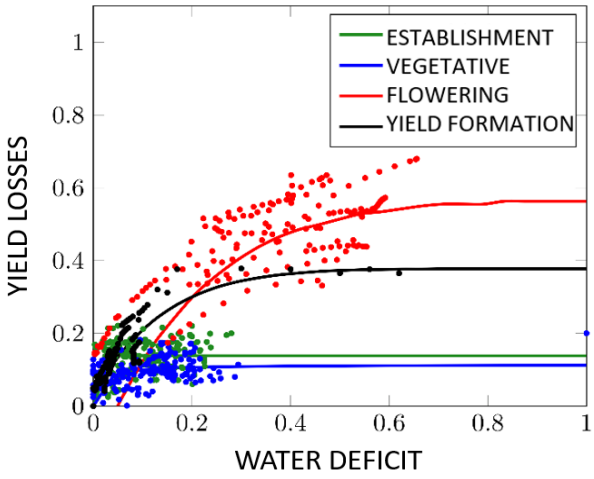

Figure 1. Winter wheat vulnerability curves for the province of Cremona for each single growth stage.

The developed curves, tailored on the specific context of the Po River basin for winter wheat, represent a useful tool to support water resources management and allocation during water crises. During a drought, those curves can help farmers to better manage irrigation scheduling. Furthermore, in case of an expected worsening of drought conditions, vulnerability curves can help decision-makers to implement effective water resources management strategies for reducing losses (e.g., introducing restriction in water uses in other sectors, re-pricing water resources or with mandatory rationing, etc).

References

Bozzola M, Swanson TM (2014) Policy implications of climate variability on agriculture: Water management in the Po river basin, Italy. Environmental Science & Policy 43: 26-38

Crespi A, Borghi A, Facchi A, Gandolfi C, Maugeri M (2020) Spatio-temporal variability and trends of drought indices over Lombardy plain (northern Italy) from meteorological station records (1951–2017). Italian Journal of Agrometeorology 2: 3-18

FAO (2021) AQUASTAT - FAO's Global Information System on Water and Agriculture

Musolino D, Vezzani C, Massarutto A (2019) Drought Management in the Po River Basin, Italy. In: Iglesias A et al. (eds.) Drought: Science and Policies, Wiley

Musolino D, de Carli A, Massarutto A (2017) Evaluation of the socio-economic impacts of the drought events: the case of the Po River Basin, European Countryside 1: 163-176

Rey D, Holman IP, Knox JW (2017) Developing drought resilience in irrigated agriculture in the face of increasing water scarcity. Reg Environ Change 17, 1527–1540. https://doi.org/10.1007/s10113-017-1116-6.

Rosa L, Chiarelli DD, Rulli MC, Dell'Angelo J, D'Orico P (2020) Global agricultural economic water scarcity. Science Advances 6(18): eaaz6031

Steduto P, Hsio TC, Fereres E, Raes D (2-12) Crop yield response to water. Food and Agriculture Organization

12th World Congress on Water Resources and Environment (EWRA 2023)
"Managing Water-Energy-Land-Food under Climatic, Environmental and Social Instability"
Thessaloniki, Greece, 27 June - 1 July 2023

Covering heating and summer air conditioning needs of school buildings through (Natural) Swallow Geothermal (Open Loop System) installation

E. Argyropoulou[1*], A. Adamidis[1], M. Vrachopoulos[2], I. Diamantis[1]
[1] Department of Civil Engineering, Democritus University of Thrace, Xanthi, Greece
[2] General Department, National and Kapodistrian University of Athens, Athens, Greece
* e-mail: eiriargy@hotmail.com

Introduction

The paper presents the heating and summer air conditioning needs of school buildings through the application of an open normal geothermal system.

The purpose of the geothermal system is to use the heat that can be extracted from the surface subsoil fluids that throughout the year maintain their temperature in conditions much closer to the seasonal requirements of the building, while at the same time their thermal storage is much greater than that of air. During this work, initially the energy requirements of the complexes were studied, as defined by the heating and summer air conditioning regulations (Technical Guideline 20701 2017) as well as the annual variation of these needs as defined by National European and International regulations. For this reason, the open-loop geothermal system was simulated using models and measurements of the surface fluid quantity and quality potential of the area (MODFLOW 2005, MT3DMS). By solving the groundwater flow and transport model, maps are obtained that represent the piezometric and thermal changes of the groundwater, due to the pumping and reintroduction of the water in the geoexchangers. The aim of the above process is to determine if the system chosen is effective, if problems arise directly or indirectly either in the system or in the subsoil, and if such an investment-implementation is economically advantageous compared to a corresponding conventional heating/cooling system.

Materials and methods

The underground water circulates through the open circuit and by making use of the already existing subsoil temperature (around 17^{o}C), it is possible to use it to meet the building's air conditioning needs. The buildings examined here are two school buildings within the same plot in the city of Alexandroupolis. Before the implementation of the open circuit system, it is necessary to investigate its functionality, the control of which was carried out through the simulation of the system in a QGIS environment.

For the simulation it was assumed that the thickness of the studied soil layer is 110m consisting entirely of a layer of brown clayey sand with gravel. The area was delineated and then the location of four production wells and four reintroduction wells was assessed within the open area of the block. Then followed the assessment of the needs of the buildings in terms of annual calorie consumption and the system supplies for heating and cooling respectively were calculated, while the temperatures of pumping and re-introducing the water into the wells were also estimated. During the design of the open circuit system, the use of a Geothermal Heat Pump (G.H.P.) was chosen, which uses the constant temperature water of the underground aquifer, to cover the heating and cooling air conditioning needs of the buildings.

The simulation of mass (water) and heat transfer models was carried out using the FREEWAT platform, integrated into the QGIS interface, where the data is managed through a SpatiaLite Database Management System (DBMS), allowing the assessment of water balances and water resource availability in space and time. The MODFLOW 2005 (Harbaugh 2005) was used to simulate the groundwater flow, which solves the flow equation by the finite difference method, while the MT3DMS (Zheng and Wang 1999) was used to simulate the heat transfer, which solves the heat transfer equation also by the finite difference method. The model created operates daily four hours per day in constant flow conditions. In winter months, the system absorbs heat from the underground water, which with the help of the heat pump is used to heat the buildings, while in the summer, heat is absorbed in the water, which is used to cool them.

By solving the underground flow and heat transfer model, maps were obtained that represent the piezometric and thermal changes of groundwater respectively, due to the pumping and re-introduction of water in geoexchangers (Figure 1). These maps serve to create appropriate diagrams and conclusions from their interpretation.

Figure 1. Isothermal curves and piezometric surface of groundwater on 31th January (left) and 31th July (right).

Finally, a comparison was made of the open circuit system with a corresponding conventional system for heating and cooling the buildings where the depreciation of the G.H.P. installation is achieved in approximately 9.5 years, taking a discount rate of 5%.

Results and concluding remarks

From model's solution, satisfaction was found in terms of the full coverage of the air conditioning needs of the two school buildings, without any problems being observed in the system while at the same time it is economically beneficial in the long term.

In order to avoid future problems, over-pumping as well as interference between neighboring wells should be avoided (Vrachopoulos et al. 2015), because they reduce the systems efficiency.

By expanding the use of shallow geothermal energy, it could be additionally utilized to produce hot water for the building's needs, but also extended so that all public and municipal buildings in the city can cover their needs through shallow geothermal energy, with low energy footprint.

References

Harbaugh AW (2005) MODFLOW-2005, The U.S. Geological Survey Modular Ground-Water Model: The Ground-Water Flow Process, Book 6, Chapter 16, U.S. Geological Survey

Technical Guideline 20701-1/2017 (2017) Analytical National specifications of parameters for the calculation of the energy efficiency of buildings and the issuance of the energy performance certificate, Ministry of Environment and Energy, Athens

Vrachopoulos M, Koukou M, Karytsas K (2015) Normal Geothermy – Design Principles of Geothermal Systems and Applications, Kallipos, Open Academic Editions, Athens

Zheng C, Wang PP (1999) MT3DMS: A modular three-dimensional multispecies transport model for simulation of advection, dispersion and chemical reactions of contaminants in groundwater systems. Documentation and User's Guide, US Army Corps of Engineers, Washington

Socioeconomic assessment of nature-based solutions to support water-energy-food-environment nexus challenges: An ecosystem-based approach

G. Bottaro*, C. Righetti, M. Masiero, D. Pettenella
Department of Land, Environment, Agriculture and Forestry, University of Padova, Legnaro, Padova, Italy
** e-mail: giorgia.bottaro@unipd.it*

Introduction

Water is a key driver of economic and social development while it also contributes to maintaining the integrity of the natural environment. An integrated water resource management to integrate the needs of different economic sectors has been conceptualised during the Bonn 2011 Nexus Conference (Hoff 2011) where the water-energy-food-ecosystem (WEFE) nexus concept was launched. The nexus considers the WEFE elements as interdependent and aims to manage synergies/trade-offs that may occur among them (Scott et al. 2016).

Ecosystem-based approaches have a huge potential to face WEFE nexus challenges both from a societal and an environmental perspective. Among the ecosystem-based approaches, Nature-based Solutions (NBS) are given special emphasis by European Commission policies (EC 2015). The rationale behind the adoption of NBS is that well managed ecosystems can provide a broad range of services that are beneficial to humans and that can reduce ecosystems vulnerability to risks and disturbances. These services are referred to through the umbrella term "ecosystem services" (ES). One relevant aspect of ES is that most of them, above all many regulating and cultural ES, do not have an explicit economic value. A lack of, or inadequate, ES valuation can lead to the overexploitation of resource stocks, result in poorly informed decisions in the design of policies, projects or investments, and finally lead to an unfair spreading of the benefits proceeding from ES. This paper aims to explore, both in theoretical and practical terms, how the biophysical and socioeconomic valuation of ES may support decision making about NBS development.

Materials and methods

To operationalize an ES-based approach to the WEFE nexus and assess socio-economic benefits deriving from the development of NBS, a general methodological framework was developed and then tested for the Koiliaris river area in north-western Crete (Greece).

Methodological framework: A preliminary in-depth literature review about ES definitions, classification systems and ES-based approaches was conducted to set the conceptual background for the framework. Multiple challenges faced within the WEFE nexus domain were identified via an expert-based approach involving local experts and managers for the pilot case studies identified within the Rexus and Lenses projects. Challenges were linked to one or more ES and/or non-ES strategies. The latter consist of consumption and management options, policies, or governance of natural resources. For each identified ES tailored socioeconomic indicators were identified to assess ES supply, demand and economic value.

Finally, specific NBS that could support the provision of the selected ES were identified via an extensive literature review and discussion with pilot case studies. Selected NBS were assessed in terms of potential ES supply and the associated economic value (benefits). To this aim a cost-benefit analysis (CBA) was implemented, analysing ES benefits via-a-vis the NBS implementation and maintenance costs.

Testing the framework: The framework was tested for the case study of Koiliaris river, assuming the restoration of a riparian forest as the targeted NBS. Due to the explorative nature of the study, the benefits associated to the selected NBS focused on a subset of ES, namely moderation of extreme events and climate regulation via carbon sequestration. ES supply was assessed via InVEST 3.9.1 models. As for the economic valuation, the replacement cost method was used for the moderation of extreme events, and the market price method for climate regulation. Costs considered included implementation and maintenance costs (assume to be equal to 5% of the implementation costs) of the selected NBS. A 3.5% discount rate

was considered (Dicks et al. 2020) over a 20 year-long period.

Results and concluding remarks

Table 1 reports the outcomes of the biophysical evaluation of ES supply and economic value, while Table 2 summarizes the outcomes of the CBA. ES have been evaluated according to a "*with and without*" approach, i.e., as a difference between values accounted under the NBS scenario and the baseline conditions.

To calculate the economic value of the moderation of extreme events a lamination basin has been used as substitute good, assuming an average unit cost of 400€/m^3. The economic value for climate regulation has been calculated considering an average market price per ton of CO_2 (7.70€ per tCO_2eq).

Table 1. Moderation of extreme events and climate regulation assessment under the baseline and NBS scenario.

	A. Baseline (without NBS scenario)	B. With NBS scenario	B-A	€
Retained runoff volume (m^3)	17,931.96	20,620.84	2,688.88	1,075,554.07
Carbon storage (tons of CO_2)	5,977.32	5,819.71	21,358.35	164,459.32

Table 2. Outcomes of the cost-benefit analysis.

Net present value (€)	Benefit/cost ratio	Internal rate of return	Payback period (years)
11,364,940.45	7.67	40.49%	5

The test allowed validating and calibrating the framework, confirming it can be effectively run at the pilot scale, though being strongly tied to data availability. Since this study is a preliminary implementation of the framework and further refinements might occur, results should be considered with caution. A precautionary approach might consist in lowering – according to a given buffer – the expected benefits to consider possible adverse events – either naturally occurring or human-induced – that might affect ES supply and value over time. Nonetheless, though considering only two out of the many possible ES delivered as co-benefits by the selected NBS, the CBA shows that socioeconomic benefits exceed the costs.

Based on our results, the proposed framework and methodology can represent a practical solution to support decision making and to guide the selection of NBS, however they should not be considered as stand-alone tools, rather they should be integrated with other approaches, including participatory ones to include stakeholders' needs and preferences when planning, designing and implementing NBS solutions.

Acknowledgments: The study has been possible thanks to the support of the H2020 REXUS project (ID: 101003632) and the EU PRIMA LENSES project (Topic 1.4.1-2020 (IA).

References

Dicks J, Dellaccio O, Stenning J (2020) Economic costs and benefits of nature-based solutions to mitigate climate change. Final Report. Cambridge Econometric, UK

European Commission (2015) Nature-Based Solutions & Re-naturing Cities. Final Report of the Horizon 2020 Expert Group on 'Nature-Based Solutions and Re- Naturing Cities'. Directorate-General for Research and Innovation–Climate Action, Environment, Resource Efficiency and Raw Materials

Hoff J (2011) Understanding the nexus. Background Paper for the Bonn 2011 Conference: The Water, Energy and Food Security Nexus, Bonn, Germany, 16–18 November 2011, Stockholm Environment Institute (SEI): Stockholm, Sweden

Scott CA, Crootof A, Kelly-Richards S (2016) The urban water-energy nexus: drivers and responses to global change in the 'urban century. Environmental Resource Management and the Nexus Approach: Managing Water, Soil, and Waste in the Context of Global Change. Hettiarachchi H, Ardakanian R (eds) (Berlin: Springer), pp 113–40

Stakeholders' perceptions on water-ecosystem-food nexus challenges in a Mediterranean rural agricultural region

A. Panagopoulos*, D. Malamataris, A. Chatzi, K. Babakos, E. Hatzigiannakis, V. Pisinaras
Soil and Water Resources Institute, Hellenic Agricultural Organization "DEMETER", Sindos 57400, Greece
** e-mail: a.panagopoulos@swri.gr*

Introduction

Population increase significantly magnifies the pressures imposed on the water, ecosystem and food sectors, resulting in the progressive decline of the services they offer. An estimated 26% of the global population are affected by food insecurity in 2019, 28% still lack safe access to drinking water (Carmona-Moreno 2021), and about 9% of global species face very high risk of extinction at 1.5°C rise in global mean surface air temperature (Parmesan 2022). Water, ecosystem and food (WEF) sectors are strongly interrelated, and thus, a holistic approach incorporating different stakeholders' viewpoints has to be ensured. An effective stakeholders' engagement approach can contribute to resources security improvement and thus, sustainability.

Materials and methods

Agia watershed in which the Pinios Hydrologic Observatory (PHO) is developed (Pisinaras et al. 2018), and Pinios River Delta (PRD) are both situated in Pinios River Basin which constitutes the most agriculturally productive plain of Greece. The current WEF state in these pilot areas is outlined as follows.

Water Sector: Insufficient agricultural management practices implementation since the mid-1980s trigger water quality deterioration in both pilot areas. Water overexploitation and inability to sufficiently cover demands is experienced only in specific sub-areas during prolonged drought periods.

Ecosystem Sector: Mainly PRD but also PHO are considered as two of the most important hydro-ecosystems in central Greece, with the 45% and 29% of their total area, respectively, being characterized as EU Natura 2000 protected areas and Important Bird Areas.

Food Sector: According to data provided by the Hellenic Payment and Control Agency for Guidance and Guarantee Community Aid for year 2021, the dominant crop in PHO is orchards (61.5%), while the main crop in PRD is forage (21.7%), followed by energy crops (17.5%) and orchards (14.9%).

A series of personal interviews with 19 stakeholders, and a LENSES stakeholders' workshop were carried out in 2022 to identify the most critical WEF challenges. The integrated methodology followed covering all nexus sectors constitutes a prerequisite to ensure sustainability.

Results and concluding remarks

Out of the personal interviews and workshop, comprehensive lists of crucial problems were drawn up per sector for PHO (Figure 1a) and PRD (Figure 1b) pilot areas, as stated by the interviewees.

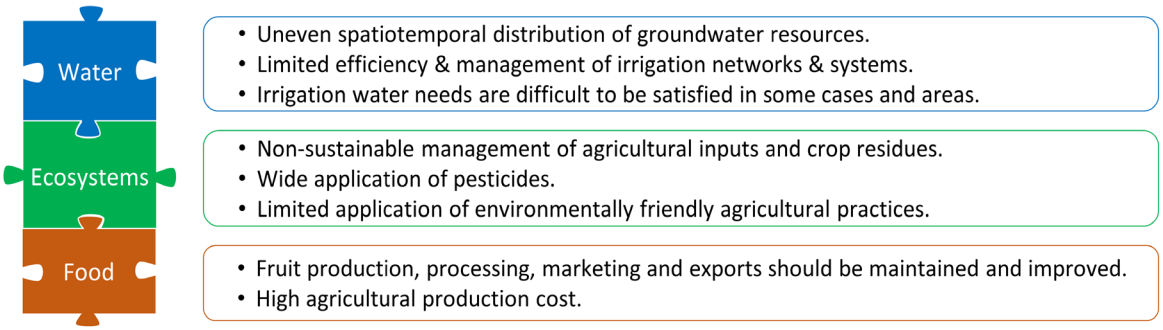

(a)

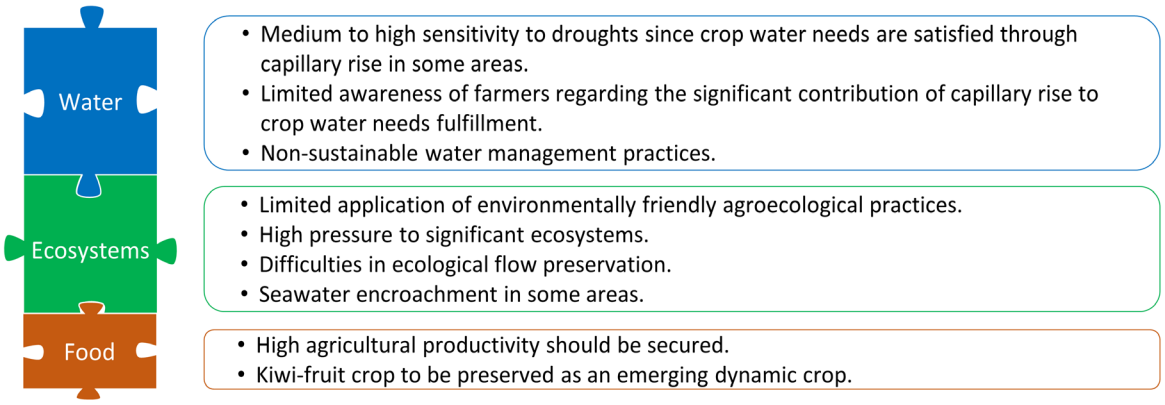

(b)

Figure 1. Identified problems in (a) PHO and (b) PRD pilot areas.

These problems were further processed and clustered in 3 distinct challenges (Figure 2), that need to be addressed towards resilience building that will ensure sectoral security.

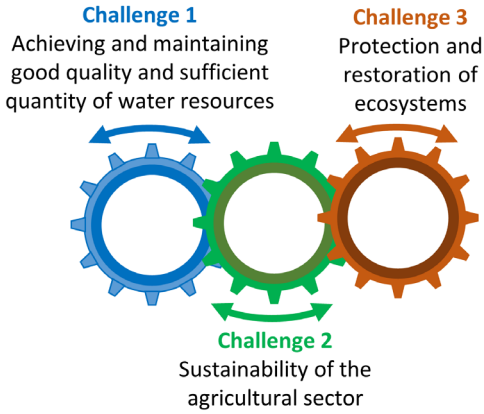

Figure 2. Critical challenges to be addressed in the pilot areas.

Even though each of the challenges identified is primarily related to a sector, clearly a strong interrelation and interdependency occurs amongst them, that calls for concerted action. Synthesis of real-world nexus challenges across various complex systems constitute an essential procedure in unraveling nexus knowledge. The presented work offers an integrated insight and exemplifies the current WEF nexus situation in pilot areas. Quantification of WEF challenges constitutes a forthcoming pursuit to provide sustainable development strategies in a dynamic and complex world.

Acknowledgments: This paper was realized in the framework of the PRIMA programme supported by the European Union. GA n° [2041] [LENSES – Learning and action alliances for Nexus environments in an uncertain future] [Call 2020 Section 1 Nexus IA].

References

Carmona-Moreno C, Crestaz E, Cimmarrusti Y, Farinosi F, Biedler M, Amani A, Mishra A, Carmona-Gutierren A (2021) Implementing the Water-Energy-Food-Ecosystems Nexus and Achieving the Sustainable Development Goals. United Nations Educational, Scientific and Cultural Organization (UNESCO), Paris, France.

Parmesan C, Morecroft MD, Trisurat Y, Adrian R, Anshari GZ, Arneth A, Gao Q, Gonzalez P, Harris R, Price J, Stevens N, Talukdarr GH (2022) Terrestrial and Freshwater Ecosystems and Their Services. In: Climate Change 2022: Impacts, Adaptation and Vulnerability. Contribution of Working Group II to the Sixth Assessment Report of the Intergovernmental Panel on Climate Change, Pörtner H-O et al. (eds), Cambridge University Press, Cambridge, UK and New York, NY, USA, pp. 197–377. https://doi.org/10.1017/9781009325844.004

Pisinaras V, Panagopoulos A, Herrmann F, Bogena HR, Doulgeris C, Ilias A, Tziritis E, Wendland F (2018) Hydrologic and geochemical research at Pinios Hydrologic Observatory: Initial results. Vadose Zone Journal 17(1): 1-16

Crop switching optimization in the indo-gangetic plain for water and food sustainability

R. Chakraborti[1], S. Ghosh[1,2*]
[1] Department of Civil Engineering, Indian Institute of Technology Bombay, Mumbai 400076, India
[2] Inter Disciplinary Programme in Climate Studies, Indian Institute of Technology Bombay, Mumbai 400076, India
* e-mail: subimal@iitb.ac.in

Introduction

Water and food security in the Indo-Gangetic Plain (IGP) is severely affected due to the growing population, intensive irrigated agriculture, and changing climate. Switching from a water-intensive rice-wheat system to alternative cereals can improve water and food security, as suggested in many recent studies (Davis et al. 2017, 2018). But the feasibility of such crop switching depends on multiple factors, such as farmers' interests considering the profit from selling the crops, meeting the calorie needs and other nutritional demands of the population, etc. Here, we present a multi-objective optimization framework for switching crops based on three objectives: minimization of water use, maximization of farmers' profit, and maximization of calorie production. Our findings show that adopting crop switching based on the optimization framework improves all three objective parameters.

Materials and methods

We have used the Aqua Crop model (Steduto et al. 2009) to simulate crop growth. The crop simulation aims to understand the climate and regional sensitivity of different crops under rainfed and irrigated conditions. The simulated yield values are later used in the optimization model as inputs along with the crop area, irrigated area, and MSP (Minimum Support Price) observed data. In the simulation of crop yield with FAO-aqua crop model, we have used the crop parameters (FAO datasets: https://www.fao.org /fileadmin/user_upload/faowater/docs/AquaCropV40Annexes.pdf) which represent estimates obtained in calibration/validation exercises of Aqua Crop with experimental data. This calibration/validation process is extensive and it is based on the geographical location, limiting conditions and years of experiments.

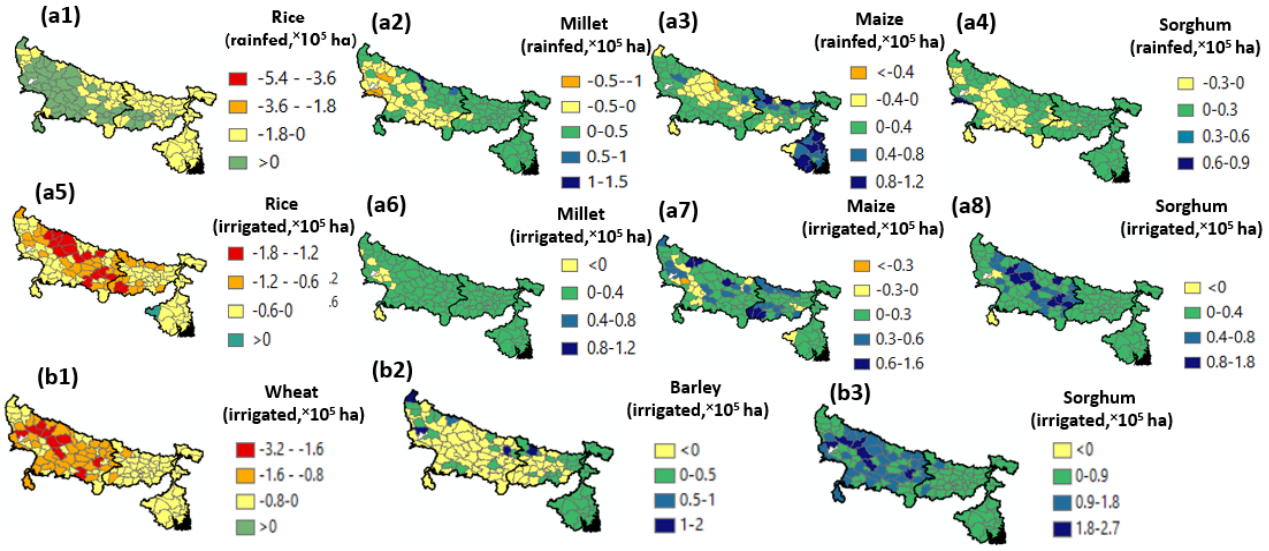

Figure 1. Proposed changes in crop areas considering simulated yield value for Kharif and Rabi season a1 – a4: Proposed changes in rainfed Kharif crop areas. a5 – a8: Proposed changes in irrigated Kharif crop areas. b1 – b3: Proposed changes in irrigated Rabi crop areas (Proposed changes in rainfed Rabi crop areas are not shown as these are significantly small comparing to irrigated area).

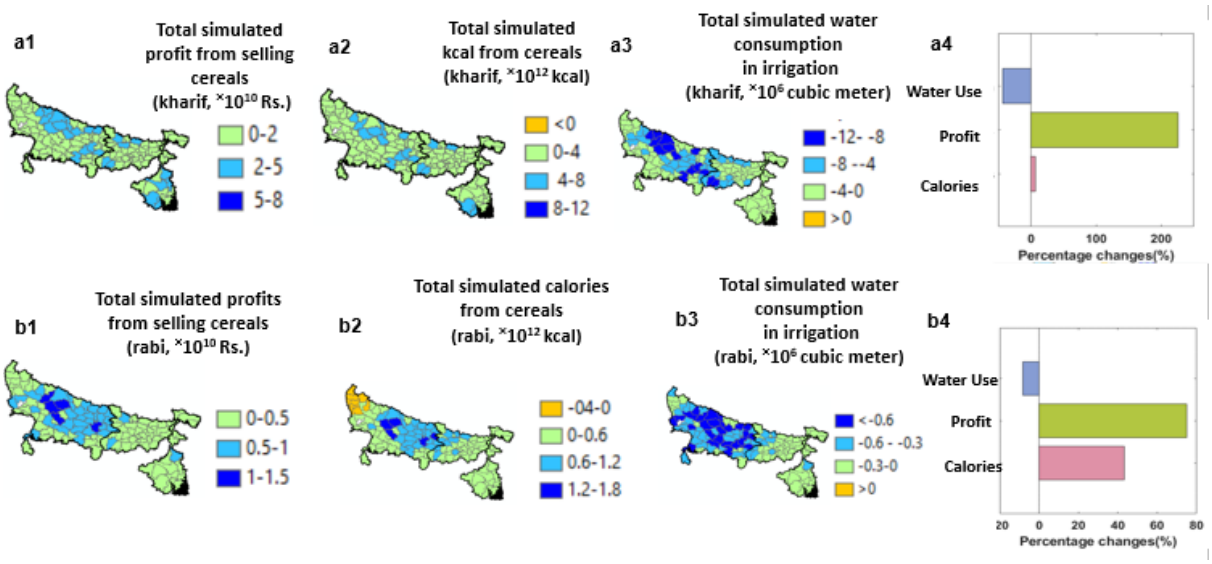

Figure 2. a1 – a3: Optimized changes in profit, calorie production and irrigation water consumption for kharif crops. a4: Percentage changes in profit, calorie and water consumption considering the summation over the study region in kharif season b1 – b3: Optimized changes in profit, calorie production and irrigation water consumption for Rabi crops. b4: Percentage changes in profit, calorie and water consumption considering the summation over the study region in Rabi season.

We used the max-min approach of multi-objective optimization. Here, the goal is to maximize the minimum satisfaction of all the goals, such as maximization of farmers' profit and calorie production and minimization of water use. The decision variables are the area fraction for the cereal crops, considering that the irrigated fraction will not change with respect to the current practice. Irrigated and Rainfed cereal crop areas are optimized for both Kharif and Rabi seasons.

Results and concluding remarks

We applied the crop switching optimization model to the three important states (Uttar Pradesh, Bihar, and West Bengal) in the IGP. Also, to meet the water demand for crop production, farmers often rely on groundwater irrigation due to the unpredictability of monsoon rainfall in the changing climate; the depleting water resources further increases the cost associated with food production and food insecurity.

Figure 1 represents the proposed changes in the crop areas subtracting the observed crop areas from the proposed optimized crop areas. Here we observe that rice area is significantly reduced over all districts, whereas millet, maize, and sorghum increase is suggested in the Kharif season. In the Rabi season, wheat areas are being replaced by alternative crops such as barley and sorghum. It is visible that less water-consuming climate-resilient crops are replacing water-intensive rice and wheat. Figure 2 shows that the goals of increasing the farmer's profit and calorie production are also satisfied with the goal of reducing irrigation water use. District-wise mapping and overall improvements in water consumption, profit, and calories, are shown in Figure 2. Applying the crop switching optimization model can provide a novel solution for sustainable agricultural practices that improve water and food security for any region threatened with water and food scarcity.

References

Davis KF, Chiarelli DD, Rulli MC, Chhatre A, Richter B, Singh D, DeFries R (2018) Alternative cereals can improve water use and nutrient supply in India. Science Advances 4(7): eaao1108. https://doi.org/10.1126/sciadv.aao1108

Davis KF, Rulli MC, Seveso A, D'Odorico P (2017) Increased food production and reduced water use through optimized crop distribution. Nature Geoscience 10(12): 919–924. https://doi.org/10.1038/s41561-017-0004-5

Steduto P, Hsiao TC, Raes D, Fereres E (2009) Aquacrop-the FAO crop model to simulate yield response to water: I. concepts and underlying principles. Agronomy Journal 101(3): 426–437. https://doi.org/10.2134/agronj2008.0139s

A participatory approach for water-energy-food nexus analysis and management: The Isonzo-Soča river basin

V.R. Coletta[1*], A. Imbò[2], A. Pagano[2], F. Lombardo[3], F. Zaffanella[3], M. Ferri[3], U. Fratino[1], R. Giordano[2]

[1] DICATECh, Polytechnic University of Bari, Bari, Italy
[2] Water Research Institute, National Research Council, Bari, Italy
[3] Autorità di Bacino Distrettuale delle Alpi Orientali, Venezia, Italy
* e-mail: virginiarosa.coletta@poliba.it

Introduction

In these times of high-resources stress, an integrated approach to water resources and environment management is needed for identifying sustainable sectoral and cross-sectoral strategies. The Water-Energy-Food domains are strictly and dynamically interdependent; the increasing demand for resources for human activities creates trade-offs that are exacerbated by the impacts of climate change (e.g., flood and drought) and, for this reason, needs to be better coordinated and utilised promoting positive synergistic impacts (Ma et al. 2020). Although the Water-Energy-Food approach is well-known for its ability of assessing the interrelationships of resource systems ("Understanding the Nexus"), the strong linkages between the sectors are rarely incorporated into strategies ("Nexus Doing"). As with other complex socio-technical challenge, the paradigm shift toward Nexus Doing needs to place people and institutions at the centre of the solution approach.

In this context, the aim of the present research is to develop an approach that, considering the co-evolution paths of different sub-systems, supports decision-makers in designing sustainable and actionable forward-looking solutions that cope with challenges across sectors. Participatory modelling techniques and integrated modelling able to perform multi-scenario analysis for the assessment of management strategies for different timescales, are used for this purpose. Specifically, a participatory System Dynamics (SD) modelling approach is applied because of its ability of adopting a systemic approach together with a process of social deepening to address a set of dynamically complex issues (see e.g., Sterman 2000; Simonovic 2009). It allows for i) analysing the complex of elements that constitute the Water-Energy-Food sectors, understanding their interactions; ii) supporting the implementation of the results of sectoral models; iii) ensuring the involvement of stakeholders; and iv) analysing how the system would behave under different scenarios of intervention, with clear options for decision-makers.

Specific reference is made to one of the pilots of the REXUS project, namely the Isonzo-Soča watershed between Italy and Slovenia, for which current cross-border flow regulation agreements are insufficient to guarantee a good status of ecosystem services in the Italian territory.

Materials and methods

The adopted approach, organised in several steps, is based on a common framework replicable in different study contexts. The shared ground for the different phases of the methodology is the active participation of stakeholders, supported by different methods. The methodological framework allows for the analysis of the dynamic Water-Energy-Food Nexus, ultimately supporting decision-makers in identifying bundles of actions (i.e., strategies) for its management. It uses the SD principles, namely System Thinking and Dynamic Simulation (see e.g., Sterman 2000 for more details), integrating conceptual and numerical modelling tools with different technical analysis and methods for the active participation of stakeholders. Firstly, Causal Loop Diagrams (CLD, the qualitative SD tool) are co-developed with stakeholders during a workshop and merged in a single CLD useful for obtaining a holistic description and understanding of the causality and interrelations between components within the system as well as influences from outside the system. Secondly, the CLD analysis is completed with a Stock and Flow model (SF model, the quantitative

SD tool) quantifying the interactions between the sectors and simulating the behaviour of the system in the current situation (Business As Usual - BAU - scenario). It allows for precise specification of all the system's parts and their interrelation and, although it may be affected by data-related uncertainty, it can reveal complex systems behaviour that could not be understood through qualitative diagramming only. Specifically, results of sectoral models/analysis (e.g., hydrological models) are used as inputs in the SF model. Multiple 'thematic' SF sub-models – closely interconnected - are developed and then aggregated in a single model, which integrate qualitative ('soft' or intangible) and quantitative variables ('hard' or physical). Once the dynamic simulation of the system in the BAU scenario is obtained, a second workshop with stakeholders is organised to identify some management measures that cope with challenges across sectors. Their effects on the system are then assessed with reference to different multidimensional future scenarios. Lastly, the obtained information is synthesised to be useful for planning and strategic purposes. For this reason, indices that aggregate representative variables of the system behaviour are constructed in this work.

Results and concluding remarks

The methodological framework was applied to the Isonzo-Soča watershed between Italy and Slovenia, which is characterised by a complex geographical and political context. In the past, an agreement between the two countries was necessary to guarantee the minimum vital downstream flow, but it did not produce the desired results. Nowadays, the Italian riverbed is subject to variations in daily flows (hydropeaking) due to the Slovenian Salcano hydroelectric dam. This leads to some difficulties, especially during summer, in irrigation and in fish reproduction. Hydropeaking constitutes an impact with heavy repercussions on the hydro-morphological and biological state of the river as well as on the entire ecosystem. There is therefore the need to identify actions for the improvement of the river habitat, mitigation of the river regime and improvement of the ecological and hydro-morphological quality of the Isonzo river.

Following the proposed methodology, pressures, resources, activities, and infrastructure acting on the system and their interactions were identified by stakeholders during participatory exercises and encapsulated into a CLD representing the conceptual view of the analysed system. In this way, a shared vision of the system with regard to different aspects (social, environmental, economic, etc.) was obtained and preliminary hypothesis on the behaviour over time of key system variables (e.g., agricultural production) were made. Currently, the translation of the CLD into the SF model is ongoing. For this reason, a technical characterisation of the analysed problem is being carried out. For example, hydropeaking indicators and ecosystem services indicators are being calculating for the assessment of both river flow alteration and benefits that humans obtain from the ecosystem in the current situation. They will be some of the inputs of the quantitative SD model. Then, some sectoral and cross-sectoral management measures for the study area will be identified with stakeholders and fed into the simulation model to assess its effects on the system under different multidimensional future scenarios.

Acknowledgments: The work described fits into the ongoing activities of the REXUS project (H2020, Grant Agreement No 101003632).

References

Ma Y, Li YP, Huang GH, Liu YR (2020) Water-energy nexus under uncertainty: Development of a hierarchical decision-making model. Journal of Hydrology 591: 125297. http://doi.org/10.1016/j.jhydrol.2020.125297

REXUS project. https://www.rexusproject.eu/

Simonovic SP (2009) Managing Water Resources: Methods and Tools for a System Approach. UNESCO, Earthscan

Sterman JD (2000) Systems Thinking and Modeling for a Complex World. McGraw-Hill, New York

Drought impact on agriculture in Northwest Bulgaria

S. Matev, N. Nikolova*, J. Svetozarevic
Faculty of Geology and Geography, Sofia University "St. Kliment Ohridski", Sofia, Bulgaria
** e-mail: nina@gea.uni-sofia.bg*

Introduction

Drought is the result of a decrease in precipitation over a long period of time. Prolonged meteorological droughts cause a decrease in soil moisture, which leads to the occurrence of agricultural droughts when soil moisture is insufficient to meet plant water needs and proper agricultural management (Qin et al. 2021). Several drought events have been analyzed in the scientific literature, which affected large areas and caused yield losses (Kim et al. 2019), soil degradation (Peters et al. 2020; Samaniego et al. 2018), and increased need for crop irrigation (Rey 2017). Despite the numerous publications on the impact of drought on agriculture in Bulgaria a thorough statistical and geographical analysis is needed to be performed to answer questions about drought impact at regional and local levels.

The present study aims to clarify the climate–water–food nexus by evaluating drought's impact on main agricultural crops in Northwest Bulgaria (maize, wheat, and sunflower). To achieve this, crop yields were analyzed in relation to the occurrence of drought and the consumptive use of blue (fresh surface or groundwater) and green (precipitation) waters are determined.

Materials and methods

Drought impact on agriculture was evaluated for Northwest Bulgaria, which is one of the main agricultural areas but on the other side, it is the economically least developed region of the country. The climate data (monthly air temperatures – average, mean, and maximum – and monthly precipitation) and agricultural data (average yield of maize, wheat, and sunflower) were used for the research. The reference period for calculating climate normal was 1961-1990.

To clarify the water-food nexus, green and blue components of the water footprints (WF) of maize production for dry (2012) and wet (2014) years were calculated. The WF of agricultural production represents the volume of water used by agricultural crops during the growing season. The green component in the WF of growing a crop (*WFgreen*, m^3/ton) is calculated as the green component in crop water use (*CWUgreen*, m^3/ha) divided by the crop yield (*Y*, ton/ha). The blue component (*WFblue*, m^3/ton) is calculated in a similar way. The green and blue components in crop water use (*CWU*, m^3/ha) are calculated by the accumulation of daily evapotranspiration (*ET*, mm/day) over the complete growing period (Hoekstra et al. 2011).

Results and concluding remarks

Data on average yields of maize and sunflower per hectare for the period 2001-2021 show a significant decrease in the dry years of 2007 and 2012, while in the wet years of 2010, 2014, 2017, yields were higher (Figure 1). Wheat yield data follow this trend but show smaller deviations in dry and wet years. An analysis of the seasonal precipitation found that in both dry years (2007 and 2012) there were three seasons with negative precipitation anomalies. In 2007, spring and summer precipitation were slightly below the climate normal, while in 2012 summer is only 53% of the normal. Precipitation was below normal in March, April, June, and July. In April 2007 monthly precipitation was only 8% of normal. In both years (2007 and 2012), precipitation in May was high, but it was not sufficient for good agricultural results, due to the dry March and April and even drier June and July. The temperature conditions during these years are also important - in 2012, the warmest summer was recorded in Bulgaria, and in 2007, June and July were extremely warm with prolonged and long heatwaves.

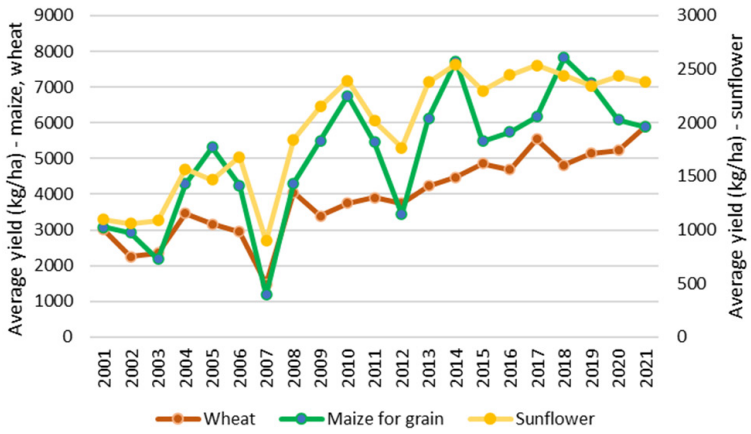

Figure 1. An average yield of selected crops in Northwest Bulgaria.

In years with higher average yields (e.g., 2010 and 2014) spring and summer precipitation were above normal. In March, April, and July of 2014, the exceedance of the monthly norms was between 2 and 3 times. In 2014, the annual air temperature for areas with an altitude of up to 800 m a.s.l. was on average 1.2°C above the norm but no prolonged extremely hot periods were observed. In wet conditions, temperatures are not as important as in dry years.

The results of the calculation of green and blue WF of maize production in the regions of selected meteorological stations are given in Table 1. Station Vidin is located in the northwest part of the region and station Lovech is in the southeast part. The total WF (green+blue) in the wet year 2014 presents 37% of WF in the dry year (2012). In 2012 blue WF was between 67% (for the region of Vidin) and 73% (for the region of Lovech) of total (green+blue) WF.

Table 1. Water footprints of maize production (m^3/ton).

Regions	2012			2014		
	WFgreen	WFblue	Total	WFgreen	WFblue	Total
Vidin	557.1	1126.8	1683.8	344.9	278.1	623.0
Lovech	442.9	1187.4	1630.3	359.9	247.5	607.4

In conclusion, the following could be pointed out: 1) the low cereal production in Bulgaria during recent years is in conjunction with the occurrence of dry periods and 2) during the dry years irrigation is very important in order to provide optimal conditions for crops. It is expected that this research work will contribute to the performance of water-food nexus assessments with a focus on agricultural production conditions in Bulgaria which could be used as a basis for developing and implementing measures to reduce and probably eliminate the risk of water scarcity and drought.

Acknowledgments: This study has been carried out in the framework of the project The Nexus Approach in Agriculture. The water-food nexus in the context of climate change, supported by the Ministry of Education and Science (MES) of Bulgaria (Agreement № КП-06-КОСТ-2/17.05.2022.

References

Hoekstra AY, Chapagain AK, Aldaya MM, Mekonnen MM (2011) The Water Footprint Assessment Manual. Earthscan, London, Washington, DC

Kim W, Iiyumi T, Nishimori M (2019) Global patterns of crop production losses associated with drought from 1983 to 2009. Journal of Applied Meteorology and Climatology 58(6): 1233–1244

Peters W, Bastos A, Ciais P, Vermeulen A (2020) A historical, geographical and ecological perspective on the 2018 European summer drought. Phil. Trans. R. Soc. B 375: 20190505. http://dx.doi.org/10.1098/rstb.2019.0505

Qin NX, Wang JN, Hong Y, Lu QQ, Huang JL, Liu MH, Gao L (2021) The drought variability based on continuous days without available precipitation in Guizhou Province, southwest China. Water 13: 660

Samaniego L, Thober S, Kumar R, Wanders N, Rakovec O, Pan M, Zink M, Sheffield J, Wood EF, Marx A (2018) Anthropogenic warming exacerbates European soil moisture droughts. Nature Climate Change 8(5): 421–426

Rey D, Holman IP, Knox JW (2017) Developing drought resilience in irrigated agriculture in the face of increasing water scarcity. Reg Environ Change 17: 1527–1540

The use of nature-based solutions to support sustainable water-ecosystems-food NEXUS management: The LENSES approach

S. Vanino[1], A. Di Fonzo[2*], V. Baratella[1], F. Pucci[2], N. Nikolaidis[3], M. Bea[4], A. Pagano[5], R. Giordano[5], S. Fabiani[2]

[1] *Council of Research in Agriculture and Analysis of Agricultural Economics, Research Centre for Agricultural and Nutrition, Via della Navicella, 2, Rome, 00187, Italy*

[2] *Council of Research in Agriculture and Analysis of Agricultural Economics, Research Centre for Agricultural Policies and Bio-economy, Via Barberini, 36, Rome, 00187, Italy*

[3] *Technical University of Crete, Tuc University Campus, Konoupidiana, 73100, Chania, Greece*

[4] *EcoAdapta, Calle Magdalena 38, 28012, Madrid, Spain*

[5] *Water Research Institute – Natial Research Council (IRSA-CNR), viale F. de Blasio, 5, Bari, 70132, Italy*

** e-mail: antonella.difonzo@crea.gov.it*

Introduction

The sustainable use of natural resources, particularly in Mediterranean region is conditioned by resources availability (water and land), changing climatic conditions, and increasing socio-economic stresses. In this context, the project "LEarning and action alliances for NexuS EnvironmentS in an uncertain future" (LENSES) is developing a stepwise approach to identify local Water, Ecosystems and Food (WEF) challenges that can be addressed in a new practical and conceptual framework, under the nexus perspective. All these activity are based on the building of an exchange and sharing environment, namely Learning & Action Alliances (LAAs) and on the implementation of participatory process (Participatory System Dynamics Modelling -PSDM) allowing the definition of specific local Nature Based Solutions (NBSs).

The proposed paper focuses on the methodology developed in the LENSES aiming to improve water allocation, enhance food security while preserving ecosystems and aiding climate change adaptation through a collecting learning process which supports the operationalization of the Water, Ecosystems and Food Nexus. Project activities involve 7 research centres, 5 SMEs and 1 NPO, with six demonstration pilot sites distributed across 6 countries in the Mediterranean basin (Figure 1) and are oriented toward the development of a new replicable methodology to define specific solutions (Nature Based) to specific issues coming from a participatory approach and stakeholder engagement process.

Figure 1. Lenses Pilot areas.

Materials and methods

To achieve this purpose, LENSES follows a mixed approach: a) on one hand, it refers on the concept of "managing" the Nexus and accepting the reality of trade-offs and synergies, thus the inherent nature of negotiation and mediation to any nexus management process. In accordance to this, LENSES sees the alternance of conflicts and cooperation as a continuum process allowing to go deeper into the system to

understand divergence of interest and social norms to work with this as part of a deep, transformative participatory approach. LAAs drive this transformation; b) on the other hand, PSDM approach focused on Group Model Building will be used for SDM development with the aim of unravelling the complexity of WEF systems and support an improved understanding of their behaviour. Through the PSDM approach, LENSES pursues a twofold goal. Firstly, it aims at enhancing the legitimacy of the decision-making processes for the WEF nexus management by integrating different kinds of knowledge and problem understandings. Secondly, will enhance the understanding of the complex web of interactions affecting the nexus by using algorithms which link the different domains and run dynamic scenarios. Under this perspective, LENSES postulates that transition towards resilient WEF Nexus systems is only possible through the true engagement of all relevant parties in the policy-dialogue and decision-making across the domains while incorporating uncertainty.

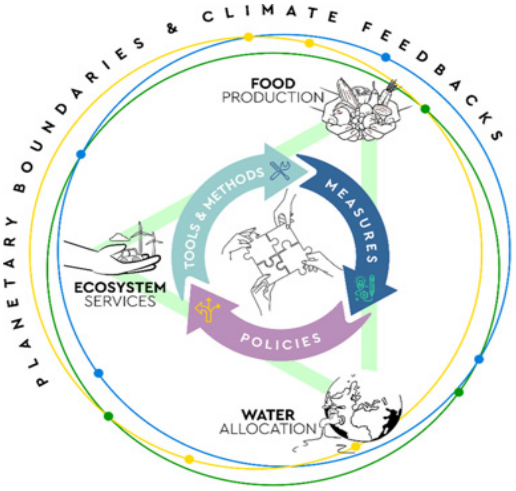

Figure 2. LENSES conceptual framework to support Learning & Action in Nexus Environments.

Results and concluding remarks

Identified NBSs aims to co-achieve multiple Nexus Domain Objectives (i.e., sectoral goals) activating Nexus Resilience Qualities that should facilitate the transition towards more efficient and resilient Nexus systems. In this study, these measures address vulnerabilities identified in 7 pilot areas distributed across the Mediterranean region and linked to (i) socio-institutional frame, and (ii) climate change. Building on the assumption that biodiversity is the only viable pathway to guarantee water-food security, the NBS will support the delivery of ecosystem services and provide evidence-base for the broader Nexus policy dialogue. Our finding provides an evaluation framework includes a comprehensive catalogue of Nexus related NBSs, whose suitability needs to be evaluated at local level to achieve a better use of protected/natural ecosystems, increase the sustainability and multi-functionality of managed ecosystems, design and manage new ecosystems. To this end, we discuss on local WEF challenges identified in the pilot areas of the project, through a participatory process, which counted on the engagement of a diverse set of relevant stakeholders from across different level. Then, we identify potential NBSs that can help addressing these challenges and increasing the resilience of the WEF nexus, for the long-lasting benefit of local ecosystems. Ultimately, we focus on the deep transformations processes required to our social and economic systems, and the crafting of integrative governance systems and co-design aspects that are needed to operationalize the WEF nexus and bring to effect these deep systemic changes. Our findings can inform policy makers at local and national level and support the drawing of improved policies and decisions that foster a fair and sustainable allocation of resources, thus accelerating the achievement of Sustainable Development Goals.

Acknowledgments: The Authors acknowledge the project LENSES, which has received funding from the PRIMA Programme supported by the European Union.GA n°2041 (LENSES). This paper and the content included in it do not represent the opinion of PRIMA Foundation, PRIMA foundation is not responsible for any use that might be made of its content.

Crop suitability projections in Pinios region

J.M. Galve[1*], J. Gonzalez-Piqueras[1], J. Garrido[1], M. Llanos López[2], E. Henao[2], C. Papadaskalopoulou[3], M. Antoniadou[3], D. Tassopoulos[3]
[1] IDR-UCLM, Campus Universitario s/n, 02071 Albacete, Spain
[2] Agrisat Iberia S.L., P. Científico y Tecnológico, Ed. Emprendedores, Paseo de la Innovación nº 1, 02006 Albacete, Spain
[3] DRAXIS Environmental S.A., 54-56 Themistokli Sofouli str., 54655 Thessaloniki, Greece
* e-mail: joanmiquel.galve@uclm.es

Introduction

FAO framework describes land evaluation as the process of predicting land use potential based on its characteristics (FAO 1976). The rational and suitable use of natural resources is a key of economic development without compromising the needs of future generations. Land suitability assessment procedures requires the use of different variable databases and ranking methods depending on the pair crop - soil evaluated. A Land Use Suitability methodology mapping has been implemented based on the databases about crop suitability using the knowledge on crop management under local soil and climate conditions.

A particular application has been selected in the Pinios region in Greece since crops like cotton or wheat ares an important crop in the river valley for decades, providing a source of income for many farmers in the region. The crop related industry in Greece has also helped to support local businesses and communities. The Pinios river valley has a Mediterranean climate, which is well-suited for cultivation of crops like cotton and wheat. The soil in the Pinios river valley is fertile and well-draining, which is favourable for those crops cultivation.

The results obtained show the maps of Land Suitability for crop cultivation in the area applied to climate projections that will be validated with stakeholders and will help as a decision support for water and land use managing.

Materials and methods

The FAO framework performed a system to analyse the land use suitability. Given a set of maps and their corresponding thresholds, we obtain a result in classifying areas suitable for the crop depending on its needs. These needs include climate conditions, landscape, soil characteristics and the management in the period evaluated. Figure 1 provides an overview of the data input, modelling, implementation and outputs.

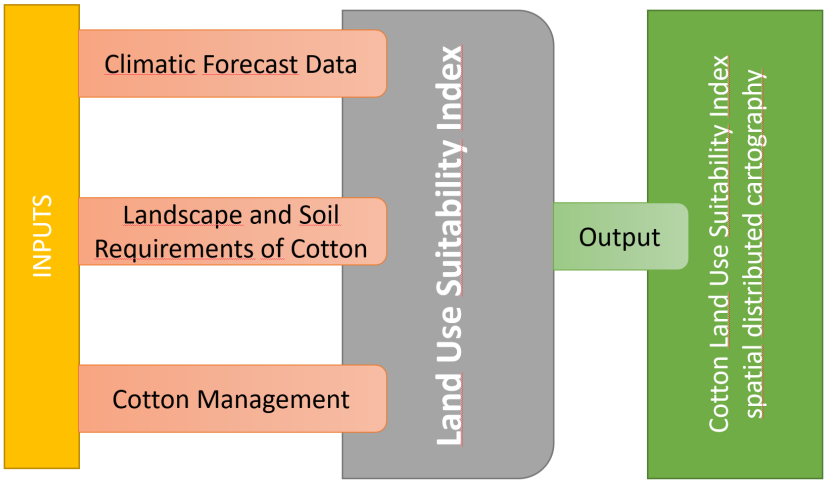

Figure 1. Inputs requirements and outputs delivered overview for the Land Use Suitability-based indicators model.

The approach involves standardizing the suitability maps, assigning relative importance weights to the suitability maps, and then combining the weights and the standardized suitability maps to obtain a suitability score. The decision maker directly assigns the "relative importance" weights to each layer of the attribute map; in this case, input has been received from local experts those crops.

Local team of experts suggest suitable conditions and thresholds of all variables concerning of the good development. A quantification of the performance of each input parameter between 0 to 100% is calculated according to the indications provided by experienced crop managers. The importance of each variable is not the same in all cases then a weight for every variable is determined following an Analytical Hierarchical Process (AHP) method (Saaty 2008). These weights are used in the suitability index of each variable and combined linearly to obtain the suitability value (0-100). Once this value is obtained, we regroup these results assuming the classification proposed by FAO framework (Table 1).

Table 1. Scheme for Land Evaluation (FAO 1976). The performance and score were proposed by Sys et al. (1991).

FAO Sutability classes	**Characterization**	**Performance / Score**
S1	Highly suitable	100-85
S2	Average suitable	85-60
S3	Marginal Suitable	60-40
N1	Temporary unsuitable	40-25
N2	Permanently unsuitable	<25

Results and concluding remarks

Crop LUS map at the Pinios River Basin 11,000 km^2, located in Greece have been developed and are evaluated. Once the LUS is estimated, a collection of yearly thematic maps over both river basins is ready for use by local stakeholders, regarding different climate change scenarios (RCP 4.5 and RCP 8.5).

These results are part of the EU Horizon 2020 project REXUS (Managing Resilient Nexus Systems Through Participatory Systems Dynamics Modelling), in which local stakeholders, from farmers to land use managers, are collecting and evaluating the information to implement nexus strategies for climate change adaptation. Our final goal is to provide spatial information for future climate change scenarios that increase land-use knowledge and enhance decision-making policies.

Acknowledgments: This paper is done under the umbrella of a research EU Horizon 2020 project called REXUS (*Managing Resilient Nexus Systems Through Participatory Systems Dynamics Modelling, reference 101003632*). Authors want to express their deeper gratitude to the local teams for providing valuable modelling input data. Thanks to Andreas Panagopoulos, Vassilis Pisinaras and Dimitris Malamataris from Soil and Water Resource Institute of Greece (SWRI) for their coordination in the team of experts needed for the present work.

References

FAO (1976) A framework for land evaluation, Rome: Agriculture Organization of the United Nations.

Saaty TL (2008) Relative measurement and its generalization in decision making why pairwise comparisons are central in mathematics for the measurement of intangible factors the analytic hierarchy/network process. Rev. R. Acad. Cien. Serie A. Mat. 102: 251–318. https://doi.org/10.1007/BF03191825

Sys C, Ranst V, Debaveye J (1991) Requirements, Land Evaluation Part I Principles in Land Evaluation and crop production calculations, Brussels Belgium: General Administration for development Cooperation

Climate risk assessment for the food system in Pinios river basin, Greece

C. Papadaskalopoulou[1*], D. Tassopoulos[1], M. Antoniadou[1,2]
[1] *DRAXIS Environmental S.A. 54-56 Themistokli Sofouli str., 54655, Thessaloniki, Greece*
[2] *Department of Meteorology and Climatology, School of Geology, Faculty of Sciences, Aristotle University of Thessaloniki, GR54124, Thessaloniki, Greece*
** e-mail: chpapadaskalopoulou@draxis.gr*

Introduction

The water and food systems are inextricably linked so that actions in one policy area commonly have impacts on the other, as well as on the energy system that natural resources and human activities ultimately depend upon. All three elements – water, energy, food (WEF) – are crucial for human well-being, poverty reduction and sustainable socio-economic development. Climate is strongly connected to the WEF systems, as it provides vital sources for their functionality while a changing climate may have adverse effects on them. The thorough analysis of the WEF and Climate nexus not only needs to account for the interactions taking place today, but also to consider how future climate will affect them. The current analysis presents the climate risk assessment of the food system for Pinios River Basin, one of the five pilot areas of REXUS project.

Materials and methods

The methodology for the assessment of climate risks on the Water – Energy – Food Nexus was developed based on the conceptual framework set by the Intergovernmental Panel on Climate Change (Reisinger et al. 2020). In specific, risks are assessed as the result of the dynamic interactions between the climate-related hazards with the exposure and vulnerability of the affected systems to the hazards. On the other hand, adaptive capacity is considered to reduce risk. In the framework of the current assessment, each of the aforementioned risk components constitutes a composite indicator consisting of one or more sub-indicators. In specific, a set of hazard indicators is used to reflect the climate related hazards for the WEF systems (e.g., heat stress, aridity, flood, frost) based on the climate projections for two climatic scenarios RCP4.5 and RCP8.5. The assessment of hazard is carried out for the period 2031-2050 in comparison to the reference period 1986-2005. For estimating the exposure of elements in an area where hazard events might occur, geospatial data on the areas cultivated with crops are used. For assessing vulnerability, several socio-economic indicators were used, as well as indicators that reflect the level of existing stress of the WEF systems, such as the Water Exploitation Index (WEI), the agricultural water consumption and the agricultural income. For assessing adaptive capacity, two sub-indicators are selected, i.e. (i) the adaptation readiness referring to the institutional capacity of a given region, and (ii) the economic capacity of a country reflected by its Gross Domestic Product (GDP). In specific for the assessment of the former, local stakeholders were asked to evaluate and weigh five institutional capacity factors through the analytical hierarchy process method.

Results and concluding remarks

In this section the results of the risk assessment for the Pinios river basin are provided. Starting with the hazard indicators, the results of the projections related to the aridity indicator show a shift from the prevalence of humid to semi-arid conditions at the Pinios pilot area in the reference period to mostly semi-arid and arid conditions in the future period, according to both scenarios. With respect to the hazard indicator of flood recurrence for a 50year return period, it was shown that while an increase is expected on average for the whole area according to both scenarios, there are several areas within the pilot for which a decrease is expected, especially in the case of RCP8.5. The projections of the hazard indicator related to the number of Growing Degree Days (GDD), show an increasing trend for both RCP4.5 (17%) and RCP8.5 (27%),

compared to the reference period, thus indicating a positive effect of climate change on crop growth. The projected relative change of the number of heat stress days >25°C shows an increase of 38% on average, with small differentiation among the two scenarios. On the other hand, the number of frost days (minimum temperature >0°C) is expected to decrease by 40% on average, with no significant difference between the scenarios, which is beneficial for crop growth. With respect to the exposure component of the assessment, it was shown that the crops under study are cultivated in great extent (18-35%) at most of the municipalities of the pilot area. As for the vulnerability component, three indicators were examined. The first indicator, the WEI of Thessaly river basin district where the Pinios pilot area is located, is estimated to be 0.4 which is the threshold above which, water stress may begin to be a limiting factor on economic development. Additionally, the indicator of water consumption for agriculture in the Pinios river basin (>90% of total water consumption) is very high, therefore a potential reduction in water availability due to climate change would be critical for the agricultural sector of the area. The agricultural income indicator for the region of Thessaly is 210% higher compared to the national average, which indicates a high dependency of the country to the agricultural income of the region. With respect to the adaptive capacity, the institutional capacity indicator for the Pinios pilot area was evaluated as medium. Finally, the GDP indicator for Greece is 54% of the EU average, thus reflecting a low to medium economic capacity of the pilot. The overall results of the climate risk assessment, with respect to the food system, are depicted in Figure 1. As it can be seen, a medium level risk is expected for more than half of the municipalities of the pilot, while the risk for the other municipalities is characterized from low to low-medium.

Table 1. Qualitative climate risk assessment for the food system per risk component.

Risk components	Index	Level
Hazard	Frost	Low
	Heat stress	Medium-High
	Aridity	Medium-High
	Decrease of growing degree days	None
	Increase of floods	Medium
Exposure	Cultivated area	Medium
Vulnerability	Agricultural water consumption	High
	Water exploitation	High
	Agricultural income	High
Adaptive Capacity	Institutional capacity	Medium
	GDP	Low-Medium

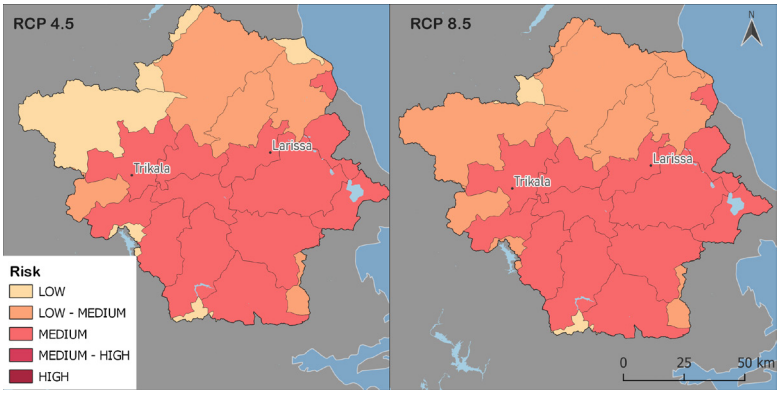

Figure 1. Qualitative climate risk assessment for the food system per municipality.

Acknowledgments: This study was conducted in the framework of the REXUS project which has received funding from the European Union's Horizon 2020 research and innovation programme under grant agreement No 101003632.

References

Reisinger A, Howden M, Vera C (2020) The Concept of Risk in the IPCC Sixth Assessment Report: A Summary of Cross-Working Group Discussions. Intergovernmental Panel on Climate Change, Geneva, Switzerland, 15p https://www.ipcc.ch/site/assets/uploads/2021/02/Risk-guidance-FINAL_15Feb2021.pdf

Applying the Farm Process for assessing irrigation demand and water management in Arta, Greece

K.S. Panagiotaropoulos*, C. Pouliaris, E. Chrysanthopoulos, M. Perdikaki, K. Markantonis, A. Kallioras
School of Mining and Metallurgical Engineering, National Technical University of Athens, Athens, Greece
** e-mail: kostaspan96@yahoo.gr*

Introduction

This study presents the results of the application of a hydrologic model aiming at assessing irrigation strategies in an agricultural area. The alluvial plain field of Arta is the case study area; the area has an extent of 271 km^2 and it is covered with a wide variety of cultivations, namely kiwi, olive trees, citrus trees and potatoes. The paper involves the application of the Farm Process of MODFLOW OWHM (Hanson et al. 2014) in the area, including the cultivations that are the most crucial for the agricultural and economic development of the area. A calibrated MODFLOW 2005 (Harbaugh 2005) model is used as the base model of the simulation. The aim is to estimate the irrigation water demand for various types of crops in different fields in order to assess different water management scenarios in the area. The results of such studies can give new insights in the management of irrigation water in various scales, especially if connected to the energy demand for pumping and distribution of water.

Materials and methods

As mentioned, the Farm Process model is based on a preexisting MODFLOW 2005 model (Pouliaris et al. 2022). For the needs of the simulations, the model was transferred to the FREEWAT platform (De Filippis et al. 2019 and references therein), which is a plugin included in QGIS 2.18 that allows the user to build, run and visualize groundwater related models, using the MODFLOW family of codes.

Regarding the cultivations present in the area, each one of them represents a water consumption unit which is called 'farm'. The simulation has been applied for each farm.

The irrigation and drainage networks are included in the simulation for providing irrigation water in the adjacent farms and improving the drainage of the cultivated fields.

The wells included in the simulation are also connected with the farms by defying the maximum well capacity (m^3/day).

Results and concluding remarks

Results show the Farm's Budget which has been presented by three diagrams (Figure 1):

- The first concerns the total water inflows to the water unit which is the sum of the supply from precipitation, evaporation from groundwater and the surface water delivery which is the supply from the irrigation network.
- The second concerns the total water outflows from the water unit which is the sum of: i) Evaporation from: a) irrigation, b) precipitation and c) groundwater, ii) Transpiration from a) irrigation and b) precipitation, iii) Runoff and iv) Deep percolation.
- The third concerns the Total Farm Delivery Requirement (TDFR) which is practically the farm's water irrigation requirement.

By observing the third diagram, it can be concluded, that the total farm delivery requirement has been satisfied only by the irrigation network and there is no need to have groundwater supply from pumping wells.

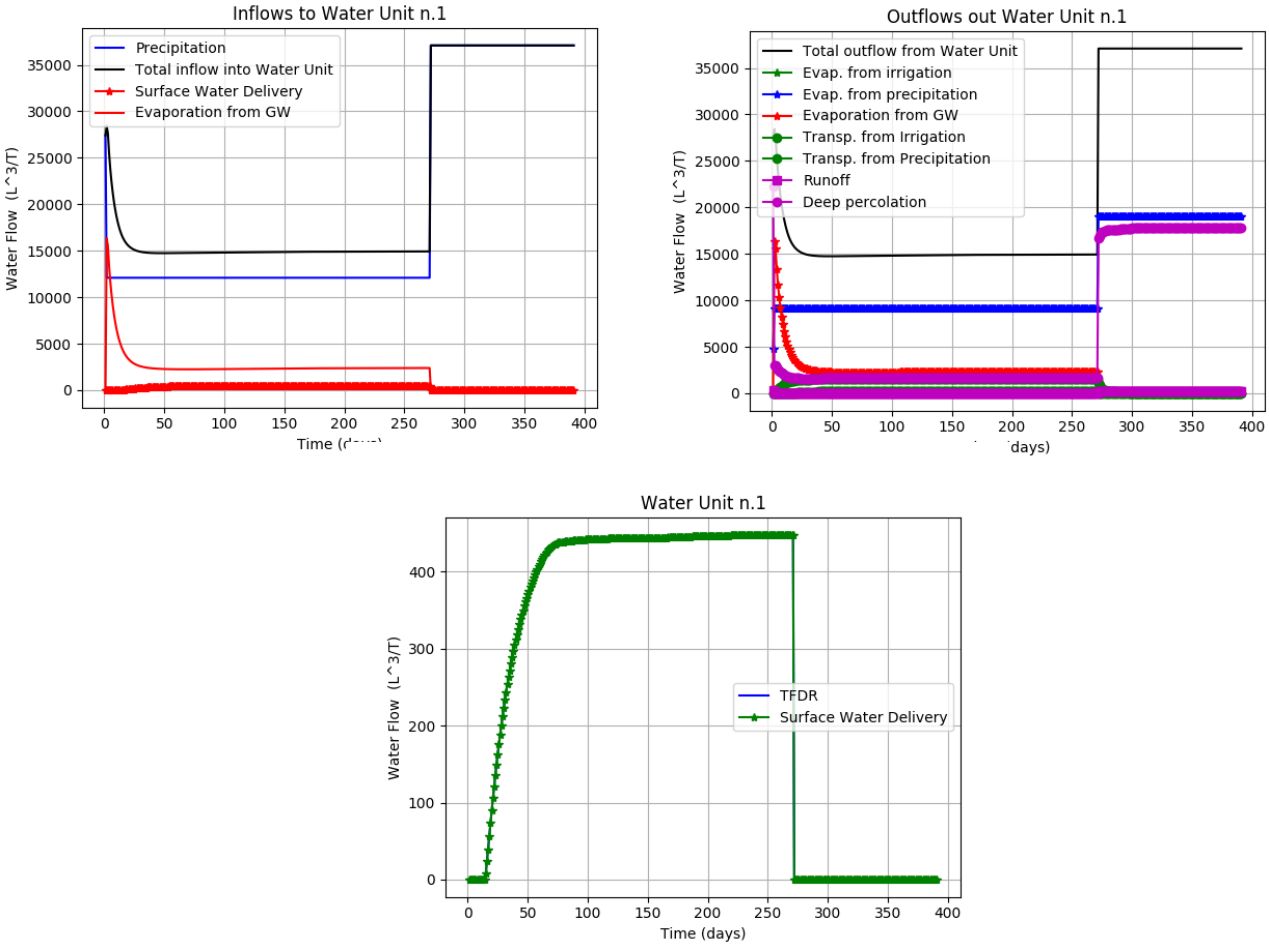

Figure 1. Results of the simulation showing the total water inflows to the Farm 1 (kiwi), the total water outflows and the total irrigation demand.

Acknowledgments: We acknowledge support of this work by the project "e-Pyrros: Development of an integrated monitoring network for hydro-environmental parameters within the hydro-systems of Louros-Arachthos-Amvrakikos for the optimal management and improvement of agricultural production" (MIS 5047059) which is implemented under the Action "Reinforcement of the Research and Innovation Infrastructure", funded by the Operational Programme "Competitiveness, Entrepreneurship and Innovation" (NSRF 2014-2020) and co-financed by Greece and the European Union (European Regional Development Fund).

References

De Filippis G, Pouliaris C, Kahuda D, Vasile TA, Manea VA, Zaun F, Panteleit B, Dadaser-Celik F, Positano P, Nannucci MS, Grodzynskyi M, Marandi A, Sapiano M, Kopač I, Kallioras A, Cannata M, Filiali-Meknassi Y, Foglia L, Borsi I, Rossetto R (2020) Spatial Data Management and Numerical Modelling: Demonstrating the Application of the QGIS-Integrated Platform at 13 Case Studies for Tackling Groundwater Resource Management. Water 12: 41. http://doi.org/10.3390/w12010041

Hanson RT, Boyce SE, Schmid W, Hughes JD, Mehl SM, Leake SA, Maddock T, Niswonger RG (2014) One-Water Hydrologic Flow Model (MODFLOW-OWHM): U.S. Geological Survey Techniques and Methods 6-A51, 120 p, http://dx.doi.org/10.3133/tm6A51

Harbaugh AW (2005) MODFLOW-2005, The U.S. Geological Survey modular ground-water model—the Ground-Water Flow Process: U.S. Geological Survey Techniques and Methods 6-A16

Pouliaris C, Chrysanthopoulos E, Perdikaki M, Koltsida E, Myriounis C, Markantonis K, Kallioras A (2022) Groundwater modelling and data dependence: Getting insight on the simulated processes through Fit-Independent Statistics, 16th International Congress of the Geological Society of Greece, 17-19 October, Patras, Greece

Unravelling the complexity of water-ecosystems-food nexus through integrated modelling: The Doñana case study in SW Spain

C. Panciera[1], A. Pagano[2*], R. Giordano[2], I. Portoghese[2], P. Vergine[2], M. Bea[3], M. Najar[4], M.C. Gunacti[5], G. Onusluel Gul[5]
[1] DICATECh, Politecnico di Bari, Bari, Italy
[2] Water Research Institute- National Research Council (IRSA- CNR), Bari, Italy
[3] Asociación ECOADAPTA, Madrid, Spain
[4] GIS Department, Islamic University of Gaza, Gaza, Palestine
[5] Department of Civil Engineering, Faculty of Engineering, Dokuz Eylul University, Izmir, Turkey
* e-mail: alessandro.pagano@ba.irsa.cnr.it

Introduction

This work describes the development of a model for supporting an improved Nexus understanding and management in a complex context with multi-dimensional problems and conflicts. Phenomena such as the demographic and economic growth of an area, as well as the impacts of climate change, lead to competition between sectors such as agriculture, domestic and industrial uses and the environment (Karamouz et al. 2021). The sustainable exploitation of water is a challenging task particularly in protected areas such as the Doñana National Park (DNP), a coastal area in SW Spain. Several research projects already focused on this area and, currently, the LENSES project is proposing new modelling approaches in which local knowledge and scientific tools are integrated to better investigate the interplay between marshland state and water exploitation, for both irrigation and drinking purposes. The main aim of our work is the development and implementation of an integrated socio-ecological model for the area that allows building a holistic view of the system, combining quantitative hydrological modelling with the dynamic interactions that involve resources and users (Pulido-Velazquez et al. 2023). This integrated modelling approach is based particularly on the use of hydrological modelling, water resources allocation modelling and Participatory System Dynamic modelling techniques. It aims to explicitly include the local stakeholders' knowledge and perception in all activities, from model definition to scenario analysis. The present work mainly focuses on the conceptualization of the study area and aims to provide an improved understanding of the interconnections among multiple uses and users of natural resources.

The ultimate goal of the adopted approach, therefore, is to operationalise the Water-Ecosystems-Food (WEF) Nexus, supporting decision- and policy-makers in finding solutions for a more sustainable and resilient Nexus management, exploring multiple scenarios which include e.g. new infrastructures, different management conditions and Nature-based Solutions (NbS).

Materials and methods

The main problem affecting Doñana area concerns the overexploitation of surface water bodies and groundwater, mainly due to the high irrigation demand (with legal and illegal withdrawals) and tourism in the coastal area. This exploitation, along with the imbalances due to climate change, leads to alterations in the marshland regimes, with severe environmental effects. Furthermore, the pristine hydrological state of the marshland has been highly altered by flow regulation works that disconnected the water-dependent environments. Even some high water-demanding crops such as berries contribute to the imbalances in the area. The interactions between all these hydrogeological, infrastructural and human factors needs to be carefully investigated to define sustainable pathways for the area. The proposed modelling approach is based on the integration of hydrological modelling with a water allocation model and Participatory System Dynamics Modelling (PSDM). The first step of the proposed approach is related to the definition of baseline knowledge for building a consistent conceptual scheme of the system. Starting from the review of the available literature, key elements of interest are identified based on their function, e.g. points of demand

such as urban areas or crops that need irrigation, or storage points such as groundwater bodies or dams. The functional interconnections among these elements are drawn (i.e. streams-drainage channels-wetlands) using the Hydrologic Modeling System (HEC-HMS) for a suitable representation of main hydrological processes in the Doñana sub-catchments. The hydrological model is also determinant to quantify the impact of climate change on the system, and then to realize input for the scenarios that will be subsequently implemented. The literature information is then augmented through the evidence of a series of participatory activities (semi-structured interviews and workshops), oriented to understand the interdependencies among different users and uses of resources. Such conceptual model allows identifying not only the hydrological connections but also the causal ones, which are fundamental for scenarios design and analysis. The second step is carried out using WEAP (Water Evaluation And Planning) software. The conceptual scheme is basically translated into a WEAP model, and all the numerical data needed are reviewed and included into the model. In such a complex context, the main value added of the WEAP model is to explicitly consider to the water balance the quantitative modelling of stakeholders' needs, as well as the role of environmental needs. A baseline scenario is then created, which reflects present system conditions and likely evolution. The third step is based on the integration of the outcomes of WEAP with PSDM tools, namely Causal Loop Diagrams and stock and flow models. The interaction is twofold: i) PSDM can inform the WEAP analysis providing a set of key scenarios to analyse; ii) PSDM can then test the multidimensional impacts that different management measures can have on the system, based on the Nexus approach.

Preliminary results and overview of future activities

A conceptual scheme has been created for the system and translated into HEC-HMS and WEAP models, which provide a snapshot of current system conditions and potential imbalances. A comprehensive overview of the system will allow inserting and modifying nodes and connections, guaranteeing a conceptual understanding of interconnections that can be considered in scenario analysis. In particular, the scenario analysis will help assessing the impact of different strategies, i.e. a combination of measures (ranging from different water management criteria, to infrastructural changes and NBS), which will be co-designed through PSDM exercises. PSDM is currently being developed (in the form of both Causal Loop Diagrams and Stock and flow model) to build a holistic system picture, which reflects in a consensual way the system perception of multiple stakeholders, as well as the multi-dimensional impacts of such strategies. The coupling between different models will ultimately provide actionable information for decision- and policy makers involved in the area, based on an improved understanding of the impacts of multiple stressors and measures on the system as a whole.

Acknowledgments: The present work has been funded by the LENSES project (PRIMA Programme, GA n°2041). This paper and the content included do not represent the opinion of PRIMA Foundation, PRIMA foundation is not responsible for any use that might be made of its content.

References

Karamouz M, Barkhordari H, Ebrahimi E (2021) Dynamics of Water Allocation: Tradeoffs between Allocator's and Farmers' Benefits of Irrigation Practices. Journal of Irrigation and Drainage Engineering Online 147(6). http://doi.org/10.1061/(ASCE)IR.1943-4774.0001550

Pulido-Velazquez D, Baena-Ruiz L, Mayor B, Zorrilla-Miras P, López-Gunn E, de Dios Gómez-Gómez J,de la Hera-Portillo Á, Collados-Lara AJ, Mejías Moreno M, García Aróstegui JL, Alcalá FJ (2023) Integrating stakeholders' inputs to co-design climate resilience adaptation measures in Mediterranean areas with conflicts between wetland conservation and intensive agriculture. Science of The Total Environment 870: 161905. https://doi.org/10.1016/j.scitotenv.2023.161905

12th World Congress on Water Resources and Environment (EWRA 2023)
"Managing Water-Energy-Land-Food under Climatic, Environmental and Social Instability"
Thessaloniki, Greece, 27 June - 1 July 2023

The Remote Sensing-based Agricultural Water Accounting and Footprint (RS-AWAF) for different river basins and crop management conditions

J. Garrido-Rubio[1], J. González-Piqueras[1], A. Ossan[2], A. Calera[1]
[1] Remote Sensing and GIS group, IDR-UCLM, Campus Universitario s/n, 02071 Albacete, Spain
[2] Agrisat Iberia S.L., P. Científico y Tecnológico, Ed. Emprendedores, Paseo de la Innovación nº 1, 02006 Albacete, Spain
* e-mail: jesus.garrido@uclm.es

Introduction

Aside from raising public awareness, gathering indicators on the sustainability of productive human sectors provides invaluable information in the administration of political decision-making (Giljum et al. 2008; Čuček et al. 2015). Among the environmental indicators available today, the water footprint approach brings to the agriculture sector the opportunity to distinguish the water source used along the crop development between the surface or groundwater resources (blue water) or the precipitation events (green water). This information converted later in the agricultural water footprint allows water managers to achieve a better understanding of their territories. While a considerable number of researchers employed tabulated values for crop parametrization, the use of remote sensing temporal series received less attention (Feng et al. 2021).

According to that, the present paper presents an innovative approach that uses the strength of dense time series for crop monitoring over large areas (Tasumi and Allen 2007), to derive biophysical parameters such as basal crop coefficient, to be used within a remote sensing-based soil water balance (Garrido-Rubio et al. 2020), and to estimate later the temporal and spatially distributed crop adjusted evapotranspiration (ET_{cadj}) and net irrigation requirements (NIR). Finally, these two components are included in the agricultural water footprint framework (Hoekstra et al. 2011), to obtain again temporal and spatially distributed thematic maps of the green and blue crop water use (CWU_{green} and CWU_{blue}) as well as the green and blue water footprint (WF_{green} and WF_{blue}) remotely sense assisted. Therefore, the combination of earth observation images, the soil water balance and the water footprint approach configure the Remote Sensing-based Agricultural Water Accounting and Footprint (RS-AWAF).

Materials and methods

The RS-AWAF approach presented is applied over different river basins across the European continent: Júcar (Spain 2017, 42.735 Km^2), Pinios (Greece 2017, 11.000 Km^2), Isonzo-Soča (Italy and Slovenia 2018, 3.400 Km^2), and an area enclosed in the Lower Danube river basin near Craiova (Romania 2018, 14.000 Km^2). The common and most cultivated crops in all areas are wheat and maize, although citric, vineyards, vegetable orchards, stone fruits or cotton are well represented at least in one study area. All areas present irrigated and rainfed crops that finally are developed under different crop management. The Köppen-Geiger climate classification (Beck et al. 2018) states Júcar and Pinios as arid, steppe and cold climate (Bsk) and temperate with dry and hot summer climate (Csa); in Lower Danube, the climate is cold with no dry season and hot summer (Dfa) like in the Slovenian part in Isonzo- Soča area although in the Italian part, the climate is temperate with no dry season and hot summer (Cfa).

In parallel, the inputs for RS-AWAF are: i) remote sensing time series of images from satellite Sentinel-2 were processed to obtain NDVI (at 10 m spatial resolution scale); ii) daily climatic records of Precipitation and reference evapotranspiration from local agroclimatic networks or from the Agri4Cast Resource Portal (https://agri4cast.jrc.ec.europa.eu/); iii) crop characteristics such as root depth or evapotranspiration depletion fraction for soil water balance from local experts or FAO56 guidelines; iv) crop yield from local surveys or national statistics; and v) the soil characteristics such as total available water or soil limit depth to root development from the European Soil Database (https://esdac.jrc.ec.europa.eu/).

As said, the RS-AWAF combines two globally accepted and used methodologies. Firstly, the remote

sensing-based soil water balance is based on FAO56 methodology (Allen et al. 1998) that provides temporal and spatially distributed crop adjusted evapotranspiration (ET_{cadj}) and net irrigation requirements (NIR). Later, these two components are monthly aggregated and then included by equations (1) and (2) along the crop cycle into the agricultural water footprint approach to obtain the thematical maps of the four components cited in the introduction section CWU_{green}, CWU_{blue}, WF_{green} and WF_{blue}.

$$CWU_{blue} = 10 \sum NIR \quad (1)$$

$$CWU_{green} = 0 \text{ when } (ET_{cadj} - NIR) < 0 \textit{ otherwise } CWU_{green} = 10 \sum (ET_{cadj} - NIR) \quad (2)$$

Results and concluding remarks

Results from RS-AWAF are thematical maps at 10 m pixel spatial scale of CWU_{green}, CWU_{blue}, WF_{green} and WF_{blue}. While the first two components are provided at monthly and yearly temporal scales the final two are based on the crop campaign (just yearly). Evaluation values regarding irrigation water demand or gross irrigation water consumed at Júcar and Isonzo-Soča river basins were provided. Its comparison with remote sensing-based estimated values was adequate.

In addition, zonal statistical values were computed by crop type at different spatial scales aggregation. Focusing on maize at Pinios and Júcar river basin scale (that present a similar average crop yield value of 12.3 and 13.6 t/ha respectively) the WF_{green} varies from 210 to 90 m^3/t respectively and WF_{blue} varies from 360 to 410 m^3/t respectively. This range of values is due to a difference in the type of crop water usage because in Júcar the blue crop water use is higher than in Greece and vice versa (2,620 versus 1,280 m^3/ha for CWU_{green} and 4,430 versus 5,520 m^3/ha for CWU_{blue} both in Pinios and Júcar areas respectively).

Among the principal concluding remarks, we highlight the novelty approach to obtain appropriate agricultural water accounting and footprint values along different areas with different crop management practices based on remote sensing dense temporal series and in a remote sensing-based soil water balance. Hence, the RS-AWAF provides the private or public water managers with temporal and spatial distributed thematical maps of CWU_{green}, CWU_{blue}, WF_{green} and WF_{blue}. Its strength lies in distributed information for political decision-making that contributes to enlarging the knowledge database of a territory. Oppositely, the authors highlight that more years should be included in the present study as the agricultural water footprint framework states to provide more independent values regarding different climatological conditions.

Acknowledgements: This paper is done under the umbrella of a research EU Horizon 2020 project called REXUS (*Managing Resilient Nexus Systems Through Participatory Systems Dynamics Modelling*). The authors want to express their deeper gratitude to the local teams for providing valuable modelling input data.

References

Allen RG, Pereira LS, Raes D, Smith M (1998) Crop evapotranspiration - Guidelines for computing crop water requirements. FAO Irrigation and Drainage Paper No 56. FAO, Rome, Italy

Beck HE, Zimmermann NE, McVicar TR, Vergopolan N, Berg A et al. (2018) Present and future Köppen-Geiger climate classification maps at 1-km resolution. Sci. Data 5: 180214. https://doi.org/10.1038/sdata.2018.214

Čuček L, Klemeš JL, Varbanov PS, Kravanja Z (2015) Significance of environmental footprints for evaluating sustainability and security of development. Clean Technol. Environ. Policy 17(8): 2125–2141. https://doi.org/10.1007/S10098-015-0972-3

Feng B., Zhuo L, Xie D, Mao Y, Gao J et al. (2021) A quantitative review of water footprint accounting and simulation for crop production based on publications during 2002–2018. Ecol. Indic. 120: 106962. https://doi.org/10.1016/J.ECOLIND.2020.106962

Garrido-Rubio J, González-Piqueras J, Campos I, Osann A, González-Gómez L et al. (2020) Remote sensing–based soil water balance for irrigation water accounting at plot and water user association management scale. Agric. Water Manag. 238: 106236. https://doi.org/10.1016/j.agwat.2020.106236

Giljum S, Hinterberger F, Lutter S (2008) Measuring Natural Resource Use: Con- text, Indicators and EU Policy Processes. Background Paper 14. SERI, Vienna

Hoekstra AY, Chapagain AK, Aldaya MM, Mekonnen MM (2011) The Water Footprint Assessment Manual. Earthscan, London

Tasumi M, Allen RG (2007) Satellite-based ET mapping to assess variation in ET with timing of crop development. Agric. Water Manag. 88(1–3): 54–62. https://doi.org/10.1016/j.agwat.2006.08.010

Development and implementation of a HRES in Leros island

S. Skroufouta*, A. Lemonis, E. Baltas
Department of Water Resources and Environmental Engineering, School of Civil Engineering, National Technical University of Athens, 5 Iroon Polytechniou, 157 80, Athens, Greece
** e-mail: sofiaskroufouta@chi.civil.ntua.gr*

Introduction

Water scarcity is a vital problem, troubling humankind all around the world in the last decades. The problem is more severe in cases, where the accessibility to renewable water resources, like rivers; is the case of Greece and, especially, of the Greek islands. Therefore, the cost of drinking water is very high, since it is transferred by watercraft. Aiming also to reduce the dependence on fossil fuels world widely, there is an effort to include renewable energy resources (RES) more and more in the energy balance. Exploiting RES and combining them with desalination could be the answer to the world's remote offshore locations' water shortage and unstable electrical systems (Belessiotis et al. 2016; Miller 2003; Khare 2016; Emmanouilidis and Karalis 2001; Ghaffour et al. 2015). Even though the use of RES is a great step towards sustainability, it is necessary to be able to store the produced energy, in order to allocate it where and when is needed and increase the reliability of the system; leading the solution to the hybrid renewable energy systems (HRES) (Papaefthymiou et al. 2012; Anagnostopoulos and Papantonis 2007; Farrokhifar 2016; Giatrakos et al. 2009; Ribeiro et al. 2012).

The under-study HRES is located in Leros, Greece and consists of a wind park (4.2 MW), 2 desalination plants (total capacity of 2,000 m^3/day), a seawater hydroelectric plant (flow capacity of 5 m^3/s, capacity of 780,000 m^3 at 170 m above sea level), a pumping station (2 MW) and a desalinated water reservoir (785,000 m^3). The main objectives of the sizing of the HRES, with a 40-year lifespan, are the coverage of drinking water, irrigation and energy needs, as well as the reduction of CO_2 emission.

Materials and methods

The first important step in this simulation is the data processing of the input timeseries. Due to the project's 40-year lifespan, the uncertainty of the natural processes and often their data deficiency, the use of stochastic methods seems to be crucial. In the case of wind speed, the production of the hourly synthetic timeseries is based on the method of Negra et al. (2008), while, for the production of rainfall and temperature timeseries, the chosen stochastic method is ARMA (1,1) (Mimikou et al. 2016).

Subsequently, it is important to estimate the needs, that the HRES aims to meet. Drinking water needs are estimated, assuming a typical consumption per capita per day (150 L/day/capita for the permanent population and 200 L/day/capita for the tourists), taking into account the population increase and the seasonal increased needs due to high temperatures. Irrigation needs are estimated with the Blaney-Criddle method, since it is the recommended method in the Greek area, using as inputs the synthetic timeseries of rainfall and temperature (Hargreaves and Samani 1982). Lastly, the energy needs deduced from the neighboring island of Patmos, which has similar social-economic features.

The HRES' operation prioritizes first drinking water supply (i.e. the desalination plant) and then irrigation and electricity. Therefore, 30% of the electricity produced by the wind park is sent directly to the grid, while the remaining 70% powers the desalination plant. If there is any surplus energy after producing the necessary drinking and irrigation water, it is stored using the Pumped Storage Hydroelectricity (PSH) technique, which has the shape of a reversible HP and is both suitable and environmentally beneficial, as well as being an economical means of storing electricity for the Greek islands.

Results and concluding remarks

The simulation of the HRES seems to produce remarkably good results, since drinking water needs, the

primary goal of the HRES, is met with 85% reliability. The first 20 year period, however, where geometric population growth is less conservative, the reliability rises to 99%. The considerable volume of the desalinated water reservoir and the supply of the required energy for the desalination plant's operation account for this great reliability. The coverage of energy needs derives 26% from the Public Power Corporation (PPC) network, 22% from the wind park and 52% from the HPP. The ability of each energy source (hydropower, wind energy, and energy from the PPC network) to provide the island's complete energy needs. Although the national network of PPC and the wind park contribute more power on average each month than hydropower does, there are some months when PPC is primarily responsible for meeting the demand. The maximum yearly production is 35,000 MWh, while the greatest annual demand is 46000 MWh; with the overall annual energy production consistently above 28,000 MWh. Lastly, the coverage of irrigation water needs amounts to 63.92%. Essentially, the average annual reliability of drinking water and irrigation is decreased, because not enough energy is produced to meet the island's and the desalination plant's peak energy demands during the summer months when energy needs are higher.

References

Belessiotis V, Kalogirou S, Delyannis E (2016) Thermal Solar Desalination: Methods and Systems. Elsevier

Miller JE (2003) Review of Water Resources and Desalination Technologies. Materials Chemistry Department, Sandia National Laboratories

Khare V, Nem S, Baredar P (2016) Solarwind hybrid renewable energy system: a review. Renew. Sustain. Energy Rev. 58: 23-33

Emmanouilidis G, Karalis G (2001) Desalination Plants in the Arid Islands of the Aegean, Technologies, Institutional Framework, Use of RES and Case Studies: Patmos, Lipsi, Thirasia. Ios-Aegean Energy Office - Consultant of the Islands in Energy

Ghaffour N, Bundschuh J, Mahmoudi H, Goosen MFA (2016) Renewable energy driven desalination technologies: a comprehensive review on challenges and potential applications of integrated systems. Desalination 356: 94-114

Papaefthymiou SV, Papathanassiou SV, Karamanou EG (2012) Application of pumped storage to increase renewable energy penetration in autonomous island systems. In: Wind Energy Conversion Systems, Springer, London 295-335

Anagnostopoulos JS, Papantonis DE (2007) Pumping station design for a pumpedstorage wind-hydro power plant. Energy Convers. Manag. 48(11): 3009-3017

Farrokhifar M (2016) Optimal operation of energy storage devices with RESs to improve efficiency of distribution grids; technical and economical assessment. Int. J. Electr. Power Energy Syst. 74: 153-161

Giatrakos GP, Tsoutsos TD, Mouchtaropoulos PG, Naxakis GD, Stavrakakis G (2009) Sustainable energy planning based on a stand-alone hybrid renewable energy/hydrogen power system: application in Karpathos island, Greece. Renew. Energy 34: 2562-25

Ribeiro LA de S, Saavedra OR., Lima SL, de Matos JG, Bonan G (2012) Making isolated renewable energy systems more reliable. Renew. Energy 45: 221-231

Negra NB, Birgitte BJ, Sorensen P (2008) Model of a Synthetic Wind Speed Time Series Generator. Wind Energy 11(2): 193 - 209

Mimikou MA, Baltas EA, Tsihrintzis VA (2016) Hydrology and Water Resource Systems Analysis. CRC Press-Taylor & Francis Group, Boca Raton, FL, USA

Hargreaves GH, Samani ZA (1982) Estimating potential evapotranspiration, J. Irrigat. Drain. Eng. 108: 223-230

Strengthening water-food-ecosystem nexus management through learning and action alliances: Insights from REXUS and LENSES projects

B.Willaarts[1*], R. Giordano[2], I. Portoghese[2], A. Pagano[2], M. Bea[1,3], E.López-Moya[1,3]
[1] I-CATALIST S.L., Madrid, Spain
[2] Water Research Institute - National Research Council (IRSA- CNR), Bari, Italy
[3] Asociación ECOADAPTA, Madrid, Spain
* e-mail: bwillaarts@icatalist.eu

Introduction

This communication introduces the work currently conducted within REXUS and LENSES projects for supporting the elaboration of participatory strategic roadmaps towards resilient WFE (Water-Food-Ecosystems) Nexus in 12 pilots. This approach is being integrated with participatory system dynamic modelling (PSDM) within the framework of local and project Learning and Action Alliances (LAAs).

Socio-ecological systems are *complex* and highly uncertain, requiring the development of integrated approaches, also called "nexus approaches" to manage often conflicting views and goals. *Conflicts* arise between users and stakeholders with different priorities, as well as competing regulations, which undermine the potential of the Nexus approach for sustainable development and social prosperity. A *Nexus approach* can help to solve these conflicts by aiming for optimal, sustainable, and fair resource allocation, fostering a collaborative paradigm, and overcoming sectorial isolation.

To address these challenges, REXUS (funded under Horizon 2020) and LENSES (funded by PRIMA foundation) projects are using a similar approach for *stakeholder engagement and mobilisation*. Both projects aim to contextualise Resilient Nexus Systems and create a common vision and action plan to address chronic stresses and acute shocks in diverse pilot contexts. Visioning is being developed as a core part of the participatory activities, with Learning and Action Alliances (LAAs) integrating stakeholder discussions and knowledge sharing activities into a structured visioning process. This will lead to the elaboration of action plans, also called *transition roadmaps* for managing and operationalising the Water-Food-Ecosystem Nexus in a plausible, realistic, and holistic manner.

The process of *visioning prosperous nexus communities* begins with sharing knowledge among stakeholders in a participatory way to address conflicts. LAAs involve multi-level and multi-scale stakeholders who will produce shared visions and find tangible ways to put in place methods and tools through cooperation. The co-creation process in the LAA is the development of transformative scenarios for resilience building through the integration of explorative models and participatory activities. At the pilot level, this approach will allow for knowledge exchange and will improve stakeholders' scientific and technical capacities about the Water-Food-Ecosystem Nexus, as well as a roadmap for their implementation. At the project level, LAAs enable a multiplicity of stakeholders to set up a collaborative Nexus space across the Mediterranean region to socialise and scale up solutions. LENSES and REXUS aim not only to share but also to integrate methods to develop applicable tools/services for the Nexus.

Materials and methods

The task focuses on the design and development of a series of visioning exercises through a participatory process also integrating the elaboration of participatory system dynamic modelling at the pilot scale.

REXUS and LENSES combine for 12 pilots facing different Nexus challenges: *Deir Alla (Jordan)* tests unconventional water resources to address food production challenges. *Doñana region (Spain)* balances water needs of agriculture with conservation of wetland ecosystem. *Hula Valley (Israel)* tests agro-voltaic technology and nature-based solutions to increase water use efficiency in agriculture. *Koiliaris Critical Zone in Crete (Greece)* reduces water demands in avocado crops and assesses nature-based solutions. *Menemen*

plain (Turkey) develops ecosystem-based basin management to ensure sustainable agriculture and food supply. *Tarquinia plain (Italy)* addresses water quantity and quality in agricultural areas, and improves collaboration and data sharing. *Pinios Hydrologic Observatory and Pinios River Basin (Greece)* improves water management practices and efficiency in agriculture. *Isonzo/Soča river basin (Italy/Slovenia)* integrates nature-based solutions and advanced technologies to improve water use efficiency. *Lower Danube region (Bulgaria/Romania/Serbia)* develops a visioning exercise to address continued exploitation of Danube River resources. *Nima river watershed (Colombia)* balances water allocation conflicts between different stakeholders through a visioning exercise. *Peninsular Spain* addresses unequal availability of water between northern and southern regions and promotes sustainable water use and management practices. *Pinios River Basin (Greece)* implements integrated water resources management plans through stakeholder engagement and participation.

The visions are represented under the form of scenarios through a participatory planning process to be complemented with the use of backcasting techniques for building narratives that can lead from the business as usual scenario towards the consensus consensual vision of the group of local and regional stakeholders. As a final step, this process will be synthesised in the form of LENSES strategic roadmaps describing bundles of strategies and actions that can support the achievement of the long-term desirable visions.

Results and concluding remarks

Preliminary results from workshop the first workshop (conducted in all pilots) relates to the validation of the causal relations between the system elements, as an outcome, the validation of a causal-loop diagram which will serve as the basis of the PSDM vas validated with stakeholders, as well as the core challenges at each area, which were collectively translated from sectorial to nexus challenges. The second workshop will focus on developing BAU/green visions and the the strategic roadmaps will be produced within the final stage of both projects (i.e. by 2024). These results are expected to provide a good diagnosis of what are the preferred solutions and desired pathways for many regions facing similar challenges in the Nexus management.

Acknowledgments: The present work has been funded by the LENSES project (PRIMA Programme, GA n°2041) and by the REXUS project (funded by the European Union's Horizon 2020 research and innovation programme under grant agreement No 101003632). This paper and the content included do not represent the opinion of PRIMA Foundation and the European Commission, and strictly reflect the authors' views.

References

Karamouz M, Barkhordari H, Ebrahimi E (2021) Dynamics of Water Allocation: Tradeoffs between Allocator's and Farmers' Benefits of Irrigation Practices. Journal of Irrigation and Drainage Engineering Online 147(6). https://doi.org/10.1061/(ASCE)IR.1943-4774.0001550

Pulido-Velazquez D, Baena-Ruiz L, Mayor B, Zorrilla-Miras P, López-Gunn E et al. (2023) Integrating stakeholders' inputs to co-design climate resilience adaptation measures in Mediterranean areas with conflicts between wetland conservation and intensive agriculture. Science of The Total Environment 870: 161905. https://doi.org/10.1016/j.scitotenv.2023.161905

The REXUS project: From nexus thinking to nexus doing

J. González-Piqueras[1*], A. Osann[2]
[1] Remote Sensing & GIS Group, IDR, University of Castilla-La Mancha, 02071 Albacete, Spain
[2] AgriSat Iberia SL, Paseo de la Innovación 1, 02006 Albacete
* e-mail: jose.gonzalez@uclm.es

Introduction

The interdependencies between the Water, Energy, Food and Environment sectors has grown in recent years, along with the realisation that purely sectoral viewpoints or traditional silo models cannot lead to sustainable solutions (Weitz et al. 2017). Growing demand for resources create trade-offs, which are complicated by the impact of climate change. The Water-Energy-Food-Environment Nexus approach is a powerful concept for addressing the interrelationships of resource systems and moving towards better coordination and utilisation of natural resources, taking into account existing trade-offs and moving towards synergies. However, progress in terms of incorporating Nexus thinking in practical policymaking has been slow. This issue is important for society, taking into account the competition between some sectors like the energy industry and agriculture sharing the water resources and land. Agriculture is a strategic sector for food security, economic, social, and environmental sustainability. Access to energy is a key factor for economic development. In essence, political strategies must look for addressing the interdependency between the nexus domains, with the adequate and sustainable management of resources.

The REXUS Project aims to close the gap between science and policy, moving from Nexus thinking to Nexus doing. It brings together the scientific tools and the integrated vision necessary to analyze real-world conditions, including frictions and climate risks. This issue is addressed employing Systems Dynamic Modelling, it is designing sustainable and actionable forward-looking solutions that increase resilience across sectors, integrating the big data available (Earth Observing Data, soil, climate, crops, etc.) and feedback from stakeholders. These solutions, clearly visualised, will form the basis of forward-looking and participatory decision making.

Materials and methods

REXUS is devoted to establish a high participation level of stakeholders (Water Managers, Policymakers, Farmers, Energy producers and distributors, Consultants, Scientifics, Technicians, etc.) in the five pilot areas studied, Nima-Cauca Watershed in Colombia, the Pinios River Basin in Greece, the Peninsular Spanish area, and two transboundary river basins as Lower Danube in the border between Romania-Bulgaria-Serbia and Isonzo/Soča between Italy-Slovenia. It has been created the named Learning Action Alliances (LAAs), on each pilot area composed by actors from the different domains and at different institutional levels. These alliances have been active defining the main challenges on each area, the boundaries of the system, providing qualitative and quantitative inputs to the models applied. In parallel, the main laws and regulations concerning the management of water, energy, food/agricultural sector as well as the main bodies relevant for decision-making in these areas have been identified. There is an Observatory in the terms of a server to share data between the consortium in a way that they feed the Participatory System Dynamics Models (PSDM), Nature Based Solutions (NbS) and Ecosystem-based Adaptation (EbA) proposed on pilot areas. It includes a complete study of climate projections mapping and climate risk assessment; the energy accounting and carbon footprint (Garrido et al. 2023); the Land Use suitability for the main crops in the study areas (Galve et al. 2023); and a selection of socioeconomic indicators for nexus systems in all pilots. The integration of the data allowed to define pilot-specific Causal Loop Diagrams to describe the complexity of interconnections between sectors, based on the integration of stakeholders' knowledge with baseline information. A roadmap to assist a variety of decision-makers at different levels in identifying

potential Nature-based Solutions (NBS) to be implemented under the perspective of the Water-Energy-Food Nexus has been developed.

REXUS is an essentially human-centered process, and this sets the required tone of a project that follows a scientific and fact-based approach, but always with the human element at the centre. A diagram about the implementation of the project is shown on Figure 1.

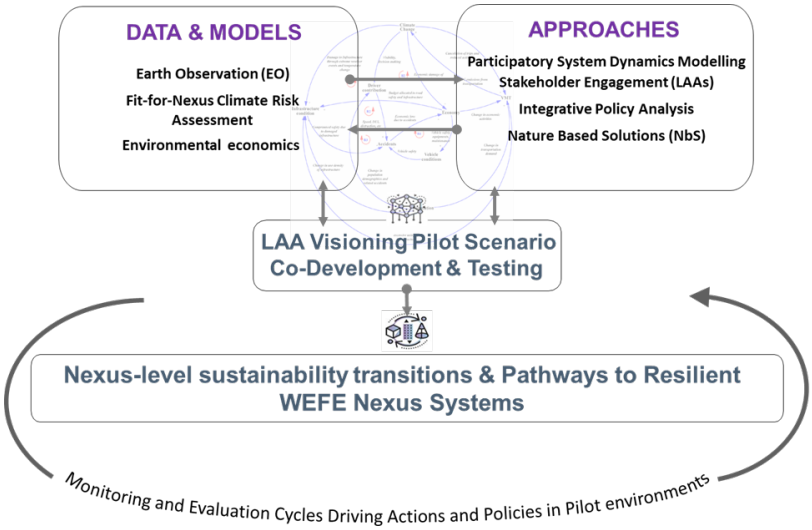

Figure 1. Diagram with the implementation of REXUS project, including the identification and integration of models and approaches.

Results and concluding remarks

REXUS goes beyond the state of the art in many ways, with innovations that support each other in their effectiveness and impact. REXUS LAAs are integrating discussion and knowledge sharing activities with a structured visioning process that concludes in the elaboration of transition roadmaps for the management and operationalisation of the WEFC nexus and explores multiple ways in which Nexus operational management can be progressed through innovative use of Earth Observation. Novel energy and water accounting and footprint estimation methods have been proposed, based on dense time series of high spatial resolution images (free from Sentinel-2). With the support of PSDM, REXUS enables evidence-based multi-objective policy design, which can help aligning overarching policies in distinct domains. For the first time, REXUS attempts to establish and mainstream a strong link between climate adaptation (NDCs of the Paris Agreement) and Nexus management. Moreover, the proposed EbA is a recognized, suitable vehicle to greening the CAP.

REXUS will contribute to reducing institutional fragmentation whilst increasing cross water, energy, food collaboration and inclusive multistakeholder engagement by using a specifically designed LAA process. Will help water diplomacy to include Nexus considerations, supporting the development of “diplomatic” instruments and mitigate conflicts through cooperation and promotes regional stability.

Acknowledgments: To the EU Horizon 2020 project REXUS (Managing Resilient Nexus Systems Through Participatory Systems Dynamics Modelling, reference 101003632).

References

Galve J, Gonzalez-Piqueras J, Garrido J, Llanos López M Ll, Henao E, Papadaskalopoulou C, Antoniadou M, Tassopoulos, D (2023) Cotton suitability projections in Pinios Region. In: Proceedings of 12th EWRA World Congress (EWRA2023), 27 June - 1 July 2023, Thessaloniki, Greece

Garrido-Rubio J, Calera A, Arellano I, Belmonte M, Fraile L, Ortega T, Bravo R, González-Piqueras J (2020) Evaluation of remote sensing-based irrigation water accounting at river basin district management scale. Remote Sensing 12(19): 3187. https://doi.org/10.3390/rs12193187

Weitz N, Strambo C, Kemp-Benedict E, Nilsson M (2017) Closing the governance gaps in the water-energy-food nexus: Insights from integrative governance. Global Environmental Change 45: 165-173. https://doi.org/10.1016/j.gloenvcha.2017.06.006

Evaluation of rainwater and greywater as sustainable water sources in central European countries

A. Stec*, D. Słyś
Department of Infrastructure and Water Management, Rzeszów University of Technology, Poland
** e-mail: stec_aga@prz.edu.pl*

Introduction

The world's growing population, increasing urbanization and climate change are having an adverse impact on the environment and contribute to the overexploitation of natural resources, including water resources. Therefore, increasing attention is being directed toward more sustainable management of these resources. One solution that fits into such a management model is the closed-loop economy, which enables the reuse, recycling and reduction of water resources (Velenturf and Purnell 2021). Rainwater harvesting systems (RWHS) and greywater recycling systems (GWRS) are most often implemented as alternative water sources in buildings (Pacheco and Alves 2023; Campisano et al. 2017; Zavala et al. 2016). RWHS are most often used for non-potable purposes, such as toilet flushing, laundry, watering vegetation and housekeeping. As studies have shown, depending on local conditions, technical parameters of the systems, and variants of cooperation of these solutions, RWHS and GWRS can significantly reduce the use of potable water, up to 94% (de Sá Silva et al. 2022; Kim et al. 2022; Li et al. 2010).

When analysing the literature on unconventional water systems located in European countries, it was noted that this topic had received limited interest so far, especially with regard to Central and Eastern European countries. Despite the fact that these solutions are increasingly used, research on their effectiveness and cost-effectiveness of implementation is carried out on a much smaller scale than is the case in other regions of the world, such as the United States, Brazil, Australia or Western Europe. Taking this into account, a study was conducted with the main objective to determine the feasibility of using alternative water sources in residential buildings in selected cities in Poland, Slovakia, the Czech Republic and Hungary.

Materials and methods

In the study on the hydraulic efficiency of the RWHS a simulation model by Słyś (Słyś 2009), whose computational algorithm is based on the YAS (yield-after-spillage) operating rule, was applied. The simulations were carried out using 10 years of actual daily precipitation data from meteorological stations located in the analysed cities. The study assumed that rainwater would be used only for non-potable uses: toilet flushing, washing and garden watering. The focus was on single-family buildings, since, according to Eurostat data, more than 50% of the residents of the countries under consideration live in such buildings (Eurostat 2020). The results of the simulation study were the input data to determine the volumetric reliability (Vr) for different tank capacities, and this in turn made it possible to determine the optimal tank capacity. The model's variable parameters were roof area, water demand for non-potable uses and tank capacity.

In the next stage of the research, a financial analysis of various installation variants was performed, also taking into account the unconventional RWHS and GWRS water systems. The studies using the Life Cycle Cost (LCC) methodology were carried out for single-family buildings located in four selected European countries. The use of the LCC technique is recommended by the European standard ISO 15686-5, which enables the achievement of the United Nations Organization Sustainable Development Goals (SDGs). Unit prices for water, wastewater and electricity were set for each location. The research was extended with scenario sensitivity analysis. The following variants were considered:

- Variant 0 – traditional installation,
- Variant 1 – RWHS for toilets flushing,

- Variant 2 – RWHS for toilets flushing and washing,
- Variant 3 – RWHS for toilets flushing, washing and garden watering,
- Variant 4 – GWRS for toilets flushing,
- Variant 5 – hybrid installation with RWHS and GWRS for toilets flushing, washing and garden watering.

Results and concluding remarks

The simulation studies carried out showed that the level of volumetric reliability Vr depended on the variant of the installation equipped with RWHS and local climatic and technical conditions. The highest Vr value (84%) for Variant 1 was obtained for the RWHS location in Budapest, for other cities (Warsaw, Prague and Bratislava) it was 80%. It was also found that the differences between Vr for Variant 1 and Variant 2 were insignificant. For Variant 3, where rainwater was used for flushing toilets, laundry and watering the garden, the maximum Vr value for all locations was similar and it was around 90%.

Based on the results of the financial analysis, it was found that only in the case of Prague it was profitable to use the rainwater harvesting system, and then only in the case of Variant 3. The implementation of unconventional water systems is not financially beneficial for their locations in Warsaw, Budapest and Bratislava. In the case of these cities, the lowest value of the LCC indicator was obtained for the traditional installation solution (Variant 0). The highest level of LCC was found in variants that included recycling of greywater (Variant 4 and Variant 5).

Taking into account all the research results, it can be generally stated that the implementation of alternative water sources in single-family buildings in the case of the cities under the analysis was completely unprofitable since the water savings over the period of 30 years did not cover the investment outlays and the costs of replacing filters and pumps in RWHS and GWRS. However, when comparing both unconventional water sources, it was noticed that much more favourable financial results were obtained for rainwater harvesting systems.

References

Campisano A, Butler D, Ward S, Burns M, Friedler E, DeBusk K, Fisher-Jeffes L, Ghisi E, Rahman A, Furumai H, Han M (2017) Urban rainwater harvesting systems: Research, implementation and future perspectives. Water Research 115: 195-209, https://doi.org/10.1016/j.watres.2017.02.056

de Sá Silva ACR, Bimbato AM, Balestieri JAP, Vilanova MRN (2022) Exploring environmental, economic and social aspects of rainwater harvesting systems: a review. Sustain Cities Soc 76, 103475. https://doi.org/10.1016/j.scs.2021.103475

Eurostat (2020) https://ec.europa.eu/eurostat/statistics-explained/index.php?title=Living_conditions_in_Europe_-_housing#Housing_conditions (Accessed April 2023)

ISO 15686-5:2017 Buildings and constructed assets — Service life planning — Part 5: Life-cycle costing

Kim J, Humphrey D, Hofman J (2022) Evaluation of harvesting urban water resources for sustainable water management: Case study in Filton Airfield, UK. Journal of Environmental Management 322: 116049. https://doi.org/10.1016/j.jenvman.2022.116049

Li Z, Boyle F, Reynolds A (2010) Rainwater harvesting and greywater treatment systems for domestic application in Ireland. Desalination 260(1): 1-8. http://dx.doi.org/10.1016/j.desal.2010.05.035

López Zavala MÁ, Castillo Vega R, López Miranda RA (2016) Potential of Rainwater Harvesting and Greywater Reuse for Water Consumption Reduction and Wastewater Minimization. Water 8(6):264. https://doi.org/10.3390/w8060264

Pacheco GCR, Alves CA (2023) The Influence of Deep Uncertainties in the Design and Performance of Residential Rainwater Harvesting Systems. Water Resour Manage 37: 1499–1517. https://doi.org/10.1007/s11269-023-03436-w

Słyś D (2009) Potential of rainwater utilization in residential housing in Poland. Water Environ J 23:318-325. https://doi.org/10.1111/j.1747-6593.2008.00159.x

Velenturf AP, Purnell P (2021) Purnell Principles for a sustainable circular economy. Sustain Prod Consum 27: 1437-1457. https://doi.org/10.1016/j.spc.2021.02.018

Time-scale comparative analysis of hydrological alteration by hydropower generation in the Cheakamus and Squamish rivers, Canada

M.D. Bejarano[1*], F. González[1], D. Tuzlak[2], F. Poulsen[3], F. Knight[2]
[1] Natural Systems and Resources Department, Universidad Politécnica de Madrid, Madrid, Spain
[2] Squamish River Watershed Society, Squamish, British Columbia, Canada
[3] Ashlu Environmental Consulting, Squamish, British Columbia, Canada
* e-mail: mariadolores.bejarano@upm.es

Introduction

Hydropower generation can cause significant impacts on fluvial ecosystems as a result of its drastic changes in the long- and short-term flow regime characteristics. In the long-term, large hydropower plants and reservoirs reduce the annual peak flows and seasonality of flows, whereas in the short-term they trigger unnatural sudden, rapid, and frequent sub-daily flows and water level fluctuations termed as "Hydropeaking".

The main objective of this study was to analyze a real case of hydrological alteration caused by a large hydropower plant affecting the Cheakamus and Squamish rivers in British Columbia (Canada). For this aim we first characterized the natural and altered flow regimes of the two rivers and subsequently we evaluated the changes of the flow regimes due to hydropower by comparing the natural and altered flows. We used a set of indices based on both, mean daily flows and hourly flows. Finally, the advantages and disadvantages of using different time-scale flow data for characterization and flow alteration evaluation were analysed.

The results suggested a high degree of hydrological alteration in the two studied rivers. In the Cheakamus River, the implementation of the Daisy Lake dam and reservoir and the transfer of a large part of its flow to the Squamish River basin were the source of the hydrological disturbance. On the other hand, in the Squamish River, the increase in flow and the hydropeaking phenomena were the main hydrological alterations due to the transferred water and the operation of the power station, respectively. Whereas the impacts for the former river were detected through the analyses with daily flows, the impacts for the latter river were only visible when sub-daily flows were used.

Materials and methods

To carry out the comparative analysis, real hydrological information was taken on a daily and hourly scale, from the Squamish and Cheakamus rivers, approximately 60 km north of Vancouver, in Canada, where the Cheakamus Hydroelectric Generating Station has existed since 1957. The generation system is comprised of the Daisy Lake Dam and Reservoir on the Cheakamus River, with a storage capacity of 55 million cubic meters, at approximately 378 meters above sea level. From the reservoir, the water is conducted through a canal to Shadow Lake, which is located at a similar height above sea level, to later be transported through a diversion tunnel 11 km long and 5.5 m in diameter, to the central generation, which is located on the left bank of the Squamish River, 38 meters above sea level (BC Hydro 2005).

The flow series used for the analysis correspond to hourly flow series associated with points upstream and downstream from the disturbance in each river, that is, upstream and downstream from Daisy Lake Reservoir on the Cheakamus River and upstream and downstream from the hydroelectric plant discharge into the Squamish River. The periods of the revised series were 11 years for the Squamish and 15 years for the Cheakamus.

Initially, an analysis of hydrological alteration was carried out on a daily scale, for which the daily series of flows were obtained in each case, as the daily average of the 24 hourly flow data, and subsequently the daily information of the 4 points was processed using the IHARIS software, widely used for the characterization and identification of daily hydrological alteration in rivers (Martínez y Fernández 2021).

Next, the analysis of hydrological alteration was carried out on an hourly scale at the 4 study points, using the specialized software InSTHAn, for hydrological analysis in rivers at a sub-daily level (Bejarano et al. 2020).

This made it possible to carry out, on the one hand, an analysis of the hydrological alteration caused by the disturbances in each river, independently. We run different analyses for each river at the two time scales. On the other hand, it also allowed a comparative analysis of the results of hydrological alteration at the two time scales.

Results and concluding remarks

First of all, the Cheakamus and Squamish rivers suffered from different hydrological alterations which were related to the different pressures they were subject. Furthermore, the identification of these alterations depended on the time scale of the flow data. Whereas the daily flows allowed to identify the peak flows decrease of the Cheakamus river, we needed hourly flows to detect the Hydropeaking phenomenon characteristic of the Squamish river. This can be clearly seen in Figure 1a. It shows a week in March 2008 in the Squamish River, in which Hydropeaking is completely imperceptible on a long time scale, but totally evident on a short time scale. The different parameters provided by IHARIS and InSTHAn sofwares highlighted these differences between time scales. Figure 1b shows how the parameter Number of Inversions (Trev) for the Squamish River (the one suffering from Hydropeaking) behaves practically the same in the natural and altered regimes when calculated on a daily basis whereas it has a very different behaviour for the two types of regimes on an hourly basis, identifying the Hydropeaking.

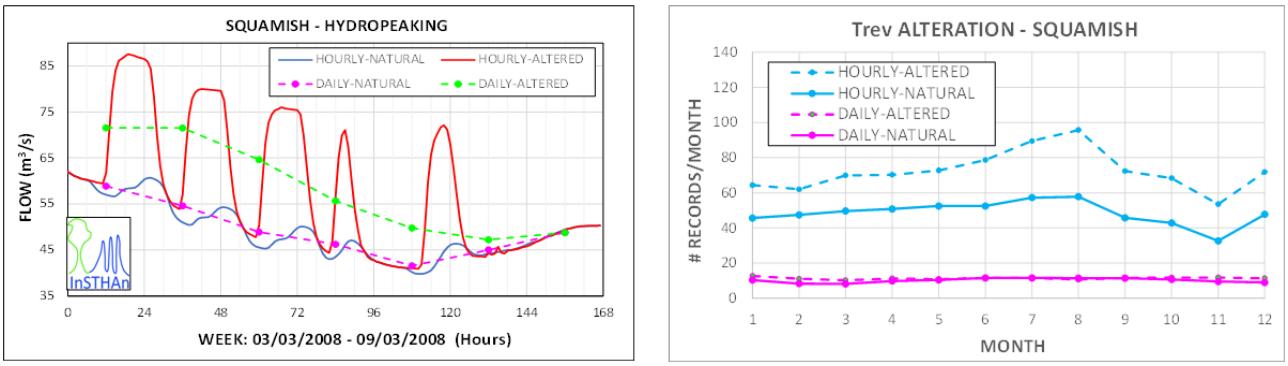

(a) *(b)*

Figure 1. (a) Identification of hydropeaking on an hourly scale in the Squamish River; (b) Behavior of the parameter of Number of Inversions (Trev) for an average year in the Squamish River (natural/altered regime and daily/hourly scales.

In this particular case, it was concluded that the hydrological alteration in the Cheakamus River could be established on a daily time scale, while the hydrological alteration in the Squamish River and, therefore, the identification of Hydropeaking, could only be evidenced on an hourly time scale.

The results obtained suggest that in order to identify and characterize disturbances in fluvial ecosystems, it is necessary to carry out the corresponding analyses at the same temporal scale in which they occur. This represents a great challenge for the scientific community and particularly for environmental authorities, to support decisions that allow a truly sustainable development, preserving ecosystems.

References

BC Hydro (2005) Cheakamus Project Water Use Plan. Report for review for acceptance by the comptroller of water rights

Bejarano MD, García-Palacios JH, Sordo-Ward A, Garrote L, Nilsson C (2020) A new tool for assessing environmental impacts of altering short-term flow and water level regimes. Water 12: 2913

Martínez Santa-María C, Fernández Yuste JA (2021) Índices de alteración hidrológica en ríos (IAHRIS 3.0). Manual de referencia metodológica. Ed. Dirección General del Agua (MITECORD), Madrid

VII. Ecosystems and Environmental Processes

Estimation of soil hydraulic conductivity from disc infiltrometer

I. Logothetis, D. Koka*, G. Kargas, P.A. Londra
Department of Natural Resources Management and Agricultural Engineering, School of Environment and Agricultural Engineering, Agricultural University of Athens, Athens, Greece
** e-mail: dimkokas@aua.com*

Introduction

Hydraulic conductivity (K_0) is a fundamental requirement of physically based models in several scientific disciplines such as agronomy, hydrogeology, and environmental sciences. Several researchers (Ankeny et al. 1991; Zhang 1997) have studied the three-dimensional infiltration of water in soil in order to obtain valid and accurate estimates of hydraulic conductivity under either saturated or unsaturated conditions. One of the most popular devices used in infiltration experiments for pressure heads $H \leq 0$ is the Tension Infiltrometer (TI) (Kargas et al. 2022).

There are two different approaches by which the infiltration data can be analyzed. The first approach is based on the study of steady-state flow data. The majority of methods that have been proposed are based on Wooding's equation (Wooding, 1968) such as the method of Ankeny et al. (1991). The second approach studies the transient flow data and the equations that have been proposed have in common that they are identical to the two-term equation of the one-dimensional infiltration equation of Philip (1957):

$$I = C_1 t^{1/2} + C_2 t \quad (1)$$

where I (L) is the cumulative infiltration, t (T) is the time, C_1 ($L\ T^{-1/2}$) and C_2 ($L\ T^{-1}$) are coefficients that differ depending on the model applied. The aim of this paper is to compare the method of Ankeny et al. (1991), which is a steady-state flow method, with Zhang's (1997) method, which is based on transient flow, in clay soil under unsaturated conditions.

Materials and methods

Laboratory experiments of three-dimensional infiltration in disturb clay soil at negative pressure heads close to saturation were carried out.

Water infiltration in our experiments was performed using a Tension Infiltrometer with a disc radius of 10 cm. The applied heads were -15, -7, -3 and -1 cm. No contact material was used between the disc and the soil in any of the experiments.

For the method of Ankeny et al. one infiltration experiment was carried out starting from pressure head -15 cm. When a steady flow was achieved the pressure head was changed to the next one (i.e. -7 cm). The experiment was terminated when a steady flow was achieved at pressure head -1 cm. The data were processed based on the equations reported by Ankeny et al. (1991).

In Zhang's case, four infiltration experiments were carried out, one at each applied pressure head (-15, -7, -3 and -1 cm). Each experiment was terminated when a steady flow was observed. The time needed to obtain steady flow was 29, 33, 22 and 37 min at the respective pressure heads. Zhang's method correlates coefficients C_1 and C_2 of equation (1) with sorptivity and hydraulic conductivity respectively and more specifically:

$$C_1 = S_0 A_1 \text{ και } C_2 = K_0 A_2 \quad (2)$$

where A_1 and A_2 are dimensionless parameters depending on various soil parameters. More specifically, Zhang correlated the parameters A_1 and A_2 with the coefficients of van Genuchten equation (a and n) which describe the characteristic soil moisture curve.

In order to calculate the parameters C_1 and C_2, the method of cumulative linearization (CL) of Smiles and Knight (1976) was applied.

Results and concluding remarks

Figure (1a) shows the relationship i(t) for each negative pressure head. Figure (1b) illustrates the relationship of Smiles and Knights (1976) for each applied pressure head. From the relationships in figure (1b), the parameters C_1 and C_2 were obtained from which K_0 and S_0 of Zhang's method were calculated. The relationships are considered to be linear as R^2 at all heads exceeds 0.94.

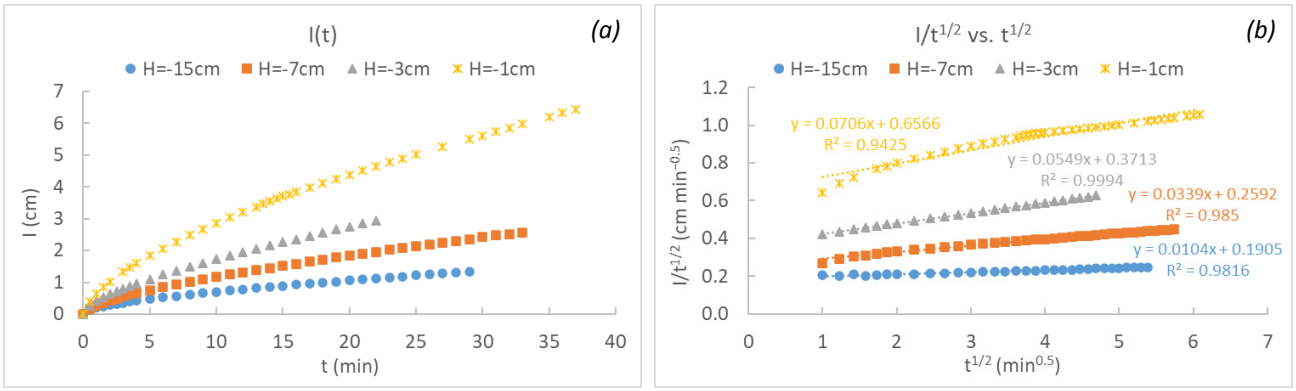

Figure 1. (α) Cumulative infiltration (I) versus time (t). (b) Relationships of Smiles and Knight (1976) method for finding the parameters C_1 and C_2 at all applied pressure heads.

Table 1. Hydraulic conductivity (K_0) of the Zhang (1997) and Ankeny et al. (1991) methods at all applied pressure heads.

H (cm)	K_0 (cm/min) [Zhang (1997)]	K_0 (cm/min) [Ankeny et al. (1991)]
-15	0.0050	0.0131
-7	0.0240	0.0349
-3	0.0473	0.0783
-1	0.0670	0.1087

From Table 1 it is observed that the method of Ankeny et al. (1991) tends to give higher values of K_0 than Zhang's (1997) method at all heads. These differences may be due to the values of van Genuchten's coefficients (a and n) taken from literature for Zhang's method. The time parameter seems to also play a crucial role in the case of Zhang's method since using the method only at initial times tends to give similar values to those of Ankeny et al. However, this observation needs further investigation as the exact way of finding the useful experimental time for transient flow experiments has not been clarified yet.

The advantages of Zhang's method over Ankeny et al. are that it is a simple method, relatively short as it is based on transient flow data and needs only one pressure head, and it provides the possibility of iteration. There is also the capability of finding sorptivity if the initial and final volumetric soil water content are measured. The disadvantage is that it requires more data to estimate hydraulic conductivity, such as knowledge of the infiltration curve i(t) as well as soil type or soil characteristic retention curve.

References

Ankeny MD, Ahmed M, Kaspar TC, Horton R (1991) Simple field method for determining unsaturated hydraulic conductivity. Soil Science Society of America Journal 55(2): 467-470. https://doi.org/10.2136/sssaj1991.03615995005500020028x

Kargas G, Koka D, Londra PA (2022) Evaluation of Soil Hydraulic Parameters Calculation Methods Using a Tension Infiltrometer. Soil Systems 6(3): 63. https://doi.org/10.3390/soilsystems6030063

Philip JR (1957) The theory of infiltration: 4. Sorptivity and algebraic infiltration equations. Soil Science 84(3): 257-264. https://doi.org/10.1097/00010694-195709000-00010

Smiles DE, Knight JH (1976) A note on the use of the Philip infiltration equation. Soil Research 14(1): 103-108. https://doi.org/10.1071/SR9760103

Wooding RA (1968). Steady infiltration from a shallow circular pond. Water Resources Research 4(6): 1259-1273. https://doi.org/10.1029/WR004i006p01259

Zhang R (1997) Determination of soil sorptivity and hydraulic conductivity from the disk infiltrometer. Soil Science Society of America Journal 61(4): 1024-1030. https://doi.org/10.2136/sssaj1997.03615995006100040005x

12th World Congress on Water Resources and Environment (EWRA 2023)
"Managing Water-Energy-Land-Food under Climatic, Environmental and Social Instability"
Thessaloniki, Greece, 27 June - 1 July 2023

Influence of soil properties on soil bulk electrical conductivity readings using EMI and FDR technology in non-saline soils of Greece

P.A. Petsetidi*, G. Kargas, K. Sotirakoglou
Department of Natural Resources Development and Agricultural Engineering, Agricultural University of Athens, Greece
** e-mail: toniapets@hotmail.com*

Introduction

The measurement of the bulk soil electrical conductivity, *σb* has been extensively used as a rapid mean of soil salinity assessment, particularly in arid and semi-arid regions, where sustainable water management practices are essential. The soil factors that define the value of *σb* include the pore water electrical conductivity, *ECp*, soil water content, proportion and type of clay, organic matter, soil bulk density, and soil temperature (Kargas et al. 2022). Over the last decades, there have been developed advanced sensors for the *σb* measurements relying on methodologies such as electromagnetic induction (EMI) and frequency domain reflectometry (FDR). Hence, researchers have conducted numerous studies in order to elaborate the relationship between individual soil properties as the water content and the *σb* for various commercial devices. However, due to the complexity regarding the contribution of soil properties' spatial variability on the measured *σb,* as long as the distinct signal responses of the available instruments, these relationships are site-specific and may be inconsistent across fields with different soil and water status.

As a matter of fact, in non-saline soils where salinity is considered negligible, texture and soil water content, among other soil parameters are reported to be the most dominant factors affecting the *σb* measurements. Nevertheless, under these field conditions, determining and interpreting the magnitude of the effect of each static and dynamic variable on the accuracy of *σb* and thus on designing proper irrigation systems is still a challenging task. In this respect, Brevik and Fenton (2002) using multiple linear regression correlated the EM-38 measurement with soil moisture, clay content, temperature and carbonate minerals whereas, most recently, Visconti and de Paz (2021) estimated the share of influence of every including soil attribute. Acknowledging the importance of defining the multiple interrelations of *σb*, the objective of this work was to investigate the contribution of soil properties on bulk soil electrical conductivity, *σb* in a non-saline field as is measured by two popular, efficient devices, an EM38-MK2 (EMI) and a WET-2 sensor (FDR).

Materials and methods

The field survey was carried out during April 2022 in north Lakonia, at Greece. A total of 24 points were selected for the measurements of *σb* which were made by the Geonics EM38-MK2 and the dielectric WET-2 sensor. Firstly, by employing the appropriate calibration of the instrument, the EM38-MK2 was used. Placed on the surface of the ground, once in horizontal ($ECH_{0.5}$) and then in vertical mode ($ECV_{0.5}$), there were acquired two *σb* readings for each point. Afterwards, the WET-2 probe was inserted to the center of each point below EM38-MK2 and recorded the measurements of *σb* ($WET_{\sigma b}$), water content *ϑ,* bulk dielectric permittivity, *εb* and temperature, *T*. Then, 24 soil samples, one from each site were collected from top soil of 0-30 cm, packed and transferred to the laboratory. After air drying and sieving (2 mm), each sample was analysed to determine the electrical conductivity of saturated soil paste extract (ECe), soil texture and $CaCO_3$, according to standard methods. Finally, to evaluate the dependency of *σb*, a multiple linear regression (MLR) was performed for each device based on the obtained *σb* values as the dependent variables. The attributes of texture (e.g. Clay content), $CaCO_3$, ECe, εb and T were included as independent. The coefficient of determination, R^2 was applied as validation criteria for the regression models.

Results and concluding remarks

The study area was characterised by clay loam texture with mean sand content around 27.3% and clay

content at 35.7%. The water content measured in the field by the WET sensor had a mean value of 11% and the $CaCO_3$ was determined around 9%. Regarding the ECe levels, they ranged from 52.9 to 148.2 mSm^{-1} affirming the absent concentration of salts in the soil surface depth (0-30 cm). The average value of $WET_{\sigma b}$ was 6.3 mSm^{-1} while the $ECH_{0.5}$ and $ECV_{0.5}$ had an average value of 10.7 and 15 mSm^{-1} respectively.

*Table 1. Multiple Linear Regression (MLR) models of the **σb** for the EM38-MK2 and the WET-2 sensor.*

Probe	Mode	MLR model (mS m^{-1})	R^2 (%)
EM38- MK2	H 0.5	$\mathbf{ECH_{0.5}} = 3.72\ \boldsymbol{\varepsilon b^{0.5}}$	97.6
	V 0.5	$\mathbf{ECV_{0.5}} = 5.46\ \boldsymbol{\varepsilon b^{0.5}}$	89.6
WET-2		$\mathbf{WET_{\sigma b}} = 8.95\ \boldsymbol{\varepsilon b^{0.5}} - 0.86\ \mathbf{T} - 0.14\ \mathbf{Clay}$	97.6

As presented in Table 1, both $ECH_{0.5}$ and $ECV_{0.5}$ MLR models showed a strong correlation to the $\varepsilon b^{0.5}$ of WET sensor. This variable was used as a substitute for soil moisture ϑ since the relationship between ϑ and $\varepsilon b^{0.5}$ resulting from the use of the WET-2 sensor is strongly linear for many soil types. More specifically, the $\varepsilon b^{0.5}$ explained 97.6% of the variability on the EM38-MK2 σb as measured in the horizontal mode and 89.6% as taken in the vertical mode. The higher R^2 of the horizontal regression comes to agreement with the greater sensitivity of the instrument on the surface variability which in this case exhibits a dry surface layer.

In contrast to Brevik and Fenton (2002) findings, the clay fraction, the temperature and the carbonate minerals appeared to have no effect on the EM38-MK2 σb. Visconti and de Paz (2021) likewise reported the effect of soil texture in low salinity fields, an incidence that was not observed in our case study. This deviation could be explained by the different moisture conditions of the in situ measurements and by the fact that in such occasions the prominent influence of water content may obscure the minor changes of clay and carbonate content.

As regards the WET-2 sensor, the MLR model revealed $\varepsilon b^{0.5}$, T and clay as the strongest contributors on the measured σb with R^2 value up to 97.6% (Table 1). In particular, the regression coefficient of $\varepsilon b^{0.5}$ seemed to have the greatest magnitude followed by the temperature and the clay content which have an inverse relation to the σb. This MLR product displays the high dependence of the $WET_{\sigma b}$ on the εb and eventually its relationship with ϑ as well the negative effect of clay minerals and T on its dielectric behavior.

Considering the results of the present survey, soil volumetric water content, ϑ was identified as the most powerful factor controlling the σb of the sensors in the non-saline soil, supporting the existing literature. Nonetheless, other stable soil features such as clay content, which were expected to contribute to the EM38-MK2 σb, found to be statistically unrelated, highlighting the site dependency of the EMI σb. Instead, WET σb indicated the impact of clay content and temperature, even though negative. The detection of these variations may be attributed to the WET's smaller soil volume of measurement and the sensitivity of its dielectric characteristics to the soil texture and temperature.

The significant correlation of EM38-MK2 with the WET's $\varepsilon b^{0.5}$ as an outcome of MLR was able to reflect the main cause of the surface variability in the low salt soil, producing a good potential for εb to be used as a reliable covariate for monitoring the field-scale moisture conditions. The approach of rapid and non-invasive EMI σb measurements combined with easily acquired soil moisture FDR data could be beneficial in precision irrigation. By applying a site-specific calibration, the low cost WET-2 probe's linear relationship $\varepsilon b^{0.5}$ - ϑ could provide a detailed knowledge of the spatial patterns of water content occurring in the non-saline field of interest and reduce the amount of soil samples. Consequently, this method may enhance the interpretation of the complex σb interactions but further research is recommended to determine its efficacy in predicting individual targeted soil properties, as this has not been thoroughly evaluated.

References

Brevik EC, Fenton TE (2002) The relative influence of soil water content, clay, temperature, and carbonate minerals on soil electrical conductivity readings taken with an EM-38. Soil Survey Horizons 43: 9–13. https://doi.org/10.2136/sh2002.1.0009

Kargas G, Londra PA, Sotirakoglou K (2022) Evaluation of soil salinity using the dielectric sensor WET-2. Soil Research https://doi.org/10.1071/SR22163

Visconti F, de Paz JM (2021) Sensitivity of soil electromagnetic induction measurements to salinity, water content, clay, organic matter and bulk density. Precision Agriculture 22(5): 1559-1577. https://doi.org/10.1007/s11119-021-09798

Analysis of the relevant legal setting, processes and actors on climate change in Albania

E. Keci
Department of Natural and Applied Sciences, Faculty of Professional Studies, "Aleksander Moisiu" University, Durres, Albania
e-mail: erjolakeci@yahoo.it

Introduction

Albania received European Union candidate status in June 2014. As such, it is expected to align with and implement EU legislation, the acquis Communautaire. Albania's EU accession process is a driving force in the reform of the environment sector and of cross-sectorial coordination needful for climate change responses. EU integration directly implies compliance with EU regulations. Albania has developed a political and strategic framework reflecting on the significance of climate change and the natural environment for the country's sustainable development providing entry points for the national adaptation and mitigation process to climate change. Moreover, Albania has developed different policy instruments which will contribute to reducing vulnerabilities and enhancing adaptive capacity in the various sectors. Several initiatives at the international level, policy documents and legislation at the national level, and some measures at the regional/ local level have been taken in this regard and described in the sections below.

Despite some level of preparation in the field of climate change, the recent EC-Albania Progress Reports note that progresses remain limited (CSWD 2021). They note the need to align with the Acquis on Monitoring and Reporting Mechanism, to adopt a comprehensive climate policy consistent with the EU 2030 framework and fully integrated climate considerations into all relevant sectoral policies, to implement Paris Agreement, develop integrated National Energy and Climate Plans, to considerably strengthen the administrative capacity, sustainable financing of the sector and awareness-raising activities.

Materials and methods

Albania was the first country in the Balkan region to endorse a Strategy on Climate Change, and related Action Plans on Mitigation and Adaptation. The National Climate Change Strategy, 2020 – 2030, adopted in 2019, is the country's low carbon development strategy within the meaning of the Paris Agreement.

This paper presents an analysis of the relevant legal setting, processes, and actors on Climate Change in Albania.

A legislative gap analysis has provided a clear view as to what domestic legislation exists and/or is in compliance/compatible with the EU acquis; and what further legislative steps are required. Tables of Concordance, where each article or requirement of the national legislation is set out in comparison to the reference of the relevant article of the International Legislation, were used for legal analysis.

The comparison of the Albanian laws, institutions, and procedures with the requirements of the EU on Climate Change mitigation and Adaptation, has been carried out, and the achievements and gaps to be filled from the Country related to Climate change mitigation and adaptation identified.

Results and concluding remarks

Although Albania is making progress with transposing and implementing the Chapter 27 of the Acquis, a lot of work is still required to complete the alignment. The country has achieved some level of preparation for tackling climate change by adopting in December 2020 the climate law, however the alignment with the *climate acquis* remains limited.

Table 1. Analyses of achievements, gaps and rsults related to climate change setup in Albania.

	Progress	Gap
2014	Adoption of the DCM No. 865, "For the reduction and stabilization of fluorinated greenhouse gases"	The implementation of the DCM is still at initial stage.
2016	Adoption of the Law 75/2016 ratifing the Paris Agreement, within the Framework Convention of the United Nations, on climate change, made in Paris on 12 December 2015.	
2018	Albania submitted its third national communication under the United Nations Framework Convention on Climate Change	
2019	In January Albania has ratified the Kigali Amendment to the Montreal Protocol, which will reduce use of HFCs. In July Albania adopted a National Strategy On Climate Change for 2019-2030, with objectives for 2050. The strategy focuses on energy, transport, agriculture, land use and forestry, with a 32% renewable energy target. In January the DCM No. 10 "On the rules to produce, import, export, placing in the market and use of ozone depleting substances as well as for the export, import, placing in the market and use of products and equipment containing these substances" was adopted.	The Climate Strategy requires updating due to the new climate targets set by the EU. The DCM No. 10 only partially transposes Regulation 1005/2009/EC Ozone Depleting Substances. Its implementation remains at an initial stage. No emissions register is in place.
2020	Albania adopted the Law on Climate Change.	The Law on Climate Change only partly transposes provisions the EU Emissions Trading Directive. The implementation of the Law requires further implementing measures to be initiated under the Minister in charge of environment.
2021	Albania adopted revised National Determined Contribution (NDC) in October, increasing the ambition from 11.5% to 20.9% of emissions reduction for the period 2021-2030. Albania adopted a National Energy and Climate Plan (NECP) in December.	Albania has some level of preparation for tackling climate change, but alignment with the EU *acquis* still remains limited. Relevant legislation which need to be transpose including: Directive 2009/31/EC Carbon Capture and Storage; Directive 2008/101/EC Emissions Trading System Aviation Activities (EU ETS); Regulation 2019/631 Setting CO_2 emission performance standards, and Regulation (EU) NO 2018/841 LULUCF. Capacities in the public administration to understand the climate change impacts on Albania and to mainstream climate change in sectoral strategies and plans remain very limited, and capacity building is very much needed in this regard. Capacities in the public administration to understand the climate change impacts on Albania and to mainstream climate change in sectoral strategies and plans remain very limited, and capacity building is very much needed in this regard. Climate risks management plans need therefore to be adopted at all level.

References

CSWD (Commission Staff Working Document) (2021) Albania 2021 Report. Communication from the Commission to the European Parliament, the Council, the European Economic and Social Committee and the Committee of the Regions. 2021 Communication on EU Enlargement Policy. https://ec.europa.eu/neighbourhood-enlargement/albania-report-2021_en

European Commission (2020) Economic Reform Programme of Albania (2020-2022). https://data.consilium.europa.eu/doc/document/ST-7468-2020-INIT/en/pdf

Knez S, Š trbacand Š, Podbregar I (2022) Climate change in the Western Balkans and EU green deal: Status, mitigation and challenges. Energy, Sustainability and Society 12: 1. https://doi.org/10.1186/s13705-021-00328-y

Republic of Albania (2021) National Adaptation Planning to Climate Change in Albania. https://unfccc.int/sites/default/files/resource/National_Adaptation_Plan_Albania.pdf

Republic of Albania (2016) Third National Communication of the Republic of Albania under the United Nations Framework Convention on Climate Change. https://unfccc.int/sites/default/files/resource/Albania%20NC3_13%20October%202016.pdf

USAID (2016) Climate Change Risk Profile – Albania. https://www.climatelinks.org/sites/default/files/asset/document/2016%20CRM%20Fact%20Sheet%20-%20Albania%20%28003%29.pdf

Vuković A, Vujadinović Mandić M (2018) Study on climate change in the Western Balkans region. Regional Cooperation Council Secretariat. https://www.rcc.int/download/docs/2018-05-Study-on-Climate-Change-in-WB-2a-lowres.pdf/06af8f7432484a6ce384ebcb8c05e8d7.pdf

Investigation of harmful cyanobacterial proliferations in Lake Sevan, Armenia

G. Gevorgyan[1*], A. Hovsepyan[1], T. Khachikyan[1], A. Hayrapetyan[1], M. Schultze[2], K. Rinke[2]
[1] Scientific Center of Zoology and Hydroecology, National Academy of Sciences of RA, Yerevan, Armenia
[2] Helmholtz-Centre for Environmental Research – UFZ, Magdeburg, Germany
* e-mail: gor.gevorgyan@sczhe.sci.am

Introduction

Lake Sevan, Armenia, is the largest freshwater resource in the Caucasus region and one of the great freshwater high mountain lakes worldwide. Being a very important freshwater resource in Armenia with major significance for irrigation, fisheries, hydropower, recreation, and tourism, as well as for sustaining valuable freshwater-associated communities and endemic species, Lake Sevan was subjected to tragic events in the past. The lake water level fell dramatically due to the large-scale hydrotechnical transformation and excessive use of water supplies for energetic and agricultural purposes from 1933 to 1990s. In combination with the severe decrease in the water level by about 19 m, the land use was noticeably intensified contributing to the changes in nutrient regime. Parallel to all these changes, the lake was subjected to eutrophication (Gabrielyan et al. 2022). After undertaking restoration measures by reducing water withdrawal and diverting water from the Arpa catchment into Lake Sevan, the lake showed a tendency of improvement in ecological status. However, recently the lake has again shown signs of eutrophication which are clearly expressed by substantial shifts in phytoplankton community towards cyanobacterial dominance in summer (Gevorgyan et al. 2020). The aim of the present study was to characterize the harmful cyanobacterial developments and their drivers in Lake Sevan.

Materials and methods

Lake Sevan is located in the eastern part of Armenia, in 40°19' north latitude and 45°21' east longitude at an altitude of 1900 m above sea level and consists of 2 sub-basins, Small Sevan (surface area approximately 338 km^2) with a maximum depth of 81 m and Big Sevan (surface area approximately 939 km^2) having a maximum depth of 32 m.

The first step in our analysis was a literature review on historical occurrences of cyanobacteria in the lake. Sampling and measurements were done in both sub-basins, Small and Big Sevan, of the lake. Lake surface water samples for cyanobacterial quantification and taxonomic identification as well as nutrient analyses were collected monthly with a bucket (attached with rope) from January to December 2022 at 3 locations. The samples for cyanobacterial analysis were preserved with formalin. During each sampling, measurements of cyanobacterial chlorophyll-*a* were performed with a portable fluorometer (AlgaeTorch, bbe Moldaenke). Surface water temperature was also measured monthly from January to December 2022 with a multiparameter sonde equipped with temperature sensor (EXO3, YSI). In the laboratory, the nutrient (phosphate, ammonium, nitrate, nitrite) concentrations in the water samples were determined by photometry (HI83200, Hanna Instruments; DV-8200, Drawell Scientific). The fixed cyanobacterial samples were concentrated by the sedimentation method and subsequently identified microscopically to the lowest taxonomic level and counted in a Nageotte counting chamber.

A surface water sample for the investigation of the growth rates of cyanobacteria blooming in the lake was taken with a bucket (attached with rope) in July 2022 at one location. In the laboratory, the sample was incubated at different temperature and light conditions. The optical densities of the sample during the incubation were measured with a spectrophotometer (DV-8200, Drawell Scientific).

Surface sediment samples for akinete analysis were taken with a Van Veen grab sampler in March 2022 at 2 locations. The samples were centrifuged, and the supernatant was preserved with formalin until microscopic quantification of akinetes in a Nageotte counting chamber.

Results and concluding remarks

The observation of historical dynamics of cyanobacteria in Lake Sevan showed that the first harmful cyanobacterial development, expressed as a cyanobacterial bloom, was registered in 1964 and became a stable phenomenon until 1972 (Legovich 1968, 1979). Another cyanobacterial bloom was recorded in 1975 (Parparov 1979). These blooms were mainly caused by the rapid growth of *Anabaena* (now *Dolichospermum*) and rarely mediated by *Aphanizomenon* (Legovich 1968, 1979; Parparov 1979).

The current observations in Lake Sevan recorded a massive cyanobacterial bloom in July 2022, which was mediated by the rapid growth of *Dolichospermum*. The cyanobacterial abundance reached up to 198000 cells mL^{-1}, and the cyanobacterial chlorophyll-*a* concentration attained 190 $\mu g\ L^{-2}$. An investigation conducted in Lake Sevan in July 2018 also revealed a massive cyanobacterial bloom (*Dolichospermum*) and the presence of microcysins and numerous other partly toxic metabolites in phytoplankton (Gevorgyan et al. 2020).

The investigation of temporal nutrient dynamics in the lake in 2022 showed an almost complete depletion of phosphate in August and September (0.00-0.02 $mgP\ L^{-1}$). The noticeably low phosphate concentrations recorded after the cyanobacterial bloom can be explained by the phosphate uptake by *Dolichospermum*, a nitrogen-fixing cyanobacterium. It can be stated that mineral phosphorus was a limiting factor of the cyanobacterial bloom in Lake Sevan. Based on the multi-year monitoring data of Environmental Monitoring and Information Center of the Ministry of Environment of RA, in the lake, the average phosphate concentration for May increased more than 10 times during 2006-2018. Therefore, the high concentration of mineral phosphorus can be considered as a driver of cyanobacterial blooms in the lake.

In July 2022 during the mass development of cyanobacteria, the surface water temperature of the lake reached around 18°C. This was almost the maximum for 2022 (20°C) which was reached in August. A similar pattern was also observed in 2018 (Gevorgyan et al. 2020). This allows to conclude that the high water temperature also constitutes a driver of cyanobacterial blooms in the lake, probably by facilitating a competitive superiority of cyanobacteria in comparison to other algae.

Cyanobacterial akinetes in the bottom sediment of Lake Sevan were also studied to assess the potential contribution of akinetes to harmful developments of cyanobacteria. The results showed that the number of akinetes in the bottom sediment of Big Sevan was noticeably higher compared to Small Sevan. It is worth mentioning that the massive cyanobacterial blooms in the lake originated from Big Sevan. Therefore, the akinete germination also can be concluded as a factor favouring the cyanobacterial blooms.

In different ecological conditions, the growth rates of cyanobacteria blooming in Lake Sevan were investigated. The results of laboratory experiments showed that the high water temperature caused intensification of bloom but reduction of bloom duration, and the absence of light led to bloom decline.

The findings of this study indicate that Lake Sevan shows harmful cyanobacterial blooms driven by high phosphate availability and thermal regime. As little can be done in the short term to mitigate the expected global and regional warming, the nutrient input reductions are the only instrument to control such unfavorable dynamics of cyanobacteria in the long-term and need to be initiated as soon as possible.

Acknowledgments: This work was supported by the Science Committee of MESCS RA in the frame of the research project no. 20TTCG-1F002 and by the German Federal Ministry of Education and Research in the frame of the research project SEVAMOD2 (funding ID 01DK20038).

References

Gabrielyan B, Khosrovyan A, Schultze M (2022) A review of anthropogenic stressors on Lake Sevan, Armenia. Journal of Limnology 81(S1): 2061. https://doi.org/10.4081/jlimnol.2022.2061

Gevorgyan G, Rinke K, Schultze M, Mamyan A, Kuzmin A, Belykh O et al. (2020) First report about toxic cyanobacterial bloom occurrence in Lake Sevan, Armenia. International Review of Hydrobiology 105(5-6): 131-142. https://doi.org/10.1002/iroh.202002060

Legovich NA (1979) About “bloom” of the water of Lake Sevan. Proceedings of Sevan Hydrobiological Station 17: 51-74 (in Russian)

Legovich NA (1968) Changes in the qualitative composition of phytoplankton of Lake Sevan under the influence of a decrease in its level. Biological Journal of Armenia 21(12): 31-42 (in Russian)

Parparov AS (1979) Primary production and chlorophyll-a content in the phytoplankton of Lake Sevan. Proceedings of Sevan Hydrobiological Station 17: 89-99 (in Russian)

12th World Congress on Water Resources and Environment (EWRA 2023)
"Managing Water-Energy-Land-Food under Climatic, Environmental and Social Instability"
Thessaloniki, Greece, 27 June - 1 July 2023

Impact of solar net radiation input data source on accuracy of Penman-Monteith reference evapotranspiration values

V. Rattayová[1*], M. Garaj[2], K. Hlavčová[1], K. Mikulová[2]
[1] Department of Land and Water Resource Management, Faculty of Civil Engineering, Slovak University of Technology, Bratislava, Slovakia
[2] Department of the Climatological Service, Slovak Hydrometeorological Institute, Bratislava, Slovakia
* e-mail: rattayovaviera@gmail.com

Introduction

Evaporation has an important role in hydrological processes by water loss; it transfers rainfall water back to the atmosphere from the land surface, related to surface energy fluxes. Knowledge about the spatial and temporal distribution of this meteorological variable is necessary for many hydrological, climatological, and agricultural tasks, mainly during the decades affected by climate change. Changes in meteorological variables, especially air temperature and precipitation, lead to changes in evapotranspiration and consequently to changes in runoff, groundwater storage and storage of soil water. Evaporation value is affected by meteorological parameters, their yearly cycles, temporal changes and relationships, and land characteristics (landuse and land cover), mainly affected by anthropogenic influence. Although diverse methods for estimating evapotranspiration are exist for many decades, ranging from basic empirical formulas to data processed from satellite measurements, the model providing relevant results for every region without high input demand is still unavailable. In many regions, hydrological engineers and researchers use habitual models to estimate evapotranspiration without verifying their accuracy. The unsuitability of some models for local conditions necessarily leads to low accuracy of results. This problem is gaining importance in recent times, when evapotranspiration is commonly used in hydrological models for the estimation of increasingly occurred hydrological extremes affecting human security - floods and drought. Another equally important subject affecting the usability of the model are input parameter requirement of the model. In many regions, we still do not have good accessibility of measured data. For this reason, it is necessary to select a suitable model regarding local data availability and, after evaluating the model's accuracy in a local condition. The new direction for data acquisition in research could provide datasets based on remote sensing observations. Increasing availability and free access to datasets based on remote sensing data could provide a favorable source of data for many tasks, mainly because of their spatial character. However, their accuracy is affected by the used model, the accuracy of input variables and local conditions. Verification of the accuracy of these datasets can lead to increased independence of researchers on local institutions and policy and improvement punctuality of research results, consequently, their better applicability in engineering practices.

This research is aimed to compare the impact of selected methods for the estimation of Solar net radiation data to the results of reference evapotranspiration in 36 meteorological stations in Slovakia. A set of stations was selected according to a length of sunshine duration measurement between 1980-2020, where the main requirement was the availability of more than 60% of measurement in a specified time window.

Materials and methods

FAO method (Allen et al. 1998), which is widely recommended as a reference method, was used for the estimation of reference evapotranspiration in daily time steps.

Meteorological data was accessed from the Slovak Hydrometeorological Institute database. The usability of this method in the region of research is limited by a wide range of input data required for calculation due low availability of this data. The unavailability of a sufficient dataset of sunshine duration measurement caused the main problem. Information about sunshine duration is required as an input

parameter for calculating Solar Net Radiation. However, this parameter is hard to compute from other measurements, and a satellite-based dataset of these estimates is unavailable. For this reason, a dataset of Solar net radiation estimated from measured input data was directly gap filled by remote sensing-based Solar Net radiation datasets - Era5, Merra-2, Fluxcom datasets and Merra2(RS). Reference evaporation was estimated by the FAO Penman-Monteith method, using datasets of net solar radiation from measure-based and satellite-based sources. The results in daily time step were compared by the Pearson correlation coefficient (CC) and the BIAS assessment.

Results and concluding remarks

Comparison analyses realized using data from the reference FAO method showed good correlation for all datasets and all stations, with the highest mean value of 0,92 for Merra2 based dataset, 0,94 for the Fluxcom CRES-based dataset and a mean value of 0.87 for the ET_0 dataset using Era and Era5 land. Results of the BIAS comparison showed slightly higher accuracy of the Merra2 dataset (mean BIAS = - 0,78%) and Fluxcom CRES-based dataset (mean BIAS= -7,5%) than Era5 and Era5 land (with mean BIAS 48,2% and 46,75%).

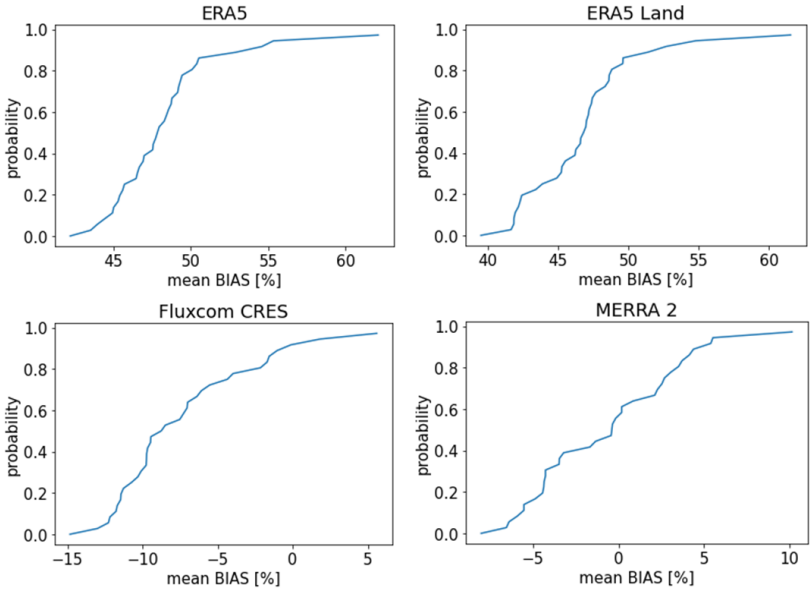

Figure 1. Bias of ET_0 datasets based on different source of radiation data.

A more detailed analysis of local conditions influence on dataset accuracy does not show any influence of station altitude and long-term mean daily evapotranspiration in stations on the results of CC and BIAS.

The impact of the variance of reference evapotranspiration daily values on the accuracy of remote sensing datasets was detected in both datasets. Although the ability of RS datasets to detect changes in ET_0 does not relate to the variance of ET_0 values very significantly, in the case of the Era5 dataset, the increasing variance of the daily ET_0 values in stations are in positive correlation relationship with BIAS (R2=0.58). The impact of driving factors of evapotranspiration on this phenomenon will be the task of consequent research.

Acknowledgments: "This publication is the result of the project implementation: „Scientific support of climate change adaptation in agriculture and mitigation of soil degradation" (ITMS2014+ 313011W580) supported by the Integrated Infrastructure Operational Programme funded by the ERDF; and was supported by the Slovak Research and Development Agency under Contract No. APVV-18-0347; and grant number VEGA 1/0782/21."

References

Allen RG, Pereira LS, Raes D, Smith M (1998) Crop evapotranspiration - Guidelines for computing crop water requirements. FAO Irrigation and drainage paper 56. https://doi.org/10.1016/j.eja.2010.12.001

12th World Congress on Water Resources and Environment (EWRA 2023)
"Managing Water-Energy-Land-Food under Climatic, Environmental and Social Instability"
Thessaloniki, Greece, 27 June - 1 July 2023

Impact of fertilizer management practices and land cover dynamics on nitrate transport to surface waters

M.C. Gunacti[1*], H. Boyacioglu[2], F. Barbaros[1]
[1] Dokuz Eylül University, Faculty of Engineering, Department of Civil Engineering, Izmir, Turkey
[2] Dokuz Eylül University, Faculty of Engineering, Department of Environmental Engineering, Izmir, Turkey
* e-mail: mert.gunacti@deu.edu.tr

Introduction

Water resources management becomes a crucial topic under the impacts of climate and land cover change. Extreme meteorological conditions are driven by climate change, causing increasing surface runoff and flooding, and severe droughts. Land cover change is a less afflicting factor on basin hydrology and water quality than climate change. Excess nitrogen in water bodies causes eutrophication and accordingly algae blooms (Mahmoodi et al. 2021; Yang et al. 2018). Soil Water Assessment Tool (SWAT) has been employed by researchers to investigate and study the hydrological cycle and water quality under climate and land cover change. SWAT is one the most comprehensive models that can simulate both the quantity and quality of surface water and groundwater. Results of several SWAT studies on water quality management concluded that changes in the hydrological cycle could directly affect the transport of various water pollutants including but not limited to nitrogen and phosphorus.

The presented study investigated the impact of fertilizer management scenarios combined with land cover change on water quality based on land cover estimations of 2035, 2065, and 2085 created by ANN-oriented approaches in the case of Küçük Menderes River Basin (KMRB), Turkey. In this scope, SWAT was used to evaluate the impact of land cover changes superposed with fertilizer management scenarios on surface water nitrate content under various scenarios.

Materials and methods

The case study area, KMRB is located in Western Turkey, where the Mediterranean climate is observed. The land cover of the basin is mainly dominated by agriculture (about 58%) and since there are intensive agricultural activities, the deficit of surface water is one of the main issues in the region. As a result, agricultural communities in the basin seek to meet their irrigation water needs by exploiting groundwater resources with increasing demand.

The LCM, a TerrSet software tool created by Clark Labs, was used to model land cover change. The LCM tool uses the Multi-Layer Perceptron (MLP) and Markov Cellular Automata (MCA) techniques to forecast future land cover classes (Ansari and Golabi, 2019). The model's general process includes spatial change analysis for historical land cover data, defining the relevance of the driver variables with the model data, developing a transition sub-model (MLP-MCA), validating the sub-model, and making future predictions. As a result, land cover maps representing the years 2035, 2065, and 2085 were generated to examine future period conditions.

As the first part of the nutrient modeling study, hydrologic simulation was performed to estimate nitrogen fluxes in the study area. In this scope, monthly discharge at the outlet streamflow gauging station was modeled using the SWAT. The SWAT model delineated the study area into 50 sub-basins, and simulation results were evaluated for these sub-basins individually. Input variables needed in SWAT modeling studies can be classified as (a) physical inputs and (b) meteorological inputs. The physical inputs consist of a representable DEM, a detailed soil map, and a land cover map. The meteorological inputs are maximum and minimum temperatures, solar radiation, precipitation, wind speed, and relative humidity representing the investigated area. SWAT is compatible with daily or monthly meteorological inputs acquired from the relevant national authorities of Turkey such as the State Hydraulic Works (DSI), and the Turkish State Meteorological Service (MGM).

Fertilizer consumption rates were either obtained from local authorities or estimated based on the literature values. Under the management scenarios consumption rates were reduced by 50% to investigate

its impacts on water quality. Furthermore, combined with predicted land cover maps of 2035, 2065, and 2085 which are representing near, mid, and far future periods, respectively, the impact of the land cover change was also investigated.

Results and concluding remarks

Receiver Operating Characteristic (ROC) analysis method was employed for each land cover class and their Area Under Curves (AUCs) were calculated for the validation of the land cover change model. An average of 0.88 percent among AUCs of land cover classes indicated a good model fit. Nash-Sutcliffe Efficiency (NSE) and Percent bias model statistics were utilized to calibrate and validate the SWAT hydrological model. The model was judged as "very good" since the NSE values were above 0.75 for both periods (Moriasi et al. 2007).

The SWAT model was run under the scenario conditions and results showed that, by reducing fertilizer usage by half, total NO_3 loads were also reduced by 27, 25, and 23 percent for the years 2035, 2065, and 2085, respectively (Figure 1). Most of the NO_3 load reduction was observed at the outlet basin (50th sub-basin) by 35, 32, and 28 percent for the years 2035, 2065, and 2085, respectively. Results also show that while NO_3 loads did not differ much among future scenarios, which would indicate the lesser impact of the land cover change, a slight increase was observed throughout the future. In this case, the total NO_3 loads increased by 3% between 2035 and 2065 and by 2% between 2065 and 2085.

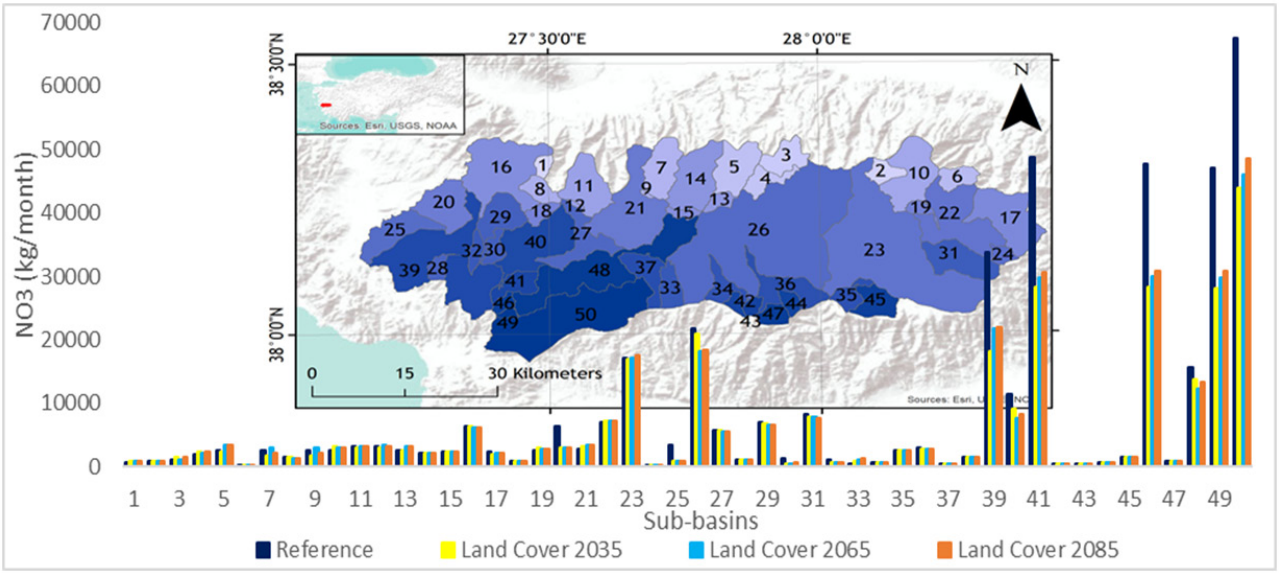

Figure 1. NO_3 loads calculated at hydrological model subbasin outlets.

Acknowledgments: This research was supported by the 1003 Programme of the Scientific and Technological Research Council of Turkey (TUBITAK) under Grant Agreement No 116Y423. We thank the project team members who provided insight and expertise that greatly assisted the research.

References

Ansari A, Golabi MH (2019) Using Ecosystem Service Modeler (ESM) for Ecological Quality, rarity and Risk Assessment of the wild goat habitat, in the Haftad-Gholleh protected area. International Soil and Water Conservation Research 7(4):346–53. https://doi.org/10.1016/j.iswcr.2019.08.004

Mahmoodi N, Wagner PD, Kiesel J, Fohrer N (2021) Modeling the impact of climate change on streamflow and major hydrological components of an Iranian Wadi system. Journal of Water and Climate Change 12(5): 1598–1613. https://doi.org/10.2166/wcc.2020.098

Moriasi D, Arnold J, Van Liew M, Bingner R, Harmel R, Veith T (2007) Model evaluation guidelines for systematic quantification of accuracy in watershed simulations. Transactions of the ASABE 50(3): 885 https://doi.org/10.13031/2013.23153

Yang X, Warren R, He Y, Ye J, Li Q, Wang G (2018) Impacts of Climate Change on TN Load and its Control in a River Basin with Complex Pollution Sources. Science of the Total Environment 615: 1155-1163. https://doi.org/10.1016/j.scitotenv.2017.09.288

12th World Congress on Water Resources and Environment (EWRA 2023)
"Managing Water-Energy-Land-Food under Climatic, Environmental and Social Instability"
Thessaloniki, Greece, 27 June - 1 July 2023

Assessment of environmentally minimum level in Lake Volvi based on morphological features

C. Doulgeris[1*], R. Nikolaidou[1,2], D. Bobori[2]
[1] Soil & Water Resources Institute, Hellenic Agricultural Organisation, 574 00 Sindos, Central Macedonia, Greece
[2] Laboratory of Ichthyology, School of Biology, Aristotle University of Thessaloniki, 541 24 Thessaloniki, Greece
* e-mail: ch.doulgeris@swri.gr

Introduction

Surface water bodies are a source of water to support society's economic activities, while on the other hand, there is a moral and legal obligation that modern societies should sustain the water bodies' ecosystems. Pressures on aquatic ecosystems of lakes and reservoirs are highly associated with the need of their water level management, considering that the water volume of a lake or a reservoir is an easily available source of water to meet human requirements. Thus, the assessment of a minimum water level is a key factor for their sustainable management, as the minimum water level is the critical level below which no further withdrawal should take place to further decrease the water level, ensuring the protection of their ecosystems.

Yet, several methods exist for the assessment of the environmentally minimum flow in rivers (Tharme 2003; Jain 2012); however, only few assessment methods exist to define a minimum water level in lakes and wetlands. In addition, minimum water level assessment methods have rarely been used to assist water resources management in lake ecosystems. In general, minimum water level assessment methods include the historical lake level method (Leeper and Ellison 2015), lake morphology analysis method (Li et al. 2007; Shang 2013), habitat analysis method and species-environment models (Abbaspour and Nazaridoust 2007; Mjelde et al. 2013). In this work, a lake morphological analysis based on the lake surface area-volume relationship is evaluated to assess the environmentally minimum water level of Lake Volvi in Central Macedonia, Greece.

Materials and methods

Lake Volvi is located in Northern Greece, at a distance of around 50 km east of the city of Thessaloniki. Lake's hydrological catchment area is 1,293 km^2; the lake itself is the second largest natural lake in Greece with a surface area of 72.5 km^2 and stored water volume of 911 hm^3 at water level of 36 m a.m.s.l.. Its average depth is 13.5 m while its maximum depth is approximately 24.5 m, according to lake's water level-surface-volume relationship, that was recently studied by the Greek Biotope/Wetland Centre (http://biodiversity-info.gr) in the context of the National Water Monitoring Network.

In general, lake surface area increases with the lake volume, but the increase rate, or in other words, the slope of surface area-volume (S-V) relationship, may increase or decrease with the volume depending on lake morphology. Thus, a critical lake storage exists at which the lake surface area does not change significantly. The critical storage corresponding to the breakpoint of the lake surface area-volume curve can be used to define the minimum water level in lakes, similarly to the wetted perimeter method for determining the minimum environmental flow in rivers (Gippel and Stewardson 1998).

The lake surface area method (Shang 2013) may define the minimum ecological lake level by considering both the protection of lake ecosystems and meeting water requirements of economic activities. Specifically, the minimum water level could be calculated from the multiobjective optimization model (Shang 2008; 2013). The lake surface area method has also been applied by Doulgeris et al. (2017) to estimate the minimum water level in lakes Vegoritida, Petron, Cheimaditida and Zazari.

Results and concluding remarks

The minimum water level in Lake Volvi is estimated to 32.5 m considering its maximum water level at 36 m (Table 1). At this minimum level, the lake's surface area, which is an appropriate index for the protection of lake ecosystems as lake biodiversity increases with its surface area (Browne 1981), decreases by 11%. At the same time, 26% of the lake's water volume could be available to meet water requirements of economic activities. However, it should be noted that the water potential of lakes' hydrological catchment should be sufficient to recover each year the water level from its minimum to its maximum level (Doulgeris et al. 2020). If water inflow from lake's catchment is not sufficient to rise water level to its maximum level, then a higher value for minimum water level should be considered for Lake Volvi. In addition, seasonal thresholds for the proposed minimum water level of Lake Volvi should also be examined based on the analysis of requirements of biological species, such as macrophytes, benthic macroinvertebrates and fish fauna.

Table 1. Maximum and proposed minimum water level in Lake Volvi based on its morphological features - compared with water level values in other four lakes as proposed by Doulgeris et al. (2017).

	Volvi	**Vegoritida**	**Petron**	**Cheimaditida**	**Zazari**
Maximum Water Level, m a.m.s.l.	36.0	518.0	573.1	592.0	599.7
Minimum Water Level, m a.m.s.l.	*32.5*	516.2	571.1	591.3	596.0
Lake level lowering, m	*-3.5*	*-1.8*	*-2.0*	*-0.7*	*-3.7*

Acknowledgments: This work was carried out in the framework of the project "Assessment of ecological water level in Lake Volvi", which is supported by the Natural Environment & Climate Change Agency.

References

Abbaspour M, Nazaridoust A (2007) Determination of environmental water requirements of Lake Urmia, Iran: an ecological approach. International Journal of Environmental Studies 64(2): 161–169. https://doi.org/10.1080/00207230701238416

Browne RA (1981) Lakes as islands: biogeographic distribution, turnover rates, and species composition in the lakes of central New York. Journal of Biogeography 8(1): 75–83. https://doi.org/10.2307/2844594

Doulgeris C, Georgiou P, Apostolakis A, Papadimos D, Zervas D, Petriki O, Bobori D, Papamichail D, Antonopoulos V, Farcas C, Stålnacke P (2017) Assessment of the environmentally minimum lake level based on hydromorphological features. Eur. Water 58: 197–202

Doulgeris C, Koukouli P, Georgiou P, Dalampakis P, Karpouzos D (2020) Assessment of Minimum Water Level in Lakes and Reservoirs Based on Their Morphological and Hydrological Features. Hydrology 7(4): 83. https://doi.org/10.3390/hydrology7040083

Gippel CJ, Stewardson MJ (1998) Use of wetted perimeter in defining minimum environmental flows. Regulated Rivers: Research & Management 14(1): 53–67. https://doi.org/10.1002/(SICI)1099-1646(199801/02)14:1%3C53::AID-RRR476%3E3.0.CO;2-Z

Greek BiotopeWetland Centre. Available online: http://biodiversity-info.gr (accessed on 5 February 2020).

Jain SK (2012) Assessment of environmental flow requirements. Hydrological Processes 26(22): 3472–3476. https://doi.org/10.1002/hyp.9455

Leeper DA, Ellison DL (2015) Proposed Minimum and Guidance Levels for Lake Hancock in Polk County, Florida. Southwest Florida Water Management District. Brooksville, Florida

Li XH, Song YD, Li YT et al. (2007) Calculation methods of lowest ecological water level of lake. Arid Land Geography 30(4): 526–530

Mjelde M, Hellsten S, Ecke F (2013) A water level drawdown index for aquatic macrophytes in Nordic lakes. Hydrobiologia 704: 141–151. http://dx.doi.org/10.1007/s10750-012-1323-6

Shang SH (2008) A multiple criteria decision-making approach to estimate minimum environmental flows based on wetted perimeter. River Research and Applications 24(1): 54–67. http://dx.doi.org/10.1002/rra.1047

Shang SH (2013) Lake surface area method to define minimum ecological lake level from level–area–storage curves. J Arid Land 5(2): 133−142. http://dx.doi.org/10.1007/s40333-013-0153-3

Tharme RE (2003) A global perspective on environmental flow assessment: Emerging trends in the development and application of environmental flow methodologies for rivers. River Research and Applications 19(5–6): 397–441. https://doi.org/10.1002/rra.736

12th World Congress on Water Resources and Environment (EWRA 2023)
"Managing Water-Energy-Land-Food under Climatic, Environmental and Social Instability"
Thessaloniki, Greece, 27 June - 1 July 2023

Machine learning in environmental modeling: A case study with ground-truth data from Seich–Sou suburban forest, Greece

M.J. Diamantopoulou
Faculty of Agriculture Forestry and Natural Environment, School of Forestry and Natural Environment, Aristotle University of Thessaloniki, Greece
e-mail: mdiamant@for.auth.gr

Introduction

Forests are a key resource serving a multitude of functions. Sustainable forest management ensures that the behaviour of forest ecosystems is environmentally and socio-economically acceptable. Sustainability in forests management needs the use of reliable and accurate models. The development of new models and methods to improve prediction of attributes of trees related to the survival and productivity of the forests has become a highly relevant topic both in forest and environmental policy. Forest biometric characteristics and especially the tree volume, which highly related to the tree stem form, is the first step and the main source of information for the rational management of forest ecosystems (Dau et al. 2015; Kershaw et al. 2016; Güner et al. 2022). Especially, when the forest is located near residential areas, the wood stock of these forests, among other important benefits, is considered as a significant part in the reduction of the dangerous sequencies of the human's intervention, by aiming to clean the atmosphere from many quantities of carbon dioxide gas and to provide recreation to people.

Natural resource modeling searches for new models and methods so as to find optimal solutions, which will satisfy the conditions of the maximum possible accuracy along with the optimal cost of the estimated parameters of the forest ecosystem (van Laar and Akça 2007). Due to the machine learning (ML) strength (Vapnik 2000; Breiman 2001; Haykin 2009), the Support Vector Regression (SVR) and the Random Forest (RFr) ML techniques were utilized and evaluated for the accurate and reliable trees stem form quotient estimation, which can be considered as the main significant tree volume estimation "correction factor" in forest ecosystems.

Materials and methods

Tree diameters along the stem generally decrease from the base to the tip. The way in which this decrease occurs defines the stem form which varies from tree to tree and, due to the irregular shape of the tree stem, is consider complex. The stem form quotient (k_i) is a measure that can describe the stem form and is calculated as the ratio of the stem diameter in a height *i* above the 1.3 meters, to the stem diameter at 1.3 meters. In order to accurately estimate different stem form quotients (k_{is}), depending on the numerator's diameter value, a random sample of 110 pine trees (*Pinus brutia*) from the Seich–Sou suburban forest of Thessaloniki, Greece, were measured. This forest is an almost pure planted pine forest. Tree measurements included diameter at 1.3 m height above ground ($d_{1.3}$), diameters at one-meter height interval above 1.3 m., diameter at a height halfway between 1.3m and total tree height ($d_{0.5h}$), and total height (h_{total}) of the sampled trees. Tree bole diameter values at different heights of the tree stem provide the necessary stem form quotient information needed for the accurate volume computation of the standing tree boles.

In forest research, the machine learning (ML) standing out characteristic is its methodologies generalization ability and the potential of learning from noisy or incomplete data by detecting inherent complex nonlinear relationships between output and input variables. The basic concept of the SVR methodology (Vapnik 2000) is to find an optimal surface lie within the margin determined by the Support Vectors (SV), using a loss function in a way that the regression error of all training samples (x_i's) is minimized. As a part of ML, the algorithm of Random Forest regression (RFr) technique (Breiman 2001), can be used to derive the estimation values of continuous variables. This algorithm constitutes an ensemble

supervised machine learning model, which makes use of the decision trees learning process to optimize the learning procedure. The statistical evaluation of the constructed models was made by the correlation coefficient (r), the maximum absolute error (maxab), and the mean squared error (mse), between the observed (measured on the trees) and the estimated by the models' values. For the construction of the SVR and RFr models, scikit-learn libraries (Pedregosa et al. 2011) in the Python programming language (van Rossum and Drake 2011; Python Software Foundation 2022) were used.

Results and concluding remarks

The basic concept of the SVR methodology used, is to find an optimal surface lie within the margin determined by the Support Vectors (SV), using a loss function. The *ε*-insensitive loss function supported by the radial basis kernel functions (RBF) in non-linear ε-SVR algorithm, was used. The trial-and-error method was applied for selecting the best parameters' values. The best combination of the values of the three meta-parameters that controls the compound of the estimation error, the Kernel's spread and the simplicity of the constructed model, that is the *ε* parameter, the gamma parameter (γ) and the cost parameter (C), was found 0.01, 0.27 and 35, respectively. The random forest (RFr) model estimation was calculated as the average of the estimations produced by the optimization of the decision trees included in the analysis. The technique of bagging (bootstrapping) has been followed. The number of the 100 regression trees and the number of 10 branches in each tree were selected after trials, to serve as the depth of the system and the tree, to avoid the learning over-parameterization of each decision tree.

The evaluation criteria of both models are given in Table 1. As can be seen (Table 1), the RFr model showed better adaptation to the data as compared to the ε-SVR model. In particular, the mse value for the RFr model, was found equal to 0.00358, that is 20% less than the corresponding mean square error of the *ε*-SVR model. The residual analysis showed that both models revealed normally distributed errors, with a small and homogeneous variance, which supports the statistically correct construction of the models.

Table 1. Models' evaluation criteria.

Model	Dependent var.	r	maxab	mse
ε-SVR	ki	0.9245	0.3258	0.00429
RFr	ki	0.9325	0.2856	0.00358

The effectiveness of the machine learning models that fitted to the available data, is compared with the observed data in hand and evaluated. The investigation has shown that each one of the constructed models can be used for the tree stem form quotient estimation. Furthermore, the RFr model showed superior adaptation to our data in hand as compared with the SVR investigated model and can be considered as a reliable alternative methodology, under its constrains, in order to achieve the accuracy of the information provided, saving time and effort in field.

References

Breiman L (2001) Random Forests. Machine Learning 45: 5–32. https://doi.org/10.1023/A:1010933404324

Dau JH, Mati A, Dawaki SA (2015) Role of Forest Inventory in Sustainable Forest Management: A Review. International Journal of Forestry and Horticulture (IJFH) 1(2): 33-40.

Güner S, Diamantopoulou MJ, Poudel K, Özçelik R (2022) Employing artificial neural network for effective biomass prediction: An alternative approach. Computers and Electronics in Agriculture 192(2022): 106596. https://doi.org/10.1016/j.compag.2021.106596

Haykin S (2009) Neural networks and Learning Machines. 3rd ed. Prentice Hall, UK.

Kershaw Jr JA, Ducey MJ, Beers TW, Husch B (2016) Forest Mensuration. 5th ed. John Wiley & Sons. Hoboken, NJ. https://doi.org/10.1002/9781118902028

Pedregosa F, Varoquaux G, Gramfort A, Michel V, Thirion B, Griesel O, et al. (2011) Scikit-learn: Machine learning in Python. Journal of Machine Learning Research 12: 2825–2830.

Python Software Foundation (2022) Python 3.9. https://docs.python.org/3.9/index.html

van Laar A, Akça A (2007) Forest Mensuration. 2nd ed. Springer, Dordrecht, The Netherlands. https://doi.org /10.1007/978-1-4020-5991-9

van Rossum G, Drake Jr FL (eds) (2011) The Python Language Reference Manual release 3.2 Network Theory Ltd.

Vapnik VN (2000) The Nature of Statistical Learning Theory. Springer, NY. https://doi.org/10.1007/978-1-4757-3264-1

Application of eDNA in fisheries: The case of Polifitou dam-lake (Greece)

A. Laggis[1,2*], K. Gkagkavouzis[1,2], O. Petriki[3], C. Ntislidou[3], T.M. Perivolioti[3], K. Michailidis[3], D. Petrocheilou[3], A. Kouletsos[3], A. Triantafyllidis[1,2], D. Bobori[3]

[1] *Department of Genetics, Development and Molecular Biology, School of Biology, Aristotle University of Thessaloniki, Thessaloniki, Greece*

[2] *Genomics and Epigenomics Translational Research (GENeTres), Center for Interdisciplinary Research and Innovation (CIRI-AUTH), Balkan Center, Thessaloniki, Greece*

[3] *Department of Zoology, School of Biology, Aristotle University of Thessaloniki, Thessaloniki, Greece*

** e-mail: alaggi@bio.auth.gr*

Introduction

Lake water can be thought of as an organismal genetic soup since it contains among others, skin cells and metabolic waste. This environmental DNA (eDNA) has emerged as a promising tool for assessing species diversity and abundance. When compared to traditional methods, eDNA collection is considered less invasive, easier to sample, faster, and less expensive (Rourke et al. 2022).

The Polifitos reservoir is situated in the municipality of Kozani, which sits in the Northwest of Greece. It was created, artificially in 1973, by the Public Power Corporation, using the Aliakmonas River, for the provision of electrification to Greece via hydro energy. Polifitos covers a surface of 5.630 km^2 (flooded). In total, 33 fish species (belonging to 17 families) and 3 crayfish species (Astacidae family) have been reported in the Aliakmonas drainage (Economidis et al. 2000; Oikonomou et al. 2009; Perdikaris et al. 2017). Here, we present the preliminary results of the first attempt to extract, amplify and sequence eDNA derived from the aforementioned aquatic ecosystem. The aim is to develop a model for assessing fish stocks by applying molecular methodologies used for eDNA analysis.

Materials and methods

Water sampling was performed seasonally at five stations in Polifitou dam-lake in 2022. In every station, two replicate samples (1.5 l each) were collected from the subsurface (i.e., 0.5 m below the surface) and the bottom (i.e., 0.5 m above the lake floor). The depth of the water body at the sampling stations varied between 6 and 8 m. A negative field control, comprising double-distilled water, was included in each seasonal sampling. To prevent DNA degradation, 1.5 ml of benzalkonium chloride (10%) was added to every water sample (negative control included). Water samples were transported to the laboratory in coolers and kept at 4°C until filtration. Each sample was filtered using Sterivex™ Millipore® (0.45 μm pore size). Afterwards, filters were stored at -20 °C until DNA extraction. All equipment were sterilized with commercial bleach (<5% NaOCl) for at least 20 min and rinsed with tap and distilled water. In the field, further rinsing was performed to the sampling equipment with water from the sites. To minimize contamination disposable gloves and bags were used.

Subsequently to water samplings, fish samplings was conducted with benthic multimesh gill nets, to assess the structure and biomass of fish communities at each sampling site. Furthermore, collapsible drum traps were used to catch crayfish. Water temperature (°C), dissolved oxygen (DO, mg/l), pH and conductivity (EC, μS/cm) were measured *in situ* both on the surface and above the lake floor using the Aqua Read AP-2000 probe (Kent, GB). Water transparency was determined with a Secchi disk (m).

DNeasy® PowerWater® Sterivex™ Kit was used to extract eDNA, whereas DNA from fish and crayfish tissue was extracted by CTAB. Isolated samples were quantified using Nanodrop™ and preserved at -20 °C. Primers amplifying mitochondrial genes (12S and 16S for fish, and COI and 16S for crustaceans) were tested by PCR. Tissue amplification was carried out to evaluate the performance of the primers for non-available species sequences. Mix tissues (i.e., DNA from various species tissues) and eDNA amplification was also performed to determine the appropriate PCR conditions. Exploratory library sequencing was performed on Illumina iSeq using MiFish-U primers (Miya et al. 2015).

Results and concluding remarks

Filtrated water volumes were in between 900 and 1500 ml. Filtration time ranged from 15 minutes to 2 hours. Low filtered volumes and extended duration of filtration occurred due to filter clogging. Most of the water filtrations resulted in volumes higher than 1.4 l. The latter is perceived as adequate in order to be used for species identification (Mächler et al. 2014). The mean value of eDNA concentration was higher during the summer season followed by spring, winter, and autumn (9.7, 5.5, 2.69 and 2.16 ng/μl, respectively).

In total, 9 fish species (attributing to 6 families) and crayfish species *Astacus leptodactylus* (family Astacidae) were caught. The most abundant species in terms of numbers and biomass was *Rutilus rutilus* followed by *Perca fluviatilis* and *Alburnus thessalicus.* The highest catches, in terms of specimen number and biomass values, were recorded in summer, followed by spring, autumn, and winter. It is important to note that catch seasonality was similar to the observed eDNA concentrations.

Tissue amplification showed that the tested primers were appropriate for species identification. However, species-specific primers for *Astacus leptodactylus* – genetic clade III (Agersnap et al. 2017) indicated a possible amplification of other Astacidae species. Mixed extracted DNA tissues could be used as a starting point for determining appropriate PCR conditions to minimize the use of eDNA samples. Amplification and sequencing of some eDNA samples were positive for fish. Further analysis of the acquired samples and their comparison to fish abundance and biomass data are needed to clarify this issue.

Acknowledgments: The research forms part of the "Innovation in fisheries using intelligent molecular approaches" project, co-funded by the European Maritime and Fisheries Fund and the Hellenic Ministry of Rural Development and Food.

References

Agersnap S, Larsen WB, Knudsen SW, Strand D, Thomsen PF, Hesselsøe M, Bondgaard Mortensen P, Vrålstad T, Møller PR (2017) Monitoring of noble, signal and narrow-clawed crayfish using environmental DNA from freshwater samples. PLoS One 12(6): e0179261. https://doi.org/10.1371/journal.pone.0179261

Economidis PS, Dimitriou E, Pagoni R, Michaloudi E, Natsis L (2000) Introduced and translocated fish species in the inland waters of Greece. Fisheries Management and Ecology 7(3): 239-250. https://doi.org/10.1046/j.1365-2400.2000.00197.x

Mächler E, Deiner K, Steinmann P, Altermatt F (2014) Utility of environmental DNA for monitoring rare and indicator macroinvertebrate species. Freshwater Science 33(4): 1174-1183. https://doi.org/10.1086/678128

Miya M, Sato Y, Fukunaga T, Sado T, Poulsen JY, Sato K, Minamoto T, Yamamoto S, Yamanaka H, Araki H, Kondoh M, Iwasaki W (2015) MiFish, a set of universal PCR primers for metabarcoding environmental DNA from fishes: detection of more than 230 subtropical marine species. Royal Society open science 2(7): 150088. https://doi.org/10.1098/rsos.150088

Oikonomou A, Zogaris S, Hatjinikolou G, Giakoumis S, Tachos V, Vardakas L, Skoulikidis N, Dimitriou H, Mousoulis H, Economou E (2009) Study of the fish fauna and proposals for its conservation in the Hilarion hydroelectric power plant construction area. (in Greek)

Perdikaris C, Konstantinidis E, Georgiadis C, Kouba A (2017) Freshwater crayfish distribution update and maps for Greece: combining literature and citizen-science data. Knowledge & Management of Aquatic Ecosystems (418): 51. https://doi.org/10.1051/kmae/2017042

Rourke ML, Fowler AM, Hughes JM, Broadhurst MK, DiBattista JD, Fielder S, Wilkes Walburn J, Furlan EM (2022) Environmental DNA (eDNA) as a tool for assessing fish biomass: A review of approaches and future considerations for resource surveys. Environmental DNA 4(1): 9-33. https://doi.org/10.1002/edn3.185

12th World Congress on Water Resources and Environment (EWRA 2023)
"Managing Water-Energy-Land-Food under Climatic, Environmental and Social Instability"
Thessaloniki, Greece, 27 June - 1 July 2023

Use of gridded data for the evaluation of ten radiation-based potential evapotranspiration models in a forest ecosystem in Greece

A. Bourletsikas[1*], N. Proutsos[1], I. Argyrokastritis[2]
[1] Institute of Mediterranean Forest Ecosystems, Hellenic Agricultural Organization DIMITRA, Athens, Greece
[2] Department of Natural Resources Management & Agricultural Engineering, Agricultural University of Athens, Greece
* e-mail: abourletsikas@elgo.gr

Introduction

Accurate estimation of potential evapotranspiration (PET) is crucial in forest hydrology, as it is an important input parameter for forest stand and watershed hydrological models. However, obtaining the necessary input parameters for PET estimation especially in forests can be very difficult and expensive. Recent studies have used high-resolution gridded meteorological datasets with different spatial and temporal resolutions (Hassan et al. 2020), produced by applying various interpolation methods to the records of nearby agro-hydro-meteorological stations (Crespi et al. 2021), to estimate PET. The accuracy and the quality of these datasets depend on the data assimilation system and the methodology followed for the homogenization of the time series.

This work aims to investigate the uncertainties introduced in the estimation of daily PET when using the AGRI4CAST gridded interpolated dataset, in the environment of a Mediterranean forest as well as to evaluate the performance of 10 widely used radiation-based PET estimation models.

Materials and methods

The study focuses on an evergreen broadleaved forest stand in Western Greece (latitude 38°50′46′′, longitude 21°18′18′′, 340 m a.s.l). An automatic meteorological station (AMS) located 420 m away from the forest stand was used to measure various variables, on an hourly time-step for a period of 23 years (1996-2018). These variables include minimum, maximum, mean air temperature (°C), relative humidity (%), global solar radiation (W/m^2) and wind speed (m/s). Precipitation was measured using four rain gauges. To estimate daily reference evapotranspiration (PM_{ground}), a ground dataset containing 7,554 daily values was used covering 90% of the time period from 1996 to 2018. In addition, the gridded dataset AGRI4CAST "Gridded Agro-Meteorological Data in Europe" – node 51149 (Toreti 2014), which provides daily meteorological data for the period 1979-2020, was also employed to estimate PET (PM_{grid}). The PM_{grid} estimates from FAO56 Penman-Monteith and 10 other radiation-based methods were compared against the FAO56 Penman-Monteith method using ground data (PM_{ground}), for the common period 1996-2018. The performance of all models was evaluated by several statistical indices: coefficient of determination (R^2), intercept (a) and slope (b) of the linear regression factors of the least squared regression analysis, mean bias error (MBE), mean absolute error (MAE), weighted determination coefficient (wR^2), model efficiency (EF) and long-term average ratio (rt) (Bourletsikas et al. 2018).

Results and concluding remarks

The daily results of PM_{grid} were generally satisfactory, although an underestimation of 7.8% is observed in its mean value (Table 1). On the other hand, the radiation-based methods showed highly variable results. PM_{ABT}, PM_{HAM}, PM_{MAK} and $PM_{P\text{-}T}$ return underestimated mean PET values of 8.9%, 24.5%, 16.1% and 0.7% respectively, whereas PM_{CAP}, PM_{DeB}, PM_{F24}, PM_{HAN}, $PM_{J\text{-}H}$ and PM_{MCB} showed overestimated mean values of 30.0%, 1.0%, 15.7%, 0.4%, 16.3%, 18.2% respectively. The best MBE (0.013 mm) and rt (1.004) were displayed by PM_{HAN}, while PM_{ABT} returned the best intercept coefficient, wR^2 and EF indices. Overall, $PM_{P\text{-}T}$ had the best performance comparing all the examined statistical parameters. Compared with the results of Bourletsikas et al. (2018) results, an increase in mean R^2 of 3.0% (range 2.4%-4.4%) and a mean decrease in

rt of 12% (3.1%-16.5%) were observed for all models. These results indicate the necessity of a cross-calibration analysis on the gridded data, mainly by the administrators of the data products which will result in an improvement to the three-dimensional regression model techniques (Thornton 2021) or by the user, carrying out a comparative analysis with the ground data (Ramirez-Cuesta 2017).

Table 1. Statistical analysis using gridded agrometeorological data for the estimation of daily PET (PMgrid) and 10 radiation-based methods against the PMground model during the study period (1996–2018, n=7554).

Method	a	b	R^2	MV	SD	rt	MBE	MAE	wR^2	EF
PM_{ground} Penman Monteith				3.34	2.20					
PM_{grid} Penman Monteith	1.1270	0.1314	0.918	3.08	1.87	0.922	-0.260	0.549	0.747	0.892
ET_{ABT} Abtew	0.9559	0.4317	0.922	3.04	2.20	0.911	-0.297	0.521	0.889	0.902
ET_{CAP} Caprio	0.7057	0.2759	0.882	4.34	2.92	1.300	1.002	1.177	0.706	0.521
ET_{DeB} DeBruin	0.9234	0.2237	0.878	3.37	2.23	1.010	0.035	0.601	0.834	0.871
ET_{F24} FAO24	0.8318	0.1242	0.919	3.86	2.53	1.157	0.531	0.712	0.832	0.825
ET_{HAM} Hamon	1.6328	0.7766	0.821	2.52	1.22	0.755	-0.818	1.148	0.413	0.559
ET_{HAN} Hansen	1.0739	0.2606	0.901	3.35	1.94	1.004	0.013	0.537	0.756	0.897
ET_{J-H} Jense-Haise	0.7576	0.3962	0.914	3.88	2.77	1.163	0.545	0.811	0.758	0.759
ET_{MAK} Makkink	1.2324	0.1131	0.901	2.80	1.69	0.839	-0.538	0.699	0.659	0.809
ET_{MGB} MacGuiness-Bordne	0.9204	0.2941	0.840	3.95	2.19	1.182	0.608	0.824	0.766	0.757
ET_{P-T} Priestley-Taylor	0.9241	0.2759	0.882	3.31	2.23	0.993	-0.024	0.588	0.842	0.876

In summary, point application of gridded datasets for the estimation of daily PET is very useful but the selection of the dataset is very important because of the cumulative error of the different variables used in complicated equations. These findings can be valuable to other experts in hydrological and climate research.

Acknowledgements: The authors would like to thank the Institute of Mediterranean Forest Ecosystems (Department of Forest Ecology and Hydrology) for the data provision and the Hellenic Ministry of Environment and Energy for funding research programmes in the study area.

References

Allen R, Pereira L, Raes D, Smith M (1998) Crop Evapotranspiration. Guidelines for Computing Crop Water Requirements. FAO Irrigation and Drainage Paper No 56, FAO, Rome, p 300

Bourletsikas A, Argyrokastritis I, Proutsos N (2018) Comparative evaluation of 24 reference evapotranspiration equations applied on an evergreen-broadleaved forest. Hydrology Research 49(4): 1028-1041. https://doi.org/10.2166/nh.2017.232

Crespi A, Matiu M, Bertoldi G, Petitta M, Zebisch M (2021) A high-resolution gridded dataset of daily temperature and precipitation records (1980–2018) for Trentino-South Tyrol (north-eastern Italian Alps). Earth System Science Data 13(6): 2801-2818. https://doi.org/10.5194/essd-13-2801-2021

Fuka DR, Walter MT, Macalister C, Degaetano AT, Steenhuis TS, Easton ZM (2014) Using the Climate Forecast System Reanalysis as Weather Input Data for Watershed Models. Hydrological Processes 28: 5613-5623. https://doi.org/10.1002/hyp.10073

Hassan I, Kalin RM, White CJ, Aladejana JA (2020) Evaluation of Daily Gridded Meteorological Datasets over the Niger Delta Region of Nigeria and Implication to Water Resources Management. Atmospheric and Climate Sciences 10: 21-39. https://doi.org/10.4236/acs.2020.101002

Ramírez-Cuesta JM, Kilic A, Allen R, Santos C, Lorite IJ (2017) Evaluating the impact of adjusting surface temperature derived from Landsat 7 ETM+ in crop evapotranspiration assessment using high-resolution airborne data, International Journal of Remote Sensing 38(14): 4177-4205. https://doi.org/10.1080/01431161.2017.1317939

Thornton PE, Shrestha R, Thornton M, Kao SC, Wei Y, Wilson BE (2021) Gridded daily weather data for North America with comprehensive uncertainty quantification. Scientific Data 8(1): 1-17. https://doi.org/10.1038/s41597-021-00973-0

Toreti A (2014) Gridded Agro-Meteorological Data in Europe. European Commission, Joint Research Centre (JRC) [Dataset] http://data.europa.eu/89h/jrc-marsop4-7-weather_obs_grid_2019

12th World Congress on Water Resources and Environment (EWRA 2023)
"Managing Water-Energy-Land-Food under Climatic, Environmental and Social Instability"
Thessaloniki, Greece, 27 June - 1 July 2023

An approach for assessing the sustainability of Mediterranean wetlands through a tailored handling of drought indices

A. Kuzucu[1], M. Najar[2], A. Gul[3*], G. Onusluel Gul[3], C.P. Cetinkaya[3]
[1] Graduate School of Natural & Applied Sciences, Dokuz Eylul University, Izmir, Turkey
[2] GIS Department, Islamic University of Gaza, Gaza, Palestine
[3] Department of Civil Engineering, Faculty of Engineering, Dokuz Eylul University, Izmir, Turkey
* e-mail: ali.gul@deu.edu.tr

Introduction

Wetlands constitute rich biodiversity reserves and hotspots associated with extensive ecosystem functions globally. Wetlands in the Mediterranean transect of Turkey, which are greatly referred to international significance and conservation concerns, are unfortunately under intensifying threats because of the gradually (sometimes quite rapidly) changing hydro-climatic conditions and mostly the emergence of droughts. This fact requires the use of scientific approaches in these areas to guide protective/restorative policy actions and to orient engineering solutions. Yet, such efforts will certainly require solid records of river discharge data that can sufficiently represent inlet hydrologic conditions to the wetlands of interest, while it is observed that either no hydrographic station is available or the data series lacks either the required quality or the length. Based on this knowledge and understanding, the methodology that is partly exemplified in the present study provides an analytical framework tailored towards the use of hydro-meteorological drought indices in assessing wetland sustainability. The study on the use of drought indices in a novel handling for the annual series of maximum drought severities is an extension of the approach that was previously suggested by Onuşluel Gül et al. (2022) and Kuzucu and Onuşluel Gül (2023). The results on targeted assessments for detecting trends in significant drought characteristics are presented over a series of spatially distributed wetland systems that distinctively represent Mediterranean hydrologic conditions.

Materials and methods

The study approach for assessing hydrologic sustainability conditions and emerging trends in arising negative consequences of droughts is based on the use of Standardized Precipitation Index (SPI) (McKee et al. 1993), but with a temporally diversified algorithm that yields daily index values rather than the monthly ones. The approach was illustrated in the case studies of some selected wetland systems located alongside the western and southern coastal regions of Turkey. The daily precipitation data that is spatially distributed in the study area was compiled from the data repository "CHELSA-EarthEnv daily precipitation product" in the form of global daily 1 km land surface precipitation based on cloud cover-informed downscaling. The dataset is mentioned with an improved temporal accuracy compared to ERA5, an additional improved spatial accuracy and much better representation of precipitation in complex terrain (Karger et al. 2021). The daily data series cover the period 2003-2015 and was used in computing daily values of the SPI index through the use of a special algorithm that was developed in Python language by Adams (2022).

From the daily SPI time series that were computed on a spatially grid representation, areal averages of the SPI values that correspond to the accumulating catchments of the wetland areas were obtained using batch processing algorithms developed in the ArcGIS software of ESRI. Here, a total of 28 wetlands identified in both Aegean and Mediterranean ecological regions of Turkey were considered in exemplifying the methodology (Figure 1a). For these, catchment zonal averages of the SPI values were computed accordingly inside the corresponding catchments (Figure 1b).

Spatially averaged daily drought index values were then used in generating the series of annual maximum severities, calendar days of the annual maximum drought event start, the lengths of the annual maxima, and some other relevant characteristics that included, for example, the length of the total period

of days associated with the drought conditions within the years of the covered period.

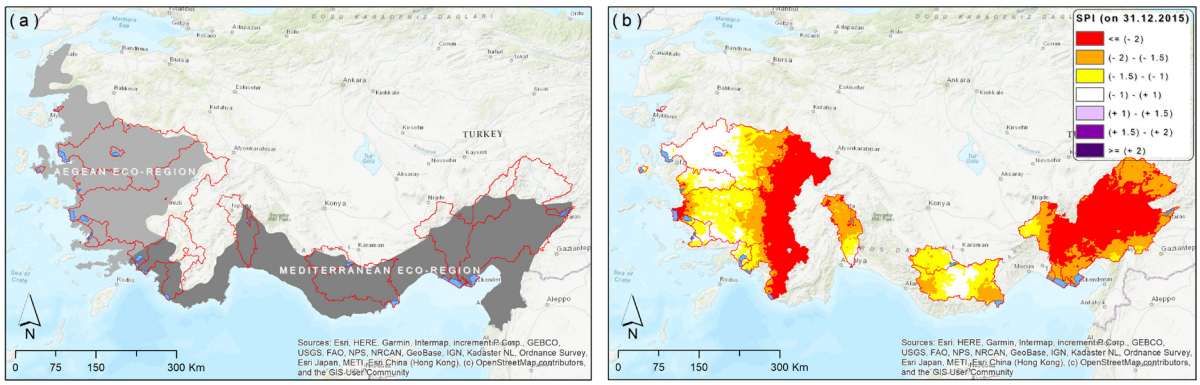

Figure 1. (a) Wetlands (in blue polygons) identified inside the two ecoregions and corresponding catchment areas; (b) spatial distribution of the daily SPI values (as in the example of the date 31.12.2015) inside the catchments.

Results and concluding remarks

The preliminary results obtained in the study indicate that overall sustainability concerns should be raised for the wetland systems of national and international significance along the Aegean and Mediterranean coastal transects of Turkey. This is explicitly due to the emerging conditions that greatly associate with decreasing precipitations (as far as being captured with the capacity of an index based purely on precipitation input), while unstably increasing temperatures in the region also need to be considered as another significant driver. The spatial appearance of the drought conditions in the catchments belonging to the analysed wetland systems of interest may still indicate some positive appearances especially in micro-climatic regions where flooding threats are also estimated in favour of wetland restoration. However, this still should not preclude the anticipation of the emerging drought conditions in the Mediterranean climate zones of Turkey from the perspective of climate change impacts felt in larger spatial domains with regionally homogeneous drought signals.

Acknowledgments: This presented study is partly funded under the research support of the MCST (Malta) & TUBITAK (Turkey) 2022 Thematic Area 1: Water Management project "UNIfied framework to cope with droughts under MEDiterranean climate change condition (UNIMED)".

References

Adams J (2022) Climate_Indices Documentation Release 1.0.10: an open source Python library providing reference: implementations of commonly used climate indices. https://github.com/monocongo/climate_indices

Karger DN, Wilson AM, Mahony C, Zimmermann NE, Jetz W (2021) Global daily 1 km land surface precipitation based on cloud cover-informed downscaling. Scientific Data 8: 307. https://doi.org/10.1038/s41597-021-01084-6

Kuzucu A, Onuşluel Gül G (2023) Analysis of drought dynamics over annual maximum drought severity series based on daily index definitions. Water Resources Management 37(3): 1421-1436. https://doi.org/10.1007/s11269-023-03434-y

McKee TB, Doesken NJ, Kleist J (1993) The Relationship of drought frequency and duration to time scales. Eighth Conference on Applied Climatology, 17-22 January 1993, Anaheim, California

Onuşluel Gül G, Gül A, Najar M (2022) Historical evidence of climate change impact on drought outlook in river basins: analysis of annual maximum drought severities through daily SPI definitions. Natural Hazards 110(2): 1389-1404. https://doi.org/10.1007/s11069-021-04995-0

The habitats' state in the Natura 2000 site "GR2310001" in river Acheloos delta

A. Psilovikos, T. Papathanasiou*
Laboratory of Ecohydraulics & Inland Water Management (ECO–HYDRO Lab), Department of Ichthyology & Aquatic Environment, University of Thessaly, Fytoko St., 38446, N. Ionia Magnisias
** e-mail: tpapathanasiou@uth.gr*

Introduction

River Acheloos Delta is a wetland of international importance, protected by Ramsar Treaty and Natura 2000. It is a complicated hydrosystem of natural lakes and artificial dam-lakes, lagoons and parts of river Acheloos. It is characterized by very competitional uses of water, which the most important of them are: a) Hydroelectric Production, b) Irrigation, c) Anti-flooding control, d) Domestic water supply and e) Ecological Preservation. The natural environment has been transformed into a fully anthropogenic one, after the construction of the dams of Kremasta in 1965, Kastraki in 1969 and Stratos I & II in 1989 from Public Power Corporation of Greece (DEH) for hydroelectric production, but also serves the uses above. Kremasta dam is the biggest reservoir in Greece, with approximately 4,75 x 10^9 m^3 of water. According to the Legislations (129264/23-05-2007 & 205198/18-11-2011 Ministerial Agreements) the human intervention due to anthropogenic activities in Acheloos Delta, needs to be investigated, if they are compatible with the protection and preservation of Natura 2000 habitats area *"GR2310001 Delta Acheloou, Limnothalassa Mesolongiou – Aitolikou, Ekvoles Evinou, Nisoi Echinades, Nisos Petalas"*. A monitoring program took place, for the documentation of these areas, under the cooperation of PPC with ECO–HYDRO Lab.

Materials and methods

According the European Environment Agency (EEA) (2022), the classification of the site "GR2310001" has been confirmed as SCI (Site of Community Importance) in 09/2006 and its definition as SAC (Special Area of Conservation) took place in 03/2011. The table below shows all the habitats of "GR2310001".

The site "GR2310001" includes 3 types of priority habitats: a) 1120 – Posidonia beds (Posidonion oceanicae), b) 1150 – Coastal lagoons, and c) 2250 – Coastal dunes with Juniperus spp. Concerning on the wild fauna, the most important species are: Elaphe quatuorlineata, Emys orbicularis, Testudo marginata, Mauremys rivulata, Alosa fallax, Aphanius fasciatus, Cobitis trichonica, Telestes pleurobipunctatus, Silurus aristotelis, Pelasgus stymphalicus, Testudo hermanni and Tropidophoxinellus hellenicus (EEA 2022). In order to preserve and protect the habitats and the landscapes of the area of interest, it is considered valuable to investigate the compatibility of anthropogenic pressures with the legislations of the specific Natura 2000 area. For this purpose, on-site visits and fieldwork were carried out in the area, using Drone Mavic 2JS II camera, for the photographic documentation, together with analysis of orthophotomaps of the Hellenic Cadaster (2015 – 2016), as well as utilization of previous literature. It is emphasized that the anthropogenic pressures of River Acheloos Delta can be distinguished mainly in agriculture, livestock farming, fishery, tourism, artificial dams, other technical constructions, waste etc (Psilovikos et al. 1995; Ministry of Environment 1999; Psilovikos et al. 2021).

Results and concluding remarks

After the field work, the documentation of the habitats and the mapping of the study area, it appears that the current state of Acheloos Delta has not been significantly affected and the complicated hydrosystem has reached a dynamic equilibrium between the natural processes combined with the anthropogenic interventions. In Acheloos Delta, the fluvial processes do not drastically and practically affect the preservation of the habitats (both flora and fauna) (Psilovikos et al. 2021). In addition, a stabilized

situation appears to have occurred, exactly as described in previous studies and research that preceded it. Non significant degradation is shown in populations and condition of the habitats. Moreover, the conditions of the Environmental Flows, have been taken into account (Konstantinidis et al. 2022).

Table 1. The Description of the habitats found in the site "GR2310001" (EEA 2022).

Habitats	Description	**Habitats**	Description
1120	Posidonia beds (*Posidonion oceanicae*)	**3290**	Intermittently flowing Mediterranean rivers of the Paspalo-Agrostidion
1130	Estuaries	**5210**	Arborescent matorral (*Juniperus* spp)
1150	Coastal lagoons	**5330**	Thermo-Mediterranean and pre-desert scrub
1160	Large shallow inlets and bays	**5420**	*Sarcopoterium spinosum* phryganas
1170	Reefs	**8210**	Calcareous rocky slopes with chasmophytic vegetation
1210	Annual vegetation of drift lines	**8310**	Caves not open to the public
1240	Vegetated sea cliffs of the Mediterranean coasts with endemic *Limonium* spp	**91F0**	Riparian mixed forests along the great rivers (Ulmenion minoris)
1310	Salicornia and other annuals colonizing mud-sand	**92A0**	*Salix alba* and *Populus alba* galleries
1410	Mediterranean salt meadows (*J. maritimi*)	**92C0**	*Platanus orientalis* and *Liquidambar orientalis* woods (*Platanion orientalis*)
1420	Mediterranean and thermo-Atlantic halophilous scrubs (*S. fruticosi*)	**92D0**	Southern riparian galleries and thickets (*Nerio-Tamaricetea* and *Securinegion tinctoriae*)
2110	Embryonic shifting dunes	**9320**	Olea and Ceratonia forests
2120	Shifting dunes along the shoreline with Ammophila arenaria ('white dunes')	**9350**	*Quercus macrolepis* forests
2250	Coastal dunes with *Juniperus* spp	**9540**	Med/nean pine forests with endemic pines

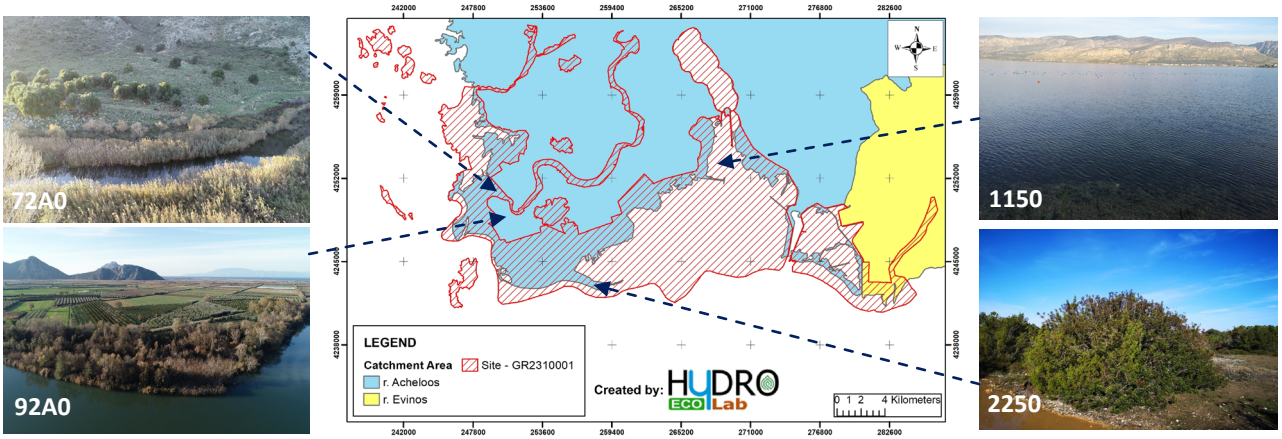

Figure 1. The boundaries of the site "GR2310001" and photographs from representative habitats (personal archive of Aris Psilovikos).

References

European Environment Agency (EEA) (2022) N2K GR2310001 Dataforms. Database release: End 2021-06/10/2022. https://natura2000.eea.europa.eu/natura2000/SDF.aspx?site=GR2310001

Konstantinidis A et al. (2022). Investigation of the Hydrologic Regime and Flow Modeling of River Acheloos, Downstream of the Hydroelectric Plants of Kremasta, Kastraki and Stratos I & II with the Utilization of Geoinformation Technologies. Research Program, Public Power Corporation of Greece (DEH). Technical Report, Research Committee International Hellenic University, Thessaloniki, Greece

Ministry for the Environment, Regional Planning and Public Works (YPEXODE) (1999) Special Environmental Study of the Wetland Complex of Messolonghi – Aitoliko. Athens, Greece

Psilovikos A et al. (2021). Investigation of the Effects of the Dams' Operation in Natura 2000 Protected Areas GR2310001 & GR2310015 in River Acheloos Delta. Research Program, Public Power Corporation of Greece (DEH). Technical Reports A, B, C. Research Committee University of Thessaly, Volos, Greece

Psilovikos A et al. (1995). Research for the Assessment and Management of the Water Resources of Lower Acheloos Basin for the Development and Environmental Improvement of the Delta, the Lagoons and the Entire Area. Research Program, Ministry of Environment and Public Works, Technical Reports A1, B1, B2, B3, C1, C2, C3, C4, D1, D2, D3. Research Committee Aristotle University of Thessaloniki, Thessaloniki, Greece

12th World Congress on Water Resources and Environment (EWRA 2023)
"Managing Water-Energy-Land-Food under Climatic, Environmental and Social Instability"
Thessaloniki, Greece, 27 June - 1 July 2023

Decadal-scale reconstruction of water storage changes of the Chagan lake of China Ramsar wetland using a machine learning approach

B. Hu[1,2], Y. Wu[1], G. Zhang[1*]
[1] Northeast Institute of Geography and Agroecology, Chinese Academy of Sciences, Changchun, Jilin 130102, China
[2] University of Chinese Academy of Sciences, Beijing 100049, China
* e-mail: zhgx@iga.ac.cn

Introduction

The global water cycle and ecological equilibrium depend heavily on lakes. Numerous lake's area, water level and storage have changed significantly over the past few decades as a result of continuous climate change and increased human activities(Pickens et al. 2020). Many studies now concentrate on large-scale research owing to remote sensing techniques, which substantially aids in disclosing the characteristics of lake alterations in various worldwide locations (Fan et al. 2021).

The primary objective of this study is to reconstruct the hypsometric curve of Chagan lake over the past decades. We measured the bathymetry of Chagan lake and integrated the data from altimetry and water surface images to rebuild the hypsometric curve and examine the water storage change. Furthermore, the machine learning algorithm is used to extend the water storage series and investigate the long-term relationships between hydrological and climatic variables. This study is expected to advance scientific understanding of the characteristics of lake water balances in response to climate change and fluctuation of Chagan lake.

Materials and methods

Data sets are divided into four categories: (1) Bathymetry surveying was conducted in the deep-water and water-land regions of the Chagan lake in 2021; (2) The Hydroweb database, which was developed by LEGOS and freely provides the water level time series of 230 lakes and water storage fluctuations. The data set passes a number of traditional corrections, including tropospheric corrections, polar and solid Earth tides, and sea state bias. Sentinel-3 altimetry data was obtained from the Copernicus Data Hub, and the outlier was removed before combining the two data sources by cross-validation to rebuild the water level series; (3) Google Earth Engine's Lansat NDWI algorithm was used to gather data on water surface area. In this study, images with less cloud contamination and an acquisition date that was close to the Sentinel-3 altimetry water level date were used. The Landsat 5, 7, and 8 satellites were used to create the JRC global surface water Mapping Layer in Version 1.4, a data collection that offers statistics on the extent and change in the water surfaces. In this study, maximum extent and occurrence bands of JRC data were produced to determine the land-water boundary; (4) The CRU data set was used to get the information on precipitation, temperature, and potential evapotranspiration. Then, using delta techniques in accordance with meteorological observation stations located inside the basin of Chagan Lake, we downscale the CRU data to 1 km scale.

The hypsometric curce were reconstructed based on the multisource remote sensing data to estimate the water storage time series of Chagan lake. The steps of the proposed method for the water storage analyze of Chagan lake are shown in Figure 1. The next three key stages are described as follows: (1) The measured terrain data and the deep water contours were generated using the in-situ data; (2) The lake shorelines were extracted from the image data, and the correspond altimetry water levels were assigned as the shoreline elevations to obtain the contours in the shallow water belts; (3) A complete hypsometric curve was constructed by combing the contours of deep and shallow water zones. The water storage series of Chagan lake was extended using the extreme gradient boosting tree (XGBoost) model with the independent variables of precipitation, temperature, and potential evapotranspiration. The equation that represents the XGBoost model is as follows:

$$OBJ = \sum_{i=1}^{n} l(yi, \hat{y}i) + \sum_{K=1}^{K} \Omega(fk) \quad (1)$$

$$\Omega(fk) = \gamma T + \frac{1}{2}\lambda \sum_{j=1}^{T} \omega_j^2$$

where the l(y_i, $\hat{y}_i$) represents the difference. n represents the sum of samples in the training data set. $\Omega(f_k)$ is the complexity of the trees, where K is the sum number of decision trees in the XGBoost model. γ and λ represent the regularization coefficients, T and ω represent the number of leaves and the leaf weights, respectively.

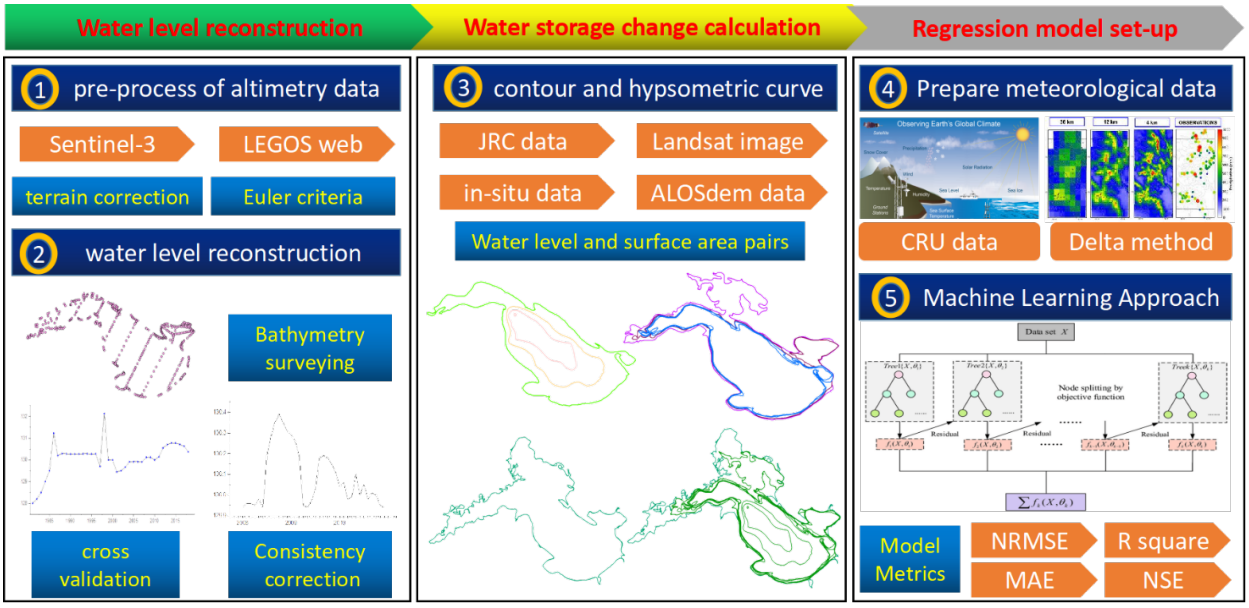

Figure 1. The workflow of the method proposed for analyzing the water storage change of Chagan lake.

Results and concluding remarks

Since records have been kept, Chagan Lake has never had water below 128 meters, and since the local government began ecological replenishment efforts, it has always been above 130 meters, peaking at 130.78 meters in 2014. The lake's area varies from 315.69 km² to 360.72 km², and its storage volume ranges from 487 million m³to 745 million m³. The absolute error of the XGboost regression model is 0.32, while the mean square deviation is 0.12, both of which show high accuracy. Further evidence that the equation is valid comes from the fact that the water area is 306 km² and the corresponding storage volume is 548 million m³. These values are identical to the official numbers. Finally, the factors affecting the water level change are precipitation, temperature and potential evapotranspiration in order.

Acknowledgments: This work was supported by the National Natural Science Foundation of China (41877160 and 42101051), the Strategic Priority Research Program of the Chinese Academy of Sciences, China (XDA28020501 and XDA28100105) and The National Key Research and Development Program of China (2021YFC3200203).

References

Pickens AH, Hansen MC, Hancher M, Stehman SV, Tyukavina A, Potapov P et al. (2020) Mapping and sampling to characterize global inland water dynamics from 1999 to 2018 with full Landsat time-series. Remote Sensing of Environment 243: 111792

Fan C, Song C, Liu K, Ke L, Xue B, Chen T, Congsheng F, Cheng J (2021) Century-scale reconstruction of water storage changes of the largest lake in the inner mongolia plateau using a machine learning approach. Water Resources Research 57(2): e2020WR028831

Wetland mitigation functions on hydrological droughts

Y. Wu[1*], J. Sun[1,2], L. Chen[1,3], M. Blanchette[4], A.N. Rousseau[4], Y.J. Xu[5], B. Hu[1,2], G. Zhang[1]
[1] Northeast Institute of Geography and Agroecology, Chinese Academy of Sciences, Changchun, Jilin 130102, China
[2] University of Chinese Academy of Sciences, Beijing 100049, China
[3] State Key Laboratory of Earth Surface Processes and Resource Ecology, Beijing Normal University, China
[4] INRS-ETE / Institut National de la Recherche Scientifique - Eau Terre Environnement, 490 rue de la Couronne, G1K 9A9 Quebec City, Quebec, Canada
[5] School of Renewable Natural Resources, Louisiana State University Agricultural Center, 227 Highland Road, Baton Rouge, LA 70803, USA
* e-mail: wuyanfeng@iga.ac.cn

Introduction

Wetlands have been singled out as a potential nature-based solution for improving the resilience and reducing the risks of hydrometeorological extremes. Previous research efforts have assessed and discussed the effects of wetlands on hydrological droughts, and specifically on baseflow or low flow support services. Most studies assessed these support services using comparative methods, where wetland scenarios (with and without wetlands, drained and undrained wetlands, varying proportions of wetlands, etc.) were simulated (e.g., Bullock and Acreman 2003; Kadykalo and Findlay 2016; Wu et al. 2020). However, wetland loss and drainage can also increase minimum summer low flows and dry period flow volume to some extent (Lee et al. 2018; Wu et al. 2020); demonstrating that wetlands may sometimes worsen droughts. Furthermore, although baseflow can be used as a proxy to characterize hydrological droughts of a basin, it cannot fully portray the specific characteristics of droughts, such as duration, severity, and more importantly propagation patterns (e.g., development and recovery processes). Thereby, there persists a knowledge gap on how to quantify wetland regulation services on hydrological droughts.

In this study, we hypothesize that wetlands can largely affect a river basin's resilience to hydrological drought events. To test the hypothesis, we propose a general framework to answer whether and to what extent wetlands can affect hydrological droughts and underlying propagation processes of meteorological droughts to hydrological droughts at the basin scale. Specifically, we perform two tasks: (i) quantifying wetland effects on hydrological droughts characteristics (duration, severity, development, and recovery processes); (ii) assessing changes in the propagation of meteorological droughts to hydrological droughts given wetland regulation services. The findings of this study can provide new insights to mitigate droughts given the hydrological regulation services of wetlands.

Materials and methods

We selected a distributed hydrological modelling platform including wetland hydrology modules (i.e., isolated and riparian wetlands modules) to simulate basin hydrological processes. We first used the monthly precipitation (basin-average) and simulated streamflow (hydrological stations) to calculate the Standardized Precipitation Index (SPI, McKee et al. 1993) and the Standardized Runoff Index (SRI, Shukla and Wood, 2008), respectively. We then applied the run theory (Yevjevich 1967) and pooling method (Guo et al. 2020) to recognize and characterize (drought duration, severity, and propagation time) meteorological and hydrological droughts. Further, we explored the relationship between meteorological droughts and hydrological droughts using the Pearson correlation coefficient, temporal shift method and cross wavelet transforms. Finally, we compared the multiple characteristics and the relationship under with and without wetland scenarios to discern whether and to what extent wetlands can affect hydrological droughts and modify the propagation from meteorological to hydrological droughts at the basin scale.

Results and concluding remarks

To validate the proposed framework, two river basins located at China and Canada (the Gan River Bain and the Nelson River Bain), with distinct land cover, were chosen to perform hydrological modelling and quantify wetland effects. The results indicate that wetlands mainly contribute to alleviating hydrological droughts by decelerating the development process, accelerating the recovery, shortening the duration, and reducing the severity of the hydrological drought events. However, the effects are variable as they may have weak impacts and even worsen drought conditions. Wetlands can extend drought propagation time and weaken the transition of meteorological to hydrological droughts. The likelihood of hydrological drought formation due to meteorological decreased by 19% and 18% respectively, for the Gan River Bain and Nelson River Bain, thanks to the mitigation services of wetlands. These findings highlight the drought-mitigation roles of wetlands and the proposed modelling framework has the potential to be useful in beneficial in assisting basin management on drought risks in the context of climate change mitigation.

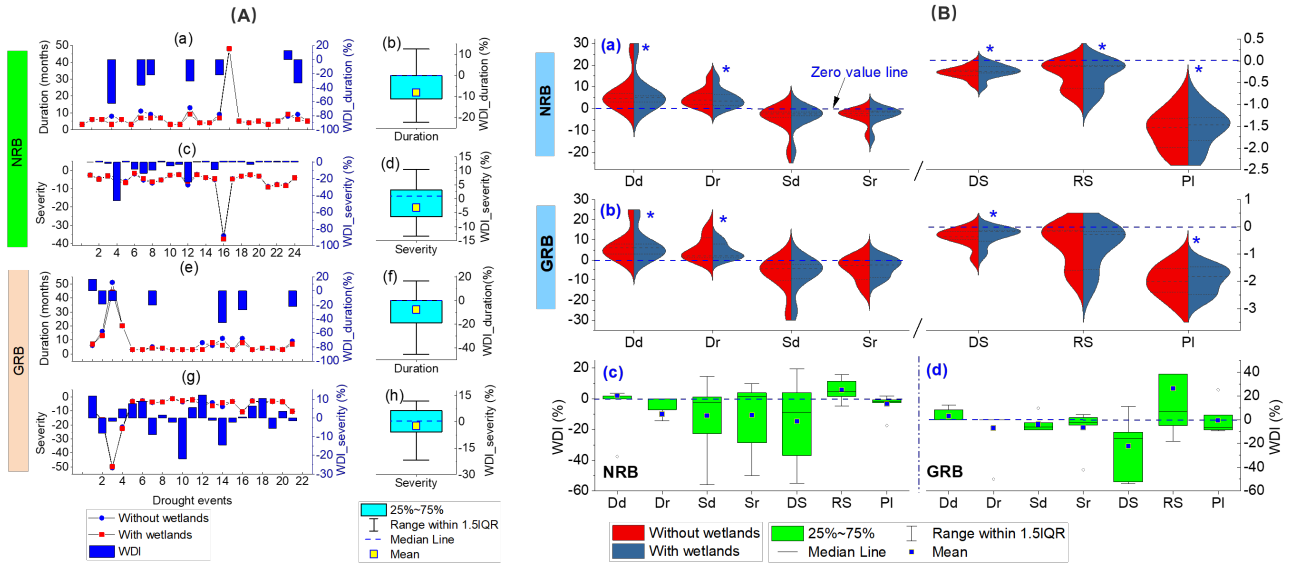

Figure 1. Wetland effects on drought propagation characteristics for the Nelson River Basin and Gan River Basin. In Fig. (A), the left panel shows the duration and severity of each drought event and wetland impacts (WDI) for the with/without wetland scenarios. The right panel shows a box plot of WDI. The number on the x-axis for the left panel refers to the drought events' number. In Fig. (B), the first two rows show changes in the severity and duration and the with/without scenarios and the last row show the effects of wetlands on hydrological droughts during the development (subscript d) and recovery (subscript r).

Acknowledgments: This work was supported by the National Natural Science Foundation of China (42101051 and 42207088), Project Supported by State Key Laboratory of Earth Surface Processes and Resource Ecology (2021-KF-02), the Postdoctoral Science Foundation of China (2021M693155 and 2022M723129), the Strategic Priority Research Program of the Chinese Academy of Sciences, China (XDA28020501 and XDA28100105) and The National Key Research and Development Program of China (2021YFC3200203).

References

Bullock A, Acreman M (2003) The role of wetlands in the hydrological cycle. Hydrology and Earth System Sciences 7(3): 358-389

Kadykalo AN, Findlay CS (2016) The flow regulation services of wetlands. Ecosystem Services 20: 91-103

Lee S, Yeo IY, Lang MW (2018) Assessing the cumulative impacts of geographically isolated wetlands on watershed hydrology using the SWAT model coupled with improved wetland modules. Journal of Environmental Management 223: 37-48

Wu YF, Zhang GX, Rousseau AN, Xu YJ (2020) Quantifying streamflow regulation services of wetlands with an emphasis on quickflow and baseflow responses in the Upper Nenjiang River Basin, Northeast China. Journal of Hydrology 583: 124565

VIII. Groundwater Contamination and Management

Groundwater resources evaluation in a mountainous aquifer system in NE Greece

I. Empliouk[1*], F.-K. Pliakas[1], A. Kallioras[2], D. Kaliampakos[2], T. Tzevelekis[1]
[1] Democritus University of Thrace, Department of Civil Engineering, 67100 Xanthi, Greece
[2] School of Mining and Metallurgical Engineering, National Technical University of Athens, 15773, Athens, Greece
* e-mail: ismail.empliouk1@gmail.com

Introduction

Groundwater flow in mountains areas has been a topic of research for several decades, spanning regional flow characterization (Freeze and Witherspoon 1967; Forster and Smith 1988), interaction with mountain and valley bottom streams (Constantz 1998; Winter et al. 2003; Covino and McGlynn 2007) and mountain block recharge (Manning and Solomon 2005). The present work deals with the collection and processing of data regarding the groundwater resources evaluation in the aquifer system of Myki Municipality in the mountainous area of Xanthi Prefecture, NE Greece.

Materials and methods

The Municipality of Myki is located in the northern mountainous area of Xanthi Prefecture, NE Greece, and belongs to the Administrative Region of Eastern Macedonia and Thrace (Figure 1). The area of the Municipality is 633.3 km^2 and its population is 14,521 people according to the 2021 census. The relief morphology of the wider area appears intensely diverse with a dense hydrographic network, a characteristic of the impermeable rocks, which constitute the largest area of the mountain mass. The relevant hydrogeological research work was performed in October 2021 and covered fifty-two (52) points (forty-seven (47) springs and five (5) groundwater wells) in the study area, which is part of the Municipal Community of Myki. After groundwater sampling from these points, in situ measurements of the parameters: pH, Electrical Conductivity (EC), and temperature were conducted. Table 1 presents the relevant measurements for October 2021 as this time period is considered more interesting regarding water scarcity.

Results and concluding remarks

Based on the results of relevant chemical analysis of groundwater samples from the fifty-two (52) points in the study area, it was concluded that these groundwater samples can be characterized from a hydrochemical point of view, in the first approach, suitable for water supply. However, it was found that the available water resources to meet the water needs of the Myki Municipality are insufficient. The observed water shortage can be attributed to the limited capacity of aquifers in some places, some bad groundwater recovery facilities, as well as water losses in the water supply system.

The problem of water shortage in Myki Municipality remains unsolved for many years due to the required costly projects. It has essentially been studied whether any of these fifty-two (52) springs and wells can supply water to more than one settlement. The results of the research showed that springs S6, S13, S14, S17, S20, S29, S30, S31, S37, S38, and S52 (Table 1, data in *italics*) can supply drinking water to more than one settlement due to the high value of discharge.

In the context of the improvement and upgrade of the existing water infrastructures in the study area and to avoid significant water loss and quality degradation problems, the following actions are proposed: (a) construction of works for the protection of the narrow area of the springs, (b) protection of the water supply system, (c) concentration of individual springs in a central spring network, (d) design and construction new groundwater recovery systems in locations of selected springs.

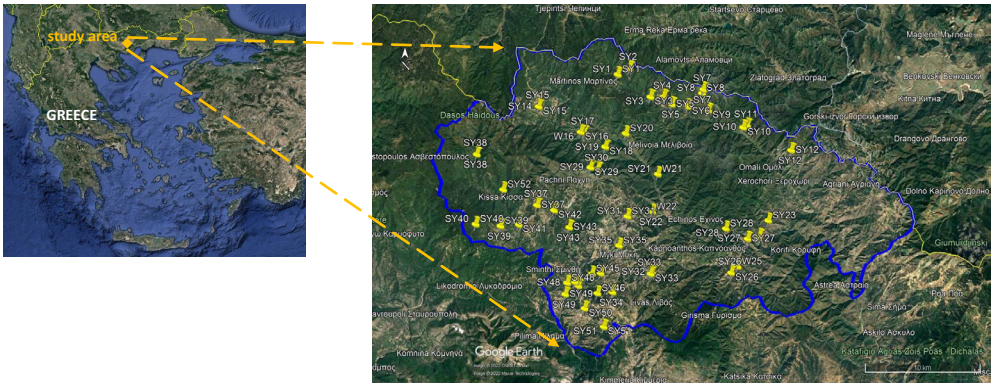

Figure 1. Study area and the network of monitoring springs/wells (Google Earth 2022).

Table 1. In situ measurement of groundwater spring/well discharge, pH, Electrical Conductivity (EC) and temperature at the study area (October 2021) (data in italics: supply of drinking water to more than one settlement).

Spring (S) / Well (W)	Discharge (m^3/h)	EC (μS/cm)	Temperature (^oC)	pH	**Spring (S) / Well (W)**	Discharge (m^3/h)	EC (μS/cm)	Temperature (^oC)	pH
S1	1.78	99.3	14.1	6.33	**S27**	0.36	495	14.3	7.74
S2	0.50	202	14.0	7.35	**S28**	0.95	282	13.3	7.19
S3	0.52	337	13.7	7.25	***S29***	*10.58*	*106.4*	*14.2*	*6.7*
S4	8.47	228	13.9	7.20	***S30***	*7.86*	*123.4*	*14.8*	*6.92*
S5	8.93	545	17.2	7.47	***S31***	*8.27*	*132.4*	*14.1*	*6.46*
S6	*10.85*	*356*	*16.2*	*7.35*	**S32**	0.38	255	13.9	6.15
S7	0.59	184.4	14.6	6.02	**S33**	2.46	280	13.6	6.70
S8	1.53	234	13.7	7.33	**S34**	1.71	425	14.3	7.32
S9	3.86	627	18.3	7.36	**S35**	4.73	580	14.1	7.32
S10	4.22	135	14.7	6.77	**W36**	30.00	543	17.4	7.67
S11	0.90	401	14.6	7.62	***S37***	*22.00*	*159*	*13.6*	*7.74*
S12	0.16	188.1	14.7	7.12	***S38***	*15.18*	*156.3*	*12.7*	*6.55*
S13	*12.20*	*126.8*	*13.1*	*6.37*	**S39**	3.40	71.4	13.9	6.32
S14	*29.06*	*94.2*	*12.2*	*6.29*	**S40**	0.78	85.4	13.5	6.20
S15	4.18	126.6	13.7	6.38	**S41**	0.55	130.3	14.7	6.26
W16	17.80	170.6	16.5	7.10	**S42**	1.24	297	13.7	7.49
S17	*15.89*	*116*	*14.2*	*6.10*	**S43**	1.23	331	14.1	6.56
S18	1.95	128.8	14.1	7.17	**S44**	0.64	375	14.8	8.03
S19	0.66	344	14.9	7.80	**S45**	1.37	547	13.2	7.29
S20	*12.25*	*315*	*14.7*	*7.56*	**S46**	0.50	232	13.1	6.82
W21	15.00	499	17.4	7.30	**S47**	0.56	514	13.8	7.50
W22	15.00	389	17.2	8.08	**S48**	0.56	590	14.8	7.26
S23	0.55	434	14.5	7.52	**S49**	0.88	319	14.3	7.57
S24	0.48	483	14.3	8.09	**S50**	0.87	424	14.4	7.70
W25	10.00	353	16.0	8.43	**S51**	0.29	467	13.9	7.32
S26	0.95	449	13.9	7.10	***S52***	*18.00*	*73.2*	*13.1*	*6.35*

References

Constantz J (1998) Interaction between stream temperature, streamflow, and groundwater exchanges in alpine streams. Water Resources Research 34(7): 1609–1615

Covino TP, McGlynn BL (2007) Stream gains and losses across a mountain-to-valley transition: impacts on watershed hydrology and stream water chemistry. Water Resources Research 43: W10431. https://doi.org/10.1029/2006WR005544

Forster C, Smith L (1988) Groundwater flow systems in mountainous terrain 2. Controlling factors. Water Resources Research 24(7): 1011-1023

Freeze RA, Witherspoon PA (1967) Theoretical analysis of regional groundwater flow. 2. Effect of water-table configuration and subsurface permeability variation. Water Resources Research 3(2): 623-634

Manning AH, Solomon DK (2005) An integrated environmental tracer approach to characterizing groundwater circulation in a mountain block. Water Resources Research 41: W12412. https://doi.org/10.1029/2005/WR004178

Winter TC, Rosenberry DO, LaBaugh JW (2003) Where does the groundwater in small watersheds come from? Ground Water 41(7): 989-1000

12th World Congress on Water Resources and Environment (EWRA 2023)
"Managing Water-Energy-Land-Food under Climatic, Environmental and Social Instability"
Thessaloniki, Greece, 27 June - 1 July 2023

Groundwater resources hydrochemical evaluation in Ooeides aquifer system, NE Greece

A. Adamidis[1*], A. Kallioras[2], I. Gkiougkis[1], P. Angelidis[1], F.-K. Pliakas[1]
[1] Democritus University of Thrace, Department of Civil Engineering, 67100 Xanthi, Greece
[2] School of Mining and Metallurgical Engineering, National Technical University of Athens, 15773, Athens, Greece
* e-mail: adamidi@otenet.gr

Introduction

Zhang (2015) mentions that the use of groundwater as a free source of water has been an effective means to meet the ever-increasing water demands and addressing the problems of surface water scarcity. Gkiougkis et al. (2021) argue that accurate conceptual model is directly related to a thorough investigation of the natural system involving subsurface investigations (groundwater well logging, geophysical investigations, pumping tests), hydrological (groundwater level monitoring, surface and unsaturated zone studies) and hydrochemical measurements (groundwater sampling and analyses). Groundwater resources play the most important role in the supply of irrigation water to rural communities in Orestiada Region in Evros Prefecture, NE Greece, while surface water sources are related to rivers Evros and Ardas. This work deals with the groundwater hydrochemical evaluation in the aquifer system of Ooeides, Orestiada Region contributing to the assessment of groundwater and surface water interaction in the study area.

Materials and methods

The study area is located in River Evros Trough, Orestiada Region in Evros Prefecture, NE Greece (Figure 1a) covering a narrow land strip of 160 km^2, called "Ooeides", which means oval because of its shape. The eastern border is River Evros. The lithological composition of the study area is made up of Holocene alluvials, consisting of alternations of cobbles, sands, gravels and clays in interlocking horizons in vertical and horizontal sense creating a heterogeneity in the material (Adamidis et al. 2022a) (Figure 1a). According to Adamidis et al. (2022b), the sedimentation of Plio – Plistocene represents the main formation of the study area. Located to the edges of River Ardas basin and the Neochori stream basin, continues submerged under the alluvial depositions. Irrigation needs for rural activities are met by pumping of groundwater from over a hundred wells, then supplied through a pipe network. Hydrogeological and hydrochemical research were carried out in a selected network of monitoring wells. The research included groundwater sampling and chemical analysis at the Laboratory of Engineering Geology and Groundwater Research, Department of Civil Engineering, DUTH, and design of relevant hydrochemical diagrams (August 2018, 2019 and 2020) (Figures 1b, e, f). The chemical parameters examined were the following: Ca^{2+}, Mg^{2+}, SO_4^{2-}, HCO_3^-, PO_4^{3-}, NO_3^-, NO_2^-, NH_4^+, Cl^-, Electrical Conductivity (EC), TDS, pH, K^+, Na^+, Fe^{2+}, Mn^{2+}.

Results and concluding remarks

Spatial distribution of clay and sand-gravel formations create the assumption of interactions between solid and liquid phases according to two cases: a) weathering of rock-forming minerals and b) weathering of trace minerals (Figures 1c, d). According to Adamidis et al. (2022a) the Gibbs diagrams (Figure 1b) illustrate the main procedure affecting groundwater hydrochemistry evolution due to ionic exchange. In order to define ion origin of interaction, end-member diagrams were created (Figure 1e). Groundwater samples were observably situated in and around the evaporite dominance, suggesting that evaporite dissolution is the dominant source for the major ions, while samples of campaign 2018, 2019 and 2020 are situated around the silicate dominance, indicating that silicate weathering was dominant source. Additionally, to detect hydrochemical process between surface and groundwater, a molar ratio diagram of the ratios NO_3^-/Na^+ and SO_4^{2-}/Ca^{2+} were used (Figure 1f). The land use concerns agricultural lands and

human settlements in the study area. Agricultural application of sulfate fertilizers is an important source of chemicals in groundwater and evidence of surface and groundwater influence.

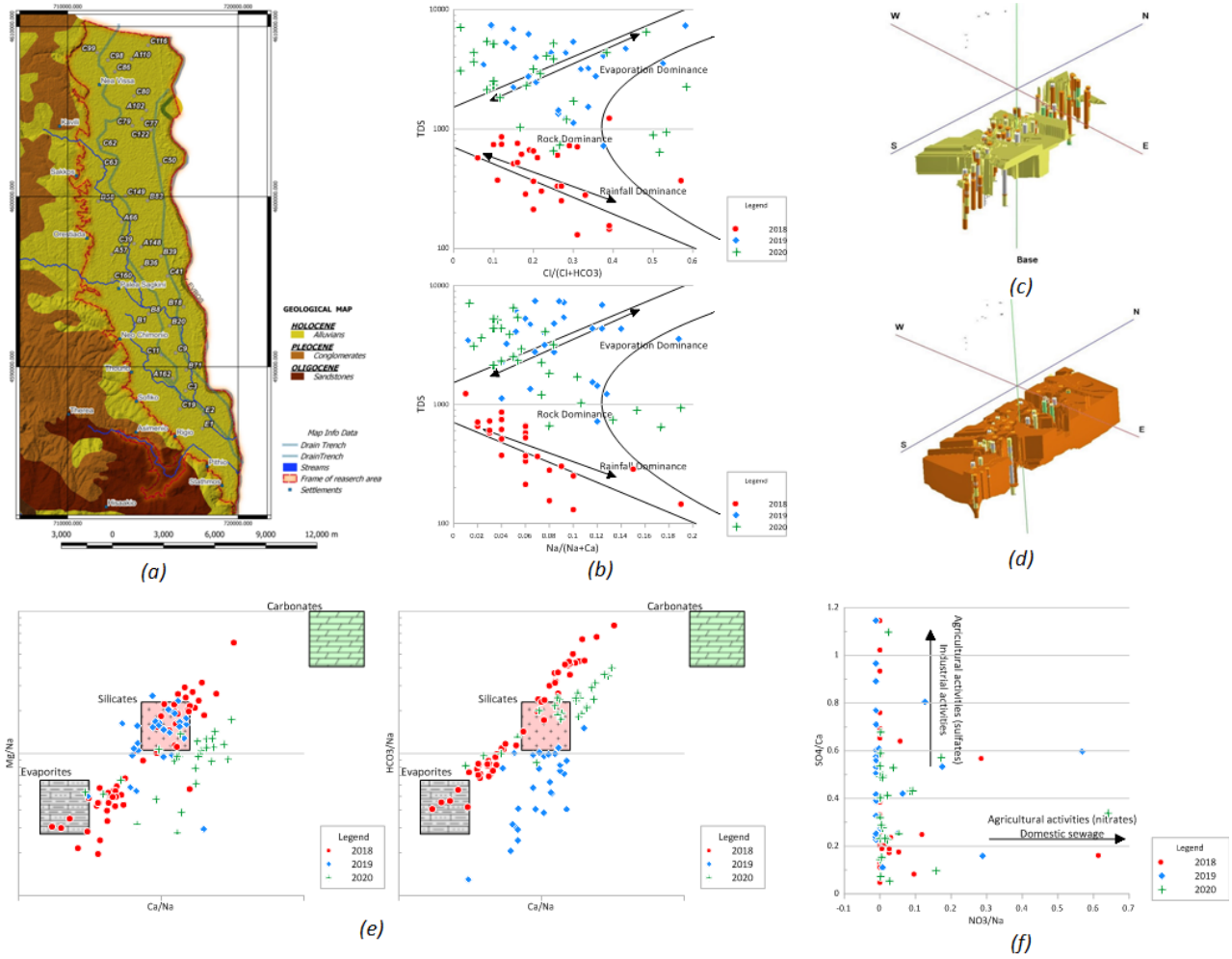

Figure 1. (a) Geological map of the study area (dashed red line) and monitoring wells and settlements; (b) Gibbs diagrams illustrating the natural principal mechanisms governing groundwater chemistry; (c) Spatial distribution of sand-gravel formation; (d) Spatial distribution of clay formation; (e) End-member diagrams representing the main rock type involved in the water–rock interactions; (f) Molar ratios of the NO_3^-/Na^+ and SO_4^{2-}/Ca^{2+}.

References

Adamidis A, Kallioras A, Angelidis P, Gkiougkis I, Pliakas FK (2022a) Assessment of Groundwater Quality in Ooeides Aquifer System, NE Greece. Bulletin of the Geological Society of Greece, Special Publication, Vol. 10, 2022, Book of Extended Abstracts, 16th International Congress of the Geological Society of Greece, 17-19 October 2022, Patras, Greece, Ext. Abs. GSG2022-165, pp.474-475

Adamidis A, Despotakis I, Kallioras A, Angelidis P, Pliakas FK (2022b) Conceptual model of an aquifer system in the region of Orestiada, North Greece. Proceedings of the 12th International Hydrogeological Congress of Greece and Cyprus / Nicosia, 2022, Book of Extended Abstracts, 52-55.

Gibbs RJ (1970) Mechanisms controlling world water chemistry. Science 170: 1088–1090

Gkiougkis I, Pouliaris C, Pliakas FK, Diamantis I, Kallioras A (2021) Conceptual and Mathematical Modeling of a Coastal Aquifer in Eastern Delta of R. Nestos (N. Greece). Hydrology Journal MDPI 8(1): 23. https://doi.org/10.3390/hydrology8010023

Zhang X (2015) Conjunctive surface water and groundwater management under climate change. Frontiers in Environmental Science 3: 59. https://doi.org/10.3389/fenvs.2015.00059

Application of the GALDIT method for the study of groundwater vulnerability in river Laspias coastal aquifer system, NE Greece

I. Gkiougkis*, E. Tzini, D. Karasogiannidis, C. Pliaka, I. Empliouk, A. Adamidis, F.-K. Pliakas, E. Evangelou, T. Tzevelekis
Democritus University of Thrace, Department of Civil Engineering, 67100 Xanthi, Greece
** e-mail: jgiougis@civil.duth.gr*

Introduction

Vulnerability of coastal aquifers is considered an issue of ample importance in water resources management, directly connected to aquifer ecosystem services and therefore affecting both natural as well as human environment. GALDIT groundwater vulnerability method has been either used directly to assess seawater intrusion problems (Lobo Ferreira et al. 2005; Chachadi and Lobo-Ferreira 2005, Santha Sophiya and Syed 2013; Recinos et al. 2015; Pedreira et al. 2015) or certain techniques have been developed to improve it or adjust it to certain hydrogeological problems (Luoma et al. 2017). This paper refers to the assessment of groundwater vulnerability to seawater intrusion in River Laspias coastal aquifer system, NE Greece (Figure 1). The paper presents the application of GALDIT method for the study of groundwater vulnerability in River Laspias coastal aquifer system, NE Greece, as well as the design of appropriate vulnerability maps to identify the aquifer parts where there is a serious potential for groundwater resources qualitative degradation due to seawater intrusion for the year 2021.

The plain area of River Laspias is coved by clay, sandy clay, sand and in some cases pebbles. The wider study area faces serious environmental problems due to seawater intrusion and quality degradation of fresh water from different sources such as applied fertilizers and pesticides, irrigation return flows and disposal of municipal and industrial waste (Gkiougkis et al. 2022).

Materials and methods

According to Eminoglou et al. (2017), the most important factors controlling seawater intrusion in the context of the development of GALDIT vulnerability index (GVI) are the following: Groundwater occurrence (aquifer type; unconfined, confined and leaky confined); Aquifer hydraulic conductivity; Depth to groundwater Level above the sea; Distance from the shore (distance inland perpendicular from shoreline); Impact of existing status of sea water intrusion in the area; and Thickness of the aquifer, which is being mapped. The acronym GALDIT is formed from the highlighted letters of the previous parameters. The procedure includes the use of a numerical ranking system which contains three significant parts: weights, ranges, and ratings. Each GALDIT factor is evaluated in relation to the other to define the relative significance of each factor. Each of the six indicators has a predefined fixed weight indicating its relative importance to seawater intrusion. The values of the GALDIT index are derived by calculating the individual index scores and summing them according to the following equation:

$$GVI = \sum(W_i R_i)/ \sum W_i \quad (1)$$

where W_i is the weight of the i^{th} indicator and R_i is the importance rating of the i^{th} indicator.

Based on the results obtained from the application of the GALDIT method, vulnerability (GVI) maps were designed for the study area for the time periods of July and October 2021 respectively (Figure 1). All relevant parameters were measured and calculated in the framework of previous hydrogeological research in the study area carried out in July and October 2021 (Gkiougkis et al. 2022). Based on results derived from relevant in situ measurements and chemical analyses from this research in July 2021, high Electrical Conductivity (EC) values were detected in the study area (>3200 μS/cm), while at the same area, the chloride (Cl^-) concentration values ranged from 60 to more than 700 mg/L, while Revelle values ranged from 0.28 to 10.78. These parameters' distribution maps were correlated against the GVI map. It was

concluded that at the southern part of the study area, there is a coincidence between the zone of high vulnerability based on GVI (> 9.0) and the high Revelle, Cl^- and EC values.

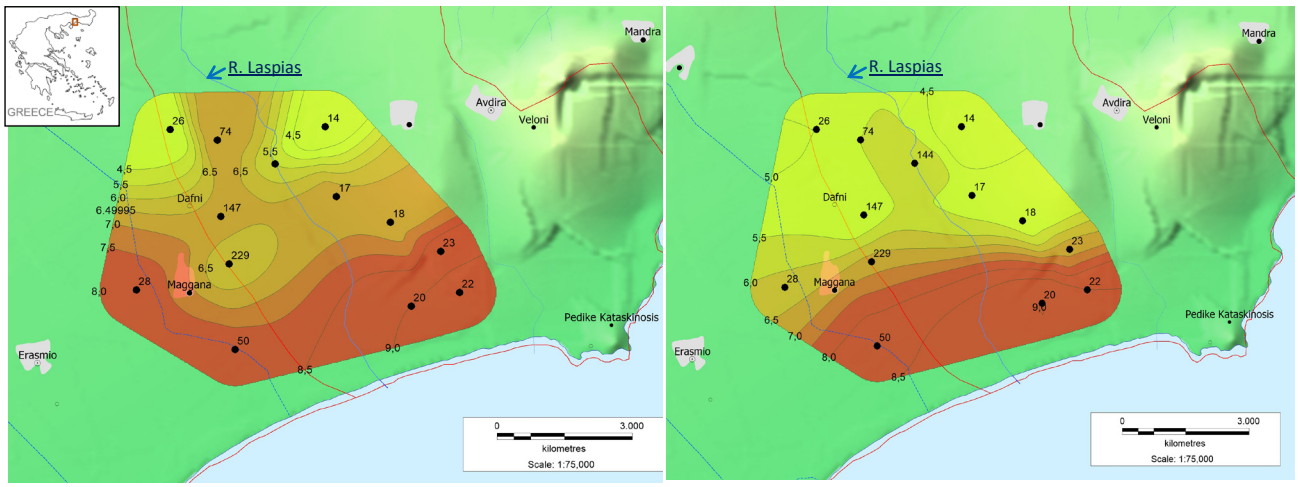

Figure 1. Left: GVI map (July 2021). Right: GVI map (October 2021).

Results and concluding remarks

Based on the findings of this research work, the need for further relevant investigation arises in order to approach better and more reliably the valuation process of the values of the GALDIT index for the coming years, both at the level of numbers and at the level of spatial distribution.

Acknowledgments: The research was funded by Eye4Water project (eye4water.com), implemented under the action: "Support for Research Infrastructure and Innovation" by the Operational Program "Competitiveness, Entrepreneurship and Innovation" in the framework of the Co-financed by Greece and the European Union-European Regional Development Fund.

References

Chachadi AG, Lobo-Ferreira JP (2005) Assessing aquifer vulnerability to sea-water intrusion using GALDIT method: Part 2 - GALDIT Indicators Description. Fourth Inter-Celtic Colloquium on Hydrogeology and Management of Water Resources, 11–14, July 2005, Portugal

Eminoglou G, Gkiougkis I, Kallioras A, Pliakas FK (2017) Updated groundwater vulnerability evaluation at a coastal aquifer system in NE Greece. European Water 57: 423-428

Gkiougkis I, Adamidis A, Emplioukl I, Karasogiannidis D, Pliaka C, Tzevelekis T, Pliakas FK (2022) Research for The Conceptual Model Development of River Laspias Coastal Aquifer System, NE Greece. Bulletin of the Geological Society of Greece, Special Publication, Vol. 10, 2022, Book of Extended Abstracts, 16th International Congress of the Geological Society of Greece, 17-19 October 2022, Patras, Greece, Ext. Abs. GSG2022-087, pp. 452-453

Lobo-Ferreira JP, Chachadi AG, Diamantino C, Henriques MJ (2005) Assessing aquifer vulnerability to seawater intrusion using GALDIT method: Part 1 Application to the Portuguese Aquifer of Monte Gordo. Fourth Inter-Celtic Colloquium on Hydrogeology and Management of Water Resources, 11–14, July 2005, Portugal

Luoma S, Okkonen J, Korkka-Niemi K (2017) Comparison of the AVI, modified SINTACS and GALDIT vulnerability methods under future climate-change scenarios for a shallow low-lying coastal aquifer in southern Finland. Hydrogeology Journal 25: 203. https://doi.org/10.1007/s10040-016-1471-2

Pedreira R, Kallioras A, Pliakas F, Gkiougkis I, Schuth C (2015) Groundwater vulnerability assessment of a coastal aquifer system at River Nestos eastern Delta, NE Greece. Environmental Earth Sciences 73: 6387–6415

Recinos N, Kallioras A, Pliakas F, Schuth C (2015) Application of GALDIT index to assess the intrinsic vulnerability to seawater intrusion of coastal granular aquifers. Environmental Earth Sciences 73: 1017–1032

Santha Sophiya M, Syed TH (2013) Assessment of vulnerability to seawater intrusion and potential remediation measures for coastal aquifers: a case study from eastern India. Environmental Earth Sciences 70: 1197. https://doi.org/10.1007/s12665-012-2206-x

Numerical simulation of seawater intrusion under the influence of groundwater exploitation in the Annaba aquifer system, Algeria

S. Hani[1*], N. Bougherira[1], I. Shahrour[2], F. Toumi[1], A. Hani[1], L. Djabri[1], H. Chaffai[1]
[1] Water Resources and Sustainable Development Laboratory (REDD). Badji Mokhtar Annaba University, BP 12, 23000, Algeria
[2] Civil Engineering and Geo Environment Laboratory (LGCgE). University of Lille, 59650 Villeneuve d'Ascq Cedex, France
* e-mail: hani.samir@outlook.fr

Introduction

Coastal areas are generally the most populated regions in the world (Chang and Yeh 2010). To meet the water needs of public water supply, agriculture and industry, groundwater resources have been seriously overexploited in recent decades.

In the present research, the study of saltwater intrusion in the coastal plain of Annaba is approached using the MODFLOW code (McDonald and Harbaugh, 1988) coupled to the MT3DMS model. The objective of using the Modflow is to analyze the effects of the intensification of pumping in the plain. The use of the MT3DMS model involves calibrating the salinity of the water in steady state and then transient over a period of 13 years. The calculated parameter is the salinity of the water expressed as chloride concentration (Cl^-).

Material and methods

The studied area is situated in the extreme North Eastern of Algeria. The aquifer system is composed of Mio-Pliocene and Quaternary sediments of Ben-Ahmed and Ben-M'hidi graben. The filling sediments of these two grabens are heterogeneous, they include an alternation of sandy clays, sands and gravels where a superficial aquifer made up of silts, a semi-permeable and finally a main aquifer made up of gravels and pebbles (Lamouroux and Hani 2006).

Many piezometric level readings and geochemical analyzes were monitored from 2009 to 2012. The analyzes are carried out on a network of 45 water points in the lower Seybouse. Electrical conductivity (EC) was measured in situ using a WTW multiparameter (Multiline P3 PH/LF SET). Chloride and sodium concentrations were determined by the volumetric method. The strontium contents were measured by ICP-MS with an accuracy of 5%. The collected hydrogeological data is used for the preparation of the groundwater flow and mass transport model.

Results and concluding remarks

To highlight the influence of the distance to the coast on the quality of groundwater, we present here the results of the evolution of the contents of chlorides Cl^-, sodium Na^+, strontium Sr and the values of electrical conductivity EC carried out along three S-N profiles perpendicular to the Mediterranean. The high levels of chlorides and sodium observed in the coastal zone are explained by contamination of the aquifer by sea water. The piezometric level measured in this sector is lower than sea level. Towards the south, after a drop, the content of these elements rises again. The increase in strontium in this part may reflect the influence of evaporitic formations on the Cl and Na contents in the water (Bougherira et al. 2015).

A multilayer model was developed to synthesize the hydrological data. Groundwater flow was modeled using the Modflow code (McDonald and Harbaugh 1988) with a mesh of 500 x 500 m. The model is made up of three layers; the surface alluvial aquifer, the semi-permeable horizon made up of sandy clays and the deep captive aquifer. The piezometric behavior of aquifers, observed over the period 2003-2015, could be reconstructed in most piezometers with an average deviation of 0.3 m. In particular, to the north where we find on the calculated piezometric maps the various depressions visible on the measured maps. On the other hand, on the eastern edge of the discretized domain, the reconstruction of the curves is less well

restored on the calculated maps. This is probably due to the low number of meshes in this area. A finer definition would have allowed a better similarity with the reference piezometry. As for the surface aquifer, the model reproduces the measured piezometry fairly well except at a few points where the deviations can reach 0.8 m (Figure 1). The calculated budget indicates that the contribution due to the marine intrusion for 2015 represents nearly 16% of the total contributions to the aquifer (Table 1).

Table 1. Summary of inputs and outputs of the aquifer system for the year 2015.

Incoming Flows (m^3/d)				Outgoing Flows (m^3/d)		
By the limits	**Recharge**	**Sea Water**	**Total**	**Pumping**	**To the sea**	**Total**
54795	0.13	9810.90	62512	53657	0.00	62512

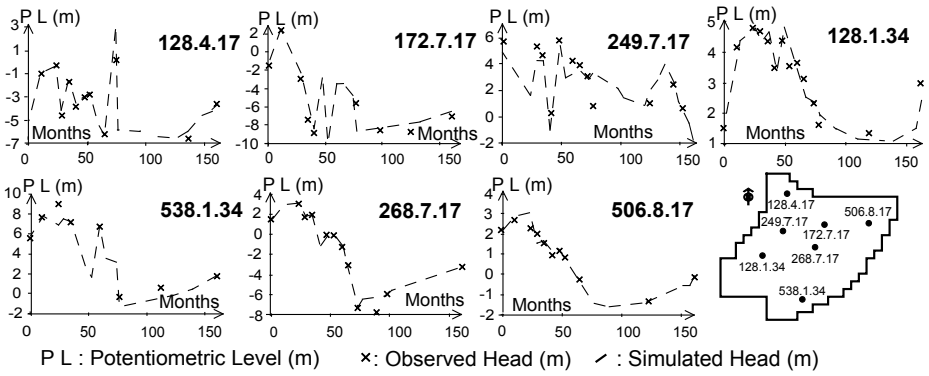

Figure 1. Transient model calibration (control piezometers).

The modeling of the transfer of Cl made it possible to simulate the salinity of the waters of the aquifer for the years 2009, 2012, 2015 and 2045 (Figure 2). For the Wells in the southern and central sector, the model shows that the exploitation of the aquifer, at its current level, can be done in a sustainable manner without significant degradation of the salinity. On the other hand, the Wells located further north seem to destabilize the fresh-brackish water balance. According to the results of the model in 2013, only a few wells in the north were affected by high values of Cl (500-800 mg/l), whereas in 2015 these same wells reached concentrations of 800 to 1100 mg/l.

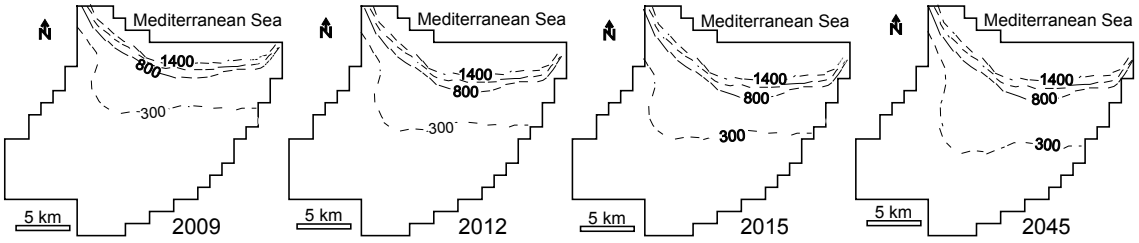

Figure 2. Simulations of marine intrusion in the lower Seybouse aquifer system.

This research allowed the location and delimitation of the salt front which advances continuously, from the year 2009 to 2015, inland, inducing increasingly high chloride concentrations. Forecasts for the year 2045 show that the salt front would progress inland by 300 to 400 m on the eastern edge, by 700 m in the center of the plain and would reach 2500 m further west of the plain.

References

Bougherira N, Hani A, Toumi F, Haied N, Djabri L (2015) Impact des rejets urbains et industriels sur la qualité des eaux de la plaine de laMeboudja (Algérie). Hydrological Sciences Journal 62(8): 1290-1300. https://doi.org/10.1080 /02626667.2015.1052451

Chang CM, Yeh HD (2010) Spectral approach to seawater intrusion in heterogeneous coastal aquifers. Hydrol. Earth Syst. Sci. 14: 719–727

Lamouroux C, Hani A (2006) Identification of groundwater flow paths in complex aquifer systems. Hydrol. Process. 20: 2971-2987

McDonald M, Harbaugh AW (1988) A Modular Three-Dimensional Finite Difference Ground-Water Flow Model. In: Techniques of Water-Resources Investigations, Book 6, U.S. Geological Survey, 588

Water resources management scenarios under climate change in the Mediterranean Almyros basin, in Greece

A. Lyra[1*], A. Loukas[2]
[1] Laboratory of Hydrology and Aquatic Systems Analysis, Department of Civil Engineering, School of Engineering, University of Thessaly, 38334 Volos, Greece
[2] Laboratory of Hydraulic Works and Environmental Management, School of Rural and Surveying Engineering, Aristotle University of Thessaloniki, 54124 Thessaloniki, Greece
* e-mail: klyra@uth.gr

Introduction

This paper evaluates the quantity and quality of water resources for various water resources development and agronomic scenarios under climate change conditions in an agricultural and coastal basin, Almyros Basin, Thessaly, Greece. The climate of the region is typical semi-arid climate. The main economic activity in Almyros Basin is agriculture, which is the main water consumer in the basin, followed by the urban water supply. Alfalfa, cereals, cotton, maize, olive groves, trees, vegetables, vineyards, and wheat are the main crops cultivated and irrigated by unsustainable groundwater pumping from the Almyros aquifer. Mean annual groundwater pumped for irrigation is estimated at about 30 hm^3 and it caused large groundwater deficit. The decline of the groundwater table due to unsustainable groundwater pumping and the heavy fertilization over the previous years also caused severe problems of nitrate pollution and seawater intrusion affecting crop production.

Materials and methods

A multi-model Med-CORDEX ensemble for RCP85 climate change scenario for precipitation and temperature has been configured, bias corrected with Quantile Empirical Mapping method and used in the analysis (Lyra and Loukas 2023b). The simulation has been performed using an Integrated Modelling System that consists of coupled models of surface hydrology (UTHBAL), reservoir operation (UTHRL), groundwater hydrology (MODFLOW), nitrate leaching/crop growth (REPIC), nitrate pollution (MT3DMS) and seawater intrusion (SEAWAT). Two groups of water resources management strategies have been examined, Strategy A in which only groundwater used for irrigation (baseline), and Strategy B in which surface water reservoirs would be developed for irrigation and urban water supply use and water is supplied by the conjunctive use of groundwater pumping and reservoir-water. Various agronomic scenarios have been developed and simulated for both water resources management strategies coupling historical irrigation, deficit irrigation and rain-fed cultivation along with reduced fertilization, as shown in Figure 1. The future groundwater abstractions, the groundwater budget, the salinity hazard both for crops and groundwater system, and the agronomic efficiency of cultivation practices are assessed with the Standardized Chloride Hazard Index and the Nitrogen Use Efficiency. The Standardized Chloride Hazard Index is estimated as shown in equation (1):

$$SCHI = (Cl_i - Cl_{mean}) / \sigma_{Cl} \quad (1)$$

where Cl_i is the spatial average of the chlorides concentrations as simulated by the IMS, Cl_{mean} is the monthly average and σ_{Cl} is the standard deviation of the timeseries. SCH Index scores lower than -1.2 indicated low hazard with normal yields, lower than -0.9 low-moderate hazard with yield decrease of sensitive crops, lower than -0.1 moderate hazard with yield decrease of crops, lower than 0.7 high hazard with yield for tolerant crops, and more than 1.5 extremely high hazard with yields for tolerant crops (Lyra and Loukas 2023a). Typical NUE scores for cereal crops range between 70 and 90 kg of grain yield per kg of nutrient applied (Fixen et al. 2015). The Nitrogen Use Efficiency Index (NUE) is estimated with equation (2):

$$NUE = \text{Crop Yield} / \text{Nitrogen Applied} \quad (2)$$

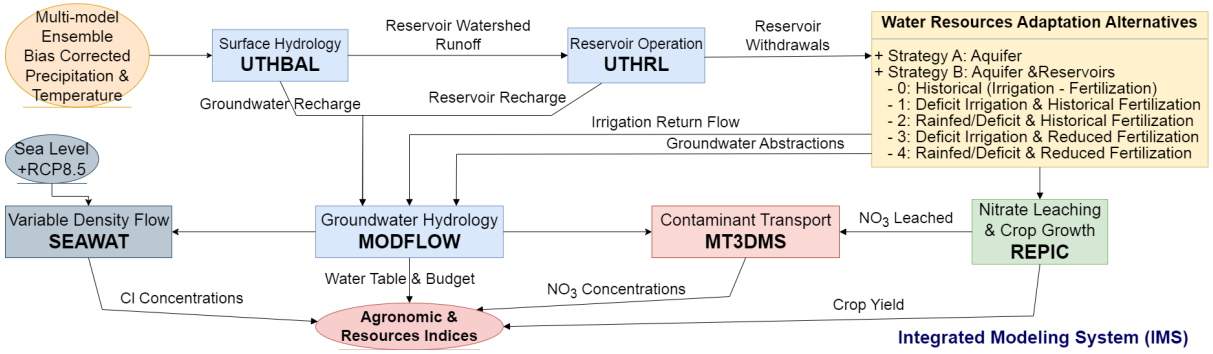

Figure 1. Flowchart of the Integrated Modelling System (IMS) applied in the Almyros Basin, Thessaly, Greece.

Results and concluding remarks

The results of Table 1 show that groundwater withdrawals will be increased in 2019-2050 as compared to the historical period 1991-2018 (Baseline A0), even with the operation of reservoirs.

Table 1. Annual water withdrawal, water budget, Seawater Intrusion, and SCHI and NUE Indices for historical and future 2019-2050 periods.

Management Scenarios	**Baseline A0**	**A0**	**A1**	**A2**	**A3**	**A4**	**B0**	**B1**	**B2**	**B3**	**B4**
Period	**1991-2018**					**2019-2050**					
Groundwater withdrawal (hm^3)	31.4	36.2	31.2	18.6	31.2	18.6	34.3	29.4	18.0	29.4	18.0
Water budget (hm^3)	-13.5	-18.1	-14.6	-7.3	-14.6	-7.3	-15.8	-9.8	-6.3	-9.8	-6.3
Seawater Intrusion (hm^3)	0.1	1.1	0.5	0.1	0.5	0.1	1.5	0.3	0.1	0.3	0.1
SCHI [1]	-1.0	-0.8	-1.1	0.1	-1.1	0.1	-0.8	-1.0	0.1	-1.0	0.1
NUE [1]	87.6	78.0	77.1	99.4	80.7	100.1	81.0	80.8	106.0	80.7	100.1

If only groundwater is used for irrigation in the period 2019-2050, then rain-fed cultivation and deficit irrigation will alleviate the groundwater water deficit. If reservoirs are constructed and operated in 2019-2050, then, in all scenarios the water budget will be relieved. However, according to the volume of seawater that intrudes the aquifer, and the SCHI scores, the salinity hazard will be low-moderate in deficit irrigation and will cause yield decrease of salt-sensitive crops while moderate in rainfed/deficit irrigation that will cause generalised decrease of crop yields during 2019-2050. This is verified by NUE values as well, which will decrease under current practices for the period 2019-2050. NUE rates are inversely proportional to the volume of groundwater used for irrigation, increased under the proposed agronomic practices, and even more increased under the use of stored freshwater for irrigation.

Acknowledgments: "This research is co-financed by Greece and the European Union (European Social Fund- ESF) through the Operational Programme «Human Resources Development, Education and Lifelong Learning» in the context of the project "Strengthening Human Resources Research Potential via Doctorate Research" (MIS-5000432), implemented by the State Scholarships Foundation (IKY)". This work was based on the Med-CORDEX initiative (www.medcordex.eu).

References

Fixen P, Brentrup F, Bruulsema T, Garcia F, Norton R, Zingore S (2015) Nutrient/fertilizer use efficiency: measurement, current situation and trends. In: Drechsel P et al. (eds.), Managing water and fertilizer for sustainable agricultural intensification, International Fertilizer Industry Association

Lyra A, Loukas A (2023a) Modelling Water Resources Adaptation and Agronomic Efficiency under Climate Change in a Mediterranean Coastal Watershed. 7th International Electronic Conference on Water Sciences (ECWS–7), 15–30 March 2023, Adaptive Water Resources Management in an Era of Changing Climatic, Environmental and Social Conditions, https://ecws-7.sciforum.net/

Lyra A, Loukas A (2023b) Simulation and Evaluation of Water Resources Management Scenarios Under Climate Change for Adaptive Management of Coastal Agricultural Watersheds. Water Resources Management 37: 2625–2642. https://doi.org/10.1007/s11269-022-03392-x

Spatiotemporal analysis of historical groundwater drought in a regional UK aquifer based on numerical modelling and the SGI index

V. Christelis, M.M. Mansour, C. Jackson, L. Wang
British Geological Survey, Keyworth, United Kingdom
** e-mail: vc@bgs.ac.uk*

Introduction

Drought is a complex natural phenomenon which varies in space and time across water catchments and can be broadly classified as meteorological, agricultural, and hydrological (Tsakiris et al. 2013). The latter category includes, among others, accumulated shortfalls in groundwater variables, the response of which to weather stresses is determined by various factors such as antecedent groundwater levels, storage, and hydraulic properties of the aquifer system (Van Loon 2015). Models of varying complexity have been employed in the literature to simulate groundwater response to meteorological drought (e.g. Peters et al. 2006; Marchant and Bloomfield 2018).

Distributed groundwater numerical models represent a comprehensive approach for studying groundwater drought in a catchment, as they can include the spatial variability of aquifer properties and complex hydraulic features over the area of interest. In this work, we employ an updated instance of a real-world groundwater model over the Marlborough and Berkshire Downs catchment, part of Thames Catchment in southeast England, to analyse the response of groundwater levels to historical drought events. The groundwater model has been enhanced with important river networks of the catchment and the analysis is undertaken considering transient groundwater flow and simulated non-uniform recharge.

Materials and methods

This study focuses on the Chalk aquifer in the Marlborough and Berkshire Downs in central-southern England (Figure 1) which is one of the major aquifers in England (Allen et al. 1997) supplying more than 70% of the water used for public supply in south-east England. Long-term average rainfall is approximately 725 mm/year and annual potential evapotranspiration is approximately 600 mm/year. Infiltration recharge occurs through the Chalk outcrop at an average rate of approximately 225 mm/year and is the main groundwater flow driver. The aquifer system mainly is under unconfined conditions because the water table location is deep below the ground surface and only to the southeast of the study area, the Chalk is confined. Groundwater is discharged mainly through the major River Thames tributaries such as the River Kennet, the River Lambourn, and the River Pang, in addition to discharge through springs located along the Chalk escarpments.

The modelling approach followed in this paper includes calculation of spatially variable daily recharge for the 1971-2004 period (Mansour et al. 2018) and used to drive the BGS in-house ZOOMQ3D groundwater flow simulator (Jackson and Spink 2004). ZOOMQ3D simulations were undertaken on a daily time step with recharge varying on a weekly basis. The characterization of historical groundwater drought events is based on the standardised groundwater index (SGI) (Bloomfield and Marchant 2013) and the results are contrasted to the widely applied meteorological drought index SPI (McKee et al. 1993). The identification of the spatio-temporal patterns of groundwater droughts in the catchment is facilitated by using a dimensionality reduction method, namely principal component analysis (PCA), to capture the overall behaviour of the catchment during the examined simulation period.

Results and concluding remarks

Although 1976 is considered a benchmark meteorological drought year for the UK, our groundwater model-based analysis indicates that the 1992 drought event propagated as a more severe groundwater drought in the catchment. Also, the leading PCA components of the SGI and SPI of the 12-month

accumulation period showed a maximum cross-correlation at a lag of 2 months. However, the SPI-based analysis identified a prominent drought event in 2003 where historical groundwater records do not support any impact on groundwater. The SGI-based analysis on the simulated groundwater levels adequately captured the expected groundwater resilience to rainfall deficits of that period. Furthermore, the spatial pattern of groundwater droughts in the catchment, through our model-based analysis, indicates that the inclusion of the updated river network is important as it appears to have a dominant role in the development of groundwater drought variability in the catchment.

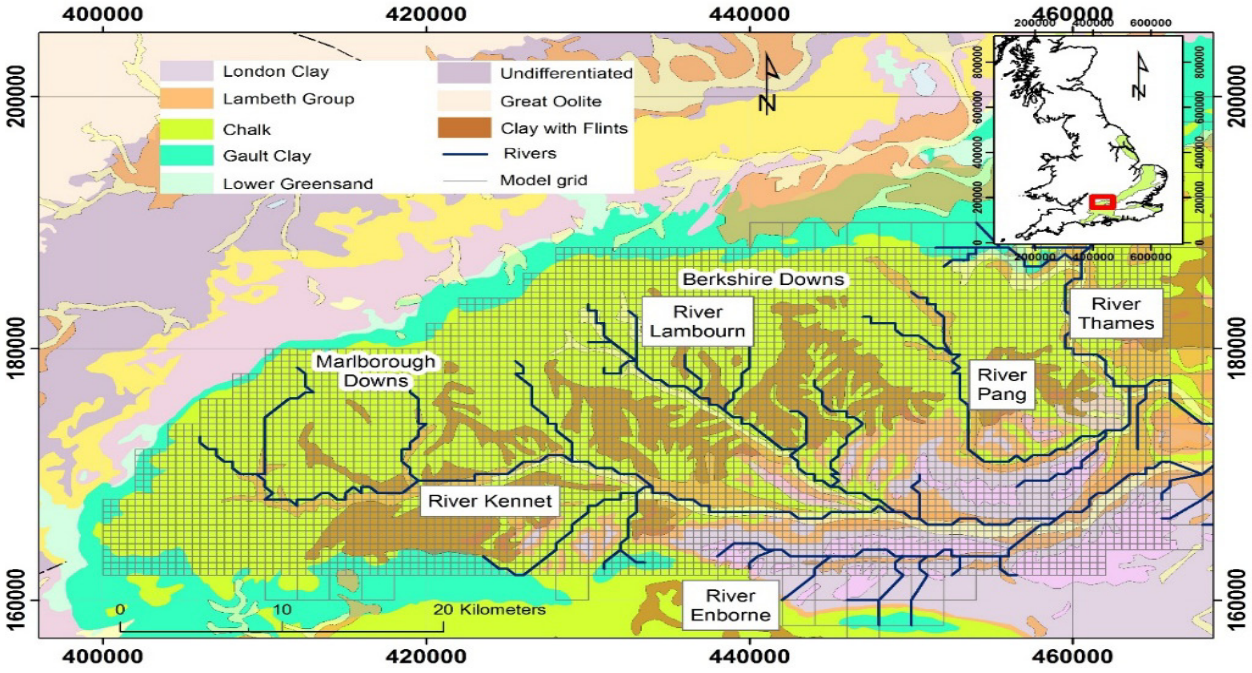

Figure 1. Simplified geological map of the study area, river networks and model grid.

Acknowledgments: This work was undertaken through funding provided by the UK Natural Environment Research Council (NERC) IMPETUS project (NE/L010178/1).

References

Allen DJ, Brewerton LJ, Coleby LM, Gibbs BR, Lewis MA, MacDonald AM, Wagstaff SJ, Williams AT (1997) The Physical Properties of Major Aquifers in England and Wales. BGS Technical Report WD/97/34, Environment Agency R&D Publication 8, Keyworth, Nottingham, UK

Bloomfield JP, Marchant BP (2013) Analysis of groundwater drought building on the standardised precipitation index approach. Hydrology and Earth System Sciences 17(12): 4769-4787

Jackson CR, Spink AEF (2004) User's manual for the groundwater flow model ZOOMQ3D.

Marchant BP, Bloomfield JP (2018) Spatio-temporal modelling of the status of groundwater droughts. Journal of Hydrology 564: 397-413

Mansour MM, Wang, L, Whiteman M, Hughes, AG (2018) Estimation of spatially distributed groundwater potential recharge for the United Kingdom. Quarterly Journal of Engineering Geology and Hydrogeology 51(2): 247-263

McKee TB, Doesken NJ, Kleist J (1993) The Relationship of drought frequency and duration to time scales. Eighth Conference on Applied Climatology, 17-22 January 1993, Anaheim, California

Peters E, Bier G, Van Lanen HA, Torfs PJJF (2006) Propagation and spatial distribution of drought in a groundwater catchment. Journal of Hydrology 321(1-4): 257-275

Tsakiris G, Nalbantis I, Vangelis H, Verbeiren B, Huysmans M et al. (2013) A system-based paradigm of drought analysis for operational management. Water Resources Management 27(15): 5281-5297

Van Loon AF (2015) Hydrological drought explained. Wiley Interdisciplinary Reviews: Water 2(4): 359-392

Laboratory methods for estimating the hydraulic properties of undisturbed soil samples

E. Chrysanthopoulos[1*], C. Pouliaris[1], K. Markantonis[1], I. Tsirogiannis[2], A. Kallioras[1]
[1] Laboratory of Engineering Geology and Hydrogeology/School of Mining and Metallurgical Engineering, National Technical University of Athens, Athens, Greece
[2] Department of Agriculture, University of Ioannina, Arta, Greece
* e-mail: echrysanthopoulos@metal.ntua.gr

Introduction

The hydraulic properties of the unsaturated zone, a crucial component of the pedosphere, are critical in understanding its hydrological processes, which are essential for various applications including agriculture, geotechnology, and environmental management. The saturated hydraulic conductivity (Ksat) and the correlation between volumetric water content and water tension (matric suction) are considered the principal soil hydraulic properties of the unsaturated zone, and their explicit knowledge is prerequisite to model the water flow and storage within that hydrologic zone. Several methods either field or laboratory have been thoroughly described in literature (Amoozegar and Warrick 1986; Whalley et al. 2013) for determining the key hydraulic properties of the unsaturated zone. In this study, the selection of methods is examined focused on the preservation of soil structure of the samples during the conductance of the experiments. Soil structure formation varies between soil groups based on climate, geology, hydrology and biological activity and determines the conditions of water movement through the unsaturated zone.

Materials and methods

Several undisturbed soil samples, up to 1 m below the soil surface, have been collected from an experimental kiwi field in the Arta's plain, located within Aracthos and Louros rivers on the east, west boundaries respectively and Amvrakikos wetlands in the south. A gasoline powered percussion hammer in combination with percussion gouges were used to conduct the drilling within the field. Soil samples were placed in PVC sample tubes (liners), which are installed inside the gouges during the drilling.

As a way of estimating saturated hydraulic conductivity of undisturbed samples, the falling head permeability method was selected. After a thorough sampling campaign within the field, using a hand auger and collecting soil samples from 2 depths (0 - 30 cm and 30 - 60 cm, respectively), pore size distribution of samples was identified, combining sieve and hydrometer analysis. Every single sample has been categorized as silty clay based on USDA particle sizes, entailing low hydraulic properties.

Falling head permeability method is conventionally used for disturbed soil samples, however in this study a new permeability cell was constructed in order to carry out permeability experiments on undisturbed soil samples. The new permeability cell was designed in such a way to fit perfectly with the dimensions of the liner. The 1 m soil sample was separated in 10 pieces in the laboratory, consequently the saturated hydraulic conductivity was determined every 10 cm, providing explicit insights into the vertical distribution of hydraulic conductivity.

For matric suction measurement and soil water characteristic curve (SWCC) definition, correlating volumetric water content with matric suction, several field and laboratory methods have been proposed (Whalley et al. 2013), with several limitations either in the range of measurements or in the depth of conductance of the experiment. In this study, two methods were used, the centrifuge and salt solution method. The latter is considered as conventional method of determining SWCC and matric suction and the centrifuge method is deemed as contemporary method, from which matric suction is determined rapidly in large range of suctions. The suction range is strongly related with the angular velocities of the centrifuge, during this experiment. Both methods have been described as methods for geotechnical characterization of a soil sample (Rahardjo et al. 2019) and in this study were implemented in the context of soil hydrology,

combining the use of undisturbed samples maintaining soil structure.

The salt solution method was conducted using an air-tight desiccator and is based on the theoretical view that matric suction in a soil – water system is linked to a specific relative vapour pressure of the water. A salt solution of sodium chloride was prepared and the weight of soil samples was measured in a tactical base, until there was no discernible change in the mass of soil specimen. The suctions measured with this method were above -2000 kPa.

The centrifuge is used for the low to medium suction range (1-400 kPa) and the measurement time is relatively less than other conventional methods, since the experiment can be completed in less than 8 hours for the whole range of suctions. The centrifuge buckets used in this experiment are able to rotate at angular velocities of 400 to 10.000 rpm. Special custom moulds have been constructed in order to fit the centrifuge buckets. The undisturbed soil sample inside the liner was placed at the base of the mould, which has been shaped with perforations to channel the water of the sample at the bottom of the bucket. The soil samples were saturated for 24h before the conductance of the experiment and then were subjected to various angular velocities for about 2 hours. In every step, when the rotation had been completed, the weight of the sample was recorded.

Results and concluding remarks

The selected methods for determining soil suction, centrifugal and salt solution method, confer the advantage of estimating matric suction in the whole range of interest. The combination of the two methods provides an opportunity to define field capacity and permanent wilting point, within the whole extent of unsaturated zone using the long undisturbed samples, in a rapid and efficient way. The outcomes of the experiments conform with literature values of that group of soils. In combination with the results of the falling head test in the undisturbed soil samples the hydraulic properties of the unsaturated zone in the field reveal the effects of conventional farming. In the upper layer of the unsaturated zone, the rizosphere, the hydraulic water flow was facilitated due to practices followed in conventional farming, such as tillage, in contrast to the lower layers of the unsaturated zone.

Taken together the results of the methods concerning saturated hydraulic conductivity (Ksat) and matric suction, a complete characterization of the hydraulic properties of the unsaturated zone was performed, considering soil structure. These results constitute the hydraulic inputs of the hydrological models of unsaturated zone, which in most cases use estimated and not calculated values for these inputs, which do not represent the actual properties of the soil water system.

Acknowledgments: This research is part of the Project “e-Pyrros: Development of an integrated monitoring network for hydro-environmental parameters within the hydro-systems of Louros-Arachthos-Amvrakikos for the optimal management and improvement of agricultural production” (MIS 5047059) and received financial funding from the Operational Programme “Competitiveness, Entrepreneurship and Innovation 2014-2020 (EPAnEK)”.

References

Amoozegar A, Warrick AW (1986) Hydraulic Conductivity of Saturated Soils: Field Methods. In: Methods of Soil Analysis (pp. 735–770). John Wiley & Sons, Ltd. https://doi.org/10.2136/sssabookser5.1.2ed.c29

Rahardjo H, Satyanaga A, Mohamed H, Yee Ip SC, Shah RS (2019) Comparison of Soil–Water Characteristic Curves from Conventional Testing and Combination of Small-Scale Centrifuge and Dew Point Methods. Geotechnical and Geological Engineering 37(2): 659–672. https://doi.org/10.1007/s10706-018-0636-2

Whalley WR, Ober ES, Jenkins M (2013) Measurement of the matric potential of soil water in the rhizosphere. Journal of Experimental Botany 64(13): 3951–3963. https://doi.org/10.1093/jxb/ert044

Anthropogenic sources and hydrogeochemical characteristics of groundwater in Mediterranean regions

M.M. Ntona[1,3*], K. Kalaitzidou[2], M. Mitrakas[2], G. Busico[1], M. Mastrocicco[1], N. Kazakis[3]
[1] *Department of Environmental, Biological and Pharmaceutical Sciences and Technologies, Campania University "Luigi Vanvitelli", Caserta, Italy*
[2] *Department of Chemical Engineering, Analytical Chemistry Laboratory, Aristotle University of Thessaloniki, Thessaloniki, Greece*
[3] *Department of Geology, Laboratory of Engineering Geology & Hydrogeology, Aristotle University of Thessaloniki, Thessaloniki, Greece*
** e-mail: mariamargarita.ntona@unicampania.it*

Introduction

In Mediterranean countries, groundwater (GW) is an almost ubiquitous source of fresh water and covers about 60% of the water demand. Indisputably, preserving GW reserves is of utmost importance to support economic activities (food production, tourism, industry, energy), as well as to ensure the health of humans and ecosystems. Due to its importance, the phenomenon of GW depletion needs to be further studied, adopting innovative methods and integrated approaches. Three areas in which GW depletion has been documented to have influenced GW quality have been studied. Two areas are located in Greece (Anthemountas and Mouriki basins) and one in Italy (Volturno basin). Different hydrogeological regimes including porous/unconsolidated, fractured rock, and karst aquifers are determined in the three basins. The current work is part of a thorough hydrogeological research on GW quality and quantity variations in the areas under investigation.

Materials and methods

Land use: Agricultural activities occupy most of the study areas (Figure 1) affecting the quality of GW. Agricultural, livestock, and industrial water demands are met by GW resources in the Anthemountas basin (Kazakis and Voudouris, 2015; Busico et al. 2021). In the Mouriki basin, the main crops are corn, cereals, fruit trees, vegetables, and legumes (Patrikaki et al. 2012; Busico et al. 2021). In the Italian region, agricultural, livestock activities, and mixed forests and pastures constitute the land cover of the area, while the main crop types are vineyards, cereals, vegetables, and orchards (Cuoco et al. 2016).

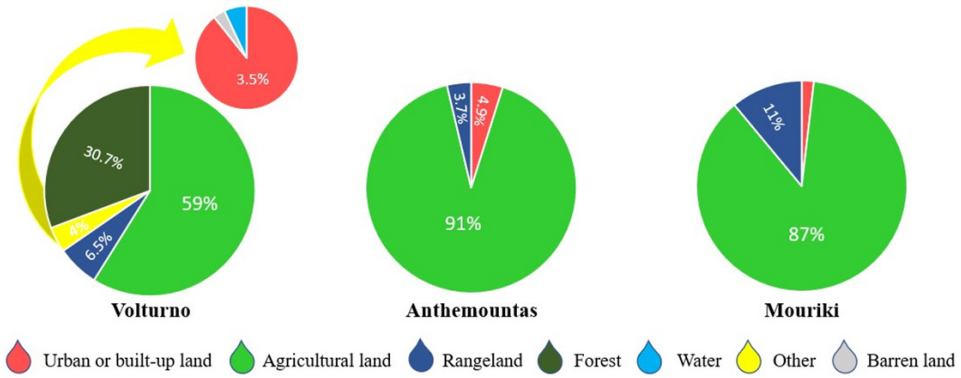

Figure 1. Pie diagrams of land use in the study areas (from Corine Land Cover 2018).

Samples collection: GW samples were collected during the dry period of 2022 (month of June) from agricultural wells in the three study areas. To give good spatial coverage over the entire studied areas, the sampling wells covered all the extent of the catchments, where it was possible. The main ions were determined according to the respective Standard Methods for the Examination of Water and Wastewater (Rice et al. 1999).

Results and concluding remarks

The obtained analytical values of the GW samples were plotted on the Piper diagram (Figure 2). The results showed that the GW samples in Volturno and Mouriki mainly have the following cations $Ca^{2+} > Mg^{2+} > Na^{+}+K^{+}$, while $HCO_3^{-} > Cl^{-} > SO_4^{2-}$ are the main anions. On the other hand, the samples from the Anthemountas basin show lower concentrations of Ca^{2+} and Mg^{2+}. Moreover, NO_3^{-} concentrations in the areas vary from 1 to 128 mg/L and depict the extensive use of fertilizers in the study areas, where the higher values belong to samples from the Volturno basin. Obviously, the formation of the hydrochemical facies/water types is a result of the geochemistry of the GW, which is further controlled by the geological structure and mineralogy of the aquifers, while external factors such as anthropogenic activities also affect the water quality. Thus, the hydrochemical analysis will be analyzed in spatial and temporal steps in all the basins. A multi-analysis of the provided data can help enhance the findings' validity and reliability. In this aspect, the current research data could be combined in various ways with other indexes and simulation processes. Different methods of GW protection have to be applied in the study areas taking into account the hydrogeological regime, artificial aspects, and climate variability.

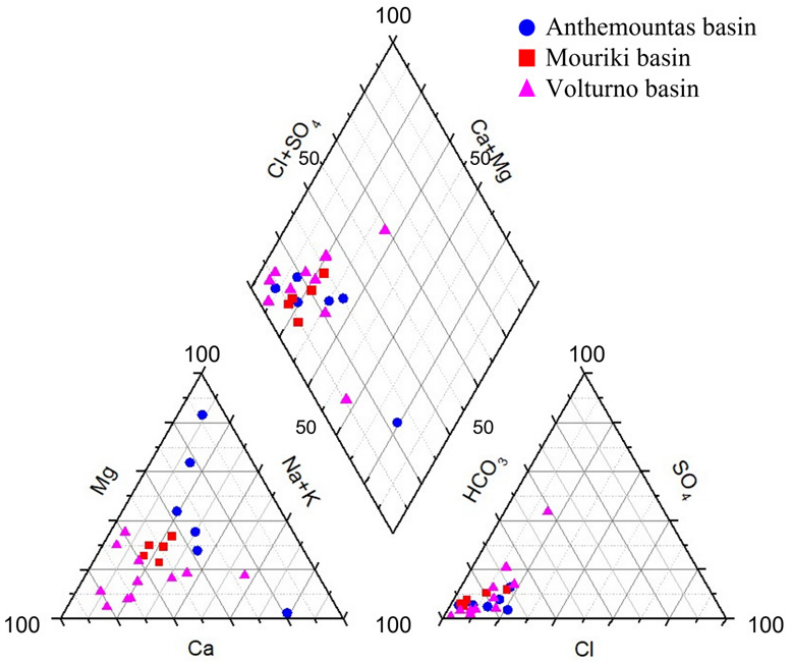

Figure 2. Classification of the GW samples in a Piper diagram.

Acknowledgments: This research project was supported financially by the Hellenic Foundation for Research and Innovation (H.F.R.I.) under the "Second Call for H.F.R.I. Research Projects to support Post-Doctoral Researchers" (Project Number: 00138). The scholarship and research activities of Maria Margarita Ntona were part of the Environment, Design and Innovation PhD Program funded by the V:ALERE 2020 Program (VAnviteLli pEr la RicErca) of the University of Campania "Luigi Vanvitelli".

References

Busico G, Ntona MM, Carvalho SCP, Patrikaki O, Voudouris K, Kazakis N (2021) Simulating Future Groundwater Recharge in Coastal and Inland Catchments. Water Resource Management 35: 3617-3632

Cuoco E, Colombani N, Darrah TH, Mastrocicco M, Tedesco D (2016) Geolithological and anthropogenic controls on the hydrochemistry of the Volturno river (Southern Italy). Hydrological Processes 31(3): 627-638

Kazakis N, Voudouris K (2015) Groundwater vulnerability and pollution risk assessment of porous aquifers to nitrate: Modifying the DRASTIC method using quantitative parameters. Journal of Hydrology 525: 13-25

Patrikaki O, Kazakis N, Kougias I, Patsialis T, Theodossiou N, Voudouris K (2018) Assessing Flood Hazard at River Basin Scale with an Index-Based Approach: The Case of Mouriki, Greece. Geosciences 8(2): 50

Rice EW, Baird RB, Eaton AD, Clesceri LS (1999) Standard Methods for the Examination of Water and Wastewater. 21st ed, American Water Works Association, American Public Works Association, Water Environment Federation, Washington DC

Comparison of physics-based and data-driven surrogate models in coastal aquifer management

G. Kopsiaftis[1*], M. Kaselimi[1], A. Voulodimos[2], E. Protopapadakis[3], I. Rallis[1], A. Doulamis[1], N. Doulamis[1], A. Mantoglou[1]
[1] School of Rural, Surveying and Geoinformatics Engineering, National Technical University of Athens, Greece
[2] School of Electrical and Computer Engineering, National Technical University of Athens, Greece
[3] School of Information Sciences, Department of Applied Informatics, University of Macedonia, Greece
* e-mail: gkopsiaf@survey.ntua.gr

Introduction

Surrogate models are becoming increasingly popular in scientific research and engineering as they provide an efficient alternative to the time-consuming models used to simulate complex physical phenomena. A surrogate model is a simplified representation of a complex system or process that can be used to quickly and accurately predict its behaviour. This is achieved by using data from the original model to train a surrogate model that can make predictions based on a smaller set of inputs. During the last few decades, the growing trend in the use of surrogate models can be also observed in the field of water resources. For example, in coastal aquifer management many researchers have used surrogate models (e.g., Mantoglou et al. 2004; Kourakos and Mantoglou 2009; Christelis and Mantoglou 2016, 2019; Kopsiaftis 2019a), which, in general, could be grouped in the following two categories: 1) the physics-based models, that simulate simplified versions of the original physical phenomenon, and 2) the data-driven models, that are constructed based on dataset, without considering the underlying mechanisms of the examined physical process.

In this work we examined the efficiency of surrogate models from both the aforementioned categories. In particular, in a first step, a widely-used sharp-interface (SI) model (Strack 1976) and two corrections of the model (Pool and Carrera 2011; Werner 2017) are applied on a simplified coastal aquifer of rectangular shape. Furthermore, a simple ensemble of all the SI models, in the form of the average of their SWI prediction is also examined. Subsequently, a number of machine learning (ML) algorithms are utilized to simulate the seawater intrusion (SWI) phenomenon in the same aquifer. All the examined methods are compared with respect to their accuracy in reproducing the extent of SWI, using the variable density (VD) approach as a benchmark model.

Materials and methods

A 3D VD model was developed for a rectangular-shaped coastal aquifer, which represents a typical example of aquifer in relatively small islands of the Mediterranean region. The aquifer is pumped by 10 productive wells and is replenished by recharge from the top surface of the aquifer and by lateral inflow from its inland boundary. A total number of 5000 pumping were generated using the Latin Hypercube Sampling statistical method. The simulation period was 30 years for all the examined scenarios. Both recharge rate and the well pumping rates were assumed constant for the entire simulation, therefore, steady-state flow conditions were achieved at the end of each scenario. By keeping the specific parameters constant, the simulations were considerably shortened, enabling the experiments to be finished within a reasonable timeframe. Following the work of Kopsiaftis et al. (2019), that highlighted the importance of the initial distribution of concentration in the aquifer, we adopted a similar approach and the input dataset for the ML methods consisted of the following variables: (i) the pumping rates of the 10 wells, and (ii) the initial location of the SWI toe. It should be noted that the 0.1 kg/m^3 concentration was selected as the critical value for the determination of the SWI extent. The output dataset consisted of the final location of the same isohaline. Four ML methods were applied on the same input/output datasets: (i) Gaussian Process Regression (GPR), (ii) Support Vector Machines (SVM), (iii) Linear Regression (LR), and (iv) Random Forests (RF).

In order to compare the efficiency of the data-driven surrogate models with the SI approach, which represents the physical-based surrogate models a pumping optimisation framework was applied on the coastal aquifer, using the benchmark VD model. The optimal pumping rates were applied on all the examined surrogate models, which were then compared in terms of their ability to reproduce the SWI extent of the VD approach.

Results and concluding remarks

Preliminary results indicate that the GPR and SVM methods outperform the remaining surrogate models examined in this paper. The original Strack SI approach tends to overestimate the extent of SWI. The SI modifications proposed by Pool and Carrera (2011) and Werner (2017), as well as the ensemble of SI model predictions, despite the improvement in the location of the SWI toe, they significantly differ from the VD results, especially in high pumping rates (Figure 1).

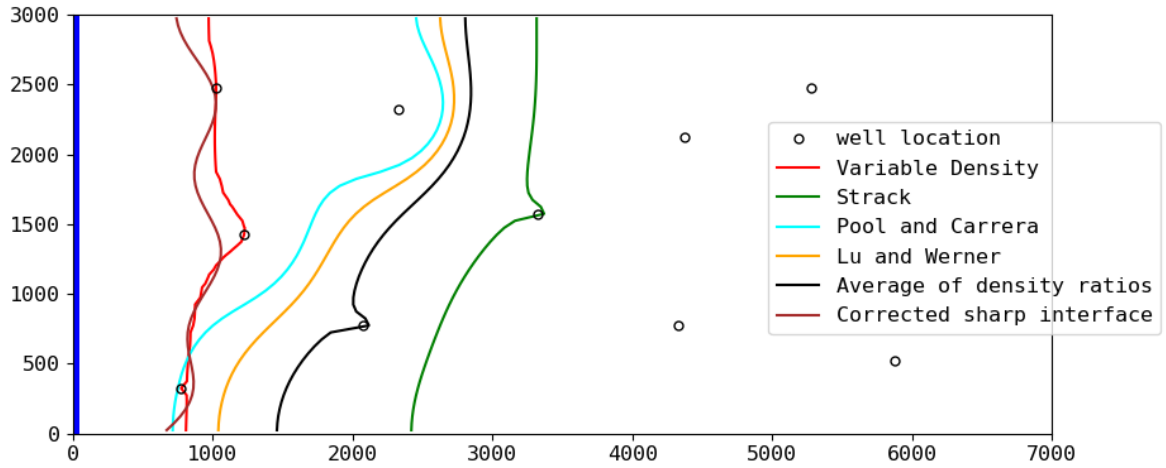

Figure 1. Location of the SWI extent, based on the examined surrogate models.

Acknowledgments: This paper is supported by the European Union Funded project euPOLIS "Integrated NBS-based Urban Planning Methodology for Enhancing the Health and Well-being of Citizens: the euPOLIS Approach" under the Horizon 2020 program H2020-EU.3.5.2., grant agreement No 869448. Also, this work was supported by computational time granted from the National Infrastructures for Research and Technology S.A. (GRNET) in the National HPC facility ARIS- under project ID pa211104 (MLGM).

References

Christelis V, Mantoglou A (2016) Pumping optimization of coastal aquifers assisted by adaptive metamodelling methods and radial basis functions. Water Resources Management 30(15): 5845-5859

Christelis V, Mantoglou A (2019) Pumping optimization of coastal aquifers using seawater intrusion models of variable-fidelity and evolutionary algorithms. Water Resources Management 33: 555-568

Kopsiaftis G, Protopapadakis E, Voulodimos A, Doulamis N, Mantoglou A (2019) Gaussian process regression tuned by bayesian optimization for seawater intrusion prediction. Computational Intelligence and Neuroscience 2019: 2859429

Kopsiaftis G, Christelis V, Mantoglou A (2019) Comparison of sharp interface to variable density models in pumping optimisation of coastal aquifers. Water Resources Management 33: 1397-1409

Kourakos G, Mantoglou A (2009) Pumping optimization of coastal aquifers based on evolutionary algorithms and surrogate modular neural network models. Advances in Water Resources 32(4): 507-521

Mantoglou A, Papantoniou M, Giannoulopoulos P (2004) Management of coastal aquifers based on nonlinear optimization and evolutionary algorithms. J Hydrol 297: 209–228

Pool M, Carrera J (2011) A correction factor to account for mixing in Ghyben-Herzberg and critical pumping rate approximations of seawater intrusion in coastal aquifers. Water Resources Research 47(5): W05506

Strack ODL (1976) A single-potential solution for regional interface problems in coastal aquifers. Water Resources Research 12: 1165–1174

Werner AD (2017) Correction factor to account for dispersion in sharp-interface models of terrestrial freshwater lenses and active seawater intrusion. Advances in Water Resources 102: 45-52

Assessment of groundwater vulnerability to agricultural pollution in River Lissos Coastal Aquifer System, NE Greece

V. Karahontzitis[1*], A. Papadopoulou[1], I. Gkiougkis[1], A. Kallioras[2], A. Panagopoulos[3], F.-K. Pliakas[1]
[1] Democritus University of Thrace, Department of Civil Engineering, 67100 Xanthi, Greece
[2] School of Mining and Metallurgical Engineering, National Technical University of Athens, 15773, Athens, Greece
[3] Hellenic Agricultural Organisation, Soil and Water Resources Institute, 57400 Sindos, Greece
* e-mail: vasiliskarachontzitis@gmail.com

Introduction

DRASTIC is a vulnerability assessment method that is introduced by the US Environmental Protection Agency (US EPA) (Aller et al. 1987) and a wide range of applicability of this environmental assessment tool is recorded in the literature (Sener et al. 2009). DRASTIC specifically involves the investigation of aquifer vulnerability with respect to nitrate loads, as a diffuse source of contamination from the surface area of the hydrogeological domain. Margane (2003) states that DRASTIC method is a popular approach to groundwater vulnerability assessments because it is relatively inexpensive, straightforward, and uses data that are commonly available or estimated. Pedreira et al. (2015) mention that DRASTIC final product is addressed to decision makers, administrators and authorities to support the assessment of the groundwater vulnerability to different sources of contamination. This paper refers to the assessment of groundwater vulnerability to agricultural pollution in River Lissos coastal aquifer system in NE Greece, resulted from the application of DRASTIC vulnerability method.

Materials and methods

The study area (Figure 1) involves a coastal catchment with an unconsolidated aquifer system, that is heavily exploited for agricultural activities. The geological setting of the study area mainly involves recent alluvial deposits from Lissos River hydrographic network, that overlay Neogene deposits or Paleogene deposits of Rhodope massif. The main irrigation activities are related to extensive cotton production throughout the entire aquifer, whereas groundwater salinization conditions within the southern part of the aquifer have also limited such agricultural activities (Pliakas et al. 2007). The aquifer system of the study area contains clay materials and appears in the form of successive layers composed of clay-sands and sands with a width ranging from 1 to 10 m, with many interferences of clay layers (Kallioras et al. 2011).

DRASTIC acronym is formed from a combination of seven (7) hydrogeological parameters: Depth to groundwater (D), net Recharge (R), Aquifer media (A), soil media (S), topography (T), influence of the vadose zone (I); and hydraulic Conductivity (C). The linear additive combination of the above parameters with the ratings and weights, is used to calculate the DRASTIC Vulnerability Index (DVI) as given below (Aller et al. 1987; Sener et al. 2009):

$$DVI = DrDw + RrRw + ArAw + SrSw + TrTw + IrIw + CrCw \quad (1)$$

where r is the rating for corresponding ranges and w the weight for each parameter.

Results and concluding remarks

Groundwater vulnerability indices are proved a valuable tool for assessing the vulnerability of groundwater aquifers to different types of contamination. Most of the cases involve the investigation of agricultural areas, focusing on the intrinsic vulnerability of the system to nitrate contamination from diffuse sources. In this area, a significant number of vulnerability indices are available, that can be modified to fit better the local conditions of each study site. The main argument against the application of vulnerability indices is the subjectiveness when it comes to assigning rating values in the model; however, they are widely accepted as an effective scientific tool for the assessment of vulnerability of groundwater aquifers.

The hydrogeological research included the analysis and interpretation of DRASTIC vulnerability indices with respect to the spatial distribution of nitrate (NO_3^-) concentration values. The typical and pesticide vulnerability indices were calculated for April 2017 and 2018, and October 2017 and 2018, while eight (8) relevant vulnerability maps were designed presenting the typical (T) and pesticide (P) DRASTIC groundwater vulnerability indices (DVI) distribution during April and October 2017, 2018. Five (5) vulnerability zones are presented in these maps (DVI values: < 100, 100-120, 120-140, 140-160, >160) showing the high vulnerability zones located in the NE part of the study area (Figure 1).

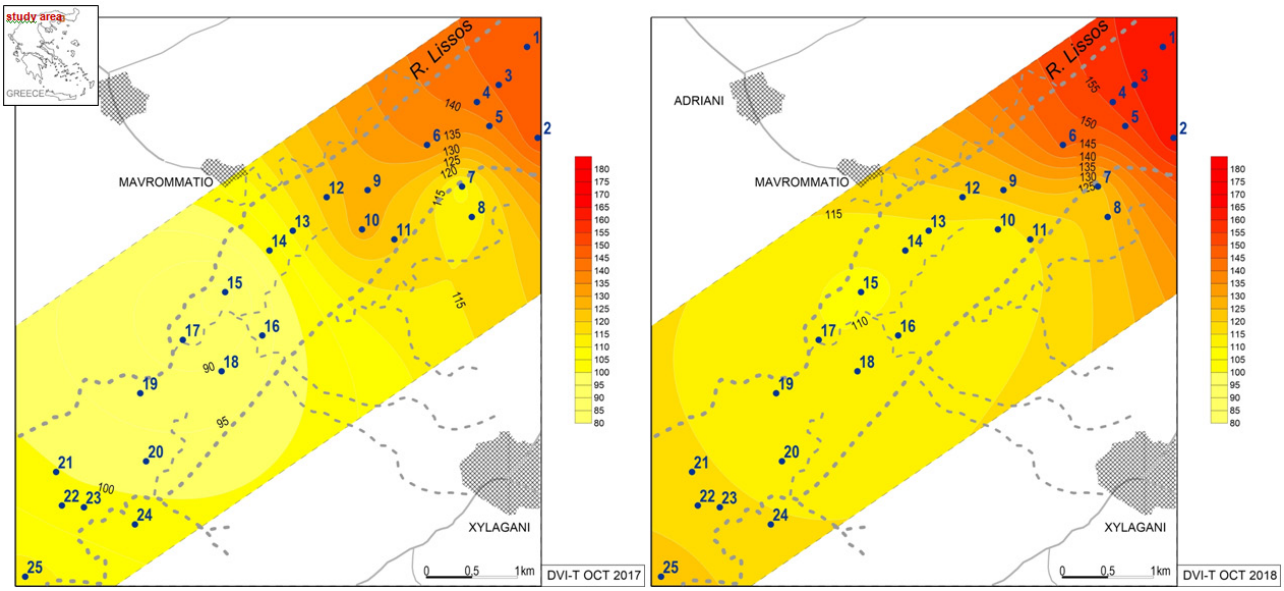

Figure 1. Selected typical (T) DRASTIC groundwater vulnerability indices (DVI) maps (October 2017, 2018).

From the comparison of the present research with relevant research works during the years 2006, 2015 (Eminoglou et al. 2017), which have preceded in the study area, the gradual groundwater quality degradation from 2006 to 2021 is evident. This finding is also reflected in the respective DVI maps of the corresponding years.

The designed DVI maps can contribute to the planning of actions and interventions by water users, stakeholders and the state, for the rational management and protection of groundwater resources in the study area.

References

Aller L, Bennett T, Lehr JH, Petty RJ, Hackett G (1987) DRASTIC: a standardized system for evaluating ground water pollution potential using hydrogeologic settings. EPA-600/2-87-035, EPA, Washington, DC

Eminoglou G, Gkiougkis I, Kallioras A, Pliakas FK (2017) Updated groundwater vulnerability evaluation at a coastal aquifer system in NE Greece. European Water, E.W. Publications, 57: 423-428

Kallioras A, Pliakas F, Skias S, Gkiougkis I (2011) Groundwater vulnerability assessment at SW Rhodope aquifer system in NE Greece. Advances in the Research of Aquatic Environment, Environmental Earth Sciences 2: 351-358

Margane A (2003) Guideline for Groundwater Vulnerability Mapping and Risk Assessment for the Susceptibility of Groundwater Resources to Contamination. Technical Cooperation Project Management, Protection and Sustainable Use of Groundwater and Soil Resources in the Arab Region. Technical Cooperation no: 1996.2189.7. ACSAD Damascus, BGR Hannover, 184 p.

Pedreira R, Kallioras A, Pliakas F, Gkiougkis I, Schuth C (2015) Groundwater vulnerability assessment of a coastal aquifer system at River Nestos eastern Delta, NE Greece, Environmental Earth Sciences 73: 6387–6415

Pliakas F, Mouzaliotis A, Kallioras A, Diamantis I (2007) Hydrogeological assessment of the salinization problem of Xilagani – Imeros aquifer system in SW plain area of Rhodope Prefecture, Greece. In: Proceedings of the 11th International Conference of the Geological Society of Greece, 24 - 26/5/2007, Athens, Greece, 2: 536-547

Sener E, Sener S, Davraz A (2009) Assessment of aquifer vulnerability based on GIS and DRASTIC methods: a case study of the Senirkent-Uluborlu Basin (Isparta, Turkey). Hydrogeology J. 17: 2023–2035

Estimating groundwater recharge from precipitation in a coastal Mediterranean aquifer: The case of Marathon

M. Perdikaki*, A. Kallioras
School of Mining and Metallurgical Engineering, National Technical University of Athens, Athens, Greece
** e-mail: mperdikaki@metal.ntua.gr*

Introduction

Understanding the mechanism of natural recharge in aquifers is necessary for effective groundwater management, especially in arid and semi-arid regions such as the Mediterranean, where dry summers make groundwater a valuable freshwater resource (Moeck et al. 2020). Amongst other sources, direct recharge from precipitation is a significant inflow of freshwater in unconfined aquifers (Perdikaki et al. 2022). Numerous methods for calculating inflow from precipitation have been developed and applied from various researchers throughout the years (e.g. Gumuła-Kawęcka et al. 2022; Hamdi et al. 2020; Şen 2019).

In this research, different hydrological methods were employed in order to calculate the remaining water from precipitation that percolates into the saturated zone. The case study is a typical Mediterranean coastal aquifer located in Mararathon plain, Greece. The proposed methodology targets to identify the hydrological balance of the area, the timeframe of groundwater recharge and the lag time between precipitation and groundwater recharge.

Materials and methods

The coastal aquifer of the study is located in Marathon plain, at the NE of Attica, Greece. The weather conditions in the area are characterised by mild winters and dry and hot summers. The mean annual precipitation is around 500 mm while the annual temperature ranges between -1.8 °C in the winter up to 43 °C during summer time (http://penteli.meteo.gr/stations/neamakri/). The hydrogeological system is formed in a multilevel aquifer of an alluvial unit and an underline karstic formation. The proposed methodological framework, was applied in the upper unconsolidated formation.

Daily precipitation (P) and weather data were obtained from a meteorological station that is located at Marathon plain. To estimate rainfall excess (RE), Soil Conservation Service Curve Number (SCS-CN) approach (Mckeever et al. 1972) was used. Potential evapotranspiration (PET) was calculated with the Penman-Monteith method (Allen 2005) while the Soil Moisture Balance (SMB) (Thornthwaite and Mather 1957) method was then utilized to estimate the Actual Evapotranspiration (SMB). Finally, infiltration (I) and percolation (R_n) were estimated as part of the hydrologic balance, considering specific water capacity of the soil (S_B). The methods and/or the equation that was utilized for each component are summarized in Table 1.

Table 1. Components of hydrologic balance.

Hydrologic balance component	Method/ equation
RE	SCS-CN
PET	Penman-Monteith
AET	SMB
I	P-RE-AET
RE	$I-S_B$

Results and concluding remarks

Marathon hydrologic balance was computed for five hydrologic years (2015-2020) on a daily timestep. Figure 1 presents indicative results for the hydrologic year 2019-2020. The annual cumulative volumes for the specific hydrologic year are: 658 mm of precipitation (P), 141.41 mm of rainfall excess (RE), 408 mm of

actual evapotranspiration (AET) and 62.2 mm of percolation (Rn).

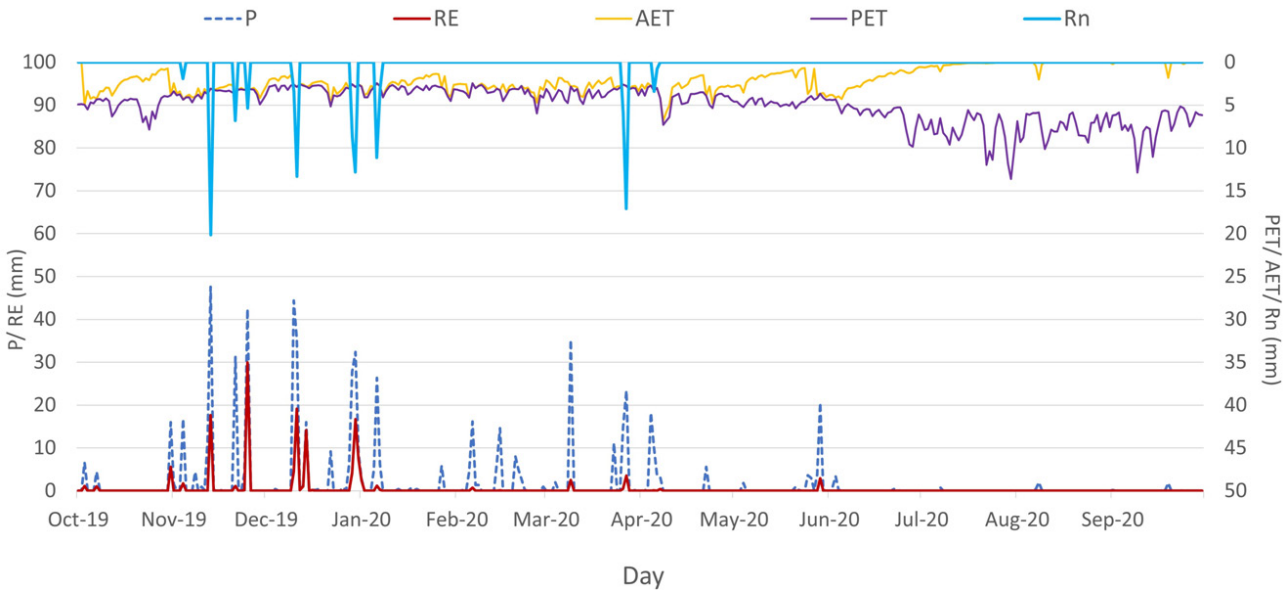

Figure 1. Water balance of 2019-2020 hydrologic year for the alluvial aquifer of Marathon.

The results of the research indicated that for the alluvial aquifer of Marathon:

- Natural recharge mainly occurs after several consecutive days of rainfall, when the unsaturated zone reaches the maximum water capacity;
- The maximum percolation volume occurs from November to April, as the storm events are more frequent;
- During the dry period natural recharge from precipitation does not occur. The limited rainfall events in conjunction with high temperatures and dry weather results in evaporation of rainwater and partially infiltration in the unsaturated zone.

References

Allen R (2005) Penman–Monteith equation. Encyclopedia of Soils in the Environment. Elsevier, pp 180–188

Gumuła-Kawęcka A, Jaworska-Szulc B, Szymkiewicz A et al. (2022) Estimation of groundwater recharge in a shallow sandy aquifer using unsaturated zone modeling and water table fluctuation method. Journal of Hydrology 605: 127283. https://doi.org/10.1016/J.JHYDROL.2021.127283

Hamdi M, Goïta K, Jerbi H, Zagrarni M (2020) Modeling of the natural groundwater recharge under climate change: Sisseb El Alem Nadhour Saouaf basin (Central Tunisia) case study. Environmental Earth Science 79: 285. https://doi.org/10.1007/s12665-020-09010-6

Mckeever V, Owen W, Rallison R, Engineers H (1972) National engineering handbook section 4 - Hydrology. Soil Conservation Service

Moeck C, Grech-Cumbo N, Podgorski J, Bretzler A, Gurdak JJ, Berg M, Schirmer M (2020) A global-scale dataset of direct natural groundwater recharge rates: A review of variables, processes and relationships. Science of Total Environment 717: 137042. https://doi.org/10.1016/j.scitotenv.2020.137042

Perdikaki M, Makropoulos C, Kallioras A (2022) Participatory groundwater modeling for managed aquifer recharge as a tool for water resources management of a coastal aquifer in Greece. Hydrogeology Journal 30: 37–58. https://doi.org/10.1007/s10040-021-02427-8

Şen Z (2019) Groundwater Recharge Level Estimation from Rainfall Record Probability Match Methodology. Earth Systems and Environment 3: 603–612. https://doi.org/10.1007/S41748-019-00130-Z/FIGURES/9

Thornthwaite CW, Mather JR (1957) Instructions and Tables for Computing Potential Evapotranspiration and the Water Balance. Drexel Institute of Technology. Publications of Climatology, New Jersey

Pollution risk assessment and vulnerability of aquifer due to nitrates using the DRASTIC LU and Canter LU methods in Almyros, Thessaly, Greece

S. Lepuri[1*], A. Loukas[1], A. Lyra[2]
[1] School of Rural and Surveying Engineering, Aristotle University of Thessaloniki, Thessaloniki, Greece
[2] Department of Civil Engineering, School of Engineering, University of Thessaly, Volos, Greece
* e-mail: sibiankalepuri@gmail.com

Introduction

The paper evaluates the aquifer pollution risk and vulnerability due to nitrates using the DRASTIC LU and Canter LU methods in the rural and coastal Almyros basin, Thessaly, Greece. Unsustainable groundwater abstractions for irrigation, as well as high nitrates concentrations owing to overfertilization, have degraded the quality and quantity of the Almyros aquifer system. The DRASTIC and Canter methods have been modified by adding the parameter of land use and the assessment was carried out for three different time periods (Lepuri 2021).

Materials and methods

The aquifer pollution risk assessment and vulnerability has been assessed for the periods 1992-1997, 2004-2009, 2010-2015 using the typical DRASTIC index method (Aller et al. 1987; Kazakis and Voudouris 2015) and the Canter index method (Canter 1997) by adding the parameter of land use (Lepuri 2021). The rating and the weight of the parameter of land use have been evaluated according to bibliography (Kazakis and Voudouris 2015) for the three different time periods. The calculations of both modified indices have been conducted by using GIS tools. The maps were reclassified into five classes (Very low to Very high) by using the geometrical interval method. The results have also been validated against observed nitrates concentrations using the Pearson 's correlation analysis (Lepuri 2021).

Results and concluding remarks

The results for the DRASTIC LU and Canter LU indices are presented in Table 1 for the period 1992-2015. High and very high risk cumulative values are observed that occur for a large percentage of the aquifer area, i.e. 38.5% and 41.6% for the DRASTIC LU and the Canter LU index, respectively. The average vulnerability values of the indices show a small difference between them of the order of 3.7%. Low and very low risk cumulative values occupy a percentage of 40.46% and 33.63% for DRASTIC LU and Canter LU, respectively.

Table 1. Percent area (%) for each risk class estimated with DRASTIC LU and Canter Lu for the period 1992-2015.

Risk Classes	DRASTIC LU	Canter LU
Very high	14.2	14.3
High	24.3	27.3
Medium	20.9	24.6
Low	23.5	10.9
Very Low	16.9	22.7

In both methods, an increased risk of pollution was observed in the periods 1992-1997 and 2010-2015 as compared to the period 2004-2009, due to the change in land uses, the low recharge of these periods and the change in the depth of the unsaturated zone. Specifically, there was a replacement of the vineyard cropland, based on Corine 1990, with cultivation of olive groves and other irrigated crops, and an increase in the depth of the unsaturated zone was observed in the years of 2006, 2007 and 2008. In the period of 2010-2015, a decrease in the depth of the unsaturated zone was observed, which in combination with the already existing land uses, led to very high and high risk scores for the aquifer. The spatial distribution of

the pollution risk assessment is presented in Figure 1.

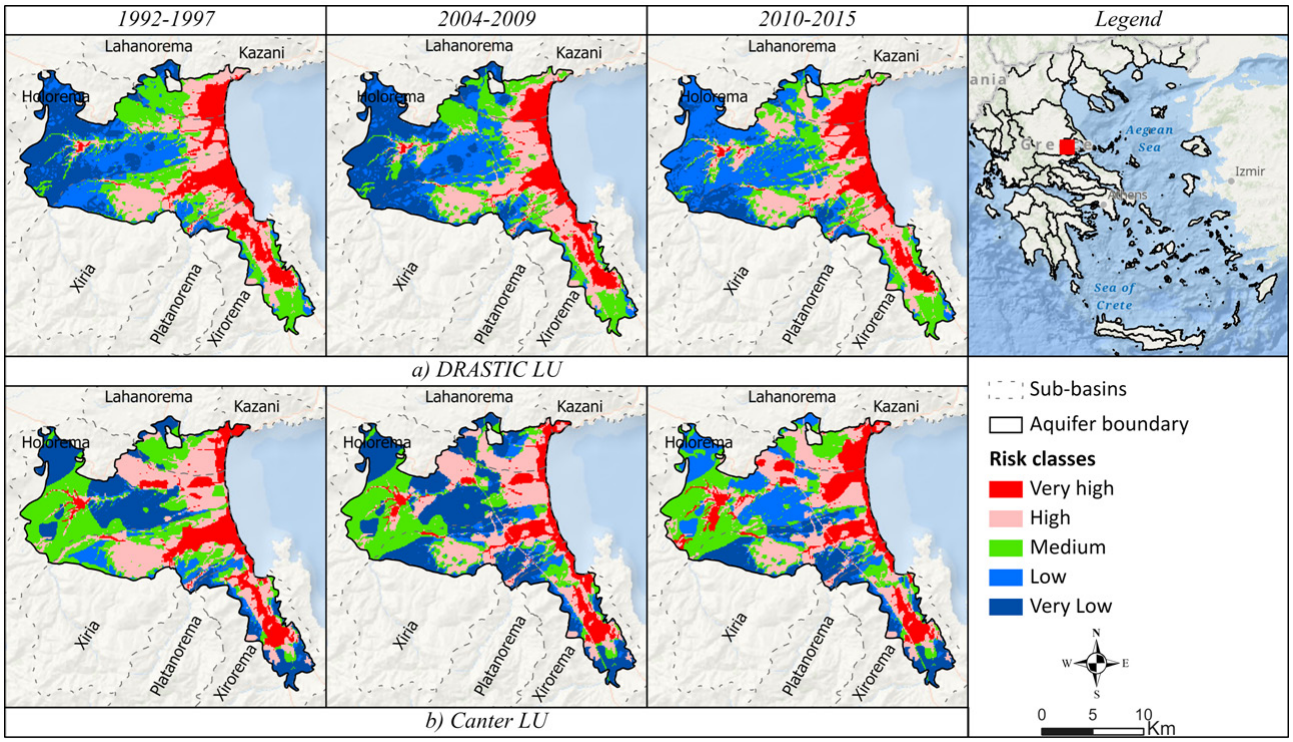

Figure 1. The spatial distribution of the pollution risk estimated with DRASTIC LU and Canter LU for the periods 1992-1997, 2004-2009 and 2010-2015.

According to Figure 1, the risk for the aquifer for the periods of 1992-1997, 2004-2009 and 2010-2015, ranges from very low to very high risk. The very high and high values, for all studied periods, appear in the NE area of the aquifer, i.e. the Lahanorema sub-basin, the coastal area of the aquifer, and the central part of the Xiria sub-basin, and also in the SE of the aquifer, in the Xirorema sub-basin. The above indices were evaluated based on the correlation with the observed nitrate concentrations in 74 observation wells, distributed all over the aquifer area. The observed nitrate concentrations were checked for their normality, and the application of the Pearson correlation test indicated that the DRASTIC LU index shows a strong positive correlation for all three studied periods 1992-1997 (r=0.57), 2004-2009 (r=0.70) and 2010-2015 (r=0.71) for p=0.000. The Pearson correlation test for the Canter LU index shows small to moderate correlations for the three studied periods (i.e. r=0.37, r=0.43 and r=0.36, respectively). These results show that the nitrate pollution risk and vulnerability is better indicated by the DRASTIC LU index than the Canter LU index.

References

Aller L, Bennet T, Lehr JH, Petty RJ, Hackett G (1987) DRASTIC: a standardized system for evaluating ground water pollution potential using hydrogeologic settings. Robert S. Kerr Environmental Research Laboratory, Office of Research and Development, US Environmental Protection Agency, Ada, Oklahoma

Canter LW (1997) Nitrates in Groundwater. 1st ed., Lewis Publishers, Florida, USA

Kazakis N, Voudouris S (2015) Groundwater vulnerability and pollution risk assessment of porous aquifers to nitrate: Modifying the DRASTIC method using quantitative parameters. Journal of Hydrology 525: 13-25. https://doi.org/10.1016/j.jhydrol.2015.03.035

Lepuri S (2021) Vulnerability of aquifers of agricultural and coastal basins due to nitrate pollution and sea water intrusion. The case of Almyros basin, Magnesia, Greece. MSc Thesis, P.M.S. "Water Resources", School of Rural and Surveying Engineering, Aristotle University of Thessaloniki, Thessaloniki (In Greek). https://doi.org/10.26262/heal.auth.ir.336336

SEAWAT application to implement the climates change induced impacts and responses of the Neretva coastal aquifer system in the south-eastern Croatia

I. Aljinović*, V. Srzić
Faculty of Civil Engineering, Architecture and Geodesy, University of Split, Matice hrvatske 15, 21000 Split, Croatia
** e-mail: iva.matic@gradst.hr*

Introduction

Seawater intrusion has been evidenced as a threat in many agricultural areas along the coastal areas worldwide. Besides the reduction in ground and surface water quality due to salinization, one of the utmost negative effects caused by seawater intrusion, is a reduction of the agricultural crops' yields and consequently reduced income.

Neretva coastal aquifer system is a 4500 ha low-lying agricultural area in south-eastern Croatia with a melioration infrastructure implemented during the 1960s and 1970s. Due to the fact that the average ground level is found below the mean sea level, this coastal system is subjected to active seawater intrusion which results in total groundwater column salinization including the pedological layer. Climate change projections imply the increase of the Adriatic Sea level, the reduction of the precipitation rate, and the increase of the characteristic air temperature at the area of interest. All the aforementioned factors contribute to more extreme conditions enhancing the seawater intrusion effects. To mimic the natural conditions, we establish a 3D variable density flow and transport model as a main tool to perform water management within the Neretva coastal aquifer system. The latter implies the calibration and the validation of the model which is used as a tool to mimic the conditions induced by climate change. Finally, several mitigation measures either to prevent or minimise the seawater intrusion effects have been implemented and tested for their efficiency.

Materials and methods

Geological settings of the Neretva coastal aquifer system have been derived from available datasets obtained through extensive fieldwork coupled with geotechnical boreholes up to 125 m depth, ERT, geoelectrical sounding, seismic reflection, and tidal methods application (Srzić et al. 2020). During the borehole performance, cores have been taken and analysed in the laboratory to determine effective porosity and hydraulic conductivity values. In this way, the litho-stratigraphic definition of the model domain has been set up (Figure 1).

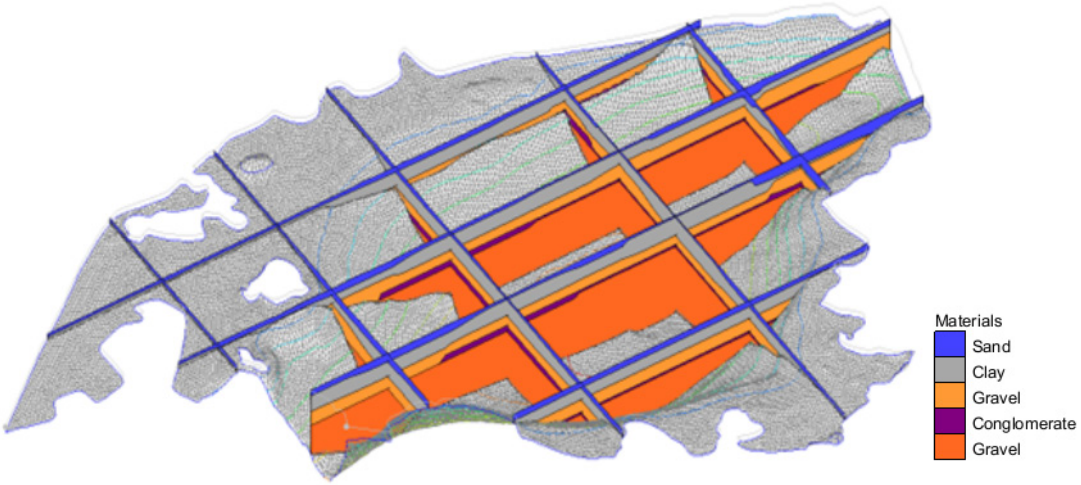

Figure 1. Geological setting of the Neretva river coastal aquifer system.

Available time series of both sea level and river Neretva surface elevation have been used as the transient flow Dirichlet boundary conditions with a 1-hour time step. Boundary condition at the sea side has been set as a Dirichlet one corresponding to the salinity concentration as observed from the sea offshore from the model domain. River Neretva represents a boundary condition separately for the rain and dry period. During the rainy season, increased recharge reflects the sea water cline diminishing from river Neretva bed thus creating a freshwater boundary. opposite is implemented during the dry season, usually taking place from late April mid-October.

SEAWAT model simulations are initially run to obtain the steady state flow which enables the initial condition for the transport steady state simulation. After the convergence of the transport steady state simulation, the transient coupled flow and transport simulations are set up to get insight into the transient nature of the groundwater salinity along the study area. The flow calibration has been performed based on the time series from the monitoring system (Lovrinović et al. 2021) for: i) groundwater head data sets obtained from the shallow unconfined aquifer, ii) groundwater head data sets obtained from the deep confined aquifer, iii) surface water elevation data sets obtained from the pumping stations intake basins and melioration channels. The similar process has been followed to calibrate the transport component where salinity time series from the aquifer geological units were used (Lovrinović et al. 2022).

Climate change induced changes are successfully implemented by changing the mean sea level and the precipitation rates. In accordance with the national long-term water management level, a barrier has been planned and implemented into the model within the river Neretva bed, 6.5 km upstream from the Neretva River's mouth, to prevent the seawater from penetrating upstream. This mitigation measure has been tested separately and in combination with a 5 km long recharge channel located along the left bank of Neretva river.

Results and concluding remarks

The results of the flow simulation demonstrate successful calibration performance. Hereby, the dominant groundwater flow direction has been identified from the inland to the Adriatic Sea. The model emphasizes the presence of active seawater intrusion close to the shore and significantly stratified groundwater salinity along the central area of the model domain.

Implementation of the climate changes into the model highlights the global increase in groundwater salinity. The Neretva River barrier disables the seawater intrusion upstream from the barrier, which consequently leads to the improvement of the Neretva River's water quality upstream from the barrier. The increase of the surface water elevation upstream hereby enhances the recharge of the aquifer system with freshwater. Implementation of the recharge channel along the left bank of Neretva River significantly contributes to the improvement of both surface and groundwater in the Neretva Valley.

Acknowledgments: This research is funded by the contribution from the EU co-financing and the Interreg Italy-Croatia CBC Programme 2014–2020 Restricted call (Priority Axes: Safety and Resilience) through the European Regional Development Fund as a part of project Saltwater intrusion and climate change: monitoring, countermeasures and informed governance (SeCure) (PID: 10419304).

References

Srzić V, Lovrinović I, Racetin I, Pletikosić F (2020) Hydrogeological Characterization of Coastal Aquifer on the Basis of Observed Sea Level and Groundwater Level Fluctuations : Neretva Valley Aquifer, Croatia. Water (Switzerland) 12, 348. https://doi.org/10.3390/w12020348

Lovrinović, I, Bergamasco, A, Srzić, V, Cavallina, C, Holjević, D, Donnici, S, Erceg, J, Zaggia, L, Tosi, L (2021) Groundwater Monitoring Systems to Understand Sea Water Intrusion Dynamics in the Mediterranean: The Neretva Valley and the Southern Venice Coastal Aquifers Case Studies. Water 13(4): 561. https://doi.org/10.3390/w13040561

Lovrinović, I, Srzić, V, Matić, I, Brkić, M (2022) Combined Multilevel Monitoring and Wavelet Transform Analysis Approach for the Inspection of Ground and Surface Water Dynamics in Shallow Coastal Aquifer. Water 14(4): 656. https://doi.org/10.3390/w14040656

Assessment of the hydrochemical status through the application of AkvaGIS tool for an alluvial aquifer in Greece

K.S. Panagiotaropoulos*, M. Perdikaki, C. Pouliaris, A. Kallioras
School of Mining & Metllurgical Enginnering, National Technical Univercity of Athens, Athens, Greece
** e-mail: kostaspan96@yahoo.gr*

Introduction

Groundwater is a valuable source of freshwater in agriculture, especially in arid/semi-arid areas where surface water is limited during dry season. Optimal management of groundwater in rural areas involves the knowledge and assessment of the hydrochemical status of the aquifer. To evaluate the hydrochemical regime for irrigation purposes, different methods have been proposed in past and recent studies (e.g. Ma et al. 2022).

This study presents the interpretation of groundwater samples hydrochemical analysis through a graphical approach in order to assess the quality of groundwater in a coastal rural area in Greece. The analysis conducted through AkvaGIS tool that is utilized for the analysis of groundwater quality datasets (Perdikaki et al. 2022). The results indicated a good groundwater quality status in the area of interest.

Materials and methods

The study area, Arta plain, is located in Epirus region, at the west part of Greece and it is an area of about 270 km^2. At its biggest extent, the plain is occupied by agricultural irrigated land. The rivers Louros and Arachthos in the area, provide water to an extensive irrigation network, while part of the irrigation demands is satisfied through numerous drills throughout the plain. The most important hydrogeological unit in the area is a system of superimposed alluvial aquifers of great thickness (more than 200 m) while at the biggest part of the plain artesian conditions is recorded (Pouliaris et al. 2022).

Several sampling campaigns have been conducted throughout the plain since 2020. For the purpose of the present study, the results of October 2022 (including 37 samples), are analyzed through the application of AkvaGIS tool which is integrated in the FREEWAT platform (Rossetto et al. 2018; http://www.freewat.eu/). The main goal of AkvaGIS module is to manage groundwater quality parameters. It is used to analyze, interpret, compare, and visualize hydrochemical measurements in a free GIS environment (QGIS). Firstly, the data are stored in SQL database and then several hydrochemical spatial queries can be created. The main use of hydrochemical queries is to create hydrochemical diagrams (i.e. piper, SAR, SBD plots), hydrochemical parameter time plots for a specific sample in different campaigns, chemical ions balance report and chemical parameter map of a specific parameter.

Results and concluding remarks

Application of AkvaGIS tool in Arta plain was proved valuable for the interpretation of hydrochemical analysis results of October 2022 campaign. Figure 1 and Figure 2 present Piper and SAR plot respectively.

The analysis of the plots is summarised in the following conclusions:

- High concentration of Ca^{+2} and HCO_3 in most of the samples indicate that there is inflow of water from the adjacent karstic aquifer of the area to the alluvial unit.
- Absorption Ratio (SAR) index is medium (S2) for the majority of the samples and high for only a few samples, indicating a good quality of irrigation water in general.
- The majority of samples have a relatively low Electrical Conductivity (EC<1000 μS/cm).
- The irrigation network of Louros and Arachthos have provided a better groundwater quality in the area, since the aquifer system is not overexploited.

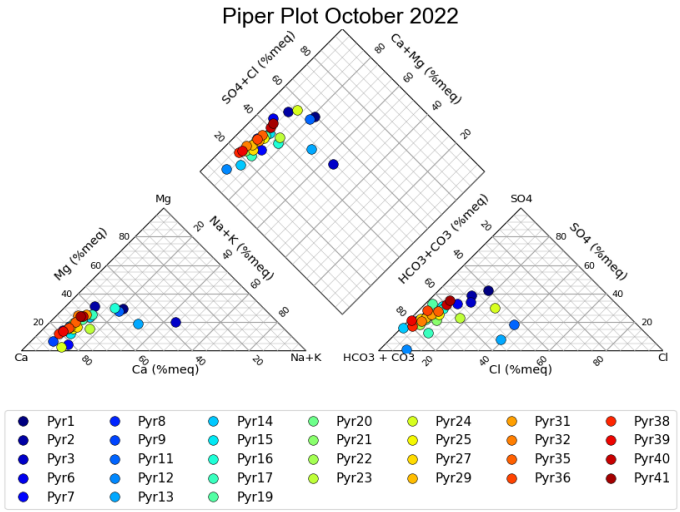

Figure 1. Piper plot for Arta plain groundwater samples (October 2022).

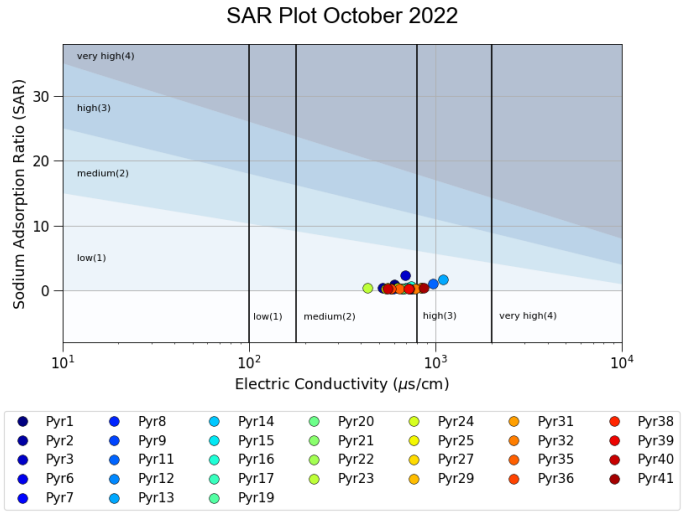

Figure 2. SAR plot for Arta plain groundwater samples (October 2022).

Acknowledgments: We acknowledge support of this work by the project “e-Pyrros: Development of an integrated monitoring network for hydro-environmental parameters within the hydro-systems of Louros-Arachthos-Amvrakikos for the optimal management and improvement of agricultural production” (MIS 5047059) which is implemented under the Action “Reinforcement of the Research and Innovation Infrastructure”, funded by the Operational Programme "Competitiveness, Entrepreneurship and Innovation" (NSRF 2014-2020) and co-financed by Greece and the European Union (European Regional Development Fund).

References

Rossetto R, De Filippis G, Borsi I, Foglia L, Cannata M, Criollo R, Vázquez-Suñé E (2018) Integrating free and open source tools and distributed modelling codes in GIS environment for data-based groundwater management. Environmental Modelling and Software 107: 210–230. https://doi.org/10.1016/j.envsoft.2018.06.007

Ma J, Chen S, Ding D, Zhao J (2022) Hydrochemical characteristics and groundwater quality appraisal for irrigation uses in the Lan-gan region, Northern Anhui Province, East China. Water Supply 22: 686–696. https://doi.org/10.2166/ws.2021.241

Perdikaki M, Manjarrez RC, Pouliaris C, Rossetto R, Kallioras A (2020) Free and open-source GIS-integrated hydrogeological analysis tool: an application for coastal aquifer systems. Environmental Earth Sciences 79: 348. https://doi.org/10.1007/S12665-020-09092-2

Pouliaris C, Chrysanthopoulos E, Myriounis C, Markantonis K, Kallioras A (2022) Identification of artesian aquifer characteristics in Greece: the case of Arta plain, Epirus. In: 12th International Hydrogeological Congress of Greece and Cyprus, Nicosia, Cyprus

Hydrological modelling of a fractured volcanic aquifer for understanding the role of climate and anthropic uses of water resources on the natural system

M. Silipigni[1], I. Borzì[1*], C. Di Salvo[2], E. Preziosi[3], B. Bonaccorso[1]
[1] Department of Engineering, University of Messina, Italy
[2] Institute of Environmental Geology and Geoengineering, National Research Council, Rome, Italy
[3] Water Research Institute, National Research Council, Rome, Italy
* e-mail: iolanda.borzi@unime.it

Introduction

Groundwater resources represent the largest reservoir of fresh water in the world. At the European level, about 75% of EU inhabitants depend on groundwater for drinking water supply; besides, groundwater resources represent an important source for industry and agriculture (EC 2000).

Groundwater overuse and depletion, especially in arid and semiarid regions, are already causing irreversible environmental damage; in addition, groundwater recharges are threatened by climate change. To this end, it is extremely important to understand the aquifer response to climate drivers and anthropogenic activities by means of appropriate modelling tools.

The Alcantara River Basin is in North-Eastern Sicily (Italy), encompassing the north side of Etna Mountain, the tallest active volcano in Europe (Borzì 2019, 2020). On the right-hand side of the river, the mountain area is characterized by volcanic rocks with a very high infiltration rate. Here, precipitation and snow melting feed a large aquifer whose groundwater springs at the mid/downstream of the Alcantara river, mixing with surface water and contributing to the river baseflow also during the dry season. In the upstream, a maximum of 520 l/s are extracted for municipal use through wells and an infiltration gallery supplying the Alcantara Aqueduct.

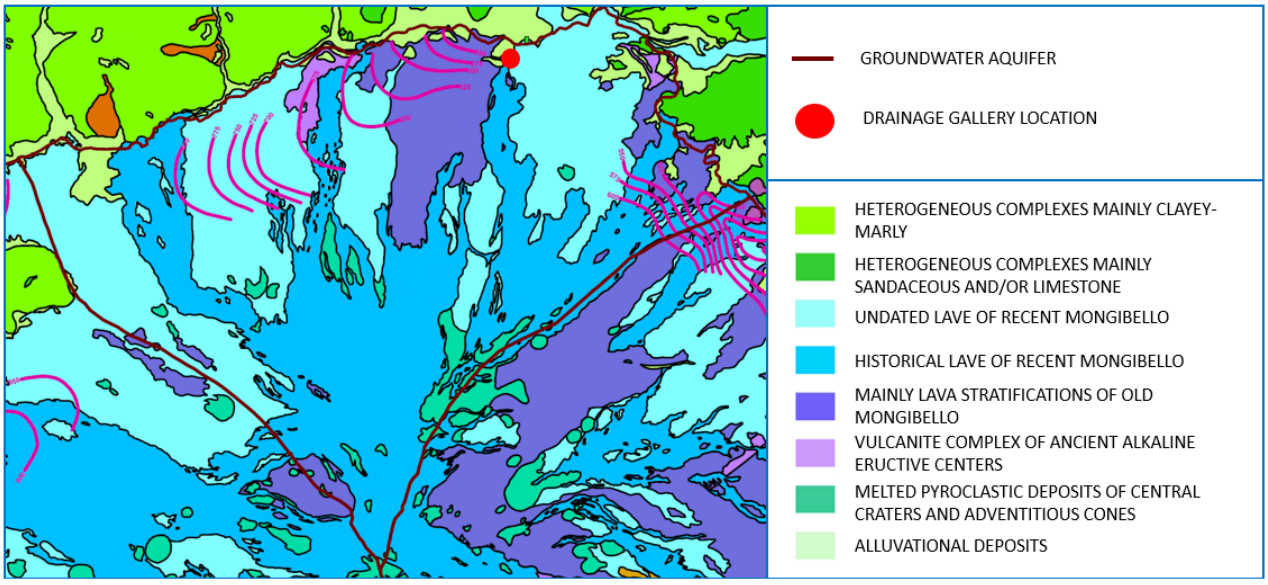

Figure 1. Groundwater aquifer, drainage gallery ubication and terrain characteristics.

Recently the river has suffered a significant decrease in spring discharge. In particular, in summer 2020 and 2021, the Alcantara river suffered a prolonged dry phenomenon in the middle-valley stretch with a serious loss of fish fauna, due to significant spring depletion along the stream most likely determined by a meteorological drought.

The main object of this study is then to understand the respective role of climate variability and groundwater withdrawal on the river flow regime and its impacts on the connected ecosystem.

Materials and methods

The aquifer has been modelled by MODFLOW 6, a USGS software (Harbaugh 2005) which implements a finite-difference numerical model, and its graphical interface MODELMUSE (Winston 2009). In Figure 1 the no-flow boundaries of the aquifer are shown.

Through the numerical model, changes in the groundwater level and in the interconnection between surface and groundwater can be evaluated for two different scenarios: 1) the current condition of the aquifer system under groundwater extraction and 2) a theoretical scenario with no groundwater extraction. Comparison between the two scenarios allows to understand impacts of groundwater extractions on water tables and spring discharges, and consequently to attribute recent dry phenomenon to anthropogenic uses, climate changes or both.

The model recharge in terms of net precipitation and snowmelt was estimated at the monthly time step using data from 2009 to 2021.

The model was calibrated in steady state mode by comparing simulated and observed water heads as well as the groundwater budget. Model calibration shows an MSE value of 0,02 and a R^2 value of 0,38 Then the simulation was run in transient mode at the monthly time step for the period 2014–2021. A delay of about 4 months in the monthly recharge was necessary to best represent the observed discharge of the infiltration gallery. Also, a warmup of 19 cycles of 13 years was necessary to ensure model convergence and independence with respect to initial conditions.

Results and concluding remarks

Results from comparison between the two above mentioned scenario highlights influences of groundwater extraction from drainage gallery on natural spring discharge. In particular, spring discharge simulated in the real configuration shows a reduction between 12,9% and 16,8% with respect to the spring discharge values simulated in absence of drainage gallery. Figure 2 shows the influence of drainage gallery (i.e. groundwater withdrawal) on natural spring discharge, in percentage. This value changes over time, showing higher values during spring months and lower values in winter ones. This suggests that, for a sustainable water resources management and for protecting the natural environment, attention should be pointed to proper strategies regarding groundwater extraction taking also into account seasonal characteristics of the hydrological regime of the river.

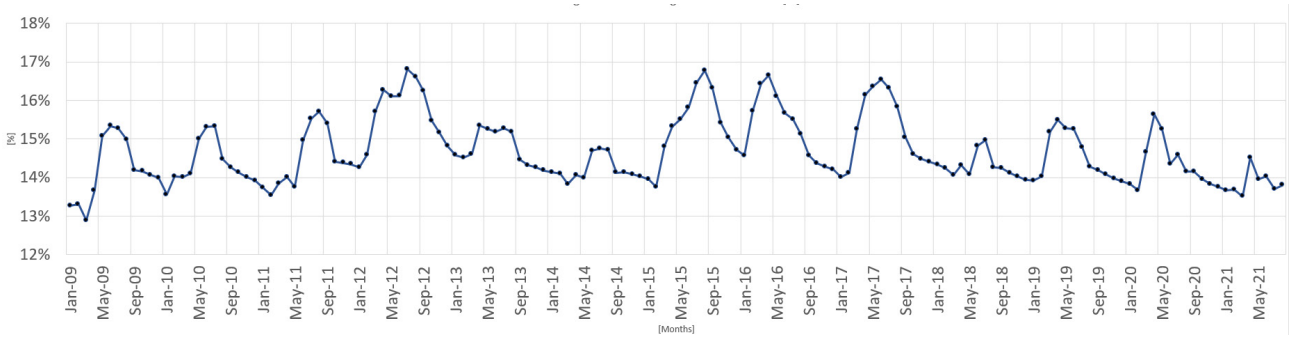

Figure 2. Influence of drainage gallery on natural spring discharge in percentage (%).

References

EC (2000) Directive 2000/60/EC of the European Parliament and of the Council of 23 October 2000 establishing a framework for Community action in the field of water policy

Borzì I, Bonaccorso B, Fiori A (2019) A Modified IHACRES Rainfall-Runoff Model for Predicting the Hydrologic Response of a River Basin Connected with a Deep Groundwater Aquifer. Water 11: 2031

Borzì I, Bonaccorso B, Aronica GT (2020) The Role of DEM Resolution and Evapotranspiration Assessment in Modeling Groundwater Resources Estimation: A Case Study in Sicily. Water 12: 2980

Harbaugh AW (2005) MODFLOW-2005, the U.S. Geological Survey modular ground-water model -- the Ground-Water Flow Process: U.S. Geological Survey Techniques and Methods 6-A16.

Winston MLA, Richard B (2009) ModelMuse a Graphical User Interface for MODFLOW-2005 and PHAST. Geological Survey, Reston, Va, USA

Using integrated methods of artificial aquifer recharge in dry regions with direct participation of stakeholders

S.A. Sajadi[1,3*], M. Ranjbar Minab[2], M. Mollaei[3]
[1] Department of Irrigation & Reclamation Engineering, University of Tehran, Karaj, Iran
[2] Hormozgan Regional Water Co, Bandar Abbas, Iran
[3] Sadrab Niroo Consulting Engineers Co, Urmia, Iran
* e-mail: s_ahmadsajadi@ut.ac.ir

Introduction

Groundwater is a vital natural resource that can be renewable or non-renewable, depending on the specific case. In arid and semi-arid regions, groundwater plays a crucial role in fulfilling water needs, particularly for agriculture and drinking purposes. As such, changes in the quantity and quality of groundwater in these areas are more pronounced than in other regions. A variety of factors, including increased agricultural and industrial activity, population growth, reduced rainfall, excessive extraction of groundwater, and the use of agricultural pesticides, as well as the leakage of pollutants over time, have contributed to a decrease in groundwater levels and quality, prompting concern among organizations and governments. Therefore, the quantitative and qualitative management of aquifers is essential for the sustainable exploitation of groundwater resources. One management practice that can help preserve and improve aquifers is artificial groundwater recharge, which involves using measures to recharge aquifers artificially during seasonal floods, thus promoting sustainable exploitation of water resources (Bize et al. 1972; Mohanty et al. 2010). However, given the high cost of artificial groundwater recharge schemes, selecting the appropriate location and method for groundwater recharge is crucial. Hence, climatic, geographical, and social conditions should be taken into account when selecting the optimal method.

In Iran, an arid and semi-arid country, artificial groundwater recharge is seen as a sustainable solution to address water crises (Madani 2014). As a case study, the Gezir plain, located in the southern part of Iran with an average rainfall of 85 mm/year, has experienced a drop in groundwater levels and an increase in salinity due to excessive consumption, rendering the water in the aquifer unsuitable for drinking. In a recent study, a combined method of Geographical Information System (GIS) and Shannon Entropy was used to identify suitable locations for artificial recharge (Sajadi et al. 2019). The appropriate method of artificial groundwater recharge was then determined by considering the aquifer's conditions in terms of water flow rate, the material of the aquifer layer, and social participation.

Materials and methods

Taking social and environmental factors into consideration, along with expert opinion and a previous study by Sajadi et al. (2019) utilizing Geographical Information System (GIS) and Shannon Entropy, suitable locations for artificial aquifer recharge were determined. After conducting field surveys and considering economic conditions and stakeholder participation, the appropriate method was chosen to be the use of direct artificial recharge, incorporating local knowledge and taking advantage of two seasonal rivers with controlled floods. Water is stored in storage pools, transferred through a transmission line, and injected directly into the aquifer through dual-purpose wells, without pumping from the wells to allow water to penetrate and recharge the aquifer. Additionally, the well walls are protected with a cement block to prevent collapse during injection, considering the material of the upper layer of the aquifer.

Results and concluding remarks

The utilization of artificial groundwater recharge presents a two-fold challenge that entails identifying appropriate recharge locations and selecting the optimal method, taking into account economic conditions, ease of implementation, exploitation, and social considerations. This study addresses these challenges

through the implementation of an artificial recharge plan that considers the aforementioned conditions and has led to active participation from the region's users and farmers, thereby facilitating sustainable benefits. The results of well sampling following flood control and artificial recharge indicate a significant improvement in water quality, as evidenced by a notable decrease in electrical conductivity from 8000 micromos/cm to 3000 micromos/cm. Moreover, after three years of implementing this plan, the groundwater level drop has plateaued, with an average increase of 40 cm in the aquifer. The method of artificial recharge employed in this study offers several advantages, including minimal evaporation of stored water, maximal efficiency in water penetration into the aquifer layer, high speed of the effectiveness of the artificial recharge of the aquifer, and productivity and stability.

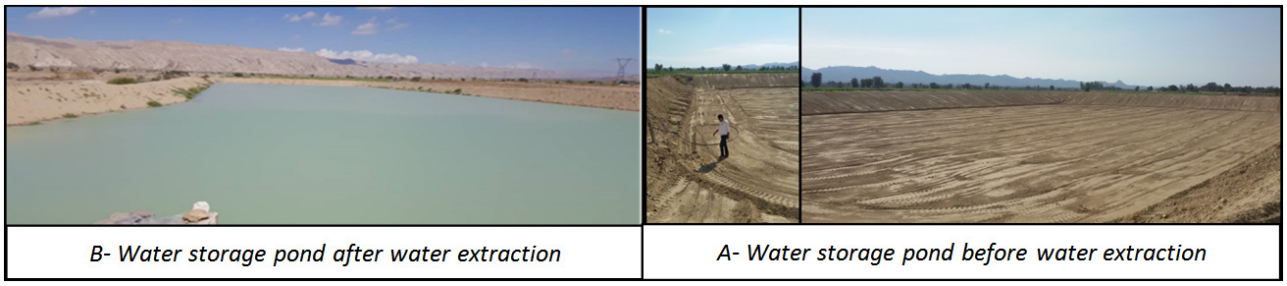

Figure 1. Water storage ponds before and after water extraction.

Figure 2. Recharge well- pumping before and during injection.

References

Bize J, Bourguet L, Lemoine J (1972) L'alimentation artificielle des nappes souterraines (Artificial groundwater recharge of aquifers). Masson Publisher, Paris, France, 199 p

Mohanty S, Jha M, Kumar A, Sudheer KP (2010) Artificial neural network modeling for groundwater level forecasting in a river island of eastern India. Water Resources Management 24(9): 1845-1865. https://doi.org/10.1007/s11269-009-9527-x.

Madani K (2014) Water management in Iran: what is causing the looming crisis? Journal of Environmental Studies and Sciences 4(4): 315-328. https://doi.org/10.1007/s13412-014-0182-z.

Sajadi SA, Shojaie S, Kholghi M (2019) A hybrid GIS-Shannon' Entropy framework for artificial recharge in arid regions plain. In: Proceedings of 11th World Congress on Water Resources and Environment: Managing Water Resources for a Sustainable Future, 387-388, Madrid, Spain. http://ewra.net/pages/EWRA2019_Proceedings.pdf

Prediction of seawater intrusion using the LSTM Deep Learning method

G. Kopsiaftis[1*], M. Kaselimi[1], A. Voulodimos[2], E. Protopapadakis[3], I. Tzortzis[1], I. Rallis[1], A. Doulamis[1], A. Mantoglou[1]
[1] School of Rural, Surveying and Geoinformatics Engineering, National Technical University of Athens, Greece
[2] School of Electrical and Computer Engineering, National Technical University of Athens, Greece
[3] School of Information Sciences, Department of Applied Informatics, University of Macedonia, Greece
* e-mail: gkopsiaf@survey.ntua.gr

Introduction

During the last decades there is a heightened demand for groundwater, making it one of the most vulnerable water resources. Prediction of seawater intrusion (SWI) extent is a key factor in addressing challenges related to well-being and public health, especially in small islands in arid and semi-arid regions, where groundwater is the main source for a number of activities, such as water supply and irrigation. The variable density (VD) model is considered the most accurate approach in simulating SWI, since it incorporates the dispersion mechanisms and the water density variability. The VD model uses a coupled differential equation system that includes fluid flow and solute transport equations, which are solved iteratively using numerical methods such as finite differences or finite elements. Although the VD simulations are accurate, they are time-consuming and CPU-intensive, making them unsuitable for applications requiring a large number of iterations, such as pumping rate optimization and uncertainty analysis. To address this issue, researchers have proposed various methods, including fast approximation models that can replace the VD model while maintaining accuracy (e.g., Christelis and Mantoglou 2016; Kopsiaftis et al. 2019) In this work, a deep learning (DL) method is utilized to mimic the complex and nonlinear relation between the time-dependent parameters of the SWI model. Specifically, the long-short term memory (LSTM) networks were utilized to simulate the location of SWI toe on a monthly basis. LSTM is one of the most widely used DL architectures for modeling nonlinear dynamic systems (Voulodimos et al. 2018; Kaselimi et al. 2021).

Materials and methods

A 3D VD model was developed for a coastal aquifer of Kalymnos Island, which is located at the eastern Aegean Sea. The total recharge of the aquifer was calculated based on the ERA5 reanalysis meteorological data (Copernicus Climate Change Service 2017). The remaining VD model parameters (e.g., hydraulic conductivity) were derived from previous studies (e.g., Mantoglou et al. 2004). A total number of 75 pumping scenarios was generated using the Latin Hypercube Sampling statistical method. A monthly timestep was applied on all the time-dependent parameters (i.e., recharge and pumping rates), and the simulation period for all the examined scenarios was 50 years. The 0.1 kg/m^3 concentration was selected as the critical value for the determination of the SWI extent.

The input set for the LSTM method includes the following variables: 1) the recharge rates, 2) the pumping rates and 3) the initial position of the SWI, expressed as the distance between the critical isohaline (0.1 kg/m^3) and the well location. It should be noted that each of the above variables is a timeseries with a monthly timestep. The average duration of each one of the simulations was approximately 2 h. The output set consists of the following data: 1) the hydraulic head at the well locations, and 2) the distance between each well and the 0.1 kg/m^3 isohaline at the bottom of the aquifer. The values of the examined variables are calculated at the end of each stress period. The proposed LSTM method assumes that the location of the critical isohaline can be predicted in each timestep based on its location in the previous timestep and two key parameters that play a critical role in dictating the flow regime in coastal aquifer.

Results and concluding remarks

Preliminary results indicate that the LSTM model approximates sufficiently the time-dependent parameters of seawater intrusion. Figure 1 presents indicative results of the proposed method for one of the 11 wells of the Kalymnos Island aquifer. For this specific well, the mean absolute error (MAE) and root mean square error (RMSE) are 4.12 m and 4.73 m for the location of the SWI toe and 2.01 m and 3.94 m for the hydraulic head. The results indicate that the LSTM approach tends to underestimate extreme hydraulic head values. However, it should be noted that in most Mediterranean islands the low recharge seasons coincide with the seasons of increased water demand. This combination leads to large hydraulic head variations, which cannot be easily predicted by the LSTM model. Also, the relatively high MAE and RMSE for the hydraulic head could be attributed to the fact that the calculations refer to the well locations, where the value range is considerably higher due to the intensified pumping.

The proposed method could provide an estimate of the aquifer condition at the beginning of each month, based on the measurements of the previous months. Despite the challenges arising from the computational burden required to create a sufficient dataset, the LSTM approach could become a useful tool towards the sustainable adaptive management of coastal aquifers.

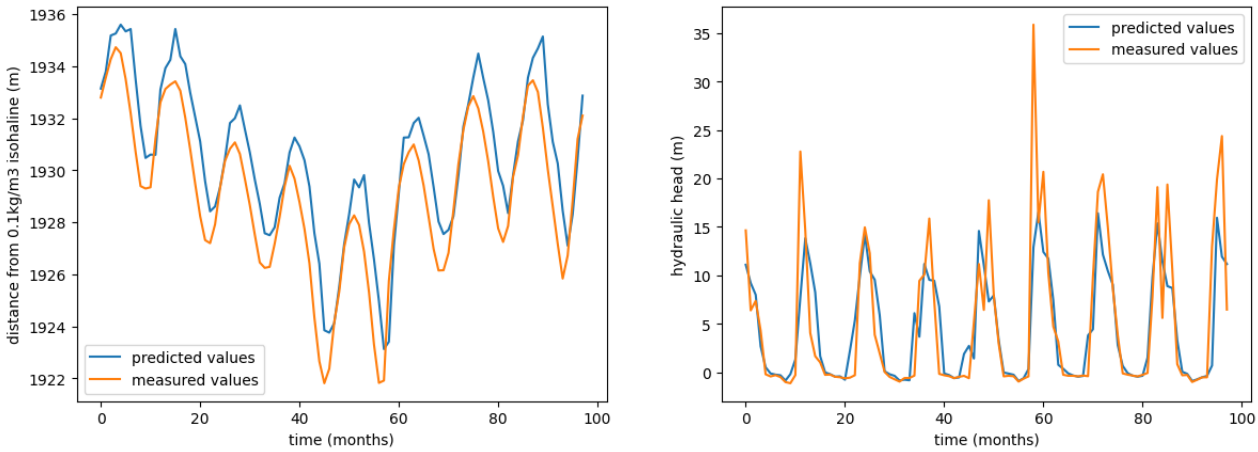

Figure 1. Indicative results of the LSTM method depicting the measured and predicted values for both the hydraulic head and the distance between the well location and the 0.1 kg/m^3 isohaline.

Acknowledgments: This paper is supported by the European Union Funded project euPOLIS "Integrated NBS-based Urban Planning Methodology for Enhancing the Health and Well-being of Citizens: the euPOLIS Approach" under the Horizon 2020 program H2020-EU.3.5.2., grant agreement No 869448. Also, this work was supported by computational time granted from the National Infrastructures for Research and Technology S.A. (GRNET) in the National HPC facility ARIS- under project ID pa211104 (MLGM).

References

Christelis V, Mantoglou A (2016) Pumping optimization of coastal aquifers assisted by adaptive metamodelling methods and radial basis functions. Water Resources Management 30(15): 5845-5859

Copernicus Climate Change Service (C3S) (2017) ERA5: Fifth generation of ECMWF atmospheric reanalyses of the global climate. Copernicus Climate Change Service Climate Data Store (CDS), date of access. https://cds.climate.copernicus.eu/cdsapp#!/home

Kaselimi M, Voulodimos A, Doulamis N, Doulamis A, Delikaraoglou D (2021) Deep recurrent neural networks for ionospheric variations estimation using gnss measurements. IEEE Transactions on Geoscience and Remote Sensing

Kopsiaftis G, Protopapadakis E, Voulodimos A, Doulamis N, Mantoglou A (2019) Gaussian process regression tuned by bayesian optimization for seawater intrusion prediction. Computational Intelligence and Neuroscience 2019: 2859429

Mantoglou A, Papantoniou M, Giannoulopoulos P (2004) Management of coastal aquifers based on nonlinear optimization and evolutionary algorithms. J Hydrol 297: 209–228

Voulodimos A, Doulamis N, Doulamis A and Protopapadakis E (2018). Deep learning for computer vision: A brief review. Computational Intelligence and Neuroscience 2018: 7068349

IX. Geoinformatics, Remote Sensing and Big Data Handling

12th World Congress on Water Resources and Environment (EWRA 2023)
"Managing Water-Energy-Land-Food under Climatic, Environmental and Social Instability"
Thessaloniki, Greece, 27 June - 1 July 2023

Fusion of MODIS TERRA and SENTINEL SLSTR land surface temperature products for minimizing gaps in basin scale hydrological studies

O.G. Şahin[1*], O. Gündüz[2]
[1] Department of International Water Resources, Izmir Institute of Technology, Izmir, Turkey
[2] Department of Environmental Engineering, Izmir Institute of Technology, Izmir, Turkey
* e-mail: onursahin@iyte.edu.tr

Introduction

Land Surface Temperature (LST) is an essential parameter for predicting energy balance, soil moisture, and evapotranspiration estimations, which varies spatiotemporally due to atmospheric and land surface conditions. It is used in numerous scientific fields including but not limited to hydrology, meteorology, and ecology (Hulley and Ghent 2019). Evapotranspiration constitutes a strongly correlated parameter to LST. Soil moisture is also a key input parameter used in drought and flood monitoring, agricultural production planning, and hydrological modeling. However, coarser spatial resolutions (9-50 km) of soil moisture data sets a limit to hydrological studies at the basin and regional scales (Zhao et al. 2018) due to information lost on the soil properties and other regional characteristics. In this context, machine learning techniques can be used to determine the non-linear relationships between soil moisture and auxiliary parameters such as LST and are increasingly being used in recent years for downscaling coarser resolution to high (1 km) and hyper (30 m) spatial resolution soil moisture data (Abowarda et al. 2021).

Since LST is highly correlated with soil moisture, it is commonly utilized as an auxiliary variable for any downscaling procedure. High-resolution LST data can be derived from thermal infrared sensors based on numerous satellite missions (e.g., Aqua, Terra, Sentinel SLSTR). However, spatial discontinuities may occur in LST maps due to adverse atmospheric conditions, sensor failures, orbital gaps, etc. (Wu et al. 2021).Cloud density is the reason for spatial and temporal discontinuities as it negatively affects thermal infrared measurements. Nevertheless, seamless LST maps are necessary for proper downscaling of soil moisture products, and gaps in LST maps can be minimized by the fusion of LST datasets derived from multiple missions. Li et al. (2018) combined Moderate Resolution Imaging Spectroradiometer (MODIS) satellites Aqua and Terra and produced two daily (mid-daytime and midnight-time) LST maps. Based on this theory, this study aims to analyze and form continuous LST data by using MODIS Terra and Sentinel SLSTR satellites with similar overpass times and spatial resolutions for data fusion purposes. The study is conducted in Küçük Menderes Basin (KMB) in Western Anatolia, Türkiye, for a period of one-month in August 2022 for demonstrating and testing the effectiveness of the fusion procedure.

Materials and methods

KMB is located between 37.65°-38.68° N latitude, 26.23°-28.42° E longitude in the Aegean Region and covers a total area of approximately 7000 km^2. The Mediterranean climate is predominant in the basin with hot and dry summers, and cold and rainy winters. Terra and Aqua satellites are the two main parts of the MODIS mission, which launched in 1999 and 2002, respectively. Two satellites collect earth observations data from multi-spectral bands consisting of Thermal Infrared (TIR) and Passive Microwave (PMW) (Hulley and Ghent 2019). Terra crosses the equator from north to south, descending (10:30) and south to north, ascending (22:30) twice daily. Sentinel 3A was launched in February 2016 and produces surface temperature data by using 11 different bands like MODIS satellites with the Sea and Land Surface Temperature Instrument (SLSTR), which uses split-window algorithm with S8 and S9 nadir view (Polehampton et al. 2022). In addition to TIR measurements, SLSTR uses auxiliary variables (land, vegetation cover, etc.) to produce LST. Level 3 Terra LST data (Wan et al. 2021) were obtained for KMB in August 2022 using the application developed for extracting and exploring analysis ready samples software (AppEEARS, 2023). LST values were then removed from the dataset if the LST error was larger than 2°K. A

Python script was prepared to download SLSTR LST data by sending HTTP requests to Copernicus OData API. If LST data is offline for any day, the script triggers the link, and data can be downloaded with 1-2 hours delay. Pixels under cloud cover and pixels with an uncertainty level of >2°K were removed using the quality criteria specified in the user handbook (Polehampton et al. 2022).

Overall, 31 and 24 LSTs are available in Terra and SLSTR satellites' day (descending) and night (ascending) passes, corresponding to 1- and 1.5- days temporal resolution, respectively. SLSTR observes the study area between the time intervals 07:46 – 09:05 and 19:14 - 20:30, whereas Terra passes from the area between the time intervals 08:00- 09:45, and 19:10 – 20:55 for day and night products. Because of the similar passing times of the satellites, when LST values are available for both satellites, the mean of the two LSTs are computed and assigned for a pixel (P1); otherwise, available LST from Terra or SLSTR were used to fill the pixel (P2) on a specific day. About 90% percent of the data satisfied the constraint and LST values existed for both satellites.

Results and concluding remarks

The absolute mean differences were analysed for SLSTR and Terra, respectively, yielding maximum (7.65, 3.38°C), minimum (1.02, 0.19°C), and mean (3.95, 2.48°C) values for day and night LSTs, under clear sky conditions. Valid LST pixels were then counted, and Terra gaps can be decreased dramatically by using SLSTR data. For example, on August 16, there was nearly no good quality LST pixel in Terra; however, SLSTR has had 2090 and 10209 good quality pixels for the same day and night products, respectively. At the opposite extreme, minor improvements were observed in the percentages of gap-filled pixels for August 04 (2.38%), August 07 (6.4%), August 19 (2.22%), and August 18 (4.07%). 7-day and 8-night LSTs were improved by more than 50% percent (rates of gap-filled pixels) when SLSTR and Terra were used together compared to the sole use of Terra.

While the methodology proposed here generates a more homogeneous and gap-free LST product that can be utilized in hydrometeorological analysis, it should be implemented carefully to avoid any potential discrepancies between P1 and P2 pixels if LST differences were recorded to be too high for SLSTR and Terra. Additional studies are necessary to further analyse the accuracies of the hybrid data generated by this methodology with data acquired from ground stations' observations.

References

Abowarda AS, Bai L, Zhang C, Long D, Li X, Huang Q, Sun Z (2021) Generating Surface Soil Moisture at 30 m Spatial Resolution Using Both Data Fusion and Machine Learning toward Better Water Resources Management at the Field Scale. Remote Sensing of Environment 255: 112301. https://doi.org/10.1016/j.rse.2021.112301

AppEEARS Team (2023) Application for Extracting and Exploring Analysis Ready Samples (AppEEARS). Ver. 3.22.1. NASA EOSDIS Land Processes Distributed Active Archive Center (LP DAAC), USGS/Earth Resources Observation and Science (EROS) Center, Sioux Falls, South Dakota, USA. https://appeears.earthdatacloud.nasa.gov

Hulley GC, Ghent D (eds) (2019) Taking the Temperature of the Earth: Steps towards Integrated Understanding of Variability and Change. Elsevier, https://doi.org/10.1016/C2017-0-01600-2

Li X, Zhou Y, Asrar GR, Zhu Z (2018) Creating a Seamless 1 Km Resolution Daily Land Surface Temperature Dataset for Urban and Surrounding Areas in the Conterminous United States. Remote Sensing of Environment 206: 84–97. https://doi.org/10.1016/j.rse.2017.12.010

Polehampton E, Smith D, Cox C, Ghent D, Xu W, Wooster M, Brunique J, Dransfeld S (2022) Copernicus Sentinel-3 SLSTR Land User Handbook. OMPC.ACR.HBK.002, ESA

Wan Z, Hook S, Hulley G (2021) MODIS/Terra Land Surface Temperature/Emissivity Daily L3 Global 1km SIN Grid V061 [Data set]. NASA EOSDIS Land Processes DAAC. https://doi.org/10.5067/MODIS/MOD11A1.061

Wu P, Yin Z, Zeng C, Duan SB, Gottsche FM et al. (2021) Spatially Continuous and High-Resolution Land Surface Temperature Product Generation: A Review of Reconstruction and Spatiotemporal Fusion Techniques. IEEE Geoscience and Remote Sensing Magazine 9(3): 112–37. https://doi.org/10.1109/MGRS.2021.3050782

Zhao W, Sánchez N, Lu H, Li A (2018) A Spatial Downscaling Approach for the SMAP Passive Surface Soil Moisture Product Using Random Forest Regression. Journal of Hydrology 563: 1009–24. https://doi.org/10.1016/j.jhydrol.2018.06.081

Assessment of upstream backwater length on account of extreme inflow events

A. Sahu, I. Ahmad[1*]
Department of Civil Engineering, National Institute of Technology, Raipur, India
** e-mail: iahmad.ce@nitrr.ac.in*

Introduction

Floods are the most common and widespread disaster in a tropical country like India. The backwatering effect adds to the devastating effects of flooding in monsoon season. When reservoirs are full, they revert huge amount of water coming from upstream. The backwatering effect can reach more than 150 Km upstream of dam (Amarnath and Thatikonda 2020). Upstream from dams, backwater fluctuations induce sediment deposition, cause more frequent and higher valley-floor inundation, increase groundwater level, and change channel morphology and riparian vegetation (Liro 2019). Due to backwatering effect, many croplands and vegetation get submerged on the upstream side of the dam, causing huge loss to livelihood of farmers. Backwatering effect is an important phenomenon to provide compensation for loss and plan the mitigation measures. The main objective of the study is to model a river geometry and simulate it under extreme flow scenario in HEC-RAS environment to assess the length of effect of backwatering caused by dam. In the present study, backwater length is evaluated on upstream of Hirakud Dam situated over Mahanadi River at Sambalpur district, Odisha State of India.

Materials and methods

River geometry is prepared using the ALOS PALSAR 12.5 m Digital Elevation Model (DEM). Daily and monthly flow data at different gauging and discharge sites are collected from Chhattisgarh Water Resources Department and India Water Resources Information System (WRIS) portal respectively. The study area map is presented in Figure 1. The river reach selected for the study starts from Shivrinarayan Barrage up to Hirakud Dam on Mahanadi River. Two main left bank tributary, Hasdeo river and Mand river join the Mahanadi River.

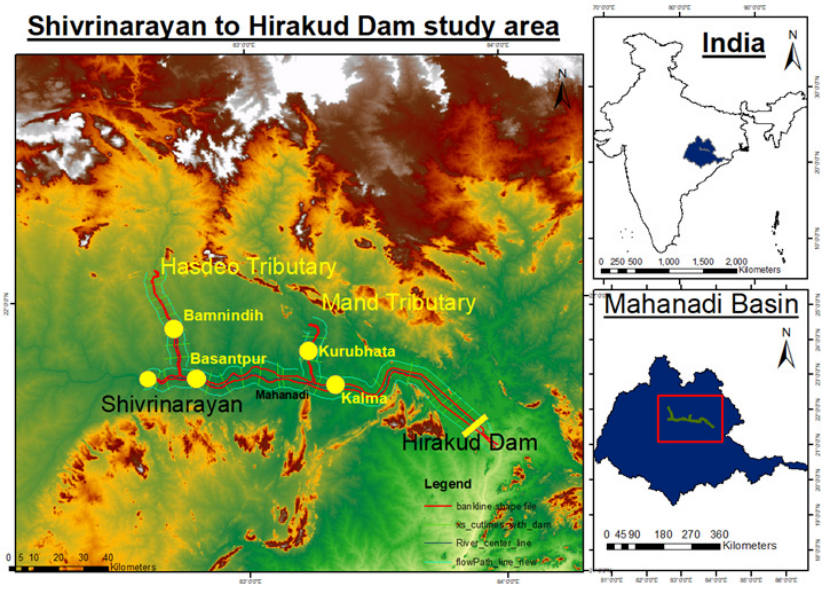

Figure 1. Selected river reaches on Mahanadi River.

DEM is processed and imported to RAS Mapper for preparing the river geometry having river centre

line, bank line, flow path line and cross section cut lines. To overcome the issue of preparing cross section across the catchment area of Hirakud Dam, the terrain is interpolated to get a DEM without dam. This interpolated DEM is processed to prepare 1D river geometry with and without dam. The modelling is done according to HEC-RAS manual (Brunner 1995). Monthly discharge data ranging from 1971 to 2019 for concerned Gauge and Discharge sites are used for steady flow analysis in 1D model. Maximum monthly flow data for different gauging and discharge sites viz. Shivrinarayan (184325.4 m^3/s), Basantpur (208435.0 m^3/s), Kalma (101320.3 m^3/s), Bamnidihi (49625.4 m^3/s) and Kurubhata (21962.25 m^3/s), were given as input for steady flow simulation. Table 1 represents the backwatering effect as a difference in water level at different cross sections without and with dam.

Results and concluding remarks

The results of 1D steady flow run considering i) maximum monthly flows from historical data, ii) dam height up to crest level of spillway, shows that water surface elevation has risen due to introduction of dam, confirming that there is an effect of backwater due to dam approximately 157 Km upstream of dam. The Mahanadi River reach longitudinal profile without and with dam is shown in Figures 2(a) and (b) respectively. In this study, an approach is presented to identify the backwatering length of dam on upstream side of dam. 1D steady flow run has proven that even when the dam height is considered up to crest level of spillway, there is a backwater effect. The authors acknowledge, Chhattisgarh Water Resource Department, India for providing monthly historical discharge data and India WRIS web portal for providing the daily discharge data.

Table 1. Obtained effect of backwatering as difference in water level considering dam height up to spillway crest.

River Reach	Distance upstream of Dam (Km)	Water surface elevations		
		Without Dam (m)	With Dam (m)	Difference (m)
Mahanadi Upper (at Shivrinarayan)	156.757	238.67	238.83	0.16
Mahanadi Middle (at Basantpur)	134.511	232.71	232.71	0
Mahanadi Lower (at Kalma)	79.399	215.92	215.93	0.01
Mahanadi Lower	18.378	184.65	193.59	8.94

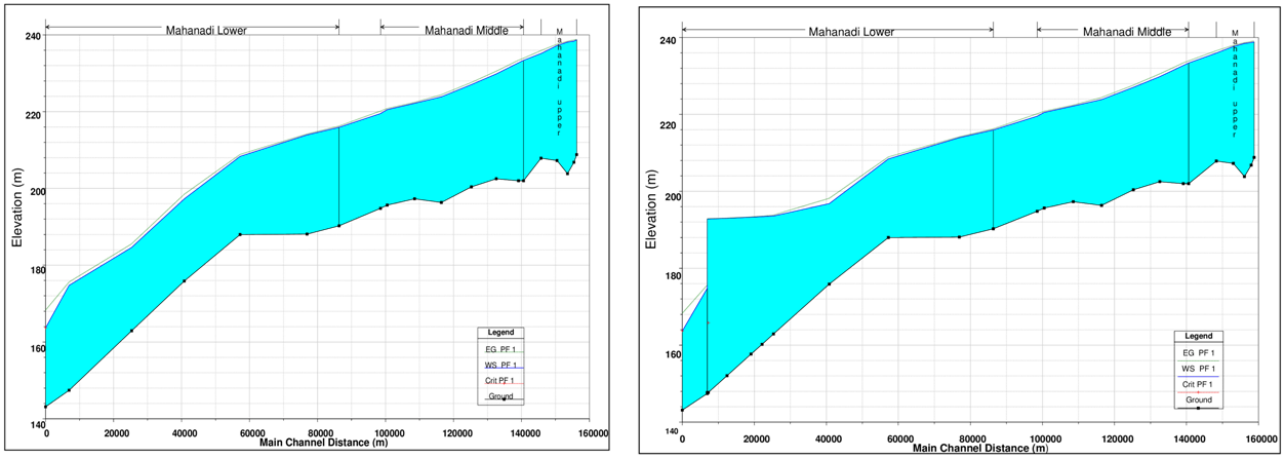

(a) *(b)*

Figure 2. (a) Longitudinal backwater profile without dam; (b) Longitudinal backwater profile with dam.

References

Amarnath CR, Thatikonda S (2020) Study on backwater effect due to Polavaram Dam Project under different return periods. Water 12(2): 576

Brunner GW (1995) HEC-RAS River Analysis System. Hydraulic User's Manual. Version 1.0. Hydrologic Engineering Center Davis CA

Liro M (2019) Dam reservoir backwater as a field-scale laboratory of human-induced changes in river biogeomorphology: A review focused on gravel-bed rivers. Science of the Total Environment 651: 2899-2912

CN-panEU: Development of a pan-European Curve Number (CN) dataset

I.M. Kourtis[1], M. Perdikaki[2], I. Zotou[1], H. Vangelis[1], A. Kallioras[2], V.A. Tsihrintzis[1]
[1] Center for the Assessment of Natural Hazards and Proactive Planning & Laboratory of Reclamation Works and Water Resources Management, National Technical University of Athens, Greece
[2] Laboratory of Engineering Geology and Hydrogeology, School of Mining and Metallurgical Engineering, National Technical University of Athens, Greece
* e-mail: gkourtis@mail.ntua.gr

Introduction

In hydrological applications the Curve Number (CN) empirical approach, now called NRCS (Natural Resources Conservation Service) CN method, constitutes one of the most widely used empirical methods for estimating direct runoff in both rural and urban studies (e.g., Kourtis et al. 2021; Vangelis et al. 2022). In addition, the SCS-CN method has been incorporated in various hydrological models (HEC-HMS, SWAT, SWMM, etc.) as it can be easily implemented with the aid of a Geographical Information System (GIS) and as the data requirements are rather low. In order to estimate the CN for the watershed, the only data needed as input are soil and land-use data.

Various researchers have used global remote sensing data for estimating CN at regional and/or global scales (e.g., Zeng et al. 2017; Jaafar et al. 2019). For instance, Jaafar et al. (2019) developed the first freely available global CN dataset, at a spatial resolution of about 250 m, based on the freely available Hydrological Soils Group dataset developed by Ross et al. (2018) and the global land cover data developed by the European Space Agency (2015). In the present work, we developed a pan-European CN gridded dataset, based on the Harmonized World Soil Database (HWSD) and the land use/land cover data from the Corine Land Cover (2018). The dataset covers the following countries: Albania (AL), Austria (AT), Belgium (BE), Bosnia and Herzegovina (BA), Bulgaria (BG), Croatia (HR), Cyprus (CY), Czechia (CZ), Denmark (DK), Estonia (EE), Finland (FI), France (FR), Germany (DE), Greece (EL), Hungary (HU), Iceland (IS), Ireland (IE), Italy (IT), Latvia (LV), Lithuania (LT), Luxembourg (LU), Malta (MT), Montenegro (ME), Netherlands (NL), North Macedonia (MK), Norway (NO), Poland (PL), Portugal (PT), Romania (RO), Serbia (RS), Slovakia (SK), Slovenia (SI), Spain (ES), Sweden (SE), Switzerland (CH), Turkey (TR), Ukraine (UA), and the United Kingdom (UK).

Materials and methods

Figure presents the methodological approach used for developing the pan-European CN gridded dataset. As depicted in Figure , three main inputs were used to generate the dataset: (i) the 2018 Corine land cover; (ii) the hydrologic soil groups estimated using the HWSD database along with the Digital Soil Map of the World (DSMW); and (iii) the CN look up tables acquired by the Greek Flood Risk Management Plans. The DSMW dataset was used to fill null values of the HWSD dataset. It should be mentioned that the CN values vary according to the Antecedent Moisture Conditions (AMC); thus, three datasets were developed: for AMC I (dry conditions), AMC II (average conditions) and AMC III (wet conditions). The CN values for AMC I and AMC III were estimated based on AMC II using the following equations, also used in the Greek Flood Risk Management Plans:

$$CN_I = \frac{0.42 \cdot CN_{II}}{1\text{-}0.0058 \cdot CN_{II}} \quad (1)$$

$$CN_{III} = \frac{2.3 \cdot CN_{II}}{1+0.013 \cdot CN_{II}} \quad (2)$$

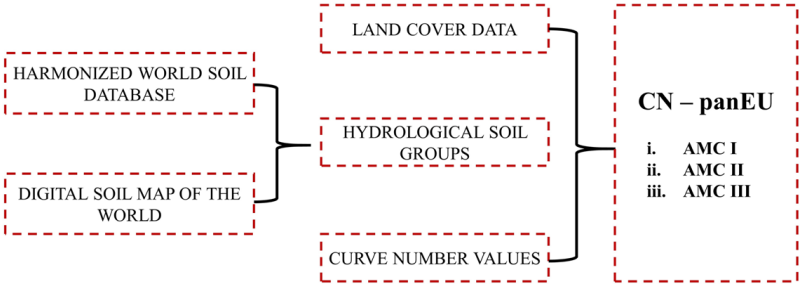

Figure 1. CN-panEU development overview.

Results and concluding remarks

We developed three datasets (Figure 2), i.e., one raster dataset for each AMC. The products are stored in GeoTiff format at about 25 m spatial resolution using the European Terrestrial Reference System 1989 (ETRS89) datum coordinate system. The results are in accordance with the results previously reported from other studies. For instance, Vangelis et al. (2022) recently reported a CN value of 68 for the Pineios basin upstream of the city of Larissa in Thessaly, Central Greece (Figure 2a). Using the developed dataset, CN was estimated at 76, 60 and 87, for AMC II, I and III, respectively.

The newly proposed CN dataset can be used from practitioners and researchers for flood vulnerability assessment and flood hazard assessment.

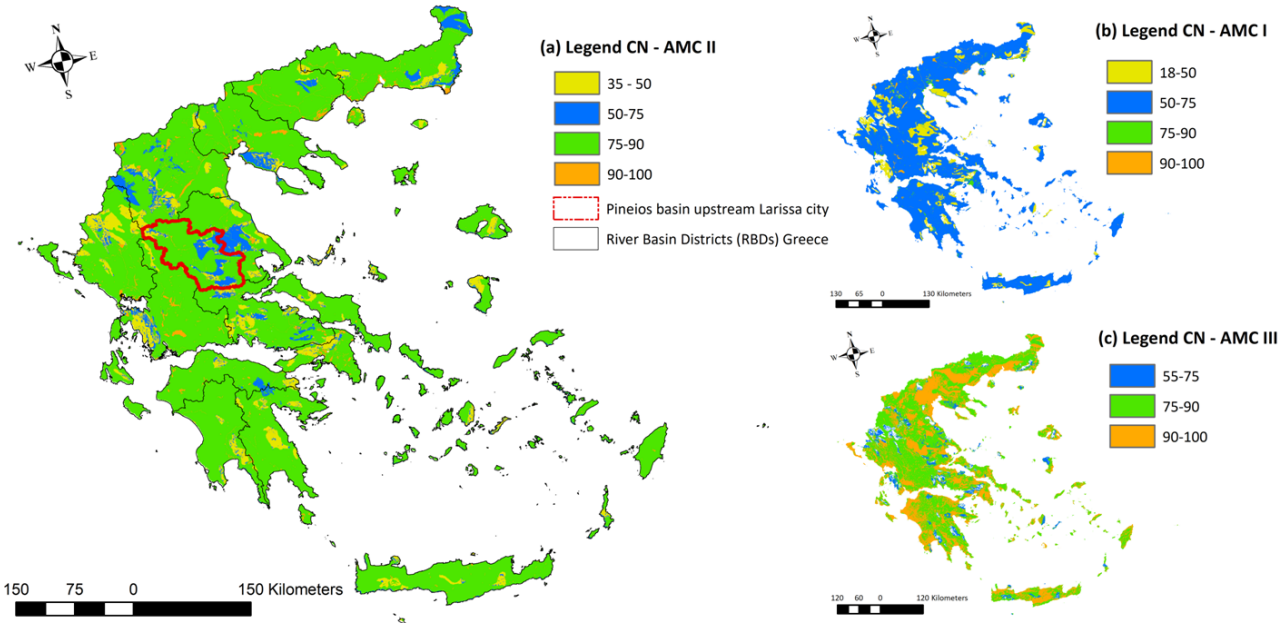

Figure 2. The Greek (EL) CN map for: (a) AMC II; (b) AMC I; and (c) AMC III.

References

European Space Agency (2018) CCI Land Cover Product User Guide version 2.4. ESA CCI LC project, https://www.esa-landcover-cci. org/?q=node/164

Jaafar HH, Ahmad FA, El Beyrouthy N (2019) GCN250, new global gridded curve numbers for hydrologic modeling and design. Scientific data 6(1): 145. https://doi.org/10.1038/s41597-019-0155-x

Kourtis IM, Bellos V, Kopsiaftis G, Psiloglou B, Tsihrintzis VA (2021) Methodology for holistic assessment of grey-green flood mitigation measures for climate change adaptation in urban basins. Journal of Hydrology 603: 126885. https://doi.org/10.1016/j.jhydrol.2021.126885

Ross CW, Prihodko L, Anchang J, Kumar S, Ji W, Hanan NP (2018) HYSOGs250m, global gridded hydrologic soil groups for curve-number-based runoff modeling. Scientific data 5(1): 1-9. https://doi.org/10.1038/sdata.2018.91

Vangelis H, Zotou I, Kourtis IM, Bellos V, Tsihrintzis VA (2022) Relationship of Rainfall and Flood Return Periods through Hydrologic and Hydraulic Modeling. Water 14(22): 3618. https://doi.org/10.3390/w14223618

Zeng Z, Tang G, Hong Y, Zeng C, Yang Y (2017) Development of an NRCS curve number global dataset using the latest geospatial remote sensing data for worldwide hydrologic applications. Remote Sensing Letters 8(6): 528-536. https://doi.org/10.1080/2150704X.2017.1297544

X. Transboundary River Basin Management and Hydro-diplomacy

Green infrastructure and agro-environmental measures for water quality management at the river basin scale

G. Ćosić-Flajsig[1*], B. Karleuša[2], M. Glavan[3]
[1] Civil Engineering Department, Zagreb University of Applied Sciences, Zagreb, Croatia
[2] Faculty of Civil Engineering, University of Rijeka, Rijeka, Croatia
[3] Department of Agriculture, Biotechnical Faculty, University of Ljubljana, Ljubljana, Slovenia
* e-mail: gcflajsig@tvz.hr

Introduction

Transboundary rural water quality management within integrated river basin management, requires at least good status of all river basin water bodies, reduction of the risk of eutrophication of waters and reduction of sediment input into waters (EU WFD 2000). Analysis of nutrient and sediment pressures and their reduction by common and new measures, including green infrastructure and agricultural measures, are presented on the Sutla River Basin case study.

Materials and methods

The Sutla River forms the border between the Republic of Slovenia and the Republic of Croatia. The size of the Sutla river basin is 590,6 km^2. After the construction of the Vonarje dam in the 1980s, the Sutla Lake/reservoir Vonarje, was constructed with a volume of 12.4 million m^3. Figure 1 presents a digital elevation model, sub-basin, hydrographic network with lakes and settlements and the location of Vonarje dam.

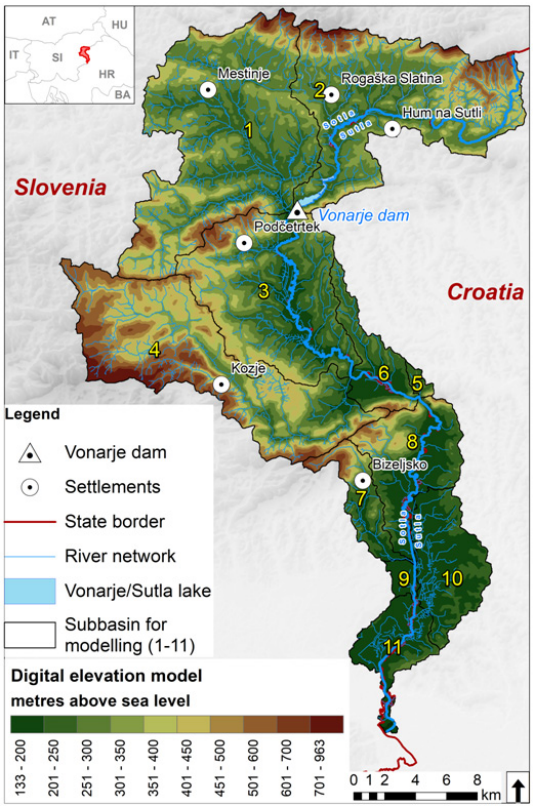

Figure 1. Transboundary rural Sutla River Basin: digital elevation model, hydrographic network with lakes, settlements, 11 subbasins and Vonarje dam.

Shortly after filling, the reservoir eutrophicated due to nutrient pollution from point and diffuse sources,

so it was emptied in 1989 and is now serving as a water retention work for flood protection (FRISCO project 2019). In this research, the Soil Water Assessment Tool Model (SWAT) has been used for the spatial quantification of nutrients and sediment and represents the BASIC SCENARIO – present scenario with basic measures. The Sutla River Basin is divided into 11 sub-basins. First the pressures in sub-basins 1 and 2 were analysed, which affected the changes in water quality in sub-basin 2 and in sub-basin 3 immediately downstream the Vonarje dam. Therefore, in sub-basin 1 and 2 for the BASIC SCENARIO, on the "hot spots" for nutrients and sediment pressures, appropriate additional "tailor-made" river basin measures have been implemented. Green infrastructure and agro-environmental measures, including best agriculture practices, show significant effects of retaining sediment, Total N and Total P. The proposed measures are based on the Nature Water Retention Measures Catalogue [NWRM] and SWAT Catalogue (Arnold et al. 2012). Selected measures are: 4 = 4.2 + 4.3 + 4.4 + 4.5, 4.1 – terracing operation, 4.2 - contouring, 4.3 – filter buffer strips, 4.4 -residue management, 4.5a – generic conservation practice - 5m, 4.5b - generic conservation practice - 15 m.

Results and concluding remarks

Selected scenarios of additional measures with different "tailor-made" agri-environmental additional measures were compared with the Sutla river basin basic scenario (Table 1).

Table 1. Results of the percentage (%) of pressure reduction for flow, sediment, total N and total P (optimal scenarios with additional measures for different measures in relation to the basic scenario).

Scenarios with additional measures	Flow (%)	Sediment (%)	Total N (%)	Total P (%)
Measure 4	1	-33	-30	-27
Measure 4.1	0	-19	-13	-14
Measure 4.2	0	-23	-16	-18
Measure 4.3	0	-4	-3	-3
Measure 4.4	0	-12	-10	-12
Measure 4.5a	0	-19	-14	-16
Measure 4.5b	0	-39	-36	-44

Table 1 shows that the selected measures significantly contribute to the reduction of sediment and nutrient pressures, especially Measure 4 and Measure 4.5b. In addition, in the future research, the presented effectiveness of the applied measures can be used to create recommendations for the application of additional measures for future climate change scenarios and for additional "tailor made" measures for the other 9 of 11 sub-basins. At the same time, the proposed measures can also be applied to, for example: smaller slopes of agricultural lands to ensure retention of sediment and nutrients in extreme hydrological situations of intense precipitation and storm runoff. The goal of this article was to present what can be achieved by SWAT model, but in order to define the optimal scenario a multicriteria analysis of all alternatives / possible scenarios, with all relevant criteria, and benchmarks should be done.

Acknowledgments: The research for this article and the publication were funded by the University of Rijeka within projects "Implementation of Innovative Methodologies, Approaches and Tools for Sustainable River Basin Management" (UNIRI-TEHNIC-18-129) and "Hydrology of Water Resources and Identification of Flood and Mudflow Risk in Karst" (UNIRI-TEHNIC-18-54) and the University of Ljubljana within the OPTAIN project (OPtimal strategies to retAIN and re-use water and nutrients in small agricultural catchments across different soil-climatic regions in Europe, cordis.europa.eu) which has received funding from the European Union's Horizon 2020 research and innovation programme under grant agreement No. 862756.

References

Arnold JG et al. (2012) Soil & Water Assessment Tool, Input/Output Documentation. Version 2012, Appendix A, Texas Water Resources Institute, TR-439, https://swat.tamu.edu/media/69296/swat-io-documentation-2012.pdf

Catalogue of Natural Water Retention Measures (NWRM) (2015) http://nwrm.eu/measures-catalogue (accessed on 11.02.2023)

European Parliament and Council (2000) EU Water Framework Directive. Directive 2000/60, European Union, Maastricht, The Netherlands

FRISCO Project (2019) www.frisco-project.eu/engl/ (accessed on 11.02.2023)

Impact of the Grand Ethiopian Renaissance Dam on the Lower Nile under different operating scenarios

A. Kuriqi[1*], E.M. Ramadan[2], I. Abd-Elaty[1]
[1] CERIS, Instituto Superior Técnico, Universidade de Lisboa, Av. RoviscoPais 1, 1049-001, Lisbon, Portugal
[2] Department of Water and Water Structures Engineering, Faculty of Engineering, Zagazig University, Zagazig 44519, Egypt
* e-mail: alban.kuriqi@tecnico.ulisboa.pt

Introduction

Water supplies in arid and semi-arid regions are critical for agriculture, industrial and domestic activities (Santana et al. 2020). Egypt is an arid region with limited water supplies; the average rainfall ranges between 50 to 200 mm per year (El-Rawy et al. 2020). Future overpopulation and climate change will influence and increase the water stress in Egypt, reducing the human water supply and increasing the water shortage (Sowers et al. 2011). This study investigates the impact of different operation scenarios of the Grand Ethiopian Renaissance Dam (GERD) on the Nile River water supply for minimum and normal flow conditions. The MODSIM model was employed to simulate the water allocation mechanism in a river basin through a sequential solution for the network flow for each period and scenario. The results of this study will be useful in evaluating the impact of GERD on Egypt and other river basins worldwide while taking effective measures.

Materials and methods

The MODSIM model was used to simulate the water allocation mechanism in a river basin, considering different filling scenarios through a sequential solution of the following network flow optimization problem for each period for different periods (Berhe et al. 2013). The model was calibrated by downstream flow with the average actual flow release downstream of Aswan High Dam (AHD) from 1991-2010. The accuracy of mathematical model prediction for the total values through the year was measured in terms of the mean percentage relative error (MPRE) (Armstrong and Collopy 1992). The results show that the error varied from +13.18% (January) to -5.13% (June), reaching 0.01% for the total flow. The MPRE through the year for the modeled flow downstream AHD with the mean monthly average actual flow from AHD was calculated at 1.89. The study used the variable density code SEAWAT to calculate the coastal aquifer's groundwater heads, water budget, and salinity.

Results and concluding remarks

The MODSIM results for the water flow reaching the AHD indicated a monthly variation of the basin hydrograph before the GERD operation (Table 1). A relatively stable water volume below about 5 BCM was estimated between December and July, followed by a rapid increase reaching about 21.35 BCM in September.

Table1. Nile discharges in BCM before and after GERD.

Month	May	Jun	Jul.	Aug.	Sep.	Oct.	Nov.	Dec.	Jan.	Feb.	Mar.	Apr.	**Total**
Nile nature flow before GERD	1.83	1.88	4.49	17.87	21.35	14.77	7.31	4.41	3.35	2.34	2.22	1.97	83.79
Modified flow after GERD	5.37	5.88	6.19	6.2	6.80	7.76	7.92	8.02	6.83	6.70	6.59	5.62	79.88
Demand from Lake Nasser	6.35	7.39	7.56	7.68	6.38	6.23	6.12	5.04	4.78	5.34	5.68	5.70	74.25

Under the GERD operation, the response of the basin hydrograph was different. A relatively more stable water volume was estimated throughout the different months, reaching its maximum in December (about 8.02 BCM). A similar stable trend defined the AHD demand. However, the highest demand is across the

summer periods, thus not following the seasonal response of the basin hydrograph, indicating the highest water volumes in autumn. Also, results show that filling of GERD at Normal (average) flow case through the operation scenarios at water elevations of 600 m, 621 m, and 645 m, respectively, will decrease the live storage of Lake Nasser (actual 90.7 BCM) by 13.29, 25.41 and 37.26 BCM through each scenario as presented in Figure 1.

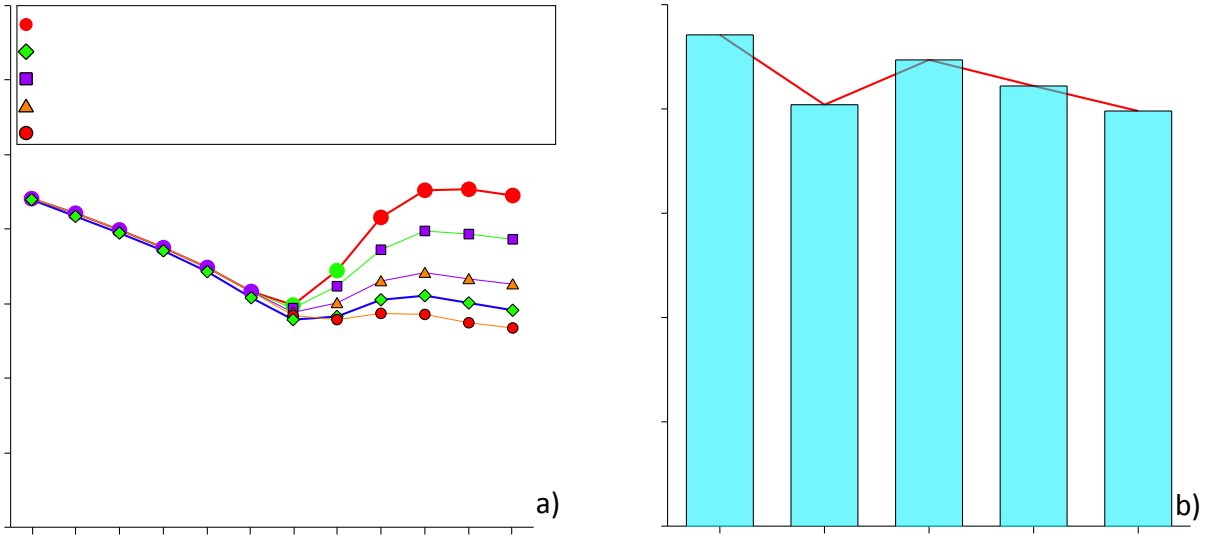

Figure 1. Water volume for different operation scenarios of GERD (a) interannual monthly average water volume and (b) total water volume.

Overall, the results indicate that GERD operation stabilizes the basin hydrograph and provides sufficient water to operate the AHD annually. More water needs to be stored in the fall and winter to ensure adequate response over the summer. In addition, our results show that filling the GERD reservoir could alter freshwater in the Nile Delta and increase aquifer salinity considerably.

Acknowledgments: Alban Kuriqi is grateful for the Foundation for Science and Technology's support through funding UIDB/04625/2020 from the research unit CERIS.

References

Armstrong JS, Collopy F (1992) Error measures for generalizing about forecasting methods: Empirical comparisons. International Journal of Forecasting 8: 69-80. https://doi.org/10.1016/0169-2070(92)90008-W

Berhe FT, Melesse AM, Hailu D, Sileshi Y (2013) MODSIM-based water allocation modeling of Awash River Basin, Ethiopia. CATENA 109: 118-128. https://doi.org/10.1016/j.catena.2013.04.007

El-Rawy M, Abdalla F, El Alfy M (2020) Water Resources in Egypt. In: Hamimi Z et al. (eds). The Geology of Egypt. Springer International Publishing, Cham. pp 687-711

Santana CS, Montalván Olivares DM, Silva VHC, Luzardo FHM, Velasco FG, de Jesus RM (2020) Assessment of water resources pollution associated with mining activity in a semi-arid region. Journal of Environmental Management 273: 111148. https://doi.org/10.1016/j.jenvman.2020.111148

Sowers J, Vengosh A, Weinthal E (2011) Climate change, water resources, and the politics of adaptation in the Middle East and North Africa. Climatic Change 104: 599-627. https://doi.org/10.1007/s10584-010-9835-4

Methodological approach for the elaboration of transboundary flood protection action plans

E. Tzanou[1], C. Skoulikaris[2], A. Chatzigiannis[3]
[1] *School of Surveying and Geoinformatics Engineering, Faculty of Engineering, International Hellenic University, Greece*
[2] *Scientific Associate - Civil Engineering Department, AUTH, Greece*
[3] *Consortis Ltd, Engineering Consultants, Greece*
** e-mail: etzanou@ihu.gr*

Introduction

Action plans are critical for effective flood protection and management. They provide a structured and systematic approach to planning, implementing, and evaluating activities aimed at reducing the impact of floods and mitigating associated risks. The scope of this study was το deliver a result-based action plan for flood protection and to present a standardized methodology that may be used in most cases, for flood-prone areas. The development of an action plan in the transboundary area of Strymon river formulated a framework that promotes a specific strategic planning for the area leading to the valuation of existing flood intervention measures and the hierarchization of newly proposed ones. The approach developed may be applied in multiple cases, since flooding events and infrastructure show similar patterns, especially in the Mediterranean region.

Materials and methods

The proposed methodology was implemented in the transboundary catchment area of Strymon river, in the Balkan Peninsula with a length of 360km, of which 242km are in Bulgarian and 118km in Greek territory. The total hydrological basin has an area of 16,550 km^2, with 6,344 km^2 located in Greece. In the area, numerous flood events take place every year with an increasing tense of occurrence, resulting in socioeconomic and natural consequences, for which stakeholders and public authorities are responsible for recovery and restoration each time. Data for the transboundary area was obtained by the collaboration with the Bulgarian managerial authorities and stakeholders, where information on flood structural and non-structural protection intervention measures were recorded and evaluated, providing feedback on the state of collaboration in the transboundary area. The methodological chain developed took into account the axes of the FRMPs (Flood Risk Management Plans) and the EU Flood Directive.

The methodological approach was applied in two distinct phases.

- The first phase delivered a valuation report and an open access Web-GIS platform as the base mechanism for the implementation of an action plan in terms of the infrastructure projects, measures and interventions that are necessary or appropriate for flood protection. It included the development of the explanatory memorandum of assessment for all the intervention measures (implemented projects/ works and planned projects/ works) related to flood protection of the area. A parametric model was developed with input elements of the current situation i.e. population density, civil works, natural environment, land use, networks, spot of special interest (industry, education, heath, landmarks) etc,by prioritizing then through Analytical Hierarchy Process. Also flood protection infrastructure (technical projects), flood protection management actions, measures taken and their so far, degree of performance were evaluated.
- The second phase was the actual elaboration of the Flood Protection action plan. It included the dynamic analysis of all protection measures recorded on phase 1, at the level of evaluating their performance, by assessing the prevailing condition of infrastructure, the performance of the implementation of the flood risk management plans so far, the documentation of the applicability and the efficiency of the measures/ interventions.

The action plan resulted in a prioritization and correlation of the interventions that should each time be implemented for flood risk or flood hazard by the competent and involved authorities, putting into effect

the mechanism and infrastructure available or by adapting directly specific actions. The action plan both covers spatial and temporal dimension of the flooding problem. The spatial dimension reflects to the location and the topological correlation with other geographical or non-geographical features, while the temporal dimension refers to the development of flood protection infrastructure over the years and their behaviour in various flood phenomena that has either occurred, appeared periodically or may occur at some point in the future. The methodological steps are presented below (Table 1).

Table 1. Step-by-step implementation of flood protection Action Plan.

Base-line reference report (phase 1)	Action plan implementation (phase 2)
• **Performance analysis** of the situation and determination of the degree of response in which both the existing and proposed flood protection projects and their existing management structures are located • Determination of the **degree of protection** they provide using benchmarking methods • Categorization of **levels of operational needs** they intend to meet. • **Evaluation of the overall effects** of the measures / interventions • Estimation of the **credibility level of effectiveness** of the implementation.	• Determination of the **operational parameters** of all intervention measures and future needs • Determination of their **levels of interaction** • Determination of the **degrees of freedom of each level of interaction** • **Evaluation of the interoperability** of the interventions in the main catchment areas by region and sub-basin • **Scenarios** of functional interconnection of intervention measures • Determination of the acceptable **cost-benefit limitations** • **Prioritization** (spatial and temporal) of proposed actions.

Results and concluding remarks

The action plan aimed to rationalize the potential risk of flooding due to the development of the transboundary region and mainly to propose measures and interventions both of permanent structural and non-structural character. Through the action plan, the priorities on the projects and intervention measures emerged. The hierarchies based on environmental, social, and economic criteria, were evaluated to reach axes and specific proposals of protection infrastructures, always in the context of the sustainable development of the region and the requirements of the vision of climate change. The action plan also aimed to demarcate, spatially and temporally, the results of interventions in relation to their implementation costs and their degree of efficiency in accordance to the feasibility of the implementation of the measures and interventions that have been proposed and followed by the Flood Risk Management Plans. Overall, developing a flood protection action plan requires a methodological approach that is grounded in scientific evidence, stakeholder engagement, and good governance practices.

Acknowledgments: This research was funded by the INTERREG V-A European Territorial Cooperation Program "Greece-Bulgaria 2014-2020 "Flood Protection-Cross Border Planning and Infrastructure Measures for Flood Protection"

References

EC (2019) International Cooperation under the Water Framework Directive (2000/60/EC) - Factsheets for International River Basins. Commission staff working document accompanying the document: Report from the commission to the European Parliament and the Council on the implementation of the Water Framework Directive (2000/60/EC) and the Floods Directive (2007/60/EC)

EC (2021) Directorate-General for Environment, Current practice in flood risk management in the European Union. September 2021, Publications Office of the European Union, https://data.europa.eu/doi/10.2779/235272

Skoulikaris C, Zafirakou A (2019) River Basin Management Plans as a tool for sustainable trans-boundary river basins' management. Environ Sci Pollut Res 26(15): 14835-14848

WHO (2017) Selecting Measures and Designing Strategies for Integrated Flood Management: A Guidance Document. Netherlands: Swiss Federal Office for the Environment, Netherlands Ministry of Infrastructure and Environment and Deltares

XI. Socioeconomic Aspects and Water Resources Policies and Governance

Determination of criteria's weights via IFWA operator and DEMATEL

T. Bakas, C. Papadopoulos, D. Latinopoulos, M. Spiliotis*, I. Kagalou, B. Papadopoulos
Civil Engineering, School of Engineering, Democritus University of Thrace, Xanthi, Greece
** e-mail: mspiliot@civil.duth.gr*

Introduction

This research aims to determine the weights of the criteria that are going to evaluate a series of alternatives in the context of rational water management of the Lissos river basin, Prefecture of Rhodope, NE Greece (Figure 1a). The Lissos river basin is extended to an area of 1486 km^2. It can be distinguished from the lowland area, which is mainly constituted of alluvial and Neogene deposits, and the mountainous where the metamorphic base of low permeability appears. The lowland part is an arable area, approximately 40 Km^2 of which are irrigated mainly by the groundwater system of Filiouri (EL1200040). Approximately 1300 private wells draw from the unconfined shallow aquifer, while there are also 100-150 municipal boreholes that draw from deeper aquifers. As concerned as the quality of groundwater, the Filiouri system is under stress in its coastal part due to sea intrusion caused by overexploitation, while certain concentrations of nitrates are observed in the center of the plain. The water balance of the groundwater appears marginally positive since the total abstractable volume is estimated at approximately 12.5-13.5x10^6 m^3, while infiltration volume is estimated at approximately 15.0x10^6 m^3. Lissos river basin is of particular research interest, with increased monitoring needs, both for the extent and intensity of the pressures it receives and the lack of available knowledge/scientific research. As it flows into bathing shores and protected coastal areas, the protection regime of the region is of high importance. It is a water body with habitat fragmentation since the former natural habitats, such as forests and fens have almost disappeared and were replaced from crops, changing the main characteristics of the river entirely. There are six natural water bodies, while three water bodies have been designated as Heavily Modified Water Bodies (HMWB) with estuaries on the east coast.

Materials and methods

A consultation (scientist workshop) was carried out in Komotini from which the opinion of experts, farmers and administrators was obtained on the problems and pressures of the Lissos River and Filiouri system. Two approaches are adopted for the determination of the criteria's weights.

The first one is based on the principle of intuitionistic fuzzy sets (IFS) which are an extension of ordinary fuzzy sets. Intuitionistic Fuzzy Sets (IFS) besides the positive information determined by the membership function in a set, also have the possibility of expressing negative information with the aid of the non-membership function. They provide also the possibility to describe and define mathematically the concept of hesitancy (i.e. uncertainty). Therefore, IFS are capable of meeting the challenge of group decision making in an uncertain environment (where uncertainty is introduced by the subjectivity of the analyst and decision maker). An IFS *A* has the form $A=\{x, \mu_A(x), \nu_A(x) \mid x \epsilon X\}$, where the second and third term denote the membership function and the non-membership function, correspondingly. Moreover, for each IFS *A* in *X* is defined the term $\pi_A(x)=1-\mu_A(x)-\nu_A(x)$ that denotes the indeterminacy degree of *x* to *A*. Initially, the opinions of twenty one experts were transformed into intuitionistic fuzzy information based on Dominguez et al. 2015. Then, the intuitionistic fuzzyfied experts' opinions were aggregated using the IFWA operator proposed by Xu (2007) (Eq. 1) to produce the criteria's weights. In the following Equation 1 *(κ)* represents the DM's, *(j)* represents the criterion, *w* the weight, and *(λ)* represents the DM's importance.

$$w_j = IFWA\left(w_j^{(1)},\ldots,w_j^{(l)}\right) = \left[1-\prod_{k=1}^{l}\left(1-\mu_j^{\kappa}\right)^{\lambda_k}, \prod_{k=1}^{l}\left(\nu_j^{\kappa}\right)^{\lambda_\kappa}, \prod_{k=1}^{l}\left(1-\mu_j^{\kappa}\right)^{\lambda_\kappa} - \prod_{k=1}^{l}\left(\nu_j^{\kappa}\right)^{\lambda_\kappa}\right] \quad (1)$$

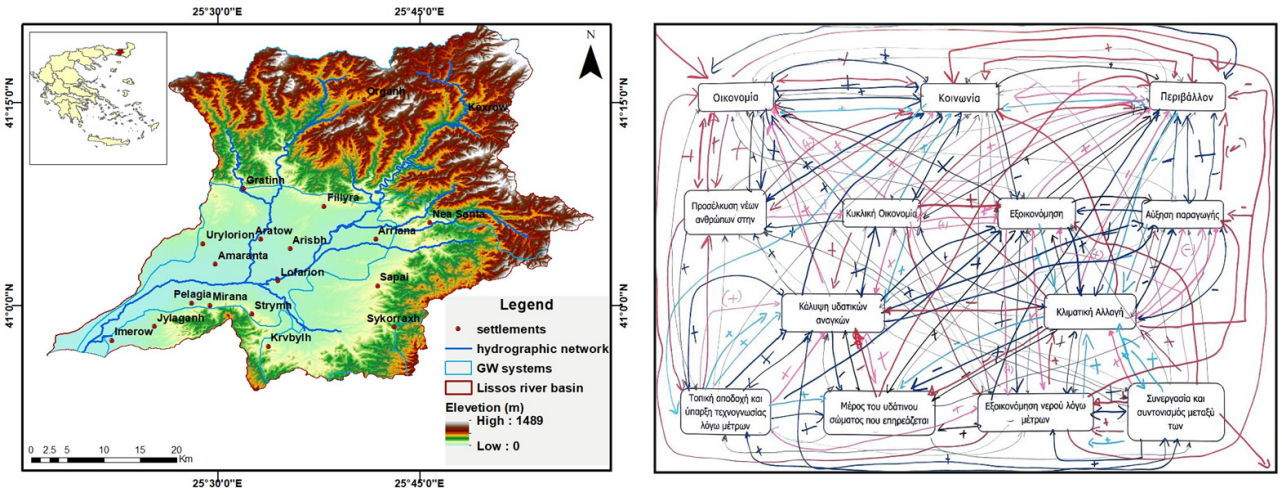

(a) *(b)*

Figure 1. a) The Lissos river basin, b) The constructed map of mind based on the DEMATEL method.

The second approach is based on the DEMATEL method developed by the Science and Human Affairs Program of the Battelle Memorial Institute of Geneva between 1972 and 1976. In general, using the DEMATEL a map of the mind of each respondent regarding the influence between the criteria can be gained (Figure 1b). Thus, based on the produced map a pairwise matrix between the criteria is constructed and normalized, while appropriate indicators are estimated. Then, according to Dalalah et al. (2011), the criteria's weights can be determined based on both the concept of prominence and relation.

Results and concluding remarks

The results show that the environmental criterion is the most important criterion for both approaches (Table 1). An interesting point is that the DEMATEL preferred universal criteria (social and financial). Furthermore, it is worth mentioning that in the DEMATEL method the nodes with the highest connectivity produced the weights with the higher importance.

Table 1. The examined criteria, fuzzy and crisp weights, and the final rankings.

Criteria	IFWA weights			Defuzzificated weights	DEMATEL weights	Ranking (IFWA)	Ranking (DEMATEL)
	μ	ν	π				
Financial	0.786	0.182	0.031	0.078	0.098	7	3
Social	0.743	0.222	0.036	0.074	0.099	10	2
Environmental	0.860	0.131	0.009	0.083	0.105	1	1
Cover of water demand	0.825	0.157	0.017	0.080	0.082	2	4
Resilience to climate change	0.819	0.167	0.014	0.079	0.080	4	6
Local acceptance and existence of know-how at prefecture level	0.767	0.209	0.024	0.075	0.067	9	9
Significance of alternative	0.810	0.165	0.025	0.079	0.047	5	13
Water saving	0.822	0.161	0.017	0.080	0.075	3	8
Synergy with other alternatives (affected part of water body)	0.733	0.232	0.035	0.073	0.066	12	10
Attracting young people to the countryside to live and work	0.778	0.197	0.025	0.076	0.058	8	12
Circular economy	0.721	0.249	0.031	0.071	0.081	13	5
Energy saving	0.740	0.230	0.031	0.073	0.078	11	7
Increasing agro-food chain production	0.803	0.171	0.025	0.079	0.064	6	11

Acknowledgments: The research was performed under Eye4Water project (MIS 5047246), Co-financed by Greece and the European Union - European Regional-Development Fund.

References

Dominguez-Perez L, Alvarado-Iniesta A, Rodriguez-Borbon I, Vergara-Villegas O (2015) Intuitionistic fuzzy MOORA for supplier selection. DYNA 82(191): 34-41

Xu Z (2007) Intuitionistic Fuzzy Aggregation Operators. IEEE Transactions on Fuzzy Systems 15(6): 1179-1187

Dalalah D, Hajaneh M, Batieha F (2011) A Fuzzy Multi-criteria Decision Making Model for Supplier Selection. Expert Systems with Applications 38: 8384-8391

12th World Congress on Water Resources and Environment (EWRA 2023)
"Managing Water-Energy-Land-Food under Climatic, Environmental and Social Instability"
Thessaloniki, Greece, 27 June - 1 July 2023

Robustness and effectiveness of Mediterranean drought regulatory framework

A. Iglesias[1*], A. Sordo-Ward[2], P. Bianucci[2], L. Garrote[2]
[1] Dep. Agricultural Economics and Social Sciences, Universidad Politécnica de Madrid, Madrid, Spain
[2] Dep. Civil Engineering: Hydraulics, Energy and Environment, Universidad Politécnica de Madrid, Madrid, Spain
* e-mail: ana.iglesias@upm.es

Introduction

The Mediterranean region has the unique characteristic of being a semi-arid region, with crucial water scarcity and social water imbalances and at the same time dramatically affected by intensified drought. Drought policies are booming in the Mediterranean region since the early 2000s. The policies have also diversified and now include societal aspects of drought risk, alongside the traditional meteorological-based risk analysis. Key policy components are driven by the EU Water Framework Directive, the EU Drought Observatory, and the UN Disaster Risk Management. Successful as the Drought Management Plans may be, their achievements are no guarantee for future excellence. The Mediterranean stakeholders involved in land and water management have relied heavily on their historical success that made possible the growth of the agricultural, industry and tourist sectors, but this strategy entails significant risks. Internal factors such as diverging interests among water users, and noncompliance by individuals, may upset the current equilibrium. External factors, such as new environmental regulations and climate change, may be equally challenging. Thinking about the future of water for all in the Mediterranean thus raises the question of how robust the current regulatory framework actually is. This issue is explored in the paper.

Materials and methods

A systematic assessment of drought management policies in the Mediterranean requires an analytical framework, a set of criteria against which performance can be evaluated. The analytical framework has two components: one institutional and one applied in the stakeholders that are affected by drought. First, institutional design principles will be applied to the current drought management framework to discuss trends in drought management plans in the Mediterranean. Second, the principles of risk management will be applied to define risk categories that are operational, focusing on evaluating the benefits of implementing drought management. These two components are then combined to explore improvements in drought management. The data are based on the information about the development of Drought Management plans, the status of other regulations, and the published scientific papers related to drought management (Alexander et al. 2016; Estrela and Sancho 2016; Garrote et al. 2016; Hagenlocher et al. 2019; Iglesias et al. 2018; OECD 2021; Raikes et al. 2019; Urquijo and De Stefano 2020).

Results and concluding remarks

Water use in the Mediterranean is very competitive, disturbing ecosystems, deteriorating water quality, and limiting the ability of being used as a production factor (i.e., for energy or food) and vital factor (i.e., for people and ecosystems). Excluding "others" from enjoying water is very difficult and is traditionally done by issuing water use permits. That is the main reason why water norms and legislation is highly developed in the region (OECD 2021). As direct consequence, drought management is highly derived from the institutional perspective and closely linked to hydrological and meteorological science (Iglesias et al. 2018).

Drought management plans tend to provide limitations on the use of water as the main action (Estrela and Sancho 2016). When water is viewed as a common good, therefore trying to limit its use is the main alternative to reach sustainable water use. The individual and collective responses responding to drought are a clear example of this tension. The lack of rain, results in increased irrigation that benefits the individual, while sharing the costs of resource degradation has an impact on other group members (i.e., the

environment). Viewing the problem in this way, the only solution for drought management is to limit the use and protecting the use of commons and practical drought management needs to include self-organised groups of individuals for governing common resources.

Despite the progress made, Drought management plans in the Mediterranean has been considered weak (OECD 2021). The decision-making and implementation process is arguably too slow to deal with the dynamic water and land use in the region. Many regulations specifically applying to the use of water are not legally binding. Those that are binding are implemented through the local legislation, leaving much room for national translation and interpretation. In addition, the rules cannot be policed and enforced effectively in the field, and they do not apply to many users that compete for water.

We propose a that drought management plans should be dynamic and adaptive, improving in the following aspects.

1. Clearly defined boundaries of the resource system, and the groups with rights to use water.

2. Proportional equivalence between benefits and costs. Rules specify the amount of water that a user is allocated related to local conditions and to rules requiring labour, materials, and/or money inputs.

3. Collective-choice arrangements. Many of the individuals affected by harvesting and protection rules are included in the group who can modify these rules.

4. Monitoring. Monitors, who actively audit biophysical conditions and user behaviour, are at least partially accountable to the users and/or are the users themselves.

5. Graduated sanctions. Users who violate rules-in-use are likely to receive graduated sanctions from other users, from officials accountable to these users, or from both.

6. Conflict-resolution mechanisms. Users and their officials have rapid access to low-cost, local arenas to resolve conflict among users or between users and officials.

7. Minimal recognition of rights to organise. The rights of users to devise their own institutions are not challenged by external governmental authorities, and users have long-term tenure rights to the resource.

8. Nested enterprises, since water resources are parts of larger systems, appropriation, provision, monitoring, enforcement, and governance activities should be organised in multiple layers.

9. Remove incentives that make water use harmful to social and environmental targets in the long run.

10. Accounting for true value and true costs of water production by sector.

11. Identify the successful actions. The results suggest that the Mediterranean groups at risk of drought already have solutions, but in some cases, politics are getting in the way.

Acknowledgments: This research was funded by the Spanish Ministry of Science and Innovation through the SECA-SRH project (PID2019-105852RA-I00) and the AG-WaMED project (PCI2022-132929), and also funded by the Universidad Politécnica de Madrid through the ADAPTA project (UPM ADAPTA).

References

Alexander M, Priest S, Mees H (2016) A framework for evaluating flood-risk governance. Environmental Science Policy 64: 38–47. https://doi.org/10.1016/j.envsci.2016.06.004

Estrela T, Sancho TA (2016) Drought Management Policies in Spain and the European Union: From Traditional Emergency Actions to Drought Management Plans. Water Policy 18: 153–176

Garrote L, Granados A, Iglesias A (2016) Strategies to reduce water stress in Mediterranean river basins. Science of the Total Environment 543: 997 - 1009

Hagenlocher M, Meza I, Anderson CC, Min A, Renaud FG, Walz Y, Sebesvari Z (2019) Drought vulnerability and risk assessments: state of the art, persistent gaps, and research agenda. Environmental Research Letters 14(8): 83002. https://doi.org/10.1088/1748-9326/ab225d

Iglesias A, Assimacopoulos, Van Lanen HAJ (eds) (2018) Drought: Science and Policy. John Wiley and Sons, Ltd

OECD (2021) Agriculture and Water Policies: Main Characteristics and Evolution from 2009 to 2019. Available online: https://www.oecd.org/agriculture/topics/water-and-agriculture/documents/oecd-water-policies-country-note-spain.pdf (accessed on 4 January 2021)

Raikes J, Smith TF, Jacobson C, Baldwin C (2019) Pre-Disaster Planning and Preparedness for Floods and Droughts: A Systematic Review. Int. J. Disaster Risk Reduct 38: 101207

Urquijo J, De Stefano L (2020) Perception of drought and local responses by farmers: a perspective from the Jucar River Basin, Spain. Water Resources Management 30(2): 577-591

Multi-criteria analysis and characterization of the integrated water resources management model in the Annaba region

A. Hani*, D. Nechem, S. Hani, N. Bougherira, F. Toumi, L. Djabri, H. Chaffai
Water Resources and Sustainable Development Laboratory. Badji Mokhtar Annaba University, BP 12, 23000, Algeria
** e-mail: haniazzedine@yahoo.fr*

Introduction

In Algeria, the ratio of water resources per inhabitant and per year which was 1500 m^3 in 1962 is only 500 m^3 today. This situation of water shortage has had serious consequences on the economy, the ecosystem, the quantitative and qualitative state of water resources.

To ensure sustainable management of water resources, this research proposes the development of a model that integrates both socio-economic data (population, income, land use, tourism connection rate, leaks, etc.), data relating to pollution pressures (solid waste, generation of domestic wastewater, pesticides, chemical fertilizers, service stations, etc.), water quality (nitrates, chlorides, nitrites, etc.), public health, the ecological impacts (mortality, loss of productivity, etc.) and the responses of decision-makers (desalination of seawater, storage of rainwater, water treatment, etc.). The DPSIR model (Driver – Pressure – State – Impact - Response) is applied to characterize the relevant variables of water management (Plan Bleu 2003; PNUE/PAM-Plan Bleu 2009; Rivm 1995). Validation is achieved through the results of expert opinion.

Materials and methods

The tools chosen for this research work were ANN, expert opinion and judgment, health risk assessment, basic statistics and multivariate techniques. There are five steps in the proposed methodology to develop a conceptual water integrated model.

Step 1: the first step expresses the creation of the ANN model, the characterization and prioritization of the effective variables and the establishment of the modelling prediction relationships.

Step 2: the second step indicates the analysis of the questionnaire undertaken to explore the expert opinion and judgment of various stakeholders using descriptive statistics. The results of Step (2) was compared with the results of ANN in Step (1) to examine the understanding and knowledge of the local experts about the actual baseline conditions of water sector.

Step 3: Transformation of data variables that were not Normally distributed, and calculation of the correlation matrix, were carried out in Step (3) for the selected variables from Step (1).

Step 4: Three techniques of multivariate analysis were undertaken in Step (4) for the selected variables, to classify them with the relevant municipalities.

Step 5: This final step explains the health risk assessment of Annaba Wastewater Treatment Plant as a contaminated hotspot. It assessed the health risks associated with the current disposal of wastewater on the sea shore close to the bathing areas. The chemicals identified as carcinogenic risks were fed back into the Conceptual Water Integrated Model in Semi-Arid Mediterranean region (CWIMSAM model).

The results of Steps (1) and (4) were also fed back to complement the CWIMSAM with the selected priority variables and geographical areas under water stresses. The whole results will be a basis and an input to evaluate the water plan through Strategic Environmental Assessment study which is beyond the scope of this research work.

In this study, we present the main results obtained from analysis of socio-economic data in addition to the synthesis of the results of the five categories analysis: socio-economic aspects, anthropogenic pollution pressures, state of water quality, public health and ecological impacts and the institutional responses.

The new conceptual water integrated model was applied to the life cycle of water resources management in Annaba region. Annaba is currently facing a serious shortage of good quality fresh water.

This region has been divided into 21 agglomerations presenting the most homogeneous geological, hydrological and socio-economic properties possible.

Results and concluding remarks

In this research a new conceptual water integrated model has been developed based on cause-effect relationships (Figure 1). The new model depicts the most important elements and sciences related to water, and indicates that water resource development and management must be within the ecological sustaining limits of available natural water resources. The new conceptual water integrated model was applied to the life cycle of water resources management in Annaba region.

The effective variables have been characterized and prioritized using multi-criteria analysis with ANN, risk assessment techniques and expert opinion and judgment. The selected variables have been classified and organized using multivariate techniques which are cluster analysis, principal component and classification analysis and factor analysis.

The conclusions of data analysis using the techniques of ANN, basic statistics, multivariate, health risk assessment and expert opinion and judgment can be summarized as follows:

All water policy and management responses are significant. Sustainable coastal aquifer management must take into consideration technical engineering as well as managerial interventions such that top priority should be given to the reuse of treated wastewater in agriculture followed by desalination of water.

Cadmium has the highest total hazard index, followed by Chromium VI, whilst copper has the lowest for both adults and children. This research also makes it possible to classify the municipalities or the group of municipalities according to their specific problems. The water plan should be reformulated to reflect priority water issues and geographical areas under pressure.

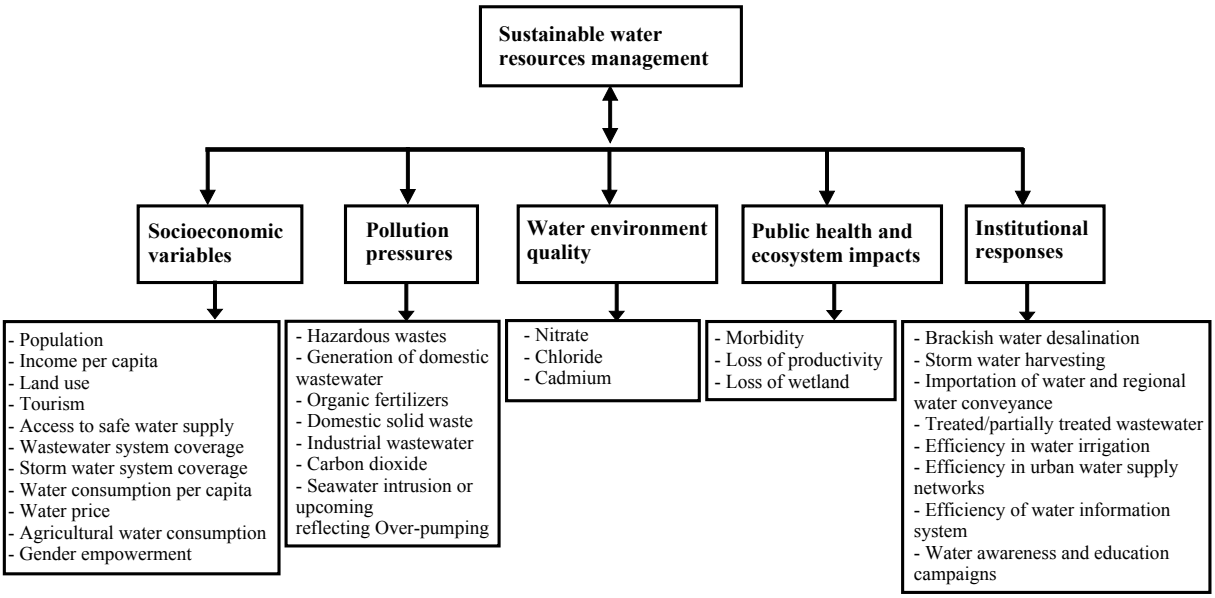

Figure 1. Conceptual water integrated model for Annaba including significant variables.

References

Plan Bleu (2003) Commission Méditerranéenne du Développement Durable, résultats du Forum de Fiuggi sur les "Avancées de la gestion de la demande en eau en Méditerranée" Constats et Propositions

PNUE/PAM-Plan Bleu (2009) Etat de l'environnement et du développement en Méditerranée. PNUE/PAM-Plan Bleu, Athens

Rivm (1995) A General Strategy for Integrated Environmental Assessment at the European Environment European Environment Agency. Copenhagen, Denmark

12th World Congress on Water Resources and Environment (EWRA 2023)
"Managing Water-Energy-Land-Food under Climatic, Environmental and Social Instability"
Thessaloniki, Greece, 27 June - 1 July 2023

Water resources in England and Wales: The rise again of national planning

A. Leonard[1*], J. Amezaga[1], R. Blackwell[2], E. Lewis[1], C. Kilsby[1]
[1] The Water Group, School of Engineering, Newcastle University, Newcastle Upon Tyne, UK
[2] Director of Water Resources West, United Utilities Water
* e-mail: a.leonard4@newcastle.ac.uk

Introduction

Water regulators in England and Wales have called on water companies to meet higher standards of supply resilience in response to growing pressures from climate change, environmental needs and growth whilst still maintaining affordability. New national and regional governance structures have been established with the aim of enabling better collaboration across water companies and other water abstractors to find and deliver the most efficient and robust water supply infrastructure schemes.

To understand how and why a more strategic direction and multi-scale structure has been introduced, this study takes a historical perspective exploring the pathway dependencies and drivers of change that led to this new approach to governance.

Although previous papers have explored the history of water resources governance in England and Wales (Kinnersley 1988; McCulloch 2009; OFWAT 2006; Taylor et al. 2009), they do not capture recent developments and the topic has not been explicitly studied in relation to multi-scale governance.

Materials and methods

This study takes a qualitative approach using data from interviews, workshops, and analysis of published planning documents and the available literature.

Twenty-four semi-structured interviews have been carried out with sixteen participants from across the water industry including regional planning leads, regulators, government officials, and water resources planners from water companies and consultancies. Two workshops were carried out with six and eight participants (respectively). Policy and planning documents and academic literature were reviewed and analysed.

The data was collated in a timeline and organised thematically using NVIVO software.

Results and concluding remarks

We find that water resources planning in England and Wales has undergone several historic shifts in scale that have occurred in a non-linear fashion, responding to a complex landscape of physical and institutional pathway dependencies, drivers, and constraints. We have demarcated six eras of water resources planning; (1) local, fragmented, and piecemeal, (2) early consolidation, (3) strategic national planning, (4) regional integrated planning, (5) privatised zonal planning and regulation, (6) rise of national and regional alongside continued company level planning, as illustrated in Figure 1. The length of each era and ultimate transition to a new scale of planning depended on a multitude of constraining and driving factors that are often peculiar to the specific time and context that surrounded the transitions.

Recently, a more strategic approach involving regional and national scale planning has emerged in response to a growing recognition that the existing planning frameworks established at privatisation were failing to increase resilience in the face of climate change, growth, and environmental pressures and unable to secure consent for large new infrastructure assets, such as reservoirs.

A new more collaborative model has been instigated with a multi-scale governance structure, including five new regional groups currently operating on a voluntary basis.

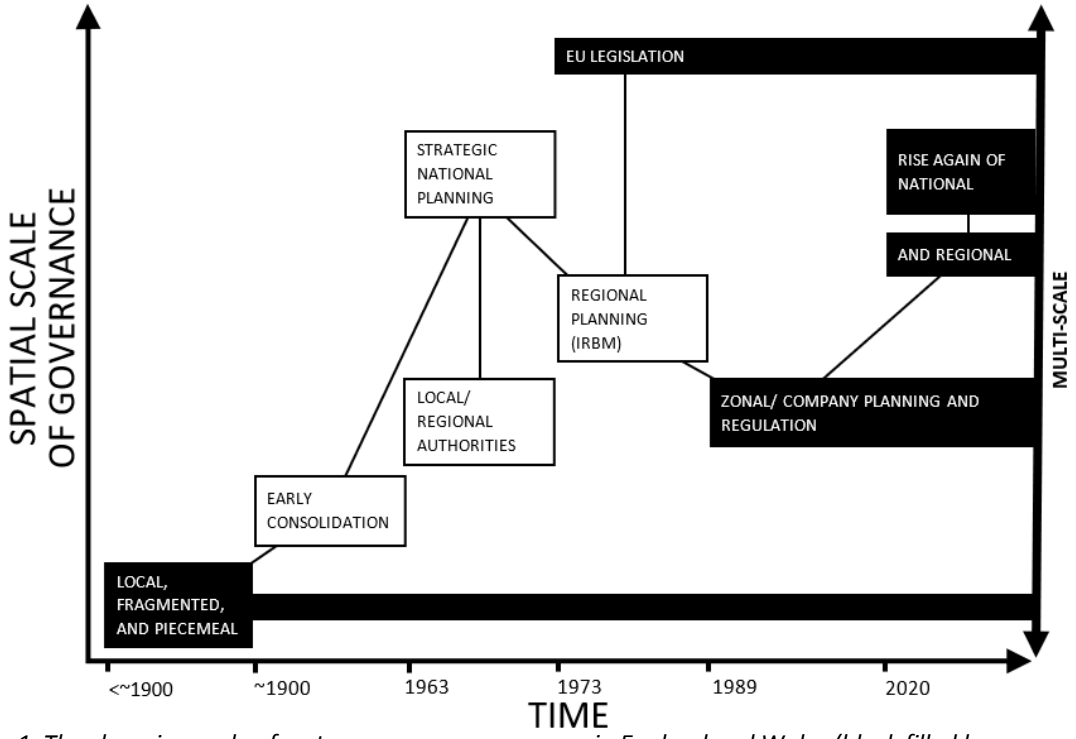

Figure 1. The changing scale of water resources governance in England and Wales (black filled boxes represent continuing governance structures, white filled boxes represent defunct governance structures).

Whilst instilling new requirements for alignment, cooperation, and resourcing, these strategic approaches are working alongside continuing legally mandated and highly regulated water company planning, which has developed and matured over the last three decades. Key to success will be overcoming constraints to enable effective communication of national strategies and priorities down to the local level, and local constraints and needs up to the national level.

The emerging governance frameworks are attempting to establish and integrate multiple scales for the first time since the sixties, and ultimately will be judged to have succeeded if the process results in aligned plans across all scales that meet long term water supply needs. Success or failure, lessons learned from this transition to a multi-scale approach may provide wider insight for decision makers involved in complex, long-term, multi-stakeholder decision making under uncertainty.

Acknowledgments: This work is funded by the UK Engineering and Physical Sciences Research Council (EPSRC) and United Utilities Water as part of the Water Infrastructure and Resilience (WIRe) Centre of Doctoral Training (CDT) (https://cdtwire.com/).

References

Kinnersley D (1988) Troubled water: Rivers, politics and pollution. Hilary Shipman. London

McCulloch CS (2009) The Water Resources Board: England and Wales' Venture into National Water Resources Planning, 1964-1973. 2(3): 15

OFWAT (2006) The development of the water industry in England and Wales. https://www.ofwat.gov.uk/wp-content/uploads/2015/11/rpt_com_devwatindust270106.pdf

Taylor V, Chappells H, Medd W, Trentmann F (2009) Drought is normal: The socio-technical evolution of drought and water demand in England and Wales, 1893–2006. Journal of Historical Geography 35(3): 568–591. https://doi.org/10.1016/j.jhg.2008.09.004

Impact of the Covid-19 on water poverty in Alicante case study

R. Abad
Interuniversitarian Institute of Geography, University of Alicante, Spain
e-mail: ricardo.abad@ua.es

Introduction

Water poverty is a recent phenomenon in Europe. It appeared after the 2008 crisis. Many households lost their income, coming to have difficulties and even not being able to pay their water bills. For this, is an urban phenomenon of affordability, which authors such as Bradshaw et al. (2013) in UK. In Spain stand out the investigations of Yoon (2017), focused on the social response. Also, Morote et al. (2018), who studied domestic fraud in Alicante. After overcoming the crisis, improving the situation of households also reduced the incidence of water poverty. But the appearance of the Covid-19, and the measures adopted such as the lockdown, devastated the economy. This crisis especially affected precarious workers, who were left without income (Llorente 2020). For this, the main hypothesis of this research is that water poverty must have increased as a consequence of this crisis, especially in those places where tourist activities have a significant weight. For this reason, Alicante was selected, as tourism has a significant impact on its economy and employment. An example is the 14.4 million tourists in this province in 2019 (GVA 2020).

To analyse the impact of Covid-19 on water poverty in the city of Alicante, the main objective was to demonstrate the significant increase in the incidence, and that it is distributed unevenly. But also, spatially locate the phenomenon of water poverty, since due to its characteristics it is difficult to locate it in the urban space. For this, it was proposed to obtain data on non-payment of water bills, analyse these data statistically, and through GIS locate and demonstrate this unequal incidence in the city. Furthermore, this is a pioneering study in locating water poverty spatially, and its recent evolution.

Materials and methods

First, an Excel file was obtained from the company Aguas de Alicante with the data on domestic contracts and defaults (2014-2021). These data are essential for statistical analysis, being of great value due to its quantitative and objective nature, and they are the best way to measure the real incidence of water poverty. These data were grouped by neighbourhoods. For this reason, the layer of census units for Alicante was downloaded from the National Institute of Statistics. This shapefile layer was loaded in the free software Quantum GIS 2.18, and the units corresponding to each neighbourhood were grouped. With this, 47 spatial objects were obtained (neighbourhoods of Alicante), each with a census code.

Within Excel, the percentages of defaults by neighbourhood were calculated, as well as the percentage of contracts with 3 or more defaults in each neighbourhood. Subsequently, the file was prepared and saved as a comma-delimited csv to be loaded in Qgis, indicating the census unit code for each neighbourhood. Next, the file was loaded into the software, and using the "joint" option, the database was joined to the layer of spatial objects, using the census code as a common identifier.

Afterwards, the results of the percentage of defaults by neighbourhood for the years 2018 and 2021 were classified by ranges. These two maps are the cartographic results of Figure 1. Finally, the Excel file was returned to analyse and compare the statistical data, an analysis that is presented in the following section on results, the most relevant being those collected in Table 1.

Results and concluding remarks

The results of the research confirm the hypothesis that the crisis derived from Covid-19 increased water poverty in Alicante. This can be seen in Figure 1, where there is an increase in urban areas with more than 10% of households in default, going from 11 areas in 2018 to 13 in 2021. While urban areas with between 7 and 10% of non-payments went from 9 in 2018 to 12 in 2020. In turn, these maps show the unequal

incidence of water poverty in the city, especially in the Carolinas – Virgen del Remedio/Juan XXIII axis. And to the west in Ciudad de Asís.

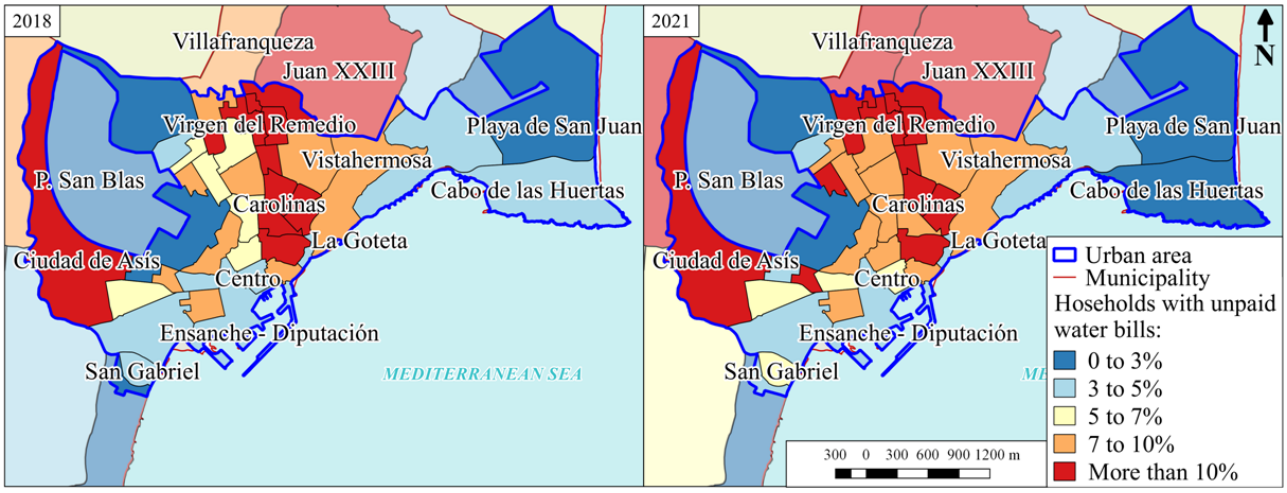

Figure 1. Households with unpaid water bills in Alicante, by neighbourhoods (2018-2021).

Table 1 also shows these results that confirm the hypothesis, evidencing the growth of water poverty after the Covid-19 crisis, worsening the situation in already highly vulnerable areas. But also, in the city as a whole, since the percentage of households with defaults went from 9.77% in 2018 (17.407 households with defaults out of 178.638), to 10.78% in 2021 (19.625 households with defaults out of 182.116).

Table 1. Evolution of the neighbourhoods with more homes with unpaid water bills (2018-2021).

	Total households in 2018	Households with unpaid water bills in 2018	Total households in 2021	Households with unpaid water bills in 2021
Colonia Requena	936	515 (59,51%)	946	597 (68,18%)
Virgen del Carmen	1.104	575 (55,07%)	1.095	653 (65,11%)
Juan XXIII	4.950	1.542 (34,46%)	4.964	1.632 (39,10%)
Virgen del Remedio	7.025	2.009 (31,96%)	7.052	2.111 (35,83%)

For this reason, Alicante's fragility in the face of water poverty is demonstrated, since a crisis can make it grow rapidly, in a city where it is already important. It has also been possible to locate it spatially, a crucial aspect since it was the main barrier to analyse it, since for this it is necessary to have data that is not easily accessible. Just as it is a field that is still little studied as it is a recent phenomenon.

Acknowledgments: This research is the result of a pre-doctoral contract funded by the University of Alicante (UAFPU2019B-01), and the research project "Assessment of water poverty in urban environments of the Mediterranean coast: case studies." founded by the MICINN (PID2019-104456RB-C22).

References

Bradshaw J, Huby M (2013) Water Poverty in England and Wales. Journal of poverty and Social Justice 21: 137-148. https://doi.org/10.1332/175982713X669835

GVA Turisme (2020) Evolution of tourist activity. Alicante province

Morote Á, Hernández M, Rico A (2018) Patterns of water consumption in tourist-residential uses on the coast of Alicante (Spain) (2005-2015). An uneven trend influenced by the urban typology and degree of occupancy. Annals of Geography of the Complutense University 38: 357-383. https://doi.org/10.5209/AGUC.62484

Llorente R (2020) Impact of COVID-19 on the labour market: an analysis of vulnerable groups. Work documents 2: 1-29

Yoon H (2017) The politicization of energy and water from vulnerable populations. The case of energy and water poverty in Barcelona. Nature, territory and city in a global world 2017: 1239-1247

12th World Congress on Water Resources and Environment (EWRA 2023)
"Managing Water-Energy-Land-Food under Climatic, Environmental and Social Instability"
Thessaloniki, Greece, 27 June - 1 July 2023

Fuzzy cognitive mapping of stakeholders' perception of water resources management

M.C. Gunacti*, C.P. Cetinkaya, A. Gul, G. Onusluel Gul, F. Barbaros
Dokuz Eylül University, Faculty of Engineering, Department of Civil Engineering, Izmir, Turkey
** e-mail: mert.gunacti@deu.edu.tr*

Introduction

Fuzzy Cognitive Mapping (FCM) is an essential qualitative soft computing method that was added to cognitive maps (CM) by Kosko (1986). Fuzzy logic, neural networks, and genetic algorithms are examples of soft computing techniques that have the potential to simplify difficult issues. FCM has received a lot of interest from researchers due to its superior capacity to model dynamic and complicated issues. FCM is a graph-based technique that, like any conventional CM, is made up of concepts and causal connections. The distinction is that in FCM, the relationships between concepts are defined by fuzzy connections and their models are fuzzy sets. Integrating FCM into the Water Resources Management (WRM) topic and combining it with various related problems such as climate change (Cakmak et al. 2013), sustainability (Bahri et al. 2020), etc., has been a relatively recent one.

The presented study investigates the perception of the Menemen Plain (MP) stakeholders on WRM through a survey, which is then evaluated by the FCM approach. MP is located at the outlet of the Gediz River Basin (GRB), which is one of the major river basins of Turkey with pressures related to anthropogenic activities and climate change. Thus, MP suffers from both water quantity and quality. The sectors' competition for water and also the increase in water demand both further aggravate water scarcity.

Materials and methods

In order to evaluate the perception of the MP stakeholders, a survey consisting of WRM-related topics has been developed. The survey simply asks participants to match the given concepts to one another. The survey was directed to invited stakeholders in a roundtable meeting organized in MP on October 2022. A total of 20 participants has taken the survey. According to their responses, average weight values between the concepts have been determined as initial values for the concepts. The links among the concepts have weight values that represent the strength of the relevant relation w_{ij} and ranges from -1 to 1. A positive weight reflects positive causation from concept C_i to concept C_j, a negative weight represents negative causality, and a zero weight represents no causality.

FCMs' collection of causal weights is represented in an NxN matrix known as a weight matrix or adjacency matrix, where N is the number of concepts in the model. The proposed graph structure for FCMs enables a system's dynamics to be analysed by conducting simple computations based on the weight matrix and the concepts' starting state values. A vector called the state vector represents the collection of concept values as follows (Eq.1).

$$C_i^{(k+1)} = F(C_i^{(k)} + \Sigma_{j=0}^{n} C_j^{(k)} \times w_{ji}) \quad (1)$$

where $C_i^{(k+1)}$ is the activation value of concept C_i at iteration k + 1, $C_i^{(k)}$ is the value of node C_i at iteration k, w_{ji} is the weight of the cause–effect relationship between C_j and C_i, and F is a threshold function (such as a sigmoid function) that is used to rescale the results of the sum into the interval between 0 and 1 or between − 1 and + 1. In this case log-normal (sigmoid) function was selected to rescale the results into -1 and +1, since the defined concepts have both negative and positive directional effects.

Results and concluding remarks

According to the responses of the survey participants, a total of 20 concepts related to WRM have been interconnected (Figure 1). The selected concepts in the survey not only represent the concepts of WRM, but also

the key challenges described by the stakeholders. The concepts are represented in a color-themed manner, i.e., blue for Water, green for the Environment, yellow for Food, and orange for Socio-economy. Furthermore, the 6 scenarios have been investigated under 3 main concepts' (i.e., water scarcity, agricultural land fragmentation, and agricultural input costs) state changes in the positive or negative direction (+100% or -100%).

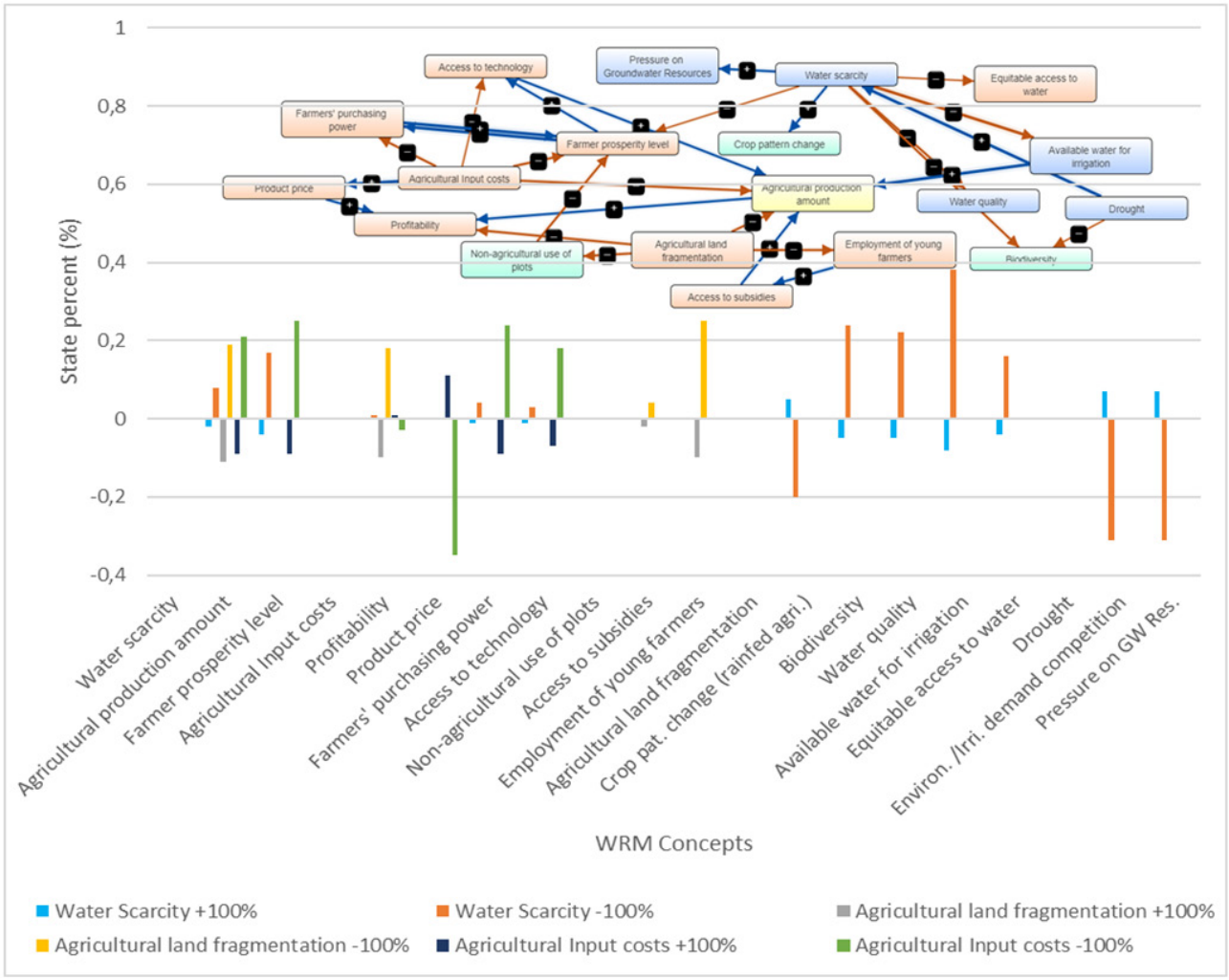

Figure 1. FCM model and its results under the investigated scenarios.

According to the results, agricultural production amount and profitability are the most vulnerable concepts within the examined model due to their tendency to respond in every scenario, excluding the response magnitude. On the other hand, the product price, available water for irrigation, environmental water needs vs. the irrigation demand competition, and the pressure on the groundwater resources have been the most vulnerable concepts, considering their response magnitude.

Acknowledgments: This study has been conducted within the frame of LENSES project (Call 2020 Section 1 Nexus IA), which is funded by the Horizon 2020 European Union Funding for Research & Innovation under the Partnership for Research and Innovation in the Mediterranean Area Programme (PRIMA).

References

Bahri O, Mourhir A, Papageorgiou E (2020) Integrating fuzzy cognitive maps and multi-agent systems for sustainable agriculture. Euro-Mediterranean Journal for Environmental Integration 5: 1-10. https://doi.org/10.1007/s41207-020-0143-8

Cakmak EH, Dudu H, Eruygur O, Ger M, Onurlu S, Tonguç Ö (2013) Participatory fuzzy cognitive mapping analysis to evaluate the future of water in the Seyhan Basin. Journal of Water and Climate Change 4: 131-145. https://doi.org/10.2166/wcc.2013.029

Kosko B (1986) Fuzzy cognitive maps. Int J Man–Mach Stud 24(1): 65–75. https://doi.org/10.1016/S0020-7373(86)80040-2

12th World Congress on Water Resources and Environment (EWRA 2023)
"Managing Water-Energy-Land-Food under Climatic, Environmental and Social Instability"
Thessaloniki, Greece, 27 June - 1 July 2023

SIGRIAN and DANIA to promote measurement of agriculture water use

V. Manganiello*, M. Ferrigno
Research Centre for Agricultural Policies and Bioeconomy (CREA-PB), Italy
** e-mail: veronica.manganiello@crea.gov.it*

Introduction

In Italy, irrigation water management is applied in a collective way by Local Agencies for Water Management (LAWM) for 50% of the irrigated utilized agricultural area and for 63% of water withdrawals for irrigation (Bellini 2014), ensuring withdrawal from water bodies, water supply (irrigation network) and defining water supplying procedures to users (irrigation practice).

The knowledge of water uses is fundamental for efficient water management and for promoting water pricing policies required by art.9 of European Water Framework Directive (WFD). In 2015, the Italian Ministry of Agriculture published the *Italian National Guidelines for the quantification of irrigation volumes by Regions (*Zucaro et al. 2019). To encourage their widespread application, an administrative procedure was defined through the joint use of SIGRIAN and DANIA, two multifunctional and highly interconnected information systems databases developed by CREA PB.

Materials and methods

The two databases have their own specific application for which they were designed.

SIGRIAN "National Information System for Water Management in Agriculture" (www.sigrian.crea.gov.it) is a GIS based platform developed by CREA-PB to provide an overview of the Italian irrigation system; it is the Italian reference Geodatabase to collect data at national scale, including the irrigation volumes data (Zucaro et al. 2017). For collective irrigation, LAWMs should transmit to SIGRIAN in a specific timing, among all, information on measured or estimated water volumes for collective irrigation (withdrawals, uses, return flows) that must be technically validated by the Regions and Autonomous Provinces. In water and agriculture policy planning (CAP, WFD) SIGRIAN data supports the definition of the context and needs of water use for irrigation.

DANIA "National Database of Investments for Irrigation and Environment" (https://dania.crea.gov.it/) was realized to help the Ministry of Agriculture in programming and monitoring infrastructural intervention plans for irrigation efficiency. It contains structural and financial information on financed and programmed projects implemented by LAWMs. The detailed information on each interventions makes it possible to catalogue them and, thus, select them basing on technical, financial, and environmental criteria. These parameters can be used both in the programming phase (Ferrigno et al. 2022) and in the monitoring phase of the financed projects, to evaluate the efficacy of the policies, through the quantification of appropriate indicators (e.g., water saving achieved) (Zucaro et al. 2021). DANIA also allows to record the compliance, by each LAWM, with the quantification of the irrigation volumes in SIGRIAN.

Beyond the specific applications, the combined use of the two databases makes it possible to expand their effectiveness. To promote use of SIGRIAN by LAWMs, the Ministry of Agriculture imposed the compliance with quantification of volume in SIGRIAN as a precondition for financing collective irrigation infrastructure in some public investment Programs, such as collective investment irrigation programme financed by Next Generation EU funds, through National Recovery and Resilience Plan. In this procedure for LAWMs not compliant with water volumes monitoring obligations, the interventions programmed in DANIA could not be selected for funding. For financed project, the maintenance of compliance is a post-financing obligation, under penalty of revocation of the funding. Therefore, in this case, the compliance with volumes monitoring obligation represents, for the beneficiaries of interventions on irrigation infrastructures, both a prerequisite for funding and an ex-post obligation (see Figure 1).

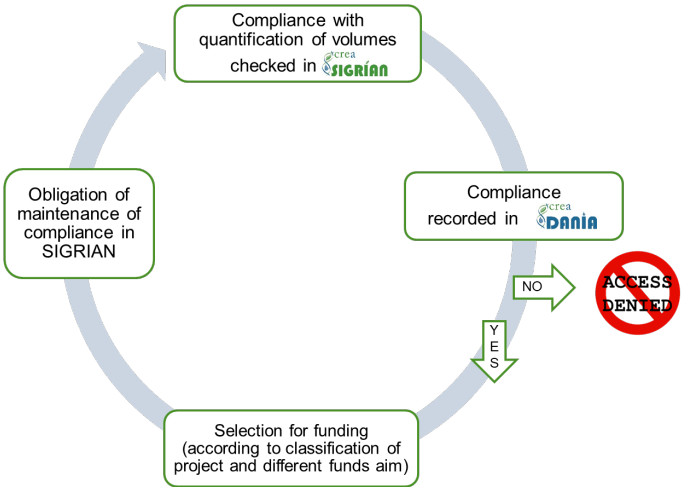

Figure 1. Procedure of checking compliance with the water volume quantification requirement.

The Italian government is recently adopted a law to extend this administrative procedure to all public authorities financing collective irrigation infrastructure, even in CAP Strategic Plan.

Results and concluding remarks

SIGRIAN contains more than 600 LAWMs of which 355 have projects registered in DANIA. The percentage of completeness of the data in SIGRIAN is equal to 43%.

According to DANIA information, 42% of LAWMs present in DANIA is compliant to volumes quantification in SIGRIAN, only 1% of them is not compliant. For the remaining 57% the information is still missing.

The procedure applied by Ministry of Agriculture to NRRP selection, led to an increase of 60% of water volumes information in SIGRIAN for the period 2016-2018, at national level.

Therefore, the application of the new law and the extension of this approach at a general level are expected to give an even greater incentive. The goal is to achieve a level of completion of SIGRIAN such as to make complete and shared data on water use available to Regions, Ministries, and River Basin District Authorities, for the purposes of planning agricultural policies and water pricing.

Acknowledgments: SIGRIAN and DANIA were developed under European Agricultural Fund for Rural Development and Development and Cohesion Fund respectively.

References

Bellini G (2014) 6° Censimento Generale dell'Agricoltura. Utilizzo della risorsa idrica a fini irrigui in agricoltura. ISTAT, 344 p

Ferrigno M, Lorenzetti R, Folino LA, Zucaro R (2022) The new Italian web database to support irrigation investment policies: DANIA, in International. Journal of Sustainable Agricultural Management and Informatics 8(1): 64-83. https://doi.org/10.1504/IJSAMI.2022.123047

Zucaro R, Giannerini G, Pepe AG, Tascone FL, Martello M (2017) Water Data Sharing in Italy with SIGRIAN WebGIS Platform. In: Salampasis M, Bournaris T (eds) Information and Communication Technologies in Modern Agricultural Development. HAICTA 2017. Communications in Computer and Information Science 953: 110-117. Springer, Cham. https://doi.org/10.1007/978-3-030-12998-9_8

Zucaro R, Ferrigno M, Manganiello V (2019) Italian approach to quantify water for irrigation. In: Garrote L, Tsakiris G, Tsihrintzis VA, Vangelis H, Tigkas D (eds.), Managing Water Resources for a Sustainable Future, Proceedings of the 11th World Congress of EWRA on Water Resources and Environment, 25-29 June 2019, pp 315-316, Madrid, Spain. http://drainage.cedex.es/site/docs/publicaciones/Garrote-et-al-(2019),-BICyL-EWRA2019_Proceedings.pdf

Zucaro R, Manganiello V, Lorenzetti R, Ferrigno M (2021) Application of Multi-Criteria Analysis selecting the most effective Climate change adaptation measures and investments in the Italian context. Bio-Based and Applied Economics 10(2): 109-122. https://doi.org/10.36253/bae-9545

12th World Congress on Water Resources and Environment (EWRA 2023)
"Managing Water-Energy-Land-Food under Climatic, Environmental and Social Instability"
Thessaloniki, Greece, 27 June - 1 July 2023

Group preference of criteria for selecting the location of pump stations: Better understanding of criteria interrelation through Bayesian BWM

Z. Srđević*, B. Srđević, S. Ždero, M. Ilić
Department of Water Management, Faculty of Agriculture, University of Novi Sad, Novi Sad, Serbia
** e-mail: zorica.srdjevic@polj.uns.ac.rs*

Introduction

Vojvodina Province, Serbia, is a lowland located in the Pannonian basin in southeast Central Europe. Due to the development of the drainage systems, especially the Danube-Tisza-Danube system with more than 20.000 km of drainage channels, Vojvodina Province is now the most important agricultural area in Serbia. To keep the system efficient, there are plans for the reconstruction of the network including the installation of new pump stations. The decision on where to locate the pumps is a complex problem that requires the participation of different sectors and analysis of different, usually conflicting, criteria. This problem is tackled using different multi-criteria methods, including analytic hierarchy process (AHP) (Srdjevic et al. 2007, 2012) and best-worst method (BWM) (Srđević et al. 2019). The methods are used in different group contexts to determine the weights of selected criteria by aggregating the preferences of involved decision-makers. The outcomes based on arithmetic or geometric averaging indicated that much of the information, especially related to (criteria) outliers, can be lost.

This paper presents the approach aimed at better understanding the interrelation of criteria for selecting the location of pump stations in Vojvodina Province, and in general, to calculate credal ordering i.e. confidence level as a measure of preference of one criterion over another by the group. The approach is introduced by Mohammadi and Rezaei (2020) as the Bayesian Best-Worst Method (B-BWM). Although new, it is used in many studies worldwide.

Materials and methods

If the decision criteria set is established, the application of the Bayesian version of the BWM can be divided into two parts. Firstly, the standard BWM is used by each decision-maker as follows: (1) the best and the worst criterion is selected; (2) pairwise comparison of best-to-other criteria are performed using 9-point ratio scale with numbers 1 for equally important to 9 for extremely more important; this way the vector A_B is created; and (3) pairwise comparisons are performed for worst-to-other criteria using the same scale, to create the vector A_W. Then, instead of calculating criteria weights based on the vectors A_B and A_W by solving optimization problems for each decision maker and then the aggregation of these vectors as in standard group BWM, the procedure continues as B-BWM with the probabilistic interpretation of inputs and outputs. Criteria are seen as random events, and their weights are thus considered as their occurrence likelihoods. Vectors A_B and A_W are modeled as a multinomial distribution, and criterion weights as Dirichlet distribution (Mohammadi and Rezaei 2020). The weights obtained for the multiple decision-makers are aggregated as the posterior distribution viewed from the probability perspective. Further, Mohammadi and Rezaei (2020) introduce a novel concept of the credal ranking "which can calibrate the degree to which one criterion is superior to one another" and provide a detailed mathematical description of their approach.

Full implementation of the B-BWM model in MATLAB and Python is provided at http:// bestworstmethod.com/software/ and is used here for the calculations and visualization of the credal ranking.

As a case study, we used the example provided by Srđević et al. (2019) and extended it with the evaluation of two more decision-makers. The objective was to find aggregated weights (importance) of the selected set of criteria for a group of three decision-makers by applying the B-BWM approach and to check what is the confidence level of criteria preferences. Criteria used for the assessment of pump station location are C1 – Economical parameters, C2 – Safety, C3 – Flood protection efficiency, C4 – Alignment with water supply planning scheme, C5 – Suitability for investment in phases, and C6 – Technical manageability.

Results and concluding remarks

The three decision-makers (DM1-DM3) provided two sets of preferences between criteria: best to others and worst to others (Table 1).

Table 1. Pairwise comparison of DM1-DM3 of best to other and other to worst criterion.

	C1	C2	C3	C4	C5	C6
Best to other criteria						
DM1 (best C2)	7	1	6	2	4	8
DM2 (best C3)	3	1	1	5	5	6
DM3 (best C3)	3	3	1	5	3	1
Other to worst criterion						
DM1 (worst C6)	2	9	5	6	4	1
DM2 (worst C5)	3	7	7	4	1	5
DM3 (worst C1)	1	7	7	3	3	5

Calculated average of the aggregated weight distribution is C1 - 0.11, C2 - 0.29, C3 - 0.22, C4 - 0.15, C5 - 0.12, and C6 - 0.12. Credal ranking graph of the criteria is given in Figure 1.

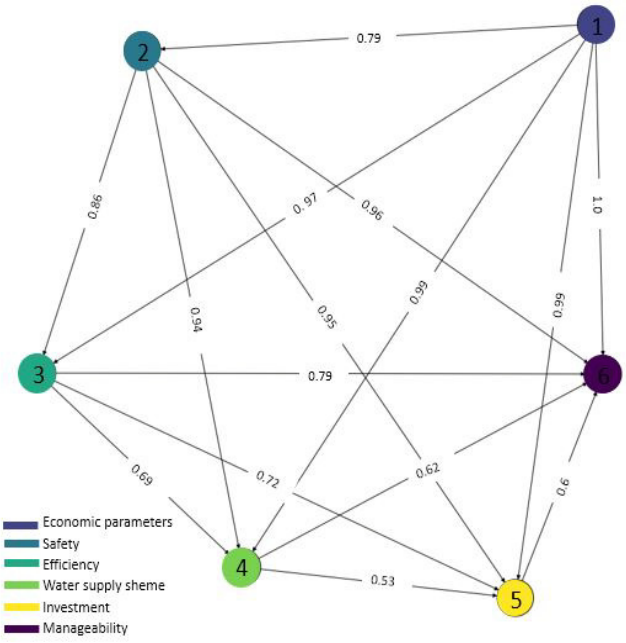

Figure 1. Credal ranking graph for the criteria C1-C6.

The values next to the arrows in Figure 1 show that criterion *X* is more important than criterion *Y* with reliability *r*. Referring to the graph, the superiority of C4 over C5 and C6 is weak (*r* = 0.53, and 0.62), as well as the superiority of C5 over C6 (*r* = 0.6). In a real-life application, this can be interpreted as a need to more carefully analyze the problem, the preferences, and the interrelation among criteria.

Acknowledgments: This work was supported by the Ministry of Education, Science and Technological Development of Serbia (Grant No.451-03-68/2023-14/200117).

References

Mohammadi M, Rezaei J (2020) Bayesian best-worst method: A probabilistic group decision making model. Omega 96, 102075. https://doi.org/10.1016/j.omega.2019.06.001

Srdjevic Z, Kolarov V, Srdjevic B (2007) Finding the Best Location for Pumping Stations in the Galovica Drainage Area of Serbia: The AHP Approach for Sustainable Development. Business Strategy and Environment 16(7): 502-511

Srđević Z, Srđević B, Bubulj S, Ilić M (2019) Primenljivost i efikasnost BEST-WORST metoda pri donošenju odluka u vodoprivredi. Vodoprivreda 0350-0519, 51(297-299): 147-154 (in Serbian)

Srdjevic Z, Bajcetic R, Srdjevic B (2012) Identifying the criteria set for multicriteria decision making based on SWOT/PESTLE analysis: a case study of reconstructing a water intake structure. Water Resources Management 26: 3379-3393. https://doi.org/10.1007/s11269-012-0077-2

Evaluating migration effects in Greece through a water, energy, and food nexus approach

K. Pappas[1,2*], C.S. Hamie[3], B. Daher[1,4], S. Williams[3], T. Rocabado-Apuri[3]
[1] Texas A&M Energy Institute, Texas A&M University, College Station, TX, USA
[2] Borders & Migration Program, Bush School of Government and Public Service, Mosbacher Institute for Trade, Economics, and Public Policy, Texas A&M University, College Station, TX, USA
[3] Bush School of Government and Public Service, Texas A&M University, College Station, TX, USA
[4] Department of Biological and Agricultural Engineering, Texas A&M University, College Station, TX, USA
* e-mail: kostis.pappas@tamu.edu

Introduction

In recent years, Europe, the U.S., and other regions globally have been facing increased refugee flows. People are forced to flee due to a legitimate fear of persecution, man-made causes (e.g., famine, war, conflict, violence), or as a result of natural disasters (e.g., environmental disaster, climate changes) (Daher et al. 2021). As of 2010, the Middle East and Europe have witnessed a surge in armed conflicts (Syria, Libya, Yemen, and recently Ukraine) that have led to increased refugee flows. With a high volume of migrants arriving in cities and refugee camps, governments and international organizations are challenged to provide adequate basic services. The challenge of maintaining adequate supplies of water, energy, and food demands becomes more nuanced in insular nations where population movements affect already vulnerable or struggling resources. The nexus approach has been used to address these interconnections in the insular context in various forms and models (Howells et al. 2013, p. 622 & 625), but none put so clear an emphasis on these as the WEF Nexus. This paper aims to conduct a scoping review of existing literature and current events in the context of the insular nation of Greece, to identify interconnections between water, energy, and food-related challenges as they relate to underlying conditions such as insularity and migration. This review will be utilized to highlight how through a Water-Energy-Food (WEF) Nexus approach (Figure 1) the way migration affects the water-food-energy systems in recipient countries, using economic, social, and environmental indicators.

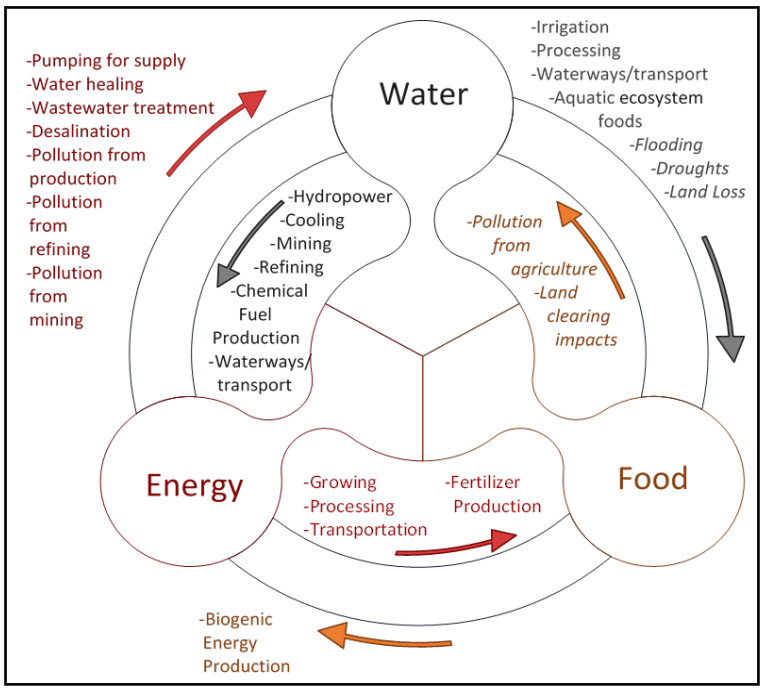

Figure 1. Water, Energy, and Food Nexus interconnections.

Materials and methods

Pressures on water, energy, and food systems in an insular context from climate change, migration patterns, and market sectors such as tourism make the use of a nexus approach vital to ensuring the sustainable livelihoods of island communities, as energy and food systems cannot function independently (Daw and Stout 2019, p. 5). The literature linking WEF with migration causes has a gap in analyzing the migration effects in destination countries using indicators related to WEF factors. This study was conducted as a scoping review of Greece's current situation. The main question that guided this review was: What are the interconnections between water, energy, and food challenges as they relate to insularity and migration in Greece? Following that, an evidence summary of more recent works on Greece's current condition was completed. Drawing on the example of Greece, based on the sustainability impact assessment methodological framework outlined by OECD (2010), combined economic, environmental, and social impacts were stressed down. The goal of this methodological framework was to identify and select contextually relevant and feasible economic, environmental, social, and political indicators relevant to migration and to investigate the utility of WEF Nexus for comprehending system interconnections and challenges at various scales. The methodology focused primarily on indicators that are or can be compiled by official statistical systems using administrative records and statistical surveys. The framework focused on quantitative as well as qualitative indicators. Efforts have been made to keep the indicators simple. The initial assessment identified possible impacts and set the focus points in the study design, breaking them down into economic, environmental, social, and political criteria.

Results and concluding remarks

Our research work to date shows that considering the case of Greece through a WEF Nexus approach is a complex undertaking that reveals many interconnections, not only between WEF Nexus factors but also between the underlying political and economic challenges and the recent migratory flows. The WEF Nexus is typically employed at a national or international level to consider large-scale resource tradeoffs. At this scale, this focus is on the continuity and security of the system as a whole. In contrast, utilizing WEF Nexus at an island level can reveal opportunities for local WEF Nexus management initiatives. E.g., our research made obvious that Greece must take into account the Nexus in planning for the sustainability of its tourism sector and ability to accept refugees and asylum seekers in its islands. The many interconnections between the WEF Nexus, recent triggering event of refugee crisis, and underlying challenges highlight the need for systems-based research that would then inform the empowerment of local WEF Nexus management initiatives. Local actors can better select management strategies that are more resilient and tailored to their constituents and to the unique local factors affecting water, energy, and food. Understanding the complex interconnections between political, economic, social, and WEF Nexus factors is key to identifying and capturing opportunities to increase WEF Nexus security and resilience and improve migration management. Understanding how migrants will impact the future size and composition of Greece’s population and its resources is important for public and private sector decision-makers who currently lack the tools for quantifying the impact of anticipated migration flows on these resource systems.

Acknowledgments: This research was made possible through the support of the Texas A&M Energy Institute Seed Grant Program.

References

Daher B, Hamie S, Pappas K, Karim NM, Thomas T (2021) Toward Resilient Water-Energy-Food Systems under Shocks: Understanding the Impact of Migration, Pandemics, and Natural Disasters. Sustainability 13: 9402. https://doi.org/10.3390/su13169402

Daw J, Stout S (2019) Building Island Resilience Through the Energy, Water, Food Nexus. Australian National Renewable Energy Laboratory, Department of Environment and Energy. Retrieved March 27, 2021, from https://www.nrel.gov/docs/fy19osti/74747.pdf

Howells M, Hermann S, Welsch, M (2013) Integrated analysis of climate change, land-use, energy and water strategies. Nature Clim Change 3: 621–626. https://doi.org/10.1038/nclimate1789

OECD (2010) Guidance on Sustainability Impact Assessment. OECD Publishing, Paris. https://doi.org/10.1787/9789264086913-en

12th World Congress on Water Resources and Environment (EWRA 2023)
"Managing Water-Energy-Land-Food under Climatic, Environmental and Social Instability"
Thessaloniki, Greece, 27 June - 1 July 2023

The complexity of the deep uncertainty in hydro-economic models: Assessment using a multi-model ensemble

H. González-López[1], C.D. Pérez-Blanco[1], F. Sapino[1], A. Hrast-Essenfelder[2], J.M. Bodoque[3]
[1] *Department of Economics and Economic History, Universidad de Salamanca, Spain*
[2] *Centro Euro-Mediterraneo sui Cambiamenti Climatici and Università Ca' Foscari di Venezia, Italy*
[3] *Faculty of Environmental Sciences and Biochemistry, Universidad de Castilla-La Mancha, Spain*
** e-mail: hector.gonzalez.lopez@usal.es*

Introduction

Climate change consequences are already obvious, threatening the water security of nearly 80% of the world's population (Vörösmarty et al. 2010). This is related not just to climate change, but also to population expansion, which increases demand for water in sectors such as agriculture (IPCC 2014), which consumes 70% of total water consumption and is a significant economic sector (Wada et al. 2017). As a result, this strategy should be founded on water economics, employing hydrological and economic models that accommodate farmers' competing interests as well as natural restrictions (such as water availability). Although hydro-economic models are designed to simulate water-human systems, the uncertainties associated with their projections are frequently overlooked. As a result, long-term strategies are increasingly employing Decision-Making Under Deep Uncertainty (DMDU) methods to assess deep uncertainty in hydrological conditions, economic development, and technological advancements, which are classified into two extreme levels of uncertainty (determinism and absolute ignorance) and four intermediate levels of uncertainty (Courtney 2001; Walker et al. 2003).

Materials and methods

This study created a multi-model ensemble framework comprised of four microeconomic models [2x multi-attribute mathematical programming (PMAUP), 1x positive mathematical programming (PMP) model, and 1x linear programming (WGP)] and the semi-distributed hydrological models Hydrologic Engineering Center-Hydrologic Modeling System (HEC-HMS) and the Soil & Water Assessment Tool (SWAT), which are linked in a modular fashion to simulate the water-human interaction scenario. As a modular approach, these interactions are linked via bidirectional protocols: i) Water management policies (increasing water prices) are implemented in the economic module, which results in land use changes based on farmer behavior. This behavior is simulated by the utility function from each micro-economic model, being defined by different attributes such as profit (in the case of PMP models) or profit, risk avoidance, and hired labor avoidance (in the case of PMAUP and WGP models). And (ii) the resulting land use and their water requirements are used as inputs to hydrological models to assess the impact of the policy shocks on the water cycle.

Results and concluding remarks

The resulting crop portfolios are shown in Figure 1. The baseline scenarios were set based on the ITACyL's land use for the calibration year, in this case, 2015. Scenarios P0.01, P0.02, and P0.03 are the obtained land use changes by the increasing prices (0.01€, 0.02€, and 0.03€). Since the calibration process varies across micro-economic models, minor disparities in each model's baseline may be observed.

The variation of the daily stored water in the Santa Teresa reservoir is calculated for the Tormes River Basin, which covers an area of 7,112 km². Each simulation from the different years has been carried out using the different micro-economics' outputs (land use changes and its water demand reductions) and altering different hydrological key parameters too (the maximum and minimum of soil storage, infiltration, and lag time values obtained among all calibrations).

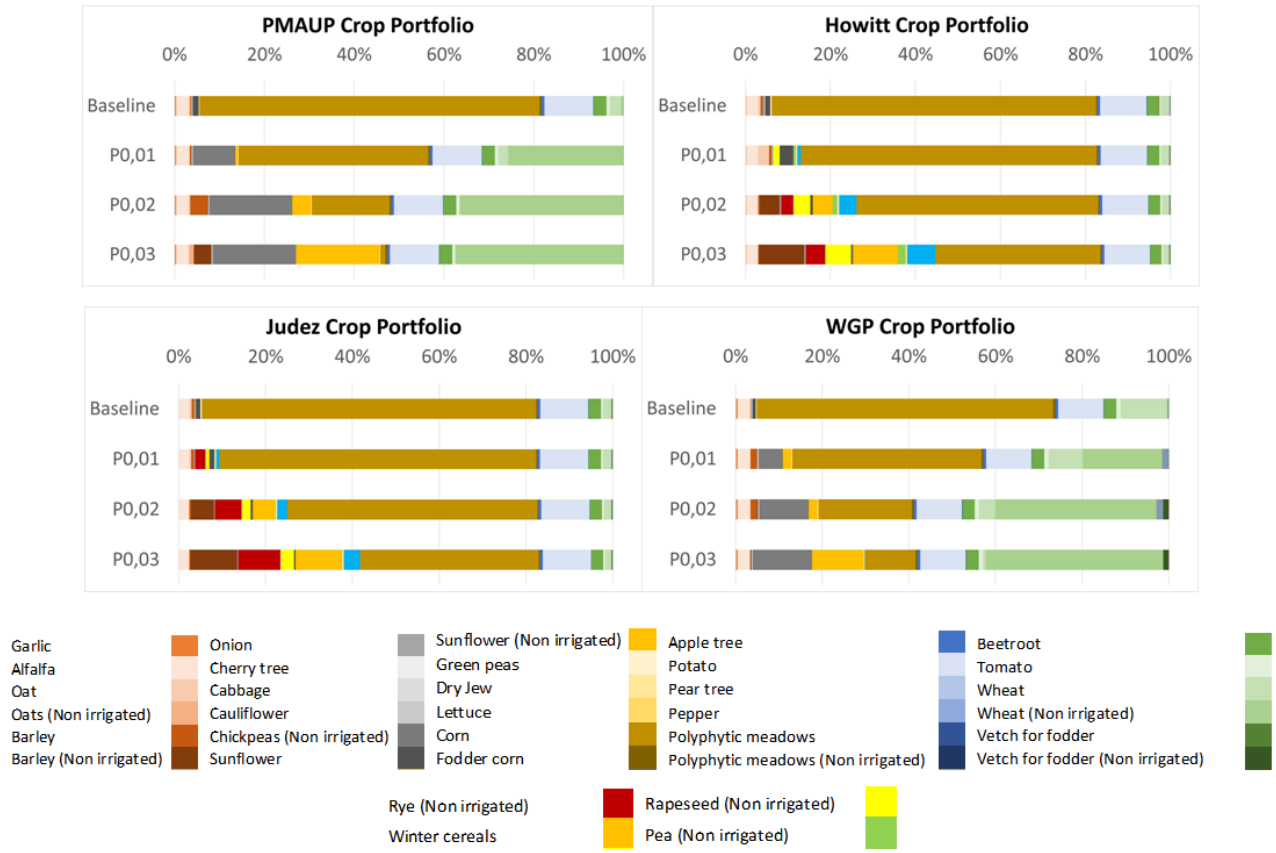

Figure 1. Simulated crop portfolio as an economic agent's response to the increased pricing policy.

As expected, the two PMP micro-economic models have almost the same response to the water management policies. On the other side, the WGP and PMAUP models present different responses to the increasing prices, showing more flexible responses in the reduction of water demand. In the WGP and PMAUP models, the economic agents' response is more likely to switch from irrigated to non-irrigated crops than in the PMP models, leading to a wider reduction in water demand as the price of water increases. The infiltration parameter has the most uncertainty, especially during the driest years.

Acknowledgments: The research leading to the results described in this presentation was carried out with the support of the TALANOA-WATER Project as a part of the PRIMA Programme, which is supported under Horizon 2020 (NUMBER 2023), the European Union's Framework Programme for Research and Innovation.

References

Vörösmarty CJ, McIntyre PB, Gessner MO et al. (2010) Global threats to human water security and river biodiversity. Nature 467(7315): 555-561. https://doi.org/10.1038/nature09440

IPCC (2014) Climate change 2014: Impacts, adaptation, and vulnerability. Part A: Global and Sectoral Aspects. Contribution of Working Group II to the fifth assessment report of the Intergovernmental Panel on Climate Change, Cambridge University Press

Wada Y, Bierkens MFP, de Roo A et al. (2017) Human–water interface in hydrological modelling: Current status and future directions. Hydrology and Earth System Sciences 21(8): 4169-4193. https://doi.org/10.5194/hess-21-4169-2017

Courtney H (2001) 20/20 Foresight: Crafting Strategy in an Uncertain World. Harvard Business School Press

Walker WE, Harremoës P, Rotmans J (2003) Defining Uncertainty: A Conceptual Basis for Uncertainty Management in Model-Based Decision Support. Integrated Assessment 4(1): 5-17. https://doi.org/10.1076/iaij.4.1.5.16466

XII. Global Water Security

12th World Congress on Water Resources and Environment (EWRA 2023)
"Managing Water-Energy-Land-Food under Climatic, Environmental and Social Instability"
Thessaloniki, Greece, 27 June - 1 July 2023

Availability and accessibility of climate and water data: Implications for water resources decision making and management in East Africa

M. Gitau[1*], V. Garibay[2], N. Kiggundu[3], S. Munishi[4], D. Moriasi[5], B. Mati[6], J .Kisekka[7], V. Kongo[8]
[1] Agricultural and Biological Engineering, Purdue University, West Lafayette, U.S.A.; [2] Informatics Institute, University of Amsterdam, Amsterdam, The Netherlands; [3] Department of Agricultural and Biosytems Engineering, Makerere University, Kampala, Uganda; [4] Civil and Environmental Engineering, University of Dar es Salaam, Dar es Salaam, Tanzania; [5] USDA ARS Oklahoma and Central Plains Agricultural Research Center, El Reno, U.S.A.; [6] Resource Plan, Nairobi, Kenya; [7] Aidenvironment, Kampala, Uganda; [8] Global Water Partnership Tanzania, Dar es Salaam, Tanzania
* e-mail: corresponding.mgitau@purdue.edu

Introduction

Surface and ground water availability in East Africa varies substantially with time and climate, and across subregions. Climate, land use, and land management changes are key factors affecting water security in the region, yet related data are generally insufficient, unavailable, or inaccessible for effective decision-making and management with respect to water resources (e.g. Näschen et al. 2018). The overall goal of this study was to evaluate current and future states of water resources with a view to providing water information, data access, and decision support for improved water resources decision-making and management in the region. This work focused on three East African countries—Kenya, Tanzania, and Uganda—as pilot study areas, selected due to their proximity to one another, as well as a common interest in water security at the regional level. For the evaluations, three key watersheds—one in each country—were selected for detailed study. These watersheds represent a variety of: landscapes from mountainous to coastal; and threats to water security including urbanization, climate change, and land degradation, thus allowing results to reflect the variety of climatic and landscape regions and to be differentiated by key threats.

Study Watersheds Description: The Sasumua River Watershed in Kenya is a 107 km^2 upstream watershed that is an important source of fresh water for the city of Nairobi. Water quality in this watershed is threatened by land degradation (Mwangi et al. 2015). Other concerns include the encroachment of agricultural land on forested areas and the limited information on the impacts of a changing climate. The 13,972 km^2 Simiyu River Watershed in Tanzania is a mixed land use watershed, which drains into Lake Victoria. Primary water uses are agriculture, fishing, and livestock production. Current threats to water security include land use and land cover change, pollutants in water courses, and high rates of erosion (Mulungu and Munishi 2007). The 40.9 km^2 Murchison Bay Watershed in Uganda supports a variety of human activities and, consequently, is impacted by anthropogenic perturbations particularly urban expansion (29%) and decreases in agricultural areas (18%), forests (6%), and wetlands (7%). These perturbations impact watershed water quantity and quality (Kiggundu et al. 2018).

Materials and methods

Baseline Data: A variety of climate and water data—including: observed water (quality and quantity) and climate data as available and shareable; continuous daily temperatures and rainfall amounts developed from climate reanalysis data (Garibay et al. 2021); and, future climate datasets derived from Coupled Model Intercomparison Project Phase 6 (CMIP6) projections—was acquired, processed, and deployed for use in this study and water resources decision making and management in the region. Spatial data were obtained from local sources in each country or from open data repositories such as the USGS Earth Explorer (https://earthexplorer.usgs.gov/) and ISRIC SOTER (https://www.isric.org/) databases. Other information necessary to support baseline modelling and scenario development was obtained from country-specific entities and local knowledge, and verified as needed through groundtruthing.

Modeling Applications: The Soil and Water Assessment Tool (Arnold et al. 1998), a continuous-simulation, daily time step, physically-based, watershed-scale model, was used in this study. The model was

selected so as to build on previous work in the study watersheds. Calibration and validation were conducted for each watershed with model performance being evaluated using pre-set performance criteria thresholds (Moriasi et al. 2015) and/or literature-based values depending on the extent and availability of measured data for use with model calibration and validation.

Scenario Evaluations: Subsequent evaluations involved quantifying: 1) impacts of various management practices and future climate scenarios on water resources (Sasumua River Watershed); 2) impacts of land use and climate change on water resources (Simiyu River Watershed); and, 3) impacts of land use changes considering historical, present, and future land uses (Murchison Bay Watershed). All scenarios were critical to policy and decision making in the respective countries.

Results and concluding remarks

Sasumua River Watershed: Results indicated that for three of four future scenarios water flows could be more than twice the values for the baseline period of 2011-2020. Filter strips were found to be the most effective single best management practice for reducing watershed sediment losses; however, combining all suitable management practices (riparian buffers, filter strips, terracing, field diversions, water harvesting ponds) would yield the best results overall.

Simiyu River Watershed: Precipitation has increased by 62% compared to the historical baseline period (1971-1999), with an anticipated increase of more than 100% in the future (2030-2060). Overland flow and total water yield are expected to increase rapidly in all future climate scenarios which could lead to increased incidences of flooding in the watershed, while sediment yield is expected to increase by more than 7% due to land use changes in the watershed.

Murchison Bay Watershed: Stream flow, surface runoff, and some nutrients have increased and are projected to increase with changing land use through 2040. Increasing population has been the leading driver of land use change and deteriorating water quality in the watershed. The implementation of vegetative filter strips at filter width of 2 m and 5 m could reduce sediment yield by 42% and 70%, respectively, while retention ponds of 20 m^3 could reduce surface runoff by 60%.

Implications for Policy and Decision Making: A primary recommendation was the need to implement a variety of management practices in anticipation of increased runoff and pollutant losses that will occur due to continued changes in climate and land use/land cover. Data availability and accessibility continued to present a challenge. As this introduces uncertainties into decision making processes, the need for updated data policies to improve curation and access to data was the strongest recommendation from this work.

Acknowledgments: This work was made possible in part through support provided by the U.S. Agency for International Development, through the LASER PULSE Program (Cooperative Agreement No. 7200AA18CA00009). The opinions expressed herein are those of the author(s) and do not necessarily reflect the views of the U.S. Agency for International Development.

References

Arnold JG, Srinivasan R, Muttiah RS, and Williams JR (1998). Large area hydrologic modeling and assessment part I: Model Development. J Am Water Resour As 34(1): 73-89. https://doi.org/10.1111/j.1752-1688.1998.tb05961.x

Garibay VM, Gitau MW, Kiggundu N, Moriasi D (2021) Evaluation of Reanalysis Precipitation Data and Potential Bias Correction Methods for use in Data-Scarce Areas. Water Resour Manag 35: 1587–1602. https://doi.org /10.1007/s11269-021-02804-8

Kiggundu N, Anaba LA, Banadda N, Wanyama J, and Kabenge I (2018) Assessing land use and land cover changes in the Murchison Bay Catchment of Lake Victoria Basin in Uganda. J Sustain Development 11(1): 44-55

Moriasi DN, Gitau MW, Pai N, Daggupati P (2015) Hydrologic and water quality models: performance measures and evaluation criteria. Trans ASABE 58(6): 1763-1785. https://doi.org/10.13031/trans.58.10715

Mulungu DMM, Munishi SE (2007) Simiyu River catchment parameterization using SWAT model. Phys Chem Earth 32: 1032-1039. https://doi.org/10.1016/j.pce.2007.07.053

Mwangi JK, Shisanya CA, Gathenya JM, Namirembe S, Moriasi DN (2015) A modeling approach to evaluate the impact of conservation practices on runoff and sediments in Sasumua watershed, Kenya. J Soil Water Conserv 70(2): 75-90. https://doi.org/10.2489/jswc.70.2.75.

Näschen K, Diekkrüger B, Leemhuis C, Steinbach S, et al. (2018) Hydrological Modeling in Data-Scarce Catchments: The Kilombero Floodplain in Tanzania. Water 10: 599. https://doi.org/10.3390/w10050599

12th World Congress on Water Resources and Environment (EWRA 2023)
"Managing Water-Energy-Land-Food under Climatic, Environmental and Social Instability"
Thessaloniki, Greece, 27 June - 1 July 2023

Development of agrohydrology in relation to critical zone science

Y. Zhao[1,2*], Y. Wang[1], E. Jobbagy[3]
[1] College of Resources and Environmental Engineering, Ludong University, Yantai 264025, Shandong, China
[2] Global Institute for Water Security, University of Saskatchewan, Saskatoon, Canada
[3] Grupo de Estudios Ambientales–Instituto de Matemática Aplicada San Luis, Consejo Nacional de Investigaciones Científicas y Técnicas, Universidad Nacional de San Luis, D5700HHW San Luis, Argentina
* e-mail: yzhaosoils@gmail.com

Introduction

According to Godfray et al. (2010), the world's population is expected to grow to nearly 10 billion by 2050, resulting in immense strain on resources like food and water. Climate change has further compounded the challenges of water and food security, necessitating innovative and sustainable methods that can improve crop yield and preserve water resources. While fresh water accounts for just 2.5% of the earth's total water supply (Gleick and Palaniappan 2010), agriculture consumes approximately 70% of all fresh water (Gan et al. 2013). This underscores the limited supply of fresh water and the conflict in allocating it between agriculture and other sectors. As climate change continues to reduce water availability in numerous regions (de Wit and Stankiewicz 2006), the water and food security issues necessitate interdisciplinary research to advance the field of agrohydrology.

Theoretical advancements in agrohydrology could benefit greatly from Critical Zone (CZ) science. The CZ is the area where rock, soil, water, air, and living organisms interact in the near-surface terrestrial environment, and it is known for its pervasive heterogeneity (Lin 2010). By combining Earth's near-surface systems across different spatiotemporal scales and gradients, the CZ concept can connect scientific knowledge that was previously disjointed.

Materials and methods

In order to tackle the issue of integrating various hydrologic subdisciplines, we suggest the introduction of a new field of research called "CZ Agrohydrology". This field takes into account the overlap between CZ processes and approaches in Hydrogeology, Hydropedology, Ecohydrology, and Hydrometeorology, while also identifying knowledge gaps. Similarly, we noticed one previous paper which proposed the concept of "CZ Hydrology" (Brooks et al. 2015). The key to the success of CZ Agrohydrology is the improvement of our understanding of the structure and processes governing water cycles in agricultural ecosystems. By doing so, we can advance CZ science, hydrology, and agriculture in a complementary way.

This perspective explores the potential for a revitalized area of study, CZ Agrohydrology, given recent advancements in the fields of CZ and agrohydrology, as well as the establishment of water-related observatories globally. The focus of CZ Agrohydrology includes clarifying the fundamental concepts of both CZ and agrohydrology, proposing a research framework to identify key characteristics and opportunities for CZ Agrohydrology, developing a comprehensive methodology for advancing the field, and discussing potential applications.

Results and concluding remarks

Critical Zone Science strengthens function-oriented agroecosystems: CZ Science is a field of study that emphasizes research and understanding across different scales and from a systematic perspective. It offers the opportunity to use knowledge from environmental and earth sciences to address real-world sustainability challenges. The CZ framework has led to a shift from reductionism to holism, which has attracted considerable attention from scientists in various disciplines. CZ Science links CZ structure, function, process, and services, integrating knowledge from disciplines such as soil science, hydrology, ecology, and agronomy to study the water and nutrient cycling processes that occur in the CZ and their

interactions with human activities. Agrohydrology can benefit from function-oriented approaches that consider the multi-functionality of CZs at different scales. Research can focus on function identification and assessment, dynamics, and associated driving forces, strategies, and models to optimize sustainable agricultural management.

New approaches in advancing AZ Agrohydrology: Researchers have recently acknowledged the necessity of interdisciplinary approaches to agrohydrology, and have made strides in developing integrated theories and approaches that can help comprehend the interactions between water and agricultural systems in the CZ. While hydrology sub-disciplines have successfully applied the integrated approaches of CZ science, this has not been the case in the field of agrohydrology. There is a need for greater coordination among different hydrologic subdisciplines in this area. The implementation of agrohydrology in the CZ is expected to offer valuable insights into enhancing agricultural management practices and promoting sustainable and resilient agroecosystems.

Application of CZ Agrohydrolgy on Modern Agriculture: Regenerate response Integrating the 5M approaches can provide a more comprehensive application of the CZ science in agrohydrology. This understanding can be used to create sustainable and resilient strategies for managing water and nutrients in agriculture. The modern agricultural sector is adopting new data-driven practices that prioritize the integration of emerging technologies. Tablets and smartphones are becoming increasingly important tools in this regard. The Internet of Things and advanced control strategies are also being leveraged to achieve improved monitoring and control of irrigation farming using node sensors in the crop field with data management via smartphone and web applications. These solutions highlight both prospects and problems, and their integration can lead to site-specific irrigation systems that are remotely controllable using a camera and smartphone. Future developments in Decision Support Systems will likely focus on integrating moisture sensors, wireless networks, and remote sensing images. Smart agriculture and intelligent agriculture are related to precision agriculture, but they focus on using data and technology to enhance decision-making in agriculture. Combining smart sensor technologies with state-of-the-art terrestrial and crop growth models can help ensure agricultural production under a changing climate. The development of CZ Agrohydrology can lead to more sustainable, resilient, and efficient agricultural systems.

References

Brooks PD, Chorover J, Fan Y, Godsey E, Maxwell RM, McNamara JP, Tague C (2015) Hydrological partitioning in the critical zone: Recent advances and opportunities for developing transferrable understanding of water cycle dynamics. Water Resour Res 51: 6973–6987. https://doi.org/10.1002/2015WR017039

de Wit M, Stankiewicz J (2006) Changes in surface water supply across Africa with predicted climate change. Science 31(311): 1917–1921. http://doi.org/10.1126/science.1119929

Gan YT, Siddique KHM, Turner NC, Li XG, Niu JY, Yang C, Liu L, Chai Q (2013) Ridge-furrow mulching systems-an innovative technique for boosting crop productivity in semiarid rain-fed environments. Adv Agron 118: 429-476. https://doi.org/10.1016/B978-0-12-405942-9.00007-4

Gleick PH, Palaniappan M (2010) Peak water limits to freshwater withdrawal and use. Proc Natl Acad Sci USA 107: 11155–11162. http://doi.org/10.1073/pnas.1004812107

Godfray HCJ, Beddington JR, Crute IR, Haddad L, Lawrence D, Muir JF, Pretty J, Robinson S, Thomas SM, Toulmin C (2010) Food security: the challenge of feeding 9 billion people. Science 327: 812–818. http://doi.org/10.1126/science.1185383

Lin H (2010) Earth's Critical Zone and hydropedology: Concepts, characteristics and advances. Hydrol Earth Syst Sci 14: 25–45. http://doi.org/10.5194/hess-14-25-2010

ISBN: 978-618-84419-1-0

PLATINUM SPONSOR

GREEN FUND

MINISTRY OF ENVIRONMENT & ENERGY

GOLD SPONSOR

RESEARCH COMMITTEE
ARISTOTLE UNIVERSITY OF THESSALONIKI

SILVER SPONSORS

TEE | TKM

SCIENTACT

YAS consulting

UNIQUE TECHNOLOGY

SPONSORS

Marathon Data Systems
www.marathondata.gr

ΠΡΑΣΙΝΟ ΤΑΜΕΙΟ

Έργο: 12ο Διεθνές Συνέδριο της Ευρωπαϊκής Ένωσης Υδατικών Πόρων (12th World Congress of European Water Resources Association)
Χρηματοδότηση Πράσινο Ταμείο
Χρηματοδοτικό πρόγραμμα και μέτρο: «Φυσικό περιβάλλον και καινοτόμες δράσεις 2023»
Άξονας Προτεραιότητας: ΑΠ.2 «Δράσεις Διατήρησης Βιοποικιλότητας, Καινοτόμες δράσεις – Έξυπνες Πόλεις – Λοιπές δράσεις»
Προϋπολογισμός Έργου: 15.000€
Τμήμα Αγρονόμων και Τοπογράφων Μηχανικών, Πολυτεχνική Σχολή, Α.Π.Θ. (Ε.Λ.Κ.Ε. Α.Π.Θ.)

http://ewra2023.ewra.net